NATIONAL TECHNICAL UNIVERSITY OF ATHENS

SCHOOL OF ELECTRICAL & COMPUTER ENGINEERING
Division of Communications, Electronic & Information Engineering

Resource Allocation and Service Management in Next Generation 5G Wireless Networks

A Thesis submitted to attain the degree of
Doctor of Philosophy

PANAGIOTIS I. VAMVAKAS

Dipl.-Ing. in Electrical and Computer Engineering
National Technical University of Athens

M.Sc. in Management, Technology & Economics
ETH Zürich

Athens, Greece - November, 2019

ΕΘΝΙΚΟ ΜΕΤΣΟΒΙΟ ΠΟΛΥΤΕΧΝΕΙΟ

ΣΧΟΛΗ ΗΛΕΚΤΡΟΛΟΓΩΝ ΜΗΧΑΝΙΚΩΝ & ΜΗΧΑΝΙΚΩΝ ΥΠΟΛΟΓΙΣΤΩΝ
Τομέας Επικοινωνιών, Ηλεκτρονικής και Συστημάτων Πληροφορικής

Κατανομή Πόρων και Διαχείριση Υπηρεσιών σε Ασύρματα Δίκτυα Νεώτερης Γενιάς

ΔΙΔΑΚΤΟΡΙΚΗ ΔΙΑΤΡΙΒΗ

ΠΑΝΑΓΙΩΤΗΣ Ι. ΒΑΜΒΑΚΑΣ

ΗΛΕΚΤΡΟΛΟΓΟΣ ΜΗΧΑΝΙΚΟΣ & ΜΗΧΑΝΙΚΟΣ ΥΠΟΛΟΓΙΣΤΩΝ ΕΜΠ
M.Sc. MANAGEMENT, TECHNOLOGY & ECONOMICS ETH ZÜRICH

Αθήνα, Νοέμβριος 2019

NATIONAL TECHNICAL UNIVERSITY OF ATHENS

SCHOOL OF ELECTRICAL & COMPUTER ENGINEERING
Division of Communications, Electronic & Information Engineering

Resource Allocation and Service Management in Next Generation 5G Wireless Networks

A Thesis submitted to attain the degree of
Doctor of Philosophy

PANAGIOTIS I. VAMVAKAS

Dipl.-Ing. in Electrical and Computer Engineering, NTUA

M.Sc. in Management, Technology & Economics, ETH Zürich

Advisory Committee: Prof. Dr. Symeon Papavassiliou, NTUA *(Supervisor)*
Prof. Dr. Dimitrios Askounis, NTUA
Asst. Prof. Dr. Ioanna Roussaki, NTUA

Approved by the seven-member examination committee on November 29, 2019

.....	.....	.....
Symeon Papavassiliou	Dimitrios Askounis	Ioanna Roussaki
Professor NTUA	Professor NTUA	Assistant Professor NTUA
.....	.....	.....
Theodora Varvarigou	Athanasios Panagopoulos	Miltiadis Anagnostou
Professor NTUA	Associate Professor NTUA	Professor NTUA

.....
Eirini Eleni Tsiropoulou
Assistant Professor UNM

Athens, Greece - November, 2019

.....
Παναγιώτης Ι. Βαμβακάς
Διδάκτωρ Ηλεκτρολόγος Μηχανικός και Μηχανικός Υπολογιστών Ε.Μ.Π.

In a dream it's typical
not to be rational

John Forbes Nash, Jr.

Abstract

The accelerated evolution towards next generation networks is expected to dramatically increase mobile data traffic, posing challenging requirements for future radio cellular communications. User connections are multiplying, whilst data hungry content is dominating wireless services putting significant pressure on network's available spectrum. Ensuring energy-efficient and low latency transmissions, while maintaining advanced Quality of Service (QoS) and high standards of user experience are of profound importance in order to address diversifying user prerequisites and ensure superior and sustainable network performance. At the same time, the rise of 5G networks and the Internet of Things (IoT) evolution is transforming wireless infrastructure towards enhanced heterogeneity, multi-tier architectures and standards, as well as new disruptive telecommunication technologies. The above developments require a rethinking of how wireless networks are designed and operate, in conjunction with the need to understand more holistically how users interact with the network and with each other.

In this dissertation, we tackle the problem of efficient resource allocation and service management in various network topologies under a user-centric approach. In the direction of ad-hoc and self-organizing networks where the decision making process lies at the user level, we develop a novel and generic enough framework capable of solving a wide array of problems with regards to resource distribution in an adaptable and multi-disciplinary manner. Aiming at maximizing user satisfaction and also achieve high performance - low power resource utilization, the theory of network utility maximization is adopted, with the examined problems being formulated as non-cooperative games. The considered games are solved via the principles of Game Theory and Optimization, while iterative and low complexity algorithms establish their convergence to steady operational outcomes, i.e., Nash Equilibrium points. This thesis consists a meaningful contribution to the current state of the art research in the field of wireless network optimization, by allowing users to control multiple degrees of freedom with regards to their transmission, considering mobile customers and their strategies as the key elements for the amelioration of network's performance, while also adopting novel technologies in the resource management problems.

First, multi-variable resource allocation problems are studied for multi-tier architectures with the use of femtocells, addressing the topic of efficient power and/or rate control, while also the topic is examined in Visible Light Communication (VLC) networks under various access technologies. Next, the problem of customized resource pricing is considered as a separate and bounded resource to be optimized under distinct scenarios, which expresses users' willingness to pay instead of being commonly implemented by a central administrator in the form of penalties. The investigation is further expanded by examining the case of service provider selection in competitive telecommunication markets which aim to increase their market share by applying different pricing policies, while the users model the selection process by behaving as learning automata under a Machine Learning framework.

Additionally, the problem of resource allocation is examined for heterogeneous services where users are enabled to dynamically pick the modules needed for their transmission based on their preferences, via the concept of Service Bundling. Moreover, in this thesis we examine the correlation of users' energy requirements with their transmission needs, by allowing the adaptive energy harvesting to reflect the consumed power in the subsequent information transmission in Wireless Powered Communication Networks (WPCNs).

Furthermore, in this thesis a fresh perspective with respect to resource allocation is provided assuming real life conditions, by modeling user behavior under Prospect Theory. Subjectivity in decisions of users is introduced in situations of high uncertainty in a more pragmatic manner compared to the literature, where they behave as blind utility maximizers. In addition, network spectrum is considered as a fragile resource which might collapse if over-exploited under the principles of the Tragedy of the Commons, allowing hence users to sense risk and redefine their strategies accordingly. The above framework is applied in different cases where users have to select between a safe and a common pool of resources

(CPR) i.e., licensed and unlicensed bands, different access technologies, etc., while also the impact of pricing in protecting resource fragility is studied. Additionally, the above resource allocation problems are expanded in Public Safety Networks (PSNs) assisted by Unmanned Aerial Vehicles (UAVs), while also aspects related to network security against malign user behaviors are examined.

Finally, all the above problems are thoroughly evaluated and tested via a series of arithmetic simulations with regards to the main characteristics of their operation, as well as against other approaches from the literature. In each case, important performance gains are identified with respect to the overall energy savings and increased spectrum utilization, while also the advantages of the proposed framework are mirrored in the improvement of the satisfaction and the superior Quality of Service of each user within the network. Lastly, the flexibility and scalability of this work allow for interesting applications in other domains related to resource allocation in wireless networks and beyond.

Keywords: Resource Allocation, Wireless Networks, Utility Function, Power Control, Rate Control, Pricing, Game Theory, Prospect Theory, Nash Equilibrium, Optimization, Multiple Services

Περίληψη

Τα ασύρματα δίκτυα νεώτερης γενιάς έχουν συνδεθεί στενά με την κατακόρυφη αύξηση της ζήτησης ως προς τον όγκο δεδομένων, τους ρυθμούς μετάδοσης, και του πλήθους των συνδεδεμένων χρηστών. Η ανάπτυξη και κυκλοφορία σύγχρονων, έξυπνων κινητών συσκευών υπό την έλευση του λεγόμενου "Διαδικτύου των Πραγμάτων" (Internet of Things), έχει συνυφαστεί με την εξέλιξη διαφορετικών μορφών επικοινωνίας και υπηρεσιών, οι οποίες ικανοποιούν διαφορετικές ανάγκες ενός ολοένα και πιο ετερογενούς και μεταβαλλόμενου πλήθους χρηστών, με διακριτές και συχνά αντικρουόμενες προτεραιότητες ως προς τα χαρακτηριστικά και τις απαιτήσεις τους.

Σύμφωνα με νεώτερες μελέτες, ο αριθμός των διασυνδεδεμένων συσκευών αναμένεται να ξεπεράσει τον παγκόσμιο πληθυσμό έως το 2021, με αναπόφευκτη την αύξηση της κίνησης και του συνωστισμού στα ασύρματα δίκτυα, ενώ η συντριπτική πλειοψηφία του όγκου πληροφορίας θα αφορά υπηρεσίες πολυμέσων. Η ανωτέρω επιτελούμενη επανάσταση σε συνδυασμό με την υλοποίηση των δικτύων 5ης γενίας (5G networks), μετασχηματίζουν ριζικά το τοπίο στον σχεδιασμό και την λειτουργία των ασύρματων δικτύων και τεχνολογιών τηλεπικοινωνίας. Σε αντίθεση με τα υφιστάμενα πρότυπα, τα δίκτυα 5ης γενιάς δεν αποτελούν μια απλή βελτίωση όσον αφορά την αύξηση του εύρους ζώνης ή της μαζικότερης συνδεσιμότητας, αλλά προτείνουν μια συνολικά διαφορετική αρχιτεκτονική ως προς την μετάδοση επικοινωνίας και την παροχή υπηρεσιών.

Βασικός πυλώνας της ανάπτυξης των σύγχρονων τηλεπικοινωνιακών συστημάτων αποτελεί η βελτιστοποίηση της ποιότητας της υπηρεσίας (Quality of Service) του εκάστοτε χρήστη εντός του δικτύου, τόσο ως προς το περιεχόμενο αλλά και την απαιτούμενη καταναλισκόμενη ενέργεια, λαμβάνοντας υπόψη την διαφορετικότητα των χρηστών και των αναγκών τους. Επιπλέον, η ελαχιστοποίηση του κόστους, η ορθολογική κατανομή των πόρων, και η ικανότητα προσαρμογής των δικτυακών συστημάτων σε ένα διαρκώς μεταβαλλόμενο περιβάλλον αποτελούν πρόσθετους παράγοντες που συμβάλλουν καθοριστικά στην λειτουργία και τις επιδόσεις των σύγχρονων αυτο-οργανώμενων (ad-hoc) ασύρματων δικτύων.

Με βάση τα ανωτέρω στοιχεία, η παρούσα διδακτορική διατριβή επιδιώκει να προσφέρει ένα ολιστικό πλαίσιο για την κατανομή πόρων σε διαδικτυακά περιβάλλοντα νεώτερης γενιάς, το οποίο επιτυγχάνει όχι μόνο την μεγιστοποίηση της ικανοποίησης και της χρησιμότητας που απολαμβάνουν οι χρήστες από την εκπομπή τους, αλλά και την συνολική βελτίωση της λειτουργίας του δικτύου. Ιδιαίτερο ενδιαφέρον δίνεται στην ζεύξη ανόδου (uplink) ως προς τους διαφορετικούς πόρους του δικτύου (εύρος ζώνης, ισχύς εκπομπής, κλπ.) για ποικίλες υπηρεσίες πραγματικού και μη χρόνου. Παράλληλα, μελετάται πλήθος μεθοδολογιών, αρχιτεκτονικών, και προτύπων επικοινωνίας με στόχο την περεταίρω βελτιστοποίηση της αποδοτικότητας του δικτύου προς όφελος των χρηστών σε σύγκριση με τις διάφορες τεχνολογίες αιχμής όπως αυτές έχουν μελετηθεί στην βιβλιογραφία.

Τα εξεταζόμενα προβλήματα μοντελοποιούνται με κριτήριο την μεγιστοποίηση της χρησιμότητας του δικτύου με βάση τις διάφορες παραμέτρους των προβλημάτων κατανομής πόρων, όπως το κέρδος καναλιού, παρεμβολές, σηματοθορυβικός λόγος, ισχύς εκπομπης, ρυθμός μετάδοσης κλπ. Με αυτόν τον τρόπο, ποσοτικοποιείται η ικανοποίηση του εκάστοτε χρήστη από την λαμβανόμενη υπηρεσία, όπως αυτή διατυπώνεται από την υιοθέτηση της συνάρτησης χρησιμότητας (utility function) ως δάνειο από την Μικροοικονομική Επιστήμη. Σε κάθε περίπτωση, τα υπό μελέτη προβλήματα διατυπώνονται ως μη συνεργατικά παίγνια σύμφωνα με τις αρχές της Θεωρίας Παιγνίων (Game Theory) και Βελτιστοποίησης, ενώ η επίλυσή τους επιβεβαιώνει την σύγκλιση σε σημεία ισορροπίας κατά Nash (Nash Equilibria), η εύρεση των οποίων επικυρώνει την ύπαρξη βέλτιστων συνθηκών επικοινωνίας εντός του δικτύου, από τις οποίες κανένας χρήστης - παίκτης δεν επιθυμεί να αποκλίνει. Κατανεμημένοι αλγόριθμοι χρησιμοποιούνται για τον πρακτικό εντοπισμό των ανωτέρω σημείων ισορροπίας, λαμβάνοντας υπόψη την μείωση της απαιτούμενης υπολογιστικής πολυπλοκότητας μέσω της αποκέντρωσης των αποφάσεων που λαμβάνονται από τους χρήστες και όχι συγκεντρωτικά από τον διαχειριστή του δικτύου. Ταυτόχρονα, κάθε ένα από τα προτεινόμενα εργαλεία προσομοιώνεται διεξοδικά υπό διαφορετικά σενάρια ώστε να αξιολογηθεί επαρκώς η συνεισφορά τους στην απόδοση του συστήματος, ενώ πραγματοποιείται πληθώρα συγκρίσεων με προβλήματα που έχουν ασχοληθεί με παρεμφερή θέματα.

Οι βασικές συνεισφορές της παρούσας διδακτορικής διατριβής σε σύγκριση με την υφιστάμενη βιβλιογραφία και έρευνα στον τομέα της βελτιστοποίησης των ασύρματων δικτύων μπορούν να συνοψισθούν ως εξής:

- Πολυμεταβλητή και πολυεπίπεδη κατανομή πόρων σε ετερογενή δίκτυα με πολλαπλές υπηρεσίες. Οι χρήστες του δικτύου στα εξεταζόμενα προβλήματα έχουν την δυνατότητα να καθορίζουν πολλαπλούς βαθμούς ελευθέριας της εκπομπής τους. Για πρώτη φορά στην βιβλιογραφία έως και τρεις παράμετροι κατανέμονται εντός του δικτύου, ενώ μικροκυψελωτά συστήματα (φεμτοκυψέλες - femtocells), ή τεχνολογίες ορατού φωτός (visible light communications) μελετώνται διεξοδικά σε θέματα βελτιστοποίησης και καταμερισμού πόρων. Επιπλέον, σε αντίθεση με συμβατικά δίκτυα στα οποία μόνο υπηρεσίες φωνής παρέχονται στους χρήστες, στα πλαίσια της διατριβής διαφορετικές υπηρεσίες πραγματικού και μη χρόνου με διακριτές απαιτήσεις ως προς τον όγκο δεδομένων παρέχονται ταυτόχρονα στους χρήστες ανάλογα με τις προτιμήσεις τους.

- Υιοθέτηση και ενσωμάτωση διαφορετικών ευέλικτων τεχνικών πρόσβασης στην διαδικασία κατανομής πόρων. Η ανάπτυξη σύγχρονων ασύρματων τεχνολογιών για τα δίκτυα νεώτερης γενιάς επιτρέπει την επέκταση και πιο ολοκληρωμένη αξιοποίηση του εύρους ζώνης, μέσω πιο εξελιγμένων μορφών συνδεσιμότητας. Στα προτεινόμενα μοντέλα της διατριβής μελετώνται διαφορετικές τεχνολογίες πρόσβασης (πχ. μη-ορθογωνική τεχνική πολλαπλής πρόσβασης, NOMA και ορθογωνική τεχνική διαίρεση συχνότητας πολλαπλής πρόσβασης, OFDMA), καθώς και συστήματα στα οποία αδειοδοτημένες και μη ζώνες συχνότητας διατίθενται ταυτόχρονα στους χρηστες, οι οποίοι έχουν την δυνατότητα να καθορίζουν την διάρθρωση της εκπομπής τους ώστε να μεγιστοποιήσουν τον βαθμό ικανοποίησής τους από την ποιότητας της υπηρεσίας τους.

- Λελογισμένη αξιοποίηση πόρων, βελτίωση της ενεργειακής αποδοτικότητας, και περιορισμός των επιπέδων ισχύος εκπομπής εντός των δικτύων. Στα πλαίσια της ανάγκης για περιορισμό των ρυπογόνων εκπομπών και της προστασίας του περιβάλλοντος, στην παρούσα εργασία καινοτόμες τεχνικές εφαρμόζονται με στόχο οι χρήστες να επιτυγχάνουν ποιοτικά ανώτερη συνδεσιμότητα και ανταλλαγή δεδομένων με χαμηλότερες ενεργειακές απαιτήσεις. Αυτό καθίσταται εφικτό με την χρήση νέων ενεργειακά ευέλικτων συσκευών που μπορούν να συνδέονται στο δίκτυο με ταυτόχρονη εκπομπή σε περισσότερες από μία τεχνικές πρόσβασης, χρήση πολυεπίπεδων και μικρών κυψελών (πχ. φεμτοκυψέλες), νέα πρότυπα περιορισμού των παρεμβολών (διαδοχική ακύρωση παρεμβολών, SIC), αλλά και προσαρμοστική φόρτιση των συσκευών ανάλογα με τις ενεργειακές ανάγκες της επικείμενης εκπομπής τους μέσω δικτύων επικοινωνιών ασύρματης φόρτισης (wireless powered communication networks). Ταυτόχρονα, ο σχεδιασμός αλγορίθμων για την ορθολογική κατανομή πόρων ανάλογα με τα χαρακτηριστικά και τις προτεραιότητες των χρηστών περιορίζει την κατασπατάλησή των πόρων και συμβάλλει στην βελτιστοποίηση της ενεργειακής απόδοσης του δικτύου.

- Σύνθεση υπηρεσιών μέσω της μεθόδου συγκέντρωσης / ομαδοποίησης προϊόντων (bundling), η οποία απευθύνεται σε διαφορετικές ομάδες καταναλωτών, λαμβάνοντας υπόψη μια πιο εμπορικά βιώσιμη διάσταση σχετικά με την διάθεση δικτυακών προϊόντων. Στις σύγχρονες τηλεπικοινωνίες, οι εκπεμπόμενες υπηρεσίες διακρίνονται όπως έχει ήδη αναφερθεί από σημαντική ετερογένεια και διαθέτουν διαφορετικά χαρακτηριστικά ως προς την ανοχή τους σε καθυστερήσεις ή τον όγκο των μεταδιδόμενων δεδομένων. Στα πλαίσια της παρούσας διατριβής, οι χρήστες εντός του δικτύου έχουν την δυνατότητα να επιλέξουν τα είδη υπηρεσιών που χρειάζονται για την εκπομπή τους, σχηματίζοντας ένα μοναδικό και εξατομικευμένο τηλεπικοινωνιακό προϊόν. Συνδυάζοντας την κατανομή πόρων με την προαναφερθείσα σύνθεση υπηρεσιών, πιθανές συνέργειες και αλληλοεξαρτήσεις δημιουργούν όλες εκείνες τις συνθήκες για την ανάπτυξη πιο αποδοτικών προϊόντων τόσο σε επίπεδο ανταπόκρισης στις ανάγκες των χρηστών, όσο και για την ενεργειακή τους συμπεριφορά και διαχείρηση του εύρους ζώνης.

- Σχεδιασμός και εισαγωγή νέων τεχνικών κοστολόγησης οι οποίες επιτρέπουν την εξατομίκευση των τιμολογιακών πολιτικών στην κατανομή πόρων, αλλά και στην ενίσχυση του ανταγωνισμού. Για πρώτη φορά σε προβλήματα βελτιστοποίησης δικτύων, το εκάστοτε κόστος της εκπομπής δεν επιβάλλεται ως μία εξωτερική ποινή για τον περιορισμό των παρεμβολών, αλλά αντιμετωπίζεται ως ένας ανεξάρτητος και πεπερασμένος πόρος, τον οποίο οι χρήστες κατανέμουν ανάλογα με τις ανάγκες τους εκδηλώνοντας τον βαθμό στον οποίο αποδέχονται να κοστολογηθούν για να εκπέμψουν και να λάβουν την εκάστοτε υπηρεσία. Με αυτόν τον τρόπο, οι πόροι (πχ. εύρος ζώνης, ισχύς εκπομπής) καταλήγουν στους χρήστες εκείνους οι οποίοι είναι διατεθειμένοι να κοστολογηθούν περισσότερο, οδηγώντας σε

πιο δίκαιες κατανομές που αντικατοπτρίζουν την συμπεριφορά των καταναλωτών εντός του δικτύου. Παράλληλα, ο σχεδιασμός διαφορετικών τιμολογιακών πολιτικών ενισχύει τον ανταγωνισμό μεταξύ των παρόχων υπηρεσιών ευνοώντας τους καταναλωτές.

- Έως τώρα, η μοντελοποίηση της συμπεριφοράς των χρηστών σε ασύρματα δίκτυα γινόταν σύμφωνα με τις αρχές της Θεωρίας Αναμενόμενης Χρησιμότητας (Expected Utility Theory), κατά την οποία οι χρήστες του δικτύου έχουν ομοιογενή συμπεριφορά επιδιώκοντας απλά την μεγιστοποίηση της ικανοποίησής τους από την ποιότητα της υπηρεσίας. Ωστόσο, η εν λόγω θεώρηση δεν κατορθώνει να καλύψει επαρκώς την συμπεριφορά των χρηστών σε ένα δίκτυο, καθώς απουσιάζει πλήρως η υποκειμενικότητα στην λήψη αποφάσεων υπό συνθήκες αβεβαιότητας. Το κενό αυτό καλύπτεται στην διατριβή αυτή με την εισαγωγή της Θεωρίας Προοπτικής (Prospect Theory), η οποία αποτελεί ένα από τα κυριάρχα εργαλεία στον κλάδο των Συμπεριφορικών Οικονομικών (Behavioral Economics), σχετικά με την μοντελοποίηση της ανθρώπινης συμπεριφοράς και την διαδικασία λήψης αποφάσεων. Αυτό οφείλεται στο γεγονός ότι οι χρήστες τείνουν να υπερεκτιμούν την επίδραση από μια ενδεχόμενη απώλεια σε σχέση με ένα θετικό αποτέλεσμα, με συνέπεια να παρεκλίνουν από τις προσδοκόμενες αποφάσεις με βάση την προσέγγιση της Θεωρίας Αναμενόμενης Χρησιμότητας. Συνεπώς, προτείνεται και σχεδιάζεται ένα πιο ρεαλιστικό πρότυπο το οποίο ανταποκρίνεται πιο συνολικά στην συμπεριφορά των χρηστών όταν πραγματικές συνθήκες εκπομπής δεδομένων λαμβάνονται υπόψη.

- Παράλληλα, για πρώτη φορά στην βιβλιογραφία, οι υπό κατανομή πόροι (και πιο συγκεκριμένα το εύρος ζώνης) σχεδιάζονται ως εύθραυστοι και πεπερασμένοι ώστε σε περίπτωση υπερβολικής ζήτησης να καταρρέουν και να μην μπορούν να γίνουν διαθέσιμοι εκ νέου στους χρήστες του δικτύου συνολικά. Επομένως, οι χρήστες αντιλαμβάνονται πλέον τις συνθήκες ρίσκου που ενέχουν οι αποφάσεις τους, καθώς μία πιο επιθετική διεκδίκηση του εύρους ζώνης εκ μέρους τους μπορεί να οδηγήσει στην κατάρρευση του και την απώλεια υπηρεσίας, σύμφωνα με τις αρχές της θεώρησης της "Τραγωδίας των Κοινών" (Tragedy of the Commons). Ως αποτέλεσμα, η αντίληψη του κινδύνου από τους χρήστες αναδεικνύεται ως βασική παράμετρος σύμφωνα με την οποία λαμβάνονται οι αποφάσεις για τον καταμερισμό των πόρων του δικτύου.

- Το πρόβλημα της κατανομής πόρων επεκτείνεται σε νέα πεδία μέσω της υιοθέτησης προηγμένων τεχνικών εξαγωγής δεδομένων και της "Νοημοσύνης των Μηχανών" (Machine Learning), ενώ αυτοοργανώμενα Δίκτυα Δημόσιας Ασφάλειας (Public Safety Networks), εγκαθίστανται σε περιβάλλοντα με αντίξοες συνθήκες επικοινωνίας (πχ. λόγω φυσικών καταστροφών, τρομοκρατίας κλπ). Πιο συγκεκριμένα, η αλματώδης αύξηση της κίνησης και της ανταλλασσόμενης πληροφορίας καθιστά αναγκαία την ανάπτυξη εργαλείων για την λήψη αποφάσεων και την διαχείριση των δεδομένων από τους χρήστες. Αυτό καθίσταται εφικτό μέσω της χρήσης τεχνικών για την αναγνώριση προτύπων αλλά και προς την κατεύθυνση της αυτοματοποίησης της βελτιστοποίησης των δικτύων. Επιπλέον, η χρήση μη επανδρωμένων ιπτάμενων οχημάτων (Unmanned Aerial Vehicles), σε δίκτυα δημόσιας ασφάλειας επιφέρει συγκριτικά πλεονεκτήματα όσον αφορά την άμεση και εύκολη εγκαθίδρυση αξιόπιστων τηλεπικοινωνιών σε επείγοντα γεγονότα ή απρόσμενες περιστάσεις, τα οποία θέτουν σε κίνδυνο την δημόσια τάξη και ασφάλεια, αλλά και συμβάλλουν στον εντοπισμό και στην αποβολή κακόβουλων χρηστών από το δίκτυο.

Ακόλουθα, παρατίθεται μια συνοπτική περιγραφή της δομής της διδακτορικής διατριβής και των σημαντικότερων προβλημάτων που μελετήθηκαν και επιλύθηκαν.

Κατανομή πόρων σε πολυεπίπεδες αρχιτεκτονικές δικτύων

Αρχικά, μελετάται διεξοδικά η διαχείριση της ισχύος εκπομπής και του ρυθμού μετάδοσης ζεύξης ανόδου σε διεπίπεδα φεμτοκυψελωτά δίκτυα πολλαπλών υπηρεσιών και σε δίκτυα επικοινωνίας ορατού φωτός. Οι εν λόγω προσεγγίσεις έχουν αναδειχθεί ως ιδιαίτερα επωφελείς λύσεις για την μείωση των εκπομπών και την αύξηση του περιθωρίου του φάσματος του δικτύου με πολύ χαμηλό κόστος εγκατάστασης αφορώντας εκπομπές μικρής γεωγραφικής έκτασης. Στην περίπτωση των φεμτοκυψελωτών δικτύων, ένα σημείο πρόσβασης συνδέεται εντός του δικτύου (μακροκυψέλης) με τους χρήστες να μπορούν να συνδεθούν σε ένα εκ των δύο. Οι χρήστες εντός της φεμτοκυψέλης απολαμβάνουν ιδιαίτερα ευνοϊκές συνθήκες εκπομπής λογώ της πολύ μικρής απόστασης από το σημείο πρόσβασης, ενώ έχουν πρόσβαση στο εύρος ζώνης χωρίς περιορισμούς σε σχέση με τους χρήστες εντός της μακροκυψέλης. Αντίστοιχα, στα δίκτυα επικοινωνίας ορατού φωτός, η ανταλλαγή δεδομένων γίνεται μέσω της χρήσης δεσμών φωτός, παρέχοντας σε κλειστούς χώρους μικρής

γεωγραφικής κάλυψης ουσιαστικά απεριόριστο εύρος ζώνης το οποίο μπορεί να αξιοποιηθεί υπό πολύ χαμηλές απαιτήσεις ενέργειας και χωρίς επιβλαβείς επιπτώσεις στην υγεία. Οι χρήστες συνδέονται σε οπτικά σημεία πρόσβασης στο εσωτερικό της μακροκυψελης σχηματίζοντας ένα διεπίπεδο δίκτυο, εξασφαλίζοντας έτσι την αποσυμφόριση της κίνησης. Όπως αναφέρθηκε, για την θεωρητική διατύπωση των προβλημάτων, σε κάθε χρήστη ανατίθεται μία χαρακτηριστική συνάρτηση χρησιμότητας με βάση το είδος της υπηρεσίας και τον κλάδο του δικτύου στον οποίο ανήκει (φεμτοκυψέλη, δίκτυο ορατού φωτός ή μακροκυψέλη).

Σε πρώτο στάδιο, ερευνάται το πρόβλημα του ελέγχου της ισχύος εκπομπής P_i των χρηστών σε διεπίπεδα ασύρματα φεμτοκυψελωτά δίκτυα. Η επίλυση των προβλημάτων βασίζεται στην χρήση μη συνεργατικών παιγνίων με στρατηγική συμπληρωματικότητα (Supermodular Games), από τα οποία επιβεβαιώνεται η ύπαρξη ενός σταθερού σημείου ισορροπίας κατά Nash. Με την χρήση κατανεμημένων αλγορίθμων και μέσω μίας σειράς αριθμητικών προσομοιώσεων, κατέστη προφανές ότι η ύπαρξη φεμτοκυψελών επιφέρει σημαντική μείωση στις ενεργειακές απαιτήσεις του δικτύου. Επιπλέον, διευκολύνεται η διαχείριση της κίνησης του δικτύου με ταυτόχρονη αύξηση του ρυθμού μετάδοσης των δεδομένων λόγω του κατακερματισμού των χρηστών σε δύο επίπεδα. Ταυτόχρονα, η πλεονεκτική τοποθέτηση των χρηστών εντός των φεμτοκυψελών στις οποίες επικρατούν ανώτερες συνθήκες κέρδους καναλιού συγκριτικά με την μακροκυψέλη, συμβάλλει επιπρόσθετα στην αναβάθμιση της ποιότητας της εκπομπής λόγω της μικρής απόστασης από το σημείο πρόσβασης.

Εν συνεχεία, το πρόβλημα επεκτείνεται ενσωματώνοντας και τον ρυθμό μετάδοσης R_i στην κατανομή των πόρων, εκ νέου σε διεπίπεδα φεμτοκυψελωτά δίκτυα. Για την επίλυση του διπαραμετρικού προβλήματος και για τον περιορισμό της πολυπλοκότητας, το πρόβλημα βελτιστοποίησης μετασχηματίζεται σε μονοπαραμετρικό μέσω του λόγου του ρυθμού μετάδοσης ως προς την αντίστοιχη ισχύ εκπομπής, $x_i = {}^{R_i}/_{P_i}$. Το πρόβλημα διατυπώνεται και σε αυτήν την περίπτωση ως μη συνεργατικό παίγνιο και επιλύεται μέσω της απόδειξης της οιονεί κοιλότητας (quasi-concavity) της συνάρτησης χρησιμότητας. Το εξεταζόμενο πρόβλημα προσομοιώθηκε για διάφορα σενάρια, με τα αποτελέσματα να αποδεικνύουν τα οφέλη από την διαχείριση δύο πόρων σε σχέση με το μονοπαραμετρικό πρόβλημα.

Στοχεύοντας σε μία πιο ολιστική αντιμετώπιση της διπαραμετρικής κατανομής, το πρόβλημα του ελέγχου της ισχύος εκπομπής και του ρυθμού μετάδοσης επιλύεται εκ νέου με δύο μεταβλητές αυτήν την φορά, μέσω της χρήσης πολυμεταβλητών μη συνεργατικών παιγνίων με στρατηγική συμπληρωματικότητα. Η εύρεση του σημείου ισορροπίας κατά Nash και η εκτενής ανάλυση της απόδοσης του προτεινόμενου μοντέλου δηλώνουν τις περεταίρω βελτιώσεις στην κατεύθυνση της πτώσης της ισχύος, την αύξηση των ρυθμών μετάδοσης, και την ανώτερη ενεργειακή αποδοτικότητα. Το πρόβλημα προσομοιώνεται για διάφορες τοπολογίες με αυξανόμενο αριθμό χρηστών, υπηρεσιών και φεμτοκυψελών καθώς και συγκριτικά με την βιβλιογραφία, με την σχετική βελτίωση σε όλα τα στοιχεία της μετάδοσης να αιτιολογούνται στην αυτονομία και τον πλήρη έλεγχο δύο μεταβλητών.

Ολοκληρώνοντας το κεφάλαιο, παρατίθεται η μελέτη του συνδυαστικού προβλήματος ισχύος και οπτικών σημείων πρόσβασης σε δίκτυα ορατού φωτός αυτήν την φορά. Το πρόβλημα επιλύεται ξεχωριστά για δύο τεχνικές πρόσβασης (NOMA και OFDMA), με τα αποτελέσματα να αναδεικνούν ενδιαφέροντα συμπεράσματα ως προς τις διαφορές και τα πλεονεκτήματα της κάθε υλοποίησης.

Κοστολόγηση πόρων σε ασύρματα δίκτυα

Στο επόμενο κεφάλαιο της διατριβής ερευνώνται θέματα σχετικά με πρωτότυπες πολιτικές κοστολόγησης συνδυαστικά με την κατανομή πόρων σε ασύρματα δίκτυα. Η εκάστοτε τιμολόγηση συνιστά βασικό παράγοντα για την βελτιστοποίηση και την εμπορική εκμετάλλευση ενός ασυρμάτου δικτύου, καθώς αποτελεί ένα ευέλικτο εργαλείο για την συμμόρφωση των χρηστών σε κοινωνικά πιο αποδεκτά πρότυπα σχετικά με την πρόκληση παρεμβολών και την δέσμευση πόρων. Η έρευνά μας φέρει την καινοτομία ότι η εκάστοτε τιμή για τον καταμερισμό ενός πόρου αφορά μια νέα μεταβλητή που μπορεί να βελτιστοποιηθεί ως ένας ξεχωριστός πόρος του συστήματος.

Αρχικά, μελετάται το πρόβλημα της ταυτόχρονης διαχείρισης του επιπέδου των τιμών και της ισχύος εκπομπής για τον κάθε χρήστη. Οι συναρτήσεις χρησιμότητας μετασχηματίζονται ανάλογα για υπηρεσίες πραγματικού και μη χρόνου ώστε να συμπεριλάβουν μία συνάρτηση κόστους με τους χρήστες εν τέλει να ορίζουν το βέλτιστο ζεύγος της ισχύος εκπομπής και της τιμής που αποδέχονται να κοστολογηθούν προκειμένου να κατορθώσουν να εκπέμψουν. Το πρόβλημα μοντελοποιείται ως μη συνεργατικό παίγνιο με δύο μεταβλητές, την ισχύ εκπομπής P_i και το αντίστοιχο κόστος c_i για κάθε χρήστη, και επιλύεται με χρήση των παιγνίων με στρατηγικά υποκατάστατα (Submodular Games) λόγω της περιοριστικής επίδρασης των υψηλότερων τιμών στην άνοδο της ισχύος εκπομπής. Η υλοποίηση του προτεινόμενου μοντέλου υπό διαφορετικά κριτήρια (πχ. με βάση το είδος της υπηρεσίας, την απόσταση από τον σταθμό βάσης ή την

πλήρη εξατομίκευση των τιμών) επιφέρει σημαντικές βελτιώσεις στην ικανοποίηση των χρηστών, εξαιτίας του ελέγχου της κοστολόγησης αναφορικά με τις πραγματικές τους ανάγκες για την λήψη της εκάστοτε υπηρεσίας.

Συνακόλουθα, το πρόβλημα επιλύεται για ένα νέο ζεύγος μεταβλητών, αυτήν την φορά του ρυθμού μετάδοσης R_i και της κοστολόγησης c_i. Η προσέγγιση αυτή δίνει μία πιο πρακτική αντιμετώπιση από πλευράς οικονομικής φύσεως, καθώς οι χρήστες δηλώνουν την τιμή που αποδέχονται να κοστολογηθούν προκειμένου να δεσμεύσουν ένα τμήμα του διαθέσιμου εύρους ζώνης υπό συνθήκες ανταγωνισμού. Η σύνδεση της ζήτησης και της προσφοράς του εύρους ζώνης επεξηγείται και επιλύεται και αυτήν την φορά μεσω των μη συνεργατικών παιγνίων με στρατηγική συμπληρωματικότητα, ως συνέπεια της τάσης των χρηστών να αποδέχονται υψηλότερες τιμές όταν οι ανταγωνιστές τους αποσπούν μεγαλύτερο μέρος του διαθέσιμου φάσματος. Τα αποτελέσματα της υλοποίησης και αριθμητικής προσομοιώσης του συστήματος ανέδειξαν τα σημαντικά οφέλη για τους επιτυγχανόμενους ρυθμούς μετάδοσης του κάθε χρήστη αλλά και συνολικά για το δίκτυο.

Η κατανομή και κοστολόγηση πόρων κλείνει με μία πολυσύνθετη προσέγγιση, κατά την οποία για πρώτη φορά επιχειρείται η επίλυση ενός τριπαραμετρικού προβλήματος. Πιο αναλυτικά, ταυτόχρονα η ισχύς εκπομπής P_i, ο ρυθμός μετάδοσης R_i, και το αντίστοιχο κόστος c_i καθορίζονται από τους χρήστες οι οποίοι ελέγχουν δυναμικά και καθορίζουν την τιμή που λαμβάνει ο κάθε ένας από τους τρεις πόρους. Το πρόβλημα απλοποιείται ορίζοντας τον λόγο x_i του ρυθμού μετάδοσης ως προς την ισχύ εκπομπής, ενώ επιλύεται εκ νέου με την χρήση των παιγνίων με στρατηγική συμπληρωματικότητα. Η εύρεση του σημείου ισορροπίας κατά Nash οδηγεί στην διαπίστωση των σημαντικών κερδών του δικτύου όσον αφορά την ποιότητα υπηρεσίας, την ενεργειακή αποδοτικότητα, και την ικανοποίηση των χρηστών λόγω των πολλαπλών βαθμών ελευθερίας που ελέγχονται από αυτούς. Επιπλέον, η πλήρης αποκέντρωση του δικτύου λόγω της μεταφοράς της ευθύνης της λήψης των αποφάσεων από τους χρήστες, συμβάλλει στην βελτιστοποίηση και την ομαλή λειτουργία του δικτύου λόγω της ισορροπημένης και εξατομικευμένης πολιτικής κοστολόγησης για τον κάθε χρήστη του συστήματος.

Επιλογή παρόχου σε αγορές ασύρματων τηλεπικοινωνιών

Στο επόμενο κεφάλαιο, μελετάται μία ακόμη επέκταση της κατανομής και κοστολόγησης πόρων σε ασύρματα δίκτυα, αυτήν την φορά ωστόσο σε ένα ευρύτερο πλαίσιο. Ειδικότερα, θεωρούμε μία ανοιχτή τηλεπικοινωνιακή αγορά, στην οποία διαφορετικοί πάροχοι υπηρεσιών ανταγωνίζονται για την απόκτηση μεγαλύτερου μεριδίου, επιβάλλοντας διαφορετικές πολιτικές κοστολόγησης. Ο αυξανόμενος αριθμός των χρηστών και οι ολοένα και περισσότερες εφαρμογές στις ασύρματες επικοινωνίες εντείνουν τον ανταγωνισμό για την κάλυψη των αναγκών των καταναλωτών, ενώ ταυτόχρονα καθίσταται αναγκαίο να ευρεθούν νέες πηγές εσόδων για τους τηλεπικοινωνιακούς παρόχους. Για τον λόγο αυτό, αποκτά ιδιαίτερο ενδιαφέρον η σύνδεση της διαχείρισης πόρων με τον τρόπο που λειτουργούν οι αγορές και να ερευνηθεί παράλληλα πώς η κοστολόγηση των υπηρεσιών και των εκπομπών μετάδοσης, όχι μόνο επιφέρει έναν πιο ορθολογικό καταμερισμό των πόρων, αλλά και οδηγεί συνολικά τις αγορές και τις οικονομίες σε σταθερές συνθήκες λειτουργίας.

Επιπλέον, μία ακόμη συνεισφορά της παρούσας διατριβής αποτελεί η προσπάθεια για την βέλτιστη δυνατή αυτοματοποίηση των αποφάσεων των χρηστών ως προς την επιλογή του παρόχου που προσφέρει την καλύτερη σχέση τιμολόγησης και ποιότητας υπηρεσίας, ενώ με τεχνικές από τον κλάδο της "Νοημοσύνης των Μηχανών" (Machine Learning), μεγαλύτερος όγκος δεδομένων μπορεί να επεξεργασθεί πιο γρήγορα και αποδοτικότερα. Οι χρήστες μοντελοποιούνται ως "μανθάνοντα αυτόματα" (Learning Automata), συλλέγοντας πληροφορίες κατά την διάρκεια της κατανομής πόρων και μέσω ενός μηχανισμού εκμάθησης μπορούν να συμπεράνουν ποιός πάροχος καλύπτει καλύτερα τις απαιτήσεις τους.

Διαφορετικά σενάρια τιμολόγησης επιβάλλονται από τους παρόχους (πχ. ομοιογενής κοστολόγηση ανάλογα με το είδος της υπηρεσίας ή με βάση την απόσταση από τον Σταθμό Βάσης) με τους χρήστες να αξιολογούν τις επιπτώσεις από την εκάστοτε τιμολογιακή πολιτική στην συνάρτηση χρησιμότητας τους, η οποία μετασχηματίζεται ώστε να περικλείει έναν παράγοντα κόστους. Κάθε πάροχος χαρακτηρίζεται από μία πιθανότητα επιβράβευσης που αντικατοπτρίζει τον δείκτη ανταγωνιστικότητάς του, με συνέπεια να διαμορφώνει σταδιακά την "φήμη" του προς τους καταναλωτές, αυξάνοντας και την πιθανότητα επιλογής του για την παροχή υπηρεσιών.

Το πρόβλημα διαμορφώνεται ως ένα διεπίπεδο μη συνεργατικό παίγνιο, στο οποίο η κατανομή πόρων συνδυάζεται με την διαδικασία επιλογής του παρόχου από την διαρκή ενημέρωση των δεικτών ανταγωνιστικότητάς τους. Μέσω της εξέτασης διαφορετικών σεναρίων κοστολόγησης, διαπιστώνουμε ότι σε κάθε περίπτωση το πρόβλημα συγκλίνει σε βέλτιστους καταμερισμούς πόρων, με τους παρόχους οι οποίοι προ-

σφέρουν τον ιδανικό συνδυασμό τιμής και ποιότητας υπηρεσίας να καταλαμβάνουν το μεγαλύτερο τμήμα της αγοράς. Με αυτόν τον τρόπο, γίνεται κατανοητός ο βαθμός στον οποίο τα επίπεδα τιμών επηρεάζουν συνολικά την βελτιστοποίηση και τον ανταγωνισμό εντός των δικτύων, αλλά και το γεγονός πως οι αποφάσεις των χρηστών όχι μόνο είναι μέγιστης σημασίας αλλά και ο τρόπος λήψης τους μπορεί σε μεγάλο βαθμό να τυποποιηθεί εξοικονομώντας πόρους και χρόνο.

Σύνθεση υπηρεσιών σε ασύρματα δίκτυα

Εν συνεχεία, αναγνωρίζοντας την διαρκώς αυξανόμενη ετερογένεια και πολυπλοκότητα των υπηρεσιών που διατίθενται στα σύγχρονα δίκτυα, εξετάζουμε το πρόβλημα της δυναμικής σύνθεσης υπηρεσιών και της συνδυαστικής κατανομής πόρων, σύμφωνα με τις αρχές της θεωρίας συγκέντρωσης / ομαδοποίησης υπηρεσιών (bundling). Αναλυτικότερα, οι μεταδιδόμενες υπηρεσίες και εφαρμογές πολυμέσων στα σύγχρονα ασύρματα δίκτυα διακρίνονται από σημαντική διαφοροποίηση ως προς το περιεχόμενο τους, τον όγκο των δεδομένων, και τις απαιτήσεις τους ως προς την ανοχή των καθυστερήσεων στην μετάδοσή τους.

Ως συνέπεια για τα δικτυακά περιβάλλοντα 5ης γενιάς, οι χρήστες απαιτούν την λήψη και διαχείριση διακριτών υπηρεσιών την ίδια στιγμή (πχ. παρακολούθηση βίντεο, τηλεδιασκέψεις, ή έλεγχος ηλεκτρονικού ταχυδρομείου κλπ.), συνθήκη η οποία έως τώρα δεν είχε επαρκώς μελετηθεί σε θέματα βελτιστοποίησης δικτύων. Στο σημείο αυτό, αναπτύσσουμε ένα πλαίσιο το οποίο επιτρέπει την κατανομή των πόρων όταν πολλαπλά είδη υπηρεσιών λαμβάνονται ταυτόχρονα από τους χρήστες. Η ανωτέρω καινοτομία συνιστά μια ουσιαστική τομή, καθώς επιτρέπει την ανάπτυξη συνεργειών και αλληλοκαλύψεων μεταξύ υπηρεσιών οι οποίες γίνονται διαθέσιμες μέσω κοινών σημάτων μετάδοσης, τόσο για την πληρέστερη υποστήριξη και ικανοποίηση των χρηστών από ένα μεγαλύτερο εύρος περιεχομένου αλλά και για την ενεργειακή αποδοτικότητά τους.

Αρχικά εξετάζουμε το βασικό πρόβλημα κατανομής ισχύος εκπομπής και ρυθμού μετάδοσης σε δίκτυα στα οποία υπηρεσίες πραγματικού και μη χρόνου ζητούνται ταυτόχρονα από τους χρήστες. Οι χρήστες του δικτύου καθορίζουν το ποσοστό των πόρων που θέλουν να διαθέσουν σε κάθε υπηρεσία, με τις συναρτήσεις χρησιμότητας να διαμορφώνονται ανάλογα. Το πρόβλημα διατυπώνεται εκ νέου ως ένα μη συνεργατικό παίγνιο και η ύπαρξη του επιζητούμενου σημείου ισορροπίας κατά Nash επιβεβαιώνεται εκ νέου μέσω των παιγνίων με στρατηγική συμπληρωματικότητα. Τα αποτελέσματα αποτυπώνουν πως η υπέρθεση υπηρεσιών δύναται να αυξήσει σημαντικά τους επιτυγχανόμενους ρυθμούς μετάδοσης λόγω της παράλληλης λήψης περισσότερων υπηρεσιών, ενώ η ενεργειακή αποδοτικότητα αυξάνεται καθώς μέσω μίας κοινής μετάδοσης καλυπτονται πολλαπλές ανάγκες των χρηστών.

Συνακολουθα, επεκτείνουμε το πρόβλημα της ομαδοποίησης τηλεπικοινωνιακών υπηρεσιών ώστε να περικλείει περισσότερες επιλογές υπό μία πιο εμπορική προσέγγιση. Πιο συγκεκριμένα, οι χρήστες πριν την έναρξη της διαδικασίας κατανομής πόρων, επιλέγουν αυτόνομα ποιά είδη υπηρεσιών επιθυμούν (πχ. έλεγχος ισχύος, σύνδεση σε φεμτοκυψέλες, υπηρεσίες μόνο πραγματικού χρόνου κλπ.) σχηματίζοντας σε κάθε περίπτωση ένα μοναδικό προϊόν το οποίο ανταποκρίνεται στις απαιτήσεις και τις προτεραιότητες τους. Προσομοιώνοντας το ανωτέρω μοντέλο παρατηρούμε μία σημαντική βελτίωση της χρησιμότητας των χρηστών, καθώς η μετάδοση της πληροφορίας πραγματοποιείται με βάση τις παραμέτρους και τα κριτήρια που οι ίδιοι καθόρισαν νωρίτερα. Επιπλέον, μελετούμε την βέλτιστη εφαρμογή κοστολόγησης για τέτοια είδη τηλεπικοινωνιακών προϊόντων.

Συγκριτικά με άλλες απλοποιημένες ή περισσότερο σύνθετες πολιτικές κοστολόγησης πολυπαραμετρικών προϊόντων, στην παρούσα εργασία επικεντρωνόμαστε στην τεχνική της κοστολόγησης δέσμης προϊόντων με βάση των αριθμό των επιλεγμένων υπηρεσιών (Bundle Size Pricing). Μέσω προσομοιώσεων, καταλήγουμε στο συμπέρασμα ότι η εν λόγω μορφή κοστολόγησης επιφέρει συγγενή αποτελέσματα με άλλες πολύπλοκες τιμολογήσεις δεσμών προϊόντων, εξασφαλίζοντας με αυτόν τον τρόπο απλοποιημένους υπολογισμούς και περιορισμό της υπολογιστικής πολυπλοκότητας των τιμών.

Δίκτυα επικοινωνιών ασύρματης φόρτισης

Στο επόμενο κεφάλαιο, διερευνούμε την διαδικασία κατανομής πόρων υπό μία άλλη οπτική, με επίκεντρο την αποδοτική και ευέλικτη ασύρματη φόρτιση των μπαταριών των χρηστών σε δίκτυα επικοινωνιών ασύρματης φόρτισης (Wireless Powered Communication Networks). Στην κατηγορία αυτών των δικτύων, ο σταθμός βάσης ή εκπομπής, υπεύθυνος για την μετάδοση των δεδομένων συνυπάρχει με έναν σταθμό φόρτισης, από τον οποίο εκπέμπονται ραδιοκύματα τα οποία φορτίζουν ασύρματα τις μπαταρίες των τερματικών. Με αυτόν τον τρόπο δεν απαιτείται η χειροκίνητη φόρτιση των συσκευών, ενώ επιτυγχάνεται υψηλή απόδοση

και επέκταση της διάρκειας λειτουργίας των μπαταριών με χαμηλό κόστος.

Στην παρούσα μελέτη, τα προβλήματα της ασύρματης φόρτισης και της μετέπειτα εκπομπής και κατανομής πόρων αναλύονται συνδυαστικά για τον κάθε χρήστη του δικτύου, σε αντίθεση με άλλες προσεγγίσεις εντός της βιβλιογραφίας, στις οποίες η προσπάθεια βελτιστοποίησης αφορούσε συγκεντρωτικά το δίκτυο. Με περισσότερες λεπτομέρειες, με βάση την μοντελοποίηση της ικανοποίησης των χρηστών μέσω των συναρτήσεων χρησιμότητας, αναπτύσσουμε μια καινοτόμο προσέγγιση στην οποία τα στάδια της ασύρματης φόρτισης και της επικοινωνίας με τον σταθμό βάσης που ακολουθεί είναι άρρηκτα συνδεδεμένες. Οι χρήστες, έχοντας γνώση των βασικών χαρακτηριστικών της εκπομπής τους (πχ. κέρδος καναλιού, είδος υπηρεσίας, περιορισμοί ως προς την ισχύ εκπομπής) είναι σε θέση να εκτιμούν τις απαιτήσεις τους σε ενέργεια, έτσι ώστε να φορτιστούν επαρκώς οι μπαταρίες τους από τον σταθμό φόρτισης, αποφεύγοντας ανεπιθύμητη κατασπατάληση ενέργειας η οποία ουσιαστικά δεν διευκολύνει την μετάδοση δεδομένων.

Επομένως, ο σταθμός φόρτισης συλλέγοντας όλες τις πληροφορίες από τους χρήστες προσαρμόζει δυναμικά την εκπομπή των ραδιοκυμάτων φορτίζοντας τους χρήστες με βάση τις πραγματικές απαιτήσεις τους. Όπως και στα προηγούμενα κεφάλαια, οι χρήστες επιδιώκουν να μεγιστοποιήσουν την ικανοποίησή τους από την εκπομπή με την ελάχιστη δυνατή κατανάλωση ενέργειας, γεγονός εφικτό από το στάδιο της ασύρματης φόρτισης που προηγείται. Το ανωτέρω διατυπώθηκε ως ένα πρόβλημα βελτιστοποίησης της ισχύος εκπομπής και φόρτισης με βάση την διάρκεια που διατίθεται εντός μίας χρονοσχισμής ώστε να φορτιστούν κατάλληλα όλες οι συσκευές. Το πρόβλημα υλοποιείται πρακτικά μέσω ενός κατανεμημένου αλγόριθμου που προσδιορίζει την ακριβή ισχύ εκπομπής και φόρτισης του εκάστοτε χρήστη. Προσομοιώνοντας την λειτουργία του προτεινόμενου μοντέλου, τα αποτελέσματα αναδεικνύουν την βέλτιστη προσαρμογή του σταδίου φόρτισης στην επικείμενη εκπομπή, τόσο όσον αφορά τον επιτυγχανόμενο ρυθμό μετάδοσης αλλά και την αύξηση της ενεργειακής απόδοσης για κάθε χρήστη του δικτύου συγκριτικά και με άλλες εργασίες από την βιβλιογραφία.

Δυναμική κατανομή εύθραυστων πόρων

Όπως έχει ήδη αναφερθεί, η ανάπτυξη δικτύων 5ης γενιάς οδηγεί τα ασύρματα τηλεπικοινωνιακά συστήματα σε μία ριζική αναδιοργάνωση από συμβατικές επικοινωνίες φωνής σε πολύπλοκες και πολυεπίπεδες δομές, οι οποίες υποστηρίζουν πολλά διαφορετικά είδη υπηρεσιών με ανώτερες προδιαγραφές σε ρυθμούς μετάδοσης και όγκο δεδομένων. Επιπλέον, όλο και περισσότεροι χρήστες με ετερογενή χαρακτηριστικά συνδέονται στο δίκτυο, των οποίων η συμπεριφορά και οι απαιτήσεις μεταβάλλονται δυναμικά, με αντίστοιχες συνέπειες στον όγκο δεδομένων και στην κατανάλωση του διαθέσιμου εύρους ζώνης.

Έχοντας ως βασικό στόχο την παροχή μίας εξατομικευμένης τηλεπικοινωνιακής εμπειρίας για τον κάθε χρήστη, στο τελευταίο τμήμα της διατριβής το πρόβλημα της κατανομής πόρων μετασχηματίζεται θεμελιωδώς, εξετάζοντας τον τρόπο με τον οποίο η συμπεριφορά και η διαχείριση του ρίσκου εκ μέρους των χρηστων επιδρά στην λειτουργία του δικτύου αλλά και συνεισφέρει στην βελτίωση της απόδοσής του συνολικά. Επιπλέον, για πρώτη φορά σε προβλήματα βελτιστοποίησης ασύρματων δικτύων, το εύρος ζώνης δεν θεωρείται ως ένας απεριόριστος και άφθαρτος πόρος, αλλά αντιμετωπίζεται υπό το πρίσμα μίας πιο ρεαλιστικής προσέγγισης και τοποθετείται ως ένας εύθραυστος και πεπερασμένος πόρος που μπορεί να καταρρεύσει συνολικά για όλο το δίκτυο σε περίπτωση υπερκατανάλωσης ή υπερβολικής ζήτησης.

Η υλοποίηση αυτή γίνεται εφικτή με την εισαγωγή της Θεωρίας Προοπτικής (Prospect Theory) που αναπτύχθηκε από τους Kahneman και Tversky, η οποία μοντελοποιεί την συμπεριφορά των ανθρώπων υπό συνθήκες αβεβαιότητας και έντονης μεταβλητότητας. Σύμφωνα με τις αρχές της Θεωρίας Προοπτικής, οι χρήστες λαμβάνουν αποφάσεις με υποκειμενικά κριτήρια, χαρακτηριζόμενα από την χρήση ενός σημείου αναφοράς, την αποφυγή των κινδύνων, την μειούμενη ευαισθησία και την βέλτιστη εκτίμηση, εκδηλώνοντας την τάση των ανθρώπων να υπερεκτιμούν γεγονότα απώλειας σε σχέση με περιπτώσεις κέρδους.

Στο παρόν μοντέλο, υποθέτουμε ότι το εύρος ζώνης διατίθεται στους χρήστες υπό δύο μορφές: ένα αυστηρά ελεγχόμενο, κλειστής πρόσβασης τμήμα (“σταθερός ή ασφαλής πόρος” - safe resource), στο οποίο ο κάθε χρήστης απολαμβάνει εγγυημένη ποιότητα υπηρεσίας αλλά με περιορισμένη αποδοτικότητα ώστε να εξασφαλίζεται ότι όλοι οι χρήστες που συμμετέχουν κατορθώνουν να εκπέμψουν. Από την άλλη, το υπόλοιπο μέρος του εύρους ζώνης διατίθεται ελεύθερα και διαμοιράζεται μεταξύ των χρηστών (“συλλογικός πόρος” - common pool of resources), το οποίο αν και μεγαλύτερης κλίμακας φάσματος μπορεί να καταρρεύσει υπό συνθήκες υπερβολικής ζήτησης κατά τις αρχές της υπόθεσης του Hardin για την “Τραγωδία των Κοινών”. Η συγκεκριμένη θεώρηση έρχεται σε αντίθεση με την Θεωρία Αναμενόμενης Χρησιμότητας, η οποία αντιμετωπίζει τους χρήστες ως ομοιογενή και μη αυτόνομα τερματικά που αποσκοπούν “τυφλά” στην μεγιστοποίηση της ικανοποίησης τους, χωρίς τα ατομικά χαρακτηριστικά ή οι προτεραιότητες των χρηστών να λαμβάνονται υπόψη, ενώ απουσιάζει η αντίληψη και εκτίμηση συνθηκών ρίσκου στην διαχείριση των πόρων.

Ως μία πρώτη εφαρμογή στην επίλυση προβλημάτων βελτιστοποίησης δικτύων με την χρήση της Θεωρίας Προοπτικής, εξετάζουμε το πρόβλημα της αποτελεσματικότερης αξιοποίησης του εύρους ζώνης όταν αδειοδοτημένες και μη αδειοδοτημένες πηγές φάσματος είναι διαθέσιμες προς τους χρήστες. Το αδειοδοτημένο εύρος ζώνης (licensed bandwidth) συμπεριφέρεται ως ο ασφαλής πόρος ο οποίος απαιτεί άδεια πρόσβασης ώστε να χρησιμοποιηθεί, ενώ το μη αδειοδοτημένο εύρος ζώνης (unlicensed bandwidth) μπορεί να προσφερθεί στους χρήστες μέσω διαφορετικών εναλλακτικών πηγών, κατά την τάση των ρυθμιστικών αρχών να διαθέσουν περισσότερες συχνότητες φάσματος για την κάλυψη των τηλεπικοινωνιακών αναγκών. Η έλλειψη μίας κεντρικής αρχής για την διαχείριση του μη αδειοδοτημένου φάσματος το καθιστά ευάλωτο στην πιθανή κατάχρησή του από τους χρήστες, με συνέπεια την κατάρρευσή του και την αναπόφευκτη απώλεια της υπηρεσίας.

Σημαντική συνεισφορά της διατριβής σε αυτόν τον τομέα είναι ο κατάλληλος σχεδιασμός των συναρτήσεων χρησιμότητας ώστε να εμπεριέχουν την πιθανότητα της κατάρρευσης του φάσματος όταν οι χρήστες μαζικά επενδύουν σε αυτό. Για να γίνει αυτό εφικτό, εισάγουμε την "παράμετρο επένδυσης" (investment parameter) η οποία αντιπροσωπεύει το ποσοστό της ισχύος που ο κάθε χρήστης διατίθεται να αφιερώσει σε κάθε πηγή φάσματος. Το μοντέλο υλοποιείται με την εκτέλεση ενός κατανεμημένου αλγορίθμου ο οποίος αναλαμβάνει την κατανομή των πόρων και την αντιστοιχη επένδυση στο αδειοδοτημένο και μη εύρος ζώνης, λειτουργώντας υπό δύο διαφορετικά σενάρια. Το πρώτο αφορά την βέλτιστη χρήση και των δύο πηγών φάσματος με όλους τους χρήστες να εκπέμπουν απρόσκοπτα, ενώ το δεύτερο σενάριο αφορά την απώλεια του μη αδειοδοτημένου εύρους ζώνης λόγω υπερβολικής ζήτησης, με μόνο όσους χρήστες κατένημαν μέρος της ισχύος τους στο αδειοδοτημένο εύρος ζώνης να κατορθώσουν να εκπέμψουν. Μέσω μίας σειράς προσομοιώσεων, αποτυπώνεται ο βαθμός στον οποίο οι αντιλήψεις των χρηστών επηρεάζουν τις επιδόσεις του δικτύου, καθώς μέσω της πιθανότητας κατάρρευσης του φάσματος αναπροσαρμόζουν την επένδυσή τους σε αυτό. Με αυτόν τον τρόπο γίνεται εμφανές το πώς η εκτίμηση του ρίσκου μπορεί να οδηγήσει σε μία πιο ορθολογική κατανομή και χρήση των πόρων, διασφαλίζοντας ουσιαστικά την ομαλή λειτουργία του δικτύου συνολικά.

Σε μία παράλληλη προσέγγιση που αποκαλύπτει την ευελιξία του προτεινόμενου μοντέλου, μελετούμε το πρόβλημα της ταυτόχρονης εκπομπής των χρηστών μέσω δύο τεχνικών μετάδοσης (NOMA και OFDMA). Οι σύγχρονες κινητές συσκευές διαθέτουν την ικανότητα να εκπέμπουν μέσω περισσότερων από μίας τεχνικών μετάδοσης, γεγονός που επιτρέπει την δυναμική αξιοποίηση του εύρους ζώνης ανά πάσα στιγμή. Κατ΄ αναλογία με προηγουμένως, η τεχνική OFDMA λόγω του κατακερματισμού του φάσματος σε διακριτά τμήματα θεωρείται ως το ασφαλές μέσο επικοινωνίας, ενώ στην τεχνική πρόσβασης NOMA αν και επιτρέπεται στους χρήστες να αξιοποιήσουν το φάσμα στο σύνολό του, αυτό καθίσταται ευάλωτο στην περίπτωση υπέρμετρης ζήτησης λόγω της ελεύθερης πρόσβασης των χρηστών σε αυτό.

Κατανοώντας τους περιορισμούς και την εύθραυστη φύση των πόρων όπως το εύρος ζώνης, επιχειρούμε να εξετάσουμε μεθόδους που μπορούν να υιοθετηθούν ώστε να διασφαλιστεί ο έλεγχος της ζήτησης και να τεθούν όρια στην υπερβολική κατανάλωση του φάσματος από τους χρήστες προωθώντας μια πιο λελογισμένη διαχείριση συνολικά για το δίκτυο. Η εισαγωγή ενός συστήματος φορολόγησης ή κοστολόγησης των πόρων προσφέρει ένα αποτελεσματικό μέσο για την πιο ρεαλιστική επένδυση σε συλλογικούς πόρους και την αποφυγή της απώλειας υπηρεσίας. Η συνάρτηση χρησιμότητας υπό την μοντελοποίησης της Θεωρίας Προοπτικής προσαρμόζεται ανάλογα με την προσθήκη μίας συνάρτησης κόστους, ενώ το πρόβλημα και σε αυτήν περίπτωση διατυπώνεται και επιλύεται ως ένα μη συνεργατικό παίγνιο με στρατηγική συμπληρωματικότητα. Τα αποτελέσματα επιβεβαιώνουν ότι η εισαγωγή κοστολόγησης των συλλογικών πόρων μειώνει την επιθετική επένδυση σε αυτούς, με τους χρήστες αυτοβούλως να διαμοιράζουν την εκπομπή τους μεταξύ του ασφαλή και συλλογικού πόρου για να μειώσουν τον κίνδυνο της κατάρρευσης του δεύτερου, γεγονός που θα ζημιώσει σημαντικά την δική τους εκπομπή.

Διαχείριση πόρων σε δίκτυα δημόσιας ασφάλειας

Στο τελευταίο κεφάλαιο της διδακτορικής διατριβής εξετάζεται η επέκταση του προβλήματος διαχείρισης πόρων σε νέα πεδία τηλεπικοινωνιών, όπως τα δίκτυα δημόσιας ασφάλειας. Η σπουδαιότητα των δικτύων αυτών γίνεται κατανοητή λόγω της ικανότητας τους να παρέχουν επαρκή και άμεση συνδεσιμότητα σε περιοχές στις οποίες φυσικές καταστροφές ή κάποιο άλλο εξωτερικό γεγονός έχει λάβει χώρα, όταν υπό άλλες συνθήκες η μετάδοση δεδομένων και η επικοινωνία μεταξύ των χρηστών δεν θα ήταν εφικτή. Ένας επιπλέον σημαντικός παράγοντας που αναδεικνύει τέτοιας φύσεως δίκτυα είναι η χρήση μη επανδρωμένων ιπτάμενων οχημάτων, που επιτρέπουν την επιτόπια εγκατάσταση και λειτουργία τους χωρίς την απαίτηση για επένδυση σε άλλες υποδομές στην περιοχή όπου επλήγη.

Λόγω των συνθηκών έντονης μεταβλητότητας αλλά και τον κίνδυνο που απειλεί να διαταράξει την διαδικασία της κατανομής πόρων, η αξιοποίηση της Θεωρίας Προοπτικής συνιστά και σε αυτήν την περίπτωση βασικό εργαλείο για την μοντελοποίηση των εκάστοτε προβλημάτων και στην καλύτερη αντίληψη των στρατηγικών των χρηστών σε αβέβαιες καταστάσεις. Οι χρήστες, εκπέμποντας κάτω από ιδιαίτερα δυσμενείς συνθήκες, δύνανται να συμβάλλουν στην λειτουργία του δικτύου επιλέγοντας με ποιό ιπταμενο όχημα να επικοινωνήσουν, υιοθετώντας μία πιο μετριοπαθή στάση στην ζήτηση του διαθέσιμου εύρους ζώνης. Τα προβλήματα που μελετώνται αφορουν πολλαπλά στατικά ή μετακινούμενα μη επανδρωμένα αυτόματα οχήματα, με την επίλυση των προβλημάτων να ακολουθεί την ίδια λογική με προηγουμένως, δηλαδή την βελτιστοποίηση της παραμέτρου επένδυσης στο κοινά διαθέσιμο εύρος ζώνης. Μέσω της θεωρητικής εύρεσης σημείων ισορροπίας αλλά και από την πρακτική προσομοίωσή τους, επιβεβαιώνεται η ευελιξία και η ικανότητα των προτεινόμενων μοντέλων να οδηγούν σε αποδοτικότερη και λελογισμένη διαχείριση των πόρων εξασφαλίζοντας την μετάδοση δεδομένων σε κρίσιμες περιστάσεις.

Ολοκληρώνοντας, εξετάζονται θέματα ασφάλειας και προστασίας δικτύων δημοσίας ασφάλειας από κακόβουλους χρήστες των οποίων η δραστηριότητα αποσκοπεί στην απώλεια υπηρεσιών και στην παύση της λειτουργίας του δικτύου. Και αυτήν την φορά, η Θεωρία Προοπτικής επιτρέπει τον σχεδιασμό της χρησιμότητας και συμπεριφοράς των χρηστών υπό διαφορετικά κριτήρια, με ένα τμήμα τους να θεωρείται ως "φυσιολογικοί" χρήστες που στοχεύουν απλώς στην βέλτιστη δυνατή επικοινωνία τους με το ιπτάμενο τερματικό, ενώ οι υπόλοιποι χρήστες αντιμετωπίζονται ως "κακόβουλοι", οι οποίοι μέσω της πολύ επιθετικής εκπομπής τους στοχεύουν στην υπερκατανάλωση των πόρων (δηλαδή του εύρους ζώνης) σε βάρος των υπολοίπων χρηστών, με συνέπεια την κατάρρευση του φάσματος του δικτύου δημόσιας ασφάλειας, θέτοντας ενδεχομένως σε κίνδυνο την προστασία των χρηστών στην περιοχή. Στην εργασία αυτή, διερευνούμε τεχνικές οι οποίες επιτρέπουν την ταυτοποίηση επιβλαβών δραστηριοτήτων εντός του δικτύου και με σύγχρονες μεθόδους να ενεργοποιούν την απόρριψη των κακόβουλων χρηστών από αυτό, εξασφαλίζοντας έτσι την προστασία και την απρόσκοπτη διαδικασία της κατανομής πόρων και της μετάδοσης δεδομένων.

Συνοψίζοντας, στην παρούσα διδακτορική διατριβή μελετήθηκε και αναλύθηκε διεξοδικά μία πληθώρα θεμάτων κατανομής πόρων. Εντοπίζοντας τα κενά στην διαθέσιμη βιβλιογραφία και αξιοποιώντας σύγχρονες τεχνολογίες τηλεπικοινωνιών, στην τρέχουσα εργασία προτείνουμε ένα πλήρες και πρωτοποριακό πλαίσιο για την διαχείριση πόρων και την βελτιστοποίηση της απόδοσης των ασύρματων δικτύων 5ης γενιάς. Βασικές κατευθύνσεις στην επίλυση των υπό εξέταση προβλημάτων αποτελούν η ενεργειακή αποδοτικότητα, η βελτίωση της ποιότητας υπηρεσίας, και η αύξηση της ικανοποίησης των καταναλωτών, προωθώντας έτσι τον ορθολογικότερο διαμοιραρμό των διαθέσιμων πεπερασμένων πόρων. Παράλληλα, έμφαση δίνεται στην ετερογένεια μεταξύ των χρηστών και στο γεγονός ότι οι ατομικές στρατηγικές και αποφάσεις του κάθε χρήστη είναι καθοριστικής σημασίας για την ισορροπημένη και βέλτιστη λειτουργία του δικτύου.

Οι παραπάνω παραδοχές είναι απόλυτα ευθυγραμμισμένες με τα χαρακτηριστικά και τις απαιτήσεις των επερχόμενων ασύρματων δικτύων νεώτερης (5ης) γενιάς, τα οποία αναλύονται ως πολυεπίπεδα και πολυμεταβλητά τηλεπικοινωνιακά συστήματα. Ο αυξανόμενος αριθμός χρηστών, η απαίτηση για μαζική και άμεση συνδεσιμότητα, και η διάθεση πολλαπλών υπηρεσιών με υψηλές προδιαγραφές ως προς τον όγκο δεδομένων, αναδεικνύουν τις μεθοδολογίες που παρουσιάζονται στην παρούσα διδακτορική διατριβή ως μία πολλά υποσχόμενη προσέγγιση για την πιο εξελιγμένη και πολυσύνθετη αξιοποίηση και διαχείριση των διαφόρων μεταβλητών του δικτύου.

Σε κάθε περίπτωση, τα προβλήματα διατυπώνονται μέσω μίας διεπιστημονικής προσέγγισης υιοθετώντας εργαλεία από διαφορετικούς χώρους, ενώ η θεωρητική επίλυσή τους επιβεβαιώνεται μέσω της εκτέλεσης πρακτικών και κατανεμημένων αλγορίθμων οι οποίοι συγκλίνουν σε βέλτιστα σημεία ισορροπίας κατά Nash. Η σύγκλιση αυτή παρατηρείται τόσο ανάμεσα στους χρήστες όσο και στο δίκτυο στο σύνολό του, την στιγμή που η απόκλιση από αυτά οδηγεί στην υποβάθμιση της απόδοσης του συστήματος. Επιπλέον, προσομοιώσεις αποδεικνύουν τα έμπρακτα οφέλη των προτάσεων μας ως προς την σημαντική βελτίωση των χαρακτηριστικών της λειτουργίας του δικτύου (πχ. ενεργειακή αποδοτικότητα, αύξηση των ρυθμών μετάδοσης) και της συνολικής ικανοποίησης των χρηστών, συγκριτικά και με άλλες παρόμοιες εργασίες στον κλάδο.

Η εν λόγω διατριβή έχει σχεδιαστεί ειδικά για να προσφέρει ένα ευέλικτο σύστημα διαχείρισης πόρων το οποίο μπορεί να επεκταθεί σε ποικίλα τηλεπικοινωνιακά συστήματα με διαφορετικούς πόρους ή τεχνολογίες. Παραδείγματα αποτελούν η κατανομή πόρων σε υπολογιστικά περιβάλλοντα στην "άκρη" του δικτύου (mobile edge computing), σε νέα πρότυπα υπηρεσιών ορατού φωτός (light fidelity), σε άμεσες επικοινωνίες μεταξύ συσκευών (machine-to-machine, device-to-device communications), κλπ. Επίσης σημαντικές ερευνητικές ευκαιρίες προσφέρονται για την εφαρμογή των προτεινόμενων μοντέλων στην κατεύθυνση της ανάπτυξης νέων τηλεπικοινωνιακών προϊόντων και πολιτικών κοστολόγησης, καθώς και στον συνδυασμό

νέων τεχνολογιών αυτοματοποίησης, αναγνώρισης προτύπων, και τεχνητής νοημοσύνης σε δίκτυα νεώτερης και μεταγενέστερης γενιάς.

Παράλληλα, η εργασία αυτή διαθέτει όλα εκείνα τα χαρακτηριστικά τα οποία επιτρέπουν την προσαρμογή της για την επίλυση προβλημάτων διαχείρισης και κατανομής πόρων σε διαφορετικούς τομείς, όχι αποκλειστικά εντός του κλάδου των τηλεπικοινωνιών αλλά και σε άλλα πεδία στα οποία οι χρήστες αλληλεπιδρούν και ανταλλάσουν πληροφορίες. Ενδεικτικά, θέματα δικτύων μεταφορών, μετάδοσης ηλεκτρικής ενέργειας ή εφαρμογές σε διασυνδεδεμένα συστήματα έξυπνων πόλεων αποτελούν μερικά μόνο παραδείγματα στα οποία οι λύσεις που παρέχονται στην παρούσα διατριβή μπορούν να επιφέρουν σημαντικά οφέλη.

Λέξεις Κλειδιά: Κατανομή Πόρων, Ασύρματα Δίκτυα, Συνάρτηση Χρησιμότητας, Έλεγχος Ισχύος Εκπομπής, Έλεγχος Ρυθμού Μετάδοσης, Κοστολόγηση, Θεωρία Παιγνίων, Θεωρία Προοπτικής, Σημείο Ισορροπίας κατά Nash, Βελτιστοποίηση, Πολλαπλές Υπηρεσίες

Γλωσσάρι

5G Networks: Δίκτυα 5ης γενιάς
Ad-hoc Networks: Αυτο-οργανώμενα δίκτυα
Behavioral Economics: Συμπεριφορικά Οικονομικά
Bundle Size Pricing: Κοστολόγηση δέσμης ως προς το πλήθος των υπηρεσιών
Bundling: Ομαδοποίηση προϊόντων
Common Pool of Resources: Συλλογικός πόρος
Device-to-device: Συσκευή προς συσκευή
Expected Utility Theory: Θεωρία αναμενόμενης χρησιμότητας
Femtocells: Φεμτοκυψέλες
Game Theory: Θεωρία Παιγνίων
Internet of Things: Ίντερνετ των Πραγμάτων
Investment Parameter: Παράμετρος επένδυσης
Learning Automata: Μανθάνοντα Αυτόματα
Licensed Bandwidth: Αδειοδοτημένο εύρος ζώνης
Machine Learning: Νοημοσύνη των Μηχανών
Machine-to-machine: Μηχανή προς μηχανή
Nash Equilibria: Σημεία ισορροπίας κατά Nash
NOMA: Μη-ορθογώνια τεχνική πολλαπλής πρόσβασης
OFDMA: Ορθογώνια τεχνική διαίρεσης συχνότητας πολλαπλής πρόσβασης
Prospect Theory: Θεωρία Προοπτικής
Public Safety Networks: Δίκτυα Δημόσιας Ασφάλειας
Quality of Service: Ποιότητα Υπηρεσίας
Quasi-concavity: Οιονεί κοιλότητα
Safe Resource: Ασφαλής πόρος
SIC: Διαδοχική ακύρωση παρεμβολών
Submodular Games: Παίγνια με στρατηγικά υποκατάσταστα
Supermodular Games: Παίγνια με στρατηγική συμπληρωματικότητα
Tragedy of the Commons: Τραγωδία των Κοινών
Unlicensed Bandwidth: Μη αδειοδοτημένο εύρος ζώνης
Unmanned Aerial Vehicles: Μη επανδρωμένα ιπτάμενα οχήματα
Uplink: Άνω ζεύξη
Utility Function: Συνάρτηση χρησιμότητας
Visible Light Communications: Επικοινωνίες ορατού φωτός
Wireless Powered Communication Networks: Δίκτυα επικοινωνίας ασύρματης φόρτισης

Acknowledgements

A PhD journey can be a lonely experience. Exploring new ideas, mathematical concepts, and new technologies is not only a discovery of the world of science and research, but also a constant quest for understanding what is important in life and how we can achieve learning ourselves deeper and becoming better individuals during this process. I have been fortunate enough to be surrounded by people to whom I would like to express my gratitude for their direct or indirect support in transforming something that originally seemed impossible into a tangible accomplishment.

First and foremost, I am indebted to my advisor Prof. Dr. Symeon Papavassiliou, Professor of Electrical Engineering at NTUA, Greece, who with his immense experience, interest, and constant involvement provided me with all the ideal conditions in order to work in different research areas and learn how to critically assess all aspects of conducting research. His support, understanding, and trust have been a decisive driver in tackling different obstacles which otherwise I would not be able to overcome. It has been an honor for me to have worked under his supervision and for sharing with me his knowledge and scientific expertise. I am proud that the work included in this thesis constitutes a small part of his significant contribution to the scientific community.

Equally important, I would like to thank my co-advisor Prof. Dr. Eirini Eleni Tsiropoulou, Assistant Professor of Electrical Engineering at University of New Mexico (UNM), USA. Getting to knowing her and working with her for my undergraduate diploma thesis at NTUA almost a decade ago, now seems to be a definitive turning point in my life. Seeing her passion and endless commitment to research and following her dreams has been an inspiration for me in never giving up when something is worth fighting for. Her fresh ideas, advice, and her proactive participation have undoubtedly stepped far beyond a simple advisory role and have become an integral part of this research work. I deeply admire and respect her scientific and personal path and I am very fortunate to have had the opportunity to associate myself and contribute to areas of her own research.

I would also like to thank Prof. Dr. Askounis, Prof. Dr. Roussaki, Prof. Dr. Varvarigou, Prof. Dr. Panagopoulos, and Prof. Dr. Anagnostou for honoring me by accepting to be members of my examination committee and for allowing me to present my research work in front of them. Additionally, I would like to acknowledge the flexibility of Professors at NTUA, Prof. Dr. Venieris, Prof. Dr. Panagopoulos, Prof. Dr. Mentzas, and Prof. Dr. Anagnostou towards the fulfillment of the course requirements as part of my PhD degree. Many thanks also go to Marinos Vomvas for his cooperation in a certain research section of this work. Moreover, I would like to express my gratitude to Mrs. Winette Krommendijk, Mr. Martin Salzmann, and especially to Mrs. Griet Hautekeete for their support and excellent cooperation with me in the last few years and for their strong interest in my academic occupations.

I would like to express my sincere thanks to my friends who during all this process supported me and showed genuine interest in my work. Special thanks to my close friends Katerina and Giorgos for their patience and the precious time they have spent with me during this journey, Michael and Theodora for the nice travel moments somewhere around the world, and Richardos and Alexandros for always checking with me how I am doing. I would also like to acknowledge the support of my friend Vasilis A. when I asked for his help in the beginning of enrolling for this degree.

Lastly, to my parents, Konstantina and Ioannis, and my sister Elisavet, words are not enough to express my gratitude for all of your sacrifices not only during the course of this PhD, but since the day I was born. You believing in me, supporting me both materially and morally has been always the basis of anything that I have managed to accomplish in my life. This work is not an exception; you unconditionally standing by my side in good and bad moments has filled me with strength and perseverance.

Panagiotis Vamvakas
October 30, 2019

Contents

Abbreviations

3G: 3^{rd} Generation
4G: 4^{th} Generation
5G: 5^{th} Generation
6G: 6^{th} Generation
ALLURE-U: ALlocation of Licensed and Unlicensed REsources under probabilistic Uncertainty
ANN: Artificial Neural Network
AP: Access Point
AWGN: Addittive White Gaussian Noise
B5G: Beyond 5^{th} Generation
BSP: Bundle Size Pricing
BENCHMARC: Bundling sErvices in wireless Networks via user CHoice in Modular ARChitecture
bps: bit per second
BR: Best Response
BS: Base Station
CDMA: Code Division Multiple Access
CPR: Common Pool of Resources
CPU: Central Processing Unit
D2D: Device to Device
dB: Decibel
DC: Direct Current
DDoS: Distributed Denial of Service
DSL: Digital Subscriber Line
DYNAMISM: DYNAMIc Spectrum Management
ECC: Emergency Control Center
EE: Energy-Efficiency
EL: Elastic
EMI: ElectroMagnetic Interference
ENTRADA: ENergy TRansfer and TRansmission Adaptation
EUT: Expected Utility Theory
EVT: Extreme Value Theory
FAP: Femto Access Point
FCC: Federal Communication Commission
FOV: Field Of View
FUs: Femtocell Users
GPS: Global Positioning System
GSM: Global System for Mobile communication
HetNet: Heterogeneous Network
Hz: Hertz
ICT: Information and Communications Technology
IDS: Intrusion Detection System
IEEE: Institute of Electrical and Electronics Engineers
IES: Intrusion Ejection Systems
IMT: International Mobile Telecommunications
INEL: Inelastic
INSPIRE-U: Investment in Network Spectrum via Pricing for Intelligent REsource Utilization
IoT: Internet of Things

IP: Internet Protocol
LAA: Licensed Assisted Access
Li-Fi: Light Fidelity
LoS: Line-of-Sight
LTE: Long Term Evolution
LTE-U: Long Term Evolution - Unlicensed
LWA: LTE-WLAN radio level Aggregation
M2M: Machine to Machine
MAC: Medium Access Control
MBS: Macro Base Station
MEC: Mobile Edge Computing
MGS: Maximum Gain Selection
MIMO: Multiple-Input Multiple-Output
ML: Machine Learning
MUPRAF: Multi-service Uplink transmission Power and data Rate Allocation distributed algorithm in two-tier Femtocell wireless networks
MUs: Macrocell Users
MUSA: MUlti-Service joint resource Allocation
NE: Nash Equilibrium
NOAPRA: Non-cooperative OAP selection and Resource Allocation
NOMA: Non Orthogonal Multiple Access
NRT: Non-Real Time
NTUA: National Technical University of Athens
OAP: Optical Access Point
OFDM: Orthogonal Frequency Division Multiplexing
OFDMA: Orthogonal Frequency Division Multiple Access
OMA: Orthogonal Multiple Access
PARIS: Prospect-theoretic Autonomous Resource Investment algorithm for public Safety
PDA: Personal Digital Assistant
PHY: Physical Layer
PNE: Pure Nash Equilibrium
PRI-PO: PRIce and uplink transmission POwer control
PROSREMA: PROvider Selection and REsource MAnagement
PS: Power Station
PSN: Public Safety Network
PT: Prospect Theory
QoS: Quality of Service
RAM: Random Access Memory
RAN: Radio Access Network
RAT: Radio Access Technologies
RB: Resource Block
REACTS: Resource & Risk Efficient ACcess Technology Selection
RF: Radio Frequency
RFI: Radio Frequency Interference
RFID: Radio-Frequency IDentification
RoR: Rate of Return
RP: Rate and Price
RT: Real Time
R-UPSTREAM: Reduced - User Personalized Price Setting TowaRds the Efficient Allocation of Multiple Resources
SAPIENSS: Security Aware Power Investment for Efficient Network Spectrum Sharing
SC-FDMA: Single Carrier Frequency Division Multiple Access
SDN: Software Defined Network
SI: Self-Interference
SIC: Successive Interference Cancellation
SINR: Signal-to-Interference-plus-Noise Ratio
S-UPRA-MSF: Single variable Utility-based uplink Power and transmission data Rate Allocation game

in Multi-Service two-tier Femtocell networks
TDMA: Time-Division Multiple Access
TETRA: (TDMA)-based Terrestrial Trunked Radio
UAV: Unmanned Aerial Vehicle
UE: User Equipment
UNM: University of New Mexico
UPC-MSF: Uplink Power Control algorithm in Multi-Service two-tier Femtocells
UPRA-MSF: Utility-based uplink Power and transmission data Rate Allocation in Multi-Service Femtocell networks
UPSTREAM: User Personalized Price Setting TowaRds the Efficient Allocation of Multiple resources
UWB: Ultra Wideband
VLC: Visible Light Communications
VPAN: Visible Light Communication Personal Area Networks
WET: Wireless Energy Transfer
Wi-Fi: Wireless Fidelity
WiMax: Worldwide Interoperability for Microwave Access
WISP: Wireless Internet Service Provider
WIT: Wireless Information Transmission
WLAN: Wireless Local Area Network
WPCN: Wireless Powered Communication Networks
WRSN: Wireless Rechargeable Sensor Networks

List of Figures

List of Tables

List of Algorithms

Chapter 1

Introduction

The demand for higher data rates, energy-efficiency, and interference improved solutions in wireless networks is unrelenting. The even-increasing support of wireless services, e.g., data transfer, voice, video streaming, e-Health, glasses / touch Internet, e-gaming, etc., via wireless networks has dictated the necessity for deploying more data supportive cellular architectures. The Ericsson Mobility Report [1] presented in June 2015, predicts 9.2 billion total mobile subscriptions (i.e., mobile broadband, smartphones, mobile PCs, tablets, and routers) by 2020, which is an increase of 30% compared to 2014. Furthermore, it is estimated that 90% of the world's population over 6 years old will have a mobile phone by 2020 [2], [3]. As a result, future mobile network is foreseen to reach several milestones with global mobile traffic to increase sevenfold by 2021, with 1.5 connected devices per capita and 75% of mobile data traffic being video services [4].

The fifth generation (5G) revolution constitutes a tectonic shift in the structure and operation of future wireless networks and telecommunications. 5G does not simply consist an advancement of existing 4G infrastructures with regards to compatibility, bandwidth availability or accommodating denser topologies, but it has emerged as a new architecture and design of networked systems under a user-centric perspective. 5G networks are engineered to be heterogeneous, flexible, and adaptable to different usage conditions towards providing seamless user experience and superior Quality of Service (QoS). Rising user diversification with regards to requirements, types of services, and massive connectivity both in numbers of users and coverage in extreme environments, as well as new intelligent devices under the Internet of Things (IoT) trend, highlight that future networks need to address issues related to cost efficiency, energy management, data rate sufficiency, and service variability.

Based on the above realizations, 5G networks are being developed with their main pillars being the use of heterogeneous wireless access technologies, the availability and opening of additional spectrum frequencies (e.g., mm-Wave), and ultra densification. This new emerging radio access network (RAN) vision is expected to attract unprecedented number of users, information data, and software driven applications, all of which pose significant challenges with regards to congestion and interference management, bandwidth allocation, regulatory and standardization requirements, as well as new disruptive business models to respond to rapidly changing market needs, [5], [6].

Hence, it can now be understood that different networks aim at different service goals, while distinct user groups may focus on varying preferences for their transmission. The rising number of degrees of freedom in telecommunication environments and the different parameters which need to be considered at each time, emphasize the need for the adoption of resource allocation techniques towards the multi-dimensional optimization of wireless networks. This should adapt to the structural characteristics of the systems and the needs of the consumers stemming from power, data rate, service type, resource pricing, time, computational complexity, etc. All the above consist crucial elements for the performance of the network, which at each single time need to adjust to the priorities of the administrator or the connected users. Therefore, the increasing complexity of the models under investigation with multiple parameters to be properly addressed, cover a broad array of optimization topics with many resource allocation problems in telecommunications to be nonlinear and nonconvex, further implicating the efforts towards a holistic and straightforward solution [7].

The next generation cellular wireless networks should be appropriately designed and amended to accommodate the ongoing growth of mobile data traffic, while in parallel improve their spectral and energy-efficiency. To cope with this trend, the current technologies and standards adopted in cellular

wireless networks, should evolve for supporting a multi-tier cellular architecture, where system's bandwidth reusability will be supported.

In this direction, multi-tier wireless network architectures, i.e., macrocell, femtocell, and Visible Light Communication (VLC) cells suggest realistic and cost effective measures to improve performance and reliability, via decongesting the macrocell and allowing the latter to redirect its resources towards providing better reception for mobile users. Network heterogeneity is reinforced by multiple levels of user connectivity, while additional interfaces allow enhanced interference management. Resource allocation becomes more agile, while at the same time users gain higher control with regards to their decision strategies and transmission priorities. A conceptual representation of a 5G multi-layered heterogeneous network is shown in Fig. 1.1

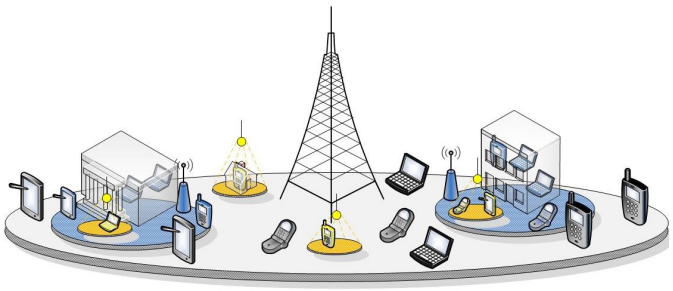

Figure 1.1: A conceptual multi-layered 5G heterogeneous network

Moreover, the rising demand of a variety of communication services poses stringent QoS requirements to Wireless Internet Service Providers (WISPs). The emergence of cloud services, machine-to-machine applications, mobile videos and capacity hungry applications, contribute to the rapid growth in demand for mobile data communications, which can be translated to increased users' consumption of system's resources [1]. As a consequence, the efficient use of the limited wireless system resources is of critical importance in order to improve system's efficiency. Users' services and demands are characterized either as elastic or inelastic [8], where the corresponding data demand can be respectively either shiftable in time, e.g., data uploading, electronic mail, or non-shiftable, e.g., voice call, video-conference. Providing the appropriate framework and creating the right incentives to the users to adjust their system's resources' usage behavior is of high research and practical importance, so as to achieve energy-efficiency and help WISPs with better resource allocation, thus contributing to the social welfare [9].

Pricing suggests an intelligent and adaptable tool towards more effective resource allocation schemes in telecommunications in the direction of more socially acceptable outcomes via guiding user behavior and recognizing individuals' preferences. Pricing mechanisms have been widely used by economists and researchers to remedy operational inefficiencies of networks and encourage users to utilize resources in a more effectual manner, while also provide an "incentive compatible" which reflects the cost of usage and reinforce measures against over-utilization and enhance revenue maximization for the WISPs. Different pricing policies mirror unique network and usage conditions in order to further improve user satisfaction from the provided services, while getting aligned with the vision of subscriber self-optimization and self-adaptation in future ad-hoc wireless networks, where sophisticated user-centric resource management approaches are required [10].

The massive expansion of connections and the subsequent growth in data traffic [4] is shedding light to the problem of spectrum shortage, with mobile users being unable to exploit bandwidth resources based on lack of infrastructure, outdated regulation policies, or limited access to data sharing. The ongoing transformation of radio cellular networks towards heterogeneity, machine-to-machine communications, and small cell deployment has shifted the interest to schemes exploiting the coexistence and use of both licensed and unlicensed spectrum bands which remain currently largely unutilized. This new paradigm creates a whole new vision of how spectrum becomes available to users, not only in terms of accessing free to use resources which are under the risk of over-exploitation, while also on how to develop adaptive models for traffic offloading and congestion management by considering though conditions of uncertainty and diverse user preferences.

Moreover, the state of the art of wireless communications systems is embracing the adoption of new access technique protocols and shared interfaces, which require a completely different philosophy with respect to how networks operate, allocate users, and prioritize interference management and energy

savings. New schemes away from traditional orthogonal multiple access (OMA) techniques have emerged, such as Non-Orthogonal Multiple Access (NOMA), identified as a preferred candidate for the imminent deployment of 5G, providing superior connectivity, flexibility, and lower transmission latency to the users, but at the same time safeguard compatibility to other technologies and wireless systems and simultaneously guarantee complexity mitigation and transmission robustness.

The above developments are leading to a rethinking of how modern networks are addressing spectrum shortages, energy-efficiency, and their capacity to manage services' heterogeneity. The corresponding challenges mirror the urgency to consider spectrum fragility in alignment with this ever growing data demand, since scarcity of spectrum is already a reality currently pushing networks to their potential limits of operation [1]. In view of this, user integration into the self-optimization process of 5G networks to achieving more efficient resource utilization and flexibility is vital for the future design and structure of wireless communication systems. This objective is expected to be further supported in future wireless networks through the use of devices with flexible access technology interfaces, where more than one access technologies [11], become simultaneously available to the users as potential options of communications and usage.

The exponential increase of data exchange and the need for more intensive information sharing has highlighted also the need in the direction of more efficient algorithms, automated decision making processes, and pattern recognition. Subsequently, Machine Learning (ML) as a subfield of computer science and computational learning theory, appears to be more interconnected with the way modern smart devices operate in order to improve energy consumption, data overhead, and computational power so as to support the increasing complexity of transmissions. In modern communication systems, designing predictive models and investing in artificial intelligence techniques can contribute to higher quality of services by better managing spectrum resources, heterogeneous services, and facilitate complicated network configurations. On the other hand, the convergence of networks offering a plethora of distinct services to different user groups has intensified competition among WISPs also due to the disruptive nature of the 5G modules and IoT adoption. WISPs aiming to ameliorate their revenue potential and increase their market reach, explore different strategies spanning from novel pricing policies, service offerings, and new transmission standards [12], [13].

Intelligence of smart devices keeps improving, and users are capable of making decisions themselves over the emerging competitive wireless environments and markets. Given the variety of 5G wireless access technologies and multiplicity of available resources of different nature and properties (e.g., power, rate, resource blocks, price), users have several degrees of freedom to access and control these parameters. Future wireless networks realized through disruptive technologies, are characterized by their user-centric nature, thus moving away from the operator-centric (as in 3G) or service-centric (as in 4G) paradigms. To succeed with these trends and proceed to successful deployment and realization of a powerful wireless world, user intelligence and user satisfaction become crucial factors.

Additionally, the wide range of modern day applications in telecommunications require that wireless networks can extent their operation to extreme environments ensuring flexibility and resiliency. Being able to maintain undisrupted communications in volatile conditions considering mobility of nodes, congestion and over-utilization, as well as fragility of resources is of outmost importance, impacting public safety and economic development. Moreover, given the significance of data privacy and high interconnection of networked systems, security against attacks and malicious behavior has received widespread attention. In view of this, the development of sophisticated solutions and algorithms protecting the safe operation of networks has arisen as one of the fundamental requirements for future network infrastructure.

On the other hand, under the blooming wireless communication systems, the problem of energy-efficiency and extending mobile devices' battery life via identifying additional energy resources is another topic of pivotal importance. Exploring alternatives which improve the operational efficiency and durability of networks in a sustainable manner, such as Wireless Powered Communication Networks (WPCNs), have been considered as promising alternatives to conventional battery-powered networks via energy harvesting techniques based on natural energy sources such as solar or wind. Those novelties are leading to a redesign of how networks function, prioritizing energy conservation without compromising performance and QoS standards.

Within such a dynamically evolving and autonomous environment, Game Theory as a branch of applied mathematics has in recent decades become an integral part of designing telecommunication systems due to its inherent characteristics of capturing interactions between several decision-makers who can have conflicting or common interests. Game theory although originally developed as a tool to be used in economics and social sciences, has found fertile ground of application in wireless network problems by

formulating them as non-cooperative games. This is mainly due to the need for incorporating decision-making rules and techniques to enable communication nodes to operate more efficiently and reach stable operating outcomes (i.e., notion of Nash Equilibrium) under conditions where the optimal strategy is generally unclear, since no player has absolute control of the situation, in contrast to classical optimization problems where an objective function is optimized given a list of constraints [14], [15].

1.1 Motivation and Scope

Given this dramatic evolution of wireless networks towards a new era of information exchange and connectivity, this thesis attempts to encompass the latest advancements in the field of telecommunications with the development of algorithms which improve the performance of the network and provide a superior user experience. Recognizing the unique opportunities and challenges coming from the continuous accomplishments of technology and the diversification of user needs, this work has been constructed upon the following four pillars:

User satisfaction and network performance

In wireless network problems, user satisfaction has been so far perceived as just a numerical value with respect to the maximization of an objective function or parameter. This work envisions to explore users' QoS and their overall transmission experience from a multi-faceted perspective, which includes not only the optimization of a specific resource, but allows users to proactively shape the nature of their transmission by adding new technologies, service modules, and personalized telecommunications products, thus, elevating the role of users in the network and adjust to their preferences and priorities. As a result, the overall network performance and resource allocation process is orchestrated by integrating the actions of individual users into an interactive framework that allows the system to evolve and converge to optimal outcomes.

Energy-efficient and sustainable communications

Understanding the significant impact of resource scarcity and the rising costs of energy for both the consumers and WISPs alike, developing information and communications technology (ICT) applications and algorithms which enhance the energy-efficiency of transmissions and data transfer does not only have a positive impact on the environment, but expands the capacity of networks towards higher connectivity, enhanced operational durability, and long-term profitability. This thesis aims at the design of algorithms and methodologies which safeguard social welfare among the users and ensure more pragmatic energy and resource management.

User centricity and self-optimizable networks

So far, users have been considered as data exchange nodes with neutral behavior inside highly concentrated and centralized network structures. The development of smart devices and the increasing diversification of service offerings dictate that decision making, needs to be adjusted dynamically based on the heterogeneous user types with varying requirements. In this work, the user is placed at the core of the resource allocation problem, with its decisions and strategy to significantly impact the performance of the network. Next generation network structures cannot be static; they should evolve autonomously according to the state of user interactions and the system's capacity to allocate the available resources in a fair and balanced manner.

A holistic solution framework for resource allocation problems

The overwhelming body of literature regarding network optimization has so far focused on solving single aspects of resource management problems in single variable and one dimensional topologies. Adding more degrees of freedom and designing scalable and generic enough network models, allows to structure resource allocation problems in a more holistic manner. This thesis encloses a novel and adaptable framework which manages to confront different aspects of resource optimization, offering stable outcomes despite the uncertainty and high variability of user interactions. As a result, the presented solution approach in

this work is not restricted to tackling problems only in the area of wireless networking, but can be easily expanded in other fields where sustainable resource allocation and user centricity are crucial elements.

1.2 Contributions

Wireless network optimization via game theoretic approaches consists a field which has received widespread attention and interest from the scientific community [16], with the literature being enriched with valuable works extensively discussed within the course of this thesis. Although significant performance accomplishments have been achieved, the vast majority of those efforts have approached the resource allocation problem from a static perspective where users are blindly aiming at the maximization of their utility by determining the numerical value of a single parameter, or focus on a system-wide performance improvement e.g., via interference mitigation or sum rate maximization. The network administrator or the WISP possesses a paramount role for the operation of the network by monopolizing the decision making process and centralizing the actions with respect to data exchange and resource distribution. Moreover, the user populations are missing the flexibility of defining the conditions of their communication by controlling limited degrees of freedom, while also lack the incentive to optimize their transmission since any system measures aiming at social fairness are enforced in the form of penalties in order to mitigate any selfish or competitive behaviors.

Our work takes a structurally different approach from the overwhelming body of existing literature in this area, by aiming to bridge the gap between the new trends in connectivity and network access enabled by the dawn of the 5G era and the ability of diverse users to dynamically determine various attributes of their transmission. Hence, users are positioned at the centerpiece of the network operation with their actions to obtain a dominant role for the optimization of the performance of the system which evolves in an autonomous manner. In more detail, the primary contributions of this work are summarized as follows:

1. ***Multi-dimensional system modeling by optimizing resources in multi-service, multi-tier heterogeneous networks:*** Modern wireless networks have evolved into a complex system of numerous interconnections between users, devices, WISPs, and data interrelations. A major novelty of this work lies in the fact that users are able to determine multiple degrees of freedom during the resource allocation process not in flat topologies, but assuming networks of various layers, architectures, and diverse services. In this thesis, for the first time, up to three different parameters are controlled by the users, while small cells (e.g., femtocells) and Visible Light Communications are utilized towards exploring alternative means of data exchange. Moreover, next generation networks have moved forward from simplistic voice-only communications to elastic (non-real time) or inelastic (real time) services with different QoS standards. Hence, in this work such offerings are designed appropriately to be synchronously provided so that users can shape their transmission according to their personal preferences and objectives.

2. ***Integration of new access and flexible technology schemes in the resource allocation process:*** The development of multiple access techniques enabled by the 5G technology breakthroughs allows the expansion of the system's capacity and enhanced flexibility in spectrum allocation and energy management. In this work, different access technologies and bands (e.g., OFDMA, NOMA, licensed and unlicensed bands) considered to be employed in future 5G installations are extensively studied and implemented in different scenarios aiming at driving network operation into higher transmission standards and at the same time achieve optimal resource allocations. Moreover, in a pioneer approach, for the first time in the literature different access techniques are simultaneously modeled into the resource optimization problem by being accessed by multi-interface ready devices, allowing for the further sophistication of the communication experience.

3. ***Prioritizing energy-efficiency and spectrum distribution optimization:*** Reducing energy consumption without deteriorating QoS has been a key target for WISPs, end users, and societies alike, in the effort to reduce operational expenditures, contain carbon dioxide emissions, and switch to long standing solutions to address the exploding number of mobile subscriptions in an environmentally friendly way. In this work, we develop concrete methodologies towards optimizing the energy-efficiency of transmissions, while ensuring superior quality of experience by expressing user satisfaction as the quantification of exchanged information to the consumed energy. This thesis exploits new technologies in smart devices (e.g., dual-access interfaces), network tiering (femtocells),

transmission protocols (e.g., NOMA, SIC) and adaptive wireless energy harvesting (WPCNs), which allow for sophisticated interference, congestion, and energy transfer management. Moreover, the joint allocation of resources like transmission power and data rate, segmentation of user groups, and service types, further optimize utilization, reduce energy waste and resource over-investment, thus ameliorating social fairness and service durability for mobile customers.

4. ***Flexible service composition via bundling to diverse user groups under a market driven perspective:*** Online end-user service demand, supported by the convergence of next generation networks, has undergone a vast transformation with respect to heterogeneity and diversity. Networks and their elements are required to provide agile and flexible services in different user groups or market segments, towards realizing future network's user-centric prospect. However, so far conventionally this has happened only as a combination of existing and often competing service options. In this thesis, we discuss a novel paradigm based on the concept of service bundling, which inherently integrates various technical service modules based on customer preferences in order to optimize resource allocation and increase user overall experience. Stemming from the commonalities and synergies among the bundled options in terms of characteristics and performance, a new and superior product is devised, enabling users to enjoy better performance under a common and standardized methodology.

5. ***Introduction of price personalization and novel pricing schemes in the resource allocation problem enhancing competition:*** For the first time in network optimization problems, price is considered as a resource expressing users' willingness to pay for the involved services instead of simply penalizing them for unfair resource consumption. The joint determination of price alongside power and / or data rate exploits network's conditions and users' real-time service demands, concluding to better service delivery to individual users and better usage of system's resources as a whole, leading to more efficient points of operation. Moreover the adoption of new pricing schemes and their implementation in competitive telecommunication markets is proven to define the strategies of WISPs and their revenue prospects, while simultaneously increase user surplus and increase allocation efficiency.

6. ***Allow for user subjectivity in decisions assuming real life conditions with the use of Prospect Theory:*** Users are not assumed to be blind utility maximizers as instructed by the majority of existing works based on Expected Utility Theory (EUT), but in this work their behavior modeling is specifically designed to reflect real life human decision making under uncertainty, highlighting individual preferences and communication priorities which may considerably vary. This piece of research constitutes one of the first approaches in the field of wireless networking to adopt the use of Prospect Theory as the main behavioral tool towards mirroring user strategies in competitive resource allocation problems with incomplete information, evaluating satisfaction in a user oriented perspective.

7. ***Introduce resource fragility and incorporate risk assessment in users' strategies during the resource allocation process:*** Although resource sharing, utilization, and over-congestion consist common phenomena in wireless network optimization problems, so far literature has considered spectrum, or network capacity as infinite or imperishable variables. On the contrary, in this thesis, for the first time we consider the probability of failure (i.e., fragility) for resource management in wireless networks in cases of over-exploitation according to the concept of the *"Tragedy of the Commons"*. The above breakthrough creates a totally different landscape on how end users and WISPs define their behavior and actions, based on risk aversion perceptions and probability weighting. This consideration allows the study and evaluation of satisfaction and resource effective utilization under more realistic and personalized assumptions.

8. ***Extend the resource allocation problem to new frontiers of intelligent communications via Machine Learning and expand in extreme communication environments:*** In order to manage the substantial traffic and congestion load, future wireless networks need to develop capacities of monitoring patterns and automate the decision making process. This work proposes schemes which are well above the conventional scope of resource allocation, with the introduction of Machine Learning methodologies, where end-users and the system develop, learn, and adapt in different conditions, improving QoS delivery and contribute to the network optimization process.

Additionally, aiming to increase coverage and service support under extreme conditions, we expand the mission of resource allocation to include Public Safety Networks (PSNs) including Aerial Unmanned Vehicles (UAVs), ensuring reliable communications in cases of urgent events or in unfavorable transmission environments. Moreover, the security aspects of resource management in such networks is considered, with this thesis to propose intelligent frameworks for capturing malicious behaviors that distort the resource allocation process and enforcing protective measures against them.

1.3 Thesis Outline

The thesis is organized as follows. Each chapter confronts a specific resource allocation topic, initially presenting the problem realization and the solution motivation, followed by a description of the current state of related work in the literature. Next, the system model is determined and the corresponding problem is mathematically formulated and solved. A distributed algorithm is devised next for the practical implementation of the problem, while a series of simulations confirm the operation and the performance gains of each approach.

In **Chapter 2**, we present resource (power and rate) allocation problems in multi-tier architectures incorporating femtocells and Visible Light Communications. The problems under consideration are gradually expanded to more complicated topologies from power control only to joint power and rate control schemes, resource block allocation, and access technology comparison between NOMA and OFDMA.

In **Chapter 3**, an overview of the use of pricing in wireless communications is presented. Price becomes a resource to be allocated alongside power and / or data rate, with each user expressing its willingness to pay allowing for customized pricing schemes alongside conventional resource allocation.

In **Chapter 4**, we expand the previous analysis for power control by exploring WISP selection methodologies given a selected pricing strategy, with users being modeled as learning automata via Machine Learning under conditions of competition.

In **Chapter 5**, the notion of service composition in resource allocation problems in wireless networks is introduced. The model is structured in a way so that users are able to utilize multiple service offerings under the principles of service bundling. The problem is initially solved via combining real and non-real time services and following, is expanded to involve multiple service modules which are individually selected by the users.

In **Chapter 6**, the problem of adaptive energy transfer is confronted with the use of Wireless Powered Communication Networks. The resource allocation problem is incorporated and adjusted to the energy requirements of the system, by linking the transmissions of the users to their energy consumption and charging requirements.

In **Chapter 7**, Prospect Theory becomes the main modeling tool for resource allocation problems. Users become risk-aware and control their decisions by evaluating the probability of collapse of spectrum, under the concept of the Tragedy of the Commons. The problem is applied to dynamic sharing of licensed and unlicensed spectrum bands, as well as by using shared access technology interfaces among NOMA and OFDMA techniques. Lastly, an investigation of how pricing can be utilized towards resource fragility protection is conducted.

In **Chapter 8**, the resource allocation problem is expanded in extreme transmission environments by exploring its application for UAV-assisted Public Safety Networks, while also security aspects of network operation against malicious user behavior are examined.

Lastly, **Chapter 9** concludes the thesis with an overall summary of the content and a review of its contributions. Additionally, a segment is devoted to the presentation of potential future research directions stemming from this work.

Remark 1. *Due to the overwhelming number of variables and parameters throughout the course of this thesis, for notational convenience in each chapter the key symbols are summarized in relevant tables. Some of the parameters used in separate chapters may represent different notations and thus, are appropriately defined in each section.*

1.4 Game Theory Preliminaries

Game Theory is considered a field of applied mathematics studying strategic decision making in conditions of conflict, holding its foundations from the book of John von Neumann and Oskar Morgenstern in *"Theory*

of Games and Economic Behavior", while it was further enriched and formalized by John Nash with his work on non-cooperative games. Game Theory, although initially developed as a tool related to social and economic disciplines, as already mentioned has been widely accepted and used as a modeling paradigm across various areas including evolutionary biology, computer science, international politics, business, and wireless networking, among others.

Game Theory is built upon the concept of a *game*, representing an interaction between different rational stakeholders, or *players*, whose individual decisions affect each other's payoff and strategies, aiming at each time to maximize their expected benefit based on their current status of information. Games are modeled based on the players' strategies, representing the set of available options to the users under which they define their optimal decisions and are determined as *pure* (when only one option is selected at all times), or *mixed* if multiple options may selected during the game. The decisions of the users lead to a certain payoff or utility, representing a quantification of users gains or losses from their corresponding strategies.

A simple example widely used towards explaining Game Theory is the well known *"Prisoner's Dilemma"* [15]. According to the formulation of this game, the hypothetical scenario of two suspects being arrested for a crime is assumed. The police does not have enough information to convict either of them, hence asks each suspect to testify, getting a reduced sentence or be released. Each of the prisoners does not have information about the decisions of the other, with the following scenarios being unveiled:

- Both deny any knowledge of the crime (cooperate - (C)): they both get the maximum payoff since they will be convicted of a lesser crime, since no further evidence can be collected against them for the real one.
- If one defects (D) while the other stays silent, the first is released while the other is convicted since evidence became available against him.
- In the last option, both prisoners confess getting a reduced sentence.

In brief the different outcomes are possible: $(C, C), (C, D), (D, C), (D, D)$. The above options can be summarized in the following matrix:

Table 1.1: Prisoner's Dilemma Payoff Matrix

	Prisoner B cooperates	Prisoner B defects
Prisoner A cooperates	(3,3)	(0,**5**)
Prisoner B defects	(**5**,0)	(**1**,**1**)

From the above it is concluded that the optimal outcome, or *equilibrium* for the system in total (i.e., the situations for the both players) is for both to defect (hence, (D, D)), given the actions of the other player.

Different variations of games exist referring to different conditions of interactions among the players based on the considered situation [14].

- *Zero-sum and non zero-sum games:* The first indicates a strictly competitive situation where the benefit of one player leads to an equivalent loss of the other player, while the second category instructs a situation where cumulative gains and losses of players are not complementary (i.e., their summation may not equal zero) being either competitive or non-competitive.
- *Static and dynamic games:* The first kind of games refers to situations where users hold a certain amount of knowledge which stays stable during the game, while dynamic games imply that users can gain information from previous decisions or actions.
- *Non stochastic and stochastic games:* In stochastic games the game is played in stages with a certain state to evolve according to a probabilistic rule.
- *Non-cooperative and cooperative games:* In cooperative games users can form alliances towards achieving optimal outcomes, while in non-cooperative games players compete with each other often with conflicting interests.

- *Games with complete and incomplete information:* Complete information games assume that the information available among the players is common knowledge, while incomplete information (or *Bayesian*) games refer to situations where users hold only partial information of the game's characteristics.
- *Games with perfect or imperfect information:* In the first type, users are fully aware of the history of the game, while in the latter this does not hold true.

Towards formalizing a game in mathematical terms, although different formulations are found, the most common representation of a game is its *Strategic Form*, defined as below:

$$\mathscr{G} = \{\mathscr{K}, \{\mathscr{S}_i\}_{i\in\mathscr{K}}, \{\mathscr{U}_i\}_{i\in\mathscr{K}}\} \tag{1.1}$$

where $\mathscr{G}$ is the game, $\mathscr{K}$ is the set of players, $\mathscr{S}_i$ is the strategy set of each player with its list of actions, and $\mathscr{U}_i$ is the utility or payoff function of each player.

For non-zero sum games, the state where all users cannot further increase their payoff by modifying their strategies is known as *Nash Equilibrium* (formally defined in Definition 2.3.4). A simplistic representation of a game with a Nash Equilibrium is shown below:

Table 1.2: Identification of Nash Equilibrium

		Player Two	
		Option 1	Option 2
Player One	Option 1	(-1,-1)	(-3, **0**)
	Option 2	(**0**,-3)	(**-2**,**-2**)

By determining the different entries, the outcome $(-2, -2)$ is the Nash Equilibrium, since no player would improve its position by modifying their decision, given the decision of the other player. If player 2 selects option 1, player 1 receives a better payoff selection when selecting option 2, while if player 2 selects option 2, again player 1 achieves a better payoff with option 2. On the other side, if player 1 selects option 1, given this decision player 2 is better off if it selects option 2. The same applies if player 1 picks option 2. Then, by combining the above options, both players benefit by selecting option 2, which is the Nash Equilibrium of the game.

Remark 2. *More definitions and explanations will be provided during the course of the thesis in later sections.*

Chapter 2

Resource Control in Multi-Tier Architectures

Aiming at achieving system's bandwidth reusability in the same physical area, the idea of cell splitting has been proposed and it is based on the hierarchical cell deployment model, where small cells with possibly different transmission technologies lie in the coverage area of a macrocell. This hierarchical infrastructure of a wireless network constitutes a heterogeneous network, i.e., HetNet [17]. However, though system capacity may increase via such an approach, several drawbacks exist in their deployment. These may include:

- The installation and maintenance of the cell towers is prohibitively expensive,
- They do not completely solve the indoor coverage problem,
- The radio frequency interference in the same bandwidth diminishes system's capacity,
- The backhaul deployment costs cannot be avoided.

Based on the above observations, more cost-effective solutions have emerged, such as femtocells and visible light communication cells.

A femtocell consists of a short-range (10-50m) low-cost and low-power (10-100mW) Femtocell Access Point (FAP) being installed by the consumers towards achieving better indoor coverage and capacity. FAPs transmit over a licensed Radio Frequency (RF) spectrum and are connected to the macrocell network via a broadband connection, e.g. Digital Subscriber Line (DSL), cable modem or via a dedicated RF backhaul channel. The main advantages of femtocells are:

1. Lower transmission power,
2. Prolongation of mobile users' battery life,
3. Higher signal-to-interference-plus-noise ratio (SINR),
4. Increased system capacity,
5. Reduced interference,
6. Low cost installation,
7. Increased number of served users in the same physical area [18].

Visible Light Communication (VLC) cells, developed by the IEEE 802.15.7 standard, operate in a different frequency band (i.e., 400 - 800 THz) compared to RF communication, thus overcoming the burden of interference with RF-based small cells. A VLC cell consists of an Optical Access Point (OAP) with small coverage area (i.e., 1–4 m). In VLC systems, the communication signal is encoded on top of the illumination light, thus resulting in energy-saving "green" communication and high-speed wireless connectivity reaching speeds of 224 Gbps [19]. The key advantages of VLC cells are:

1. Nearly infinite bandwidth,
2. Usage of free and unregulated channels,
3. They pose no health hazards, due to the non-existence of electromagnetic radiation,
4. They pose no electromagnetic interference (EMI) and / or no radio frequency interference (RFI),
5. Extremely low transmission power,
6. Almost no cost, due to the fact that light sources already exist everywhere [20].

This chapter aims to present the architecture of a multi-tier heterogeneous wireless network for each type of small-cell technology, e.g., femtocell and VLC resolving different types of resource allocation problems for varying classes of resources and access technologies towards enhancing system capacity, mitigating potential interference, while satisfying users' QoS requirements in a cost effective and energy sustainable approach [21], [22], [23].

2.1 Femtocells in Wireless Communications

Femtocells have arisen as a promising solution in order to confront users' Quality of Service (QoS) prerequisites and decongest the macrocell network [24] from the increasing number of mobile users and the corresponding caused traffic. According to the statistical data in [18], nearly 90% of data services and 60% of phone calls nowadays occur in indoor environments. Thus, femtocells usually reside in a home / office environment and consist of an access point (AP) with short range which is being connected to service provider's internet network [18]. They have attracted great attention, not only because they can provide large indoor coverage and system capacity due to the short communication distance to users, but also due to the fact that they offer significant economic benefits, given their low-cost installation over an existing macrocell network [25]. The entire overlaid network is referred as *two-tier femtocell network* and consists of femtocells and the conventional macrocell network. In order to maximize the benefits that stem from the two-tier femtocell network architecture, it is of paramount importance to control and optimize the allocation of available resources (i.e., power and transmission data rate) to the users. In this work, we focus exactly on the treatment of this problem in the uplink case, targeting at providing an autonomic user-centric optimal resource allocation mechanism, enabling users' self-optimization and self-adaptability. A conceptual representation of a two-tier femtocell network is illustrated in Fig. 2.1.

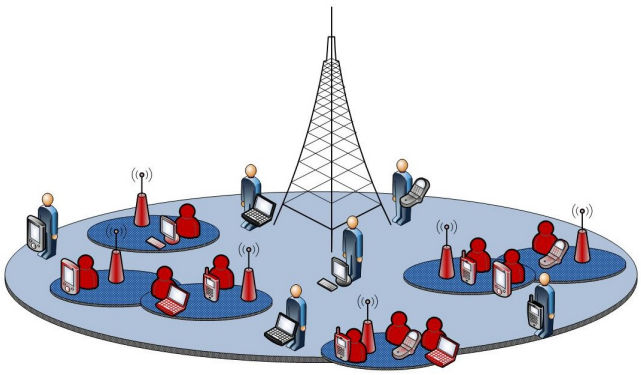

Figure 2.1: Two-tier femtocell network topology

Femtocell users (FUs) enjoy the privilege of superior indoor reception and higher data rates with lower transmission powers, due to the close proximity between themselves and their own home APs. Furthermore, FUs operate in the licensed spectrum owned by the wireless operators and share this spectrum with macrocell users (MUs), which have strictly higher priority over the FUs in accessing the underlying radio spectrum. Thus, the cross-tier interference reduction is of great importance for deploying femtocells in two-tier wireless networks.

Given the above setting and aiming at mitigating interference, the system "penalizes" FUs towards keeping their transmission powers at low levels, while trying to satisfy their QoS prerequisites. This strategy enables the MUs to maintain their service quality regardless of the deployment of femto APs [26]. Moreover, due to the absence of an overall central entity which has the global knowledge and authority to determine simultaneously the power level of each FU and MU in the uplink, a decentralized power control framework is a requirement rather than a desire.

2.2 Related Work on Resource Allocation in Femtocell Networks

In recent literature, considerable research efforts have been devoted to the problem of optimal resource allocation in the uplink of wireless networks under different architectures and technologies (e.g., single-tier, two-tier, CDMA, OFDMA, SC-FDMA [27], etc.), while special emphasis has been given on the power control problems due to the inherent convenience of single variable optimization.

Initially, for single-tier wireless network architectures, in the seminal paper [10], the authors model the power control problem as a non-cooperative game, where users act as individual players aiming at maximizing selfishly their utilities and determining their own transmission power in a distributed manner. More energy-efficient power allocations are determined in [28] and [29] via proposing a convex pricing policy with respect to the user's uplink transmission power and a linear pricing scheme as a function of signal-to-interference ratio, respectively.

Moreover, due to the necessity of supporting multiple services and aiming at maximum efficiency of system's resource allocation, considerable research efforts have been devoted to the combined problem of power and transmission data rate allocation, still in single-tier macrocell wireless networks [30, 31]. The basic approaches that have been proposed in the recent literature are mainly three. First, in [32] the authors follow a two-step approach and solve separately and in a sequential manner the problem of transmission power and data rate allocation. Second, the combined problem of power and transmission data rate allocation is considered as a single-variable problem of the ratio of uplink transmission data rate to the uplink transmission power [33], and updates both power and transmission data rate at the same time. Third, in [34], [35] the joint resource allocation has been confronted as a two variable problem and users' optimal transmission power and transmission data rate are determined simultaneously and independently.

Expanding the problem in two-tier network architectures, in [36–39], a distributed utility-based SINR adaptation algorithm has been proposed in order to alleviate cross-tier interference at macrocell from co-channel femtocells. Users are organized in two main categories femto-users (FUs) and macro-users (MUs) and they are associated with a generic utility function [38]. Furthermore, the FUs can be penalized with linear [37, 38] or convex pricing policies [40] with respect to their uplink transmission power, in order the intercell and cross-tier interference to be mitigated and give higher priority to the MUs, that unlike to the FUs have by default worse channel conditions, due to their high distance from the base station (BS). MUs and FUs satisfaction, with respect to their allocated system resources, are represented with different utility functions. Specifically in the case of MUs they simply express the minimum prerequisite of QoS in terms of SINR, while the FUs are penalized in order to reduce cross-tier interference. The overall problem of maximizing each user's satisfaction is formulated as a non-cooperative game and solved. Similar approach is followed in [41,42] where common utility functions for MUs and FUs are assumed, and the problem is addressed via the formulation of an energy-efficient power control game, which concludes to a unique feasible and stable users' uplink transmission power vector. Additional utility-based approaches are also reported in [43, 44].

Especially for two-tier femtocell networks, the main research efforts have concentrated so far only on users' uplink transmission power allocation [45], without considering the combined problem of power and transmission data rate allocation and the multi-service users' QoS prerequisites. In [40], a distributed utility based SINR adaptation algorithm has been also proposed in order to mitigate cross tier interference at macrocell from co-channel femtocells and concludes to users' power allocation. Aiming at guaranteeing a target SINR of the MUs and making as many FUs to achieve a target SINR, the authors in [46] introduce user selection and channel re-allocation complementary to the power control problem. Some initial research work has been performed in the area of spectrum allocation. In [47], the authors propose a Stackelberg game-based spectrum allocation scheme among macro base stations and femto APs aiming at a dynamic optimal frequency allocation and resulting in minimum interference to MUs and FUs. Additionally, in [48] the authors propose a resource block allocation in LTE two-tier femtocell networks. The distributed resource blocks allocation algorithm is modeled after link-state propagation routing protocols and consists of a graph formation stage, where individual APs create a view of the network and each AP assigns resources to FUs based on their throughput requirements.

However, the real joint problem of user's uplink transmission power and rate allocation in wireless networks has not yet been thoroughly examined in the literature and especially under the paradigm of two-tier femtocell networks. Some efforts have been devoted to this problem in multi-hop wireless networks. A representative example is Heat Diffusion Protocol [49] which provides a Pareto optimal

resource allocation and packet latency in interference wireless networks. Moreover, in [50], a different derivative of Back Pressure Routing Protocol has been proposed for joint resource allocation and routing in time varying wireless networks. However, those approaches still remain to be investigated regarding their applicability and extensibility in single-hop multi-tier wireless networks. An initial approach to the joint power and rate allocation problem in single-tier wireless networks has been proposed in [33], where a specific form of user's utility function is adopted (i.e., the ratio of the reliably transmitted bits to the base station divided by their corresponding transmission power) enabling the authors to change the two variable optimization problem to a single variable problem. The latter goal is achieved via substituting the ratio of user's transmission rate to the corresponding transmission power with a new variable and solve the corresponding single variable optimization problem.

The problem of optimal resource allocation in the downlink of two-tier femtocell networks, where orthogonal frequency division multiple access (OFDMA) technology is adopted has been thoroughly examined in the literature. The key problems that have been studied target at interference mitigation, [51], [52] energy-efficient resource management [53], joint subchannel and power allocation [54], and resource allocation based on usage-pricing mechanisms [55], and/or link-state propagation model [48]. However, all these approaches are centralized and their goal is to guarantee system's efficiency, e.g., maximization of system's sum rate, system's overall interference mitigation etc.

Approaching a more comprehensive resource allocation problem for two-tier femtocell networks, some initial approaches have been proposed that target mainly at system's efficiency and not at the maximization of each user's perceived satisfaction. In [56], the problem of subchannel, rate, and power allocation in two-tier OFDMA femtocell networks using fractional frequency reuse has been examined, towards maximizing only FUs throughput, while maintaining as little as possible reduction in the macrocell users' performance. In [57], the authors target at the maximization of the sum users' rate at each FAP, under the constraints of cross-tier interference between macrocell and multiple FAPs. In [58], a joint subchannel and power allocation in two-tier OFDMA femtocell networks is proposed. The formulated resource allocation problem considers only the FUs as candidate users in order to determine the subchannels that are allocated to them, as well as their transmission power towards mitigating their co-channel and co-tier interference. Furthermore, the subchannel and the power allocation problem is decomposed into two separate problems and solved. As a consequence, there is no guarantee that the obtained stable point is as efficient as the one achieved if solving the actual joint subchannel and power control problem where the two resources are updated simultaneously at the same step. Lastly, in [59], the authors study the problem of resource and power allocation in congestion cases in which femtocell demands exceed the available resources, while in [60], a distributed resource management framework that effectively manages interference across femtocells is proposed.

2.3 Power Control for Multi-Service Networks

In this section, the problem of efficient distributed power control in the uplink of two-tier femtocell networks supporting multiple services (i.e., both real-time and non-real time) with various and often diverse QoS prerequisites is addressed via a game theoretic framework. The definition and treatment of users' utility functions has been designed in a way which reflects their service QoS-aware performance efficiency according to both the tier the users belong to, as well as to the type of service they request. Such a consideration, which is reflected through the use of heterogeneous user utilities and appropriate system modeling allows for a more realistic representation of users' QoS prerequisites, while at the same time taking into account properly cross-tier and intercell interference, thus giving high priority to the MUs. However, these considerations do not allow the adoption and direct application of existing power control approaches in femtocell networks and call for different treatment of the overall problem.

2.3.1 System Model

We consider a two-tier femtocell network that consists of a central macrocell base-station B_0 serving a region $\Re$, providing a cellular coverage of radius R_0. Within the region $\Re$ reside F co-channel femtocells B_i $(i = 1, ..., F)$. Each femtocell supports a region $\mathbb{C} \subset \Re$ and consists of a disk of radius $R_c << R_0$. In our proposed framework, we consider closed access femtocells, i.e., registration is mandatory for users to be served by femto APs, thus each femto AP knows the number of users residing in its coverage area. Let us denote the set of all users by $S = S_m \cup S_f$ and the set of MUs and FUs by S_m and S_f respectively, consisting of N_m and N_f number of users. Consider that user $j \in S$ is connected to its B_i $(i = 1, ..., F)$

and denote its uplink transmission power by P_j. Let σ^2 be the variance of Additive White Gaussian Noise (AWGN) at B_i. Then, the received SINR γ_j of user j at B_i is given as

$$\gamma_j = \frac{W}{R} \frac{G_{jj} P_j}{\sigma^2 + \sum_{j \neq i} G_{ji} P_j} \tag{2.1}$$

where W $[Hz]$ is the total bandwidth, R $[bits/sec]$ is the bit rate, G_{jj} denotes the channel gain from the transmitter of user j to its receiver and G_{ji} the corresponding gain from the transmitter of user j to the receiver of user $i \neq j$. The channel gains are represented using the simplified path loss model in the IMT-2000 specification [61].

In our proposed framework, we consider QoS requirements imposed by real-time (RT) and non-real-time (NRT) services in a network topology as depicted in Fig. 2.2.

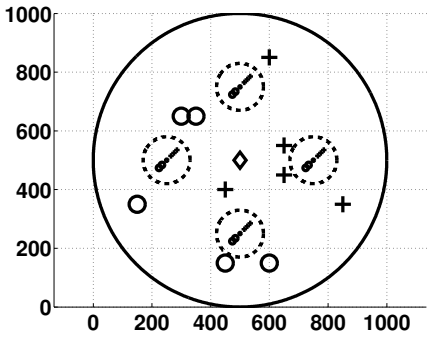

Figure 2.2: Network with macrocell and femtocells for multiple services

Therefore, aiming at supporting multiple services with diverse QoS demands, each user is associated with an appropriately selected utility function, depending on the tier that it belongs to, as well as to the service that it requests. The concept of utility is commonly used in microeconomics and refers to the level of satisfaction the decision-taker receives as a result of its actions.

Definition 2.3.1. ***Utility Function:*** *A utility function represents the quantified level of satisfaction an agent receives as a result of its actions. It is modeled as a function which assigns a numerical value to the elements of the action set A, $(u : A \rightarrow \Re)$ if for all $x, y \in A$, x is at least as preferred compared to y if and only if. $u(x) \geq u(y)$ [10].*

Thus, users' utilities can be expressed as:

$$U_j(\mathrm{p}, \mathrm{r}) = \begin{cases} \frac{R_F f(\gamma_j)}{P_j}, \ j \in S_{m,RT} \\ \frac{R_F \log(1+Df(\gamma_j))}{P_j}, \ j \in S_{m,NRT} \\ \frac{R_F f(\gamma_j)}{P_j} - c\left(e^{P_j} - 1\right), \ j \in S_{f,RT} \\ \frac{R_F \log(1+Df(\gamma_j))}{P_j} - c\left(e^{P_j} - 1\right), \ j \in S_{f,NRT} \end{cases} \tag{2.2}$$

where R_F, D are positive constants, $S_{m,RT}$, $S_{m,NRT}$, $S_{f,RT}$, $S_{f,NRT}$ denote the set of real and non-real time MUs and FUs respectively and $f(\gamma_j)$ denotes user's efficiency function [28]. Without loss of generality the following form of efficiency function is adopted:

$$f(\gamma_j) = \left(1 - e^{-A\gamma_j}\right)^M \tag{2.3}$$

Definition 2.3.2. ***Efficiency Function:*** *The efficiency function $f(\gamma_j)$ represents the successful packet transmission with respect to user's signal-to-interference plus noise ratio γ_j at fixed data rates depending on the modulation and coding schemes that are being used. The positive constant M denotes the number of bits of transmitted packets and A determines the slope of the curve.*

The main properties of the efficiency function are:

1. f is an increasing function of γ_j
2. f is a continuous, twice differentiable sigmoidal function with respect to γ_j
3. $f(0) = 0$
4. $f(\infty) = 1$

For fairness and practical purposes throughout this work, and without loss of generality, it is assumed that all users residing in the cell adopt the same modulation scheme, i.e., common form of efficiency function.

Moreover, as shown in relation 2.2, FUs are "penalized" via a convex cost function with respect to uplink transmission power, aiming at minimizing cross-tier and intercell interference, thus giving in turn high priority to the MUs QoS prerequisites fulfillment. The adoption of an appropriate pricing mechanism by the FUs generates better revenue for the system and encourages both the FUs and MUs to reclaim system resources even more efficiently [10]. Let c denote the pricing factor in relation 2.2.

Furthermore, users are organized in classes according to the type of service they request (i.e., real and non-real time service) and the tier they belong to (i.e., FU or MU). Regarding the users requesting real time (RT) services, their utility function reflects the tradeoff between the reliably transmitted bits to the BS/AP and the corresponding energy consumption. In our formulation, the ideal value of user's transmission rate, at which its service QoS prerequisites are fulfilled, is mapped to the inflection point of the sigmoidal function $R_j^*(P_j) = R_F f(\gamma_j)$ (e.g., voice service $R_j^*(P_j) = 64Kbps$). Thus, in the case that user's transmission rate is less than the value of inflection point of $R_j^*(P_j)$ function, then its utility rapidly decreases, indicating its priority/intention in occupying additional system resources. Considering users requesting non-real time (NRT) services, their utility function is formulated via adopting the Shannon formula, thus representing NRT users' greedy behavior with respect to the achievable data rate. For convenience, all symbols used in this section are summarized in Table 2.1.

2.3.2 Problem Formulation and Solution

As the system evolves, at the beginning of each time slot, a user's Uplink Power Control algorithm in Multi-Service two-tier Femtocells (UPC-MSF) is responsible for determining an appropriate uplink transmission power level towards maximizing its overall degree of satisfaction, which is reflected by the corresponding values of its utility. In this section, the main goals of UPC-MSF framework are analyzed and formally defined as a generic optimization problem in a game theoretic framework.

Since each user $j \in S = \{0, 1, ..., N = N_m + N_f\}$ in the two-tier femtocell network aims at the maximization of its utility U_j and due to the absence of coordination between the two tiers, both MUs and FUs are willing to participate to a non-cooperative resource allocation game.

Definition 2.3.3. ***Non-cooperative Games:*** *A non-cooperative game refers to a situation where each player under conditions of competition needs to take a decision in an independent manner from the rest of players, given the possible choices of the rest of the involved players and the potential impact on its own objectives or utility [15].*

Let the game be $G = [S, \{A_j\}_{j\in S}, \{U_j\}_{j\in S}]$, where S is the set of users / players, $A_j = [0, P_j^{Max}] \times \mathbb{R}^N$ is the strategy of the j^{th} user, and U_j is the user's j utility function, formally expressed in equation 2.2. Furthermore, the resulting per time slot non-cooperative game can be expressed as the following maximization problem.

$$\textbf{UPC} - \textbf{MSF Game}: \quad \max_{P_j \in A_j} U_j(P_j, \mathbf{P_{-j}}),\ \forall j \in S = S_m \cup S_f \tag{2.4}$$

Considering UPC-MSF game, we are interested in determining the equilibrium point, i.e., a vector of N users' transmission powers, wherein each user $j \in S$ individually maximizes its utility in 2.2, given the transmission powers of the rest of the users. Such an equilibrium operating point in optimization problem 2.4 denotes the Nash equilibrium (NE).

Table 2.1: Section 2.3 list of key notations

Symbol	Description
B_0	Base station
B_i	Femtocells
$\Re$, $\mathbb{C}$	Regions
R_0	Network Radius
F	Number of co-channel femtocells
R_c	Femtocell radius
S	Set of all users
S_m and S_f	Sets of MUs ad FUs
N_m and N_f	Number of MUs ad FUs
P_j	Uplink transmission power
σ^2	Variance of Additive White Gaussian Noise
γ_j	Signal-to-interference-plus-noise ratio
W	Total bandwidth
R	Data bit rate
G	Channel gain
R_F, D	Constants
$S_{m,RT}, S_{m,NRT}, S_{f,RT}, S_{f,NRT}$	Set of real and non-real time MUs and FUs
$f(\gamma_j)$	Efficiency function
M	Number of bits of transmitted packets
A	Efficiency function constant
c	Pricing factor
U_j	Utility
G	UPC-MSF Game
A_j	User strategy
$\mathbf{E}$	Set of Nash equilibria
$\mathbf{P_L}$	Largest element of Nash Equilibrium set
$\mathbf{P_S}$	Smallest element of Nash Equilibrium set

Definition 2.3.4. ***Nash Equilibrium:*** *A Nash Equilibrium is a profile of strategies such that each player's strategy is an optimal response to other players strategy [62].*

Nash Equilibrium coined by John F. Nash in 1951 [63], is concluded as a unanimous consensus among the games contestants, where none of them would obtain further performance gains by unilaterally deviating from their previously chosen strategy, considering the opponents choices.

Theorem 1. ***(UPC-MSF Nash Equilibrium:)*** *The power vector* $\mathbf{P}^* = \left(P_1^*, P_2^*, ..., P_N^*\right)$ *is a Nash Equilibrium of the UPC-MSF game, if for every* $j \in S$, $U_j\left(P_j^*, \mathbf{P}_{-\mathbf{j}}^*\right) \geq U_j\left(P_j, \mathbf{P}_{-\mathbf{j}}^*\right)$, *for all* $P_j^* \in A_j$

Given the above definition of Nash Equilibrium, it is observed that no user of the UPC-MSF game can individually improve its own utility, given the transmission powers of the rest of the users.

In the direction of establishing the existence of the above Nash Equilibrium point for the UPC-MSF game, the theory of supermodular games has been utilized. The main motivation for using supermodularity to study the properties of NE in this case (instead of using other alternatives such as ones based on quasi-concavity) stems from the fact that the users' utilities considered here are heterogeneous in nature and more importantly they are not quasi-concave functions with respect to transmission power.

Definition 2.3.5. ***Supermodular Games:*** *Supermodular are those games characterized by strategic complementarities, i.e., when one player takes a more competitive and aggressive action, then the rest of the users want to follow the same behavior [62].*

Supermodular games, an important class of the broader S-modular games introduced by Topkis [64] and Vives [65], are of great interest as an optimization tool, due to the fact that they encompass many applied models, they tend to be analytically appealing and they have the outstanding property that many solutions yield the same predictions [65], [10].

Theorem 2. ***(UPC-MSF Supermodular Game:)*** *The game $G = [S, \{A_j\}_{j\in S}, \{U_j\}_{j\in S}]$ is said to be supermodular, if and only if $\partial^2 U_j(\mathbf{P})/\partial P_j \partial P_i \geq 0$, $\forall j \neq i \in S$.*

Furthermore, a supermodular game has some desirable properties. Considering a supermodular game, a pure strategy Nash equilibrium exists, its best responses are monotonically increasing and if the equilibrium is unique, then it is globally stable. However, UPC-MSF game is not a supermodular game, based on Theorem 2. Thus, the strategy spaces of the users should be modified appropriately, in order the resulting game to be supermodular. In view of this, we use the condition given in Theorem 2, i.e., $\partial^2 U_j(\mathbf{P})/\partial P_j \partial P_i \geq 0$, $\forall j \neq i \in S$ and we obtain $\gamma_j \geq \frac{lnM}{A}$. Thus, let the modified strategy space be denoted as $\hat{A}_j = [\underline{P_j}, P_j^{Max}]$, where the smallest power $\underline{P_j}$ can be derived from $\frac{lnM}{A}$, and the largest power P_j^{Max} is implied by the physical and technical limitations of the networks. Based on the above analysis, we can easily conclude to Lemma 3, where due to space limitations the analytical proof is omitted.

Lemma 3. ***(Supermodularity of UPC-MSF game:)*** *The UPC-MSF game $G = [S, \{\hat{A}_j\}_{j\in S}, \{U_j\}_{j\in S}]$ with the modified strategy space is supermodular.*

Given by Lemma 3 that UPC-MSF game is supermodular, then its set of Nash equilibria $\mathbf{E}$ is non-empty and consists of a largest element $\mathbf{P_L}$ and a smallest element $\mathbf{P_S}$. Furthermore, according to [10], we conclude that $\mathbf{P_S} \in \mathbf{E}$ is the Pareto dominant equilibrium of UPC-MSF game, thus the best-response of a user is the Nash equilibrium with the minimum overall transmission power. Based on this attribute of UPC-MSF game, the energy-efficient resource allocation to the users is guaranteed.

Definition 2.3.6. ***Best Response:*** *Best Response refers to the strategy which produces the most favorable outcome for a player, given the strategies of the rest of the players of the game [66].*

The convergence of UPC-MSF game to its Pareto dominant Nash equilibrium can be concluded based on the properties of a supermodular game [10]. Thus, it is easily shown that given users' best-responses, i.e.:

$$BR_j(\mathbf{P_{-j}}) = P_j \in \hat{A}_j : U_j(P_j, \mathbf{P_{-j}}) \geq U_j(P_j', \mathbf{P_{-j}}), \forall P_j' \in \hat{A}_j \tag{2.5}$$

Being single-valued, then each user updates its transmission power, regardless of the starting point selected from its strategy space, and its strategies monotonically converge to the smallest Nash equilibrium $\mathbf{P_S} \in \mathbf{E}$.

Definition 2.3.7. ***Pareto Dominance and Optimality:*** *A vector $\hat{\mathbf{p}}$ is Pareto dominant to another vector $\mathbf{p}$ if for all users in a set with utility V, we have $V_j(\hat{\mathbf{p}}) \geq V_j(\mathbf{p})$ and for some $V_j(\hat{\mathbf{p}}) > V_j(\mathbf{p})$. On the other hand, Pareto optimality suggests that there exists no other vector $\mathbf{p}$ such that, for all the users in the set, $V_j(\mathbf{p}) \geq, V_j(\mathbf{p}^*)$ and for some users $V_j(\mathbf{p}) \geq V_j(\mathbf{p}^*)$ [10].*

2.3.3 Distributed Algorithm

Based on the previous analysis, in this section we introduce a distributed and iterative uplink power control algorithm that determines the Pareto dominant Nash equilibrium of UPC-MSF game. The UPC-MSF algorithm consists of two main parts, i.e., the AP's part and the user's part. The AP's part resides at each femtocell AP and is responsible for broadcasting the determined pricing factor c to the FUs, as well as for collecting from them their experienced satisfaction. The user's part resides at each MU and FU, who play non-cooperatively the proposed game and given the announced pricing factor, they determine their uplink transmission power in a distributed manner. The above described procedure is repeated iteratively till the algorithm converges to the Pareto dominant Nash equilibrium $\mathbf{P_S}$ of UPC-MSF game. The corresponding parts of the overall algorithm are as described in the following.

Concluding this section, it should be clarified that the proposed UPC-MSF algorithm can be characterized as a single valued low complexity best response distributed algorithm for every MU and FU, starting from a randomly feasible power of its non-empty modified strategy space $\widehat{A_j}$.

Algorithm 1 UPC-MSF AP/BS's Part Algorithm (c_{best} Identification)

1: Each AP announces the initial pricing factor $c = 0$ to all FUs residing in each cell. The pricing factor is assumed to be the same for all femtocells residing in the same macrocell.
2: Each FU and MU determines the Pareto dominant Nash equilibrium $P_{S_j}, \forall j \in S$ (according to UPC-MSF User's Part Algorithm) and computes its pure utility (without the penalty, i.e., the cost function, considering FUs).
3: Increase the pricing factor $c = c + \Delta c$ and each AP announces it to its FUs.
4: If the pure utilities of all users, $\forall j \in S$, do not improve, i.e., $U_j(c) > U_j(c + \Delta c)$, then stop and set as the best choice of the pricing factor $c_{best} = c$. Otherwise, go to step 2.

Algorithm 2 UPC-MSF User's Part Algorithm (Power Allocation)

1: At the beginning of each time slot t, each user, either MU or FU (i.e., $\forall j \in S = S_m \cup S_f$), transmits with a randomly selected feasible uplink transmission power $P_{S_j}^{(0)}$ (i.e., $0 \leq P_{S_j}^{(0)} \leq P_{S_j}^{Max}$). Set $k = 0$ and hence $P_{S_j}^{(0)}, \forall j \in S = S_m \cup S_f$
2: Given the uplink transmissions powers of the users, which is implicitly reported by the BS from the macrocell side and the APs from the femtocells side by broadcasting its overall interference $\sum_{j,j\in S} G_{ij}P_j$, the user computes $\sum_{j\neq i} G_{ij}P_j$ and determines its best response strategy:

$$BR_j(\mathbf{P_{-j}}) = \underset{P_j \in \widehat{A_j}}{argmax} U_j(P_j, \mathbf{P_{-j}})$$

and assigns the uplink transmission power $P_{S_j}^{(k)} = min(BR_j)$
3: If the uplink transmission powers converge (i.e., $|P_{S_j}^{(k+1)} - P_{S_j}^{(k)}| \leq \epsilon$, where ϵ is a small positive value, e.g., $\epsilon = 10^{-7}$) then stop.
4: Set $k = k + 1$ and go to step 2.

2.3.4 Numerical Results

In this section, some indicative numerical results are provided to illustrate the operation and features of the proposed framework, while through a comparative study the benefits of adopting the proposed power allocation framework are also demonstrated. Throughout our study, we consider a single macrocell CDMA system [67], where F femtocells reside within the macrocell. The number of MUs is set to 10 users, where the 5 MUs demand non-real time services (e.g., data) and the rest 5 MUs demand real-time services (e.g., voice). The MUs are distributed randomly within the macro-cell, which has a radius $R_0 = 500m$. Each femtocell has a radius $R_c = 50m$ and serves 5 FUs, where 3 users demand non-real time services and 2 users real-time services. The maximum feasible transmission power, either for MUs or for FUs is set to $P_{max} = 0.2W$, while $W = 10^6 Hz$, $R = 10^4 bits/sec$ and $\sigma^2 = 5 \times 10^{-15} W$. For demonstration purposes only and following recent studies in the literature, we assume that the efficiency function $f(\gamma_j) = (1 - e^{-0.5\gamma_j})^M$ with $M = 40$, is adopted [10].

Fig. 2.3 is constructed by reaching the Pareto dominant Nash equilibrium at each value of the pricing factor c. The increment of the pricing factor c is terminated if users' utility (either MUs or FUs) cannot be further improved (UPC-MSF AP/BS's Part Algorithm) and the best pricing factor $c = c_{best}$ is determined. It is observed by the graph that users' sum of utilities is still increasing, considering values of pricing larger then c_{best}, due to the fact that the utilities of some of the users increase rapidly, however the utilities of the rest of the users decrease slowly. As it has been proposed in UPC-MSF AP/BS's Part Algorithm, we determine the best pricing factor, at the point where the utilities of all the users increase. Thus, considering the described scenario we obtain $c = 10^3$.

In Fig. 2.4a and Fig. 2.4b, we present MUs' and FUs' uplink transmission power as a function of the iterations required for UPC-MSF algorithm to converge at the Pareto dominant Nash Equilibrium. In the same figures, we compare the results of UPC-MSF algorithm to the corresponding results of [44] proposed by Ngo et al., where the authors propose a utility-based joint power and admission control solution for distributed interference management in two-tier CDMA-based femtocell networks. We consider $F = 4$ femtocells residing within the macrocell as in Fig. (2.2). We observe that the convergence of the proposed algorithm is very fast since less than eighty iterations are required for reaching equilibrium for all MUs

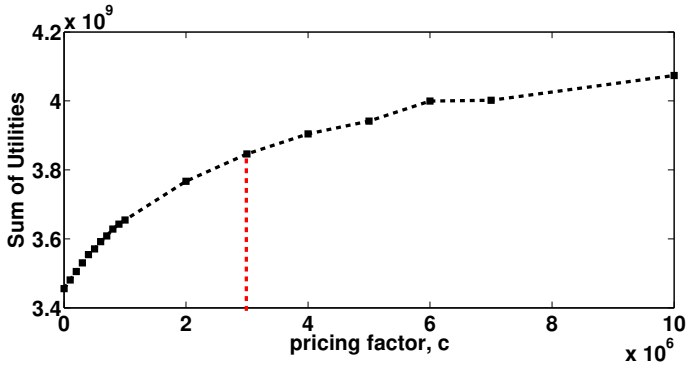

Figure 2.3: Sum of equilibrium utilities as function of the pricing factor c

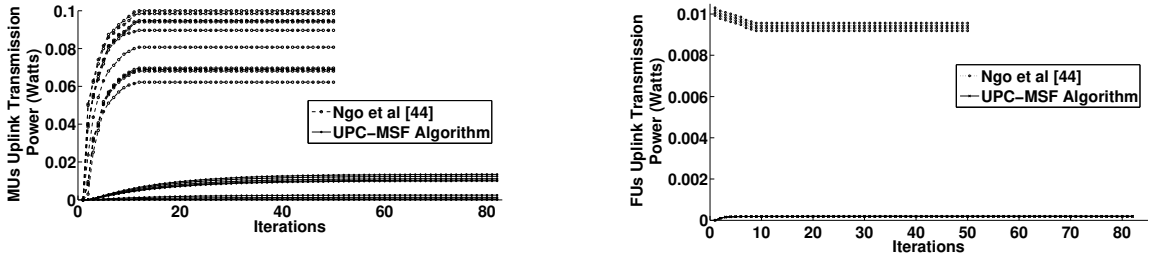

(a) Macro Users (MUs) (b) Femto Users (FUs)

Figure 2.4: Uplink transmission power convergence for MUs and FUs

and FUs, while for all practical purposes we notice that in less than thirty iterations the values of the powers have almost reached their corresponding equilibrium values. Furthermore, the results reveal that the proposed UPC-MSF framework achieves significantly lower uplink transmission power, both for MUs (Fig. 2.4a) and for FUs (Fig. 2.4b) compared to [44], due to: a) the appropriate formulation of users' utility functions, b) users' classification according to the service they request and the tier they belong to, c) the convex pricing scheme with respect to the uplink transmission power adopted, and d) the non-cooperative nature of the proposed UPC-MSF game.

Furthermore, in Fig. 2.5a and Fig. 2.5b, we compare the mean uplink transmission power of MUs and FUs respectively as a function of the number of femtocells per cell site to the corresponding values achieved through the power allocation framework proposed by Su et al. in [37]. It is observed - as intuitively expected - that as the number of femtocells per cell site increases, the mean uplink transmission power of MUs and FUs also increases, due to the increasing interference within the two-tier system. Furthermore, it is illustrated that the UPC-MSF framework has significantly better performance than the corresponding power allocation proposed in [37], in terms of power savings.

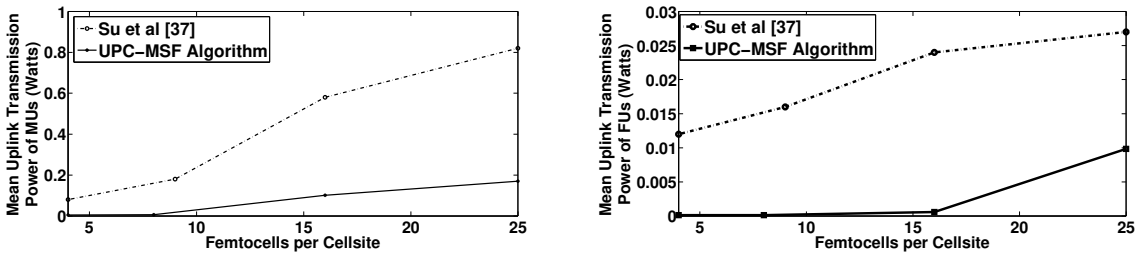

(a) Macro Users (MUs) (b) Femto Users (FUs)

Figure 2.5: Mean uplink transmission power of MUs and FUs vs number of femtocells

2.4 Power and Rate Control as a Single Parameter Problem

So far and to the best of the author's knowledge, the vast majority of approaches in the literature which concentrated on resource allocation problems considering two-tier architectures, have focused solely on controlling a unique resource at each time. Relevant research works, such as [40, 46], focus only on users' uplink transmission power allocation towards interference mitigation and satisfaction of users' multi-service QoS prerequisites [68].

Taking into account the combined power and rate allocation, in this section both power and transmission data rate are allocated to the users, considering the two variable nature of the optimization problem. In view of this, a holistic framework is presented enabling the user-centric management where the simultaneous power and transmission data rate control considering multiple services in two-tier femtocell networks support the self-properties, (e.g., configuring, optimization, and adaptation) of users who can independently conclude to their best response strategies. This multi-level structure assuming both different types of service offerings and varying connection tiers (i.e., the macro or the femtocell) allow for a sophisticated network performance management in line with the users' autonomous and parallel decisions, with respect to determining their optimal transmission characteristics towards their utility maximization.

2.4.1 System Model

For demonstration purposes, the uplink of a basic two-tier time-slotted CDMA femtocell wireless network, with $N(t)$ continuously backlogged users at time-slot t is examined, where $S(t) = S_{MRT}(t) \cup S_{FRT}(t) \cup S_{MNRT}(t) \cup S_{FNRT}(t)$ denotes their corresponding set, which consists of macro-users (MUs) and femto-users (FUs) requesting either real-time (RT) services with strict short term QoS constraints (i.e., $S_{MRT}(t)$ and $S_{FRT}(t)$) or non-real time (NRT) services (i.e., $S_{MNRT}(t)$ and $S_{FNRT}(t)$). In addition by, $N_{MRT}(t)$, $N_{FRT}(t)$, $N_{MNRT}(t)$, and $N_{FNRT}(t)$ denote the number of MUs and FUs real-time and non-real-time users respectively. For simplicity of the presentation the notation of the specific time slot t is omitted.

As before, the two-tier femtocell network under consideration consists of a central macrocell base station B_0 serving a region $\Re$, providing a cellular coverage of radius R_0. In order to construct the two-tier network, within the region $\Re$ reside F co-channel femtocells B_i $(i = 1, ..., F)$. Each femtocell support a region $\mathbb{C} \subset \Re$ and consists of a disk of radius $R_c << R_0$. We assume open access femtocells, where the registration is not mandatory for users to be served by femto Access Points (APs). It is assumed that each femto AP knows the number of users which reside within its coverage area. Consider that user $j \in S$ is connected to its B_i $(i = 0, 1, ..., F)$ and denote its uplink transmission power by p_j and its uplink transmission data rate by r_j. Due to mobile node's physical and technical limitations, user's uplink transmission power and transmission data rate are lower and upper bounded i.e., $p_{jmin} \leq p_j \leq p_j^{Max}$ and $r_{jmin} \leq r_j \leq r_j^{Max}$. A time slot is a fixed time interval and could consist of one or several packets. At the beginning of each time slot t, the users' uplink power and transmission data rate control algorithm for multi-service two-tier femtocell networks is responsible to make decisions on allocating uplink transmission power and transmission data rate to the users in a distributed manner. Furthermore, note that user's channel conditions, transmission power and transmission data rate, are assumed fixed within the duration of a time slot. Fig. 2.6 presents an indicative two-tier femtocell network topology along with the users' distribution in the cell.

The intercell interference, the thermal noise components, and the users' signals can be regarded together as an Additive White Gaussian Noise (AWGN) process, with constant power spectral density I_0 [10]. Therefore, the overall sensed interference by user $j \in S$ consists of the two-tier femtocell network interference and the AWGN background noise and is given by:

$$I(\mathbf{p_{-j}}) = \sum_{j \neq i} G_{ji} P_i + I_0 \tag{2.6}$$

where $\mathbf{p_{-j}} = \left(p_1, p_2, ..., p_{j+1}, ..., p_N\right)$ and $\mathbf{r_{-j}} = \left(r_1, r_2, ..., r_{j+1}, ..., r_N\right)$ denote the uplink transmission power and transmission data rate vector of all users except the j^{th} user, and $N = N_{MRT} + N_{FRT} + N_{MNRT} + N_{FNRT}$ denotes the total number of users residing within the two-tier femtocell network. The channel gain from the transmitter of user j to the receiver of user $i \neq j$ is denoted by G_{ji}. The channel gains are formulated here as well via adopting the simplified path loss model in the IMT-2000 specification [61]. By following the common approach adopted in the literature [18], [36], [37], [38], [39], [41], [42], and [40], [46], [68], it is assumed that the mobile users (either MUs or FUs) already know their distance

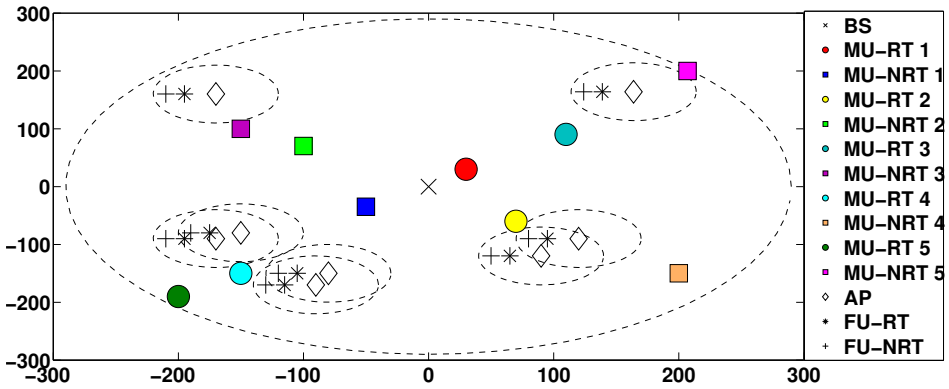

Figure 2.6: Two-tier femtocell network topology and users' distribution in the cell

from the BS or the AP, respectively. Through Global Positioning System (GPS) or as well as Global System for Mobile communication (GSM) accurate location information for outdoor users are provided, their capabilities for determining location information are limited in indoor environments, thus other techniques are limited in indoor environments, therefore in those cases other techniques are typically used as Location Positioning Systems, such as Co-Pilot Beacon for CDMA Networks, Bluetooth, Ultra wideband (UWB), Radio-frequency identification (RFID) [69], Wi-Fi positioning systems and control plane locating, where the location is determined based on the radio signal delay. In addition, it should be mentioned that newer mobule phones and PDAs typically have an integrated A-GPS chip, thus their position is easily determined.

The corresponding received signal-to-interference plus noise ratio - SINR, γ_j (i.e., [30], [31], [33], [10], [70], [71]) of user j at B_i is given by:

$$\gamma_j\left(r_j, p_j, \mathbf{p_{-j}}\right) = \frac{W}{r_j} \cdot \frac{G_{jj}P_j}{I(\mathbf{p_{-j}}) \sum\limits_{j \neq i} G_{ji}P_i + I_0} \tag{2.7}$$

where $W\,[Hz]$ denotes the available spread-spectrum bandwidth and I_0 is the AWGN power at the receiver $[W]$, [72]. As in previous section, towards supporting multiple services with diverse QoS prerequisites, each user is associated with an appropriately formulated utility function, depending on two basic factors: (a) the tier that the user belongs to, i.e., MU or FU and (b) the service that it requests, i.e., RT or NRT.

Typically, a user j, $j \in S$, residing in the two-tier femtocell network (either MU or FU), would like to achieve high SINR, γ_j, via consuming low power p_j and on the contrary transmitting at high transmission data rates, r_j. Furthermore, a user requesting NRT services, e.g., data transmission, is characterized by greedy and high throughput performance expectations, while the QoS performance requirements of a user requesting RT services, e.g., voice, video streaming etc., consist of short-term throughput and delay constraints, which result into small throughput deviations with respect to the ideal actual rate of each RT service. Therefore, the above users' QoS characteristics are formulated in a continuous and $C^{(n)}$ differentiable function U_j with respect to both user's uplink transmission power p_j and transmission data rate r_j, which depends on the tier the user belongs to and on the service it requests and is given as follows:

$$U_j(p_j, r_j, \mathrm{p_{-j}}, \mathrm{r_{-j}}) = \begin{cases} \frac{r_j f_j(\gamma_j)}{p_j}, \ j \in S_{MRT} \\ \frac{r_j \log(1+\gamma_j)}{p_j}, \ j \in S_{MNRT} \\ \frac{r_j f_j(\gamma_j)}{p_j} - c\left(e^{\gamma_j} - 1\right), \ j \in S_{FRT} \\ \frac{r_j \log(1+\gamma_j)}{P_j} - c\left(e^{\gamma_j} - 1\right), \ j \in S_{FNRT} \end{cases} \tag{2.8}$$

where $f_j(\gamma_j)$ denotes user's j, $j \in S_{MRT} \cup S_{FRT}$ efficiency function. For convenience, all of the symbols in this section are summarized in Table 2.2.

Table 2.2: Section 2.4 list of key notations

Symbol	Description
N	Number of users
N_{MRT}, N_{MNRT}	Number of macro real and non-real time users
t	Timeslot
$\Re, \mathbb{C}$	Network regions
F	Number of co-channel femtocells
N_{FRT}, N_{FNRT}	Number of femto real and non-real time users
S	Set of users
S_{MRT}, S_{MNRT}	Set of macro real and non-real time users
S_{FRT}, S_{FNRT}	Set of femto real and non-real time users
p_j, r_j	User's j uplink transmission power and data rate
p_{jmin}, r_{jmin}	User's j minimum uplink transmission power and data rate
p_j^{Max}, r_j^{Max}	User's j maximum uplink transmission power and data rate
G_{ji}	Channel gain from the transmitter of user j to the receiver of user $i \neq j$
W	Available spread-spectrum bandwidth
I_0	AWGN power at the receiver
c	Pricing factor
γ_j	Signal-to-interference-plus-noise ratio
R_0, R_c	Radius of macrocell and femtocell
$f_j(\gamma_j)$	Efficiency function
A_j	Pure-strategy space
U_j, v_j	Utility functions
G	UPRA-MSF game
x_j	Data rate to transmission power ratio
G_S	S-UPRA-MSF game
q, L	Efficiency function constants
κ, λ, l, d_j	Auxiliary parameters

The formulation of the proposed utility function in (2.8) is based on existing background information and basic formulations proposed in the literature [28], [73], where users' utility and their actual throughput utility function can be either sigmoidal-like or concave or convex functions of SINR γ_j. Thus, as mentioned before it is noted that the adopted utility function is selected to properly express users' QoS prerequisites depending on the service they request and the tier they belong to. Moreover, as it is shown in relation 2.8, a convex pricing mechanism with respect to FUs' SINR γ_j, has been introduced, due to the fundamental observation that the harm a user imposes on other users is not equivalent within the whole range of users' SINR, as linear pricing mechanisms typically assume [10], [29]. The role of the pricing mechanism is to discourage FUs from transmitting at high power and thus causing high interference to MUs. Based on this policy, the system gives higher priority to the MUs' QoS prerequisites fulfillment.

The parameter c that is included in the second term of FUs' utility function (i.e., in the pricing function), either of RT or NRT users, denotes the pricing factor. The pricing factor is announced by each Access Point to the FUs that reside in each corresponding femtocell.

Furthermore, as it is observed by relation (2.8) the users that reside within the two-tier femtocell network are organized in four basic classes, according to the service they request, i.e., real-time or non-real-time service, and the tier they belong to i.e., MU or FU, with different a utility function associated with each class. Based on the common approach that has been proposed and followed in the literature [73], users' actual uplink transmission data rate is represented by a sigmoidal-like function with respect to signal-to-interference density ratio γ_j, considering users requesting real-time services (e.g., voice, video conference, etc.) and via a concave or convex function also with respect to γ_j, considering non-real-time services (e.g., data transfer) [70]. More specifically, considering the users requesting real-time (RT) services, their utility function reflects the tradeoff between the reliably transmitted bits to the BS/AP, i.e., $r_j \cdot f_j(\gamma_j)$ and the corresponding energy consumption, p_j. In alignment with the previous section, the ideal value of user's transmission data rate in order to fulfill its QoS prerequisites, is mapped to

the inflection point of the sigmoidal function $r_j \cdot f_j(\gamma_j)$ with respect to user's SINR. This formulation of RT user's utility function provides the user with the opportunity to indicate its priority in occupying additional system resources, in the case where its uplink transmission data rate results in less SINR than the value of the inflection point of $r_j \cdot f_j(\gamma_j)$, where its utility rapidly decreases. Furthermore, considering the users requesting non-real-time (NRT) services, their utility function is formulated via approximating the capacity by a log-based function, i.e., $r_j \cdot log(1 + \gamma_j)$, where γ_j is the signal-to-interference plus noise ratio (SINR), which treats all interference as noise [30], [31], [37], [38], [41], [70]. Based on this formulation, NRT users' greedy behavior with respect to the achievable data rate is considered.

It should be stressed that each user's objective is to control and adjust its uplink transmission power and data rate in a distributed manner, in order to maximize its sensed satisfaction, i.e., utility, regardless the tier it belongs to or the service it requests. In the next section, we formulate and introduce a non-cooperative utility-based uplink power and transmission data rate control game in multi-service two-tier femtocell networks, towards maximizing each user's utility in a distributed manner.

2.4.2 Problem Formulation and Solution

In the proposed approach, the non-cooperative game is introduced, enabling users' autonomicity and self-management consisting of two separate variables, i.e., uplink transmission power and data rate, in order to maximize user's utility. Therefore, at the beginning of each time slot, a Utility-based uplink Power and transmission data Rate Allocation algorithm in Multi-Service two-tier Femtocell networks (UPRA-MSF) is responsible for determining the optimal users' uplink transmission power p_j and data rate r_j, via maximizing each user's overall degree of satisfaction, which is reflected by the corresponding values of its utility. In this section, the main objectives of UPRA-MSF framework are presented, analyzed, and formally defined as a generic optimization problem in a game theoretic framework.

A non-cooperative game in strategic form has three main elements: the set of players $j \in S$, which is a finite set $S = \{1, 2, ..., N\}$, the pure-strategy space A_j for each player j, and payoff (or utility) function U_j that gives player $j's$ utility $U_j(a)$, for each profile $a = (a_1, a_2, \ldots, a_N)$ of strategies. The players compete with each other towards converging to their best response strategy BR_j. As already mentioned, the best response is the strategy that produces the most desirable outcome for user j, given the strategies of the rest of the users.

Let $G = [S, \{P_j, R_j\}, \{U_j(p_j, r_j)\}]$ denote the UPRA-MSF game, where $S = \{1, 2, ..., N\}$ is the index set of the active MUs and FUs residing in the two-tier femtocell network, which represents the set of players (i.e., participants) of the game, $P_j = [p_{j\,\min}, p_j^{Max}]$ and $R_j = [r_{j\,\min}, r_j^{Max}]$ denote the strategy sets of user's j uplink transmission power and data rate respectively, which construct the Cartesian product $A_j = P_j \times R_j$ representing the actions available to each player at each decision point, and U_j corresponds to the objective function, as defined in Eq. (2.8), which mirrors the outcome of users' actions. The UPRA-MSF game is formulated as a distributed utility maximization problem, in which each user updates its power and transmission data rate in a selfish manner, aiming at maximizing its received satisfaction. Let the power and transmission data rate vectors $\mathrm{p}^* = (p_1^*, p_2^*, ..., p_N^*)^T \in P = P_1 \times P_2 \times ... \times P_N$ and $\mathrm{r}^* = (r_1^*, r_2^*, ..., r_N^*)^T \in R = R_1 \times R_2 \times ... \times R_N$ denote the outcome of the following game:

$$\begin{gathered} \textbf{UPRA} - \textbf{MSF Game} \\ \max_{(p_j, r_j) \in A_j} U_j(p_j, r_j, \mathrm{p_{-j}}, \mathrm{r_{-j}}), \\ s.t.\ p_{j\,\min} \leq p_j \leq p_j^{Max},\ r_{j\,\min} \leq r_j \leq r_j^{Max} \end{gathered} \tag{2.9}$$

The fundamental attribute of the non-cooperative UPRA-MSF game in (2.9) is the simultaneous and synchronous optimization of user's utility with respect not only to user's uplink transmission power, p_j, but to user's uplink transmission data rate, r_j, as well. It is observed that user's utility is a function of two variables: p_j and r_j. Furthermore, the existence of equilibrium in transmission powers or data rates individually does not guarantee that there is equilibrium in the power and transmission data rate control problem. Thus, aiming at solving the non-cooperative game (2.9) with one strategic variable, while simultaneously allocating uplink transmission power and data rate to the users, we set the ratio of rate, r_j, to the power, p_j, as the single strategic variable, as follows:

$$x_j = \frac{r_j}{p_j} \tag{2.10}$$

Therefore, the utility functions as presented in relation (2.8), can be rewritten as follows:

$$v_j(x_j)=\begin{cases} x_j\left(1-e^{-q\frac{d_j}{x_j}}\right)^L,\ j\in S_{MRT} \\ x_j\frac{\ln\left(1+\frac{d_j}{x_j}\right)}{\ln 10},\ j\in S_{MNRT} \\ x_j\left(1-e^{-q\frac{d_j}{x_j}}\right)^L-c\left(e^{\frac{d_j}{x_j}}-1\right),\ j\in S_{FRT} \\ x_j\frac{\ln\left(1+\frac{d_j}{x_j}\right)}{\ln 10}-c\left(e^{\frac{d_j}{x_j}}-1\right),\ j\in S_{FNRT} \end{cases} \tag{2.11}$$

where parameters q, L are constants from the efficiency function, $\gamma_j=\frac{1}{x_j}\cdot\frac{WG_{jj}}{I}=\frac{d_j}{x_j}$, with $d_j=\frac{WG_{jj}}{I}$, where as mentioned before, W, $[Hz]$, denotes the available spread-spectrum bandwidth, G_{jj} the channel gain from the transmitter of user j to the receiver of the same user j, and I the overall sensed interference by user $j\in S=\{1,2,...,N\}$, as it is given from equation (2.6). Thus, the UPRA-MSF game, as it was presented in relation (2.9) can be reformulated to a Single variable Utility-based uplink Power and transmission data Rate Allocation game in Multi-Service two-tier Femtocell networks (S-UPRA-MSF game). Let $G_S=[S,\{A_j\},\{v_j(x_j)\}]$ denote the S-UPRA-MSF game, which is formulated as follows:

$$\begin{gathered}\mathbf{S-UPRA-MSF\ Game} \\ \max_{x_j=\frac{r_j}{p_j}\in A_j} v_j(x_j=\tfrac{r_j}{p_j}), \\ s.t.\ p_{j\min}\le p_j\le p_j^{Max},\ r_{j\min}\le r_j\le r_j^{Max}\end{gathered} \tag{2.12}$$

In the following section, the Nash Equilibrium approach has been adopted towards seeking analytically the solution of the distributed non-convex non-cooperative S-UPRA-MSF game.

As discussed, the concept of Nash Equilibrium is the most commonly used method, towards confronting a non-cooperative game. Its basic characteristic is that it offers a predictable, stable, and definable solution of the game, where various classes of users with potentially conflicting and contradictory interests compete through autonomic self-optimization and reach a point where no user wishes to deviate. More specifically, at the equilibrium point no user has the incentive to change the combination/ratio of its uplink transmission data rate and power, since its utility cannot be further improved by making any individual changes on this one strategic variable, given the power $\mathbf{p_{-j}}$, transmission data rate $\mathbf{r_{-j}}$ and ratio $\mathbf{x_{-j}}=\mathbf{r_{-j}}/\mathbf{p_{-j}}$ vectors of all other users.

Theorem 4. ***(S-UPRA-MSF game's Nash Equilibrium:)*** *The ratio vector* $\mathrm{x}^*=(x_1^*,x_2^*,...,x_N^*)$, *where* $x_j=\frac{r_j}{p_j}$, *is a Nash equilibrium of the S-UPRA-MSF game, if for every* $j\in S=\{1,2,...,N\}$, $v_j(x_j^*,\mathrm{p}_{-\mathrm{j}}^*,\mathrm{r}_{-\mathrm{j}}^*)\ge v_j(x_j,\mathrm{p}_{-\mathrm{j}}^*,\mathrm{r}_{-\mathrm{j}}^*)$.

Based on the above definition, it is observed that no user can unilaterally improve its personal utility by individually changing its strategy, x_j, given the strategies $\mathrm{x}_{-\mathrm{j}}=\mathrm{r}_{-\mathrm{j}}/\mathrm{p}_{-\mathrm{j}}$ of the rest of the users. Moreover, it should be stressed that due to users' selfish behavior, in general a non-cooperative game does not always and necessarily has a Nash Equilibrium, because it is likely that users will not compromise with a stable outcome. However, the absence of Nash Equilibrium is translated to an inherently unstable system. Thus, one of the most important components of our framework is the investigation of the existence of Nash Equilibrium in S-UPRA-MSF game and correspondingly in UPRA-MSF game.

Various analytical methods have been proposed towards examining the existence of Nash equilibrium in a non-cooperative game, quasi-concave objective function [33], Extreme Value Theorem (E.V.T.) in conjunction with the Hessian matrix of the objective function [28], or supermodularity theory as discussed in the previous section etc. Towards solving the reformulated problem, the property of quasi-concavity of the modified utility function v_j with respect to the ratio $x_j=r_j/p_j$ has been examined, so as to prove the existence and uniqueness of the Nash equilibrium of S-UPRA-MSF game.

Lemma 5. ***(Quasi-concavity of*** v_j***:)*** *A function* v_j *is strictly quasi-concave iff, for any pair of distinct points* x_j *and* x_j' *in the convex domain* $A_j=P_j\times R_j$ *of* v_j *and for* $0<\theta<1$

$$v_j(x_j')>v_j(x_j)\Rightarrow v_j\left[\theta x_j+(1-\theta)\,x_j'\right]>v_j(x_j) \tag{2.13}$$

Furthermore, as concluded from Lemma 5, any concave function is quasi-concave, but the converse is not true.

Lemma 6. ***(Concavity of** v_j**:)*** *Given that the function* $v_j : A_j \subseteq \mathbb{R}^2 \to \mathbb{R}$ *is* $C^{(2)}$*, i.e.,* $\frac{\partial^2 v_j}{\partial x_j^2}$ *is continuous, then* v_j *is concave if and only if* $\frac{\partial^2 v_j}{\partial x_j^2} \leq 0$ *for all* $x_j \in A_j$

Based on Lemma 6, we first prove the concavity of each user's j, $j \in S = \{1, 2, ..., \}$, reformulated utility function v_j, in order to conclude to the existence and uniqueness of Nash equilibrium of S-UPRA-MSF game. Initially, we aim to have an insight of the form of the appropriately selected user's utility function for the four distinct classes, where they have been organized. Thus, in Fig. 2.7 we present the form of users' utility functions v_j with respect to the ratio x_j.

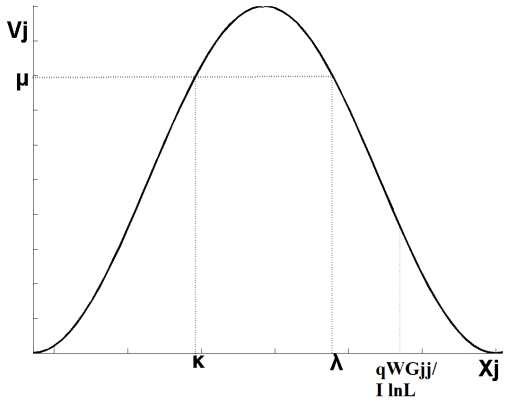

Figure 2.7: Quasi-concave form of the reformulated utility function $v_j(x_j)$

Theorem 7. ***(Quasi-concave Utility Function:)*** *User's* j, $j \in S = \{1, 2, ..., N\}$ *utility function is quasi-concave in the modified strategy space:*

$$\gamma_j > \frac{\text{lnL}}{q} \text{ or equivalently } 0 < x_j < \frac{qWG_{jj}}{I\text{lnL}} \tag{2.14}$$

Proof. Based on Lemma 6, we aim at proving the concavity of user's j, $j \in S = \{1, 2, ..., N\}$ utility function v_j, as it was defined in relation (2.11), for each of the four distinct cases in a modified strategy space. Thus, the reformulated utility function should satisfy the following condition in x_j on certain intervals, in order to be a concave function:

$$\frac{\partial^2 v_j}{\partial x_j^2} \leq 0 \tag{2.15}$$

We have examined each case of the four distinct forms of utility function individually, via determining the second order derivative and the corresponding interval of γ_j where condition (2.15) is satisfied. Specifically:

- Macro Real Time Users: $\frac{\partial^2 v_j}{\partial x_j^2} \leq 0 \Leftrightarrow \gamma_j > \frac{\text{lnL}}{q}$
- Macro Non-Real Time Users: $\frac{\partial^2 v_j}{\partial x_j^2} \leq 0 \Leftrightarrow \gamma_j > 0$
- Femto Real Time Users: $\frac{\partial^2 v_j}{\partial x_j^2} \leq 0 \Leftrightarrow \gamma_j > \frac{\text{lnL}}{q}$
- Femto Non-Real Time Users: $\frac{\partial^2 v_j}{\partial x_j^2} \leq 0 \Leftrightarrow \gamma_j > 0$

Towards completing this proof, we combine the above inequalities and determine the common interval of γ_j and correspondingly of x_j, where the condition of the second order derivative $\frac{\partial^2 v_j}{\partial x_j^2} \leq 0$ is satisfied for all the four distinct cases of users' utility functions.

Therefore, we conclude that all four given utility functions are simultaneously concave in x_j for $\gamma_j > \frac{\ln \mathrm{L}}{q}$ and since $\gamma_j = \frac{1}{x_j} \cdot \frac{WG_{jj}}{I}$ then $x_j < \frac{qWG_{jj}}{I \ln \mathrm{L}}$ □

The following theorem is stated based on the above analysis.

Theorem 8. ***(Existence and Uniqueness for S-UPRA-MSF game's NE:)*** *A Nash equilibrium exists and it is unique in S-UPRA-MSF game $G_S = [S, \{A_j\}, \{v_j(x_j)\}]$, if for all $j \in S = \{1, 2, ..., N\}$:*

1. *A_j is a non-empty, convex and compact subset of an Euclidean space $\mathbb{R}^N$*
2. *$v_j(\mathbf{x})$ is continuous in $\mathbf{x}$ and quasi-concave in x_j*

Proof. Each user has a strategy space A_j that is defined by a minimum value $x_{j\,\min} = \frac{r_{j\,\min}}{p_j^{MAX}}$, a maximum value $x_j^{MAX} = \frac{r_j^{MAX}}{p_{j\,\min}}$, where $r_{j\,\min},\ p_{j\,\min} > 0$ and all the values in between. Moreover, we assume that the maximum value x_j^{MAX} is larger or equal to the minimum value $x_{j\,\min}$, i.e., $x_j^{MAX} > x_{j\,\min}$. Thus, the first condition is satisfied. The second condition derives from Theorem 7, where it is shown that the utility function v_j is concave in $x_j \in \left(0, \frac{qWG_{jj}}{I \ln \mathrm{L}}\right) \subseteq A_j, \forall j \in S$, thus it is also quasi-concave in the corresponding interval. Furthermore, the utility function v_j is continuous in $\mathbf{x}$, as a composition of continuous functions. Concluding this proof, the set of maximizers of the continuous function v_j exists a unique maximizer in $x_j \in A_j, \forall j \in S$ of the S-UPRA-MSF game, i.e., its best response strategy, is denoted by BR_j, expressed below:

$$BR_j = \left\{x_j \in A_j : v_j\left(x_j, \mathrm{x_{-j}}\right) \geq v_j\left(x_j', \mathrm{x_{-j}}\right), \forall x_j' \in A_j\right\} \tag{2.16}$$

□

In the following analysis we will prove that $U_j(p_j, r_j)$ is also quasi-concave in (p_j, r_j) and that the UPRA-MSF game has a Nash equilibrium in $\{P_j, R_j\}$, considering the concept proposed in [33]. Based on Theorem 7, the reformulated utility function v_j with respect to x_j is quasi-concave in the interval $x_j \in \left(0, \frac{qWG_{jj}}{I \ln \mathrm{L}}\right)$. Therefore, the upper contour sets of the form $\left\{x_j \in \left(0, \frac{qWG_{jj}}{I \ln \mathrm{L}}\right) \Big/ v_j(x_j) \geq \mu\right\}$ are candidate intervals, as it is shown in Fig. 2.8.

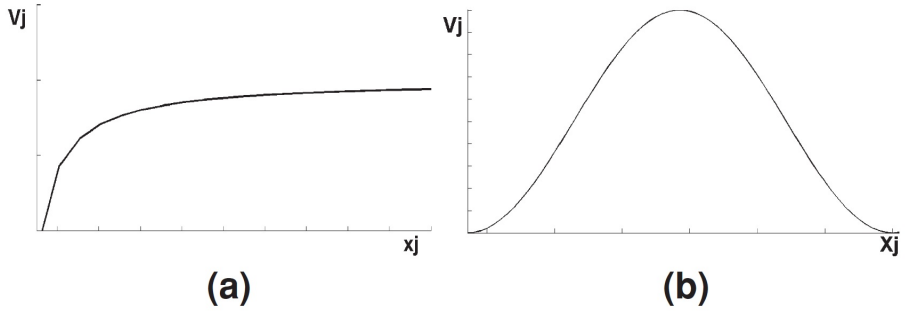

Figure 2.8: Shape of user's j utility function: (a) $j \in S_{MNRT} \cup S_{FNRT}$, (b) $j \in S_{MRT}$, where the shape of user's $j \in S_{FRT}$ can be either (a) or (b) depending on the parameter $d_j = WG_{jj}/I$

Additionally, for any real number $\mu \in \mathbb{R}$ and for any $\mathrm{p_{-j}} \in P_{-j} = P_1 \times ... \times P_{j-1} \times P_{j+1} \times ... \times P_N$ and $\mathrm{r_{-j}} \in R_{-j} = R_1 \times ... \times R_{j-1} \times R_{j+1} \times ... \times R_N$, the following relations hold true.

$$\begin{aligned}
&\left\{x_j \in \left(0, \tfrac{qWG_{jj}}{I \ln \mathrm{L}}\right) \Big/ v_j(x_j) \geq \mu\right\} = \\
&\left\{(p_j, r_j) \in \left[p_{j\,\min}, p_j^{MAX}\right] \times \left[r_{j\,\min}, r_j^{MAX}\right] \Big/ v_j\left(\tfrac{r_j}{p_j}, \mathrm{p_{-j}}, \mathrm{r_{-j}}\right) \geq \mu\right\} = \\
&\left\{(p_j, r_j) \in \left[p_{j\,\min}, p_j^{MAX}\right] \times \left[r_{j\,\min}, r_j^{MAX}\right] / U_j\left(r_j, p_j, \mathrm{p_{-j}}, \mathrm{r_{-j}}\right) \geq \mu\right\}
\end{aligned} \tag{2.17}$$

Furthermore, given the domain of user's reformulated utility function, i.e., $x_j \in \left(0, \frac{qWG_{jj}}{I\ln \mathrm{L}}\right) \subseteq A_j, \forall j \in S$, where the function v_j with respect to x_j is quasi-concave and as it is obviously observed in Fig. 2.8, can obtain the following relation:

We assume the values κ and λ for which the quasi-concave function v_j satisfies:

$$\left\{x_j \in \left(0, \frac{qWG_{jj}}{I\ln \mathrm{L}}\right) \Big/ v_j\left(x_j\right) \geq \mu\right\} = [\kappa, \lambda]: \tag{2.18}$$

Thus, the following convex set in $\mathbb{R}^2$

$$\begin{aligned} &\left\{(p_j, r_j) \in \left[p_{j\,\min}, p_j^{MAX}\right] \times \left[r_{j\,\min}, r_j^{MAX}\right] \Big/ v_j\left(\tfrac{r_j}{p_j}, \mathrm{p}_{-\mathrm{j}}, \mathrm{r}_{-\mathrm{j}}\right) \geq \mu\right\} = \\ &\left\{(p_j, r_j) \in \left[p_{j\,\min}, p_j^{MAX}\right] \times \left[r_{j\,\min}, r_j^{MAX}\right] / \kappa p_j \leq r_j \leq \lambda p_j\right\} \end{aligned} \tag{2.19}$$

Based on relations (2.8), (2.19), and Lemma 5, we conclude that U_j is quasi-concave in (p_j, r_j). Thus, following the same concept of Theorem 8 for the utility function $U_j\left(p_j, r_j\right)$, we conclude that the UPRA-MSF game $G = [S, \{P_j, R_j\}, \{U_j\left(p_j, r_j\right)\}]$ has at least one Nash equilibrium $(\mathrm{p}^*, \mathrm{r}^*)$. Therefore, for every $j \in S$

$$U_j(r_j, p_j, \mathrm{p}^*_{-\mathrm{j}}, \mathrm{r}^*_{-\mathrm{j}}) \leq U_j(\mathrm{p}^*, \mathrm{r}^*), \forall\left(p_j, r_j\right) \in A_j = P_j \times R_j \tag{2.20}$$

Let $l = \min\left(\frac{r_j^{MAX}}{p_{j\,\min}}, \frac{qWG_{jj}}{I\ln \mathrm{L}}\right)$. Two basic cases can derive from the values p_j^{MAX}, r_j^{MAX} and l.

$$Case\ A: \ \frac{r_j^{MAX}}{p_j^{MAX}} < l, \quad Case\ B: \frac{r_j^{MAX}}{p_j^{MAX}} > l \tag{2.21}$$

We show that there exists $\left(p'_j, r'_j\right) \in \left[p_{j\,\min}, p_j^{MAX}\right] \times \left[r_{j\,\min}, r_j^{MAX}\right]$ such that $x_j = \frac{r'_j}{p'_j}$, for each of the possible and examined cases. Considering Case A, two sub-cases are possible:

1. Case A1: $x_j \in \left[\frac{r_{j\,\min}}{p_j^{MAX}}, \frac{r_j^{MAX}}{p_j^{MAX}}\right]$. We take $p'_j = p_j^{MAX}$ and $r'_j = x_j p_j^{MAX}$. Moreover, the transmission data rate r'_j is lower and upper bounded due to: $r'_j \geq \frac{r_{j\,\min}}{p_j^{MAX}} p_j^{MAX} = r_{j\,\min}$ and $r'_j \leq \frac{r_j^{MAX}}{p_j^{MAX}} p_j^{MAX} = r_j^{MAX}$.

2. Case A2: $x_j \in \left[\frac{r_j^{MAX}}{p_j^{MAX}}, l\right]$. We take $r'_j = r_j^{MAX}$ and $p'_j = \frac{r_j^{MAX}}{x_j}$. Moreover, the power p'_j is lower and upper bounded due to: $p'_j \geq \frac{r_j^{MAX}}{\frac{r_j^{MAX}}{p_{j\,\min}}} = p_{j\,\min}$ and $p'_j \leq r_j^{MAX} l \leq p_j^{MAX}$.

3. Case B: $\frac{r_j^{MAX}}{p_j^{MAX}} > l$. In Case B the interval of x_j, where v_j is quasi-concave is $x_j \in (0, l) \subseteq \left(0, \frac{r_j^{MAX}}{p_j^{MAX}}\right)$. Thus, we take $p'_j = p_j^{MAX}$ and $r'_j = x_j p_j^{MAX}$ and the transmission data rate r'_j is lower and upper bounded due to: $r'_j \geq \frac{r_{j\,\min}}{p_j^{MAX}} p_j^{MAX} = r_{j\,\min}$ and $r'_j \leq \frac{r_j^{MAX}}{p_j^{MAX}} p_j^{MAX} = r_j^{MAX}$

Therefore, we conclude by (2.20) for each of the presented cases that the inequality of Nash equilibrium is satisfied:

$$U_j\left(r_j, p_j, \mathrm{p}^*_{-\mathrm{j}}, \mathrm{r}^*_{-\mathrm{j}}\right) = v_j(x_j, \mathrm{p}^*_{-\mathrm{j}}, \mathrm{r}^*_{-\mathrm{j}}) = v_j(\tfrac{r'_j}{p'_j}, \mathrm{p}^*_{-\mathrm{j}}, \mathrm{r}^*_{-\mathrm{j}}) = U_j\left(r'_j, p'_j, \mathrm{p}^*_{-\mathrm{j}}, \mathrm{r}^*_{-\mathrm{j}}\right) \leq U_j\left(r_j^*, p_j^*\right) \tag{2.22}$$

2.4.3 Distributed Algorithm

In this section, based on our previous analysis, we introduce an iterative, distributive, and low complexity Utility-based uplink Power and transmission data Rate Allocation algorithm in Multi-Service Femtocell networks (UPRA-MSF Algorithm), which determines the unique Nash equilibrium point $(\mathbf{p}^\star, \mathbf{r}^\star)$ of UPRA-MSF game and enables users' autonomic self-optimization. The fundamental attribute of the

designed algorithm is that the users update synchronously their uplink transmission power and data rate at the same iteration, thus the unique Nash equilibrium is derived simultaneously.

Specifically, the proposed algorithm is divided into two basic parts. The Access Point's Part resides at each Access Point (AP) and is responsible only for broadcasting the determined pricing factor to the users and collecting from them their experienced satisfaction, which is expressed via the values of the utility function. The second part, i.e., Macro/Femto User's Part, resides at each user, who plays non-cooperatively the UPRA-MSF game and given the broadcasted pricing factor, each user decides its uplink transmission power and data rate in a distributed manner. The above described procedure is repeated iteratively till the UPRA-MSF algorithm converges to the Nash equilibrium $(\mathbf{p}^\star, \mathbf{r}^\star)$.

According to the presented UPRA-MSF algorithm, since each user's j, $j \in S = \{1, 2, ..., \}$ power and transmission data rate is initialized at the minimum and at the maximum value respectively for all j and since the sequences $p_j^{(k)}, r_j^{(k)}$ are monotonically increasing and decreasing respectively, in bounded intervals, they are convergent to the pair $(\mathbf{p}^\star, \mathbf{r}^\star)$, which is the Nash equilibrium of the game. Furthermore, due to the monotone behavior of $p_j^{(k)}, r_j^{(k)}$ and given that they are bounded, these sequences always converge to the same optimal pair $(\mathbf{p}^\star, \mathbf{r}^\star)$, regardless the initial power and transmission data rate values.

Algorithm 3 UPRA-MSF Algorithm Part 1 (Access Point's Part)

1: Each Access Point announces the initial pricing factor $c = 0$ to its respective FUs, $j, j \in S_j$, $i = \{1, 2, ..., F\}$. The pricing factor is the same for all FUs within their corresponding FAPs (Femtocell Access Points) that reside within the same macrocell.
2: Each user, either MU or FU, determines its uplink transmission power and data rate Nash Equilibrium pair, i.e., $(p_j^\star, r_j^\star)$, according to UPRA-MSF algorithm Part II and computes its pure utility value, i.e., without the penalty factor.
3: The pricing factor is increased by the same value Δc, i.e., $c := c + \Delta c$. The new pricing factor is announced to all FUs by their corresponding AP.
4: If the pure utility values for all users, either MUs or FUs, are not improved, i.e., $U_j(c) > U_j(c := c + \Delta c)$, then stop and set $c_{best} = c$. Otherwise, go to step 2.

Algorithm 4 UPRA-MSF Algorithm Part 2 (User's Part)

1: At the beginning of time slot t and at the first iteration $k = 0$ of the algorithm, each user j, $j \in S = \{1, 2, ..., \}$ initializes its uplink transmission power and data rate. Thus, at the first iteration $k = 0$ of the algorithm we have the following power and transmission data rate vectors: $\mathbf{p} = (p_1^{(0)}, p_2^{(0)}, ..., p_N^{(0)})$ and $\mathbf{r} = (r_1^{(0)}, r_2^{(0)}, ..., r_N^{(0)})$, where $p_j^{(0)} = p_{j,min}$, $p_{j,min} > 0$ and $r_j^{(0)} = r_j^{Max}$
2: At the next iteration $k > 0$, compute the ratio $x_j^{(k)}$, as follows:

$$x_j^{(k)} = \underset{x_j \in \left[\frac{r_{j,min}}{p_j^{Max}}, \frac{r_j^{Max}}{p_{j,min}}\right]}{argmax} v_j\left(x_j = \frac{r_j}{p_j}, \mathbf{p}_{-\mathbf{j}}^{(\mathbf{k})}, \mathbf{r}_{-\mathbf{j}}^{(\mathbf{k})}\right)$$

3: Determine each user's uplink transmission power $p_j^{(k+1)}$ and data rate $r_j^{(k+1)}$ as follows:

$$\left(p_j^{(k+1)}, r_j^{(k+1)}\right) = \begin{cases} \textbf{if } \frac{qWG_{jj}}{I \ln L} > \frac{r_j^{MAX}}{p_j^{MAX}}: & \begin{cases} \left(p_j^{MAX}, x_j^{(k)} \times p_j^{MAX}\right), & \text{if } \mathbf{x_j^{(k)}} \leq \frac{\mathbf{r_j^{MAX}}}{\mathbf{p_j^{MAX}}} \\ \left(\frac{r_j^{MAX}}{x_j^{(k)}}, r_j^{MAX}\right), & \text{if } \mathbf{x_j^{(k)}} > \frac{\mathbf{r_j^{MAX}}}{\mathbf{p_j^{MAX}}} \end{cases} \\ \textbf{else } \left(p_j^{MAX}, x_j^{(k)} \times p_j^{MAX}\right) \end{cases}$$

4: If the powers and transmission data rates converge (i.e., $|r_j^{(k)} - r_j^{(k+1)}| \leq \epsilon$, $|p_j^{(k)} - p_j^{(k+1)}| \leq \epsilon$, $\epsilon = 10^{-7}$), then stop.
5: Otherwise, set $k = k + 1$ and go to step 2.

Finally, it should be noted that the only information that is exchanged between MUs, FUs, macro base station, and Access Points is the overall interference. More specifically, the only necessary information

for MUs and FUs, in order to determine their uplink transmission power and data rate $(p_j^{(k)}, r_j^{(k)})$ per iteration is the overall interference $\sum_{i,j \in S} G_{ij} P_j$ which is broadcasted by the macro base station and the Access Points, respectively. We assume that the BS and each AP has perfect channel state information of each user j, $j \in S$ and given users' uplink transmission powers, the overall interference in the two-tier femtocell network is computed based on the equation $\sum_{i,j \in S} G_{ij} P_j$. Then, the macro BS and the APs broadcast the overall interference, i.e., $\sum_{i,j \in S} G_{ji} P_j$ and each user excludes its contributing factor and determines its sensed interference caused by its neighbors, i.e., $\sum_{i,j \in S} G_{ji} P_j - G_{jj} P_j$. This information also contributes to determine the ratio and refine user's uplink transmission power and data rate, as described in steps 2 and 3, respectively, of UPRA-MSF algorithm part II (User's Part). Similar approaches have been followed in the literature, considering the implementation of the algorithm [10, 34, 35, 70, 74].

2.4.4 Numerical Results

In this section we provide some numerical results illustrating the operation and features of the proposed approach. Furthermore, the overall approach's efficiency is illustrated via representative comparisons to relevant frameworks proposed in the recent literature. Throughout our study we consider the uplink of a single-cell two tier femtocell CDMA network, supporting continuously backlogged real and non-real time users. We model users' path gains via adopting the simplified path loss model in the IMT-2000 specification [61]. Moreover, for demonstrations purposes only, we assume that each real time user, either MU or FU, adopts one common modulation and coding scheme, i.e., common efficiency function, which is expressed through a sigmoidal function $f_j(\gamma_j) = (1 - e^{-0.5 \cdot \gamma_j})^{80}$ [10]. Henceforth, we consider the following values of system parameters, as shown in 2.3.

Table 2.3: Simulation parameters values for UPRA-MSF algorithm

Parameter	**Value**
W	3.84×10^6 Hz
r_j^{MAX}	96,000 bps
$r_{j,min}$	0.1 bps
p_j^{MAX}	0.2 W
$p_{j,min}$	10^{-6} W
c_{best}	13

In the following subsections, the presented results are organized in three groups. First, we show some numerical results of UPRA-MSF algorithm aiming at evaluating its performance and convergence behavior to the determined Nash Equilibrium pair $(\mathbf{p}^\star, \mathbf{r}^\star)$. Next, we compare the results of UPRA-MSF algorithm to other approaches proposed in the literature considering a single tier network and joint uplink transmission power and data rate allocation [33, 34]. It should be stressed that as discussed before, the combined problem of power and transmission data rate allocation has not been confronted yet in two-tier femtocell networks, thus the only available comparative scenarios could refer to the one-tier macrocell architecture [33, 34]. It should be highlighted that the proposed frameworks in [33, 34] (against which we compare) could not run separately once in the femtocell tier and then to the macrocell tier (or vice versa), due to the fact that the interference caused from the one tier to the other is not negligible. Therefore, aiming at comparing our proposed framework, which performs power and data rate allocation in two-tier femtocell networks, we keep the same users' distribution and location within the macrocell for the proposed UPRA-MSF algorithm, and the algorithms in [33, 34], as well as the total number of users in the three comparative scenarios is the same. The goal of this comparison is to illustrate the benefits that stem from (a) two-tier system architecture, (b) proper formulation of users' QoS prerequisites in an appropriate and more general utility function, and (c) the well designed pricing mechanism. Finally, analytical comparative results of our proposed framework compared to [37, 68] are presented. The authors in [37] consider the problem of utility-based power allocation in two-tier femtocell network via adopting linear pricing policy with respect to user's uplink transmission power, while in [68] (i.e., the results from

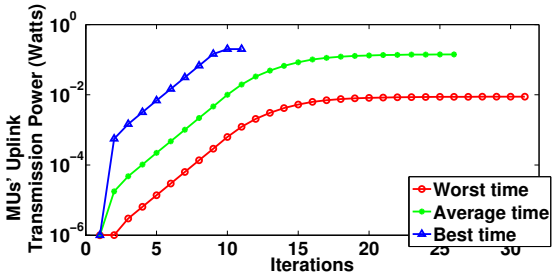

(a) MUs' uplink transmission power convergence (y-axis in algorithmic scale)

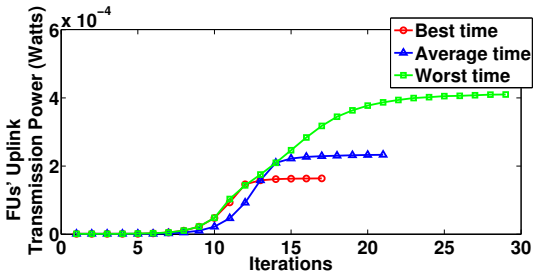

(b) FUs' uplink transmission power convergence (y-axis in algorithmic scale)

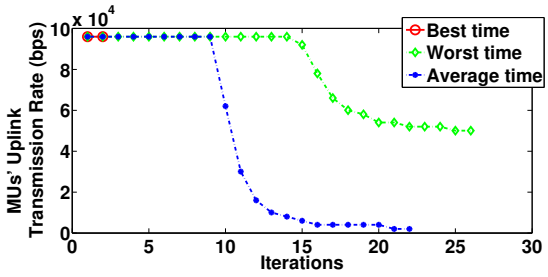

(c) MUs' uplink transmission rate convergence

Figure 2.9: Power and rate convergence under UPRA-MSF algorithm

the previous section in this chapter) suggest an efficient uplink power control in multi-service two-tier femtocell networks via adopting different user's utility function based on the tier they belong to and the service they request, as well as convex pricing policy with respect to FUs' uplink transmission power. From this comparison, we illustrate (a) the benefits of jointly allocating transmission power and rate at the same step and (b) the outperformance of UPRA-MSF framework in power saving, due to the proper design of users' utility functions and the proposed pricing mechanism, even if the authors in [37] and [68] target only on optimizing the energy consumption.

UPRA-MSF game's Nash Equilibrium Properties

In the following, we consider one single CDMA macrocell with radius $R_0 = 290\ m$ and $F = 8$ femtocells with radius $R_c = 40 - 50\ m$. The system supports 10 MUs, where $N_{MRT} = 5$ and $N_{MNRT} = 5$ and 16 FUs, where each FAP serves 2 users (one real-time and one non-real time service requested user). The corresponding users are distributed within the range of their macrocell/femtocell coverage area, where RT users are placed closer to the BS/AP contrary to the NRT users. The target rate of RT users is set to $r_{target} = 96\ kbps$. When obtaining values of rates less than the targeted one, RT user's utility decreases rapidly. According to the requested services' prerequisites (i.e., RT or NRT), as well as the tier each user belongs to (i.e., FU or MU), users are classified in four classes. The above described setup is depicted in Fig. 2.6, where users are differentiated into the four classes with different colors and symbols.

Figs. 2.9a, 2.9b and 2.9c illustrate MUs' and FUs' uplink transmission power and MUs' uplink transmission data rate as a function of the iterations required for UPRA-MSF algorithm to converge at the Nash Equilibrium. In the three figures, we present three representative users with respect to the convergence time to their equilibrium values, i.e., (a) worst, (b) best and (c) close to average convergence time. Based on the results presented in these three figures, we conclude that as MUs' mean channel conditions become worse (i.e., more distant users from the BS (Fig. 2.6)) and in order to satisfy their QoS prerequisites, their uplink transmission power increases (Fig. 2.9a), while the uplink transmission rate especially for the more distant users decreases (Fig. 2.9c), due to the increasing deterioration of their channel conditions (especially for the distant NRT users). On the other hand, considering MU-RT users, it is observed based on 2.9c) that the targeted uplink transmission rate is achieved, especially for these RT users that are reasonably close to the BS (Fig. 2.6). Furthermore, considering FUs, either RT or NRT, it is observed by Fig. 2.9b that their uplink transmission power is very low, due to the fact that they reside close to their corresponding AP, thus their mean channel conditions are good. Considering the convergence time of UPRA-MSF algorithm, we observe that the convergence of the proposed algorithm

is very fast since less than 20 iterations are required for reaching equilibrium for all MUs and FUs residing in the two-tier femtocell network, while for all practical purposes we notice that in less than fifteen iterations the values of the powers, as well as of the data rates, have reached their corresponding equilibrium values. The convergence of UPRA-MSF algorithm is characterized fast compared to the necessary number of iterations of other approaches from the recent literature [28, 29, 34, 68]. Moreover, due to the closed form and the simplified calculations in order to determine the Nash equilibrium point, the convergence of UPRA-MSF algorithm is feasible in the short duration of a time slot (i.e., slot duration $= 0.5\ msec$), considering any practical realistic scenario. In brief, it is noted that UPRA-MSF algorithm's computational complexity is low due to the simplicity of the involved calculations. The basic calculation that is performed by the mobile users is the one in step 2 of Part II (User's part) of the proposed algorithm, which is essentially the calculation of the unique maximum point of the quasi-concave function $v_j(\mathcal{X})$. Therefore, the required processing and corresponding energy consumption from mobile user's part is quite limited especially taking into account the capabilities of modern mobile devices. For example UPRA-MSF algorithm was tested and evaluated in an Intel(R) Core(TM) 2 Duo CPU T7500 @ 2.20 GHz laptop with 2.00GB available RAM and its average run time was 0.6 *msec*. We notice that the necessary time of UPRA-MSF algorithm in order to converge to the Nash equilibrium point is of the similar order of magnitude with the duration of a time slot (i.e., 0.5 *msec*, thus it can be easily adopted in a realistic scenario.

Additionally, in Table 2.4, the average number of iterations that the UPRA-MSF algorithm needs to converge to the Nash equilibrium point along with the corresponding standard deviation, under different scenarios of number of users residing in the two-tier femtocell network are presented. To further improve the convergence performance of the proposed approach several operational considerations and enhancements are discussed below. Specifically, we executed again the UPRA-MSF algorithm considering as initial values MUs' and FUs' uplink transmission power and rate values that are based on the corresponding values calculated in the previous time-slot (we refer to this scenario as "educated" case), and we observed that the average number of necessary iterations has been decreased significantly to 7.4 iterations (compared to 20.80 iterations for the original case referred to as "non-educated" case), which had also as a consequence a decrease of approximately 50% of the corresponding convergence time.

Table 2.4: Number of iterations of UPRA-MSF algorithm

Number of users	**MUs**	**FUs**	**FAPs**	**Mean iterations**	**Standard deviation**
20	10	10	5	20.80	6.76
26	10	16	8	20.92	6.15
40	10	30	15	20.94	6.38
48	12	36	18	20.95	6.54

In Table 2.5, for comparison purposes, we present the actual number of iterations required for convergence for both the educated and non educated execution of UPRA-MSF algorithm, for three representative users with respect to the convergence time to their equilibrium values, i.e., (a) worst, (b) best, and (c) close to average convergence time.

Table 2.5: Number of iterations considering educated and non-educated UPRA-MSF algorithm.

	Worst Case	**Best Case**	**Close to average case**
Non-educated UPRA-MSF algorithm	31	11	26
Educated UPRA-MSF algorithm	13	2	7

Moreover, considering that the communication environment does not change dramatically within the duration of few time slots, it is noted that in a realistic scenario the determined values for users' uplink transmission power and rate could be applied to more than one consecutive time slots. Finally, the required number of iterations and corresponding convergence time could decrease even further if we relax the convergence parameter, which now was set to $\epsilon = 10^{-7}$, fact that however provides great accuracy to our results.

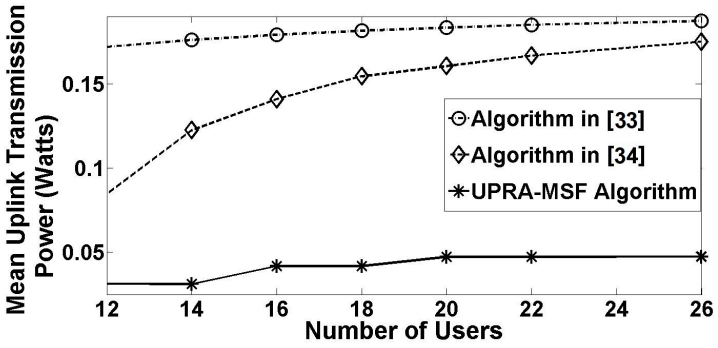

Figure 2.10: Users' mean uplink transmission power as a function of the number of users under three comparative scenarios

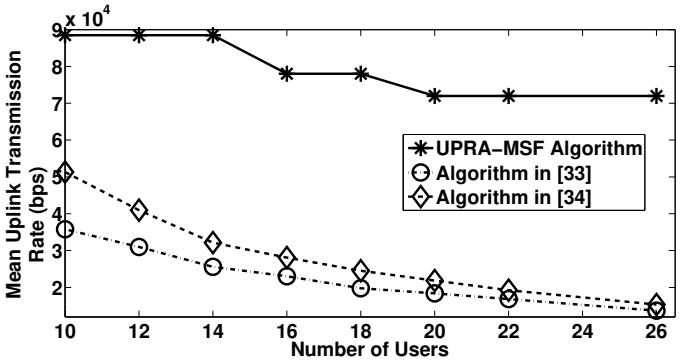

Figure 2.11: Users' mean uplink transmission rate as a function of the number of users under three comparative scenarios

Increasing number of users

In the following, we first provide some comparative numerical results illustrating the performance and superiority of the proposed UPRA-MSF framework as the number of users in the system increases, considering three different scenarios: (a) UPRA-MSF algorithm, where the 50% of users are MUs, (b) joint multi-service power and transmission data rate allocation in a single one-tier CDMA macrocell as presented in [34], where the authors consider the power and transmission data rate allocation as a two separate variable optimization problem, and (c) utility-based power and transmission data rate allocation in a single one-tier macrocell as presented in [33].

The algorithms in [33,34] have been chosen in order to present a comparative study of simultaneously allocating the power and transmission data rate to the users considering a utility-based framework. Specifically, Figs. 2.10 and 2.11 present users' average uplink transmission power and rate as a function of the overall number of users in the cell (both MUs and FUs). The results reveal that the UPRA-MSF algorithm has the best overall performance, in terms of low uplink transmission power and high data rate, due to the fact that it considers the two-tier femtocell architecture characteristics, users' specific QoS prerequisites properly expressed via well designed utility functions, and convex pricing with respect to FUs' bit energy to interference density ratio. More specifically, the comparison of the three different approaches leads to an average reduction of users' uplink transmission power of 75% and 70% respectively when comparing UPRA-MSF algorithm to the algorithms presented in [33, 34]. The corresponding gain in users' uplink transmission data rate is 270% and 204%, respectively.

Increasing number of FAPs

In the following, we present a comparative study demonstrating the benefits of the proposed UPRA-MSF algorithm as the number of FAPs residing within the macrocell increases. Specifically, we compare MUs' (Fig. 2.12a) and FUs' (Fig. 2.12b) uplink transmission powers as they are obtained based on UPRA-MSF algorithm and their corresponding values based on algorithm in [37, 68], where an energy-efficient

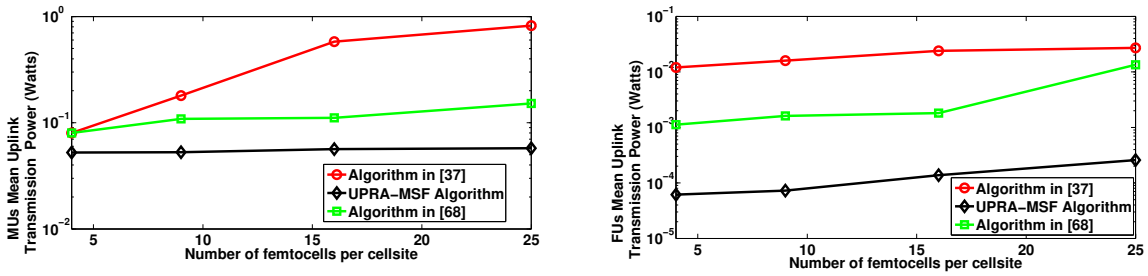

(a) Macro Users (MUs)

(b) Femto Users (FUs)

Figure 2.12: Mean uplink transmission power as a function of the number of FAPs (y-axis in logarithmic scale)

utility-based power allocation approach in single-service two-tier femtocell networks is followed.

The results reveal the superiority of UPRA-MSF algorithm in terms of power savings, due to the adoption of convex pricing mechanism with respect to FUs' bit energy to interference density ratio, in contrast to algorithms in [37,68] that adopt linear and convex pricing with respect to user's uplink transmission power, respectively. Specifically, the comparison of UPRA-MSF algorithm to the algorithms presented in [37,68] reveals that the average reduction in MUs (Fig. 2.12a) and FUs (Fig. 2.12b) uplink transmission power is 86% [37], 49% [68] and 99% [37], 97% [68], respectively. Fig. 2.13 clearly depicts the superiority of UPRA-MSF algorithm by presenting the mean energy-efficiency for MUs and FUs in units $[bits/J]$.

Definition 2.4.1. ***Energy-Efficiency:*** *The term "Energy-Efficiency" (EE)* $\left(^{bit}/_{Joule}\right)$*, has been coined to reflect the system throughput for unit-energy consumption measured in bits of transmitted information per each Joule of consumed energy (bps), [75].*

It is observed that the average increase of mean energy-efficiency via adopting UPRA-MSF algorithm is on average 230% for FUs and 145% for MUs, compared to the algorithm presented in [37], while the average increase of mean energy-efficiency is extremely high compared to [68]. Finally, it should be noted that the above presented results are the outcome of modeling and simulation, thus the corresponding practical results in real systems may slightly vary from the results presented in this work.

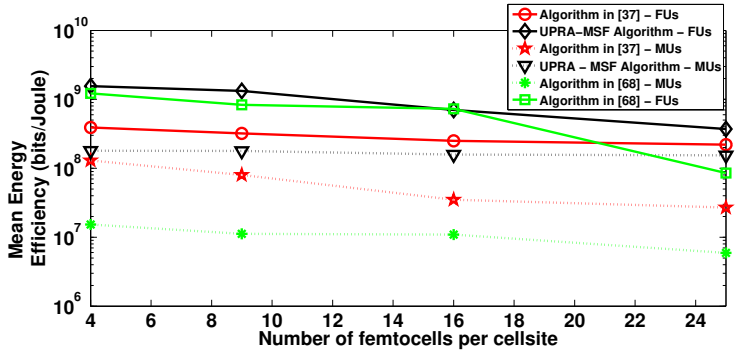

Figure 2.13: Users' mean energy-efficiency as a function of number of FAPs (y-axis in logarithmic scale)

2.5 Power and Rate Control as a Two-Parameter Problem

At this part, we further develop the resource management problem in a two-tier femtocell network by examining the joint users' uplink transmission power and data rate allocation, formulated and solved for the first time as a distinct two-variable optimization problem. The objective behind the proposed approach is to determine users' uplink transmission power and rate in a distributed manner so as to maximize their perceived satisfaction. To better reflect the latter, we design appropriate utility functions

that enable users to express their QoS demands via the independent variables of power and rate, when considering not only multiple services but the tier of the network that the user belongs to as well.

To tackle the inherent challenges stemming from the joint two-variable consideration and the resulting multidimensional competition among the users, the theory of supermodular games is applied again to the corresponding optimization problem and its Nash Equilibrium point is determined. The main novelty is that we provide two degrees of freedom, i.e., power and rate, enabling the user to better express its QoS prerequisites, achieve energy-efficiency by obtaining high transmission rates with low power consumption, while supporting both real and non-real time services [76, 77].

2.5.1 System Model

We consider the uplink of a two-tier femtocell wireless network, consisting of a macrocell base station (BS) which serves a region $\Re$ and covers an area of radius R_0, providing multiple types of services to the users. Furthermore, within the region $\Re$ there are deployed F co-channel femtocells. Each FAP supports a region $\mathscr{J} \subset \Re$ and consists of a disk of radius $R_c << R_0$.

For simplicity in the following, cell f refers to the cell served by one BS/FAP. Without loss of generality, the macrocell BS is indexed by 0 and FAPs by $1, 2, ..., F$. Therefore, in the system a user i is associated (served) by base station $B_i = 0$ if the user is MU or by FAP $B_i = 1, 2, ..., F$, if the user is FU. It is clarified that at the beginning of each time slot, the number of users per tier/cell is assumed to be known [78]. Though the cell selection problem itself is of high importance it is not within the scope of this work [79], while several approaches exist in the literature to treat it based on various criteria [78], e.g., maximum channel gain/SINR/utility criteria. This assumption does not restrict the applicability of the proposed approach due to the fact that the cell selection component can be easily included in our proposed framework prior to the resource allocation component proposed in this thesis. As previously, the FAPs considered can be either of closed access nature, i.e., the users should be registered to the FAP in order to be served, or of open access nature, where no user's registration is needed. Nevertheless, this assumption can be more easily realized in practice in the case of closed access femtocells.

We study a two-tier femtocell network, which supports users requesting either real-time (RT) services or non-real time (NRT) services. Specifically, the overall set of users is denoted by S and consists of four subset: S_{MRT}, S_{MNRT}, S_{FRT} and S_{FNRT}, representing macro (MUs) and femto (FUs) users, requesting real and non-real time services, respectively. The corresponding numbers of macro and femto users, asking for real and non-real time services are denoted by N_{MRT}, N_{MNRT}, N_{FRT} and N_{FNRT}, respectively, while the overall number of users residing in the two-tier femtocell network is N, that is $N_{MRT} + N_{MNRT} + N_{FRT} + N_{FNRT}$. Fig. (2.14) depicts a sample of users' distribution within a two-tier femtocell network, consisting of a macrocell base station and a number of FAPs.

We assume an interference limited environment where the available bandwidth (or a common band of frequencies) is co-used and shared by MUs and FUs for uplink communications. Let us denote by $B_i = l$ the BS/FAP of a user i under consideration. The channel gain of the link between user i and some BS/FAP j, $(j = 0, 1, 2, ..., F)$ in the system is denoted by h_{ij}. For simplicity these gains are modeled following the simplified path loss model in the IMT-2000 specification [61], as follows:

$$h_{ij} = \begin{cases} A \cdot \min\left(d_{i,0}^{-a}, 1\right), & i \text{ is MU, j} = 0 \\ \mathrm{B} \cdot R_c^{-b}, & i \text{ is FU, j} > 0, \text{j} = l \\ C \cdot D \cdot \min\left(d_{i,j}^{-a}, 1\right), & i \text{ is MU, j} > 0 \\ A \cdot D \cdot \min\left(d_{i,0}^{-a}, 1\right), & i \text{ is FU, j} = 0 \\ C \cdot D^2 \cdot \min\left(d_{i,j}^{-a}, 1\right), & i \text{ is FU, j} > 0, \text{j} \neq l \end{cases} \tag{2.23}$$

The exact values of the above described constants have been adopted by [61] and are presented in Table 2.6. At each time slot, each user i, $i \in S$ transmits with an uplink transmission power p_i and an uplink transmission data rate r_i, which are assumed to be upper and lower bounded continuous variables, i.e., $0 < p_i \leq p_i^{Max}$ and $0 < r_i \leq r_i^{Max}$. The uplink transmission power and data rate vector of all users residing in the two-tier femtocell network are denoted by $\mathbf{p} = [p_1, p_2, ..., p_N]$ and $\mathbf{r} = [r_1, r_2, ..., r_N]$, respectively. Therefore, the received signal-to-interference-plus-noise ratio (SINR) is denoted similarly to Eq. (2.1).

To treat users' diverse and multiple QoS prerequisites under a common optimization framework, users' utility functions are differentiated according to the tier the user belongs to, as well as to the type of requested service. It is noted that the overall proposed approach and the utility function used here allow for more general considerations compared to other frameworks in the literature as well as the

Table 2.6: Section 2.5 list of key notations

Parameter	**Symbol / Value**
Macrocell BS	B_0
Femtocell AP	$B_i = 1, 2, ...F$
Macrocell's region, radius	$\Re$, R_0
FAP's region, radius	$\mathscr{J}$, R_c
Number of FAPs	F
Set of MUs and FUs requesting RT and NRT services	S_{MRT}, S_{MNRT}, S_{FRT}, S_{FNRT}
Number of MUs and FUs requesting RT and NRT services	N_{MRT}, N_{MNRT}, N_{FRT}, N_{FNRT}
Channel gain between user i and BS/FAP j	h_{ij}
Signal-to-interference-plus-noise ratio	γ_i
User's uplink transmission power	p_i [W]
User's uplink transmission rate	r_i [bps]
System's spread spectrum bandwidth	W [Hz]
Pricing factor	c
User's strategy space	$A_i = P_i \times R_i$
Macrocell and indoor femtocell path loss exponent	$a = 4$
Indoor to outdoor femtocell path loss exponent	$b = 3$
Distance of user i (if i is an MU $i = 0$, otherwise $i \geq 1$) from BS/FAP j (if j is the BS: $j = 0$, otherwise if j is a FAP: $j \geq 1$)	$d_{i,j}$
Fixed decibel propagation loss during macrocell transmissions to the BS	$A = 28dB$
Fixed loss between FU to its corresponding FAP $j = i$	$B = 37dB$
Fixed path loss between FU to a different FAP $j \neq i$	$C = 37dB$
Partition loss during indoor to outdoor propagation	$D = 10dB$
Efficiency function	$f(\gamma_i)$
Utility function	U_i
Efficiency function constants	A, M
MUPRAF, modified MUPRAF games	G, G'
Auxiliary functions	$w(\gamma_i)$, $g(\gamma_i)$, $\tau(\gamma_i)$
Root of $\tau(\gamma_i)$	$\gamma_{i,BOL}$
Exogenous parameter	ϵ
Best response strategy	BR_i

discussion in Section 2.4, where user's perceived satisfaction depended exclusively only on the ratio of the uplink transmission data rate and power consumption. As already discussed, the latter was a strong assumption in the definition of the utilities in 2.4 by design, in order to allow the transformation of the two-variable optimization problem to a single-variable one.

In this work since we confront directly the two-variable (power and rate) optimization problem, we remove this limitation and we assume a two-variable utility function. Without loss of generality, in the following we consider the utility function presented in Eq. (2.24), where it depends on one hand on the ratio of uplink transmission rate to the uplink transmission power in order to express energy-efficiency, and on the other hand depends directly on power for the case of FUs. Other forms of the utility function can be also treated under the general framework presented in this part of the work.

$$U_i(\mathrm{p},\mathrm{r}) = \begin{cases} \frac{r_i f(\gamma_i)}{p_i},\ i \in S_{MRT} \\ \frac{r_i \log(1+f(\gamma_i))}{p_i},\ i \in S_{MNRT} \\ \frac{r_i f(\gamma_i)}{p_i} - c\left(e^{P_i} - 1\right),\ i \in S_{FRT} \\ \frac{r_i \log(1+f(\gamma_i))}{p_i} - c\left(e^{P_i} - 1\right),\ i \in S_{FNRT} \end{cases} \tag{2.24}$$

The physical meaning of the proposed formulation, as detailed below, mainly stems from two fun-

damental observations: a) user's (both MU and FU) perceived satisfaction, i.e., utility, increases as its achievable data rate increases - though in different manner for real time and non-real time services - and as its uplink transmission power decreases, the latter due to the prolongation of its battery-life; and b) MUs should receive higher priority in being served compared to FUs. Specifically, in Eq. (2.24), with reference to real time users, the achievable data rate $r_i \cdot f(\gamma_i)$ is assumed to be a sigmoidal-like function with respect to γ_i, where the inflection point is mapped to real time user's minimum QoS prerequisites. Thus, if user's SINR γ_i results in achievable data rate $r_i \cdot f(\gamma_i)$ lower than user's desirable one, then its utility decreases rapidly indicating user's starvation. Moreover, if user $i, i \in S_{MRT} \cup S_{FRT}$ achieves its desirable data rate then its utility is very slowly increasing, thus indicating to the system that it has already met its QoS prerequisites.

On the other hand, considering non-real time users' (both MUs and FUs) QoS prerequisites, we express the achievable data rate, i.e., $r_i \cdot \log(1 + f(\gamma_i))$ via adopting a log-based function with respect to user's efficiency function $f(\gamma_i)$. The proposed formulation of achievable data rate properly represents non-real time users' greedy behavior, as they are characterized by high-throughput (i.e., achievable data rate) expectations. Their overall perceived satisfaction, i.e., $U(\mathbf{p}, \mathbf{r})$, increases as they achieve higher SINR values, which in turn results in higher achievable data rate via the strictly increasing function $r_i \cdot \log(1 + f(\gamma_i))$ with respect to γ_i.

It should be noted that our framework does not limit the applicability of the proposed approach to two classes of services only (they are mainly used for demonstration purposes). Each service class (i.e., RT and NRT) could consist of other/many subclasses. For example, considering a requested real-time service, the proposed framework can support various real-time services, i.e., voice, video, etc., which consist the subclasses of real-time services, each one of them with different QoS requirements. In this case different applications can be considered and differentiated via changing the slope of the sigmoidal function $r_i \cdot f(\gamma_i)$ (i.e., appropriately selecting A, M parameters) and mapping the requested service minimum QoS requirements to the appropriate inflection point.

Furthermore, FUs are further penalized via a convex pricing function with respect to their uplink transmission power p_i, [34], [40], [58], [80], in order to mitigate their caused interference within the overall two-tier femtocell network. This way, higher priority is given to the serving of MUs, who a priori have worst channel conditions due to the fact that in general they are more distant from the base station compared to the FUs from the corresponding FAP. This is of high importance as both FUs and MUs share the same system's available spectrum bandwidth interfering with each other. The operator of the overall network enforces the FAPs to announce the strict usage-based pricing policy to the FUs being served by them, in order the FAPs to be allowed to operate within the overall network. Thus, each FAP announces the proposed convex pricing policy to the served FUs.

Parameter c refers to the pricing factor as determined by the system and adopted by the users. This parameter needs to be appropriately configured so that, through user's self-optimization, the best possible improvement in overall system's performance is achieved by forcing users to adopt a more social behavior. The determination of the appropriate value of pricing factor is discussed in Section 2.5.3. The convex pricing policy is more realistic compared to other linear pricing schemes proposed in the literature [10] due to the fact that the harm an FU imposes on other users is not equivalent within the whole range of transmission power. Previous attempts to consider non-linear pricing are not directly applicable or extensible to our formulation, mainly due to the fact that they were limited to treating cases where the ratio of uplink transmission rate to uplink transmission power appears in both users' pure utility function and their corresponding pricing function [29]. In this work, this limitation is alleviated by considering a more general formulation with respect to both utility and pricing functions, a fact that requires different treatment of the overall optimization problem.

2.5.2 Problem Formulation and Solution

As the system evolves, at the beginning of each time slot, each user determines an appropriate uplink transmission power and data rate level towards maximizing its overall perceived satisfaction, which is appropriately represented via the corresponding values of the utility function. This is obtained as a result of a user's optimal joint utility-based Multi-service Uplink transmission Power and data Rate Allocation distributed algorithm in two-tier Femtocell wireless networks (MUPRAF algorithm). In order to consider users' selfish and greedy behavior, game theory arises as a powerful and appropriate tool [10, 28, 29] and [33]. Specifically, the users act as players that compete with each other and choose a strategy space of uplink transmission power and data rate and subsequently achieve a payoff, which is represented by

their utility.

Let $G = \left[S, \{A_i\}_{i\in S}, \{U_i\}_{i\in S}\right]$ denote the Multi-service utility-based Uplink Power and data Rate Allocation game in two-tier Femtocell wireless networks (MUPRAF game), where $S = S_{MRT} \cup S_{MNRT} \cup S_{FRT} \cup S_{FNRT}$ denotes the set of users residing within the two-tier femtocell network, $A_i = P_i \times R_i$ is user's $i, i \in S$ strategy space, where $P_i = \left(0, p_i^{Max}\right]$ and $R_i = \left(0, r_i^{Max}\right]$, and U_i denotes user's payoff function. The strategy sets of each user, i.e., P_i and R_i that consist its strategy space A_i are compact and convex sets and as mentioned before, they are constrained with maximum and minimum values due to user's and system's physical and technical limitations.

The goal of each user is to maximize its utility via selecting an appropriate strategy of uplink transmission power and data rate. Therefore, MUPRAF game, is formulated as a distributed utility maximization problem, as follows:

$$\begin{gathered}\textbf{MUPRAF Game}\\ \max_{\substack{r_i\in R_i\\ p_i\in P_i}} U_i\left(\mathrm{p},\mathrm{r}\right), \forall i \in S\\ s.t.\ 0 < r_i \leq r_i^{Max},\ 0 < p_i \leq p_i^{Max}\end{gathered} \tag{2.25}$$

The solution of MUPRAF game should determine the optimal equilibrium for the system, concluded by the individual decisions of each user (either MU or FU), given the decisions made by the rest of the users. A Nash Equilibrium point of MUPRAF game is a pair of vectors of users' uplink transmission power and data rate $(\mathbf{p}^*, \mathbf{r}^*)$ i.e., $\mathbf{p}^* = (p_1, p_2, ..., p_N)^T \in P = P_1 \times P_2 \times ... \times P_N$ and $\mathbf{r}^* = (r_1, r_2, ..., r_N)^T \in R = R_1 \times R_2 \times ... \times R_N$, where the superscript T denotes the transpose operation of a vector. More precisely, the Nash Equilibrium point of the presented two-variable non-cooperative MUPRAF game can be defined as follows:

Theorem 9. ***(MUPRAF Game's Nash Equilibrium:)*** *The vectors* $(\mathbf{p}^*,\mathbf{r}^*) = (p_1^*, p_2^*, ..., p_N^*, r_1^*, r_2^*, ..., r_N^*)$ *in the strategy sets* $r_i^* \in R_i$ *and* $p_i^* \in P_i$*, is a NE of the MUPRAF game if for every user i the following condition holds true:*

$$U_i\left(p_i^*, r_i^*, \mathbf{p}_{-\mathrm{i}}, \mathbf{r}_{-\mathrm{i}}\right) \geq U_i\left(p_i, r_i, \mathbf{p}_{-\mathrm{i}}, \mathbf{r}_{-\mathrm{i}}\right) \tag{2.26}$$

for all $p_i \in P_i$ *and* $r_i \in R_i$*.*

As a result, no user has the incentive to change its strategy, due to the fact that it cannot unilaterally improve its personal utility by making any change to its own strategy, given the strategies of the rest of the users. Moreover, the existence of NE point guarantees a stable outcome of the MUPRAF game, while on the contrary, the non-existence of such an equilibrium point is translated to an unstable and unsteady situation of the system.

Towards proving the existence of at least one NE of MUPRAF game, as in a previous section, the theory of supermodular games is adopted. Considering multidimensional competition (as in MUPRAF game due to the joint users' uplink transmission power and data rate allocation), supermodular games appear suitable due to the fact that they can readily and appropriately handle multidimensional strategy spaces. Considering a two dimensional game with strategy space $A_i = X_i \times \Upsilon_i$, we have the following [65]:

Theorem 10. ***(Supermodular Games:)*** *The game* $G = \left[S, A_i = X_i \times \Upsilon_i, \{U_i\}_{i\in S}\right]$ *is smooth supermodular, if for all* $i \in S$ *the following conditions hold true:*

- $A_i = X_i \times \Upsilon_i$ *is a compact cube in Euclidean space.*
- $U_i\left(x_i, y_i\right), x_i \in X_i, y_i \in Y_i$ *is twice continuously differentiable:*
  1. *supermodular in* (x_i, y_i) *for fixed* $\left(\mathbf{x}_{-\mathrm{i}}, \mathbf{y}_{-\mathrm{i}}\right)$ *i.e.,*

$$\frac{\partial^2 U_i}{\partial x_i \partial y_i} \geq 0 \tag{2.27}$$

  2. *with increasing (or non-decreasing) differences in* $\left\{\left(x_i, y_i\right), \left(\mathrm{x}_{-\mathrm{i}}, \mathrm{y}_{-\mathrm{i}}\right)\right\}$*, i.e.,*

$$U_i(\mathbf{x}, \mathbf{y}) - U_i(\mathbf{x}, \mathbf{y}') \geq U_i(\mathbf{x}', \mathbf{y}) - U_i(\mathbf{x}', \mathbf{y}') \tag{2.28}$$

  $\forall \mathbf{x} > \mathbf{x}',\ \mathbf{y} > \mathbf{y}'$*, (i.e.,* $U_i(\cdot, \mathbf{y}) - U_i(\cdot, \mathbf{y}')$ *is non-decreasing function). If* U *is a smooth function (i.e., has derivatives of all orders), then the equivalent condition is:*

$$\frac{\partial^2 U_i}{\partial x_i \partial x_j} \geq 0, \forall j \neq i \tag{2.29}$$

given that

$$\frac{\partial^2 U_i}{\partial x_i \partial y_j} = 0, \forall j \neq i \tag{2.30}$$

In a supermodular game, external equilibria always exist: a largest element $\bar{a} = \sup\{a \in A : BR(a) \geq a\}$ and a smallest element $\underline{a} = \inf\{a \in A : BR(a) \leq a\}$ of the equilibrium set, where $BR(\cdot)$ denotes player's $i, i \in S$ best response strategy to other players' strategies [72]. If $G = \left[N, \{S = X_i \times \Upsilon_i\}, \{U_i\}_{i \in S}\right]$ is a supermodular game, then it has at least one Nash equilibrium point, where all the players converge following their best response dynamics [14, 65].

The MUPRAF game as formulated so far is not a supermodular game in $A_i = P_i \times R_i, i \in S$, thus its strategy space is appropriately modified, in order conditions (2.27), (2.29), and (2.30) to hold true. Therefore, in the following we examine separately and analytically each condition, in order to determine the modified strategy space $A_i{}'$, where MUPRAF game is supermodular. It should be noted that the original optimization problem, as introduced in equation (2.25) is not modified, but we modify the strategy space where the potential solution lies, so as to guarantee its existence.

Lemma 11. ***(MUPRAF Game Supermodularity:)*** *MUPRAF game's* $G = \left[S, \{A_i\}_{i \in S}, \{U_i\}_{i \in S}\right]$ *utility function* $U_i(\mathbf{p}, \mathbf{r})$ *as defined in (2.24) is supermodular in* (p_i, r_i) *for fixed* $\left(\mathbf{p}_{-\mathrm{i}}, \mathbf{r}_{-\mathrm{i}}\right)$*, i.e.,* $\frac{\partial^2 U_i}{\partial p_i \partial r_i} \geq 0$*, if and only if:*

$$\gamma_i \in \left[\frac{\ln M}{A}, \gamma_{i,k}\right] \tag{2.31}$$

where $\gamma_{i,k} = \min\{\gamma_{i,1}, \gamma_{i,2}\}$, $\gamma_{i,1}, \gamma_{i,2}$ are analytically determined in the following proof.

Proof. To prove that the utility function $U_i(\mathbf{p}, \mathbf{r})$ is supermodular in (p_i, r_i) for fixed $\left(\mathbf{p}_{-\mathrm{i}}, \mathbf{p}_{-\mathrm{i}}\right)$ we examine if $\frac{\partial^2 U_i}{\partial p_i \partial r_i} \geq 0$ holds true for the following four cases.

- **Case 1: Macro Real Time Users**

  The second partial derivative is $\frac{\partial^2 U_i}{\partial p_i \partial r_i} = \frac{MA^2}{p_i^2}\left(1 - e^{-A\gamma_i}\right)^{M-2} \cdot \left[\begin{array}{l} e^{-A\gamma_i}\gamma_i^2\left(1 - Me^{-A\gamma_i}\right) \\ +\frac{1}{A}\left(1 - e^{-A\gamma_i}\right)e^{-A\gamma_i}\gamma_i \\ -\frac{1}{MA^2}\left(1 - e^{-A\gamma_i}\right)^2 \end{array}\right]$. To guarantee that $\frac{\partial^2 U_i}{\partial p_i \partial r_i} \geq 0$, we examine the individual terms of relation $\frac{\partial^2 U_i}{\partial p_i \partial r_i}$. Thus, we have that $\frac{MA^2}{p_i^2}\left(1 - e^{-A\gamma_i}\right)^{M-2} \geq 0 \Leftrightarrow \gamma_i \geq 0$. Moreover, we denote as $w(\gamma_i) = e^{-A\gamma_i}\gamma_i^2\left(1 - Me^{-A\gamma_i}\right) + \frac{1}{A}\left(1 - e^{-A\gamma_i}\right)e^{-A\gamma_i}\gamma_i - \frac{1}{MA^2}\left(1 - e^{-A\gamma_i}\right)^2$. Thus, we aim to prove that there exists an interval in $\gamma_i \geq 0$ such that $w(\gamma_i) \geq 0$. To show this we apply Bolzano Theorem, which is an important specialization of Intermediate Value Theorem defined as below:

Definition 2.5.1. ***Bolzano Theorem:*** *Bolzano theorem is an important specialization of the Intermediate Value Theorem stating that a continuous function which has opposite signs inside an interval, then has a root at this interval [81].*

Function $w(\gamma_i)$ is continuous and $C^{(n)}$ differentiable $\forall \gamma_i \geq 0$. For $\gamma_i = \frac{\ln M}{A}$ it is $w\left(\gamma_i = \frac{\ln M}{A}\right) = \frac{1}{A}\left(\frac{M-1}{M}\right)\frac{1}{AM}\left(\ln M + \frac{1}{M} - 1\right) > 0$ for $M > 1$. The latter inequality is analytically proven in the following. Let us denote $q(M) = \ln M + \frac{1}{M} - 1$ where $M > 1$. From the first order derivative, we have: $\frac{\partial q(M)}{\partial M} = \frac{M-1}{M^2} > 0, \forall M > 1$. Thus, $q(M)$ is strictly increasing for all $M > 1$. Moreover, $q(1) = 0$, thus $q(M) > 0, \forall M > 1$ and therefore $w\left(\gamma_i = \frac{\ln M}{A}\right) > 0$.

For $\gamma_i = \frac{\ln 10^4 M}{A}$: $w\left(\gamma_i = \frac{\ln 10^4 M}{A}\right) = \frac{9999}{10^8 M}\left(\frac{\ln 10^4 M}{A}\right)^2 + \frac{10^4 M - 1}{10^8 M^2 A^2} \cdot \left(\ln 10^4 M + \frac{1}{M} - 10^4\right) < 0$ for various packet sizes, i.e., $M \in (1, 1000)$ and $A \in (0.1, 100)$ [10, 72]. Therefore, combining the

aforementioned inequalities, $w\left(\gamma_i = \frac{\ln M}{A}\right) \cdot w\left(\gamma_i = \frac{\ln 10^4 M}{A}\right) < 0$. Hence, there exists at least one $\gamma_{i,1} \in \left(\frac{\ln M}{A}, \frac{\ln 10^4 M}{A}\right)$ such that $w\left(\gamma_{i,1}\right) = 0$.

Assume that $\gamma_{i,1}$ is the smallest value that satisfies equation $w\left(\gamma_{i,1}\right) = 0$ and due to the fact that $w\left(\gamma_i = \frac{\ln M}{A}\right) > 0$, then it holds that $w\left(\gamma_i\right) \geq 0$ in the interval $\left[\frac{\ln M}{A}, \gamma_{i,1}\right]$. Thus, the condition $\frac{\partial^2 U_i}{\partial p_i \partial r_i} \geq 0$ when considering macro real time users is satisfied in the interval:

$$\gamma_i \in \left[\frac{\ln M}{A}, \gamma_{i,1}\right]$$

- **Case 2: Femto Real Time Users**
  Considering the second partial derivative for femto real time users: $\frac{\partial^2 U_i}{\partial p_i \partial r_i} = \frac{MA^2}{p_i^2}\left(1 - e^{-A\gamma_i}\right)^{M-2} \cdot w\left(\gamma_i\right)$. Following the same approach as in Case 1, we conclude that condition $\frac{\partial^2 U_i}{\partial p_i \partial r_i} \geq 0$ when considering femto real time users is satisfied in the interval as well:

$$\gamma_i \in \left[\frac{\ln M}{A}, \gamma_{i,1}\right]$$

- **Case 3: Macro Non-Real Time Users**
  Considering the second partial derivative for this user class, it is $\frac{\partial^2 U_i}{\partial p_i \partial r_i} = \frac{MA}{p_i^2 \ln 10} \cdot g\left(\gamma_i\right)$, where

$$g\left(\gamma_i\right) = \frac{\left(1-e^{-A\gamma_i}\right)^{M-2} e^{-A\gamma_i}\gamma_i}{1+\left(1-e^{-A\gamma_i}\right)^M} \cdot \left\{\left(1 - e^{-A\gamma_i}\right) - A\left(M-1\right)e^{-A\gamma_i}\gamma_i + A\left(1 - e^{-A\gamma_i}\right)\gamma_i\right\} + AM\left[\frac{\left(1-e^{-A\gamma_i}\right)^{M-1} e^{-A\gamma_i}\gamma_i}{1+\left(1-e^{-A\gamma_i}\right)^M}\right]^2 + \frac{\ln\left[1+\left(1-e^{-A\gamma_i}\right)^M\right]}{AM}$$

  In order to find the interval with reference to γ_i, we have to examine the inequality $g\left(\gamma_i\right) \geq 0$. In this case, Bolzano theorem is utilized again, as follows: For $\gamma_i = \frac{\ln M}{A}$, it is

$$g\left(\gamma_i = \frac{\ln M}{A}\right) = \frac{1}{AM}\left(\frac{M-1}{M}\right)^{M-1} \frac{\ln M}{1+\left(\frac{M-1}{M}\right)^M} + \frac{1}{AM}\left\{\left(\frac{M-1}{M}\right)^{M-1} \frac{\ln M}{1+\left(\frac{M-1}{M}\right)^M}\right\}^2 - \frac{\ln\left(1+\left(\frac{M-1}{M}\right)^M\right)}{AM} > 0$$

  for various packet sizes, i.e., $M \in (1, 1000)$ and $A \in (0.1, 100)$.
  For $\gamma_i = \frac{\ln 10^4 M}{A}$, $M > 1$ and given the assumption $\frac{10^4 M - 1}{10^4 M} \to 1$, then:

$$g\left(\gamma_i = \frac{\ln 10^4 M}{A}\right) = \frac{\frac{1}{10^4 M}\frac{\ln 10^4 M}{A}}{2} \cdot \left(1 + \frac{9999}{10^4}\ln 10^4 M\right) + \left(\frac{1}{2}\frac{\ln 10^4 M}{10^4}\right)^2 \frac{1}{AM} - \frac{\ln 2}{AM} < 0$$

  for various packet sizes, i.e., $M \in (1, 1000)$ and $A \in (0.1, 100)$. Thus, we conclude that $g\left(\gamma_i = \frac{\ln M}{A}\right) \cdot g\left(\gamma_i = \frac{\ln 10^4 M}{A}\right) < 0$ and due to the fact that $g\left(\gamma_i\right)$ is continuous and $C^{(n)}$ differentiable with respect to γ_i, $\forall \gamma_i \geq 0$ we conclude that there exists at least one $\gamma_{i,2} \in \left(\frac{\ln M}{A}, \frac{\ln 10^4 M}{A}\right)$, such that $g\left(\gamma_{i,2}\right) = 0$. Moreover, due to the fact that $g\left(\frac{\ln M}{A}\right) > 0$, then we conclude that $g\left(\gamma_i\right) \geq 0$ in the interval:

$$\gamma_i \in \left[\frac{\ln M}{A}, \gamma_{i,2}\right]$$

- **Case 4: Femto Non-Real Time Users**

  Considering the second order partial derivative, $\frac{\partial^2 U_i}{\partial p_i \partial r_i} = \frac{MA}{p_i^2 \ln 10} \cdot g\left(\gamma_i\right)$. Observing the latter equation we can follow the same approach as in Case 3, concluding that the required condition is satisfied in the interval

$$\gamma_i \in \left[\frac{\ln M}{A}, \gamma_{i,2}\right]$$

The proof is completed via combining relations from all 4 examined cases. Hence, MUPRAF game's utility function $U_i\left(\mathbf{p}, \mathbf{r}\right)$ is supermodular in (p_i, r_i), for fixed $\left(\mathbf{p}_{-\mathrm{i}}, \mathbf{r}_{-\mathrm{i}}\right)$, i.e., $\frac{\partial^2 U_i}{\partial p_i \partial r_i} \geq 0$ if and only if $\gamma_i \in \left[\frac{\ln M}{A}, \gamma_{i,k}\right]$, where $\gamma_{i,k} = \min\left\{\gamma_{i,1}, \gamma_{i,2}\right\}$.

□

Moreover, in the following lemma, we examine the conditions (2.29) and (2.30), considering MUPRAF game.

Lemma 12. ***(MUPRAF Game Increasing Differences:)*** *MUPRAF game's* $G = \left[S, \{A_i\}_{i\in S}, \{U_i\}_{i\in S}\right]$ *utility function* $U_i(\mathbf{p}, \mathbf{r})$ *as defined in (2.24) has increasing differences in* $\left\{(p_i, r_i), (\mathbf{p}_{-\mathrm{i}}, \mathbf{r}_{-\mathrm{i}})\right\}$*, i.e., conditions:* $\frac{\partial^2 U_i}{\partial p_i \partial p_j} \geq 0, \forall j \neq i$ *and* $\frac{\partial^2 U_i}{\partial p_i \partial r_j} = 0, \forall j \neq i$*, hold true, if and only if:*

$$\gamma_i \geq \frac{\ln M}{A} \tag{2.32}$$

Proof. Aiming at proving that the utility function $U_i(p_i, r_i)$ of MUPRAF game has increasing differences in $\left\{(p_i, r_i), (\mathrm{p}_{-\mathrm{i}}, \mathrm{r}_{-\mathrm{i}})\right\}$, we have to prove the validity of the following two conditions:

$$\frac{\partial^2 U_i}{\partial p_i \partial r_j} = 0, \forall j \neq i \quad and \quad \frac{\partial^2 U_i}{\partial p_i \partial p_j} \geq 0, \forall j \neq i \tag{2.33}$$

Four discrete cases are examined as in the previous proof.

- **Case 1: Macro Real Time Users**

  Considering the second order partial derivative,

  $$\frac{\partial^2 U_i}{\partial p_i \partial p_j} = \frac{MA^2}{p_i^2} r_i \frac{h_{ij}}{I} \left(1 - e^{-A\gamma_i}\right)^{M-2} \cdot e^{-A\gamma_i} \gamma_i^2 \left(1 - Me^{-A\gamma_i}\right)$$

  where $I = \sigma^2 + \sum_{j\neq i} h_{ij} p_j$ is the interference sensed by user i (as caused by the rest of the users). Examining each factor of the latter equation, we conclude that

  $$\frac{\partial^2 U_i}{\partial p_i \partial p_j} \geq 0, \forall j \neq i \Leftrightarrow \gamma_i \geq \frac{\ln M}{A}$$

- **Case 2: Femto Real Time Users**
  Same as in Case 1: $\frac{\partial^2 U_i}{\partial p_i \partial p_j} \geq 0, \forall j \neq i \Leftrightarrow \gamma_i \geq \frac{\ln M}{A}$

- **Case 3: Macro Non-Real Time Users**
  Considering the second order partial derivative, we have:

  $$\frac{\partial^2 U_i}{\partial p_i \partial p_j} = \frac{r_i}{p_i^2 \ln 10} \frac{h_{ij}}{I} \frac{A^2 M \left(1-e^{-A\gamma_i}\right)^{M-2} e^{-A\gamma_i} \gamma_i^2}{1+\left(1-e^{-A\gamma_i}\right)^M} \cdot \left\{1 + Me^{-A\gamma_i} \left[\frac{\left(1-e^{-A\gamma_i}\right)^{M+2}}{1+\left(1-e^{-A\gamma_i}\right)^M} - 1\right]\right\}$$

  We denote as: $\tau(\gamma_i) = 1 + Me^{-A\gamma_i} \left[\frac{\left(1-e^{-A\gamma_i}\right)^{M+2}}{1+\left(1-e^{-A\gamma_i}\right)^M} - 1\right]$ and once more apply Bolzano Theorem. For $\gamma_i = 0$, we have: $\tau(\gamma_i = 0) = 1 - M < 0, \forall M > 1$. For $\gamma_i = \frac{\ln M}{A}$, we have: $\tau\left(\gamma_i = \frac{\ln M}{A}\right) = \frac{\left(\frac{M-1}{M}\right)^{M+2}}{1+\left(\frac{M-1}{M}\right)^M} > 0, \forall M > 1$. Thus, it is obtained that $\tau(0) \cdot \tau\left(\frac{\ln M}{A}\right) < 0$ and due to the fact that function $\tau(\gamma_i)$ is continuous in $\gamma_i \in (0, +\infty)$, then there exists at least one $\gamma_{i,BOL} \in \left(0, \frac{\ln M}{A}\right)$ such that $\tau(\gamma_{i,BOL}) = 0$. We examine the sign of $\tau(\gamma_i)$ and its monotonicity via the first order derivative, i.e., $\frac{\partial \tau(\gamma_i)}{\partial \gamma_i}$. We conclude that $\frac{\partial \tau(\gamma_i)}{\partial \gamma_i} > 0, \forall \gamma_i > 0$ and $\tau(\gamma_i)$ is strictly increasing for $\gamma_i > 0$. Given the above observation, we conclude that the value $\gamma_{i,BOL} \in \left(0, \frac{\ln M}{A}\right)$, such that $\tau(\gamma_{i,BOL}) = 0$ is unique due to the monotonicity of $\tau(\gamma_i)$, $\forall \gamma_i > 0$ and $\tau(\gamma_i) \geq 0, \gamma_i \in [\gamma_{i,BOL}, +\infty)$ holds true, where $\gamma_{i,BOL} \in \left(0, \frac{\ln M}{A}\right)$, thus also exists that

  $$\frac{\partial^2 U_i}{\partial p_i \partial p_j} \geq 0, \forall j \neq i \Leftrightarrow \gamma_i \in [\gamma_{i,BOL}, +\infty)$$

- **Case 4: Femto Non-Real Time Users**
  Identical to Case 3 for $\frac{\partial^2 U_i}{\partial p_i \partial p_j} = \frac{r_i}{p_i^2 \ln 10} \frac{h_{ij}}{I} \frac{A^2 M \left(1-e^{-A\gamma_i}\right)^{M-2} e^{-A\gamma_i} \gamma_i^2}{1+\left(1-e^{-A\gamma_i}\right)^M} \cdot \tau(\gamma_i)$ it is identified that

$$\frac{\partial^2 U_i}{\partial p_i \partial p_j} \geq 0, \forall j \neq i \Leftrightarrow \gamma_i \in [\gamma_{i,BOL}, +\infty)$$

Combining all four cases, the utility function $U_i(\mathbf{p}, \mathbf{r})$ has increasing differences in $\left\{(p_i, r_i), (\mathrm{p}_{-\mathrm{i}}, \mathrm{r}_{-\mathrm{i}})\right\}$ if $\gamma_i \in \left[\frac{\ln M}{A}, +\infty\right)$.

□

From Lemmas 11 and 12, we easily conclude the following.

Lemma 13. ***(Supermodularity of MUPRAF Game in Modified Strategy Space:)*** *The MUPRAF game $G = \left[S, \{A_i\}_{i\in S}, \{U_i\}_{i\in S}\right]$ is smooth supermodular in a modified strategy space $A_i{}'$, if for all $i, i \in S$:*

$$\gamma_i \in \left[\frac{\ln M}{A}, \gamma_{i,k}\right] \tag{2.34}$$

where $\gamma_{i,k} = \min\{\gamma_{i,1}, \gamma_{i,2}\}$

It should be noted that MUPRAF game is characterized by an exogenous parameter, i.e., the pricing factor, that cannot be controlled by the users. MUPRAF game G with exogenous parameter $\varepsilon = -c$ is said to be supermodular, or it is a parameterized game with complementarities, if $U_i(p_i, r_i, \mathrm{p}_{-\mathrm{i}}, \mathrm{r}_{-\mathrm{i}}, \varepsilon)$ has increasing differences in $\left(p_i, \mathbf{p}_{-\mathrm{i}}\right)$ and (p_i, ε), as well as in $\left(r_i, \mathbf{r}_{-\mathrm{i}}\right)$ and (r_i, ε) for all $i, i \in S$.

Lemma 14. ***(Exogenous parameter for MUPRAF game:)*** *MUPRAF game with exogenous parameter $\varepsilon = -c$ is a supermodular game.*

Proof. To prove that MUPRAF game with exogenous parameter $\varepsilon = -c$ is a supermodular game, the necessary condition for supermodularity is:

$$\frac{\partial^2 U_i}{\partial p_i \partial \varepsilon} \geq 0 \quad and \quad \frac{\partial^2 U_i}{\partial r_i \partial \varepsilon} \geq 0 \tag{2.35}$$

The following table summarizes the second order partial derivatives for all types of users.

Table 2.7: Increasing differences per different user class for MUPRAF game

	RT		**NRT**	
Increasing Differences in	(p_i, ε)	(r_i, ε)	(p_i, ε)	(r_i, ε)
MU	$\frac{\partial^2 U_i}{\partial p_i \partial \varepsilon} = 0$	$\frac{\partial^2 U_i}{\partial r_i \partial \varepsilon} = 0$	$\frac{\partial^2 U_i}{\partial p_i \partial \varepsilon} = 0$	$\frac{\partial^2 U_i}{\partial r_i \partial \varepsilon} = 0$
FU	$\frac{\partial^2 U_i}{\partial p_i \partial \varepsilon} = e^{p_i} > 0$	$\frac{\partial^2 U_i}{\partial r_i \partial \varepsilon} = 0$	$\frac{\partial^2 U_i}{\partial p_i \partial \varepsilon} = e^{p_i} > 0$	$\frac{\partial^2 U_i}{\partial r_i \partial \varepsilon} = 0$

Based on the above, it is easily concluded that condition (2.35) holds true $\forall \gamma_i > 0, \forall i \in S$, hence MUPRAF game with exogenous parameter $\varepsilon = -c$ is supermodular in A_i, thus in $A_i{}' \subseteq A_i$.

□

Proving that MUPRAF game is supermodular in the modified strategy space $A_i{}' \subseteq A_i$, guarantees the existence of a non-empty set of Nash equilibria [65]. Therefore, the following holds:

Lemma 15. ***(MUPRAF Game NE Existence:)*** *Modified MUPRAF game $G' = \left[S, \left\{A_i{}'\right\}_{i\in S}, \{U_i\}_{i\in S}\right]$ has at least one NE [62], which is defined as:*

$$(p_i{}^*, r_i{}^*) = \arg\max_{p_i, r_i \in A_i{}'} U_i(\mathrm{p}, \mathrm{r}) \tag{2.36}$$

It should be noted that Lemma 15 guarantees the existence of at least one NE point of the modified MUPRAF game, while this point is not necessarily unique. Practically, the best response equation in (2.36) can be solved via multi-variable calculus (i.e., second partial derivative test) utilizing the Extreme Value Theorem [81], and the most energy-efficient Nash Equilibrium (i.e., the NE characterized by less power p_i, while guaranteeing users' QoS prerequisites' satisfaction, which is reflected by the value of uplink transmission rate r_i) is adopted by each user. However, the NE point $(\mathbf{p}^*, \mathbf{r}^*)$ is a stable solution of optimization problem in (2.25) that maximizes each user's utility function.

Convergence

In this section, the convergence of MUPRAF game to its NE point $(\mathbf{p}_\mathrm{i}, \mathbf{r}_\mathrm{i})$ is shown. Based on Lemma 15, user's best response strategy $BR_i\left(\mathbf{p}_{-\mathrm{i}}, \mathbf{r}_{-\mathrm{i}}\right)$ to the strategies $\left(\mathbf{p}_{-\mathrm{i}}, \mathbf{r}_{-\mathrm{i}}\right)$ actually chosen by other players is denoted as follows:

$$BR_i\left(\mathbf{p}_{-\mathrm{i}}, \mathbf{r}_{-\mathrm{i}}\right) = (p_i^*, r_i^*) = \underset{p_i, r_i \in A_i{}'}{\arg\max}\, U_i\left(p_i, r_i, \mathbf{p}_{-\mathrm{i}}, \mathbf{r}_{-\mathrm{i}}\right) \tag{2.37}$$

Lemma 16. ***(MUPRAF Game Convergence:)*** *Modified MUPRAF game* $G' = \left[S, \left\{A_i{}'\right\}_{i\in S}, \{U_i\}_{i\in S}\right]$ *converges to its NE point starting from any initial point.*

Proof. By definition, the NE point of a non-cooperative game has to satisfy: $BR_i\left(\mathbf{p}_{-\mathrm{i}}, \mathbf{r}_{-\mathrm{i}}\right) = (p_i^*, r_i^*)$. Aiming at showing that the modified MUPRAF game converges to its NE, we have to prove that user's best response strategy function is standard [82], [14]. A function f is characterized as standard, if the following conditions hold true:

1. Positivity: $f(\mathbf{x}) > 0$
2. Monotonicity: if $\mathbf{x} \geq \mathbf{x}^{'}$, then $f(\mathbf{x}) \geq f(\mathbf{x}^{'})$ and
3. Scalability: for all $a > 1$, $af(\mathbf{x}) \geq f(a\mathbf{x})$

for all $\mathbf{x} \geq 0$, where $\mathbf{x} = (x_1, x_2, ..., x_N)$ is a NE. Considering the modified MUPRAF game, we easily conclude that the above conditions hold true, as follows:

1. $(\mathbf{p}, \mathbf{r}) > \mathbf{0}$, thus $\mathbf{BR}(\mathbf{p}, \mathbf{r}) > \mathbf{0}$, via relation (2.37)
2. if $(\mathbf{p}, \mathbf{r}) > (\mathbf{p'}, \mathbf{r'})$ then via (2.37) it is concluded that $\mathbf{BR}(\mathbf{p}, \mathbf{r}) > \mathbf{BR}(\mathbf{p'}, \mathbf{r'})$
3. for all $a > 1$, since $\mathbf{BR}(\mathbf{p}, \mathbf{r})$ is a strictly increasing function with respect to $(\mathbf{p}, \mathbf{r})$, then $a\mathbf{BR}(\mathbf{p}, \mathbf{r}) > \mathbf{BR}(a\mathbf{p}, a\mathbf{r})$

□

2.5.3 Distributed Algorithm

In this section we propose a distributed, iterative, and low complexity algorithm, which determines the NE point of MUPRAF game starting from any initial feasible point. The algorithm is referred to as MUPRAF algorithm and consists of two parts, i.e., the Network Part and the User Part.

Considering the Network Part of MUPRAF algorithm, it is implemented at each FAP and is responsible for obtaining the best pricing factor for FUs. This pricing factor is determined via an exhaustive search following similar approaches proposed in the literature [10,28,29,80]. Starting from an initial value of c, e.g., $c = 0$, an iterative approach is followed by increasing c by Δc until an increase in c results in utility levels worse than the previous equilibrium values for at least one user. In other words, if the pure utility value of at least one user (either macro or femto user) is worse than the previous equilibrium utility, then the Network Part of MUPRAF algorithm stops and sets $c = c_{best}$. Following this process, it is noted that the best pricing factor is determined via an exhaustive search in the feasible interval of pricing factor's values, i.e., $c > 0$, however the processing time remains low, due to the simplified calculations. Moreover, as confirmed by the results presented later in Fig. 2.15, the sum of equilibrium utilities for all users obtains its highest value for $c = c_{best}$.

Algorithm 5 MUPRAF Algorithm: A. Network Part

1: Each FAP announces the initial pricing factor $c = 0$ to the FUs residing in each cell.
2: $i = 1 : N$, $\forall i \in S$
3: Determine the NE point $\left(p_i^\star, r_i^\star\right)$ (according to User Part MUPRAF algorithm).
4: Compute the pure utility $U_i\left(p_i^\star, r_i^\star\right)$ (without the penalty, i.e., cost function).
5: Increase the pricing factor $c := c + \Delta c$, where Δc is a small positive constant.
6: Announce it to all FUs.
7: If $U_i(c) < U_i(c + \Delta c)$, $\forall i \in S$, then go to step 2, else stop and declare $c_{best} = c$.
8: end.

Algorithm 6 MUPRAF Algorithm: B. User Part

1: Set $ite = 0$, where ite denotes the iteration index. Select a random feasible uplink transmission power: $p_i^{(ite=0)}$ and rate $r_i^{(ite=0)}$ from the modified strategy space A_i'.
2: The BS/FAP broadcasts the overall users' interference.
3: $i = 1 : N$, $\forall i \in S$
4: Compute the sensed interference by user i, as $I_{-i}^{(ite)}\left(p_{-i}^{(ite)}\right) = \sigma^2 + \sum\limits_{k \neq i} h_{kl} p_k$.
5: Refine $p_i^{(ite+1)}$ and $r_i^{(ite+1)}$, in accordance to Eq. (2.36)
6: $|p_i^{(ite+1)} - p_i^{(ite)}| \leq \epsilon$ and $|r_i^{(ite+1)} - r_i^{(ite)}| \leq \epsilon$ (ϵ: small positive constant), the powers and rates have converged and stop.
7: end
8: otherwise, set $ite := ite + 1$ and return to step 2.

On the other hand, the User Part is executed by each user in the network (i.e., both macro and femto users) in a distributed manner so that the NE point of MUPRAF game is determined, i.e., each user determines its optimal uplink transmission power and rate $(\mathbf{p}, \mathbf{r})$.

It should be noted that MUPRAF algorithm is executed in a distributed manner, due to the fact that the decision making process lies on the user. Assuming that the BS/FAP has perfect channel state information of each user, the only information that is broadcasted by the BS/FAP is the overall interference $\left(I^{(k)}(p^{(k)})\right)$, while each user calculates its sensed interference $\left(I_{-i}^{(k)}(p_{-i}^{(k)})\right)$, excluding its contributing factor, i.e., $h_{ii}p_i$, from $I^{(k)}(p^{(k)})$. Moreover, the convergence of MUPRAF algorithm, in terms of necessary iterations, is thoroughly evaluated in the following section, demonstrating the fast convergence property of the algorithm.

2.5.4 Numerical Results

In this section we provide some numerical results evaluating the operational features and performance of the proposed MUPRAF algorithm. Initially, we focus on the operation performance achievements of MUPRAF algorithm, in terms of uplink transmission power and achievable data rate considering that all users, i.e., both MUs and FUs request one type of service. Moreover, the fast convergence of MUPRAF algorithm is shown and the best pricing factor for FUs is determined. Then, we provide a comparative evaluation of our proposed approach against other existing approaches in the literature with respect to several metrics and considering various scenarios. Specifically, our proposed framework and the framework presented in [80] (i.e., Section 2.4), which also aims at jointly allocating users' uplink transmission power and data rate in two-tier femtocell networks, are thoroughly compared in order to illustrate the obtained gain in uplink transmission power and corresponding energy-efficiency, when user's service differentiation is considered. Following, we study cell's capacity in terms of number of users that meet their QoS prerequisites under increasing number of FAPs and users residing within the macrocell for several approaches and scenarios. Specifically, comparative results are presented that illustrate the effectiveness of MUPRAF framework, in terms of decreased users' uplink transmission power and increased uplink transmission data rate compared to other approaches proposed in the literature, i.e., [33, 34, 80].

MUPRAF Properties and Operation

In the following, we consider a two-tier femtocell system supporting 20 backlogged MUs. We assume 20 FAPs residing within the macrocell, where each FAP serves 4 users. The considered topology supports a large set of users, i.e., 100 users in total. The radius of the macrocell is set to $R_0 = 290m$ m and of each FAP $R_c = 50m$. Transmission power is $P_i^{Max} = 0.2W$, the adopted efficiency function is $f(\gamma_i) = \left(1 - e^{-1.5\gamma_i}\right)^{80}$ and the spread spectrum bandwidth is $W = 3.84 \times 10^6$ Hz [10].

In this subsection, we assume that all users (FUs and MUs), request the same type of service, i.e., target at the same uplink transmission data rate, e.g., $128kbps$ (i.e., simple video upload), in order to better illustrate and comprehend the operation characteristics and effectiveness of the MUPRAF framework. A representative topology of the scenario under consideration is the one presented in Fig. 2.14.

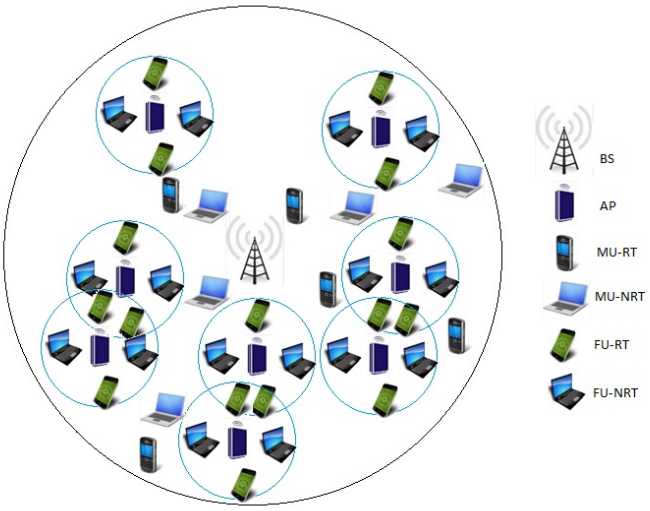

Figure 2.14: Conceptual multi-service two-tier femtocell topology

Fig. 2.15 illustrates the sum of utilities at the equilibrium point $\left(\mathbf{p}^\star, \mathbf{r}^\star\right)$ as a function of the pricing factor c. The diagram is constructed via MUPRAF algorithm (Network Part) and estimates the "best" value of pricing factor c, i.e., c_{best} which is imposed by the system to the users towards adopting a more social behavior in terms of resources' usage.

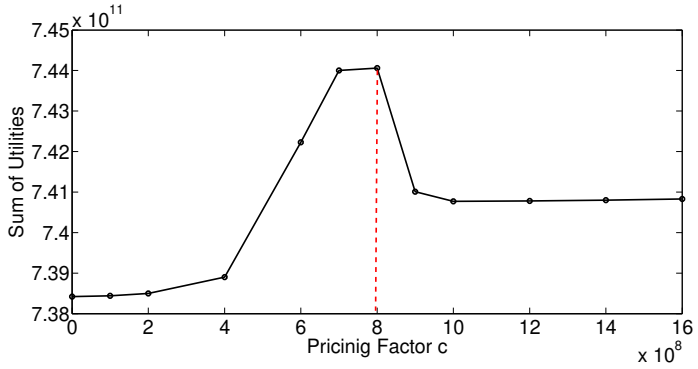

Figure 2.15: MUPRAF game sum of equilibrium utilities as a function of the pricing factor c

Fig. 2.16a illustrates users' uplink transmission power evolution as a function of the iterations required for MUPRAF algorithm to converge at MUPRAF game's Nash equilibrium point $\left(\mathbf{p}^\star, \mathbf{r}^\star\right)$ at the time slot t under consideration for the following indicative cases: a) MU closest to the BS, b) most distant MU from the BS, c) average MUs' uplink transmission power, and d) average FUs' uplink transmission power. The results reveal that as MUs channel conditions become worse (i.e., distant users from the

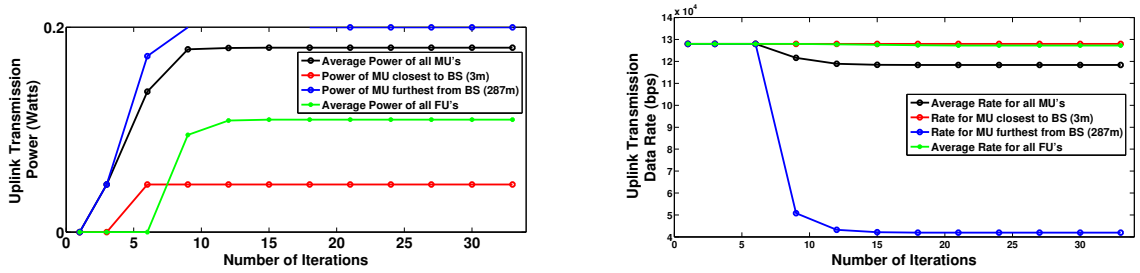

(a) MUs and FUs uplink transmission power convergence (y-axis in logarithmic scale)

(b) MUs and FUs uplink transmission data rate convergence

Figure 2.16: Convergence at Nash equilibrium under MUPRAF algorithm

base station) and in order to satisfy their QoS prerequisites their uplink transmission power increases as expected.

Moreover, average FUs' uplink transmission power is considerably lower compared to the corresponding average value of MUs, due to FUs' close proximity to the femtocell AP and the convex pricing policy that encourages FUs to utilize more efficiently their power and thus causing less interference to the MUs. Finally, the overall MUPRAF framework is characterized as energy-efficient, due to the fact that both FUs and especially MUs transmit with low uplink transmission power, i.e., they do not exhaust their maximum uplink transmission power $P_i^{Max} = 0.2W$, except for the edge MUs due to their increased distance from the BS.

Similarly, Fig. 2.16b presents the corresponding uplink transmission data rate at the Nash equilibrium point $(\mathbf{p}^\star, \mathbf{r}^\star)$ of MUPRAF game, as a function of the iterations that MUPRAF algorithm needs to converge to the stable solution, for the same cases (i.e., a) MU closest to the BS, b) most distant MU from the BS, c) average MUs' transmission rate, and d) average FUs' transmission rate). Based on the results, we observe that the majority of MUs even though they suffer from worse channel conditions compared to FUs, achieve high uplink transmission data rate, thus fulfilling their QoS prerequisites. Only the more distant users from the base station (i.e., edge users) achieve lower transmission data rate, due to their corresponding extremely bad channel conditions. Based on Fig. 2.16b, we observe that the average uplink transmission data rate of FUs is close to the target value, i.e., $128kbps$, while the corresponding average value for MUs is $120kbps$. The percentage of satisfied users, i.e., both MUs and FUs is 96%, while the corresponding percentage value considering only the MUs is 90%.

Furthermore, based on the results presented in Fig. 2.16a and Fig. 2.16b, we observe that the convergence of the proposed algorithm is very fast, since less than thirty iterations are required for reaching equilibrium for all users, starting from randomly selected initial values, while for all practical purposes we can observe that in less than fifteen iterations the values of the powers, as well as rates have very closely approximated their corresponding equilibrium values. MUPRAF algorithm – User Part as described in Section 2.5.3, is responsible to determine users' optimal uplink transmission power and rate. Its distributed nature ensures the scalability of the proposed framework, in the sense that algorithm's complexity does not directly depend on the number of users in the overall network. MUPRAF algorithm was tested and evaluated in an Intel (R) Core (TM) 2 DUO CPU T7500 @ 2.20GHz laptop with 2.00 GBytes available RAM and its runtime was 0.4 $msec$. The necessary time in order to converge to the Nash equilibrium point is of similar order of magnitude with the duration of a timeslot (0.5 $msec$), thus it can be easily adopted in a realistic scenario. It should be also noted that the convergence time of MUPRAF algorithm can further decrease, if we adopt a more "educated" implementation of the algorithm, i.e., utilize as initial values of the powers and rates the corresponding values that were calculated in the previous time slot, similar to the case studies in the previous section.

Service Differentiation and Energy-Efficiency

In this subsection, we provide some numerical results illustrating the performance of MUPRAF when service differentiation is considered. For comparison purposes, a simplified topology is considered consisting of 10 MUs and 8 FAPs, where each FAP serves 4 FUs. Two types of services are considered, i.e., real time and non-real time service. The target rate for the real time users is $r_{target} = 128kbps$. Two different scenarios are compared: (i) MUPRAF framework and (ii) the proposed combined uplink

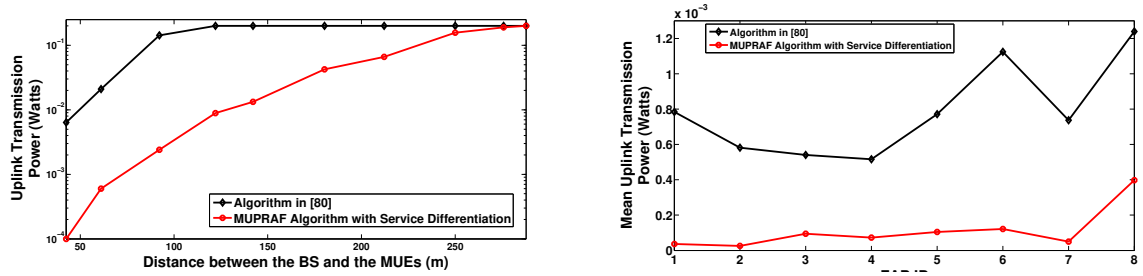

(a) MUs' uplink transmission power as a function of their distance from the BS (y-axis in logarithmic scale)

(b) FUs' mean uplink transmission power as a function of the FAP's ID

Figure 2.17: Uplink transmission power for MUs and FUs

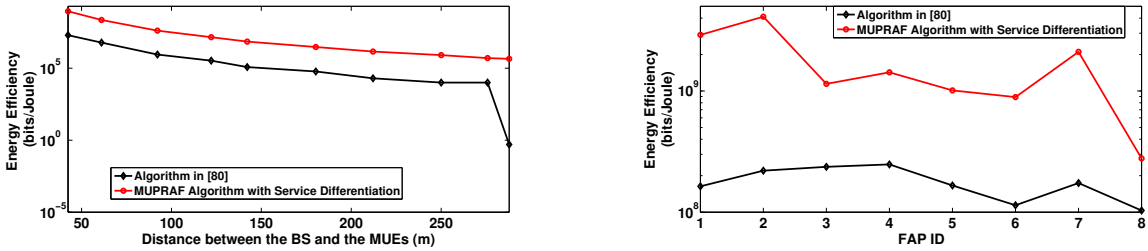

(a) MUs' energy-efficiency as a function of their distance from the BS (y-axis in logarithmic scale)

(b) FUs' mean energy-efficiency as a function of FAP's ID (y-axis in logarithmic scale)

Figure 2.18: Mean energy-efficiency for MUs and FUs

transmission power and data rate allocation in multi-service two-tier femtocell networks, as it has been presented in [80]. It is noted here that the two-variable problem in [80], as already mentioned in Section 2.4 is amended to a single variable problem via substituting the ratio of user's uplink transmission data rate to transmission power with a new single variable.

Fig. 2.17a illustrates MUs uplink transmission power as a function of their position within the macrocell, considering the two comparative scenarios. Furthermore, comparing MUPRAF algorithm with the framework of joint resource allocation in multiservice two-tier femtocell networks, as presented in [80], we observe that MUPRAF achieves an average of 56.70% reduction of users' uplink transmission power. This benefit stems from (i) formulating better users' QoS prerequisites in a two-variable utility function, (ii) solving the joint resource allocation problem as a two-variable optimization problem, where user's uplink transmission power and data rate are determined independently and updated at the same step, and (iii) imposing convex pricing policy with respect to FU's uplink transmission power.

In Fig. 2.17b we present a comparative study of FUs mean uplink transmission power within each FAP residing within the macrocell. The results reveal the superiority of MUPRAF algorithm in terms of power savings. Specifically, comparing the results of MUPRAF algorithm with service differentiation to the corresponding results of the proposed framework in [80], we observe that MUPRAF framework achieves on average 85.67% reduction with respect to power consumption. It should be noted that these great improvements in power savings are obtained, while at the same time similar performance with respect to the transmission rate is achieved for the FUs and even better rates are obtained for the MUs under the MUPRAF framework.

The combined effect of power and rate improvement is depicted in Fig. 2.18a and Fig. 2.18b, where we present MUs' energy-efficiency (EE) $[bits/Joule]$ as a function of their distance from the base station and FUs' mean energy-efficiency within each FAP residing in the macrocell, respectively. Based on these results we clearly confirm that MUPRAF algorithm outperforms the approach in [80] in terms of energy-efficiency as well.

Increasing Number of Users and FAPs

In the following, we present a comparative study illustrating the benefits of the proposed MUPRAF algorithm as the number of MUs and FAPs residing within the macrocell increases (thus respectively

the number of FUs). Specifically, we compare four different approaches: (i) MUPRAF algorithm, (ii) the algorithm presented in [80], (iii) the algorithm in [33], which determines the power and transmission data rate allocation in an one-tier macrocell wireless network via solving the problem as a single variable optimization problem, and (iv) the algorithm in [34], which determines a joint multi-service power and data rate allocation also in a single one-tier macrocell. More specifically, in [33], the combined problem of power and transmission data rate allocation is considered as a single-variable problem of the ratio of uplink transmission data rate to the uplink transmission power in a single macrocell topology and both power and transmission data rate are updated at the same time. Moreover, in [34], the joint resource allocation in a single macrocell topology has been confronted as a two variable problem and users' optimal transmission power and transmission data rate are determined simultaneously and independently.

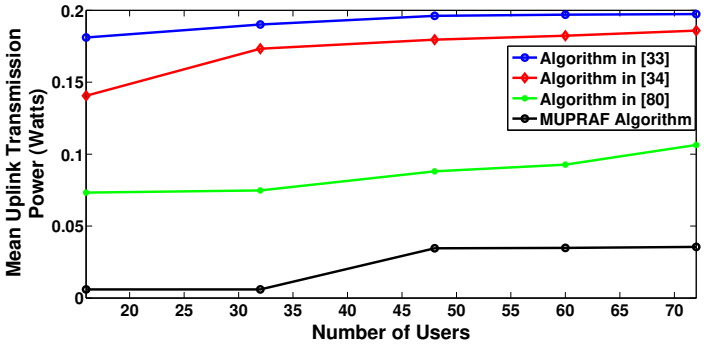

Figure 2.19: Users' mean uplink transmission power as a function of the number of users

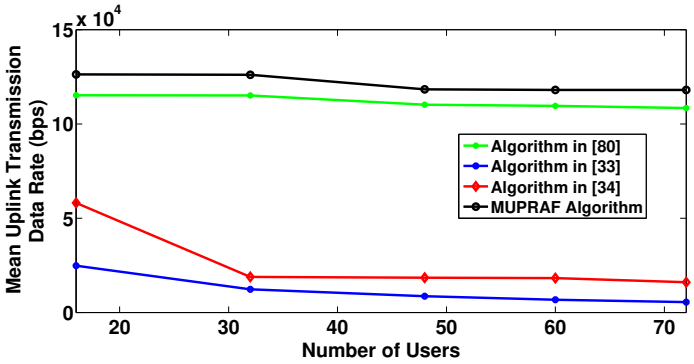

Figure 2.20: Users' mean uplink transmission data rate as a function of the number of users

Specifically, Fig. 2.19 and Fig. 2.20 present users' mean uplink transmission power and data rate as a function of the overall number of users in the cell, respectively. The specific formation of users, i.e., number of MUs and FUs, within the macrocell is presented in Table 2.8, along with the percentage reduction in mean uplink transmission power and increase of mean uplink transmission data rate achieved by the proposed MUPRAF algorithm, when compared to [33, 34, 80], respectively. The results reveal the superiority of the MUPRAF algorithm in terms of both power saving and increase of rate. Finally, it should be noted that the consideration of two-tier femtocell architecture is the key reason why both our framework and [80] significantly outperform [33] and [34] that consider single-tier macrocell architectures.

2.6 Visible Light Communications

With the growing demand for high data rate, support of multiple services with various Quality of Service (QoS) requirements, as well as the advent of numerous wireless devices, the spectrum demand is increasing rapidly. Moreover, energy-efficient solutions are required to extend mobile users' battery life and support the vision of green wireless networking. Towards this direction, Visible Light Communication (VLC) is acknowledged as a promising wireless technology that solves the bandwidth scarcity problem and enables

Table 2.8: Percentage reduction in mean uplink transmission power & increase of mean uplink transmission data rate for MUPRAF algorithm under four comparative scenarios

Number of Users			Comparison to MUPRAF algorithm without service differentiation					
			% reduction in uplink transmission power			% increase of mean uplink transmission data rate		
Only MUs [33], [34]	MUs	FUs	[33]	[34]	[80]	[33]	[34]	[80]
	MUPRAF Algorithm, [80]							
16	8	8	96.69%	95.72%	91.80%	410.02%	117.44%	9.62%
32	8	24	96.84%	96.54%	91.98%	929.02%	569.62%	9.56%
48	12	36	82.36%	80.79%	60.68%	1287.00%	543.56%	7.33%
60	12	48	82.33%	80.91%	62.46%	1660.90%	547.39%	7.71%
72	12	60	82.02%	80.89%	66.60%	2034.20%	637.43%	8.87%

decreased mobile users' transmission power [83]. VLC can ensure ubiquitous ultrahigh speed wireless communication in any indoor environment (e.g., aircraft, hospital, museum etc.) and is characterized by numerous advantages, such as high data rate, mitigated interference, harmlessness to human health, strong security, and unlicensed frequency band usage. A depiction of a two-tier VLC based network is presented in Fig. 2.21.

Prior studies have focused mainly on physical (PHY) and medium access control (MAC) optimal design, without considering mobile users' QoS provisioning [84], [85]. Therefore, in the last years the interest of research community has turned towards optimal resource allocation in order to fulfill users' QoS prerequisites. Two main transmission technologies are adopted in Visible Light Communication Personal Area Networks (VPANs), especially within the emerging era of 5G networks: Orthogonal Frequency Division Multiple Access (OFDMA) [86, 87] and Non-Orthogonal Multiple Access (NOMA). In the recent literature, considerable research efforts have been devoted to the problem of optimal resource allocation in the downlink of VPANs, where OFDMA technology is adopted. In [88], the authors propose an interference bounded opportunistic channel allocation for VPANs towards maximizing the sum rate capacity in the downlink and in parallel allowing maximum number of users with a minimum QoS prerequisite. In [89], an intercell interference coordination heuristic approach is proposed towards realizing subcarrier reuse between different transmitters, as well as power redistribution between different subcarriers. In [90], a centralized joint power and bandwidth allocation for downlink transmission is introduced to maximize system's overall capacity. The authors formulate a user's weighted sum rate maximization problem, which is solved in a centralized manner and concludes to a power and bandwidth allocation. In [91], the authors propose a joint scheduling and optimal resource allocation, via formulating a cross-layer optimization problem towards maximizing the system average throughput under the SINR constraints and solving it in a centralized manner. An interference aware time-frequency slots allocation using busy burst signaling for transmitting data is proposed in [92], where the assignment of time-frequency slots is adjusted dynamically depending on the location of an active user in the cell. In [93], the authors introduce a novel framework towards supporting rapid link recovery and visibility that minimize system's performance degradation. A resource allocation scheme that selects non-overlapping channels having best signal-to-interference-plus-noise ratio and acting indirectly on the interference levels has been proposed in [94], where the visible light multi-color logical channels are allocated in order to minimize the co-channel interference.

Considering the proposed resource allocation problems in VPANs adopting NOMA technology, the performed research is still primitive, due to the fact that NOMA technology has been recently proposed in the literature as a promising candidate for 5G wireless networks. In [95], a channel-dependent power allocation (called gain ratio power allocation) is proposed, considering users' channel conditions to ensure efficient and fair power allocation and targeting at enhancing the achievable throughput in high-rate VLC downlink networks. In [96], the authors propose theoretical expressions on the system performance, considering two different scenarios: (i) ensuring guaranteed quality of service (QoS) and providing system coverage probability and (ii) multiple users request opportunistic best-effort service and calculating system ergodic sum rate in a closed form. However, all the above approaches are centralized and mainly network-

centric and their goal is to guarantee system's welfare and efficiency, e.g., maximization of system's sum rate, system's overall interference mitigation, service provider's profit etc.

In this section, we address the problem of OAP selection and resource allocation, with respect to bandwidth and power, in the uplink of VPANs under two different enabling transmission techniques, i.e., OFDMA and NOMA. Our approach leads towards the creation of a framework where the decision making process lie at the mobile user, irrespectively of the adopted transmission technique, i.e., OFDMA or NOMA, and is well aligned with the current efforts for the realization of mobile user self-optimization functionalities. To the best of our knowledge, this is the first time in the recent literature that the problem of optimal resource allocation in the uplink of VPANs is studied. The main recent research efforts have focused on the problem of optimal resource allocation (e.g., power, bandwidth, and subcarriers) in the downlink, while the corresponding resource allocation problem in the uplink has not yet been studied. The other fundamental contribution of this work is the detailed presented comparison among OFDMA and NOMA transmission techniques, illustrating the advantages and drawbacks of adopting OFDMA or NOMA as the transmission technique in the uplink of VPANs. Detailed numerical results are provided towards better identifying the advantages of each transmission technique with respect to the resource allocation problem.

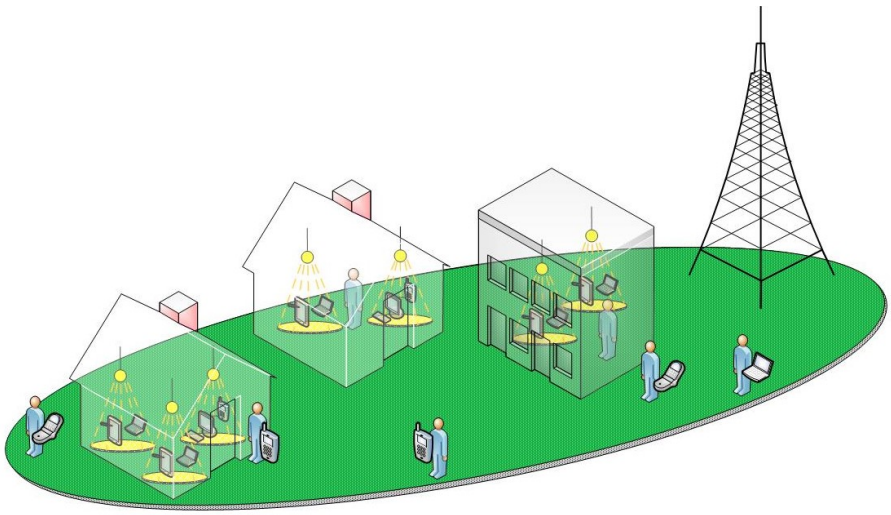

Figure 2.21: Two-tier VLC network topology

2.6.1 System Model

We consider the uplink of a multi-cell VPAN, consisting of T OAPs and U mobile users, where their corresponding sets are denoted as $\mathscr{T} = \{t = 1, 2, ..., T\}$ and $\mathscr{U} = \{u = 1, 2, ..., U\}$, respectively. It should be noted that VLC networks are expected to lie within the coverage area of a macrocell. Each OAP serves a total number of mobile users N_t. A spectrum of total bandwidth W is devoted per each OAP (and its corresponding cell) and is available for transmissions from the OAP to the mobile users and vice versa. Each mobile user $u \in \mathscr{U}$ communicates directly with an OAP $t \in \mathscr{T}$ via a communication link $l = \{u, t\}$. User's uplink transmission power $P_{u,t}$ is upper and lower bounded, i.e., $0 < P_{u,t} \leq P_{u,t}^{Max}$, due to user's physical and technical limitations. Let $H_{u,t}$ be the gain of optical communication link l between user $u \in \mathscr{U}$ to OAP $t \in \mathscr{T}$. The line-of-sight (LOS) DC gain between mobile user $u \in \mathscr{U}$ and OAP $t \in \mathscr{T}$ is given by [97]:

$$H_{u,t} = \begin{cases} \frac{(m+1)A}{2\pi d^2} \cos^m(\varphi)\, T_s(\psi)\, g(\psi) \cos(\psi), & 0 \leq \psi \leq \psi_c \\ 0, & otherwise \end{cases} \tag{2.38}$$

where A denotes the photodetector area, φ the angle of irradiance, $T_s(\psi)$ the signal transmission coefficient of an optical filter, ψ angle of incidence, and m is the order of the Lambertian emission, which is given by:

$$m = -\frac{\ln 2}{\ln\left(\cos \phi_{1/2}\right)} \tag{2.39}$$

where $\phi_{1/2}$ is the transmitter semi-angle at half power. Moreover, $g(\psi)$ denotes the channel gain of an optical concentrator and is given by

$$g(\psi) = \begin{cases} \frac{\alpha^2}{\sin^2(\psi_c)}, & 0 \leq \psi \leq \psi_c \\ 0, & otherwise \end{cases} \tag{2.40}$$

where a denotes the refractive index of the optical concentrator, ψ_c user's field of view (FOV), and d the distance between the OAP and the user. Throughout this work, it is assumed that the proposed OAP selection and resource allocation is based on perfect knowledge of path gain information both at the user and at the OAP. The corresponding optical communication link geometry, as well as the overall topology of the multi-cell VPAN are presented in Fig. 2.22.

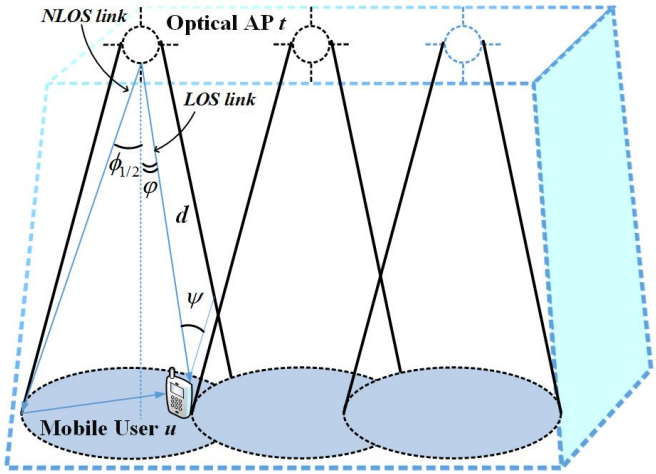

Figure 2.22: Visible light Communication Personal Area Network (VPAN) topology

Transmission Techniques in VPANs

In VPAN, two different transmission technologies have been considered, i.e., OFDMA and NOMA. In the following, some basic background information considering each transmission technology is provided.

Definition 2.6.1. ***OFDMA:*** *Orthogonal Frequency Division Multiple Access (or simply, OFDMA) dictates that bandwidth of each OAP (or any AP) is divided into subcarriers, which are organized into resource blocks (RBs) being allocated to the users. Within the same OAP, each RB is uniquely reserved by one user of the same OAP. The same RBs can be reused among different OAPs, which in turn can cause co-channel interference.*

Let $\mathscr{R} = \{r = 1, 2, ..., R\}$ be the set of available RBs. In the proposed system model, we assume the flat-fading model, i.e., mobile user's channel gain is not differentiated per RB. The signal-to-interference-plus-noise ratio (SINR), $\gamma_{u,t}^{(r)}$ of user $u \in \mathscr{U}$ served by the OAP $t \in \mathscr{T}$ at RB r can be expressed as follows:

$$\gamma_{u,t}^{(r)} = \frac{R_{PD} H_{u,t} P_{u,t}^{(r)}}{\sum\limits_{u'=1, u' \neq u, t \in \mathscr{T}}^{U} H_{u',t} P_{u',t}^{(r)} + \xi} \tag{2.41}$$

where R_{PD} denotes the responsitivity of the photodiode, $H_{u,t}$ the line-of-sight (LOS) path gain between user $u \in \mathscr{U}$ and OAP $t \in \mathscr{T}$ for RB r, and ξ is the cumulative noise power, which is given by

$$\xi = 2qR_{PD}I_{amb}B_{noise} + \frac{4K_BTB}{R_F} \tag{2.42}$$

where $q = 1.6 \cdot 10^{-19}C$, I_{amb} denotes the ambient light intensity, B_{noise} the equivalent noise bandwidth, K_B Boltzmann's constant, T the absolute temperature, and R_F the transimpedance amplifier gain.

Definition 2.6.2. ***NOMA:*** *Non-Orthogonal Multiple Access (NOMA) transmission technique is designed on the principle that users accommodated in the same OAP (or cell in general) can simultaneously exploit the entire bandwidth, thus concluding to significant enhancement in the achievable rate. More specifically, users are multiplexed in the power domain using superposition coding at the transmitter's side and successive interference cancellation (SIC) at the receiver. Based on SIC technology, the multi-user interference is mitigated and signals' decoding is performed in the order of decreasing channel gain in the uplink of the network. Based on this order, each user can correctly decode the signals of all users with worse channel gain. The interference from users with better channel gain is not mitigated, thus it is treated as noise.*

Therefore, user's SINR in the NOMA technology can be calculated as follows:

$$\gamma_{u,t} = \frac{R_{PD}H_{u,t}P_{u,t}}{\sum\limits_{u'>u,t\in\mathrm{T}}^{U} H_{u',t}P_{u',t} + \xi} \tag{2.43}$$

where u' is the first user in the OAP having worse channel gain compared to u.

User's QoS Requirements Utility Function

Towards verifying users' preference relations that are specific to the examined problem, the concept of utility function that satisfies this structure is similarly used in this section as well. A mobile user should transmit with low uplink transmission power in order to extend its battery lifetime and at the same time cause less interference in the multi-cell VPAN environment. Furthermore, mobile users' satisfaction increases by achieving high uplink transmission data rate, which is appropriately reflected by the number of reliably transmitted bits to the OAP. Based on these observations, each user adopts a utility function, which represents its degree of satisfaction in relation to the expected tradeoff between the number of information bits that are successfully transmitted to the OAP and user's corresponding power consumption. Therefore in alignment with the above claims the utility functions assumed here for the OFDMA and NOMA cases are as follows:

$$\begin{aligned} OFDMA:\ U_{u,t}^{(r)} &= \frac{W \cdot f_u\left(\gamma_{u,t}^{(r)}\right)}{N_t \cdot P_{u,t}^{(r)}} \\ NOMA:\ U_{u,t} &= \frac{W \cdot f_u\left(\gamma_{u,t}\right)}{P_{u,t}} \end{aligned} \tag{2.44}$$

where N_t denotes the number of users served by the OAP t, W is OAP's $t \in \mathscr{T}$ bandwidth, and $f_u(\cdot)$ is the efficiency function.

Optical Access Point Selection

The topology that is considered in this case is a multicell VPAN. As presented in Fig. 2.22, a mobile user can reside within the coverage area of multiple OAPs. Therefore, a sophisticated OAP selection mechanism should be proposed towards mitigating the overall interference in the multicell VPAN. The proposed OAP selection methodology is based on Maximum Gain Selection (MGS) policy. According to the MGS policy, each user residing in the multi-cell VPAN selects the OAP to which it will be associated based on the highest path gain $H_{u,t}$ between itself, i.e., $u \in \mathscr{U}$ and all available OAPs $t \in \mathscr{T}$ that it is able to connect to. This method provides a near-optimum solution achieving multi-user, as well as multiple OAPs diversity and channel gain diversity. However, it should be noted that MGS policy is neither necessary nor sufficient for optimality. More specifically, the matrix $\mathbf{H}$ is created, which is structured based on the line-of-sight (LOS) channel gain $H_{u,t}$ between each user $u \in \mathscr{U}$ and OAP $t \in \mathscr{T}$.

$$\mathbf{H}(u,t) = \begin{bmatrix} H_{1,1}H_{1,2}...H_{1,T} \\ H_{2,1}H_{2,2}.... \\ ..... \\ ..... \\ H_{U,1}H_{U,2}...H_{U,T} \end{bmatrix} \tag{2.45}$$

According to users' path gain matrix $\mathbf{H}$, each user selects the OAP to connect to and communicate with based on MGS policy as follows:

$$l^* = \{u^*, t^*\} = \arg\max_{t \in \mathrm{T}} \mathbf{H}(u,t) \tag{2.46}$$

It should be noted that after the OAP selection process, each OAP $t \in \mathscr{T}$ knows the number of users N_t that are connected to its corresponding cell. It is obvious that the number of users N_t, residing in each OAP's cell is a time-varying parameter due to users' mobility. Moreover, users' path gains $H_{u,t}$ are also time-varying variables, thus the problem of OAP selection should be solved periodically per time-slot. For clarity, we assume static users' positions within the multi-cell indoor environment. All notations used in this section are summarized in Table 2.9.

Table 2.9: Section 2.6 list of key notations

Symbol	**Description**
T	Number OAPs
U	Number of mobile users
$\mathscr{T}$	Set of OAPs
$\mathscr{U}$	Set of users
N_t	Total number of mobile users
l	Communication link
$P_{u,t}$	Uplink transmission power
$H_{u,t}$	Optical communication link gain
A	Photodetector area
φ	Angle of irradiance
$T_s(\psi)$	Signal transmission coefficient of an optical filter
ψ	Angle of incidence
m	Order of the Lambertian emission
$\phi_{1/2}$	transmitter semi-angle at half power
$g(\psi)$	Channel gain of optical concentrator
a	Refractive index of the optical concentrator
ψ_c	Field of view
d	Distance between OAP and user
$\mathscr{R}$	Set of available RBs
$\gamma_{u,t}^{(r)}$	Signal-to-interference-plus-noise ratio
R_{PD}	Responsitivity of the photodiode
$H_{u,t}$	Line-of-sight path gain
ξ	Cumulative noise power
q	Constant
I_{amb}	Ambient light intensity
B_{noise}	Noise bandwidth
K_B	Boltzmann's constant
T	Absolute temperature
R_F	Transimpedance amplifier gain
$U_{u,t}$	Utility function
$f_u(\cdot)$	Efficiency function
A_u	Set of user's uplink transmission power

2.6.2 Problem Formulation and Solution

Resource Allocation in the Uplink of VPAN

In an OFDMA VLC wireless network, two main resources should be allocated to the users considering the uplink scenario: (i) resource blocks and (ii) user's uplink transmission power. Based on the number of RBs, i.e., R, and considering non-reusability of the RBs within the same OAP, the maximum capacity of the OAP in terms of number of users is fixed, i.e., R. Given that the flat-fading model is adopted, the RBs are not differentiated considering user's channel gain per RB, thus a simplified RBs allocation is adopted.

In the case that $U < R$, we ensure that each user $u \in \mathscr{U}$ occupies at least one RB in the OAP $t \in \mathscr{T}$ and the remaining RBs are allocated to the users based on their order with respect to the channel gain $H_{u,t}$. In the case of $U > R$, users are ordered based on their channel gain and the first R users occupy the R RBs, while the rest of the users, i.e., $U - R$, cannot be served by the OAP and they are rejected. Finally, it should be noted that in the case of selective-fading channel model, an RBs allocation based on MGS policy could be also adopted. Therefore, the overall framework proposed in this work is not applicable only in the flat-fading channel model.

Power Allocation

In this section, we aim to formulate users' transmission power allocation in the uplink of VPANs either adopting OFDMA or NOMA transmission technique. More specifically, as the system evolves, at the beginning of each time slot a user's Non-cooperative OAP selection and Resource Allocation algorithm (NOAPRA algorithm) is responsible for determining an optimal uplink transmission power $P_{u,t}^{(r)}$ for the case of OFDMA (resp. $P_{u,t}^{(r)}$ for the case of NOMA). User's optimal uplink transmission power maximizes its overall perceived satisfaction, which is appropriately represented via the corresponding values of the utility function, as it is given by equation (2.44) considering either OFDMA or NOMA transmission technique. Towards supporting mobile user's autonomicity, as well as to consider user's selfish behavior, we propose a distributed approach.

As mentioned before, user's uplink transmission power is upper bounded, due to some physical and technical limitations. Therefore, the feasible set of user's uplink transmission power is denoted as $A_u = \left(0, P_{u,t}^{Max}\right]$. Let $R_{u,t}$ denote the number of RBs allocated to user $u \in \mathscr{U}$ residing in the OAP $t \in \mathscr{T}$. In the power allocation problem, users have a selfish behavior and their goal is to maximize their utility considering the occupied resources. Therefore, the power allocation is formulated as a distributed maximization problem as follows:

$$\textbf{NOAPRA Game}:$$
$$\begin{array}{ll} OFDMA: \max\limits_{P_{u,t}^{(r)}} U_{u,t}^{(r)}\left(P_{u,t}^{(r)}, \mathrm{P}_{-\mathrm{u,t}}^{(\mathrm{r})}\right) & NOMA: \max\limits_{P_{u,t}} U_{u,t}\left(P_{u,t}, \mathrm{P}_{-\mathrm{u,t}}\right) \\ s.t.\ 0 < P_{u,t}^{(r)} \leq \frac{P_{u,t}^{Max}}{R_{u,t}} & s.t.\ 0 < P_{u,t} \leq P_{u,t}^{Max} \end{array} \tag{2.47}$$

The distinctive novelty of the above proposed power control problem, which was formulated as a distributed optimization problem, lies in the fact that this is the first approach in the recent literature, where the problem of users' uplink transmission power allocation in VPANs towards supporting QoS provisioning is addressed. Towards solving the proposed optimization problem in equation (2.47), an optimization method is followed. Let $\mathbf{P}^{(r)*} = \left[P_{1,t}^{(r)*}, P_{2,t}^{(r)*}, ..., P_{u,t}^{(r)*}, ..., P_{U,t}^{(r)*}\right]$ for OFDMA (resp. $\mathbf{P}^* = \left[P_{1,t}^*, P_{2,t}^*, ..., P_{u,t}^*, ..., P_{U,t}^*\right]$ for the case of NOMA) denote the optimal solution of the optimization problem in equation (2.47). Considering the first order derivative of $U_{u,t}^{(r)}$ (resp. $U_{u,t}$) with respect to $P_{u,t}^{(r)}$ (resp. $P_{u,t}$) we have the following expression:

$$\begin{array}{c} \frac{\partial U_{u,t}^{(r)}}{\partial P_{u,t}^{(r)}} = 0 \Leftrightarrow \frac{\partial f_u\left(\gamma_{u,t}^{(r)}\right)}{\partial \gamma_{u,t}^{(r)}} \cdot \gamma_{u,t}^{(r)} - f_u\left(\gamma_{u,t}^{(r)}\right) = 0 \\ \left(resp.\ \ \frac{\partial U_{u,t}}{\partial P_{u,t}} = 0 \Leftrightarrow \frac{\partial f_u\left(\gamma_{u,t}\right)}{\partial \gamma_{u,t}} \cdot \gamma_{u,t} - f_u\left(\gamma_{u,t}\right) = 0\right) \end{array} \tag{2.48}$$

where the equation $\frac{\partial f_u\left(\gamma_{u,t}^{(r)}\right)}{\partial \gamma_{u,t}^{(r)}} \cdot \gamma_{u,t}^{(r)} - f_u\left(\gamma_{u,t}^{(r)}\right) = 0$, (resp. $\frac{\partial U_{u,t}}{\partial P_{u,t}} = 0 \Leftrightarrow \frac{\partial f_u\left(\gamma_{u,t}\right)}{\partial \gamma_{u,t}} \cdot \gamma_{u,t} - f_u\left(\gamma_{u,t}\right) = 0$) has

unique positive solution $\gamma_{u,t}^{(r)*}$, (resp. $\gamma_{u,t}^{*}$), due to the sigmoidal form of $f_u(\cdot)$ with respect to $\gamma_{u,t}^{(r)}$ (resp. $\gamma_{u,t}$). Furthermore, the SINR is an one-to-one function with respect to user's uplink transmission power, thus resulting to a unique solution, as follows:

$$\begin{aligned} OFDMA: \qquad P_{u,t}^{(r)*} &= \min\left\{ \frac{\gamma_{u,t}^{(r)*}\cdot\left(\sum\limits_{\substack{u'=1\\ u'\neq u\\ t\in \mathrm{T}}}^{U} H_{u',t}P_{u',t}^{(r)}+\xi\right)}{R_{PD}H_{u,t}}, \frac{P_{u,t}^{Max}}{R_u} \right\} \\ NOMA: \qquad P_{u,t}^{*} &= \min\left\{ \frac{\gamma_{u,t}^{*}\cdot\left(\sum\limits_{\substack{u'>u\\ t\in \mathrm{T}}}^{U} H_{u',t}P_{u',t}+\xi\right)}{R_{PD}H_{u,t}}, P_{u,t}^{Max} \right\} \end{aligned} \tag{2.49}$$

2.6.3 Distributed Algorithm

In this section, a decentralized, iterative, and low-complexity algorithm is proposed, which determines users' OAP selection and resource allocation in a distributed manner. The proposed algorithm is called NOAPRA algorithm and is divided into two basic parts. In the Optical Access Point Selection Part, each user selects the OAP to connect to based on the Maximum Gain Selection (MGS) policy. Additionally, in the Resource Allocation Part the RBs are allocated to the users in the OFDMA module and user's uplink transmission power is determined in accordance to Equation (2.49) in a distributed manner. The proposed procedure in the second part of the algorithm is repeated iteratively till the algorithm converges to its unique solution. The above described parts of the overall NOAPRA algorithm are as follows.

Algorithm 7 NOAPRA Algorithm: Optical Access Point Selection Part

1: At the beginning of each time slot, given that we assume that each user u, $u \in \mathscr{U}$, residing in the multicell environment has perfect knowledge of path gain information, create the matrix $\mathbf{H}(u,t)$, as presented in Equation (2.45). Set $k=1$, and $U^{(0)} = \{1,2,...,U\}$.
2: Each user u^* selects to connect to the OAP t^* via creating the communication link $l^* = \{u^*, t^*\}$ based on the highest path gain $H_{u,t}$ (MGS policy) as follows:

$$l^* = \{u^*, t^*\} = \underset{u^*\in\mathscr{U}, t^*\in\mathscr{T}}{\arg\max}\, \mathbf{H}(u,t)$$

3: Set $k := k+1$, delete user u^* in the set of users, i.e., $U^{(k+1)} = U^{(k)} - \{u^*\}$.
4: if $U^{(k+1)} = \emptyset$ then stop. Otherwise go to step 2.

Algorithm 8 NOAPRA Algorithm: Resource Allocation Part - RBs Allocation (only for OFDMA)

1: Based on the previous part of the algorithm, each OAP $t \in \mathscr{T}$ is aware of the number of users residing in it, i.e., U.
2: If $R = U$ allocate one RB $r \in \mathscr{R}$ to each user $u \in \mathscr{U}$, else if $R < U$, allocate at least one RB $r \in \mathscr{R}$ to each user $u \in \mathscr{U}$, sort the users based on their channel gain $H_{u,t}$ and allocate the remaining RBs, i.e., $R-U$ to the users based on the order of their channel gain, else if $R > U$, sort the users based on their channel gain $H_{u,t}$ and allocate the RBs R to the first R users with the best channel gain conditions, while the rest of the users are rejected from the OAP $t \in \mathscr{T}$.

2.6.4 Numerical Results

In this section we provide some indicative numerical results illustrating the operation and features of the proposed framework and the NOAPRA algorithm. Throughout our study, we consider a VPAN,

Algorithm 9 NOAPRA Algorithm: Resource Allocation Part - Users' Uplink Transmission Power

1: Each user, u, $u \in \mathscr{U}$ has already decided the OAP that it is connected to and initially it transmits with a randomly selected feasible uplink transmission power, i.e., $0 < P_{u,t}^{*(r)(0)} < \frac{P_{u,t}^{Max}}{R_{u,t}}$ (resp. $0 < P_{u,t}^{*(0)} < P_{u,t}^{Max}$). Set $k \coloneqq 0$ and hence $P_{u,t}^{*(r)(0)}$ (resp. $P_{u,t}^{*(0)}$), $u \in \mathscr{U}$ and $t \in \mathscr{T}$

2: Given that the single central controller of the OAPs collects the information of the overall interference within the multi-cell environment, each OAP announces this information, i.e., $\sum_{\substack{u=1 \\ t \in \mathrm{T}}}^{U} H_{u,t} P_{u,t}^{(r)}$ (resp. $\sum_{\substack{u=1 \\ t \in \mathrm{T}}}^{U} H_{u,t} P_{u,t}$) to all users residing within its coverage area, via broadcasting. Each user computes its sensed interference $\sum_{\substack{u'=1 \\ u' \neq u \\ t \in \mathrm{T}}}^{U} H_{u',t} P_{u',t}^{(r)}$ (resp. $\sum_{\substack{u'>u \\ t \in \mathrm{T}}}^{U} H_{u',t} P_{u',t}$).

3: Set $k \coloneqq k+1$. Each user updates its uplink transmission power, i.e., $P_{u,t}^{*(r)(k)}$, (resp. $P_{u,t}^{*(k)}$), $u \in \mathscr{U}$ and $t \in \mathscr{T}$, based in Equation (2.49)

4: If $\left| P_{u,t}^{*(r)(k+1)} - P_{u,t}^{*(r)(k)} \right| \leq \varepsilon$ (resp. $\left| P_{u,t}^{*(k+1)} - P_{u,t}^{*(k)} \right| \leq \varepsilon$), e.g., $\varepsilon = 10^{-5}$ stop. Else go to step 2.

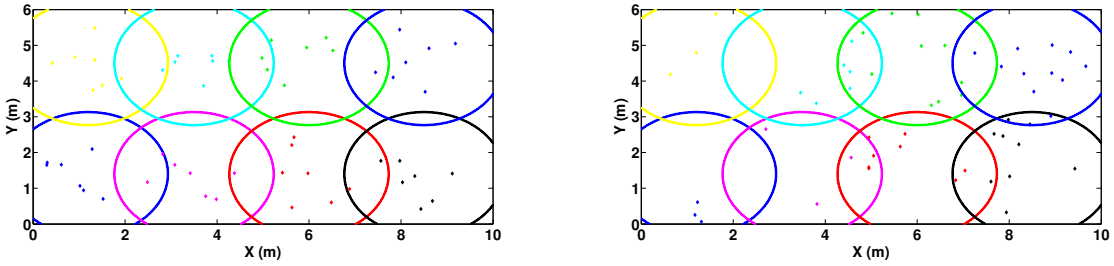

(a) Uniform distribution (b) Unbalanced distribution

Figure 2.23: Users' distribution in a VPAN network

where $T = 8$ OAPs are established within a room of size $10m \times 6m \times 3m$ ($W \times L \times H$) and U users are distributed within the room. In the OFDMA transmission technique, the number of RBs is set to $R = 7$. The responsitivity of the photodiode is set to $R_{PD} = 0.63$ $^{A}/_{W}$, users' maximum feasible uplink transmission power is $P_{u,t}^{Max} = 1$ $Watt$, and the OAP's bandwidth is $W = 20$ MHz. The cumulative noise power is $\xi = 0.03 \cdot 10^{-18}$ W, the photodetector area is $A = 3 \cdot 10^{-6} m^2$, the transmitter semi-angle at half power $\phi_{1/2} = \pi/6$ rad, user's field of view (FOV) $\psi_c = \pi/3$ rad, the signal transmission coefficient of an optical filter $T_s(\psi) = 1$, the order of the Lambertian emission $m = 1$, and the refractive index of the optical concentrator is $a = 1.5$. The adopted efficiency function is $f_u\left(\gamma_{u,t}^{(r)}\right) = \left(1 - e^{-A \cdot \gamma_{u,t}^{(r)}}\right)^M$ (resp. $f_u\left(\gamma_{u,t}\right) = \left(1 - e^{-A \cdot \gamma_{u,t}}\right)^M$), where $A = 0.2$ and $M = 1.61$.

In the following, we consider that $U = 56$ users reside within the room under two different distributions: (i) uniform distribution, i.e., 7 users reside per OAP (which is the OAP's maximum capacity in terms of users for the OFDMA transmission technique due to the fact that the number of RBs is $R = 7$) and (ii) non-uniform (unbalanced) distribution, i.e., some OAPs are overloaded in terms of users while some others are less congested, as presented in Fig. 2.23a and Fig. 2.23b, respectively.

In Fig. 2.24a and 2.24b, users' average uplink transmission power per OAP is presented for both users' distributions. Similarly corresponding users' average uplink transmission rate per OAP is presented in Fig. 2.25a and 2.25b, respectively. Considering users' uniform distribution, it is observed that for the OFDMA transmission technique, users' average uplink transmission power is lower compared to the corresponding values in the unbalanced users' distribution. This observation stems from the fact that in the latter case more users are concentrated in a specific physical area of the room, thus users from different OAPs who share the same RB will cause extremely high interference to their neighbors, resulting in increasing uplink transmission power. On the other hand, considering the NOMA transmission technique, users' average

transmission power also increases in the unbalanced users' distribution compared to the uniform one, however users' average transmission power's increase is smoother compared to the aforementioned increase in the OFDMA transmission technique. This observation holds true due to the successive interference cancellation (SIC) technique, which is an embedded module at the receivers in NOMA. Based on SIC, even if users' concentration in a specific physical area is increased, i.e., unbalanced users' distribution, the receiver is able to cancel part of the increased caused interference, fact that does not hold true in the OFDMA transmission technique.

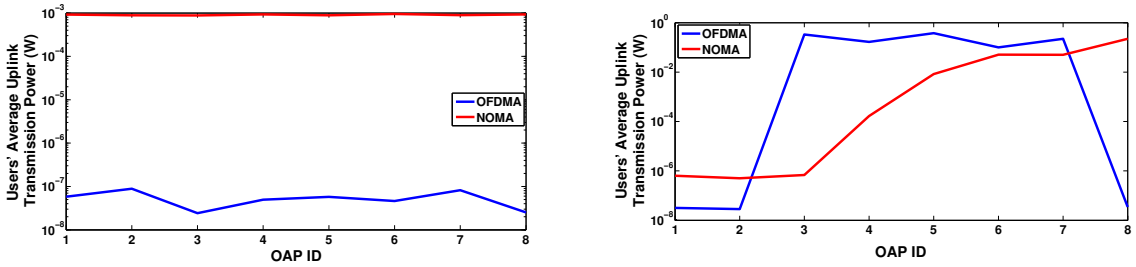

(a) Uniform users' distribution (b) Unbalanced users' distribution

Figure 2.24: Users' average uplink transmission power per OAP

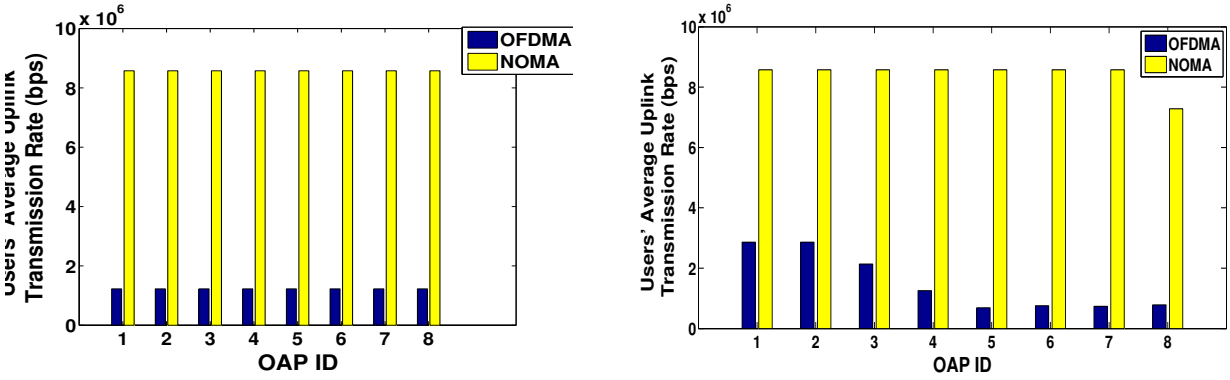

(a) Uniform users' distribution (b) Unbalanced users' distribution

Figure 2.25: Users' average uplink transmission rate per OAP

On the other hand, considering users' average uplink transmission rate per OAP, it is observed that both for the uniform (Fig. 2.25a) and the unbalanced (Fig. 2.25b) users' distribution, NOMA transmission technique results in higher users' average uplink transmission rate compared to OFDMA transmission technique, due to the fact that in the former transmission technique, i.e., NOMA, users exploit the whole bandwidth towards transmitting.

Finally, in Fig. 2.26a and 2.26b we present the total consumed uplink transmission power (Fig. 2.26a) and the total achieved uplink transmission rate (Fig. 2.26b) in the system of $T = 8$ OAPs, while the number of users increases, both for the OFDMA and NOMA transmission technique. It should be noted that system's maximum capacity in terms of number of users is fixed for the OFDMA transmission technique, i.e., $U = 56$ users, due to the finite number of non-reusable RBs per OAP, i.e., $R = 7$ RBs per OAP. Thus, it is observed that system's total transmission power and rate remain constant for number of users larger than 56 users in the OFDMA technique, while the supplementary users are rejected by the system. On the other hand, the system can accommodate and serve a larger number of users via adopting NOMA transmission technique.

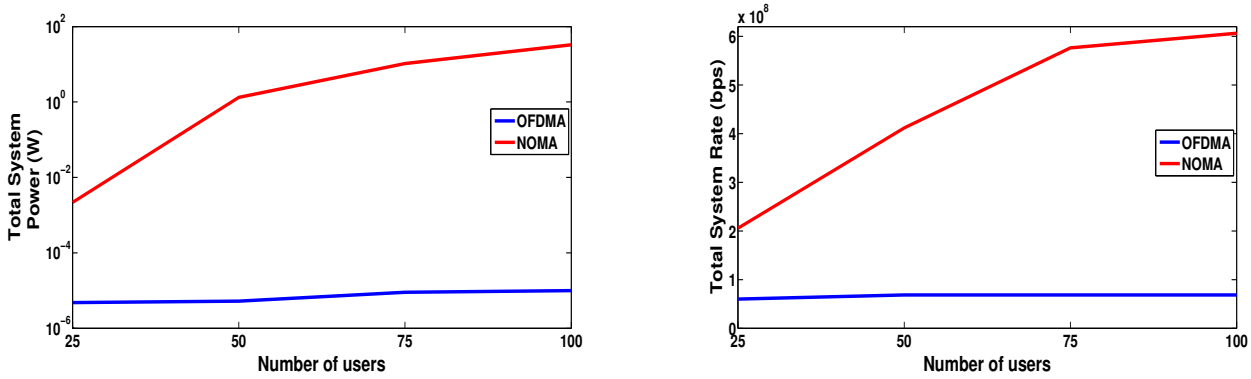

(a) Uplink transmission power

(b) Uplink transmission rate

Figure 2.26: System's total uplink transmission (a) power and (b) rate versus the increasing number of users

2.7 General Summary

In a nutshell, Chapter 2 holistically studied the problem of resource allocation in two-tier femtocell and Visible Light Communication based networks. Aiming at providing a broader analysis of the different aspects of the network performance and optimization process, both rate and power control have been considered for different types of services (real and non-real time). At each problem, users were assigned with a generic utility based function representing their perceived satisfaction with respect to the achieved energy-efficiency, based on the requested service type and the tier that the user belongs to (i.e., macro user or femto user equipment).

Originally, the problem of efficient uplink power control in two-tier femtocell networks was addressed. The considered problem was formulated as a non-cooperative game solved under the principles of supermodular games, while its convergence to its Nash Equilibrium point was determined via the iterative and low complexity UPC-MSF algorithm. The performance of the proposed scheme was evaluated via a series of numerical results and its superiority against other power control approaches in the literature for two-tier femtocell networks was demonstrated.

Following, the problem was expanded to combine both power and rate control in two-tier femtocell networks, towards enabling users to determine additional aspects of their transmission by controlling two degrees of freedom this time. In order to solve the two-variable power and rate control under a low complexity and fast converging approach, the optimization problem was converted to a single strategic variable problem by considering the ratio x_j of data rate to its corresponding transmission power. Hence, the reduced joint allocation problem was confronted as a non-cooperative game whose convergence to its Nash Equilibrium point was determined via proving the quasi-concavity of the users' utility functions and practically obtained by the application of the UPRA-MSF algorithm. The performance of the scheme was evaluated under different scenarios for increasing number of users and FAPs, while its comparison with other approaches confirmed its superiority due to the two-tier and two-variable consideration, against works that assumed only power control in femtocell-based structures, or macrocell-only networks where joint power and rate control was implemented.

In the next section, we further increased the scope by formulating the power and rate control differently as a real two-variable problem instead of using the data rate to power ratio. The above adjustment required a totally different solution approach based on the theory of multi-variable S-modular games, which for the first time were applied in a joint resource allocation problem in two-tier femtocell networks. The existence and uniqueness of the Nash Equilibrium of the considered non-cooperative MUPRAF game was proven and its convergence to the above point was demonstrated. Lastly, the superiority of formulating and solving the joint resource allocation problem as a two two-variable optimization problem has been thoroughly evaluated via analysis and simulation, against the previous sections and the literature. Moreover, it should be noted that the proposed approach can be easily applied to include other parameters, hence not restricting its applicability in other resource allocation problems.

Finally, the last part of Chapter 2 deals with the problem of power control, but this time in the uplink of Visible Light based Communications. Again in a joint manner, we examined the problem of users'

association to OAPs and resource allocation in the uplink of VPANs under two different transmission techniques, i.e., OFDMA and NOMA. Maximum Gain Selection (MGS) policy was used for treating the users to OAPs association problem where users select an OAP to connect to, based on the highest path gain while the resource allocation problem was formulated and solved as a distributed optimization problem. NOAPRA, an iterative and low-complexity algorithm was proposed towards associating users to the OAPs and allocating the resources to them, while detailed numerical results were presented illustrating the benefits of the proposed framework and comparing the impact of OFDMA versus NOMA transmission technique in the resource allocation process.

Chapter 3

Resource Pricing in Wireless Networks

The rising demand for wireless services and the launch of new network technologies is considered a vital element towards economic development and a means of new business opportunities and unlocking of new market segments. Pricing consists an efficient tool for WISPs to discover new sources of revenue by trading a resource as well as a scheme in order to navigate user decision making and achieve a more socially desirable outcome for resource allocation.

A price represents an equilibrium point between supply and demand for a resource or a product among the WISPs and the network subscribers, and has been used as an indication to translate user satisfaction into monetary units while at the same time control the amount of information exchanged within the network. The diversification of services and the emergence of heterogeneous networks is adapting to the new needs that different user groups have, hence pricing models are constantly being revised, not only in the sense of more efficiently adjusting to user requirements and their willingness to pay for superior service offerings, but also they are used as a prevalent ingredient to direct WISP competition and evolve alongside the telecommunications product in a market driven perspective.

Focusing on the resource allocation approach, pricing techniques have been recognized as a tool to deal with externalities and have found fertile application ground in the field of wireless networks by both economists and researchers. Pricing has been utilized both as a penalty enforcement measure to mitigate unsocial or aggressive behavior of users which is associated with increased interference or unfair consumption of resources, whilst has also been implemented for guiding user behavior to more efficient and Pareto optimal operating points [10].

Varying pricing mechanisms have been so far examined in the area of resource allocation for wireless networks. Aiming at providing seamless services to an increasing number of subscribers in heterogeneous network topologies which support different traffic characteristics and varying QoS requirements, pricing cannot be flat (i.e., applying a fixed price per session independently of the traffic conditions, the capacity, and the competition among users). Examples of flat pricing include metered pricing, fixed pricing, Paris-Metro pricing, and content-based pricing, among others [98], [99].

Networks are switching from homogeneous or uniform topologies to more complex structures, where single or identical user populations are considered now obsolete. Hence, pricing is also transforming to dynamic or parameter-based methodologies, in order to adjust to different events or refer to the utilization of a specific resource, towards not only indicating the valuation of the resource allocation process, but also increase mobile customers' satisfaction. A high level classification of such pricing approaches includes auction pricing, broadcasting pricing schemes, priority pricing, adaptation pricing or assignment pricing etc., [98], [99].

In this work, pricing is applied both for the distribution of different resources (e.g., aiding power control, rate control or optimizing energy-efficiency) towards supporting the performance of the network, but also for examining the market equilibrium between price and demand in competitive telecommunication markets. A major novelty of our approach consists that price is not just a policy making tool of a central administration (e.g., the WISP), but is also a limited resource owned by the users, which they also wish to optimize and invest according to their unique QoS requirements, service preferences, and transmission priorities under a game theoretic perspective.

3.1 Related Work on Pricing in Resource Allocation

In the literature significant attention has been given to the problem of efficient resource allocation in wireless networks especially via utilizing game theoretic approaches, which support the autonomous behavior of the mobile user [100]. The traditional problem of power control in cellular networks has extensively been explored mainly from the aspect of reducing battery drain and enhancing energy-efficiency (e.g., [10, 25, 28, 29, 40, 52, 101, 102]) in various architectures of wireless networks, e.g., two-tier femtocell networks, heterogeneous networks etc., adopting different technologies, e.g., CDMA, NOMA, OFDMA etc. The main goal of the aforementioned approaches is interference mitigation, energy-efficiency, and prolongation of mobile users' battery life. More holistic approaches have also been proposed considering simultaneously multiple resources. The joint resource allocation problem of power, subchannel and/or rate has been studied towards maximizing either users' throughput [56], or each user's perceived satisfaction [31, 33, 34, 72, 80].

By adding more degrees of freedom alongside power control, data rate allocation becomes feasible with the authors in [30] to convert a two-variable problem to a single parameter optimization expressed as the ratio of rate to the respective power. Following the same paradigm, the authors in [103] propose a spectrum allocation framework in cognitive radios, following the load balancing concept in distributed computer systems. Also, centralized approaches targeting at maximizing the secrecy sum rate in a NOMA system have been proposed [104]. Although substantial improvements are achieved, in these works, rate allocation is suppressed due to the priority of minimizing power consumption [105, 106]. Considering the class of problems concentrating mainly on rate allocation, in [107], a constrained throughput maximization problem is examined including stochastic control parameters towards safeguarding fairness conditions among the users. In [108], a sum rate optimization problem for multiple-input multiple-output (MIMO) NOMA systems is studied with constraints considering the total transmission power and the minimum rate.

Recent research efforts and approaches in the literature have been devoted towards examining pricing schemes which have been widely discussed as a means of service discrimination, traffic management, power saving, interference mitigation, and overall better usage of system resources [10, 28, 29, 40]. With reference to the resource allocation problem, pricing the system resources has emerged as a very powerful tool for achieving a more socially desirable outcome and allocation, while targeting energy-efficient solutions. The pricing policies proposed in the literature for this purpose are either linear with respect to users' uplink transmission power [10] or to SINR [29], or convex with respect to power [28, 40], or SINR [31]. In most of these cases however, pricing is globally announced by the WISP to the users, being the same for all of them and forcing them to re-calculate their consumed resources in a more socially acceptable way, thus leading to less interference within the network, as well as to a fairer allocation of system's resources.

In [109, 110], the nature of prices is fixed, with the users being charged a flat rate or different classes of static prices are applied to users based on their traffic requirements, respectively. The alternative of day-ahead pricing is examined in [111], with the WISP announcing the time-dependent prices 1 day in advance. In [112], Zheng et al. study a secondary data market, in which users can buy and sell left over data caps from one another. The authors derive users' optimal behavior and propose an algorithm for the Wireless Internet service providers (WISPs) to match the buyers and the sellers. Considering a similar trading model, in [113], users' decisions about their usage at different times of the billing cycle are discussed. In [114], the authors address mobile users' data usage behavior, through the study of network effects as they emerge by the joint consideration of elements both from social domain (e.g., relationships) and the physical domain (e.g., congestion). The joint pricing and data usage management problem is formulated as a Stackelberg game, where the WISP acts as leader announcing the price to the users, who follow by determining their data usage. In [115, 116], a comprehensive literature review on applications of economic and pricing models for resource management in cloud networking and the Internet of Things, respectively, is provided.

3.2 Power and Price Allocation

Considering power control problems, pricing has been mainly applied as a congestion and interference management tool, where a cost function is optimized alongside users' utilities who strive to balance the effort between capturing more resources for their transmission, but also minimize the penalties that are centrally incurring in order to contain their aggressive behavior [10].

In this work we take a different approach from the overwhelming body of existing works in the literature, and we do not simply view pricing as a tool/mechanism utilized by the WISP to penalize users for unfair resource consumption. We rather view price as an actual resource itself to be "allocated", or in mathematical terms we consider it as a variable to be determined towards the objective of maximizing the net utility of each user without harassing the other users' net utilities. Within such a framework, price becomes an incremental and distinct component of the specifically designed net utility functions and of the overall resource allocation problem. This consideration significantly distinguishes our work from the existing literature body, where authors have mainly tried to integrate price within the resource allocation (i.e., power control) by accounting for an expansion of the single parameter user's uplink transmission power optimization problem. We propose a user-centric approach in terms of resource allocation, while at the same time determine the optimal prices of resources that the users are willing to pay towards achieving their desired QoS. Focusing on energy and power considerations, the resource considered and treated here is the user's uplink transmission power, while the treatment of other resources such as user's uplink transmission rate is also of great interest and is examined at a later section. Given the above framework and consideration, the corresponding optimization problem is approached as a two-variable problem, which requires significantly different handling than the ones applied in the respective resource allocation problems in the literature.

A key contribution of our proposal is that it allows for customized pricing. The latter is defined as a pricing strategy based on individualized estimates for each customer (user) or for groups of customers, with a personalized price reflecting consumer's willingness to pay in order to receive a specific level of service. A customized price is determined through the solution of the formulated respective optimization problem that enables the WISP to "charge" each user in a personalized manner based on the service it requests, as well as based on its uplink transmission power, which implicitly considers the harm that the user imposes to the network via its caused interference. The latter better exploits network's conditions and users' real-time service demands, concluding to better service delivery to individual users and better usage of system's resources as a whole. From user's point of view, customized prices achieve relative fairness among users, who are charged based on their demand in a real-time manner, incentivizes them to re-address and re-adjust their uplink transmission power towards combining both better service quality along with potential price reductions. It is noted that by treating price as an independent variable in user's utility function and not simply as a static parameter as done in most of relevant literature, it does dynamically adapt to system's evolving conditions and to users' personal characteristics, thus driving the entire system - in conjunction with the simultaneous power optimization - to more efficient points of operation.

In our work, both variables, i.e., price and uplink transmission power, are determined in a distributed optimal and real-time manner, while the control intelligence and the decision making process lie at the mobile node, which targets at the optimization of the tradeoff between cost of resource and satisfaction of QoS prerequisites, while maintaining minimal interaction with the WISP. It is noted however here, that though the decisions are taken at the end-user level in a distributed manner, the WISP's interest in terms of optimal resource pricing determination is expressed via the adoption of the corresponding pricing function and the boundaries of price. Aiming at jointly determining the optimal customized price and users' uplink transmission power, we formulate a joint non-cooperative utility-based PRIce and uplink transmission POwer control (PRI-PO) problem towards optimizing each user's net utility function. PRI-PO optimization problem is considered as a distributed and non-cooperative game among users and is solved via a game theoretic approach based on S-modular theory. The two-variable PRI-PO game concludes to a Nash equilibrium point determining the optimal price and users' uplink transmission powers, where no user wants to deviate from, due to the fact that it cannot further improve its perceived satisfaction by making any individual change to its strategy.

3.2.1 System Model

In this section, a representative model for the uplink in a single cell of wireless network is described. For clarity of the presentation, a simple model which highlights the possible disparity between users in such an environment is selected. The considered model assumes an interference limited environment, where the available bandwidth (or a common band of frequencies) is co-used and shared among users.

In the single cell scenario, $|N(t)|$ continuously backlogged users reside in the cell at time slot t, $(0.5\ msec)$, where $N(t) = N_{EL}(t) \cup N_{IN}(t)$ denotes their corresponding set. The set $N(t)$ of mobile users consists of the set of users that require elastic services $N_{EL}(t)$ with shiftable in time, i.e., delay-

tolerant, data demand and inelastic services $N_{IN}(t)$, where users' data demand is non-shiftable in time and the services are characterized by strict short term QoS constraints [8], [72]. Throughout the analysis, however, for simplicity in the presentation only, we omit the notation of the specific time slot t.

Remark 3. *Throughout the presentation of this thesis, the terminology used for the description of "Elastic" or "Non-Real Time" and "Inelastic" or "Real Time" services is used interchangeably to describe the same type of service based on its transmission and delay tolerance characteristics. Formal descriptions of those services are given in Definitions 5.1.1 and 5.1.2 in Section 5.1.*

User's uplink transmission power is denoted by P_i and due to mobile node's physical and hardware limitations it is upper bounded, i.e., $0 \leq P_i \leq P_i^{Max}$. The WISP defines and announces a pricing function $C(c_i, P_i)$, which contains a customized price c_i for its users, considering their system's resources consumption and their caused interference to the rest of the users residing in the cell. Each WISP also defines a maximum and minimum feasible price according to its policy, i.e., c_i^{Max}, c_i^{Min}, thus the corresponding announced price is bounded, i.e., $c_i^{Min} \leq c_i \leq c_i^{Max}$. In the analysis provided in this part, the price c_i is considered as a dimensionless quantity. Nevertheless price c_i can be translated and mapped to real monetary units in a realistic implementation, a study which is however out of scope of this work.

In the following, a snapshot of the adopted model is considered, where the channel gains G_i from the transmitter of user i to the base station, as well as price c_i and user's uplink transmission power P_i are assumed to remain unchanged during the short runtime of the time slot t (i.e., 0.5 $msec$). The basic performance measure that contributes to the mobile users' QoS prerequisites satisfaction is the signal-to-interference-plus-noise ratio (SINR): $\gamma_i(P_i, \mathbf{P_{-i}}) = \frac{W}{R_{ser}} G_i P_i / \left(\sum_{j=1, j\neq i}^{|N|} G_j P_j + I_0 \right)$, which is modeled similarly to previous sections *(See also Eq. (2.1))*. Let W $[Hz]$ be the system's spreading bandwidth, $\mathbf{P_{-i}}$ denote the users' power allocation vector excluding user i, and I_0 $[W]$ the Additive White Gaussian Noise (AWGN) power representing the background noise. The processing gain is defined by the ratio $\frac{W}{R_{ser}}$, where R_{ser} denotes user's fixed transmission rate and its specific value is related to user's corresponding requested service [29].

The concept of net utility function represents user's level of satisfaction with the perceived QoS, as well as with the price imposed by a centralized entity, i.e., the WISP. The higher the net utility is, the more satisfied are the users. In general, the net utility function consists of the pure utility function and the pricing function. The pure utility function characterizes how sensitive users are to changes in the perceived QoS, while the pricing function expresses the reduction of user's satisfaction due to the harm it imposes on the system. Various net utility functions have been proposed in the literature in order to model user's behaviour and formulate pricing policies. Saraydar et al. in [10] have proposed a net utility function that consists of a generic utility function without considering users' QoS requirements and/or type of requested service and a linear pricing function with respect to users' uplink transmission power, where the price is static and common for all users. In [29], a similar pure utility function is proposed assuming a pricing policy with respect to user's SINR and considering common price for all users. In [28], users' net utility functions are differentiated in terms of pure utility based on users' requested services and a convex pricing policy with respect to user's uplink transmission power is assumed, considering common prices for all users.

In a nutshell, the main drawbacks of those approaches are: a) the price is simply a static parameter and not an independent variable in user's net utility function as in our consideration, thus it cannot dynamically adapt to system's evolving conditions and to users' personal characteristics, and b) the majority of the proposed net utility functions in the literature cannot apply to a multiple requested services environment, which will be dominant in future wireless networks [117].

Based on the above discussion and in order to support the emerging wireless network multiple services with diverse QoS demands under a unified optimization framework, each user is associated with an appropriately selected and generic enough net utility function, which represents its degree of satisfaction in relation to the expected tradeoff between its QoS-aware performance, its uplink transmission power, and willingness to pay for the price of system's resources' usage. At each timeslot, each user requests a specific type of service, either elastic or inelastic, and adopts a corresponding form of net utility function capturing its QoS prerequisites. Therefore, user's net utility function is differentiated based on the type of service as follows:

$$U_i^{NET}(P_i, \mathbf{P_{-i}}, c_i) = \begin{cases} \frac{R_{ser} \cdot f_i(\gamma_i)}{P_i} - c_i \left(e^{P_i} - 1 \right), \; i \in N_{IN} \\ \frac{R_{ser} \cdot \log(1 + f_i(\gamma_i))}{P_i} - c_i \left(e^{P_i} - 1 \right), \; i \in N_{EL} \end{cases} \tag{3.1}$$

where $f_i(\gamma_i)$ is the already known efficiency function. Considering the numerator $R_{ser} \cdot f_i(\gamma_i)$ of the pure utility of users requesting inelastic services, it is a sigmoidal function with respect to SINR γ_i, where at its inflection point the ideal value of user's transmission rate (R_{ser}) at which its QoS prerequisites are fulfilled, is mapped. Thus, in the case that user's transmission rate is less than the value of inflection point, then its utility rapidly decreases, indicating its priority/intention in occupying additional system's resources. Based on the proposed formulation of the utility function, a user is capable of regulating its uplink transmission power and its willingness to pay, so as to achieve a corresponding SINR value that guarantees its achievable data rate R_{ser}, since both latter parameters are related as in the equation of SINR as already presented in relations (2.1) and (2.7).

On the other hand, the corresponding numerator in the pure utility function of the users requesting elastic services represents user's achievable data rate and it is a log-based function with respect to user's efficiency function $f_i(\gamma_i)$. This formulation represents users' greedy behavior when requesting "elastic" services, as they are characterized by high throughput expectations. Thus, their overall perceived satisfaction, i.e., U_i^{NET}, increases as they achieve higher SINR values, which in turn results in higher achievable data rate via the strictly increasing function $R_{ser} \cdot \log(1 + f_i(\gamma_i))$ with respect to γ_i.

Furthermore, users' net utility contains price c_i, thus the users can adapt accordingly their uplink transmission power, divulging their true willingness to pay in order to receive the requested service. In this manner, the price c_i is continuously and dynamically adjusted as an independent variable according to the changes in the system's conditions as the system evolves. It should be noted that the control intelligence lies on the user side, who considers both the price and its power and makes final decisions accordingly. From WISP's perspective, it can implicitly affect users' decisions via the announced pricing policy, i.e., the pricing function $C(c_i, P_i) = c_i\left(e^{P_i} - 1\right)$ and the boundaries of its prices, i.e., c_i^{Max} and c_i^{Min}. It should be stressed here that someone could assume that the users will always choose the lowest price, i.e., $c_i = 0$, in order to maximize their overall perceived satisfaction, i.e., U_i^{NET}. However, this does not hold true, because the proposed pricing policy acts as a mean to mitigate interference as well. Thus, a user will be willing to pay a higher price, which will result in decreased uplink transmission power and the user will be able to achieve even more increased perceived satisfaction, while transmitting with low power. All the key notations are summarized in Table 3.1.

Table 3.1: Section 3.2 list of key notations

Symbol	**Description**
$N(t)$	Set of users per timeslot
$N_{EL}(t), N_{IN}(t)$	Set of elastic and inelastic users
P_i, c_i	User's i uplink transmission power and customized price
c_i^{Max}, c_i^{Min}	User's i maximum and minimum customized price
P_i^{Max}	User's i maximum uplink transmission power
W	System's spreading bandwidth
R_{ser}	User's fixed transmission rate related to the requested service
t	Timeslot
G_i	Channel gain from the transmitter of user i to the base station
I_0	AWGN power at the receiver
$U_i^{NET}(\cdot)$	User's i net utility function
$f_i(\cdot)$	User's i efficiency function
γ_i	Signal-to-interference-plus-noise ratio
$\{\mathrm{P_i}, \mathrm{C_i}\}$	Strategy space
A, M	Efficiency function parameters
$\tau(\gamma_i)$, $q(\gamma_i)$	Auxiliary functions
d_i	Distance from base station
K_i	Shadow effect
a	Distance loss exponent
$\gamma_{i,BOL}$	Root of $\tau(\gamma_i)$

3.2.2 Problem Formulation and Solution

Following, we cast the joint utility-based customized PRIce and POwer control (PRI-PO) problem into the framework of non-cooperative game theory, mapped to the two-variable (i.e., price and power) optimization problem considered in this work. This type of optimization problem is also solved via S-modular theory [62], [64], [65], since the basic intuition of this game class is that a change in one player's actions for given actions of rivals, reinforces the desire of all players to adjust their actions accordingly. In the PRI-PO framework, an increase in one user's uplink transmission power is followed by high price, thus this behavior provides the incentive to the rest of the users to sophisticatedly select their power strategy, so as to achieve reduction of price. Based on this observation, in this work it is proven that PRI-PO optimization problem (introduced later in this section) is a submodular game.

Definition 3.2.1. ***Submodular Games:*** *Submodular games are characterized by strategic substitutes, i.e., an increase in one player's action incentivizes the rest of the players to decrease their actions [62].*

Let $G = [N, \{A_i, B_i\}, \{U_i(a,b)\}]$ denote the game, where $\{A_i, B_i\}$ is the strategy space of player i. Submodular games are defined similarly to supermodular games. Utility function U_i is a submodular function if and only if [65]:

$$\frac{\partial^2 U(a)}{\partial a_i \partial b_i} \leq 0 \tag{3.2}$$

Furthermore, submodular function $U_i : A_i \times B_i \rightarrow \mathbb{R}$ has non-increasing differences (a, b) if

$$U_i(a,b) - U_i(a,b') \leq U_i(a',b) - U_i(a',b') \tag{3.3}$$

$\forall a > a', b > b'$, or in other words, if the difference $U_i(\cdot, b) - U_i(\cdot, b')$ is a non-increasing function [62], with the equivalent condition being:

$$\frac{\partial^2 U_i}{\partial a_i \partial a_j} \leq 0, \forall j \neq i \tag{3.4}$$

Theorem 17. ***(Submodular game G:)*** *A strategic game G is said to be submodular if:*

1. *$\forall i \in N, S_i = A_i \times B_i$ is a compact subset of the Euclidean space.*
2. *U_i is submodular in a for each fixed b*
3. *U_i has non-increasing differences in (a, b)*

In line with S-modular theory, if G is a submodular game, then it has at least one Nash Equilibrium [10], [14], [62], [65], [118]. Towards determining the Nash Equilibrium of a submodular game, players' best response dynamics will be adopted which monotonically converge to the NE starting from any feasible initial strategy. The best response dynamics is a natural class of dynamics in multi-user non-cooperative games, in which each player updates its strategy to maximize its utility, given the strategies of the rest of the players.

As it has been discussed before, there have been proposed various pricing rules in wireless networks, which are heuristically or empirically determined and they are common for all users residing in a cell, aiming mainly at mitigating the overall interference. In this work, we aim to jointly determine user's optimal price and uplink transmission power, with the users to take the final decision of both optimization problem's variables. Based on this formulation, the user is able to express its willingness to pay in order to receive the requested service and follow the pricing policy imposed by the WISP as it is expressed by the corresponding pricing function and the boundaries of the price, i.e., c_i^{Max}, c_i^{Min}. On the other hand the user consumes sparingly its uplink transmission power, thus implicitly presenting a more social behavior in terms of overall interference mitigation.

Therefore, the joint utility-based customized PRIce and POwer control optimization problem is formulated as a two-variable non-cooperative game with respect to user's price c_i and uplink transmission power P_i. $G_{PRI-PO} = \left[N, \{\mathrm{P_i}, \mathrm{C_i}\}, \left\{U_i^{NET}(P_i, c_i)\right\}\right]$ is denoted as the PRI-PO game, defined as:

$$\begin{gathered}\textbf{PRI}-\textbf{PO Game}\\ \underset{\substack{P_i\in \mathrm{P}_i\\ c_i\in \mathrm{C}_i}}{max}\ U_i^{NET}\left(P_i,c_i,\mathbf{P}_{-\mathbf{i}}\right),\forall i\in N\\ s.t.\ c_i^{Min}<c_i\leq c_i^{Max},\ 0<P_i\leq P_i^{Max}\end{gathered} \tag{3.5}$$

where $\mathrm{P}_i=\left(0,P_i^{Max}\right]$ and $\mathrm{C}_i=\left[c_i^{Min},c_i^{Max}\right]$ are the strategy spaces of user i. In the following section, the Nash Equilibrium approach will be adopted towards seeking analytically the two-variable solution of the non-cooperative PRI-PO game.

Theorem 18. ***(PRI-RO Game NE:)*** *The strategy vector* $(\mathrm{P}^*,\mathrm{c}^*)=\left(P_1^*,P_2^*,...,P_{|N|}^*,c_1^*,c_2^*,...,c_{|N|}^*\right)$ *in the strategy sets* $P_i^*\in \mathrm{P}_i$ *and* $c_i^*\in \mathrm{C}_i$*, is a Nash Equilibrium of the PRI-PO game if for every user* $i,i\in N$ *the following condition is satisfied:*

$$U_i^{NET}(P_i^*,c_i^*,\mathbf{P}_{-\mathbf{i}}^*)\geq U_i^{NET}\left(P_i,c_i,\mathbf{P}_{-\mathbf{i}}^*\right) \tag{3.6}$$

for all $P_i^*\in \mathrm{P}_i$ *and* $c_i^*\in \mathrm{C}_i$

As it was analyzed in the previous section, the concept of Nash equilibrium offers a stable predictable and definable solution of a non-cooperative game, where multiple users with potentially conflicting interests compete towards realizing self-optimization and reaching a point where no user wishes to deviate. Towards proving the existence of at least one Nash equilibrium point of PRI-PO game $G_{PRI-PO}=\left[N,\{\mathrm{P_i},\mathrm{C_i}\},\left\{U_i^{NET}\left(P_i,c_i\right)\right\}\right]$. Specifically for the PRI-PO game, the following hold:

Lemma 19. ***(PRI-PO Submodular Game:)*** *PRI-PO game* G_{PRI-PO} *is submodular, if for all* $i\in N$ *the following conditions hold true:*

1. $S_i=\mathrm{P}_i\times \mathrm{C}_i$ *is a compact subset of Euclidean space.*
2. $U_i^{NET}\left(P_i,c_i\right),P_i\in \mathrm{P}_i,c_i\in \mathrm{C}_i$ *is smooth and:*
   - *Submodular in* P_i *for each fixed* c_i*, i.e.,*

$$\frac{\partial^2 U_i^{NET}}{\partial P_i\partial c_i}\leq 0 \tag{3.7}$$

   - *Has non-increasing differences in* $\{(P_i,c_i),(\mathbf{P}_{-\mathbf{i}},\mathbf{c}_{-\mathbf{i}})\}$*, i.e.,*

$$\frac{\partial^2 U_i^{NET}}{\partial P_i\partial P_j}\leq 0 \tag{3.8}$$

In such games, there exists a largest element $\left(\bar{P}_i,\bar{c}_i\right)=\sup\left\{(P_i,c_i)\in S_i:BR\left(P_i,c_i\right)\geq(P_i,c_i)\right\}$ and a smallest element $\left(\underline{P_i},\underline{c_i}\right)=\inf\left\{(P_i,c_i)\in S_i:BR\left(P_i,c_i\right)\leq(P_i,c_i)\right\}$ of the equilibrium set, where $BR\left(\cdot\right)$ denotes player's $i,i\in N$ best response strategy to other players' strategies, [62].

In the following lemma, we prove the sufficient conditions in order PRI-PO game to be submodular.

Lemma 20. ***(PRI-PO Submodular Game:)*** *PRI-PO game's* G_{PRI-PO} *net utility function* $U_i^{NET}\left(\mathbf{P},\mathbf{c}\right)$ *as defined in Eq. (3.1) is submodular in* P_i *for each fixed* c_i*, if and only if:*

$$\gamma_i\geq 0 \tag{3.9}$$

Proof. Aiming at proving that the net utility function $U_i^{NET}\left(p_i,c_i\right)$ of PRI-PO game is submodular in P_i for each fixed c_i, it needs to be $\frac{\partial^2 U_i^{NET}}{\partial P_i\partial c_i}\leq 0$. For each type of requested services, the following holds:

- **Case 1: Inelastic Services Users**
  The second order partial derivative is:

$$\frac{\partial^2 U_i^{NET}}{\partial P_i\partial c_i}=-e^{P_i}<0,\forall\gamma_i\geq 0$$

- **Case 2: Elastic Services Users**
  Similarly, the second order partial derivative is:

$$\frac{\partial^2 U_i^{NET}}{\partial P_i \partial c_i} = -e^{P_i} < 0, \forall \gamma_i \geq 0$$

Combining both cases, the utility function $U_i^{NET}(\mathbf{P}, \mathbf{c})$ as defined in relation (3.1) is submodular in P_i for each fixed c_i, i.e., condition $\frac{\partial^2 U_i^{NET}}{\partial P_i \partial c_i} \leq 0$ holds true, if and only if:

$$\gamma_i \geq 0$$

□

Moreover, in the following lemma, we examine the condition (3.8) considering PRI-PO game.

Lemma 21. ***(PRI-PO Game Non-increasing Differences:)*** *PRI-PO game's G_{PRI-PO} utility function $U_i^{NET}(\mathbf{P}, \mathbf{c})$ as defined in Eq. (3.1) has non-increasing differences in $\{(P_i, c_i), (\mathbf{P_{-i}}, \mathbf{c_{-i}})\}$, i.e., condition $\frac{\partial^2 U_i^{NET}}{\partial P_i \partial P_j} \leq 0$ holds true, if and only if:*

$$\gamma_i \in [0, \gamma_{i,BOL}] \tag{3.10}$$

where $\gamma_{i,BOL}$ is analytically determined in the following proof.

Proof. Towards proving that utility function $U_i^{NET}(\mathbf{P}, \mathbf{c})$ has non-increasing differences in $\{(P_i, c_i), (\mathbf{P_{-i}}, \mathbf{c_{-i}})\}$, we examine if $\frac{\partial^2 U_i^{NET}}{\partial P_i \partial P_j} \leq 0$, for the following two cases, as previously.

- **Case 1: Inelastic Services Users**
  The second partial derivative for the class of users requesting inelastic services is determined as:

$$\frac{\partial^2 U_i^{NET}}{\partial P_i \partial P_j} = \frac{MA^2}{{P_i}^2} R_{ser} \frac{G_i}{\sum\limits_{\substack{j=1 \\ j \neq i}}^{|N|} G_j P_j + I_0} \left(1 - e^{-A\gamma_i}\right)^{M-2} \cdot e^{-A\gamma_i} {\gamma_i}^2 \left(1 - M e^{-A\gamma_i}\right)$$

  The individual terms of the above relation are examined. It is easily observed that:

$$1 - M e^{-A\gamma_i} \leq 0 \Leftrightarrow \gamma_i \leq \frac{\ln M}{A}$$

  Morever, we denote:

$$q(\gamma_i) = \frac{MA^2}{{P_i}^2} R_{ser} \frac{G_i}{\sum\limits_{\substack{j=1 \\ j \neq i}}^{|N|} G_j P_j + I_0} \left(1 - e^{-A\gamma_i}\right)^{M-2} e^{-A\gamma_i} {\gamma_i}^2$$

  where $q(\gamma_i) > 0, \forall \gamma_i > 0$. Thus, the condition $\frac{\partial^2 U_i^{NET}}{\partial P_i \partial P_j} \leq 0$, considering users requesting inelastic services is satisfied in the interval:

$$\gamma_i \in \left[0, \frac{\ln M}{A}\right]$$

- **Case 2: Elastic Services Users**
  Considering the second partial derivative for users requesting elastic services, we have the following:

$$\frac{\partial^2 U_i^{NET}}{\partial P_i \partial P_j} = \frac{R_{ser}}{{P_i}^2 \ln(10)} \frac{G_i}{\sum\limits_{\substack{j=1 \\ j \neq i}}^{|N|} G_j P_j + I_0} \frac{A^2 M \left(1 - e^{-A\gamma_i}\right)^{M-2} e^{-A\gamma_i} {\gamma_i}^2}{1 + \left(1 - e^{-A\gamma_i}\right)^M} \cdot \left\{1 - \frac{M e^{-A\gamma_i}}{1 + \left(1 - e^{-A\gamma_i}\right)^M}\right\}$$

where we denote as: $\tau(\gamma_i) = 1 - \frac{Me^{-A\gamma_i}}{1+\left(1-e^{-A\gamma_i}\right)^M}$, hence the following equation is derived:

$$\frac{\partial^2 U_i^{NET}}{\partial P_i \partial P_j} = \frac{R_{ser}}{{P_i}^2 \ln(10)} \frac{G_i}{\sum\limits_{\substack{j=1 \\ j\neq i}}^{|N|} G_j P_j + I_0} \frac{A^2 M\left(1-e^{-A\gamma_i}\right)^{M-2} e^{-A\gamma_i} {\gamma_i}^2}{1+\left(1-e^{-A\gamma_i}\right)^M} \tau(\gamma_i)$$

It is easily proven that:

$$\frac{R_{ser}}{{P_i}^2 \ln(10)} \frac{G_i}{\sum\limits_{\substack{j=1 \\ j\neq i}}^{|N|} G_j P_j + I_0} \frac{A^2 M\left(1-e^{-A\gamma_i}\right)^{M-2} e^{-A\gamma_i} {\gamma_i}^2}{1+\left(1-e^{-A\gamma_i}\right)^M} \geq 0, \ \forall \gamma_i \geq 0$$

Hence, in order to determine the interval of γ_i, where $\frac{\partial^2 U_i^{NET}}{\partial P_i \partial P_j} \leq 0$ holds true, the inequality $\tau(\gamma_i) \leq 0$ is examined. Similarly to previous cases, we utilize Bolzano's Theorem [81]. For $\gamma_i = 0$, then $\tau(0) = 1 - M < 0, \ \forall M > 1$. For $\gamma_i = \frac{\ln M}{A}$, it is $\tau\left(\frac{\ln M}{A}\right) = 1 - \frac{1}{1+\left(\frac{M-1}{M}\right)} > 0, \ \forall M > 1$.

Thus, we conclude that: $\tau(0) \cdot \tau\left(\frac{\ln M}{A}\right) < 0$, and due to the fact that $\tau(\gamma_i)$ is smooth with respect to $\gamma_i, \ \forall \gamma_i \geq 0$, we conclude that there exists at least one $\gamma_{i,BOL} \in \left(0, \frac{\ln M}{A}\right)$ such that $\tau(\gamma_{i,BOL}) = 0$. Moreover, $\frac{\partial \tau(\gamma_i)}{\partial \gamma_i} \geq 0$ holds true, thus $\tau(\gamma_i)$ is an increasing function $\forall \gamma_i \geq 0$, thus $\gamma_{i,BOL} \in \left(0, \frac{\ln M}{A}\right)$ is unique.

Hence, the condition $\frac{\partial^2 U_i^{NET}}{\partial P_i \partial P_j} \leq 0$, considering users requesting elastic services is satisfied in the interval:

$$\gamma_i \in [0, \gamma_{i,BOL}]$$

Summarizing relations for both service categories, it is concluded that $\frac{\partial^2 U_i^{NET}}{\partial P_i \partial P_j} \leq 0$ holds true in general in the interval:

$$\gamma_i \in [0, \gamma_{i,BOL}]$$

□

Based on Lemmas 19, 20, 21, we easily conclude the following:

Corollary 21.1. *The PRI-PO game G_{PRI-PO} is submodular in (P_i, c_i), if for all $i, i \in N$*

$$\gamma_i \in [0, \gamma_{i,BOL}] \tag{3.11}$$

Based on Corollary 21.1, which concludes that G_{PRI-PO} is submodular, the existence of a non-empty set of Nash equilibria is guaranteed. Therefore, the following corollary holds:

Corollary 21.2. *The PRI-PO game G_{PRI-PO} has at least one Nash Equilibrium, which is defined as:*

$$({p_i}^*, {c_i}^*) = \arg\max_{\substack{P_i \in \mathrm{P}_i \\ c_i \in \mathrm{C}_i}} U_i^{NET}(\mathbf{p}, \mathbf{c}) \tag{3.12}$$

Convergence

Due to the similar solution approach via the use of S-modular games, convergence to PRI-PO game's Nash Equilibrium is identical to Chapter 2 Subsection 2.5.2, hence for space and convenience reasons is omitted [119].

3.2.3 Distributed Algorithm

In this section, based on our previous analysis, we introduce a distributed and iterative joint utility-based customized PRIce and POwer control algorithm (PRI-PO algorithm) that determines the Nash equilibrium point of PRI-PO game. In contrast to most algorithms presented in the literature that determine power and prices in separate steps leading to suboptimal solutions, another novelty of our work is that users' customized price and power are determined via a unified process. In PRI-PO algorithm, the decision intelligence lies on the users, who decide their willingness to pay, i.e., price, in order to receive their requested service, which is implicitly controlled by the appropriate uplink transmission power. The mobile users simultaneously define their uplink transmission powers along with the optimal acceptable prices and update both of them at the same step of the algorithm. In a nutshell, PRI-PO algorithm can be described as follows:

Algorithm 10 PRIPO Algorithm

1: The WISP announces the pricing factor sets $[c_i^{Min}, c_i^{Max}]$ to all users.
2: Each user selects a random feasible set $\left(P_i^{(0)}, c_i^{(0)}\right)$, i.e., $0 < P_i^{(0)} \leq P_i^{Max}$, $c_i^{Min} \leq c_i^{(0)} \leq c_i^{Max}$. Set $k = 0$.
3: The base station broadcasts the overall interference and each user computes its sensed interference given the knowledge of its personal channel gain only.
4: Each user refines its accepted price $c_i^{(k)}$ and its uplink transmission power $P_i^{(k)}$ following its best response strategy.
5: If the net utilities do not improve, i.e., $U_i^{NET}\left(P_i^{(k)}, c_i^{(k)}\right) > U_i^{NET}\left(P_i^{(k+1)}, c_i^{(k+1)}\right)$ for all i, $i \in N$ then stop, otherwise set $k := k + 1$ and go to step 3.

At this point it should be noted that PRI-PO algorithm's operation and decision making process is fully distributed. At Step 3, the base station broadcasts only the overall interference without taking any decision about user's uplink transmission power and price.

3.2.4 Numerical Results

In this section we provide some numerical results illustrating the operation, features and benefits of the proposed framework and the PRI-PO algorithm. The overall approach's efficiency is demonstrated via representative comparisons to relevant research works proposed in the literature. Initially, we focus on the operation performance achievements of our proposed approach by providing a comparative evaluation of PRI-PO algorithm against other resource allocation approaches existing in the literature with respect to the metric of user's uplink transmission power and energy-efficiency. For comparison purposes the following three scenarios are considered, where common prices for all users determined by the WISP are used, while the actual value of the prices is differentiated per each of the comparative scenarios as follows: (a) uplink transmission power allocation, where WISP heuristically determines price with respect to user's uplink transmission power [10], (b) uplink transmission power and rate allocation in a semi-joint manner [80], and (c) uplink transmission power allocation where common price with respect to the interference is considered [101].

Then, we discuss alternatives of possible realistic implementations of the PRI-PO framework towards achieving computational complexity mitigation of the two variable distributed PRI-PO algorithm. These alternatives are based on the adoption of different user segmentation strategies mainly from a pricing perspective, through the identification and usage of users' common characteristics, in terms of QoS prerequisites, service characteristics, concentration in specific topological areas of the network, distance from the base station, etc.

Throughout our study we consider the uplink of a single cell system supporting continuously back-logged users requesting elastic and inelastic services. Towards studying the performance of the proposed PRI-PO framework as the number of users in the system increases, the total number of users $|N(t)|$ ranges from 6 to 15, while the users are placed randomly within the cell at each simulation scenario. Moreover, given a generated topology and in order to have a good balance of both type of services we assume without loss of generality an alternating order of services, where the less distant user requests inelastic service, the second less distant user requests elastic service and so on and so forth. The target service rate of the users that request inelastic services is $R_{ser} = 64kbps$. Moreover, we performed a detailed Monte Carlo analysis over random users' positions, where we examined $10,000$ random network

topologies for all the presented numerical results. We model users' path gains using the simple path loss model $G_i = {}^{K_i}/_{d_i^a}$, where d_i is the distance of user i from the base station, a is the distance loss exponent (e.g., $a = 4$), and K_i is a log-normal distributed random variable with mean 0 and variance $\sigma^2 = 8(db)$, representing shadow effect. Moreover, for demonstration purposes only and without loss of generality, we assume that all users adopt one common modulation and coding scheme, which is expressed through the sigmoidal efficiency function $f(\gamma_i) = (1 - e^{-1.15\cdot\gamma_i})^M$, $M = 80$.

Furthermore, each user has a physical limitation on its maximum uplink transmission power, i.e., $P_i^{Max} = 0.2\ Watt$, while each WISP has a maximum and minimum price that plans to announce to its users, i.e., $c_i^{Max} = 10^{10}$, $c_i^{Min} = 0$. It is noted that the parameters A, M of the efficiency function $f(\gamma_i)$ and the boundaries c_i^{Max}, c_i^{Min} have been properly selected, so as to be realistic while the two terms of user's net utility function U_i^{NET} are almost of the same order of magnitude. Moreover, the radius of the cell is $R = 1000\ m$ and the users are physically placed within the cell. Henceforth, we consider the following values of the system parameters, as shown in Table 3.2.

Table 3.2: Simulation parameter values for PRI-PO algorithm

Parameter	**Value**	**Parameter**	**Value**
P_i^{Max}	0.2 $(Watt)$	a	4
$P_i^{\star(0)}$	10^{-4} $(Watt)$	M	80
$c_i^{(0)}$	0	A	1.15
W	10^6 (Hz)	$R_{ser(IN)}$	64 $kbps$
I_0	5×10^{-16}	$R_{ser(EL)}$	128 $kbps$

Comparative Performance Evaluation

In this subsection, as explained before, the main goal is to discuss and quantify the benefits obtained by the proposed optimal joint distributed price and power control approach, through a comparative performance evaluation study of PRI-PO framework (in the following we may refer to as optimal PRI-PO) against three other resource allocation approaches proposed in the literature (i.e., [10], [101], and [80]). Specifically, in [10], authors' main goal is power control, while a heuristic linear static centralized pricing policy with respect to users' uplink transmission power is imposed by the WISP that essentially determines common prices for all users residing in the cell. Similarly, in [101] users' uplink power control problem is considered as well, while a common price with respect to the overall interference within the cell is proposed for all users. In [80], a pure user-centric resource allocation problem is confronted, where both users' uplink transmission power and rate are determined in a semijoint manner. Aiming at a fair comparison, we assume that in all comparative scenarios, the users adopt the same pure utility function presented in Equation (3.1).

Fig. 3.1 and Fig. 3.2 present users' average uplink transmission power and average energy-efficiency (i.e., the ratio of user's achievable transmission rate to the corresponding transmission power representing the number of efficiently transmitted bits per each Joule of energy consumed), respectively, as a function of the number of users residing in the cell for the four different comparative scenarios, that is the proposed PRI-PO approach and the three approaches summarized above, [10], [101], and [80]. The results clearly reveal the superiority of the proposed PRI-PO framework in terms of both power savings and high energy-efficiency. This superior performance is due to the fact that under PRI-PO framework the user has not only one degree of freedom, i.e., power, as in algorithms in [10] and [101], but is capable of determining in an optimal and dynamic way both power and price. Furthermore, based on these results it is also evident that the PRI-PO framework performs well also for increased number of users, where other frameworks present significantly higher rate of increase in the corresponding transmission power, and in some cases even collapse, e.g., semi-joint power and rate control [80], due to their single variable nature of the implementation/solution. Specifically, the latter happens because this algorithm cannot effectively capture the significant increase in the induced interference when more users transmit, while on the other hand there are no efficient means in mitigating it, due to the absence of a dynamic pricing scheme. In a nutshell, the PRI-PO framework achieves increased power saving and high energy-efficiency for increasing number of users compared to the rest of the scenarios from the literature. It should be

noted that the improvement in the energy-efficiency mainly stems from the decreased power consumption, due to the fact that all examined scenarios achieve the fulfillment of users' QoS, i.e., achieve a target data rate.

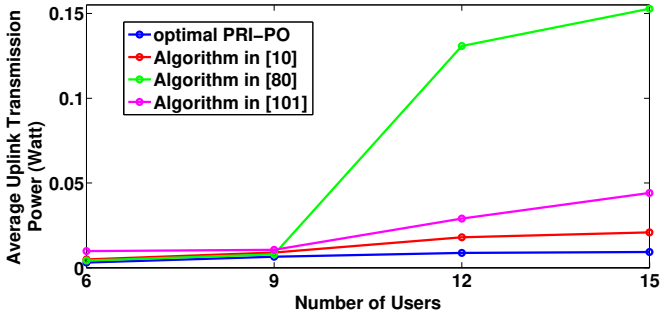

Figure 3.1: User's average uplink transmission power versus number of users considering optimal PRI-PO framework and comparative scenarios

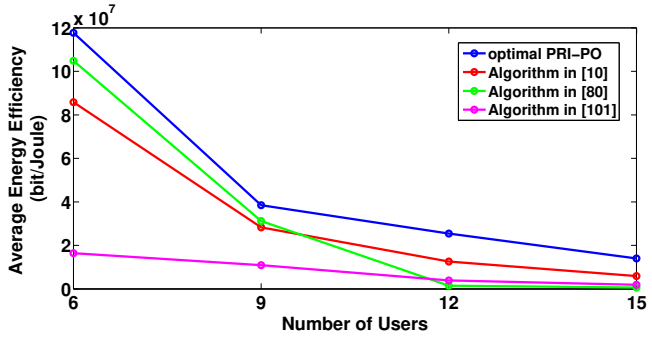

Figure 3.2: User's average energy-efficiency versus number of users considering optimal PRI-PO framework and comparative scenarios

PRI-PO Framework Implementation Alternatives: Discussions and Numerical Results

It should be noted that though the proposed optimal joint customized price and power control problem, as expressed through the PRI-PO optimization framework and corresponding algorithm presented in Section 3.2.3 (i.e., optimal PRI-PO), can achieve significant performance improvements in terms of energy-efficiency, however high computational complexity may be introduced if applied in realistic networks due to the nature of the two-variable joint optimization. In this subsection, aiming at the computational complexity mitigation we present and evaluate four realistic alternatives of implementing PRI-PO framework that still achieve satisfactory results with respect to power and energy-efficiency. These approaches are differentiated through the adoption of different user segmentation strategies mainly from a pricing perspective, while relaxing the customized price calculation at the level of group of users (i.e., common price for the users belonging to the same group) instead of obtaining a specific price for each single user. Namely, the four approaches discussed here are based on: a) centralized pricing, b) service-based pricing, c) cluster-based pricing, and d) zone-based pricing.

Firstly, the centralized pricing stands for a common price announced by the WISP to all users residing in the cell following the same pricing methodology as the one presented in [10]. The WISP announces a step increasingly universal price to all the users who recalculate and adjust their uplink transmission power. Iterating the above procedure, users converge to the two-variable Nash Equilibrium point. This pricing policy has been mainly applied to almost all cases of usage-based pricing proposed in [10], [29], [28], [40] and [31]. Secondly, the service-based pricing organizes the users in classes based on the type of service they request and their QoS prerequisites, and a common level of price is proposed for all uses within each service class. Thirdly, the cluster-based pricing exploits users' density and distribution in specific local areas of the cell towards organizing them in groups (clusters). Different levels of prices are

Table 3.3: Comparative results: average percentages of power loss, energy-efficiency loss & complexity reduction of implementations of PRI-PO approach compared to the optimal PRI-PO framework

	Power Loss	**Energy-Efficiency Loss**	**Complexity Reduction**
Zone-based pricing	7.69%	6.59%	79.26%
Cluster-based pricing	35.06%	15.34%	34.38%
Service-based pricing	39.47%	27.83%	96.83%
Centralized pricing	47.63%	47.56%	97.74%
No pricing	89.38%	68.91%	98.89%

offered to each separate group of users, who determine the optimal price and uplink transmission powers to maximize their net utilities. Fourthly, in the zone-based pricing the WISP organizes the users in different zones in relevance to their distance from the BS and a common optimal price is determined for each zone. Such an alternative can be realized by dividing the radius of the network range into distinct intervals, thus creating several non-overlapping rings (zones), where the users belonging to each "ring" (zone) are homogeneously priced.

The comparative study includes all the four aforementioned pricing approaches, as well as the approach where no pricing mechanism was considered. In Table 3.3, we present the average percentage reduction (i.e., deterioration in performance) in terms of power saving and energy-efficiency, along with the corresponding complexity percentage reduction (i.e., improvement in implementation complexity), of the four aforementioned practical implementations of PRI-PO framework when compared to the optimal approach. Specifically, we clearly observe that zone-based pricing presents an extremely efficient and effective realization of the proposed approach, as it achieves to significantly decrease the implementation complexity of PRI-PO (by 79.26% when compared to optimal PRI-PO) without paying any significant cost with respect to the obtained performance results (e.g., power, energy-efficiency, etc.), and still outperforming significantly all other alternatives in the literature as shown below. On the other hand, as seen by the results presented in Table 3.3, other alternatives achieve to further decrease implementation complexity (reaching an improvement of approximately 100%) at the cost however of higher losses in power and achieved energy-efficiency, reducing the obtained benefit, but still some of them (i.e., cluster-based pricing) performing better than the ones in the literature in terms of energy-efficiency.

Specifically, Fig. 3.3 illustrates users' average uplink transmission power as a function of the number of users residing in the cell for the four aforementioned alternatives of PRI-PO framework, the optimal PRI-PO approach, the scenario where no pricing is applied and the frameworks presented in [101] and [80]. It is noted that the centralized pricing proposed as an alternative implementation of PRI-PO algorithm follows the same pricing policy as the one presented in [10]. The results reveal that for all examined alternatives, as the number of users increases in the cell, the overall transmission conditions become more stringent and as a result their uplink transmission power increases.

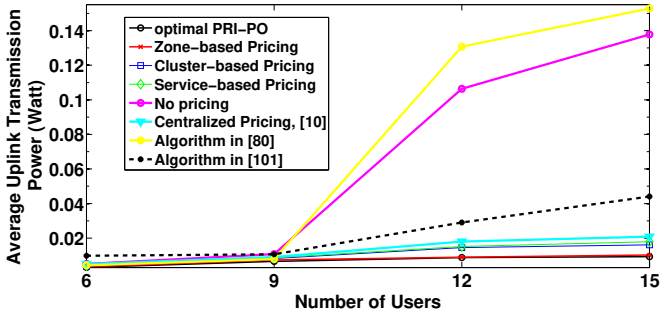

Figure 3.3: Users' average uplink transmission power under different PRI-PO framework's alternatives and comparative scenarios as a function of the number of users

The combined effect of power improvement and users' QoS prerequisites satisfaction is depicted in Fig. 3.4, where users' average energy-efficiency in $^{bits}/_{Joule}$ as a function of the number of users, is presented. Based on these results, it is clearly confirmed that zone-based pricing alternative of PRI-PO framework

outperforms the rest proposed alternatives in terms of energy-efficiency, presenting performance very close to the optimal PRI-PO. This observation holds true due to the fact that zone-based pricing better exploits network's topology, as well as users' characteristics and prerequisites due to the considered uniform distribution of users requesting different services (i.e., elastic and inelastic services) in the cell.

Furthermore, the service-based alternative of PRI-PO framework presents better results than centralized pricing. However, the results reveal that the factor of users' channel gain conditions is more dominant to power saving and energy-efficiency metrics, compared to factors associated with users' various QoS prerequisites (e.g., type of service). Thus, both cluster and zone-based pricing that mainly exploit users' channel gain conditions, conclude to better results than service-based pricing. It is obvious that customized pricing according to users' characteristics, i.e., service, cluster, and zone-based pricing, concludes to better results compared to centralized pricing that does not consider individual user's needs. Furthermore, all the alternative implementations of PRI-PO algorithm outperform the common pricing policy adopted in [101] and [80], especially for increasing number of users residing in the cell.

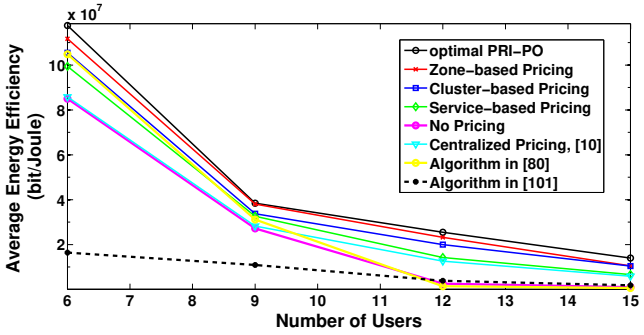

Figure 3.4: Users' average efficiency under different PRI-PO framework's alternatives and comparative scenarios as a function of the number of users.

3.3 Rate and Price Allocation

Based on the outcomes of the previous section, it becomes apparent that customized pricing can lead to significant performance gains in resource allocation problems. Controlling power consumption via pricing in wireless networks is of paramount importance in view of motivating user behavior towards a more socially acceptable behavior. However, pricing transmission power and its subsequent interference generation, can often be perceived as a strategy away from the main communication product, which is the information exchanged between the WISP and the mobile customers, translated into the data rates in bits per second.

In this part of the thesis, pricing is examined under a different angle, this time not mainly optimizing network behavior by monitoring interference generating transmissions, but by actually encouraging users to voluntarily spend more based on their QoS preferences. According to this approach, traffic from users who are willing to pay more in order to obtain higher bitstreams is prioritized against users who are not competing enough for the resources they need for their transmission. In this way, rate allocation is aligned with revenue optimization policies of the WISPs, who are able to generate more profits by offering their services to the mobile customers.

Specifically for this work, its main contributions lie in the area of enabling users to actively correlate resource allocation, QoS differentiation, and price customization towards improving their overall satisfaction under a user-centric paradigm. To the best of our knowledge, this is the first time that an intelligent mobile user is able to determine in a distributed manner its optimal rate and the corresponding price that it is willing to pay in order to achieve it. The proposed rate control and customized pricing framework has been developed aiming 5G multi-service non-orthogonal multiple access wireless networks. It should be clarified that the proposed framework is not just another work in the field of resource management which adopts game theory, but provides a novel framework dealing simultaneously with rate control and customized pricing from an autonomous user behavior point of view.

Specifically, the users, depending on prespecified/targeted signal-to-interference-plus-noise ratio (SINR) values, as they are indicated by their requested service, prioritize the allocation of the available bandwidth

among them in a real-time dynamic manner by disclosing to the WISP how much price they would accept to be charged in order to fulfill their QoS prerequisites. Hence, both variables (i.e., rate and price) are jointly determined not only in an optimal and real-time manner but also in a distributed and user-centric attitude aiming at the maximization of the users' net utilities, reflecting the overall improvement of the users' satisfaction regarding their service experience. Considering that the intelligence is provided by the mobile node, the proposed framework aims at the optimization of the naturally emerging trade-off between QoS prerequisites satisfaction and cost of resources, with reducing any interaction with the WISP. The above innovation is well aligned with networks providing heterogeneous services as in 5G systems, where each user or group of users may have considerably different demands. It is noted that in such an environment, a centrally determined pricing solution would disregard user segmentation and could damage fairness and proper resource usage instead of improving it.

Following this consideration and motivation and in order to jointly allocate the customized price and rate, an optimization problem of two variables arises which is modeled and solved as a distributed non-cooperative game. The corresponding problem is tackled by optimizing each user's net utility function and capitalizing on the principles of multi-variable S-modular theory. In the following, we refer to this problem (and corresponding game) as joint non-cooperative utility-based uplink transmission Rate and customized Price control (RP) problem.

In contrast to the preceding section [120], where the uplink transmission power control problem was treated while considering customized pricing, in this work the nature of resource is different, i.e., uplink transmission data rate, which results in completely different users' competition behavior pattern. Previously, a higher price is concluded for a specific user as a consequence of an increase in his uplink transmission power. This behavior incentivizes the rest of the group to intelligently choose their uplink power towards reaching a price reduction. In the current approach where the users have control over their transmission data rate, a higher data rate claim from some users concludes to higher prices for themselves. Thus, the rest of the users in order to withstand bandwidth competition also accept to be charged with higher prices, so as to maintain their achieved data rates. Therefore, if some users agree to pay more in order to increase their data rates, the other competing users follow the same strategy. This competition behavior pattern is captured through the supermodular games, where the actions of one player lead to similar actions from the other players and not to the opposite, as in submodular games adopted in Section 3.2.

3.3.1 System Model

In the following, the uplink of a NOMA-based wireless network including disparate user types exchanging data under system's physical limitations, is considered. To preserve simplicity in the presentation without harming the validity of our analysis and results, the notion of time slot t is omitted.

We assume $|N|$ continuously backlogged users placed around a base station (BS) with coverage radius $\Re$, requesting elastic or inelastic services, where N denotes their corresponding set. As already discussed, key characteristics of the elastic services include high throughput demand and high delay tolerance [117]. However, from a QoS satisfaction perspective, a distinctive feature of the elastic services is that they are shiftable in time, and as a consequence the corresponding users can properly reshape and adjust their demand by accounting for the respective price. On the contrary, the inelastic services are constrained by "hard" short-term data demand that needs to be achieved within a specific time frame. In turn, these requirements are translated into a specific user behavior, where the user is reluctant to consume the service when QoS drops below a pre-determined threshold.

Given the physical, technical, and economical constraints associated with both the users and the WISP, the involved resources, i.e., power, rate, and price are upper bounded $P_i^{Min} \leq P_i \leq P_i^{Max}$, $r_i^{Min} \leq r_i \leq r_i^{Max}$, and $c_i^{Min} \leq c_i \leq c_i^{Max}$ with the maximum feasible rate values being differentiated by each service type. Here as well, we consider the price to be a dimensionless unit adjustable by the users. The channel gain between the i^{th} user and the base station is denoted by G_i, and $G_i = \frac{K_i}{d_i^a}$, where K_i denotes the Rayleigh fading channel gain, a is the path loss factor, and d_i denotes the distance from the i^{th} user to the base station.

Employing the NOMA scheme in the uplink communication of a wireless network, its basic characteristic is that the users with improved channel gain sense the interference caused by the users with worse channel conditions, while the reverse does not hold true due to the successive interference cancellation (SIC) technique. Without loss of generality the channel gains are sorted as $G_1 \leq ... \leq G_{|N|}$. Following the NOMA protocol, SIC is performed at the users. Consequently, the n^{th} user detects the signal from

the i^{th}, where $n < i$ and then removes the included message from its observation in a successive manner. The signal from the n^{th} user, $i > n$, is considered as noise at the i^{th} user. Thus, it is observed that the users with worse channel gain can exclude the signals stemming from users with better channel gain in a successive manner (i.e., SIC technique) from their sensed interference. As a result, each user defines its transmission characteristics through its SINR, as defined according to the NOMA paradigm following the corresponding formulation in the seminal paper [117]:

$$\gamma_i = \frac{W}{r_i} \frac{G_i P_i}{\sum\limits_{j=i+1}^{|N|} G_j P_j + I_0} \tag{3.13}$$

The two-variables that are determined by the user are the data rate r_i and its willingness to pay for the received service, which is expressed through the price c_i. Moreover, its uplink transmission P_i is a parameter that is implicitly determined given the optimal data rate r_i^* and price c_i^*, while considering a target SINR value γ_i^{target}, as well as the physical constraints, i.e., $P_i^{Min} \leq P_i \leq P_i^{Max}$.

Cornerstone towards solving the above problem under a user-centric approach has been the adoption of pure utility functions which represent in a holistic manner user's degree of satisfaction upon receiving its requested service, while also taking into account user's QoS prerequisites (e.g., target rate) and the respective energy consumption (e.g., transmission power). Additionally, a pricing function with respect to both pricing factor c_i and SINR γ_i matches the level of the price imposed by the WISP and the user's individual willingness to pay for the desired rate based on the relevant service type. It should be noted that we strategically have chosen to express pricing function with respect to SINR, since it better captures and represents user's behavior with respect to the allocation of the system's resources, due to the fact that SINR contains both the physical resources of the uplink transmission power and rate. Therefore, if the user wants to achieve high SINR which is translated into more reliable communication, the price increases representing the fee it should pay in order to enjoy this benefit.

Utility Function

In the following, we assume that at every timeslot each user utilizes one type of service, either elastic or inelastic. Towards treating a multi-service wireless networking environment under a unified and common optimization framework, we assume that a net utility function is coupled with each user to reflect its behavior and satisfaction in terms of QoS. To achieve this objective, the introduced function maps the obtained degree of satisfaction to the expected trade-off among the parameters that depict its QoS-related performance, i.e., uplink transmission rate and eagerness to pay the price of resource usage. Hence, each user's net utility function is classified according to the type of service as follows:

$$U_i^{NET}(r_i, c_i) = \begin{cases} \frac{r_i \cdot f_i(\gamma_i)}{P_i} - c_i \left(e^{\gamma_i} - 1\right), \, (Inelastic) \\ \frac{r_i \cdot \log(1+f_i(\gamma_i))}{P_i} - c_i \left(e^{\gamma_i} - 1\right), \, (Elastic) \end{cases} \tag{3.14}$$

With regards to above relation (3.14), the efficiency function $f_i(\gamma_i)$ is modeled identically according to Eq. (2.3). With reference to the pure utility of users with inelastic services, the numerator $r_i \cdot f_i(\gamma_i)$ is a sigmoidal function of SINR γ_i, with its inflection point being mapped at the target SINR, $\gamma_i^{t \arg et}$ at which its QoS prerequisites are fulfilled. Therefore, if that user's achievable data rate is below inflection point, then a rapid reduction in its utility occurs, a fact that indicates its desire in obtaining and consuming additional system's resources. It should be highlighted that both for the elastic and inelastic services, the numerator of the pure utility function is expressed as a function of the actual transmission rate r_i and the efficiency function $f_i(\gamma_i)$, instead of only the actual transmission data rate that has been adopted so far in the literature. This formulation is proposed in order to better capture users' services' QoS prerequisites, as explained above. The aforementioned formulation of the utility function, enables a user to properly regulate its uplink transmission rate and inclination to pay, so as to obtain an SINR level that satisfies its QoS prerequisites.

Now, with reference to the users requesting elastic services, the main characteristic of the latter is their delay-tolerant and high-throughput nature. Hence, the users' goal that request elastic (i.e., non-real time) services is to achieve high throughput, thus increase their perceived satisfaction, i.e., utility. Based on this observation, users' pure utility function is strictly increasing with respect to the achievable data rate. Specifically, the respective numerator in their pure utility function represents the achievable data rate and is reflected via a log-based strictly increasing function of the user's efficiency function

$f_i(\gamma_i)$. This formulation is well aligned with the above mentioned high throughput expectations of users requesting elastic services, due to their greedy behavior. Consequently, an increase in their obtained data rate results in higher SINR values as a consequence of the nature of function $r_i \cdot \log(1 + f_i(\gamma_i))$ which is strictly increasing with respect to γ_i and therefore the overall resulting satisfaction as perceived by the users, i.e., U_i^{NET}, increases as well.

Aiming at providing a generic and stable solution for rate allocation alongside price customization, the theory of multi-variable S-modular games has again been preferred as a concrete tool towards showing the trade-off between the involved parameters. Multi-variable supermodular games as studied in [65], reflect the interrelation between the actions of one user with the rest of the players with whom it competes for the network's scarce resources. Supermodular games have been applied in multiple research works in the literature, which mainly study the resource allocation problem in wireless networks under the assumption that there is only one type of resources to be allocated among the users (especially user's transmission power), thus constituting a single variable optimization problem. We adopt multi-variable S-modular theory in order to solve a two-variable (i.e., rate and price) optimization problem, corresponding to the problem of our interest, since a user paying higher prices in order to increase its data rate is followed by a similar trend from the rest of the users, who in order to withstand bandwidth competition will also accept to be charged at higher prices so as to maintain their achieved data rates. The definition and the conditions a supermodular game needs to satisfy are summarized in Theorem 10 and the relations (2.27), (2.29), (2.30), [119] hence, for convenience are not repeated in this section.

Table 3.4: Section 3.3 list of key notations

Symbol	Description
$\|N\|$	Number of backlogged users
$\Re$	Coverage radius
P_i	Uplink transmission power
r_i	Uplink data rate
c_i	Price
G_i	Channel gain
K_i	Rayleigh fading channel gain
a	Path loss factor
d_i	Distance from base station
γ_i	Signal-to-interference-plus-noise-ratio (SINR)
W	Spreading bandwidth
I_0	Additive White Gaussian Noise
U_i^{NET}	Net utility
γ_i^{target}	Target SINR
$f_i(\gamma_i)$	Efficiency function
$\vec{r}$	Vectors of users' uplink transmission rate
$\vec{c}$	Vectors of users' uplink transmission price
$\{R_i, C_i\}$	Strategy spaces
G_{RP}	RP game
$BR(r_i, c_i)$	Best response strategy
P_i^*	Power consumption

3.3.2 Problem Formulation and Solution

Game theory has been promoted as a natural and powerful choice when dealing with users that exhibit selfish and greedy behavior. When operating in a competitive environment, the wireless network users act as players that contend against each other, and select a strategy space of data rate and willingness to pay, i.e., price, and as a result of their choices achieve a payoff expressed by their utility. In this section, we model our problem as a two-variable (Rate (r_i) and Price (c_i)) - RP game, assuming a wireless network consisting of $|N|$ users. For convenience, all notations met throughout this section are summarized in Table 3.4.

Given that the objective of each user is to maximize its utility, the RP game can be formulated as a distributed utility maximization problem. We denote the RP game $G_{RP} = \left[N, \{R_i, C_i\}, \left\{U_i^{Net}(\vec{r}, \vec{c})\right\}\right]$ as:

$$\textbf{RP Game}: \\ \max_{r_i \in R_i, c_i \in C_i} U_i^{Net}(\vec{r}, \vec{c}), \ \forall i \in N \\ s.t.\ r_i^{Min} \leq r_i \leq r_i^{Max} \ and \ c_i^{Min} \leq c_i \leq c_i^{Max} \tag{3.15}$$

where $\vec{r} = \left(r_1, ..., r_i, ..., r_{|N|}\right)$ and $\vec{c} = \left(c_1, ..., c_i, ..., c_{|N|}\right)$ are the vectors of users' uplink transmission rate and prices, and R_i, C_i denote the i^{th} user's strategy spaces in uplink transmission rate and price, respectively. The RP game should conclude to a solution that determines the optimal equilibrium (Nash Equilibrium) for the system, based on the individual decisions of each user, given the decisions made by the rest of the users.

Theorem 22. ***(RP Game NE:)*** *The strategy vector* $\left(\overrightarrow{r^*}, \overrightarrow{c^*}\right) = \left(r_1^*, ..., r_i^*, ..., r_{|N|}^*, c_1^*, ..., c_i^*, ..., c_{|N|}^*\right)$ *in the strategy sets* $r_i^* \in R_i$ *and* $c_i^* \in C_i$ *is a Nash Equilibrium of the RP game if for every user* $\forall i, i \in N$ *the following condition is satisfied:*

$$U_i^{Net}\left(r_i^*, c_i^*, \overrightarrow{r_{-i}^*}, \overrightarrow{c_{-i}^*}\right) \geq U_i^{Net}\left(r_i, c_i, \overrightarrow{r_{-i}^*}, \overrightarrow{c_{-i}^*}\right) \tag{3.16}$$

for all $r_i \in R_i$ *and* $c_i \in C_i$

Moreover, it should be noted that the existence of Nash Equilibrium point guarantees a stable outcome of the RP game, while on the other hand, the nonexistence of such an equilibrium is interpreted as an unstable state of the system. The proof of the existence of at least one Nash equilibrium of RP game, is mainly based on the use of supermodular games properties.

Lemma 23. ***(RP Supermodular Game:)*** *The RP game* G_{RP} *is supermodular in* (r_i, c_i), *if* $\forall i$, $i \in N$

$$\gamma_i \geq 0 \tag{3.17}$$

Proof. The RP game $G_{RP} = \left[N, \{R_i, C_i\}, \left\{U_i^{Net}(\vec{r}, \vec{c})\right\}\right]$ is supermodular $\forall i \in N$ if the following apply:

1. $S_i = R_i \times C_i$ is a compact subset of the Euclidean space
2. U_i^{Net} is smooth and supermodular in (r_i, c_i) i.e.,

$$\frac{\partial^2 U_i^{Net}}{\partial r_i \partial c_i} \geq 0, \ \forall i \in N \tag{3.18}$$

3. U_i^{Net} has non-decreasing differences in (r_i, c_i), $(\vec{r}_{-i}, \vec{c}_{-i})$, if:

$$\frac{\partial^2 U_i^{Net}}{\partial r_i \partial r_j} \geq 0, \ \forall j \neq i \tag{3.19}$$

given that:

$$\frac{\partial^2 U_i^{Net}}{\partial r_i \partial c_j} = 0, \forall j \neq i \tag{3.20}$$

The largest and smallest elements are denoted as $(\overline{r_i}, \overline{c_i}) = \sup\{(r_i, c_i) \in S_i : BR(r_i, c_i) \geq (r_i, c_i)\}$ and $\left(\underline{r_i}, \underline{c_i}\right) = \inf\{(r_i, c_i) \in S_i : BR(r_i, c_i) \leq (r_i, c_i)\}$, with $BR(r_i, c_i)$ denoting the best response strategy of a player given the strategies of the rest of the involved players. According to [82], BR is standard, thus guaranteeing the convergence of the RP game to its Nash Equilibrium, assuming any feasible initial solution. Combining relations (3.18), (3.19), (3.20) and requesting to hold true together, we derive the set of values of SINR, under which RP game is supermodular.

Considering the users requesting elastic services and examining the aforementioned two conditions, we have: $\frac{\partial^2 U_i^{Net}}{\partial r_i \partial c_i} = \frac{e^{\gamma_i}\gamma_i}{r_i} > 0$, $\forall i \in N$, $r_i \in \left[r_i^{Min}, r_i^{Max}\right]$, $P_i \in \left[P_i^{Min}, P_i^{Max}\right]$, $\frac{\partial^2 U_i^{Net}}{\partial r_i \partial r_j} = 0$, and $\frac{\partial^2 U_i^{Net}}{\partial r_i \partial c_j} = 0$, where $\frac{\partial \gamma_i}{\partial r_i} = -\frac{\gamma_i}{r_i}$.

Also, considering the users requesting inelastic services, based on equation (3.14) and regarding the two conditions mentioned above, we have: $\frac{\partial^2 U_i^{Net}}{\partial r_i \partial c_i} = \frac{e^{\gamma_i}\gamma_i}{r_i} > 0$, $\forall i \in N$, $r_i \in \left[r_i^{Min}, r_i^{Max}\right]$, $P_i \in \left[P_i^{Min}, P_i^{Max}\right]$, $\frac{\partial^2 U_i^{Net}}{\partial r_i \partial r_j} = 0$, and $\frac{\partial^2 U_i^{Net}}{\partial r_i \partial c_j} = 0$.

Thus, we conclude that the RP game is supermodular in (r_i, c_i), if $\forall i \in N$ the following condition holds true:

$$\gamma_i \geq 0$$

□

Based on condition (3.17), we practically conclude that the RP game is supermodular in the whole strategy space, i.e., $R_i \times C_i = \left[r_i^{Min}, r_i^{Max}\right] \times \left[c_i^{Min}, c_i^{Max}\right]$. Since the game is confirmed to be supermodular, we conclude that a non-empty set of Nash Equilibria exists as follows:

Lemma 24. ***(RP Game Existence of NE:)*** *$\left(\overrightarrow{r^*}, \overrightarrow{c^*}\right) = \left(r_1^*, ..., r_i^*, ..., r_{|N|}^*, c_1^*, ..., c_i^*, ..., c_{|N|}^*\right)$ is a strategy vector within the strategy sets $r_i^* \in R_i$ and $c_i^* \in C_i$ which is a Nash Equilibrium for the RP game $\forall i \in N$. Hence, no user can further increase its utility taking as granted the choices of the other users, i.e.:*

$$(r_i^*, c_i^*) = \arg\max U_i^{Net}\left(\vec{r}, \vec{c}\right), \ \forall r_i \in R_i \ and \ c_i \in C_i \tag{3.21}$$

The proof follows a similar approach as in [65], [82], [10], and [118].

Power Consumption

Based on Lemma 24, the users determine their optimal data rates $\overrightarrow{r^*}$ and their optimal customized prices $\overrightarrow{c^*}$ in a distributed manner, while considering the existing physical and external constraints, i.e., $r_i^{Min} \leq r_i \leq r_i^{Max}$ and $c_i^{Min} \leq c_i \leq c_i^{Max}$, respectively. In our proposed approach, each user has control over the variables of the data rate r_i and the customized price c_i, which determine its corresponding perceived satisfaction that is appropriately expressed via the adopted net utility function. However, each user has an extra constraint considering its energy-availability, which is appropriately presented via the feasible transmission power interval, i.e., $P_i^{Min} \leq P_i \leq P_i^{Max}$. The lower bound P_i^{Min} expresses the minimum necessary transmission power in order user's signal to be demodulated by the receiver. The upper bound P_i^{Max} stems from mobile user's available energy.

In this work, the power consumption P_i^* of each user results from its optimal uplink transmission data rate r_i^* and its target SINR value γ_i^{target}. It is noted that the power consumption is not constant, but dynamically determined via the control parameters of the system, i.e., optimal data rate r_i^* and customized price c_i^*. Thus, the power consumption for each user is determined as follows:

$$P_i^* = \min\left(\max\left(\frac{\gamma_i^{target}}{WG_i} r_i^* \left(\sum_{j=i+1}^{|N|} G_j P_j^* + I_0\right), P_i^{Min}\right), P_i^{Max}\right) \tag{3.22}$$

It should be clarified that the RP game may have multiple NEs. However, each mobile user selects the NE point *(See Eq. (3.21))* which concludes to its minimum corresponding power consumption, as determined in Eq. (3.22), in order to improve its achieved energy-efficiency.

Convergence

Towards proving the convergence of the RP game to a Nash Equilibrium point based on the use and properties of best response dynamics, by check that users' net utility function is a standard one. User's best response strategy in the Euclidean space $R_i \times C_i = \left[r_i^{Min}, r_i^{Max}\right] \times \left[c_i^{Min}, c_i^{Max}\right]$, expressed as:

$$BR_i\left(r_i, c_i\right) = \left(r_i{}^*, c_i{}^*\right) = \underset{\substack{r_i \in R_i \\ c_i \in C_i}}{\arg\max} U_i^{NET}\left(\vec{r}, \vec{c}\right) \tag{3.23}$$

Lemma 25. ***(RP Game Convergence to NE:)*** *The RP game G_{RP} converges to its Nash Equilibrium point starting from any initial feasible solution, (i.e., $\left(r_i^{(0)}, c_i^{(0)}\right)$, $r_i^{Min} \leq r_i \leq r_i^{Max}$ and $c_i^{Min} \leq c_i^{(0)} \leq c_i^{Max}$), provided that user's best response strategy is a standard function.*

Proof. The basic step to prove that RP game converges to its Nash equilibrium $\left(\overrightarrow{r^*}, \overrightarrow{c^*}\right) = \overrightarrow{BR}\left(\vec{r}, \vec{c}\right)$ is to show that user's best response strategy belongs to the family of standard functions [82], [14]. The steps followed are identical to Chapter 2 Subsection 2.5.2 properly adjusted to the rate and price allocation case [119]. □

3.3.3 Distributed Algorithm

In the following, we present a low complexity algorithm associated with the convergence to the Nash Equilibrium of the RP game, which operates in an iterative and distributed manner. Besides providing a stable and universally applicable solution, the RP algorithm integrates within the same scheme both the rate allocation as well as the price setting for each user at the moment of receiving the required service. The algorithm is referred to as RP algorithm. The descriptive/pseudocode steps of the RP algorithm are defined as follows.

Algorithm 11 RP Algorithm

1: The feasible pricing factor sets $[c_i^{Min}, c_i^{Max}]$ are disclosed by the WISP to the users. Each user selects a random initial feasible uplink transmission power $P_i^{(ite=0)} \in [P_i^{Min}, P_i^{Max}]$ for the initialization of the transmission. Set $ite = 0$, where ite represents the number of iterations.
2: The users, given the network's physical constraints, define their optimal data rate $r_i^\star \in [r_i^{Min}, r_i^{Max}]$ and their willingness to pay, i.e., price $c_i^\star \in [c_i^{Min}, c_i^{Max}]$, as in Equation (3.23). Set $ite = ite + 1$.
3: The WISP broadcasts the imposed interference to all users $\sum_{j=1}^{N} G_j P_j$ and each user i defines its sensed interference, as described in the NOMA technique.
4: The users compute their respective transmission power $P_i^{(ite+1)} \in [P_i^{Min}, P_i^{Max}]$ given their predetermined/target SINR values and the optimal data rate $r_i^\star$ based on Equation (3.22).
5: If the pure utilities of each one of the users do not improve $U_i\left(r_i^{ite}, c_i^{ite}\right) > U_i\left(r_i^{ite+1}, c_i^{ite+1}\right)$, terminate; else go to Step 2.

A key property of the RP algorithm is its distributed operation, owing to the fact that the final decisions are concluded by each mobile user individually. Each mobile user takes the decision about its best response strategy based on its own available personal information, i.e., channel gain G_i, and a global information broadcasted by the base station, i.e., overall interference $\sum_{j=1}^{N} G_j P_j$. Therefore, in the RP algorithm, the message exchange overhead is rather limited. It should be clarified that, at Step 3, the base station simply announces the total interference to the users. The task of deciding the uplink transmission data rate and price is performed by the users themselves. Thus, the only message exchange overhead from the base station to the mobile users is the broadcasting of the values c_i^{Min}, c_i^{Max} at the beginning of the RP algorithm's execution and the total interference at each iteration of the algorithm. Also, it is highlighted that the base station broadcasts the aforementioned information, thus the users are not burdened with additional signaling exchange. Therefore, the complexity of the algorithm is not impacted by an increase on the number of the users served by the cell. Additional results regarding the computational time and complexity of various implementations of the proposed RP framework are presented below in Section 3.3.4.

3.3.4 Numerical Results

In this section, the performance evaluation of the proposed framework is conducted through modeling and simulation. Indicative numerical results are presented to gain some insight about and demonstrate the key properties and advantages of the introduced framework and the RP algorithm. In order to better appreciate and comprehend the benefits and overall operational efficiency of the proposed approach, its performance achievements and improvements are demonstrated via a comparative evaluation study against relevant state of the art research works existing in the literature.

Initially, in order to adapt the RP framework into different resource allocation scenarios and obtain insightful, comparative results and show how the adopted pricing scheme may influence the equilibrium point, we consider again the four different pricing alternatives as described in Section 3.2. For convenience, we briefly summarize them again:

(a) Customized pricing, where each user separately declares the price it would accept in order to achieve the desired QoS upon receiving the required service,
(b) Central pricing, where the WISP charges all users with a common price for their transmission,
(c) Service pricing, where the users are priced according to their requested service type, and lastly,
(d) Zone pricing, where several non-overlapping rings (zones) are created within each cell, while within each zone homogeneous pricing, is applied to all users belonging to that zone.

Stemming from the above, it is possible to segment the users into groups according to specific criteria (e.g., service, location). Hence, the selected pricing mechanisms serve different purposes depending on the priorities of the users and/or the WISP regarding complexity and computational resource consumption reduction, interference mitigation, or the utilization of network's capacity. Furthermore, the aforementioned different versions of the RP algorithm are compared against [34], where data rates are jointly allocated among the users alongside transmission powers, and [107], where the system is designed towards maximizing its uplink sum rate. For fairness in the comparison, the approaches proposed in [34, 107] have properly been adopted to the NOMA access scheme.

Model and assumptions

Throughout our evaluation analysis, the uplink of a single cell system is considered where users place requests for elastic and inelastic services. To study the behavior of the proposed RP framework under different network sizes, we varied the number of users $|N(t)|$ from 10 to 40, while they were assumed to be randomly placed within the cell of radius $R = 1000\ m$ for each simulation scenario. For any considered network topology, the order of requested services was alternating among the users, in the sense that the closest to the base station user requests inelastic service, the second closest requests elastic service, and so on. Such a setting allows for a balanced distribution, both physical (location) and logical (type of service), of the services and users in the system. Users requesting inelastic services are assumed to have service rate target of 96 *kbps* (e.g., simple video upload). For statistical purposes, a Monte Carlo simulation was adopted, where for all the presented results we studied 10, 000 random topologies considering randomly generated users' positions. Users' path gains and efficiency function are modeled for the conducted simulations identically as in Section 3.2.4.

For practical purposes, we assume that every user imposes a strict constraint on its maximum uplink transmission power, i.e., $P_i^{Max} = 0.1\ Watt$, and the WISP has specific pricing boundaries that announces ranging between a maximum and minimum price, i.e., $c_i^{Max} = 2{\cdot}10^6$, $c_i^{Min} = 0$. Throughout our numerical evaluation all the relevant parameters, including the efficiency function $f(\gamma_i)$ and the bounds c_i^{Max}, c_i^{Min} have been appropriately chosen and configured, so as to be realistic on one hand, while on the other hand to ensure almost the same order of magnitude for both terms of user's net utility function U_i^{NET}.

Performance and discussions

Figures 3.5 and 3.6 present the performance of the considered six approaches (i.e., the four alternatives of the RP framework, and the approaches in [34,107], in terms of users' average uplink transmission rate achieved and average energy-efficiency (in $^{bits}/_{Joule}$), respectively, versus the network size. The results clearly reveal the superiority of all four alternatives of the proposed RP framework in terms of both high achievable data rate and energy-efficiency. This enhanced performance stems from the fact that under RP approach the user can control both data rate and price, as well as the intelligence of determining them dynamically and in an optimal way, as the system evolves. Furthermore, the achieved high energy-efficiency represents in a combined metric the objective of simultaneously achieving lower transmission power and higher data rate. Moreover, based on the presented numerical results, it becomes evident that the RP framework performs well as the network grows in size, while the rest of the considered frameworks, e.g., [34, 107], present significantly lower data rate and energy-efficiency, and in some cases even collapse due to the absence of control over the corresponding price that the end user is penalized by the WISP. The customized pricing policy proposed in our framework outperforms the rest of the implementation alternatives, i.e., zone, service, and central pricing, in terms of increased data rate and energy-efficiency awards, due to its attribute to adapt well to each user's QoS prerequisites and willingness to pay in order to fulfill them. The results with reference to the rest of the pricing alternatives of our framework present a trade-off among the achievable data rate, energy-efficiency, and computational complexity when compared to the customized pricing policy. Specifically, zone-based pricing policy presents a well-balanced alternative implementation both in terms of efficiency and effectiveness, as it achieves an improvement in the computational time efficiency of approximately 28% when compared to

the custom pricing implementation without paying any significant cost as far as the achieved data rate and energy-efficiency is concerned. On the other hand, the rest of the implementation alternatives, i.e., central and service pricing, achieve to further improve the computational time efficiency by 98% and 90% compared to the custom pricing implementation, paying the penalty however of increased losses in the obtained data rate (i.e., 28.08% and 14.85%, respectively) and energy-efficiency (i.e., 20.91% and 16.14%, respectively). Comprehensive comparative results with respect to the metric of computation time efficiency of all the considered approaches, as compared to the baseline scenario of custom pricing implementation, are presented in Table 3.5.

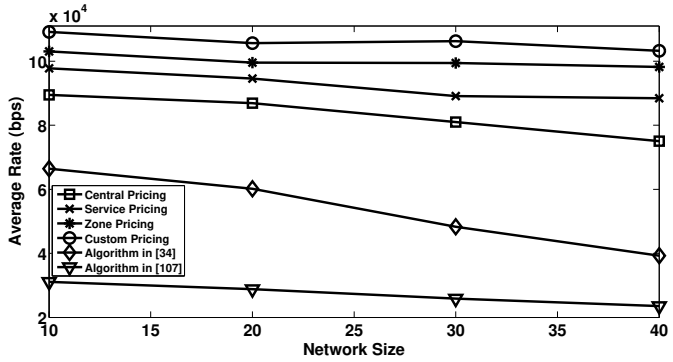

Figure 3.5: Users' average uplink transmission data rate versus the number of users considering RP framework and comparative scenarios

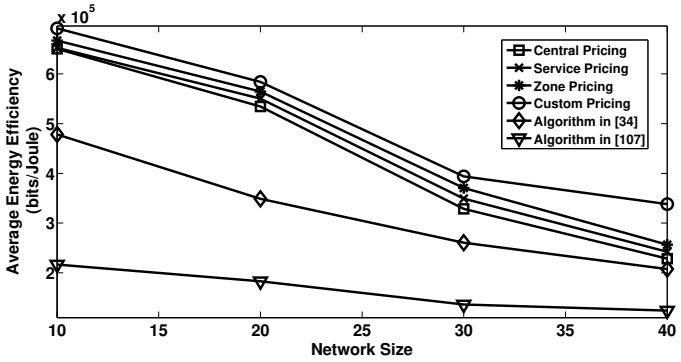

Figure 3.6: Users' average energy-efficiency versus the number of users considering RP framework and comparative scenarios

Based on these results, it is highlighted that a practical potential limitation of the custom pricing policy is its increased computational time compared to the alternative heuristic approaches (i.e., central, service and zone pricing), as well as compared to [34, 107]. Additionally, we have extended our study to the computational complexity per iteration of each of the comparative approaches, which is quantified via the average computational time per iteration per user, given the distributed nature of the algorithms. The results are presented in the last column of Table 3.5 as well. We observe that the average computational time per iteration per user for the custom pricing implementation is quite low; however, given the two-variables optimization problem that is solved, we need more iterations to converge to the optimal solution. This is the reason that the overall computational time of the custom pricing framework is increased compared to the other approaches, as discussed above.

Figures 3.7a, 3.7b and 3.8, 3.9 present similar results as in Figs. 3.5 and 3.6 - reflecting average uplink transmission rate (Fig. 3.7a, 3.7b) and energy-efficiency (Fig. 3.8, 3.9) - separately for the users that request inelastic and elastic services, respectively, in order to gain insightful information about the influence of the type of requested service on the equilibrium values of data rate and pricing. It is noted that for each simulated scenario considering increasing number of users from 10 to 40, half of them request inelastic services and the rest of them elastic services. Observing the results of Figs. 3.7a, 3.7b and 3.8, 3.9, we conclude that the custom pricing implementation of RP algorithm outperforms both the rest

Table 3.5: Comparative results for computation time efficiency and average time per iteration per user for RP algorithm

Scenario	**Increase in average computation time efficiency (against custom price)**	**Average time per iteration per user (seconds)**
[107]	97.67%	0.005200
[34]	75.97%	0.031000
RP: central price	97.56%	0.001800
RP: service price	90.81%	0.000792
RP: zone price	21.81%	0.000699
RP: custom price	(Baseline scenario)	0.000693

of the implementation alternatives of RP algorithm (i.e., zone, central, service pricing), as well as the alternatives in the literature (i.e., [34,107]), in terms of increased achieved data rate and energy-efficiency for any type of user, i.e., irrespective of the requested service type (i.e., inelastic or elastic).

Table 3.6: Comparative results for average sum rate and energy-efficiency of for RP algorithm against various scenarios - compared to Papavassiliou and Li (EURASIP, 2019)

Scenario	**Increase in average sum rate**	**Increase in average energy efficiency**
[107]	-	-
[34]	94.00%	33.15%
RP: central price	205.29%	163.83%
RP: service price	240.61%	171.76%
RP: zone price	269.58%	180.10%
RP: custom price	291.71%	202.62%

In Table 3.6, we summarize the average percentage increase in terms of achievable data rate and energy-efficiency for each algorithm, considering the six comparative scenarios. Based on these results, we observe that the different implementations of the RP algorithm considerably improve the attainable rates and energy-efficiency, achieving approximately up to 292% increase of data rate and 203% increase of energy-efficiency when compared to [107].

As mentioned before, the performance improvement of the RP implementation with customized pricing is achieved at the cost of increased computational complexity. The convergence time of the RP algorithm can be further improved via adopting several operational considerations and enhancements as discussed below. Initially, in order to derive the presented results, we execute the RP algorithm per timeslot. Towards improving the convergence performance, we can execute the RP algorithm considering as initial value of users' transmission data rate and price the ones that were calculated in the previous timeslot, i.e., "educated" implementation of RP algorithm. Taking into consideration that in reality the examined wireless communication environment is not expected to undergo significant changes within the duration of few timeslots, for all practical purposes, the users' uplink transmission rate and price values as obtained by the RP framework could be applicable to several consecutive timeslots, thus further reducing the corresponding implementation overhead.

Figure 3.10 represents the actual values of price c_i imposed to the users as a function of user's ID considering the four pricing alternatives of RP framework, i.e., (i) custom, (ii) zone, (iii) service, and (iv) central pricing. It should be noted that for demonstration purposes only, the price c_i is a dimensionless quantity. However, in a practical implementation of RP framework, the price c_i could be mapped to real monetary units reflecting the realistic economic dimension of this work. The prices that are presented in Fig. 3.10 are the Nash Equilibrium values of RP algorithm for each user. Considering the service pricing implementation, the results reveal that the users who request elastic service conclude to higher prices due to their need to achieve higher uplink transmission rates. On the other hand, in the zone pricing implementation, it is noted that the less distant users, i.e., first zone, are penalized less due to their good channel gain conditions that conclude to high transmission data rate with lower cost. Additionally,

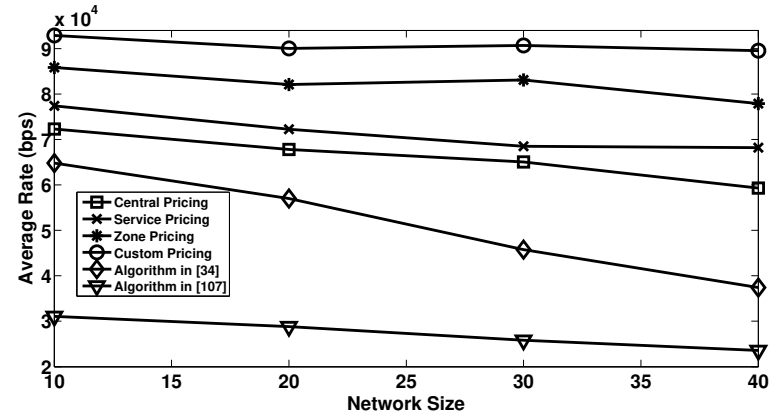

(a) Inelastic services

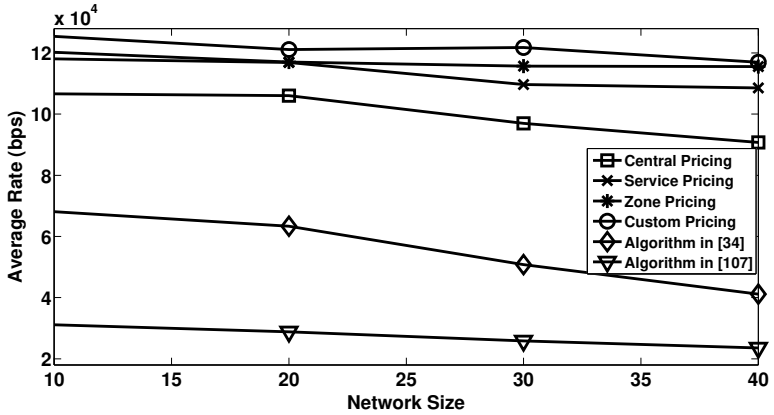

(b) Elastic services

Figure 3.7: Average uplink transmission data rate versus the number of users requesting (a) inelastic and (b) elastic services considering the RP framework and comparative scenarios

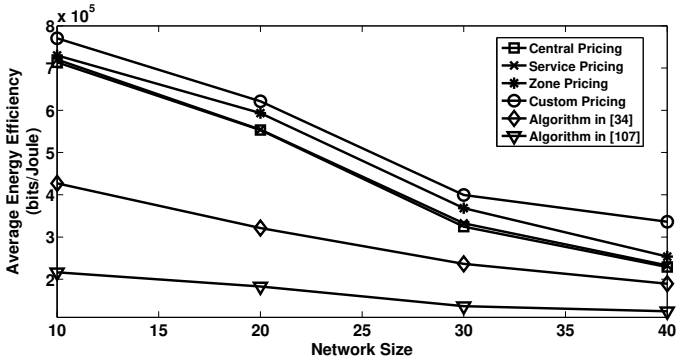

Figure 3.8: Average energy-efficiency versus the number of users requesting inelastic services considering the RP framework and comparative scenarios

in order to account for the disadvantage of the more distant users due to their deteriorated channel conditions, these users are assigned lower prices as their distance increases. The custom pricing also follows the same concept (i.e., relation of pricing and users' channels' conditions/distance from the base station). Finally, the central pricing implementation alternative of RP algorithm is the less "aggressive" one with respect to the imposed price to the users, due to the fact that it should consider the heterogeneous characteristics (i.e., requested service, channel conditions) of all the users.

Moreover, towards examining the behavior of the RP algorithm under the scenario of users' mobility within the cell, we study the impact of user's mobility on its transmission characteristics, i.e., data rate

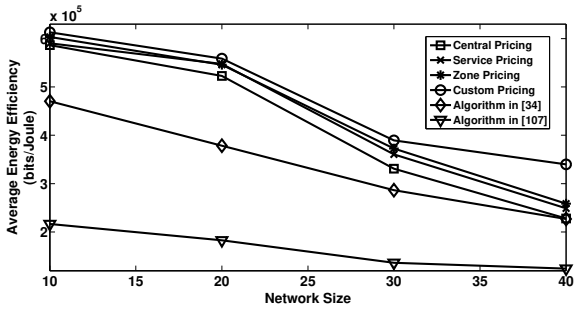

Figure 3.9: Average energy-efficiency versus the number of users requesting elastic services considering the RP framework and comparative scenarios

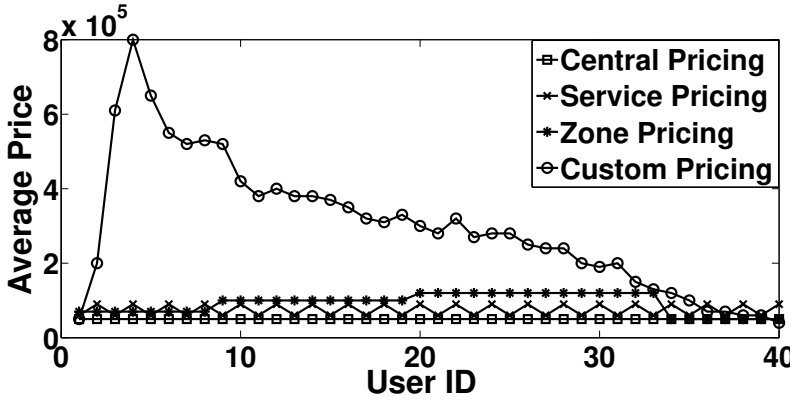

Figure 3.10: Average price (dimensionless) versus user's ID considering the alternative implementations of RP framework

and power, and on his willingness to pay for the requested service, i.e., price. It is highlighted that the duration of a timeslot is 0.5 *msec*, [80]; thus, user's intracell mobility can be considered rather limited per timeslot. As a result, the users can readjust their position coordinates within the cell per timeslot without significantly distorting the resource allocation process. For demonstration purposes, we study the impact of user's mobility to his transmission characteristics for a time-window where the user can move up to 10 m. The results reveal that the change in the rate and price allocation process is minor (approximately 0%), whereas a slight increase in the transmission power is observed (less than 0.1%). This implies that the RP algorithm maintains steady outcomes concerning the power and rate allocation, since the users constantly aim to achieve the data rates as close as possible to the feasible upper bounds. Hence, a change in user's location will not affect its data rates requirements, besides a small adjustment to the transmission power levels, so as to claim the same data rate levels. Moreover, the adoption of the NOMA SIC technique maintains the intracell interference to low levels; thus, user's mobility impact within the duration of a timeslot cannot have amplifying impact on the main transmission characteristics of the users. Additionally, by considering stochastic user's mobility, a high degree of offset among new users' positions can take place, with a number of users slightly improving their transmission (e.g., slightly better channel gain conditions) and counterbalance any negative transmission impact from the users who deteriorate their transmission capabilities in the new positions.

3.4 Multi-Resource Allocation and Pricing

Capitalizing on the previous extensive analysis of jointly allocating transmission power or data rates alongside the corresposing pricing for each mobile customer, at this section we further expand the problem to provide full control to the user over multiple resources, i.e., uplink transmission power and data rate, while simultaneously allowing it to dynamically express its desire to pay (i.e., reflected through price) to the service provider in order to satisfy its QoS prerequisites.

In the above sense, users do not focus on reaching a price equilibrium with the WISP in their aim

to transmit with the optimal penalties for their interference causing behavior or for claiming a higher portion of the available speed by accepting higher prices. This time, users since they simultaneously "negotiate" with the WISP the price that will pay for both for transmitting (in Watts) and purchasing the exchange of data (in bits per second), they eventually optimize their corresponding energy-efficiency performance (in bits per Joule) given the price that their transmission would cost them.

To the best of our knowledge, this is the first time in literature that three parameters (or resources) are jointly optimized in a wireless network resource allocation problem and consists one of the first approaches that steps out of the conventional power or data rate pricing model. This time the users target to increase their satisfaction in a more holistic manner, not only by claiming more resources in terms of bandwidth, but also to rationally calculate their transmission power as part of optimizing their overall energy-efficiency.

As a result, a User Personalized Price Setting TowaRds the Efficient Allocation of Multiple Resources (UPSTREAM) is proposed. In the UPSTREAM framework, the mobile user is able to actively correlate the multi-resource allocation, QoS differentiation, and price customization, towards improving its overall satisfaction under a user-centric paradigm.

3.4.1 System Model

The uplink of a NOMA 5G wireless network with $|N|$ users is considered, where N denotes the corresponding set of users. Let also denote by p_i and r_i the user's i uplink transmission power and data rate respectively, with $p_i^{Min} \leq p_i \leq p_i^{Max}$ and $r_i^{Min} \leq r_i \leq r_i^{Max}$. A pricing function $c\left(c_i, p_i\right)$, is also related to each user, which contains the customized price c_i, $c_i^{Min} \leq c_i \leq c_i^{Max}$ taking into account each user's $i, i \in N$ consumed resources and its caused interference via its transmission power p_i to the rest of the network players. Again, the price c_i is considered as a dimensionless quantity without harming the validity of our analysis.

The received signal-to-interference-plus-noise ratio (SINR) is similar as defined in Eq. (3.13) from previous section regarding the NOMA transmission technique [121]. Let $W\ [Hz]$ denote the system's spreading bandwidth, $I_0\ [W]$ the Additive White Gaussian Noise (AWGN) power representing the background noise, G_{jj} the channel gain from the transmitter of user i to the base station (BS), and G_{jj} the channel gain from the transmitter of user i to the receiver of user $j, j \in N$. Employing the NOMA scheme in the uplink communication, it follows that users with improved channel gain sense the interference caused by users with inferior channel conditions, while the reverse does not hold true owing to the successive interference cancellation (SIC) technique. Let us assume that the channel gains are sorted as $G_1 \leq ... \leq G_{|N|}$.

Similarly to previous discussions as in Chapter 3.2.1, the utility functions consist of two parts: the pure utility and the pricing part. The pure utility part represents the ratio of the achievable data rate over the corresponding power consumption during the uplink transmission. On the other hand, the pricing function is announced by the WISP, who penalizes the mobile users with respect to the SINR γ_i in a non-linear manner via the customized pricing factor c_i. Therefore, the mobile users, who present a greedy behavior within the 5G wireless network, i.e., increased SINR target value in order to achieve a better QoS, are penalized more by the WISP due to their trend to impose increased interference within the network via their dominant transmission. Consequently, a mobile user who requests an increased QoS, should be inclined to pay a higher price c_i.

Based on the above discussion, the utility function of each mobile user $i, i \in N$ residing in the NOMA 5G wireless network can be written as follows:

$$U_i(\mathrm{p}, \mathrm{r}, \mathrm{c}) = \frac{r_i \cdot f(\gamma_i)}{p_i} - c_i \left(e^{\gamma_i} - 1\right) \tag{3.24}$$

where $f(\gamma_i)$ is the already well known efficiency function with its parameters as defined in Eq. (2.3). For convenience, all key notations in this section are summarized in Table 3.7.

3.4.2 Problem Formulation and Solution

Let $G = \left[N, \{P_i, R_i, C_i\}, U_i\left(p_i, r_i, c_i\right)\right]$ denote the UPSTREAM game, where $N = \{1, ..., |N|\}$ is the set of actors (users), while $P_i = \left[p_i^{Min}, p_i^{Max}\right]$, $R_i = \left[r_i^{Min}, r_i^{Max}\right]$ and $C_i = \left[c_i^{Min}, c_i^{Max}\right]$ stand for the corresponding strategy sets of user's i power, rate, and price, which create the overall strategy space $A_i = P_i \times R_i \times C_i$. U_i denotes the objective function, as expressed in Eq. (3.24). Consequently, the

Table 3.7: Section 3.4 list of key notations

Symbol	Description
p_i	Uplink transmission power
r_i	Uplink transmission data rate
c_i	Price
N	Users set
W	System's spreading bandwidth
I_0	Additive White Gaussian Noise (AWGN)
G	Channel gain
γ_i	Signal-to-interference-plus-noise ratio
$f(\gamma_i)$	Efficiency function
$\{P_i, R_i, C_i\}$	Strategy sets
x_i	Single strategic variable
$v_i(\mathbf{x}, \mathbf{c})$	Reformulated utility
I	Interference
G	UPSTREAM Game
G_T	R-UPSTREAM Game
A_i	Overall strategy space
U_i	Utility function
A, M	Efficiency function parameters
$BR\left(x_i, c_i\right)$	Best response
ξ	Constant
$\varphi\left(\gamma_i\right)$	Auxiliary function

UPSTREAM game becomes a distributed utility maximization problem, where each user updates its controllable parameters p_i, r_i, c_i, in an autonomous manner targeting at its satisfaction maximization. Let the corresponding uplink transmission power, data rate, and price vectors $\mathbf{p}^* = \left(p_1^*, ..., p_i^*, ..., p_{|N|}^*\right)$, $\mathbf{r}^* = \left(r_1^*, ..., r_i^*, ..., r_{|N|}^*\right)$ and $\mathbf{c}^* = \left(c_1^*, ..., c_i^*, ..., c_{|N|}^*\right)$ represent the solution of the game.

UPSTREAM Game

$$\begin{aligned} &\max_{(p_i, r_i, c_i) \in A_i} U_i\left(\mathrm{p}, \mathrm{r}, \mathrm{c}\right) \\ &s.t.\, p_i^{Min} \leq p_i \leq p_i^{Max},\ r_i^{Min} \leq r_i \leq r_i^{Max},\ c_i^{Min} \leq c_i \leq c_i^{Max} \end{aligned} \tag{3.25}$$

Towards converting the three-variable optimization problem (3.25) to a two-variable one, we substitute the ratio of data rate to the power with a single strategic variable, as: $x_i = \frac{r_i}{p_i}$. Hence, the utility function in (3.24), can be written as $v_i(\mathbf{x}, \mathbf{c}) = x_i \cdot f(\gamma_i) - c_i\left(e^{\gamma_i} - 1\right)$, where the reformulated SINR is expressed as $\gamma_i = \frac{W}{x_i}\frac{G_{ii}}{I}$ and $I = \sum_{j=i+1}^{|N|} \frac{r_j}{x_j} G_{ij} + I_0$. Therefore, UPSTREAM game, as defined in relation (3.25) can be in turn transformed to a Reduced two-variable game, i.e., R-UPSTREAM game denoted by $G_T = \left[N, \{A_i\}, v_i\left(x_i, c_i\right)\right]$ and formulated as below:

R-UPSTREAM Game

$$\begin{aligned} &\max_{\substack{x_i = \frac{r_i}{p_i} \in P_i \times R_i \\ c_i \in C_i}} v_i\left(x_i, c_i\right) \\ &s.t.\, p_i^{Min} \leq p_i \leq p_i^{Max},\ r_i^{Min} \leq r_i \leq r_i^{Max},\ c_i^{Min} \leq c_i \leq c_i^{Max} \end{aligned} \tag{3.26}$$

Aiming at determining the Nash Equilibrium (NE) of R-UPSTREAM game, the theory of multi-variable supermodular games is used again towards showing the tradeoff between the involved parameters [65]. The supermodular games guarantee the existence of at least one NE within the multi-space strategy set $A_i = P_i \times R_i \times C_i$, thus overcoming the notions of convexity and differentiability.

Lemma 26. ***(R-UPSTREAM Supermodular Game:)*** *The R-UPSTREAM game G_T is supermodular in (x_i, c_i), if $\forall i, i \in N$, $x_i \in \left(0, \frac{AWG_{ii}}{I \ln \mathrm{M}}\right)$.*

Proof. The R-UPSTREAM game G_T is supermodular $\forall i, i \in N$ if the following applies: (i) A_i is a compact subset of the Euclidean space, (ii) v_i is smooth and supermodular in (x_i, c_i), i.e., $\frac{\partial^2 v_i}{\partial x_i \partial c_i} \geq 0, \forall i \in N$, and (iii) v_i has non-decreasing differences in (x_i, c_i), $(\mathbf{x_{-i}}, \mathbf{c_{-i}})$, if $\frac{\partial^2 v_i}{\partial x_i \partial x_j} \geq 0, \forall j \neq i$ given that $\frac{\partial^2 v_i}{\partial x_i \partial c_j} = 0, \forall j \neq i$. Due to the properties of supermodular games where external equilibria are always identified, the largest element is $(\bar{x}_i, \bar{c}_i) = \sup\{(x_i, c_i) \in A_i : BR(x_i, c_i) \geq (x_i, c_i)\}$ and the smallest element $(\underline{x_i}, \underline{c_i}) = \inf\{(x_i, c_i) \in A_i : BR(x_i, c_i) \leq (x_i, c_i)\}$ denoting the best response strategy of a player given the strategies of the rest of the involved players. According to [14], BR is standard, thus guaranteeing the convergence of the R-UPSTREAM game to its NE starting from any feasible initial point. Combining conditions (ii), (iii) and requesting to hold true together, we derive the set of values of x_i, where the R-UPSTREAM game is supermodular. Considering the condition (ii), we have:

$$\frac{\partial^2 v_i}{\partial x_i \partial c_i} = \frac{1}{x_i} e^{\gamma_i} \gamma_i > 0, \ \forall \gamma_i > 0 \tag{3.27}$$

Thus, condition (ii) is satisfied for $\gamma_i > 0$. Also, condition (iii) is satisfied, as $\frac{\partial^2 v_i}{\partial x_i \partial c_j} = 0, \forall j \neq i$ holds true $\forall x_i \in P_i \times R_i$ and $\forall c_i \in C_i$, and we have:

$$\frac{\partial^2 v_i}{\partial x_i \partial x_j} = \frac{\gamma_i r_i G_{ij}}{I x_j^2} \left\{ A^2 M \left(1 - e^{-A\gamma_i}\right)^{M-2} e^{-A\gamma_i} \left(1 - M e^{-A\gamma_i}\right) + c_i \frac{1}{x_i} e^{\gamma_i} \left(1 + \gamma_i\right) \right. \tag{3.28}$$

where we observe that for the individual factors of (3.28), $\frac{\gamma_i r_i G_{ij}}{I x_j^2} > 0$, $A^2 M \left(1 - e^{-A\gamma_i}\right)^{M-2} e^{-A\gamma_i} > 0$, $c_i \frac{1}{x_i} e^{\gamma_i} \left(1 + \gamma_i\right) > 0$, $\forall x_i \in P_i \times R_i$ and $\forall c_i \in C_i$. We set $\varphi(\gamma_i) = 1 - M e^{-A\gamma_i}$. It is $\varphi(\gamma_i) \geq 0 \Leftrightarrow \gamma_i \geq \frac{\ln M}{A} \Leftrightarrow x_i \leq \frac{AWG_{ii}}{I \ln M}$. Combining the above results, we conclude that R-UPSTREAM game G_T is supermodular in $(x_i, c_i), \forall i \in N$ if $x_i \in \left(0, \frac{AWG_{ii}}{I \ln \mathrm{M}}\right), \forall c_i > 0$ □

Lemma 27. ***(R-UPSTREAM Game Existence of NE:)*** *There exists a strategy vector* $(\mathbf{x}^*, \mathbf{c}^*) = \left(x_1^*, ..., x_i^*, ..., x_{|N|}^*, c_1^*, ..., c_i^*, ..., c_{|N|}^*\right)$ *within the strategy sets* $\forall x_i^* \in P_i \times R_i$ *and* $\forall c_i^* \in C_i$*, which is an NE for R-UPSTREAM game* $\forall i \in N$*.*

$$(x_i^*, c_i^*) = \arg\max v_i(\mathbf{x}, \mathbf{c}), \ \forall x_i \in \left(0, \frac{AWG_{ii}}{I \ln \mathrm{M}}\right), \ c_i \in C_i \tag{3.29}$$

Proof. If the R-UPSTREAM game is supermodular, as shown in Lemma 26, then it has at least one NE [65], [14].

Let $\xi = \min\left(\frac{r_i^{Max}}{p_i^{Min}}, \frac{AWG_{ii}}{I \ln \mathrm{M}}\right)$. Two basic cases can derive from the values p_i^{Max}, r_i^{Max} and ξ, i.e., Case A: $\frac{r_i^{Max}}{p_i^{Max}} < \xi$ and Case B: $\frac{r_i^{Max}}{p_i^{Max}} > \xi$. We show that there exists $(p_i', r_i') \in P_i \times R_i$ such that $x_i = \frac{r_i'}{p_i'}$, for each of the possible and examined cases. Regarding Case A, two subcases are possible:

- Case A1: $x_i \in \left(\frac{r_i^{Min}}{p_i^{Max}}, \frac{r_i^{Max}}{p_i^{Max}}\right)$. We consider $p_i' = p_i^{Max}$ and $r_i' = x_i p_i^{Max}$. The uplink transmission data rate r_i' is lower bounded, i.e., $r_i' \geq \frac{r_i^{Min}}{p_i^{Max}} p_i^{Max} = r_i^{Min}$ and upper bounded, i.e., $r_i' \leq \frac{r_i^{Max}}{p_i^{Max}} p_i^{Max} = r_i^{Max}$.

- Case A2: $x_i \in \left(\frac{r_i^{Max}}{p_i^{Max}}, \xi\right)$. We consider $r_i' = r_i^{Max}$ and $p_i' = \frac{r_i^{Max}}{x_i}$. The uplink transmission power p_i' is lower bounded, i.e., $p_i' \geq \frac{r_i^{Max}}{\frac{r_i^{Max}}{p_i^{Min}}} = p_i^{Min}$, due to $\frac{r_i^{Max}}{p_i^{Min}} > \frac{r_i^{Max}}{p_i^{Max}}$ and upper bounded, i.e., $p_i' \leq \frac{r_i^{Max}}{\xi} \leq p_i^{Max}$

- Case B: We have $x_i \in (0, \xi) \subseteq \left(0, \frac{r_i^{Max}}{p_i^{Max}}\right)$. Thus, we take $p_i' = p_i^{Max}$ and $r_i' = x_i p_i^{Max}$, where the uplink transmission data rate is lower bounded, i.e., $r_i' \geq \frac{r_i^{Min}}{p_i^{Max}} p_i^{Max} = r_i^{Min}$ and upper bounded, i.e., $r_i' \leq \frac{r_i^{Max}}{p_i^{Max}} p_i^{Max} = r_i^{Max}$.

Hence, we conclude that the inequality of NE is satisfied for each of the presented cases:

$$\begin{aligned} U_i(p_i, r_i, c_i^*, \mathrm{p}_{-i}, \mathrm{r}_{-i}, \mathrm{c}_{-i}) \leq v_i(x_i, c_i^*, \mathrm{p}_{-i}, \mathrm{r}_{-i}, \mathrm{c}_{-i}) = v_i(\tfrac{r_i{}'}{p_i{}'}, c_i^*, \mathrm{p}_{-i}, \mathrm{r}_{-i}, \mathrm{c}_{-i}) \\ = U_i(r_i', p_i', c_i^*, \mathrm{p}_{-i}, \mathrm{r}_{-i}, \mathrm{c}_{-i}) \leq U_i(p_i^*, r_i^*, c_i^*, \mathrm{p}_{-i}^*, \mathrm{r}_{-i}^*, \mathrm{c}_{-i}^*) \end{aligned} \tag{3.30}$$

□

Convergence

Again, since the solution involves the standard S-modular games approach, convergence of UPSTREAM game to its Nash Equilibrium even for the extended three parameter scenario is similar to Chapter 2 Subsection 2.5.2, [119].

3.4.3 Distributed Algorithm

In the following, an algorithm which determines the NE $\left(\mathbf{p}^\star, \mathbf{r}^\star, \mathbf{c}^\star\right)$ of UPSTREAM game in an iterative and distributed way, is presented, enabling user's autonomous self-optimization. The key aspect of the UPSTREAM algorithm is that users' various controllable parameters are updated in a synchronous manner, thus the NE is derived simultaneously.

Algorithm 12 UPSTREAM Algorithm

1: The WISP discloses the feasible pricing factor sets $\left[c_i^{Min}, c_i^{Max}\right]$ to the users.
2: Each user selects an initial random feasible uplink transmission power, i.e., $p_i^{ite=0} \in \left[p_i^{Min}, p_i^{Max}\right]$, data rate, i.e., $r_i^{ite=0} \in \left[r_i^{Min}, r_i^{Max}\right]$, and price, i.e., $c_i^{ite=0} \in \left[c_i^{Min}, c_i^{Max}\right]$. Set $ite = 0$, where ite represents the number of iterations.
3: The users, given the network's physical constraints, define their optimal uplink transmission power, $p_i^{\star(ite+1)}$, data rate, $r_i^{\star(ite+1)}$, and their willingness to pay, i.e., price $c_i^{\star(ite+1)}$, where:

$$\left(p_i^{\star(ite+1)}, r_i^{\star(ite+1)}\right) = \begin{cases} \textbf{if } \frac{AWG_{ii}}{I \ln M} > \frac{r_i^{Max}}{p_i^{Max}} : & \begin{cases} \left(p_i^{Max}, x_i^{(ite)} \times p_i^{Max}\right), \text{ if } \mathbf{x_i^{(ite)}} \leq \frac{\mathbf{r_i^{Max}}}{\mathbf{p_i^{Max}}} \\ \left(\frac{r_i^{Max}}{x_i^{(ite)}}, r_i^{Max}\right), \text{ if } \mathbf{x_i^{(ite)}} > \frac{\mathbf{r_i^{Max}}}{\mathbf{p_i^{Max}}} \end{cases} \\ \textbf{else } \left(p_i^{Max}, x_i^{(ite)} \times p_j^{Max}\right) \end{cases}$$

Set $ite := ite + 1$.
4: If the utilities of each one of the users do not improve, then terminate; else go to Step 3.

3.4.4 Numerical Results

Through modeling and simulation, a detailed numerical evaluation of the proposed framework is conducted, in terms of its operation efficiency and performance effectiveness. Initially, the achievable performance of the UPSTREAM framework is compared to the scenarios, where (a) a common centralized pricing is provided by the WISP to all the users without considering their personal willingness to pay in order to achieve better QoS levels, and (b) no pricing is assumed and only the allocation of users' optimal data rate and power is performed. All the aforementioned scenarios are compared and evaluated in terms of users' consumed power, achievable data rate, energy-efficiency, and intelligent price allocation by the WISP. The objective of this evaluation is to gain some insight into the benefits of personalized pricing. At the second part of our analysis, a comparative study is performed among the UPSTREAM framework and two different customized pricing based resource allocation approaches, namely: (a) an interference-based pricing approach [55], where the users are penalized based on their interference contribution to the network, and (b) a customized pricing and power allocation, i.e., two-degrees of control in shaping and determining user's perceived satisfaction in the 5G network [120]. The objective of this evaluation is to assimilate the benefits obtained by the simultaneous consideration of three degrees of freedom to the user, i.e., two degrees corresponding to two different physical resources and one-degree representing pricing.

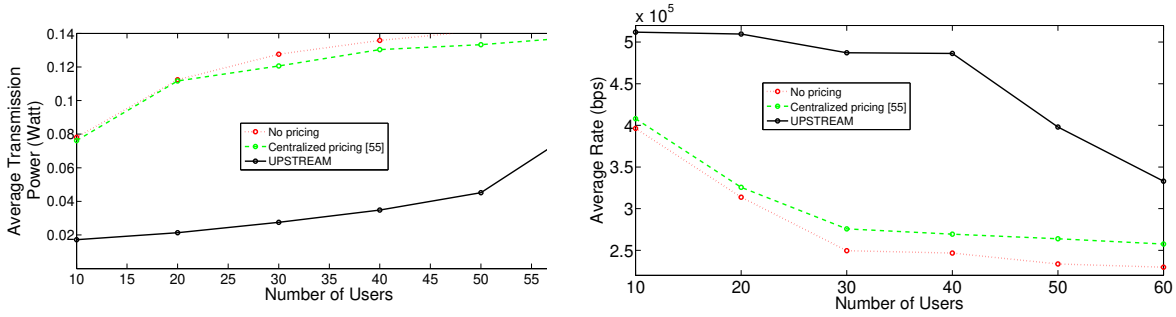

(a) (b)

Figure 3.11: (a) Average transmission power and (b) data rate vs number of users for three comparative pricing policies

For our simulations, we consider a single cell NOMA setting of radius $R_0 = 3.5km$ and the base station is placed at the center of the cell. Towards providing scalability results regarding the UPSTREAM framework, the number of users residing within the cell ranges from 10 to 60 users. The network's total bandwidth is assumed to be $20Mbps$. The simulation parameters and their corresponding values are summarized in Table 3.8. All following results are obtained through a detailed Monte Carlo analysis, considering 1000 runs for randomly generated topologies for each examined case with respect to the network size, i.e., $|N| = 10, 20, ..., 60$.

Table 3.8: Simulation parameters for UPSTREAM algorithm

Parameter	**Value**
p_i^{Max}, p_i^{Min}	$0.2W$, $0W$
r_i^{Max}, r_i^{Min}	$512kbps$, $0kbps$
c_i^{Max}, c_i^{Min}	5000, 0
$\|N\|$	$10 - 60$
A, M	1.15, 80

UPSTREAM Peformance Analysis

Fig. 3.11a and 3.11b depict users' average transmission power and the average achievable data rate, respectively, versus the network size considering the UPSTREAM framework, the centralized pricing scenario [55] and the scenario without pricing. The results reveal that the UPSTREAM framework provides the enhanced flexibility to the users to better adapt to the network's conditions, via offering them personalized pricing and thus controlling their perceived satisfaction through three different degrees, i.e., transmission power, transmission data rate, and price. Thus, the users are able to achieve lower average transmission power and higher data rates under the UPSTREAM framework compared to the centralized or no pricing scenarios. Also, an increase in the number of users results at an increase in the corresponding user's average transmission power and a decrease in the average achievable data rate, due to the increased interference within the network which deteriorates users' communication conditions and prevents them from achieving their desirable QoS levels. Furthermore, it is observed that the benefits of the centralized pricing in terms of power savings and achievable data rate are significantly smaller that the benefits of the UPSTREAM, as the first does not consider the personal characteristics of each user and penalizes all of them in the same manner.

Complementary to the aforementioned numerical results, Fig. 3.12 presents user's average energy-efficiency as a function of the number of users. The results show the combined benefits of power savings and high achievable data rate under the UPSTREAM framework, which conclude to improved energy-efficiency levels compared to the centralized and the no pricing approaches. The user's average energy-efficiency decreases rapidly as the number of users increases due to the joint influence of the increasing

user's transmission power and the corresponding decreasing achievable data rate.

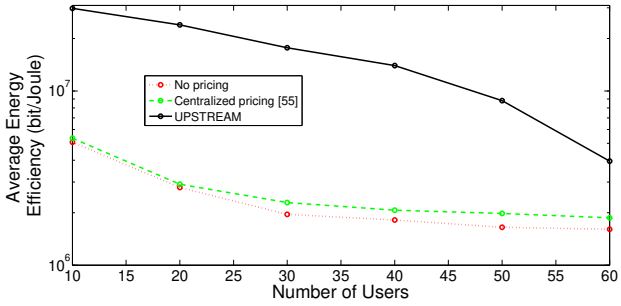

Figure 3.12: Average energy-efficiency vs number of users for three comparative pricing policies (logarithmic scale)

UPSTREAM Comparative Evaluation

In this section, a comparative evaluation analysis is provided among the UPSTREAM framework and (a) a centralized pricing mechanism based on the user's caused interference [55] and (b) a customized pricing and power allocation framework from Section 3.2, [120]. In both comparative scenarios, i.e., [55] and [120], the only resources that are allocated to the users are the transmission power and the price, where the latter is expressed in terms of user's willingness to pay.

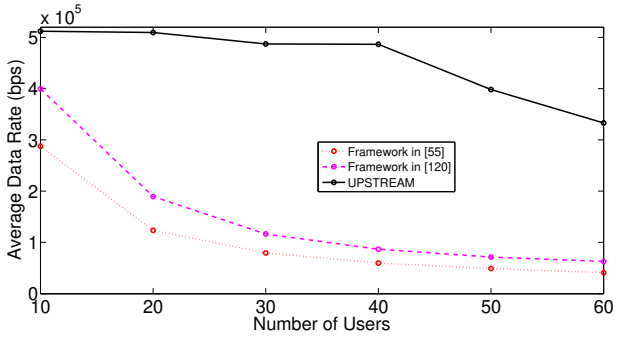

Figure 3.13: Average transmission data rate vs number of users

Fig. 3.13 demonstrates users' average achievable data rate as a function of network size considering the three examined scenarios. The results reveal that the UPSTREAM framework achieves significantly greater QoS levels compared to the rest approaches and the users' average achievable data rate decreases slowly as the number of users increases. On the other hand, the two other comparative scenarios present the same trend in terms of achievable data rate, due to the fact that in both cases the users have only two-degrees of control over their perceived satisfaction, i.e., transmission power and price. The UPSTREAM framework provides three-degrees of control to the users through dynamically adjusting two physical parameters, i.e., transmission data rate and power, and the price. Furthermore, given that the total bandwidth is assumed to be 20 *Mbps*, the average bandwidth utilization for the number of users ranging from 10 to 60 is 12.51% in [55], 18.42% in [120] and 74.39% for the UPSTREAM scenario. These results clearly demonstrate that the latter framework allows the users to better exploit the system's resources and therefore improve their overall satisfaction.

The key benefits of the UPSTREAM framework are achieved through the personalized pricing, which acts as an additional degree of control for the users via determining their pricing factor c_i, that expresses their willingness to pay to achieve a higher QoS level. Fig. 3.14 illustrates the actual value of the pricing factor as a function of users' ID for the three comparative scenarios. The users are placed in step distance from the base station. The research work in [55] announces a centralized common price to all the users considering the interference imposed on the network by all of them. The research work in [120], announces a personalized pricing to each user considering only users' transmission power levels,

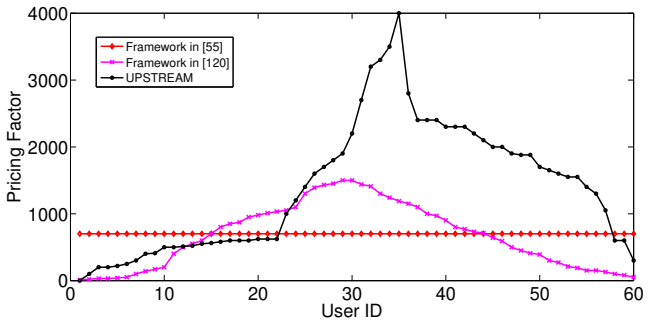

Figure 3.14: Pricing factor vs user's ID

thus it is less strict than the UPSTREAM algorithm, which in addition considers users' transmission data rates. Furthermore, in both cases of personalized pricing, i.e., UPSTREAM framework and [120], the users with average distance from the base station (i.e., 15 to 50) are penalized more to mitigate their selfish behavior which incentivizes them to increase their transmission power levels, due to both their deteriorated channel conditions and the interference they sense from the users with larger ID due to NOMA-SIC technique, as explained before.

3.5 General Summary

Pricing network resources consists an element of high importance with respect to network performance optimization and customer satisfaction. In this Chapter, we unfolded a novel approach where pricing consists an additional resource expressing a user's willingness to pay for the receipt of its requested service, in contrast to the literature, where pricing has been regarded mainly as a penalizing measure to minimize interference levels and enforce users towards a more socially acceptable behavior. Another major breakthrough analyzed is the ability to customize prices based on different criteria each time, adding more degrees of freedom in the network optimization process alongside power and / or rate control. For each of the problems, the involved net utility functions were appropriately designed in order to represent users' perceived satisfaction in terms of QoS fulfillment with respect to power, rate, and the corresponding charged price.

Firstly, the problem of joint power control and price customization was studied and solved as a two-variable submodular game assuming multiple (elastic and inelastic) services. The optimization problem was formulated as a non-cooperative price and power (PRI-PO) game, whose convergence to its Nash Equilibrium point was analytically proven. In order to mitigate the computational complexity of price customization, the WISPs can apply different pricing policies to different user segments under various criteria and still achieve satisfactory performance results. Finally, the different implementation scenarios were tested through indicative simulations, while the proposed approach was compared against other works in the literature, confirming the merits of applying a non-uniform pricing policy tailored to the needs of each user.

Next, the problem was examined under a different perspective, assuming that the involved resource to be allocated alongside price is data rate, instead of transmission power. Following a user-centric paradigm, data rate consists the most crucial parameter during the transmission, since it represents users' information exchange needs under their heterogeneous QoS prerequisites, also from a market perspective, since the users are willing to be charged in order to receive the requested service, especially under conditions of competition. Again, the problem was addressed as a two-variable rate and price (RP) supermodular game, with its solution (i.e., Nash Equilibrium point) to be analytically shown, while an iterative algorithm was devised to obtain it in a distributed manner. The performance of this framework was in depth examined through a series of simulation experiments, including again varying pricing strategies, whereas the superiority of the proposed approach was clearly demonstrated by comparing it with other research works in the literature. Specifically, it has been shown that the different implementations of the RP algorithm succeed in providing considerably higher data rates in all different user classes while at the same time maintaining transmission power at relatively low levels. This was achieved by applying customized pricing schemes to each user/user groups, thus precisely extracting consumer surplus regarding the QoS

prerequisites.

Based on the two previous solutions, in the last section of this Chapter and for the first time in the literature, a triple-parameter, power, data rate, and customized price (or willingness to pay) optimization problem was investigated in order to offer an even more holistic approach with regards to resource allocation and deliver as many degrees of freedom to the users as possible. In brief, aiming at tackling computational complexity, the original problem is reduced to a two-variable problem by optimizing the rate to power ratio x_i alongside the customized price. In this way, users are technically able to determine both the data rate and the corresponding energy consumption, by eventually improving their energy-efficiency and accept an appropriate price to be charged. As previoulsy, the (UPSTREAM) game under consideration was solved as a multi-variable supermodular game allowing for faster convergence to its unique Nash Equilibrium point. The realized performance gains in terms of both energy-efficiency and superior QoS levels due to the capability of handling various degrees of control have been confirmed via a comparative study of the proposed approach against various user segmentation methodologies and other important approaches in the literature.

Chapter 4

Provider Selection & Learning in Communication Markets

4.1 Machine Learning for Resource Allocation

Tomorrow's wireless network is expected to assess increasing volumes of information towards massive connectivity and data hungry services. This ongoing transformation instructs that networked systems need to develop built in functions so that they can manage resource distribution in a more efficient manner and develop pattern recognition and data analytics capabilities aiming at proactively adjusting the operation of the network to external factors and stimuli. From the above, we realize that such approaches can no longer be perceived as luxury features but need to be considered as a must-have characteristic of 5G ready networks.

Integrating Machine Learning (ML) algorithms and techniques can facilitate the interaction of smart wireless devices with the core of the network in order to handle in real time aspects like traffic, data exchange, energy management, content requests etc. Machine Learning can support the network to learn from its environment and adjust the resource allocation to the needs of its users by introducing intelligent resource management tools related to cell association, spectrum management, power control etc.

Furthermore, Machine Learning methodologies (i.e., supervised learning, reinforcement learning etc.) can be applied to different scenarios and can play an important role for the network to operate more autonomously and automatically optimize many of its functions. In such a way, the network can organize itself and lead to decentralized structures, with the users to become part of the decision making process without pushing large volumes of data to the network administrator, developing a parallel processing capacity which accelerates the communication and minimizes unnecessary transmissions and delays. Subsequently, the network can optimize its resources by better understanding the priorities of its connected users, mitigate interference, and manage congestion in order to deliver superior quality of services and an overall more holistic experience. The above are already a reality in recent networking paradigms (mobile edge caching, mobile edge computing etc.), hence it is of vital importance to invest more in designing Machine Learning techniques into network operations, [122–127].

4.2 Competition in Wireless Communication Markets

Within the blooming communications market where the number of mobile devices and connections reached 7.9 billion in 2015, and by the high penetration of smart devices that accounts for 89% [128] of the global mobile data traffic, it is expected that the competition among Wireless Internet Service Providers (WISPs) covering similar geographical areas and/or groups of users will only intensify. In 2021, the mobile subscribers are expected to reach 10 billion [129], hence WISPs in order to maintain their market share need to provide their potential customers with a multitude of options, ranging from different QoS offerings, to different resource allocation schemes and pricing policies.

Moreover, the deregulation of the telecommunication industry increases the flexibility of users to dynamically switch to the provider that offers the best tradeoff of price and services. Users are rational economic agents, henceforth they are able to select the service package that adjusts to their needs in the most sufficient manner, such as channel gain conditions, service variety which is in line with their

willingness to pay, [130] etc. Thus it is of great interest to jointly study the rising competition in wireless telecommunications markets where multiple WISPs strive to lock in as many customers as possible, with the mobile consumers who are becoming more critical of their preferred service provider due to the variety of alternatives they are provided. This indicates that the examined resource allocation problem requires more efficient management of the available information in an automated way to facilitate data exchange and minimize resource waste.

As a result, in this Chapter we examine the combined problem of WISP selection by the mobile customers and the corresponding power allocation, in order to meet user expectations and satisfaction in a competitive wireless communication market with several coexisting WISPs by adopting Machine Learning techniques. Each WISP is characterized by a price and service-based reputation, formed based on its adopted pricing policy and its success to satisfy customers' QoS prerequisites, the latter implicitly characterizing the specific WISP's market penetration factor. The customers act as learning automata and select the most appropriate WISP through a Machine Learning based mechanism. The output of the resource allocation problem feeds the learning system in order to build knowledge and conclude to the optimal provider selection. A two-stage iterative algorithm is proposed in order to realize the Machine Learning provider selection and the distributed resource allocation.

4.2.1 Related Work on Resource Allocation in Competitive Networks

Under such a competitive communications paradigm, end users empowered by the increased computational and communications intelligence of their smart devices, will be facing several flexibilities and challenges in dynamically selecting the most appropriate WISP to be served by, in accordance with the aforementioned options and offerings (e.g., pricing policy, WISP reputation, etc.), while properly controlling their limited power resources in order to meet their service quality requirements. Pricing studies have been devoted mainly aiming at increasing WISP's revenue and profit. Two main categories of pricing policies have been reported in the literature, i.e., static and dynamic. Static pricing policies are classified as flat-rate [109], usage-based pricing [131], tiered pricing, QoS-based pricing where multiple traffic classes with different support of users' QoS prerequisites are created and charged with different static prices [110], as well as negotiated contracts [132]. Though such policies present simplicity in their implementation, their main drawback is that they do not enable the WISPs to properly adapt to real-time users' needs and adjust their prices accordingly, therefore resulting either in low user satisfaction or poor utilization of the available resources.

To overcome this drawback various dynamic pricing policies have been proposed, such as: a) raffle-based pricing, promoting the shift of user demand to off-peak periods [133], b) auction-based pricing [134], c) day-ahead pricing [111], and d) congestion-adaptable pricing, where the WISP monitors the network and adapts the announced prices based on the observed congestion in a real time manner [135]. Nevertheless, these approaches do not consider the problem of optimal pricing as most of them are either heuristic or empirical, while more importantly they a) underestimate the need to jointly consider pricing and resource allocation for supporting multiple types of services in a real time varying environment, and b) ignore the multi-provider nature of the arising wireless competitive market.

Similarly, extensive research efforts have been devoted to the problem of power allocation in interference limited environments adopting various multiple access techniques, such as code division multiple access (CDMA) and non-orthogonal multiple access (NOMA). In 5G wireless networks, NOMA technique has been adopted to provide improved spectral efficiency, massive connectivity, and low transmission latency and signaling cost. In [136], the authors propose two power allocation frameworks, based on channel state information experienced by NOMA users and on pre-defined Quality of Service (QoS) per user respectively. In [137], a power allocation framework is proposed while considering proportional fairness objective. The authors in [138] study the optimization multi-user power and channel allocation problem in NOMA systems via combining Lagrangian duality and dynamic programming in order to conclude to a competitive suboptimal solution. However, all these efforts have been treated in isolation from the critical and interrelated resource pricing problem especially under the emerging NOMA 5G wireless networks.

Additionally, several works have already been devoted to examine the problem of resource allocation in conditions of competition between a number of WISPs. In [130], the authors show that competition of resource providers leads to a globally optimal outcomes, while [139] presents a framework where an auction mechanism dynamically allocates spectrum to the WISPs based on their bids, who later provide their service offerings to end users via dynamic pricing. Similarly, in [98] dynamic pricing is used under an equilibrium pricing scheme, where each of the involved WISPs aims to maximize its profit under QoS

constraints. [140] provides an interesting overview of how econometric measures can be used to evaluate user decisions in their interactions with the WISPs, so that the latter can better distribute the available resources. However, all the above works have not explored the conditions under which the provider selection process can be streamlined under a more generic and automated framework.

In this thesis, a Machine Learning mechanism is adopted by the customers who act as learning automata and via the learning process select the most appropriate WISP to be served by. The iterative aspect of Machine Learning is important in such a dynamic environment because as models are exposed to new data, they are able to independently adapt and evolve accordingly. Considering a time-slotted system, the Machine Learning based WISP selection algorithm determines at the beginning of each time slot the user's provider choice, while after this process is completed a power allocation framework is realized towards determining users' optimal transmission powers for the preferred WISP.

Moreover, the provider selection problem is jointly solved, while the optimal power allocation of the network is determined. The output of the resource allocation problem feeds the learning system in order to build knowledge and conclude to the optimal provider selection, even when changes dynamically apply to the system, achieving to optimize and streamline the provider selection and alongside the corresponding resource allocation.

4.2.2 System Model

A single cell non-orthogonal multiple access (NOMA) wireless network is considered, while its uplink communication is studied. Within the cell, we assume that J WISPs provide multiple types of services to the mobile customers and have full coverage of the cell. Let us denote by $\mathscr{J} = \{1, 2, 3\}$ the set of WISPs, where we have assumed three different WISPs and each one adopts one differentiated pricing policy, i.e., homogeneous, topology-based, and QoS-based. Let us denote by $\mathscr{N} = \{1, ..., i, ..., N\}$ the set of mobile customers, which consists of the mobile customers requesting real and non-real time services and their sets are $\mathscr{N}_{RT}$ and $\mathscr{N}_{NRT}$, respectively. Thus, we have $\mathscr{N} = \mathscr{N}_{RT} \cup \mathscr{N}_{NRT}$. The mobile customers requesting non-real time services are characterized by delay-tolerant data demand (e.g., video uploading, email, etc.) while those requesting real-time services impose strict short term QoS constraints (e.g., online gaming, voice, video conference, etc.)

Mobile customer's uplink transmission power is denoted by p_i and due to its physical and hardware limitations it is upper and lower bounded, i.e., $p_i^{Min} \leq p_i \leq p_i^{Max}$. The channel gain of each mobile customer $i, i \in \mathscr{N}$ to the base station is denoted by G_i. Without loss of generality, the channel gains are sorted as $G_N \leq ... \leq G_i \leq ... \leq G_1$. Based on the NOMA scheme, the Successive Interference Cancellation (SIC) technique is performed at each mobile customer. Therefore, the signal of the mobile customers with the best channel gain is demodulated first, thus the mobile customers with worse channel gain are able to remove the demodulated signals based on SIC technique and sense less interference.

Moreover, let W $[Hz]$, be the system's spreading bandwidth, $\mathbf{p_{-i}}$ denote the transmission power vector of the rest of the mobile customers in the cell and I_0 $[Hz]$ be the Additive White Gaussian Noise (AWGN) power representing the background noise. The fundamental performance measure that verifies the mobile customers' QoS prerequisites' satisfaction is the signal-to-interference-plus-noise ratio (SINR). The received SINR of mobile customer $i, i \in \mathscr{N} = \mathscr{N}_{RT} \cup \mathscr{N}_{NRT}$ at the base station can be written according to the already known definition as [138]:

$$\gamma_i \left(p_i, \mathrm{p_{-i}}\right) = \frac{W}{R_{ser}} \frac{G_i p_i}{\sum\limits_{k=i+1}^{N} G_k p_k + I_0} \tag{4.1}$$

where R_{ser} denotes mobile customer's fixed transmission, while its specific value depends on the requested service by the mobile customer and $\frac{W}{R_{ser}}$ denotes the processing gain.

Pricing Model and Policies

In the following we assume that every WISP dynamically imposes a pricing policy (e.g., homogeneous, topology-based or QoS-based, as presented in Chapter 3) to the mobile customers that are being served by it, considering the system's resources that they consume (i.e., transmission power) and the interference that their transmissions cause to the overall network. The imposed pricing policy is represented by the pricing factor c_i, which is upper and lower bounded, i.e., $c_i^{Min} \leq c_i \leq c_i^{Max}$ due to wireless market existing regulations. It is noted that the pricing factor is assumed dimensionless, however it can be easily

mapped and normalized to monetary units for further market analysis, which however is not the scope of this work. For practical purposes each WISP dynamically organizes mobile customers in classes based on different criteria according to the adopted pricing policy, and the customers belonging to the same class are homogeneously addressed by the WISP that eventually announces a common price to the users of the same class per time slot. Based on the preceding pricing analysis, we consider the following policies to be applied by WISPs towards charging their customers under competitive conditions among them:

- ***Homogeneous pricing policy.*** The WISP announces per time slot a common and universal usage-based price to all mobile customers residing in its coverage area without discriminating them, as presented in Fig. 4.1a.

- ***Topology-based pricing policy.*** In this approach, the WISP considers mobile customers' distance from the base station (BS) as the basic criterion towards penalizing them for their resource consumption and the interference that they cause to the rest of the users in the network. Thus, the WISP organizes the users in different zones with relevance to their distance from the BS and a common optimal price is determined for each zone, as shown in Fig. 4.1b. Such a discrimination is justified and motivated by the argumentation that channel conditions are worse for the more distant customers compared to the less distant ones, and thus these users tend to reach higher uplink transmission power levels in order to achieve a satisfactory QoS level. Consequently, their battery life is exhausted faster while higher levels of interference are imposed to the rest of the customers.

- ***QoS-based pricing policy.*** Users in emerging wireless networks have the ability to request different services with various QoS characteristics and competitive spectrum consumption needs. Based on their QoS requirements, the users appropriately adjust their uplink transmission power in a selfish manner, thus inducing interference within the cell. Therefore, an appropriate pricing policy should impose a more social behavior driving them towards sparingly consuming the overall system's resources. Under this observation, in QoS-based pricing scheme the WISP organizes mobile customers in pricing classes based on the type of their requested services and their corresponding QoS prerequisites. In this Chapter, we have considered two service classes consisting of mobile customers that request real (RT) and non-real time (NRT) services, as shown in Fig. 4.1c. It should be clarified that though we consider two service classes for demonstration purposes the analysis can be easily extended to multiple classes.

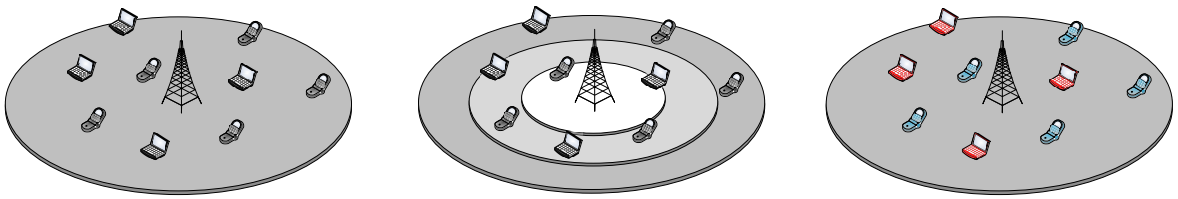

(a) Homogeneous pricing (b) Topology-based pricing (c) QoS-based pricing

Figure 4.1: Examples of pricing policies in competitive wireless communication markets

With regards to the used utility functions, they represent mobile customers' perceived satisfaction from: (i) the imposed pricing policy by the WISP, (ii) the resource allocation, and (iii) the fulfillment of their QoS prerequisites. A net utility function is adopted by each mobile customer, which as already presented throughout this thesis, it consists of the pure utility function and a cost part [28]. For both types of requested services considered (real time and non-real time), mobile customer's pure perceived satisfaction is reflected via the ratio of the achievable data rate to the corresponding consumed uplink transmission power. Thus, mobile customer's satisfaction increases if it achieves high data rate and low transmission power. The latter results in extending mobile customer's battery life and causing decreased interference to the rest of the mobile users. The utilities are again split between different service classes and are expressed as follows:

$$U_i^{NET}(p_i, \mathrm{p_{-i}}, c_i) = \begin{cases} \frac{R_{ser} \cdot f_i(\gamma_i)}{p_i} - c_i \cdot e^{p_i},\ i \in \mathrm{N_{RT}} \\ \frac{R_{ser} \cdot \log(1+f_i(\gamma_i))}{p_i} - c_i \cdot e^{p_i},\ i \in \mathrm{N_{NRT}} \end{cases} \tag{4.2}$$

where $f_i(\gamma_i)$ is the efficiency function as denoted in previous sections. Each RT mobile customer is characterized by a target SINR value, i.e., $\gamma_i^{t\arg et}$. If the target SINR value is achieved, then mobile customer's QoS prerequisites are fulfilled. Thus, the target SINR value is mapped to the inflection point of the sigmoidal function $R_{ser} \cdot f_i(\gamma_i)$, where if lower, then the perceived satisfaction decreases rapidly acting as an alert to the system that more system's resources should be allocated to the specific customer. On the other hand, for NRT mobile customers the perceived satisfaction is formulated as a logarithmic function with respect to the efficiency function $f_i(\gamma_i)$, mirroring users' greedy behavior to achieve even increased data rate. For clarity, all the parameters used in this Chapter are included in the Table 4.1.

The pricing function adopted in mobile customer's net utility function (4.2) is a convex function with respect to mobile customer's uplink transmission power p_i. This formulation has been sophisticatedly selected in order fairness to be achieved among mobile customers with respect to price. More specifically, mobile customers that transmit with high power are more penalized compared to the mobile customers that transmit with low power due to the increased interference that they cause to the overall wireless network [28], [29].

WISP Market Penetration Model

Mobile customer's decision on WISP selection is affected by its imposed pricing policy, which is expressed via the pricing factor c_i included in customer's utility function in Eq. (4.2), as well as by WISP's penetration and competitiveness in the wireless communication market. The competitiveness of a WISP $j, j \in \mathscr{J}$ is expressed via its penetration to the wireless communication market, which is translated to the total customers' achieved data rate over the total achieved data rate in the examined wireless network, i.e., $\frac{\sum_{i=1}^{N} R_{ach,i}}{\sum_{\forall j \in \mathrm{J}} \sum_{i=1}^{N} R_{ach,i}}$, where $R_{ach,i} = R_{ser} \cdot f_i(\gamma_i)$ for the RT mobile customers and $R_{ach,i} = R_{ser} \cdot \log(1 + f_i(\gamma_i))$ for the NRT customers.

4.2.3 Problem Formulation and Solution

Framework Design

At this part, the problem of joint PROvider Selection and REsource MAnagement (PROSREMA) in competitive wireless communication markets is addressed. Every time slot (or for practical purposes for every window of certain number of timeslots), each mobile customer selects the WISP that will be served from based on a Machine Learning framework. The mobile customers act as learning automata [141] gaining knowledge and experience from their past actions and they are able to intelligently sense the environment, while keeping history of their decisions in order to make more advantageous actions in the future, as time evolves. The necessary information in order to take their decision is their transmission powers $\mathbf{p}$ and the corresponding perceived utilities $\mathbf{U}^{NET}$ at the previous time slot t. Furthermore, apart from these parameters, the users consider also the competitiveness of each WISP j, i.e., reward function $r_j(t)$ (which is analytically discussed at a later section of this Chapter) in order to conclude to their final decision and action $a(t)$. Given mobile customers' actions in terms of WISP selection, a distributed non-cooperative power control game among them is performed every time slot in order to determine their optimal uplink transmission powers and their corresponding utilities. Therefore, an overall cycle of dynamic provider selection and power resource management is realized. The above described overall procedure is performed iteratively in the time, as presented in Fig. 4.2.

Provider Selection based on Machine Learning

The overall wireless network consisting of J WISPs and N mobile customers can be studied as a learning system, where customers act as learning automata that react with the environment in order to decide which WISP to select in order to be served [142, 143]. Fig. 4.2 presents the examined wireless network as a learning system and the relationship among the learning automata and their environment. Each

Table 4.1: Chapter 4 list of key notations

Symbol	Description
J	Number of WISPs
$\mathscr{J}$	Set of WISPs
$\mathscr{N}$	Set of mobile customers
$\mathscr{N}_{RT}$, $\mathscr{N}_{NRT}$	Set of users requesting real time and non-real time services
p_i	Uplink transmission
G_i	Channel gain
W	System's spreading bandwidth
$\mathbf{p_{-i}}$	Transmission power vector of the rest mobile customers
I_0	Additive White Gaussian Noise
γ_i	Signal-to-interference-plus-noise ratio (SINR)
R_{ser}	Fixed transmission data rate
c_i	Pricing factor
f_i	Efficiency function
γ_i^{target}	Target SINR value
$R_{ach,i}$	Achieved data rate
r_j	Reward function
$a(t)$, $\beta(t)$	Action and output set
$\mathbf{U}^{NET}$	Net utility function
b	Step size parameter
$\Pr_{i,j}(t)$	Probability of WISP selection
$\mathscr{P}_i$	Strategy space
λ	Constant
$\mathbf{p}^*$	Optimal transmission power vector
$\mathscr{P}_i'$	Modified strategy space
A, M	Efficiency function parameters
$g(\gamma_i)$, $h(\gamma_i)$, $\tau(\gamma_i)$	Auxiliary functions
γ_{final}	Upper value of SINR for quasi-concave utility
$BR_i(\mathbf{p})$	Best response function
R_0	Radius range
K_i	Shadow effect
n	Path loss exponent
d_i	Distance from base station
σ^2	Variance of K_i

mobile customer / learning automaton $i, i \in \mathscr{N}$ at each operation time slot has a set of action $a(t) = \{a_1, ..., a_J\}$, which represents the different choices of WISP selection, wherefrom it will be served. Towards making their decision, the mobile customers consider the output set $\beta(t) = \left\{\mathbf{U}^{NET}(t), \mathbf{p}(t)\right\}$ of their environment, where $\mathbf{U}^{NET}(t)$ and $\mathbf{p}(t)$ are the vectors of utility and power consumption of all customers. The output $\beta(t) = \left\{\mathbf{U}^{NET}(t), \mathbf{p}(t)\right\}$ is determined via performing the resource management, which will be analyzed in the next subsection. The solution of the resource management problem will be the mobile customers' optimal uplink transmission power. Based on the mobile customers' chosen actions and the corresponding reaction of the environment, we are able to determine the reward probability $r_j(t)$, which is associated with action a_j. The reward probability represents the competitiveness of the j^{th} WISP, i.e., $r_j(t) = \frac{\sum_{i=1}^{N} R_{ach,i}}{\sum_{\substack{i=1 \\ \forall j \in \mathrm{J}}}^{N} R_{ach,i}}$. The action probability vector of mobile customer / learning automaton $i, i \in \mathscr{N}$ is $\mathbf{Pr_i}(t) = \{\Pr_{i,1}(t), ..., \Pr_{i,J}(t)\}$, where $\Pr_{i,j}(t)$ expresses the probability of selecting the j^{th} WISP and following the model of learning automata, and it is updated as follows:

$$Pr_{i,j}(t+1) = Pr_{i,j}(t) - b \cdot r_j(t) \cdot Pr_{i,j}(t), \; j^{(t+1)} \neq j^{(t)} \tag{4.3}$$

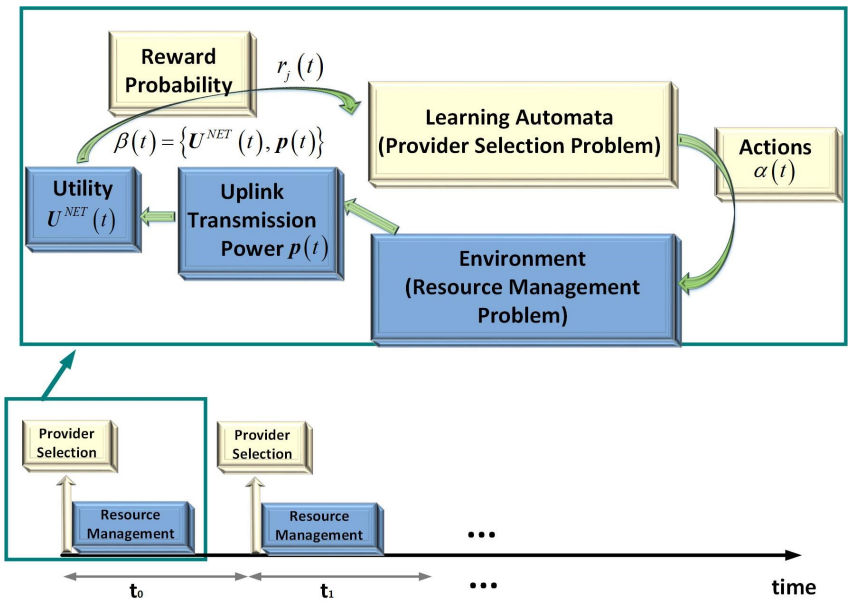

Figure 4.2: Wireless competitive communication market as a learning system

$$Pr_{i,j}(t+1) = Pr_{i,j}(t) + b \cdot r_j(t) \cdot (1 - Pr_{i,j}(t)), \; j^{(t+1)} = j^{(t)} \tag{4.4}$$

where b, $0 < b < 1$ is a step size parameter that controls the convergence time of the learning process. Equation (4.3) represents mobile customer's action probability to select a different WISP $j^{(t+1)}$ compared to the one in time slot t, i.e., $j^{(t)}$, while equation (4.4) reflects the probability of continuing the customer to be served by the same WISP, i.e., $j^{(t+1)} = j^{(t)}$.

Considering the initialization point of WISP selection, unless some more "educated" and/or historical information is available, we assume that the overall wireless network has no prior knowledge of the reward probability $r_j(t)$, $0 < r_j(t) \leq 1$ and the action probability $\mathbf{Pr}_{\mathrm{i}}(t) = \{\mathrm{Pr}_{i,1}(t), ..., \mathrm{Pr}_{i,J}(t)\}$. Therefore, the initial selection of WISP by the mobile customers could be made with equal probability, i.e., $\mathrm{Pr}_{i,j}(t=0) = \frac{1}{J}$. Finally, it is noted that the mobile customers converge to the most cost-efficient and service trustworthy WISP in a long-term period.

Power Management

Given the WISP selection, each customer aims at determining its optimal uplink transmission power p_i^* in order to maximize its perceived satisfaction, as expressed in equation (4.2). Therefore, the aforementioned mobile customers' goal is formulated as a distributed maximization problem of each customer's utility function with respect to its uplink transmission power as follows:

$$\begin{gathered} \textbf{PROSREMA Game}: \\ \max_{p_i} U_i^{NET}(p_i, \mathrm{p}_{-\mathrm{i}}, c_i), \\ s.t. \;\; p_i^{Min} \leq p_i \leq p_i^{Max}, \;\; i \in \mathscr{N} \end{gathered} \tag{4.5}$$

where $p_i \in \mathscr{P}_{\mathrm{i}}$.

Considering the distributed nature of the optimization problem (4.5) and mobile customers' selfish behavior, a game theoretic approach is adopted towards determining mobile customers' optimal transmission power vector $\mathbf{p}^* = \{p_1^*, p_2^*, ..., p_i^*, ..., p_N^*\}$. Let us denote by $G = \{\mathscr{N}, \mathscr{P}_{\mathrm{i}}, U_i^{NET}\}$ the non-cooperative power allocation game, where $\mathscr{N}$ is the set of players, i.e., mobile customers, $\mathscr{P}_i$ is the strategy space of the i^{th} customer, and U_i^{NET} its corresponding utility. The concept of Nash equilibrium is adopted towards seeking analytically the solution of the non-cooperative power allocation game. Aiming at proving the existence and uniqueness of Nash equilibrium in the non-cooperative power allocation game, we should confirm that mobile customer's utility function U_i^{NET} is quasi-concave with respect to p_i [80].

Theorem 28. ***(Quasi-concave Function for PROSREMA Game:)*** *A function U_i^{NET} is strictly quasi-concave, if for any pair of distinct points p_i and p_i' in the convex domain $\mathscr{P}_i$ and for $0 < \lambda < 1$:*

$$U_i^{NET}(p_i{}') > U_i^{NET}(p_i) \Rightarrow U_i^{NET}(\lambda \cdot p_i + (1-\lambda)\cdot p_i{}') > U_i^{NET}(p_i) \tag{4.6}$$

Based on the above, any concave function is quasi-concave.

Lemma 29. ***(Quasi-concavity of Utility Function:)*** *Mobile customer's $i, i \in \mathcal{N}$, utility function is quasi-concave in the modified strategy space $\mathscr{P}_i'$ corresponding to the SINR interval $\gamma_i \in \left(\frac{\ln M}{A}, \gamma_{final}\right)$ where $\gamma_{final} = \min\{\gamma_{RT}, \gamma_{NRT}\}$ and $\gamma_{RT}, \gamma_{\mathrm{NRT}} \in \left(\frac{\ln M}{A}, \frac{\ln 10000M}{A}\right)$, thus the Nash Equilibrium of the non-cooperative power allocation game $G = \left\{\mathcal{N}, \mathscr{P}_{\mathrm{i}}, U_i^{NET}\right\}$ exists and it is unique in the corresponding strategy space.*

Proof. Towards proving the quasi-concavity of mobile customer's utility function, we examine the sign of its second order derivative with respect to p_i. For convenience of the proof, we indicate $R = R_{ser}$ and remind that parameters A and M stem from the efficiency function modeling as in equation (2.3).

Considering the real time users, we have:

$$\frac{\partial^2 U_i^{NET}}{\partial {p_i}^2} = g(\gamma_i) + h(\gamma_i) - ce^{p_i} \tag{4.7}$$

where:

$$g(\gamma_i) = \frac{2R}{{p_i}^3}\left(1-e^{-A\gamma_i}\right)^{M-1}\left[-MAe^{-A\gamma_i}\gamma_i + 1 - e^{-A\gamma_i}\right]$$

and

$$h(\gamma_i) = \frac{MA^2R}{{p_i}^3}\left(1-e^{-A\gamma_i}\right)^{M-2} e^{-A\gamma_i}{\gamma_i}^2\left(Me^{-A\gamma_i}-1\right)$$

We examine the sign of the individual terms of equation (4.7). Considering the function $g(\gamma_i)$, we apply the Bolzano theorem, which is an important specialization of the Intermediate Value Theorem [81]. For $\gamma_i = \frac{\ln M}{A}$ we have $g\left(\frac{\ln M}{A}\right) = -\ln M - \frac{1}{M} + 1 < 0$, and for $\gamma_i = \frac{\ln 10^4 M}{A}$ we have: $g\left(\frac{\ln 10000M}{A}\right) = -\frac{\ln 10000M}{10000} - \frac{1}{10000M} + 1 > 0$, $\forall M \in (1, 1000)$. Hence, there exists a $\gamma_{RT} \in \left(\frac{\ln M}{A}, \frac{\ln 10000M}{A}\right)$ such that $g(\gamma_i) = 0$. Moreover, since $g(\gamma_i)$ is continuous, we conclude that $g(\gamma_i) < 0, \forall \gamma_i \in \left(\frac{\ln M}{A}, \gamma_{RT}\right)$. For the second term of (4.7), we have: $h(\gamma_i) < 0 \Leftrightarrow \gamma_i > \frac{\ln M}{A}$. The third term of (4.7) is always negative. Combining the above, we define the modified strategy space, where $\frac{\partial^2 U_i^{NET}}{\partial {p_i}^2} < 0$, for the real time users:

$$\gamma_i \in \left(\frac{\ln M}{A}, \gamma_{RT}\right) \tag{4.8}$$

Considering the non-real time users, we have:

$$\frac{\partial^2 U_i^{NET}}{\partial {p_i}^2} = \frac{AMR}{{p_i}^3 \ln 10}\tau(\gamma_i) - ce^{p_i} \tag{4.9}$$

where

$$\tau(\gamma_i) = \frac{\left(1-e^{-A\gamma_i}\right)^{M-2}e^{-A\gamma_i}\gamma_i}{1+\left(1-e^{-A\gamma_i}\right)^M}\left\{\ -2 + 2e^{-A\gamma_i} - A\gamma_i\left(1-Me^{-A\gamma_i}\right)\ \right\}$$
$$-AM\left(\frac{\left(1-e^{-A\gamma_i}\right)^{M-1}e^{-A\gamma_i}\gamma_i}{1+\left(1-e^{-A\gamma_i}\right)^M}\right)^2 + \frac{2\ln\left(1+\left(1-e^{-A\gamma_i}\right)^M\right)}{AM}$$

We apply again the Bolzano theorem for the function $\tau(\gamma_i)$. For $\gamma_i = \frac{\ln M}{A}$, we have:
$\tau\left(\frac{\ln M}{A}\right) = \frac{\left(\frac{M-1}{M}\right)^{M-2}\frac{1}{M}\frac{\ln M}{A}}{1+\left(\frac{M-1}{M}\right)^M}\left(-2+\frac{2}{M}\right) - AM\left(\frac{\left(\frac{M-1}{M}\right)^{M-1}\frac{1}{M}\frac{\ln M}{A}}{1+\left(\frac{M-1}{M}\right)^M}\right)^2 + \frac{2\ln\left(1+\left(\frac{M-1}{M}\right)^M\right)}{AM} < 0$ and for $\gamma_i = \frac{\ln 10^4 M}{A}$, we have: $\tau\left(\frac{\ln 10000M}{A}\right) = -\frac{1}{10000M}\frac{\ln 10000M}{2}(2+\ln 10000M) - \frac{1}{AM}\frac{1}{10000^2}\left(\frac{\ln 10000M}{2}\right)^2 + \frac{2\ln 2}{AM} > 0$ $\forall M \in (1, 1000)$ and $\forall A \in (0.1, 100)$. Hence, there exists a $\gamma_{NRT} \in \left(\frac{\ln M}{A}, \frac{\ln 10000M}{A}\right)$ such that $\tau(\gamma_i) = 0$. Moreover, since $\tau(\gamma_i)$ is continuous, we conclude that $\tau(\gamma_i) < 0$ and $\frac{\partial^2 U_i^{NET}}{\partial {p_i}^2} < 0$, for non-real time users:

$$\forall \gamma_i \in \left(\frac{\ln M}{A}, \gamma_{\mathrm{NRT}}\right) \tag{4.10}$$

Hence, combining equations (4.8) and (4.10) we conclude that all utility functions are simultaneously concave (hence quasi-concave) in the altered strategy space:

$$\gamma_i \in \left(\frac{\ln M}{A}, \gamma_{final} \right) \tag{4.11}$$

where $\gamma_{final} = \min\{\gamma_{RT}, \gamma_{NRT}\}$ □

By definition, the Nash Equilibrium of the non-cooperative power allocation game has to satisfy,

$$p_i^* = BR_i(\mathbf{p}) = \underset{p_i \in \mathrm{P_i}}{argmax}\, U_i^{NET}(p_i, \mathrm{p}_{-i}, c_i) \tag{4.12}$$

where $BR_i(\mathbf{p})$ denotes the best response function of each mobile customer $i, i \in \mathscr{N}$. The mobile customers adopt the best response dynamics and the game $G = \left\{\mathscr{N}, \mathscr{P}_\mathrm{i}, U_i^{NET}\right\}$ converges to its Nash Equilibrium, i.e., power vector $\mathbf{p}^* = \{p_1^*, ..., p_i^*, ..., p_N^*\}$, if mobile customer's best response function is standard [82], [14].

A function is characterized as standard if it satisfies the properties of: (a) positivity, (b) monotonicity, and (c) scalability for all $\mathbf{p} = \{p_1, ..., p_i, ..., p_N\}$. The above properties have already been analytically discussed in Section 2.5.2, [119]. Thus, the global convergence to the non-cooperative power allocation game's Nash Equilibrium under the proposed best response function, given by equation (4.12), is guaranteed.

4.2.4 Distributed Algorithm

In this section, we propose a two-step algorithm towards implementing the provider selection and determining the optimal power resource allocation processes, as described above. The first part of the algorithm is based on the Machine Learning framework and it is responsible to determine the provider that each user selects to be served from. It is noted that the provider selection algorithm runs once at the beginning of each time slot or alternatively in a window of time slots if the networking environment conditions do not change rapidly. On the other hand, the second part of the proposed two-step algorithm is responsible to determine the optimal power allocation in a distributed manner. The resource allocation part of the two step algorithm runs every time slot and it needs several iterations in order to converge.

Algorithm 13 PROSREMA Algorithm

1: (*Initialization*) : At the beginning of the first time slot, i.e., $t = 0$, set the initial provider selection probability vector $Pr_i(t = 0)$ as $Pr_{i,j}(t = 0) = \frac{1}{J}, \forall i \in N$. Afterwards, each mobile customer chooses a provider according to its provider selection probability vector $Pr_i(t = 0)$.

2: (*Provider Selection*) : At every time slot $t > 0$, each mobile customer chooses a provider to be served from, according to its provider selection probability vector $Pr_i(t)$ provided in relations (4.3) and (4.4).

3: (*Resource Allocation*) : Given that all customers have chosen a provider and the providers announce via broadcasting their imposed pricing, i.e., c_i, then:

4: (*Resource Allocation*) : Set $ite = 0$, where ite denotes the iteration of the resource allocation part of the algorithm. The base station broadcasts the overall interference in the network and each mobile customer determines its sensed interference.

5: (*Resource Allocation*) : Each mobile customer determines its optimal uplink transmission power in accordance to relation (4.12).

6: (*Resource Allocation*) : If $|p_i^{ite+1} - p_i^{ite}| \leq \epsilon$ (ϵ: small positive constant), the powers have converged and stop. Otherwise, return to step 4.

7: (*Provider Selection*) : Given the optimal power allocation, each provider can measure its competitiveness, which is the reward probability $r_j(t) = \frac{\sum_{i=1,j}^{N} R_{ach,i}}{\sum_{i=1,\forall j \in J}^{N} R_{ach,i}}$ and broadcasts its value to the customers.

8: (*Provider Selection*) : Each mobile customer updates its provider selection probability vector via the following rule, where $0 < b < 1$ is a step size parameter:

$$Pr_{i,j}(t+1) = Pr_{i,j}(t) - b \cdot r_j(t) \cdot Pr_{i,j}(t),\ j^{(t+1)} \neq j^{(t)}$$

$$Pr_{i,j}(t+1) = Pr_{i,j}(t) + b \cdot r_j(t) \cdot \big(1 - Pr_{i,j}(t)\big),\ j^{(t+1)} \neq j^{(t)}$$

It should be clarified that PROSREMA algorithm can be characterized as a low complexity algorithm, due to the simplicity of the calculations (i.e., closed forms) that it performs. Also, as it will be shown in detail in the section of numerical results, if the wireless communication conditions do not change rapidly, the provider selection probabilities converge fast in terms of necessary time-slots, i.e., there exists a probability $Pr_{i,j}(t)$ which is larger than a value approaching one (e.g., 0.999).

4.2.5 Numerical Results

In this section, we study the performance and operational characteristics of our proposed framework via modeling and simulation. Specifically, we initially present the framework and corresponding assumptions for the simulations and the various scenarios under consideration. Following, we concentrate on the operation and performance of the proposed framework under a series of different simulation scenarios, and we study the convergence of the PROSREMA algorithm. Finally, we conduct a comparative study of this work against two other approaches in the literature, where pricing policies have been utilized towards improving resource allocation schemes in wireless networks, demonstrating the superiority of the proposed PROSREMA approach in terms of energy-efficiency.

Simulations Assumptions

For demonstration purposes, we consider the uplink of a NOMA single cell with $N = 30$ continuously backlogged users, placed within a radius range of $R_0 = 1000\ m$. Users request Real Time (RT) or Non-Real Time (NRT) services, assuming target rates of 128 *kbps* for the first, and feasible rates of more than 360 *kbps* for the latter. Users, depending on their requested service type, are alternatively placed within the topology with increasing distance from the base station coordinates. For both user classes, each user's physical constraint towards transmission power is set at $p_i^{Max} = 0.2\ W$, while the user's path gain is modeled as $G_i = {}^{K_i}/_{d^n}$, where K_i represents the shadow effect being a log normal distributed random variable with mean 0 and variance of $\sigma^2 = 8dB$, d_i denotes the distance of the user from the respective base station that it is linked to, whereas n refers to the path loss exponent $n = 4$. Additionally, for demonstration purposes we adopted the following efficiency function $f(\gamma_i) = (1 - e^{-3.7\gamma_i})^{80}$, while the results were attained by adjusting the step size parameter $0 < b < 1$ for various values.

We consider the coexistence of three different WISPs following respectively the three different pricing policies introduced in Section 4.2.2. For simplicity and fairness considerations, we assume that all three WISPs announce their pricing policies through the base station which is positioned in the same coordinates at the center of the network $(0, 0)$. In the rest of the Chapter, we denote as WISP 1, 2 and 3, the WISP that announces the homogeneous, QoS-based, and topology-based pricing policy, respectively.

Evaluation Scenarios

As an appropriate initialization and reference point, we assume that initially each WISP supports 10 users (or 33.33% of user share), thus, initially the users are equivalently allocated among the available WISPs. Hence, via the PROSREMA algorithm, the users based on their degree of satisfaction from their transmission and service experience, have the potential at the end of each timeslot to either stay with the same WISP or switch to another WISP in order to further maximize their utilities and better exploit the offered pricing policies.

In order to investigate the efficiency of the application of the PROSREMA algorithm in assisting the users to appropriately select a WISP according to their requirements, different simulation scenarios have been designed and studied, in an evolving manner. In more detail, originally all users transmit accepting the pricing policy of the WISP that were originally allocated to (Scenario A). As a next step, as the system evolves the users based on the competitiveness of their WISP and their associated reward probability $r_j(t)$, determine whether to switch to a new WISP or not for the upcoming timeslots (Scenario B). Also, targeting at testing the proposed scheme under fiercer competitive conditions, we assume that WISP 1 (who in previous timeslots applied a homogeneous pricing policy) at some point selects to reduce its overall price levels as a step that enhances competition, while the other two WISPs do not alter their previously announced pricing policies (Scenario C). Finally, depending on the outcome of this scenario, we allow then all WISPs to engage in competition by modifying their prices attempting to win a higher share of the network's user allocation share (Scenario D). The value of the step size parameter is $b = 0.6$ considering the results presented in Table 4.2 and Figs. 4.3a and 4.3b.

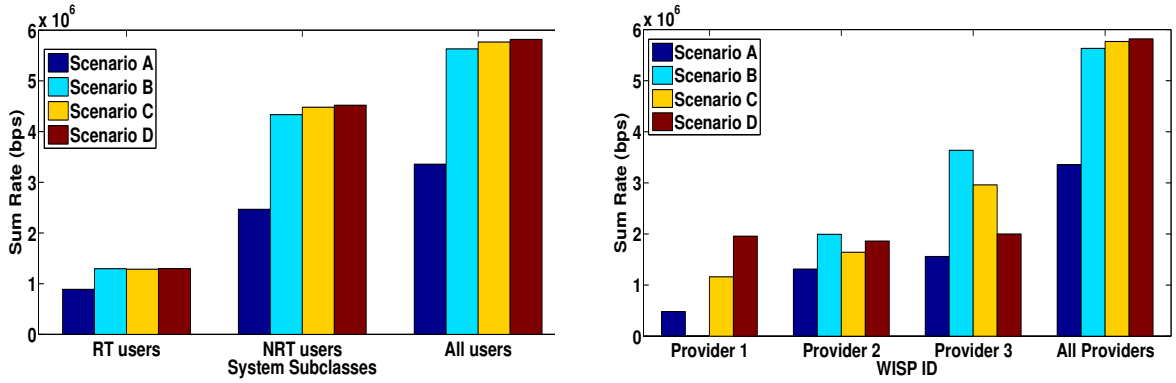

(a) Sum rate per RT, NRT and all users

(b) Sum rate per WISP and the overall system

Figure 4.3: Sum rate for under Scenarios A-D

Performance Analysis

In Table 4.2, the user share among the WISPs is presented under the aforementioned four different examined scenarios (i.e., scenario A-D), along with the achieved sum rate percentage increase with reference to scenario A, i.e., equal distribution of user shares among the three WISPs. Analyzing the results in Table 4.2, we observe that after the implementation of Scenario B, the users universally rejected WISP 1 that applied high homogeneous prices, with all of them selecting to switch to one of the other two WISPs, concluding at a share of 0.00% for the WISP 1. The vast majority of the users (including some users originally allocated to WISP 2 that applied QoS-based pricing), opted to switch to WISP 3 due to the topology-based pricing, since this scheme better fits and adapts to their transmission requirements in this scenario. Thus, WISP 3's user share almost doubled from 33.33% to 63.33%. Moreover, the new user allocation had a positive influence on the overall system's performance, since the total achieved throughput increased by 67.79% compared to the initial equal user share among the WISPs (scenario A).

Under Scenario C, WISP 1 in an attempt to mitigate the significant losses from the previous scenarios, readjusts its prices to lower levels in order to attract some of the users. Please note that for this scenario, we assume that WISPs 2 and 3 continue to charge their users under exactly the same conditions as before. As a result, under Scenario C we observe that WISP 1 manages to reclaim some of the users by increasing its share to 20.00% mostly against WISP 2, whose share has been reduced to lower levels, even lower than the original allocation (from Scenario A). On the contrary, WISP 3 still maintained the highest user share by serving half of the users, while the overall achieved throughput was further increased (by 71.79% compared to Scenario A).

Lastly, under Scenario D, all WISPs have the ability to readjust their prices, thus leading to a more balanced allocation of the users per provider. Also under these conditions, WISP 3 still maintains the lead in terms of attracted users, whereas the overall sum rate for the system was once more increased by 73.36% compared to the initial Scenario A. From all the above, it becomes obvious that the PROSREMA algorithm allows the users to dynamically adapt to the existing conditions within the network depending on the topology, service, or based on the imposed pricing policies, allowing the system to self-optimize its

Table 4.2: User share among WISPs and sum rate increase compared to equal user share (Scenario A) for PROSREMA algorithm

Scenario	Sum Rate Increase Compared to Scenario A	User Share		
		WISP 1	WISP 2	WISP 3
A	-	33.33%	33.33%	33.33%
B	67.79%	0.00%	36.67%	63.33%
C	71.79%	20.00%	30.00%	50.00%
D	73.36%	33.33%	30.00%	36.67%

overall performance. The above observations are further solidified by the results illustrated in Figs. 4.3a and 4.3b illustrating the sum rate for both classes of users (i.e., RT and NRT mobile customers), as well as for the different WISPs and the network as a whole, under all the four previously described scenarios. Observing both Figs. 4.3a and 4.3b, it becomes apparent that gradually, through the implementation of the PROSREMA algorithm and the freedom provided to the users to select the provider of their preference, the overall achieved throughput for the system increases considerably, allowing the exchange of more data among the users for the examined timeslots.

Additionally, the potential to dynamically exchange WISPs enhances competition among the service providers who are encouraged to adjust their imposed prices closer to the requirements of the users, hence leading to a fairer and more efficient allocation of the network's resources. More specifically, since the introduction of Scenario B and onwards where the WISPs readjust their prices to more rational levels in order to maintain their shares, the users are allowed to claim higher fractions of the network's available bandwidth.

Convergence Numerical Study

The step size parameter b (please refer to relations (4.3) and (4.4) in Section 4.2.3 and step 8 of the algorithm) consists an important factor for the system with respect to the convergence time of the PROSREMA algorithm towards the determination of the preferred service provider by the users. Fig. 4.4 presents the average number of timeslots required for all users to converge to the preferred WISP j with probability close to 1, i.e., $Pr_{i,j} = 0.999$, for various values of the parameter b. It can be easily observed, that for higher values of b, fewer timeslots are necessary for convergence, leading to a reduction of up to 90.57% in the number of timeslots when $b = 0.9$ compared to the case where $b = 0.1$.

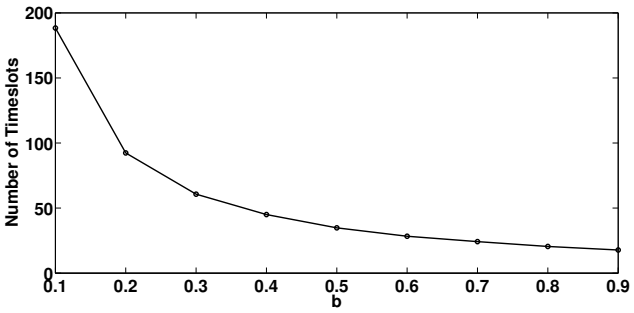

Figure 4.4: Number of timeslots for PROSREMA convergence as a function of the step size parameter b

The above observation is further confirmed via the results presented in Fig. 4.5 that depicts the evolution of the choice probabilities of a randomly selected mobile customer i when selecting one of the three available providers, as a function of the required timeslots. The evolution of the choice probabilities of mobile customer i is presented under various step size parameters, i.e., $b = 0.2$, $b = 0.5$ and $b = 0.9$. For presentation purposes we examine the behavior of user 14 ($d_i = 425$ m from the base station), who under Scenarios A and B selects to remain with the WISP 2. Similar results are observed for other users as well. It can be observed that the probability of selecting WISP 2 from the initial probability of $Pr_{14,2}(t = 0) = 0.33$, converges to $Pr_{14,2}(t = t_{final}) = 1$ regardless of the value of b, while the probabilities of the other two WISPs (1 and 3) in all cases converge to zero, since the user selects not to switch its service provider. However, it can be reaffirmed that the number of the required timeslots towards convergence decreases with higher values of the parameter b requiring only 10 timeslots for convergence when $b = 0.9$. It should be noted here that in principle, if the environment changes slowly then a large value of b would be an appropriate selection due to the fast convergence, while if we have a rapidly changing environment then a smaller value of b would be required, as for higher values of b suboptimal choices about the WISP selection may be obtained in this case.

Considering the convergence of the power control mechanism as presented in Steps 4-6 of the PROSREMA algorithm in Section 4.2.4, it is very fast since less than thirty iterations are required for reaching equilibrium for all users, starting from randomly selected initial values of uplink transmission power. PROSREMA algorithm was tested and evaluated in an Intel (R) Core (TM) 2 DUO CPU T7500 @ 2.20GHz laptop with 2.00 GBytes available RAM and the runtime of the power control mechanism was

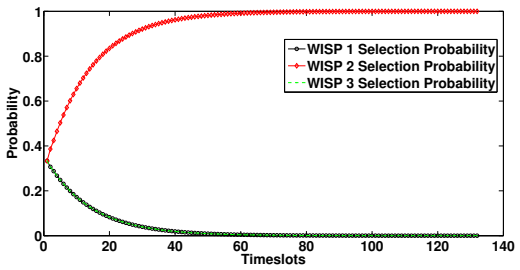

(a) $b = 0.2$

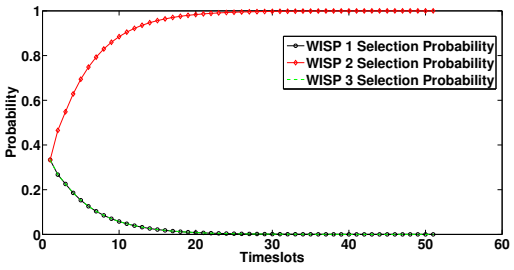

(b) $b = 0.5$

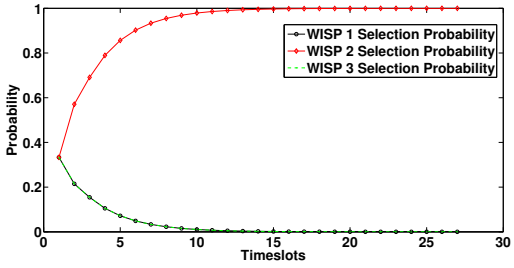

(c) $b = 0.9$

Figure 4.5: WISP selection probability under various step size parameters b of user $i = 14$

less than 0.4 *msec*. The necessary time in order to converge to the Nash Equilibrium point is of similar order of magnitude with the duration of a timeslot (0.5 *msec*), and therefore can be easily adopted in a realistic scenario. It should be also noted that the convergence time of PROSREMA algorithm can further decrease, if we adopt a more "educated" implementation of the algorithm, i.e., use as initial values of the powers the corresponding values in the previous time slot.

Comparative Results

Next, we provide a comparative study of the proposed PROSREMA framework, considering the aforementioned Scenario B, against two other fundamental works in the literature, where pricing users' resources was utilized as a basic tool towards enhancing the system's efficiency and promoting the fairness among the network's users. In [10], the authors applied universal linear pricing to all mobile customers with regards to user's transmission power, whereas in [29], a linear universally applied pricing policy as function of the SINR has been adopted. For comparison purposes, both research works, i.e., [10,29] were simulated under the NOMA transmission technique. At this point it should be noted that in this work a convex pricing policy as a function of user's transmission power has been selected, as discussed from the design of the utility functions in Section 4.2.2. Convex pricing appears to be a more pragmatic approach against linear pricing techniques, since the harm imposed by a user to its neighbors is not equivalent within the whole range of the feasible transmission power value sets. Moreover, we performed a detailed Monte Carlo analysis over random users' positions, where we examined 10,000 random network topologies.

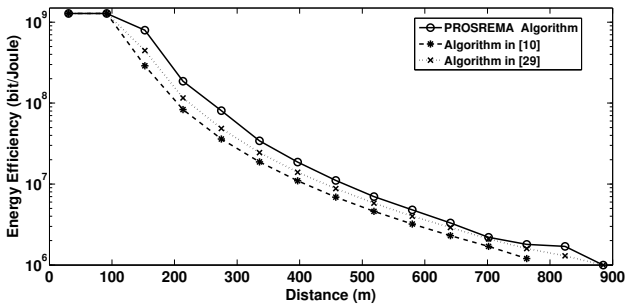

Figure 4.6: Energy-efficiency for RT users as a function of their distance from the base station (y-axis in logarithmic scale)

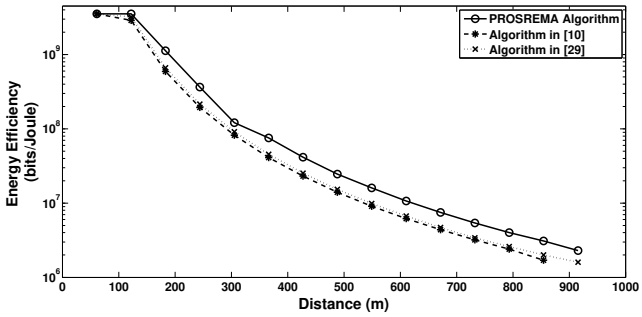

Figure 4.7: Energy-efficiency for NRT users as a function of their distance from the base station (y-axis in logarithmic scale)

Specifically, Figs. 4.6 and 4.7, (note that y-axis is in logarithmic scale) illustrate for all the three approaches under consideration (i.e., PROSREMA, [10,29]) the achieved energy-efficiency of each user as a function of its distance from the base station, for Real Time users (Fig. 4.6) and Non-Real Time users (Fig. 4.7). It is clearly observed that PROSREMA algorithm achieves higher energy-efficiency values compared to both [10] and [29] for both classes of users. This outcome stems from the flexibility that is provided to the users to select among a set of different pricing policies (i.e., homogeneous, QoS-based, topology-based). On the other hand, [10,29] adopt only a homogeneous pricing philosophy, thus offering fewer degrees of freedom to the users, who are not able to adjust the imposed pricing according to their QoS prerequisites, topology characteristics, etc. Hence, PROSREMA algorithm successfully exploits a higher portion of the system's available bandwidth, leading to a significant increase in the achievable energy-efficiency levels, reaching an improvement of up to 20.68% compared to the other approaches, allowing more data bits to be transmitted for less consumed energy.

4.3 General Summary

This Chapter tackled the problem of dynamic provider selection and the subsequent power resource management in competitive wireless communications markets. Under a Machine Learning perspective, the mobile customers act as learning automata who sense their environment and take the best decisions regarding the WISP to be served from. Regarding the resource allocation process, a well designed utility function including a pure utility and a cost function, allows the users to link their uplink transmission power control with their QoS demands, while the Machine Learning mechanism takes the outcome of the resource distribution and builds knowledge upon it. A reward function supports the users in taking their decision regarding which provider to select, with the latter to adjust their pricing policies in order to attract more customers. The problem is formulated and solved as a non-cooperative game with its corresponding Nash Equilibrium point being confirmed via the quasi-concavity of the involved utility functions. A distributed, iterative joint provider selection and resource management (PROSREMA) algorithm was proposed, combining the Machine Learning provider selection process and the distributed power resource management. The performance of the proposed framework has been thoroughly assessed via modeling, simulation, and comparative evaluation with its operational effectiveness being clearly demonstrated.

Chapter 5

Service Composition in Wireless Networks

Future mobile smart devices, new technologies as well as the capacity of emerging 5G networks to handle increasing quantities of information with superior QoS and data rates, is shaping a new landscape with regards to the services that WISPs can provide to their mobile customers. Service diversification is already a reality in telecommunications posing significant challenges to Service Providers in order to address increasing numbers of users with inherently different content and Quality of Service requirements. However, at the same time unique opportunities are offered towards responding more innovatively to new customer needs and manage network performance and resource utilization in a pioneering way.

As already mentioned before, traffic requests in wireless networks have been clustered in two main categories, elastic (or non-real time) requests and inelastic (or real time) requests, both with diverse requirements with regards to Quality of Service and are identified with different data rates and delay tolerance characteristics [8], [144], [145]. As network services are shifting from conventional voice-only offerings, new bandwidth hungry service types are emerging e.g., video streaming and content on demand, online gaming, video conferences, online messaging, voice over IP etc. which have changed how internet traffic is managed and at the same time disrupted the industry [146], [147].

In this thesis, we approach the above situation in a twofold way. We examine how composing different service types can lead to higher and more sophisticated resource utilization and the composition of multi-service packages to users, who in contrast to existing work in the literature are offered only single options at each time. Moreover, another breakthrough of this work is the market perspective under which the new technological advancements (e.g., small cells, access to higher data speeds, new access technologies etc.) available in next generation networks can become part of the overall product in a market driven perspective, a topic that has not been considered from a business point of view so far.

5.1 Real and Non-Real Time Service Bundling

In today's 5G networking era, it is highly common for a user to be using simultaneously multiple services with diverse QoS prerequisites, like streaming a video, while at the same moment checking its email or locating its position in an online map. All these services have disparate characteristics regarding their data consumption, delay tolerance etc. Those different classes of services that consist most of the traffic in modern wireless networks are between elastic (or non-real time) and inelastic (or real time) services [148]. Although mentioned before, at this point we provide a formal definition of elastic and inelastic services:

Definition 5.1.1. ***Elastic Services:*** *Elastic (or non-real time) service refers to a shiftable in time and delay tolerant transmission, like data uploading.*

Definition 5.1.2. ***Inelastic Services:*** *Inelastic (or real time) services refer to transmissions which are not shiftable in time and significantly dependent on meeting specific data rate thresholds, e.g., video streaming.*

This categorization can be further extended through a more comprehensive segmentation, thus, we should consider a plethora of new service subclasses that a mobile user may concurrently utilize.

According to the utility function and user satisfaction modeling adopted throughout this work, elastic and inelastic services due to their inherently different characteristics take distinct utility forms. More specifically, elastic services are represented through a log-based (i.e., concave) utility function meaning that the more data rate is allocated to the user by the system, the more its utility is increased, depicting the data hungry nature towards utility maximization [144]. On the other hand, inelastic services can take a sigmoidal-based form, actually adjusting to the users' requirement to consume a minimum amount of data, which is translated to a target user's transmission data rate.

Based on the above background, user's perceived satisfaction for being served for such different types of services, considering simultaneously its requested real-time and non-real time communications, is designed in a manner similar to the concept of *Service Bundling*.

Definition 5.1.3. ***Service Bundling:*** *The term service bundling has been coined to refer to the integration and offering of two or more products for which different markets exist into a unified package [149].*

This integration provides added value to users through enhanced performance, compactness, and interconnectivity, while it meets a wider spectrum of user demands. Moreover, bundling can capture higher customer surplus and transfers value among the bundled services [150]. The use of this terminology is adopted referring to the bundling of real and non-real time services. Such a bundling scheme enables mobile users to expand their perceived utility through consuming two discrete services, as well as the potential to exploit a bigger fraction of the overall throughput capacity of the network. On the other hand, the network provider is benefited by locking customers in and increasing its profit prospects by selling more services to a wider market and achieving a competitive advantage against competitors, while at the same time improves the utilization of its resources.

Since years, the practice of bundling has been applied to different market areas mostly supporting commercial and marketing purposes. Placing more than one products or services within the same package can be attractive to users since they can purchase more than one goods at a reduced price and potentially cover multiple needs with a single offering. The technique of bundling has been broadly used as a means of increasing or maintaining market power, lock customers in, and grow sales volumes.

Various types of bundling methodologies exist, from price bundling for just offering different products sold together at a common price, to product (equivalently service) bundling, where a new good is shaped with fully integrated components providing functionalities that increase total consumer valuation. This work is placed within the broader scope of product and mixed bundling, where the consumers enjoy the freedom of purchasing each of the items separately or multiple ones in a package. Under this setting, bundled options share each time specific commonalities, which allow the designer to construct a unique service.

In the modern digital economy, services, due to their nonphysical nature, provide bundling advantages that enable developers, marketing specialists, and business strategists to design service provisions that manage to enclose within the same structural architecture different user needs, via a solution with integrated options. In telecommunication markets, data rates and connectivity demand, energy saving potential, and diversity in service applications are regarded as an even growing trend, expected to monopolize consumer interest. Going one step further, the strong connection among the bundled services is clearly demonstrated through the adaptation of a utility function which captures the main user preferences when ordering and consuming services. The notion of expressing user satisfaction with a utility function is a well known practice applied in resource allocation problems. It is adopted to assign numerical values as outcome of a user's actions towards a quantification of its perception that its predefined prerequisites have been successfully met.

5.1.1 System Model

The uplink of a NOMA wireless network is considered, consisting of a base station (BS) serving a region $\Re$, covering an area of radius R_0 and providing multiple services to users. Let $\mathscr{I} = \{1, ..., i, ..., I\}$ denote the set of users who reside within the cell. Users' time varying channels are affected by fast fading, channel fading, and long-time scale variations, thus they can be modeled as a stationary time-varying stochastic process. Let G_i denote the channel gain of user i. Without loss of generality, users' channel gains are sorted in increasing order as: $G_I < ... < G_i < ... < G_1$. As already described, based on the

Successive Interference Cancellation (SIC) at the receiver's side, the messages from the users are decoded in an increasing order of their indices. Thus, the message from the user with the best channel, i.e., G_I is decoded first, and it will see the interference from the rest of the users, i.e., $i = 2, ..., I$ and so on. Therefore, the users that are characterized by poor channel conditions are able to sense decreased interference from the rest of the users residing in the cell via adopting SIC technique [137]. Based on the above description, the interference sensed by the i^{ith} user is as follows:

$$I_i(\mathbf{p_{-i}}) = \sum_{j=i+1}^{I} p_j G_j \tag{5.1}$$

where $\mathbf{p_{-i}}$, denotes the vector of users' uplink transmission power excluding user i. For convenience, all parameters from this section are included in Table 5.1.

Let us denote by p_i and r_i user's uplink transmission power and data rate, respectively. Each user is able to control its transmission power and rate (which are continuous variables) in order to achieve its QoS prerequisites. Due to mobile node's physical limitations, both uplink transmission power and data rate are lower and upper bounded, i.e., $p_i^{Min} \leq p_i \leq p_i^{Max}$ and $r_i^{Min} \leq r_i \leq r_i^{Max}$. Moreover, as already discussed, the received signal-to-interference plus-noise (SINR) ratio from user i at the base station is given by [138]:

$$\gamma_i = \frac{W}{r_i} \cdot \frac{G_i \cdot p_i}{I_i(\mathbf{p_{-i}}) + I_0} \tag{5.2}$$

where I_0 denotes the Additive White Gaussian Noise (AWGN) and $W\ [Hz]$ is the system's available spread spectrum bandwidth. In order to provide a holistic representation of the previously described service diversity paradigm, the concept of utility functions is adopted, which reflects the degree of satisfaction of a user upon receiving its required service or bundle of services.

In view of this, a unified utility framework is introduced towards service differentiation, diverse QoS requirements, as well as the simultaneous support and coexistence of disparate services (e.g., elastic or inelastic with varying data rates) for the same user:

$$U_i\big(p_i, r_i\big) = a_i \cdot \frac{r_i \cdot f(\gamma_i)}{p_i} + (1 - a_i) \cdot \frac{r_i \cdot log\big(1 + f(\gamma_i)\big)}{p_i} \tag{5.3}$$

where the first component represents the utility obtained via the satisfaction of inelastic services, while the second one corresponds to the satisfaction perceived by the elastic services' prerequisites fulfillment, with $f(\gamma_i)$ refering to the already introduced efficiency function.

Additionally, a_i, $0 \leq a_i \leq 1$ is a parameter which represents the percentage of the resources a user plans to allocate in each service type, i.e., elastic or inelastic services in the service bundling offering. For simplicity purposes we assume that the sum of all services should refer to 100% of the resources a user is capable of claiming from the network during its transmission.

In this section, user's utility function is considered to contain two types of utilities; however, this scheme can support additional service utilities regardless of the selected transmission technique, e.g., NOMA technique. Furthermore, we assume that the user has previous knowledge of its upcoming service demands, thus the a_i parameter is fixed and known at each time slot.

Aiming at reaching a stable outcome for the combination of two service types in a single offering, we again formulate the problem as a non-cooperative game which is solved under the concept of supermodular games (*See definition 2.3.5*). As previously mentioned, such games are built upon the fundamental principle that an increase in one's player's / mobile user's action for given actions of the rest of the users, reinforces the desire of all players / mobile users to increase their actions because of strategic complementarity. Hence, the system concludes to a stable solution, since supermodular games have a priori a non-empty set of Nash Equilibria in the two-variable strategy space $S_i = A_i \times B_i$, monotonically converging to a NE point that depends on player's initial state. Moreover, in the case that the examined supermodular game has a unique Nash Equilibrium point, then it is dominance solvable, while learning and adjustment rules, i.e., best response dynamics, will converge to it.

The definition and the conditions a supermodular game needs to satisfy are summarized in Theorem 10 and the relations (2.27), (2.29), (2.30) from Section 2.5.2, [119] hence, for convenience are not repeated.

Table 5.1: Section 5.1 list of key notations

Symbol	Description
$\Re$	Network region
R_0	Radius
$\mathscr{I}$	Set of users
G_i	Channel gain
I_i	Interference
$\mathbf{p_{-i}}$	Vector of users' uplink transmission power excluding user i.
p_i	Uplink transmission power
r_i	Data rate
I_0	Additive White Gaussian Noise
W	System's spread spectrum bandwidth
a_i	Percentage of resources allocated in each service type
U_i	Utility function
G	MUSA game
$S_i = A_i \times B_i$	Strategy space
$f(\gamma_i)$	Efficiency function
M,A	Efficiency function parameters
$w(\gamma_i)$	Auxiliary function

5.1.2 Problem Formulation and Solution

The MUlti-Service joint resource Allocation (MUSA) optimization problem is formulated as a two-variable non-cooperative game with respect to user's uplink transmission power p_i and data rate r_i. Let us denote $G = \big[\mathscr{I}, \{S_i = P_i \times R_i\}, \{U_i(p_i, r_i)\}\big]$ the MUSA game, which defined as follows:

$$\begin{gathered}\textbf{MUSA Game}: \\ \underset{\substack{p_i \in \mathrm{P}_i \\ r_i \in \mathrm{R}_i}}{max}\ U_i(\mathbf{p}, \mathbf{r}) \\ s.t.\ p_i^{Min} \le p_i \le p_i^{Max} \\ r_i^{Min} \le r_i \le r_i^{Max}\end{gathered} \tag{5.4}$$

where $P_i = [p_i^{Min}, p_i^{Max}]$ and $R_i = [r_i^{Min}, r_i^{Max}]$ are the strategy spaces of user i, $i \in \mathscr{I}$. Towards solving the optimization problem (5.4), similarly the concept of Nash Equilibrium is adopted. For the examined MUSA game, the considered Nash Equilibrium point is expressed as follows:

Theorem 30. ***(MUSA Game Nash Equilibrium:)*** *The strategy vector* $(\mathbf{p}^*, \mathbf{r}^*) = (p_1^*, ..., p_I^*, r_1^*, ..., r_I^*)$ *in the strategy spaces* $p_i^* \in P_i$ *and* $r_i^* \in R_i$ *is a Nash Equilibrium of MUSA game if for every user* i, $i \in \mathscr{I}$ *the following condition holds true:*

$$U_i\big(p_i^*, r_i^*, \mathbf{p}_{\mathbf{-i}}^*, \mathbf{r}_{\mathbf{-i}}^*\big) \ge U_i\big(p_i, r_i, \mathbf{p}_{\mathbf{-i}}^*, \mathbf{r}_{\mathbf{-i}}^*\big) \tag{5.5}$$

for all $p_i \in P_i$ *and* $r_i \in R_i$.

Furthermore, it is noted that the Nash equilibrium point is a critical operation point of the resource allocation problem, because it leads the overall system to a stable operation. Therefore, in order to prove the existence of MUSA game's Nash equilibrium point, the S-modular theory is adopted. Our goal is to prove that MUSA game is supermodular, thus a non-empty set of Nash equilibria exists.

Lemma 31. ***(MUSA Supermodular Game:)*** *MUSA game* $G_{MUSA} = \big[\mathscr{I}, \{S_i = P_i \times R_i\}, \{U_i(p_i, r_i)\}\big]$ *is supermodular in* (p_i, r_i), *if for all* i, $i \in \mathscr{I}$

$$\gamma_i \in \Big[\frac{lnM}{A}, \gamma_{Bol}\Big] \tag{5.6}$$

where $\gamma_{Bol} = min\{\gamma_{INEL}, \gamma_{EL}\}$ *and the parameters* γ_{INEL}, γ_{EL} *are formally defined in the Proof below.*

Proof. In order to guarantee that the utility function $U_i(\mathbf{r},\mathbf{p})$ is supermodular in $\big(r_i,p_i\big)$ for fixed $\big(\mathbf{r_{-i}},\mathbf{p_{-i}}\big)$, the following should be satisfied (according to condition (2.27), Section 2.5.2):

$$\frac{\partial^2 U_i}{\partial p_i \partial r_i} \geq 0 \tag{5.7}$$

We examine the sign of the individual components of the above utility, i.e., inelastic and elastic services.

$$\begin{aligned}\frac{\partial^2 U_i^{INELASTIC}}{\partial p_i \partial r_i} = a\frac{MA^2}{p_i^2}\big(1-e^{-A\gamma_i}\big)^{M-2}\Bigg[e^{-A\gamma_i}\gamma_i^2(1-Me^{-A\gamma_i}) \\ + \frac{1}{A}(1-e^{-A\gamma_i})e^{-A\gamma_i}\gamma_i - \frac{1}{MA^2}(1-e^{-A\gamma_i})^2\Bigg]\end{aligned} \tag{5.8}$$

$$\begin{aligned}\frac{\partial^2 U_i^{ELASTIC}}{\partial p_i \partial r_i} = (1-a)\frac{AM}{p_i^2 ln10}\Bigg\{\frac{(1-e^{-A\gamma_i})^M e^{-A\gamma_i}\gamma_i}{1+(1-e^{-A\gamma_i})^M}\big[(1-e^{-A\gamma_i}) - A(M-1)e^{-A\gamma_i}\gamma_i + A(1-e^{-A\gamma_i})\gamma_i\big] \\ + AM\Big[\frac{(1-e^{-A\gamma_i})^{M-1}e^{-A\gamma_i}\gamma_i}{1+(1-e^{-A\gamma_i})^M}\Big] - \frac{ln\big(1+(1-e^{-A\gamma_i})^M\big)}{AM}\Bigg\}\end{aligned} \tag{5.9}$$

Towards determining the sign of the above functions, since both of them are continuous and $C^{(n)}$ differentiable (i.e., smooth functions), we can apply similarly to previously Bolzano Theorem, by selecting two arbitrary values (one extremely small and the other extremely large) of γ_i, i.e., $\gamma_1 = \frac{lnM}{A}$ and $\gamma_2 = \frac{ln(10^4 M)}{A}$, the following hold true:

$$\frac{\partial^2 U_i^{INELASTIC}(\gamma_1)}{\partial p_i \partial r_i} > 0 \; and \; \frac{\partial^2 U_i^{INELASTIC}(\gamma_2)}{\partial p_i \partial r_i} < 0 \tag{5.10}$$

$$\frac{\partial^2 U_i^{ELASTIC}(\gamma_1)}{\partial p_i \partial r_i} > 0 \; and \; \frac{\partial^2 U_i^{ELASTIC}(\gamma_2)}{\partial p_i \partial r_i} < 0 \tag{5.11}$$

Hence, for both cases and for various packet size, $M \in 1,1000$ and $A \in (0.1,100)$, there exist values $\gamma_{INEL}, \gamma_{EL} \in (\gamma_1,\gamma_2)$ such that:

$$\frac{\partial^2 U_i^{INELASTIC}(\gamma_{INEL})}{\partial p_i \partial r_i} = 0 \; and \; \frac{\partial^2 U_i^{ELASTIC}(\gamma_{EL})}{\partial p_i \partial r_i} = 0 \tag{5.12}$$

By combining the above relations, $U_i(\mathbf{r},\mathbf{p})$ is supermodular in $\Big[\frac{lnM}{A},\gamma_{Bol}\Big]$, where $\gamma_{Bol} = min\big\{\gamma_{INEL},\gamma_{EL}\big\}$.

Moreover, $U_i(\mathbf{r},\mathbf{p})$ has non-decreasing differences in (r_i,p_i) for fixed $(\mathbf{r_{-i}},\mathbf{p_{-i}})$ and the following conditions (according to relations (2.29) and (2.30), Section 2.5.2) should hold true:

$$\frac{\partial^2 U_i}{\partial p_i \partial p_j} \geq 0, \; \forall i \neq j \;\; and \;\; \frac{\partial^2 U_i}{\partial p_i \partial r_j} = 0, \; \forall i \neq j \tag{5.13}$$

$\frac{\partial^2 U_i}{\partial p_i \partial r_j} = 0$ is always satisfied, thus we examine the sign of the individual terms of the utility function to prove that $\frac{\partial^2 U_i}{\partial p_i \partial p_j} \geq 0$.

- For the case of inelastic services:

$$\frac{\partial^2 U_i^{INELASTIC}}{\partial p_i \partial p_j} = a\frac{MA^2}{p_i^2} r_i \frac{G_j}{I}\big(1-e^{-A\gamma_i}\big)^{M-2}\cdot e^{-A\gamma_i}\gamma_i^2\big(1-Me^{-A\gamma_i}\big) \tag{5.14}$$

where $I_i = \sum_{j=i+1}^{I} G_j p_j + I_0$. By examining the sign of the above relation, it is concluded that:

$$\frac{\partial^2 U_i^{INELASTIC}}{\partial p_i \partial p_j} \geq 0, \; \forall j \neq i \Leftrightarrow \gamma_i \geq \frac{lnM}{A} \tag{5.15}$$

- For the case of elastic services:

$$\frac{\partial^2 U_i^{ELASTIC}}{\partial p_i \partial p_j} = (1-a)\frac{r_i}{p_i^2 ln10} \cdot \frac{G_j}{I} \cdot \frac{A^2 M\left(1-e^{-A\gamma_i}\right)^{M-2} e^{-A\gamma_i}\gamma_i^2}{1+\left(1-e^{-A\gamma_i}\right)^{M}} w(\gamma_i) \tag{5.16}$$

where $w(\gamma_i) = \left\{1 + Me^{-A\gamma_i} \cdot \left[\frac{\left(1-e^{-A\gamma_i}\right)^{M-2}}{1+\left(1-e^{-A\gamma_i}\right)^{M}} - 1\right]\right\}$. Again, by applying Bolzano Theorem for $w(\gamma_i)$, selecting $\gamma_0 = 0$ and $\gamma_1 = {}^{lnM}/_{A}$ it is obtained:

$$w(\gamma_0) < 0 \;\; and \;\; w(\gamma_1) > 0 \tag{5.17}$$

Hence, there exists a value $\gamma_w \in (\gamma_0, \gamma_1)$ such that $w(\gamma_w) = 0$. We check that $w(\gamma_i)$ is strictly increasing for $\gamma_i > 0$, so $w(\gamma_i) \geq 0,\ \forall \gamma_i \geq \gamma_w$ and consequently $\frac{\partial^2 U_i^{ELASTIC}}{\partial p_i \partial p_j} \geq 0,\ \forall \gamma_i \geq \gamma_w$.

By combining all the above conditions, $U_i(\mathbf{r}, \mathbf{p})$ has non-decreasing differences in (r_i, p_i) for fixed $(\mathbf{r_{-i}}, \mathbf{p_{-i}})$, if $\gamma_i \geq \frac{lnM}{A}$. Thus the game $G_{MUSA} = \left[\mathscr{I}, \{S_i = P_i \times R_i\}, \{U_i(p_i, r_i)\}\right]$ is supermodular in (p_i, r_i), if for all $i,\ i \in \mathscr{I}$, $\gamma_i \in \left[\frac{lnM}{A}, \gamma_{Bol}\right]$, where $\gamma_{Bol} = min\{\gamma_{INEL}, \gamma_{EL}\}$. □

Therefore, given that MUSA game is supermodular, the following lemma can be straightforwardly concluded.

Lemma 32. ***(MUSA Game Existence of NE:)*** *The MUSA game has at least one Nash Equilibrium point, which is defined as:*

$$\left(p_i^*, r_i^*\right) = \underset{\substack{p_i \in \mathrm{P}_i \\ r_i \in \mathrm{R}_i}}{argmax}\, U_i(\mathbf{p}, \mathbf{r}) \tag{5.18}$$

Given that MUSA game is supermodular, all players converge to the Nash equilibrium point following their best response dynamics and via showing that user's utility function is standard [82], [14].

5.1.3 Distributed Algorithm

In this section we propose a distributed, iterative, and low complexity algorithm towards determining the Nash Equilibrium point of the MUSA game. The proposed algorithm is referred as MUSA algorithm.

Algorithm 14 MUSA Algorithm

1: Each user selects its service percentage a_i.
2: Set $ite = 0$, where ite denoted the iteration index. Each user selects a random feasible uplink transmission power $p_i^{(ite=0)}$ and rate $r_i^{(ite=0)}$ from the strategy space $S_i = P_i \times R_i$
3: The BS sorts the users by increasing order of channel gain, e.g., $G_{\mathscr{I}} < ... < G_i < ... < G_1$ and unicasts to each user its sensed interference, e.g., user $i = 1$ receives the interference information $I_1 = \sum_{j=2}^{I} p_j G_j$, user $i = 2$ receives the interference information $I_2 = \sum_{j=3}^{I} p_j G_j$ and so on.
4: For $i = 1 : I$, $(\forall i \in \mathscr{I})$
5: Determine the optimal uplink transmission power $p_i^{(ite+1)}$ and rate $r_i^{(ite+1)}$, according to equation (5.18).
6: End
7: If $|p_i^{(ite+1)} - p_i^{(ite)}| \leq \epsilon$ and $|r_i^{(ite+1)} - r_i^{(ite)}| \leq \epsilon$ for all $i \in \mathscr{I}$, where ϵ is a relatively small positive constant, users' uplink transmission powers and data rates have converged and stop.
8: Otherwise, set $ite := ite + 1$ and go to step 2.

It is noted that MUSA algorithm is of low complexity, due to the simplicity of the involved calculations, as well as due to the fact that it runs at each user in a distributed manner, thus its complexity does not increase with respect to the number of users residing in the cell.

5.1.4 Numerical Results

In this section some indicative numerical results are provided through modeling and simulation, towards a) evaluating the performance and the operational characteristics of the MUSA framework, and b) providing a comparative study against existing works in the literature. For demonstration purposes, we consider the uplink of a single NOMA cell, with I continuously backlogged users, scattered within its radius ($R_0 = 3.5\ km$). Each user can simultaneously request different types of services (e.g., elastic or inelastic) with varying data rate requirements. We consider 2 concurrently requested basic service classes per user, real time (i.e., inelastic) services associated with target rates of 96 *kbps* (e.g., voice service), and non-real time (i.e., elastic) services with a maximum feasible rate of 256 *kbps* (e.g., simple video uploading). The physical limitation for the maximum feasible uplink transmission power is set at $p_i^{max} = 0.2\ Watts$. The users' path gain is modeled as $G_i = {}^{K_i}/_{d_i^n}$, where d_i is the distance of each user from the base station, n is the distance loss exponent ($n = 4$), and K_i denotes the shadow effect being a log normal distributed random variable having mean 0 and variance $\sigma^2 = 8db$. Moreover, we adopted the following efficiency function, $f(\gamma_i) = (1 - e^{-1.15\gamma_i})^{80}$. As previously mentioned, the parameter a_i is selected by the users according to their service preferences. Initially we consider a scenario where all users select half of each service type (i.e., $a_i = 0.5$).

Fig. 5.1 illustrates the attainable data rates for $I = 9$ users placed with increasing distance from the base station (i.e., $d = [560, 920, 1230, 1480, 1680, 2050, 2370, 2830, 3400]\ m$), compared to the maximum feasible rate per user. It is observed that for more than half of the users (i.e., 1 to 5), MUSA algorithm delivers the highest feasible achievable data rate, while from the rest of the users, only the two more distant users from the base station have considerably lower data rates, mainly due to their very high distance from the base station that deteriorates their communication channel. Moreover, the majority of the users achieve to simultaneously receive both real and non-real time services with sufficient data rates due to the joint determination of r_i and p_i in order to maximize each user's utility, meaning that they can exploit the network's capacity to its full extent.

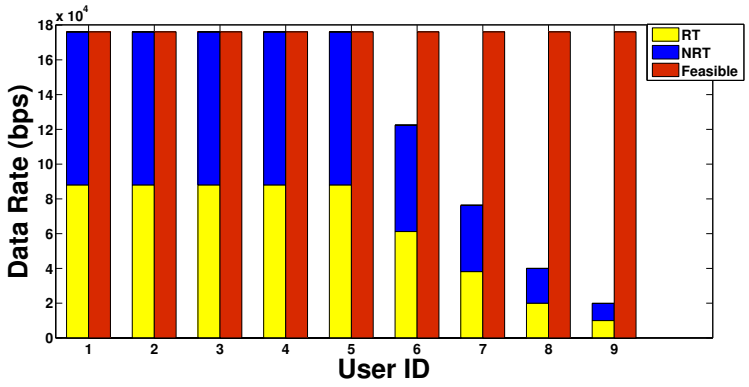

Figure 5.1: Users' data rates for $50\% - 50\%$ simultaneous request of real and non-real time services

Fig. 5.2 depicts the final rates for one selected user when it readjusts its service preferences (i.e., parameter a_i) given that all the rest of the users within the topology do not alter their selections. The case for user $i = 4$ has been considered with initially only real time services requested, i.e., $a_4 = 1$. At each new time slot, user 4 gradually increases its desire for non-real time services, while proportionally reducing its reserved real time services request. As it is observed, the user's real time data rate remains at high levels despite the user's trend to reduce its demand for this service type, while the increasing contribution of non-real time service request considerably increases its attainable data rates, until 100% of the transmission is exclusively related to the latter. This successful combination, where for most of the time both services achieve high rate levels, stems from the joint determination of the power and rate by each user as well as from the fact that the user unlocks higher bandwidth capacity in such a service bundling environment.

Additionally, the performance of MUSA framework ($a_i = 0.5$) has been compared against an approach which does not address users' requirement for joint multi service support. The simulations were universally conducted under the NOMA transmission scheme and involved the same transmission parameters as before, considering 8 users. Originally the case where each user is associated exclusively with only one service type is examined. Specifically, by assuming again joint power and rate control, at this time half of

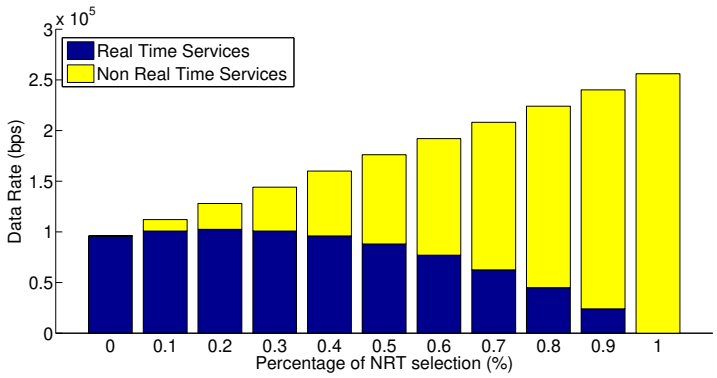

Figure 5.2: User's ($i = 4$) data rate as a function of $a\%$ of non-real time service request

the users requested only real time services, whereas the rest selected non-real time services, for fairness in the comparison with respect to the total requested services and rate. Although the available bandwidth is the same for both cases, by comparing the obtained results, the achieved system's total throughput for the MUSA framework was up to 31.88% higher than the non multi-service case. This is due to the fact that users can benefit from the service bundling by offering two services simultaneously to the users when their channel conditions allow it and take advantage of the synergies between the distinct services when they are paired within the same transmission, instead of just selecting a more data hungry one only to achieve higher data rate, thus removing valuable scarce resources from the rest of the users.

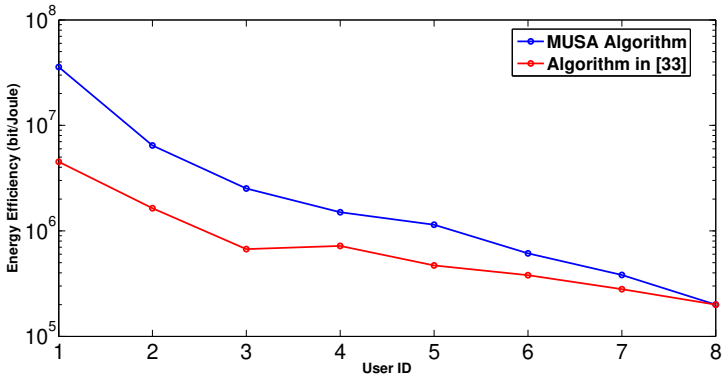

Figure 5.3: User's energy-efficiency as a function of its ID, i.e., distance from the base station (y-axis in logarithmic scale)

Furthermore, in Fig. 5.3, the energy-efficiency representing the ratio of a user's data rate to the corresponding energy consumption required for this transmission with respect to a user's distance from the base station has been compared between our work and [33]. In [33], the authors considered the joint allocation of power and rate as an one parameter optimization problem, with the utility functions expressed as the ratio of data rate to transmission power, i.e., $x_i = {}^{r_i}/_{p_i}$. For comparison purposes, [33] was also simulated under the NOMA transmission technique involving real and non-real time exclusive users' requests. The results reveal that MUSA algorithm clearly outperforms [33], since for the vast majority of users, the achieved energy-efficiency is significantly higher, translating into less consumed energy for more transmitted data bits. MUSA's average energy-efficiency per user is 201.08% higher than in [33], due to the fact that the latter does not optimally determine both parameters (i.e., power and rate) since the optimization of the utility function takes place semi-jointly through their previously set ratio. Additionally, energy-efficiency is improved under the MUSA framework, since the synthesis of two different services offsets the data hungry and more energy consuming non-real time services with the less energy demanding real time services, thus improving the overall energy consumption of the whole system. Likewise, the decision to predetermine the proportion of resources that should be reserved (by regulating the parameter a_i), incentivizes users towards consuming what is actually necessary (in terms of data rate and battery drain) for their transmission, hence enhancing social welfare and fairness inside the network.

5.2 Market-based Dynamic Multi-Service Bundling

Understanding the increasing importance of service diversity in the new 5G era of communications, user requirements are multiplying and different service classes are required each time, to ensure that all customers receive sufficient QoS support according to their unique service preferences. Based on the preceding analysis covering only two services classes for allocating resources like power and data rate [151], in this section we extend the market-based concept of service bundling [149] in the field of future wireless networking and telecommunications to include multiple service offerings under a new perspective.

This extended framework aims to provide a new vision in: a) service diversity, b) heterogeneity in terms of user requirements, c) diversity with respect to the capability of control and type of resources, and d) pricing and wider adaptability. For convenience of discussion, we discuss bundling of "technical service modules" according to user selections, with the term coined to refer to the options provided to the user in controlling any type of its resources and part of the network resources it may have access to, as well as other options that may affect its satisfaction from the final service delivery.

The introduced paradigm aspires to: a) enable the user to better adopt and customize the available technical services to its needs, profile, and requirements. This will result in directly increasing user's overall experience; b) drive the Wireless Internet Service Providers (WISPs) to apply their general expertise and common practices in the service bundling era. This will enable WISPs to maintain and/or enhance their customer basis, improve their satisfaction, and unlock utility surplus; and c) introduce a modular service composition architecture.

In this part of the thesis, a structurally different philosophy with regards to bundling services has been adopted in comparison to the resource allocation problems in existing literature. This time, users are equipped with the freedom to determine the basic strategy of their decisions, instead of simply adjusting their actions to the options provided by the network administrator. The users by disclosing the service components they are interested in significantly diversify the nature of their transmission, since a unique service request is shaped by each one of them in line with the autonomy and heterogeneity trends in the modern wireless networks.

Similarly to before, the concept of utility functions acts as a common interface where service bundling meets resource optimization under a user-centric ecosystem [152]. The created bundles now are not static, but a dynamic combination of different factors ranging from QoS prerequisites satisfaction to a completely new pricing structure. This enables and is enabled by the concept of modularity in composing separate offerings into an "as one package" in a dynamic manner. Another key contribution of this work is its extensibility to additional services or stakeholders, in harmony with the growing demands and capabilities of next generation wireless networks. Lastly, the proposed framework is envisioned to support and be supported by the evolution of software defined technology and the notion of self-optimization and adaptability, in order for the network and its elements to provide agile and flexible services in future networks.

Such sophisticated utility functions easily adapt in the structure of multiple telecommunication service packages by putting together a series of distinctive parameters critical to different aspects of a user's wireless transmission. The user by optimizing certain of these parameters (i.e., picking service components during the bundle design phase), identifies its preferences that should be prioritized for the following transmission. Hence, a fully personalized product version is formed from this prior configuration with each of the individual services being in a direct "1-to-1" relationship with the utility elements. As an outcome, the utility itself acts as an expression not only of the user satisfaction from the fulfillment of its QoS requirements, but also as a measurement of the success of the bundling design. A high utility reflects a successful transmission facilitated by an efficient and highly synergetic bundle, whereas a lower utility mirrors an inferior bundling synthesis, where the coupled services fail to generate sufficient added value. Thereafter, the utility function acts as the beacon for formalizing both the process of bundle design and reflects the outcome of the resource allocation in a uniform and quantifiable way.

5.2.1 Modular Service Architecture

Next generation wireless networks can accommodate varying services which succeed in significantly diversifying the nature of the network's operation, since two users within the same topology may request completely different services. In this work, we focus on some of the most commonly examined technical services in the resource allocation literature, which although extensively studied as stand-alone processes, have never been jointly investigated under the proposed service bundling setting.

Power Control: Power control in wireless networks is a key mechanism for managing energy-efficiency, interference mitigation, and ensuring sufficient QoS provisioning through stable SINR values.
Rate Control: Wireless networks which employ rate control ensure enhanced fairness of bandwidth allocation among the users and superior throughput utilization. Thus, users can fully utilize network's capacity and reduce congestion impact and system instability risks.
Multi-service Support: Modern communications industry has already transitioned from audio only traditional services, to a multimedia ready environment with diverse and complex data capabilities. Bridging the gap between elastic (non-real time) and inelastic (or non-shiftable in time) services, delivers a unique opportunity to optimize data management and prioritize simultaneous service support and customer satisfaction.
Ultra High Data Speed: Access to high speed networks is a defining factor regarding the use of internet nowadays and a basic contributor to the widening digital inequality problem among different regions, industries, or social segments. Broadband networks provide externalities for higher utilization of resources, agile service development, and scalable connectivity among multiple terminals under the IoT trends.
Femtocell Access: Two-tier femtocell architecture has emerged as an effective, low cost, and power saving approach in reducing macrocell load and providing users with superior channel conditions and interference management. Femtocell users enjoy superior transmission conditions due to their proximity to the Access Point operating with the same licensed spectrum alongside macrocell users, resulting in turn to increased system capacity with limited infrastructure investment [18].

In Fig. 5.4, a conceptual representation of how bundle formation and customer satisfaction with reference to the aforementioned technical services is provided for different network topologies. In particular, we highlight that customer utility (red y-axis) increases when advanced network structures (horizontal x-axis) are implemented stemming from the increased flexibility and enhanced interference management of 5G heterogeneous networks. Moreover, on another dimension, the inclusion of additional services towards forming larger bundle sizes (blue z-axis) into the customer basket increases its satisfaction as well, due to the more diverse services and wider QoS provisioning potential.

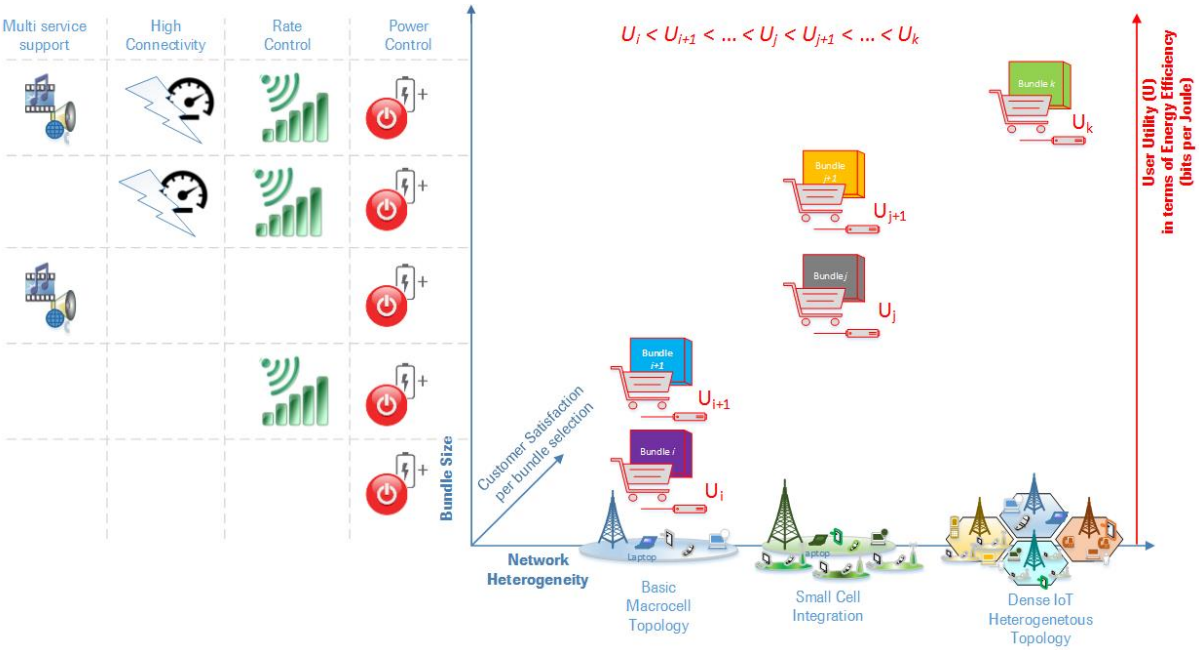

Figure 5.4: Conceptual modular bundling architecture

Without loss of generality, we adopt a utility function identical to previous section as introduced in relation (5.3). The flexible design means that all the basic variables in the utility function correspond to a technical service module, configured by the users each time. A brief summary is provided in Table 5.2.

It becomes apparent that the utility function is specifically designed to dynamically adapt to the selected service modules. Users are enabled to add extra degrees of freedom to the resource allocation

problem in accordance to the services they desire to obtain. In such a way, the perceived utility reflects the users' investment during the upcoming transmission. Moreover, the proposed utility function attains additional importance through its realistic interpretation of transmission energy-efficiency, expressing the amount of data bits transmitted per each Joule of consumed energy.

In this case as well, the solution of the resource allocation problem is confronted via a game theoretic formulation with the existence, uniqueness, and stability of the game to be guaranteed once more through the concept of Nash Equilibrium. The class of supermodular games provides again the theoretical model to easily obtain the above equilibrium point (for single or multi-variable problems) as already examined in the literature [153], [65], [151]. Due to the identical problem formulation and solution to the previous section of this Chapter, the proof has been omitted *(See sections 5.1.1 and 5.1.2 in this Chapter).*

5.2.2 Distributed Algorithm

Modular systems accommodate the easy migration of multiple individual components into new configurations which emerge as new product versions, customized according to user preferences. Modularity promotes adaptability and flexibility in a system as the needs of the market evolve, thus extending the lifespan of an offering, while also providing standardization and scalability potentials. As a result, successful aggregation of an increasing number of components is accomplished, with the new product exhibiting synergetic behavior with unique value creating features to the user [154].

The concept of a modular algorithm is in agreement with the bundling scheme in this work, while simultaneously enables decision making at the user level in a distributed manner. This modular design besides the personalization of the product reinforces information exchange and sharing. At the same time, the network administrator may accumulate and assess valuable information, acquire strategic knowledge of the trends, and finally cluster it into relevant market segments.

Market segmentation functions under the fundamental principle that certain users who value more a specific feature or attribute of a product, are expected to display similarities or a degree of predictability in their actions. Thus, service providers following market segmentation and bundling, according to [150], can obtain strategic gains by providing bundles to specific user groups with higher identified valuation of those products, and extract higher profits by imposing apt pricing policies.

Modularization and decision decentralization come to fruition from the deployment of the BENCHMARC algorithm, i.e., Bundling sErvices in wireless Networks via user CHoice in Modular ARChitecture. BENCHMARC algorithm is divided in two parts, considering the actions of both the users and the network. Initially, the users disclose to network administrator which service modules will be activated for their upcoming transmission, with their utility functions to be configured accordingly. Transmission parameters are adjusted and the degrees of freedom are determined, reflecting the selected service portfolio. At the beginning of each timeslot, each user computes its utility function given the actions of the rest of users, with the system gradually converging to a stable outcome via the determination of the non-cooperative game's Nash Equilibrium. Upon the completion of the timeslot, the users evaluate their performance from the prior bundling design, and reassess their decisions accordingly for the next transmission periods. The flow diagram of the BENCHMARC algorithm is depicted in Fig. 5.5.

Table 5.2: Parameter & service relation for BENCHMARC algorithm

PARAMETER	DESCRIPTION	COMPARABLE SERVICE
$p_i \in [p_{min}, p_{max}]$	Uplink Transmission Power	Power Control
$r_i \in [r_{min}, r_{max}]$	Uplink Data Rate	Rate Control
G_i	Channel Gain	Access Point
$a_i \in [0, 1]$	Service Selection Parameter	Multi-service Support
W_i	Bandwidth	Ultra High Data Speed Capacity

The above algorithmic framework is designed in a flexible manner so that additional services, users, or even WISPs are added without increasing the computational burdens to the resource allocation process, while simultaneously enhancing extraction of further network externalities.

Algorithm 15 BENCHMARC Algorithm

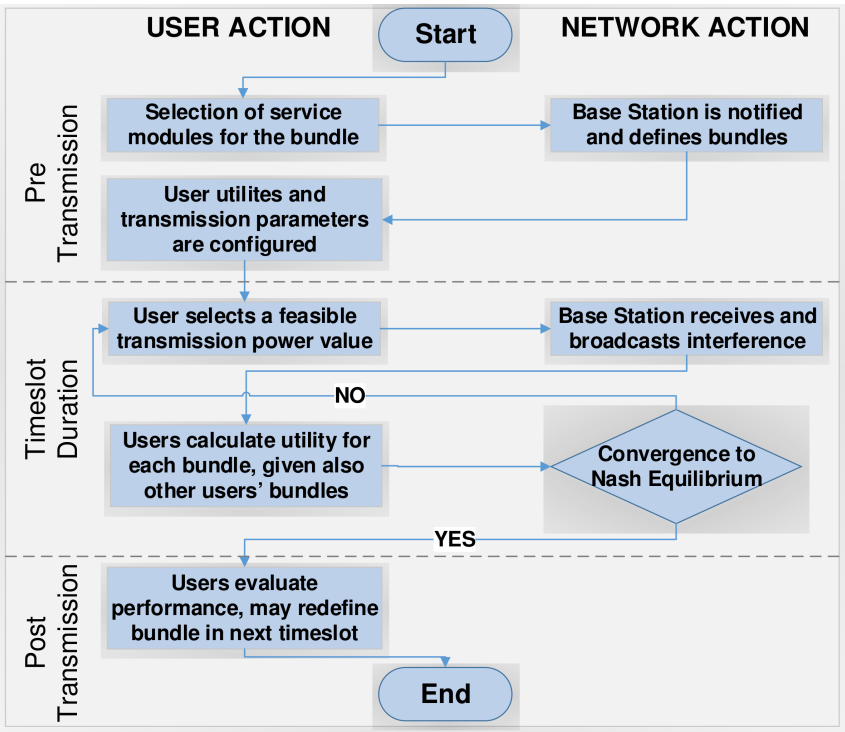

Figure 5.5: BENCHMARC algorithm flow and actions

5.2.3 Numerical Results

In order to evaluate the applicability, usefulness, and impact of the proposed paradigm, the following basic question arises and should be answered at first: Does utility increase with additional services, since the basic formulation of the utility function does not change? And if yes, is there any trade-off associated with such an increase? In this section, we initially investigate how user satisfaction is impacted by gradually adding more technical services in its portfolio. Users have the potential of selecting modules shaping a personalized product with unique characteristics, which functions differently as it adjusts to specific requirements. In our evaluation, we concentrate on the service modules presented in Section 5.2.1.

For demonstration purposes, we study a scenario of a potential bundling and resource allocation for a wireless network, adopting Non-Orthogonal Multiple Access (NOMA) transmission [155]. In order to ensure similar initial channel gain conditions, we assume a number of continuously backlogged users ($N = 8$) equally positioned around a macrocell base station, within a circular topology. At the beginning of the timeslot users select the service modules according to their preferences under a dynamic mixed bundling perspective, and disclose this information to the base station.

To gain some insight about the changes in user utility as more service components are added, we compare users' overall satisfaction from a basic and add-on free product (e.g., only power control) which gradually evolves to a comprehensive and multifaceted inclusive product with several secondary characteristics *(See Scenario C in Fig. 5.6)*. Such an overview is provided in Table 5.3, where 8 users within the network define different bundles. As observed from Fig. 5.6, when more service modules are added to the bundle, users' utilities increase, regardless of the fact that the mathematical formulation of the utility function remains unmodified.

Table 5.3: Bundle service mix (Scenario C) for BENCHMARC algorithm

	Power Control (Basic Service)	Rate Control	Elastic and Inelastic Support	Ultra High Speed	Femto Access	Final Package
User 1	✓					Bundle 1
User 2	✓	✓				Bundle 2
User 3	✓			✓		Bundle 3
User 4	✓	✓	✓			Bundle 4
User 5	✓		✓	✓		Bundle 5
User 6	✓	✓	✓	✓		Bundle 6
User 7	✓	✓	✓		✓	Bundle 7
User 8	✓	✓	✓	✓	✓	Bundle 8
Selected Options	8/8	5/8	5/8	4/8	2/8	

In combination with Table 5.3 (referring to scenario C), we observe that the user selecting the basic service (i.e., power control only), receives the lowest utility in comparison to the rest of the users. As more service options are included, utility increases and in some particular cases very rapidly. Users who opt for a bundle of two services enjoy further increase in their utilities, reaching the last user (ID=8) who achieves significantly higher utility after obtaining all available service options. Additional variations of bundling selections have been assumed and modeled as comparative cases. It should be noted that the product bundling mix is a factor considerably affecting the performance and the perceived satisfaction of the users during their transmission. For instance, it is depicted that femtocell access option notably improves channel conditions leading to utility increase as higher data rates are achieved with almost minimum transmission power.

Additionally, synergies are identified among the various service combinations. That is, different bundling mixes contribute in different ways to the final resource allocation, depending on the user's expectations and priorities. For instance, users who select both femtocell access and "Ultra high data speed" capability, fully exploit the superior connectivity and bandwidth, since maximum speed is managed with limited impact on energy consumption. On the other hand, the user who selects the modules of power and rate control only, although witnesses an amelioration in the utility, does not sense equal improvement with the users who preferred the higher bandwidth option (user IDs 2 and 3 in Scenario C in Fig. 5.6). Moreover, concurrent elastic and inelastic service support, although does not come with infrastructure investment by the users or does not occupy additional licensed spectrum, delivers higher utility because of the easier information exchange and synchronous handling of multiple services. This is observed by comparing users with ID 2 and ID 4 in Scenario C, with the latter almost doubling its quantified satisfaction.

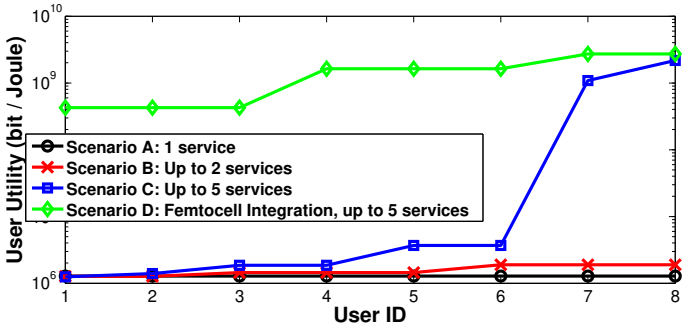

Figure 5.6: Utility per user ID for increasing number of services

5.2.4 Pricing Discussion

Bundle prices consist a significant factor which can influence the strategy that best fits the development and design of the bundle. As analyzed in [156], the reservation prices of the individual components of the bundle may follow an asymmetric distribution. However in the case of Information and Communications

Technology (ICT) services, variation of reservation prices is assumed to be low, since users are considered homogeneous in their evaluation of the same add-on. Some of the most well-known and extensively studied schemes related to pricing are listed below [157]:
Uniform (flat) pricing: Each unit is sold independently at an equable price with no discrimination on the attributes or the size of the product.
Pure bundling pricing: Only the full bundle is provided to users with a single price. All components are offered to the consumer, regardless of its preferences or valuations.
Component pricing: Each of the individual products within the market are sold at a different price. This practice is also known as unbundling, since any externalities of bundling are reversed.
Mixed bundling pricing: For every combination of goods a different price is set. For a multiproduct firm this may induce an overwhelming number of different prices assuming all the related complexity and calculation effort.

Bundling non homogeneous products without providing additional surplus to the consumers or exploiting the dominant position of a firm has been identified to lead to misallocation of resources and potential monopolistic behaviors [156]. BENCHMARC framework can sufficiently address such considerations, since alongside its flexible design, it allows for the adoption of Bundle-size pricing (BSP) [157]. Bundle-size pricing instructs charging different prices based on the size of the bundle, while simultaneously enabling users to be a priori aware of the added value they will receive upon determining their preferred bundle. This means that a bundle consisting of one service will be charged with an equal price for each different service, a bundle of two services with a second price etc., regardless of the service mix. Bundle-size pricing constitutes a pragmatic pricing structure pursuant to market conventions, since most service providers prefer to avoid complicated pricing calculations for their products.

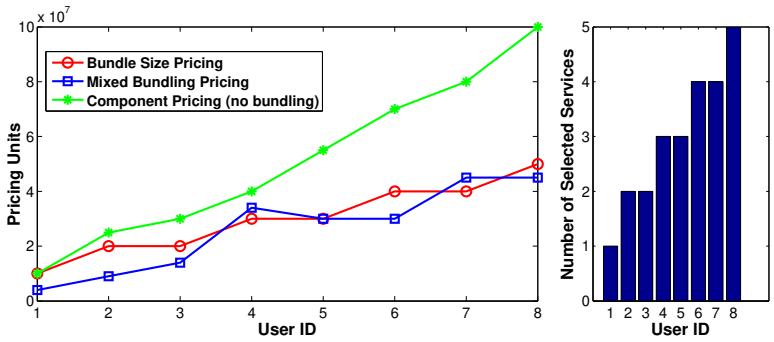

Figure 5.7: Pricing per increasing number of services

For proof of concept demonstration purposes, we assume a standard pricing structure, where prices increase linearly with the number of the services added to the bundle. For simplicity, we consider pricing to be in dimensionless units matching the format of the utility function in equation (5.3). In Fig. 5.7 a comparative investigation of different pricing policies for increasing bundle sizes is shown (in the right subfigure the bundle size considered for each user ID is shown, where users with increasing ID are assumed to have non-decreasing bundle size). It is observed that for the case of component pricing (or unbundling) where customers have to purchase each transmission service separately without any bundling potential, they have to pay significantly higher prices compared to the options where bundling is involved.

On the contrary, bundle-size pricing delivers comparable results to the case of mixed bundling, as simulated under the paradigm of [120], where users indicate the price they are willing to pay in order to achieve the QoS they request, given the customized bundle version they have previously selected. Users benefit from the bundle externalities and pay significantly reduced prices for the same network options, whereas the WISP manages to achieve economies of scale with increased service output. Bundle-size pricing, apart from its predictable and stable structure, enables users to a priori determine the price of the bundles based on their preferences and significantly mitigates computational complexity of market prices compared to mixed bundling.

5.3 General Summary

In this part of the thesis, we provided a generic enough framework towards accumulating multiple types of services within the same transmission of a mobile consumer in next generation 5G networks. New smart devices provide the necessary background and flexibility to handle multiple different functions and services at the same time, offering a unique opportunity to redesign the telecommunication product via the well known concept of service bundling. Users are given the freedom to personalize the types of services they want to include in their transmission, defining a unique product which directly adjusts to their priorities and preferences.

Initially, a novel utility function was proposed expressing user's satisfaction from the resource allocation while simultaneously requesting both elastic and inelastic services in line with the service bundling principles. The problem was applied in the uplink of a NOMA wireless network and was formulated and solved as a non-cooperative game, solved through the use of S-modular games allowing for the first time the joint resource allocation and multi-service provision. The iterative and low complexity MUlti-Service joint resource Allocation (MUSA) algorithm was designed towards practically determining the Nash Equilibrium of the game, while the performance of the proposed approach was evaluated through modeling, simulation, and extensive comparative numerical results.

Following, the problem has been considerably expanded to include multiple service options mainly from a market perspective towards examining the potential design and transmission synergies that can deliver a superior product addressing more customer needs and at the same time enable providers to increase market penetration and potential revenues. Through this work, it was realized that the flexibility, high degree of product versioning, and the potential of customization, as well as the strategic advantages of bundling theory provide exciting application areas for the design and development of new ICT services. The above framework was developed under a service composition modular architecture (implemented via the BENCHMARC algorithm), where different technical service options are selected by the users, and are reflected to a utility function which matches each of the tied-in services to its parameters to be configured. Numerical results demonstrated that a wider service portfolio is followed by higher levels of utility, providing both data rate and energy-efficiency, while it is argued that different services are evaluated differently by the consumers. Additionally, pricing alternatives in line with bundling principles were explored, with the concept of Bundle-size pricing to provide a simplified, low complexity, and efficient pricing strategy for increasing bundle sizes.

Chapter 6

Wireless Powered Communication Networks

6.1 Energy Transfer in Wireless Networks: an Overview

In Wireless Powered Communication Networks (WPCNs), the mobile devices are powered over the air by dedicated wireless power stations (PSs) via harvesting and storing energy from the RF signals during the wireless energy transfer (WET) phase [158,159]. Then, the mobile devices transmit their information signals to the base station (BS) during the wireless information transmission (WIT) phase by exploiting the saved energy [160].

Compared to conventional battery-powered networks, the fundamental benefits of WPCNs are: (a) the elimination of the need for frequent manual replacement and recharging, (b) higher throughput, (c) prolongation of devices' lifetime, and (d) low network operating cost. Moreover, WPCNs have full control over their power transfer, thus they are able to provide stable energy supply under different physical conditions and service requirements in contrast to energy-harvesting based networks, where the devices opportunistically harvest renewable energy in an environment not dedicated to power them, e.g., solar or wind power.

6.1.1 Related Work on WPCNs

The majority of the existing research works on WPCNs and WET aim at improving the system throughput [161] under various constraints imposed by network's physical characteristics [162], while neglecting the energy utilization efficiency, which is also of high importance and criticality for next generation communication systems [163]. Some initial research efforts have been devoted to the problem of energy-efficient resource allocation under the paradigm of WPCNs considering various objectives. In [164], a joint time allocation and power control framework is proposed targeting at maximizing network's energy-efficiency under different conditions, such as the initial battery energy of each user and the minimum system throughput constraints. The authors show that network's energy-efficiency depends on the trade-off between the energy harvesting time and the fulfillment of users' Quality of Service (QoS) prerequisites. In [165], the authors study a multi-user WPCN aiming at maximizing the uplink sum-rate network's performance via jointly determining the optimal energy and time resource allocation for the multiple users. This work has been extended in [166] to consider additional constraints, such as infinite or finite capacity energy storage. In [167], the authors study the problem of joint subcarrier scheduling and power allocation in orthogonal frequency division multiplexing (OFDM) WPCNs towards maximizing system's sum-rate under two scenarios: (a) perfect self-interference cancellation (SIC) where the access point fully eliminates its self-interference (SI), and (b) imperfect SIC where residual SI exists.

6.2 Adaptive Power Management in WPCNs

Though such resource management efforts and approaches present significant results towards optimizing system's welfare, their main drawback is that they cannot be properly adapted to user-centric paradigms, where the goal of the resource management problem is to optimize users' perceived satisfaction from the

occupied resources. In this part of the thesis, we aim to approach resource allocation problems from a different angle which is considered as given so far. This refers to the optimal charging of the devices' batteries in order to be able to sufficiently transmit and optimally allocate resources, truly adjusting energy consumption to the real needs of the system.

Subsequently, in order to achieve this, a user-centric distributed resource management approach is proposed, aiming at enhancing the WPCN's energy-efficiency while guaranteeing the satisfaction of users' transmission requirements. Initially, each user is associated with an appropriately designed utility function representing its degree of satisfaction with respect to its consumed energy towards achieving its QoS prerequisites. The users are able to determine in a distributed manner their energy needs via maximizing their utility function, towards communicating with the BS and fulfilling their QoS demands. Based on this information, the Power Station (PS) determines the optimal amount of energy that should be delivered to the users for meeting their QoS priorities. The PS transfers the aforementioned optimal energy supply to the users during the WET phase which precedes the WIT phase with the BS.

The key novelty of the proposed framework in providing enhanced energy-efficient communication, is the joint consideration of the needs and dependencies in both directions and phases of this process, that is the WET and WIT phase. In this way, by dynamically having the PS to adjust its transmission power levels during the WET phase to the actual requirements of the users, unnecessary energy waste is avoided. A distributed and low complexity Energy Transfer and Transmission Adaptation (ENTRADA) algorithm is proposed in order to determine the optimal charging power transmitted by the PS, while also guarantee the fulfillment of users' QoS prerequisites. The performance of the proposed framework is evaluated through modeling and simulation and its superiority compared to various state of the art approaches is illustrated.

6.2.1 System Model

A single cell WPCN is considered, while the WET and WIT phases are jointly studied. The WPCN consists of a power station (PS) broadcasting RF signals, a base station (BS) receiving users' information signals and $|N|$ continuous backlogged users, where N denotes their corresponding set. The adopted topology is presented in Fig. 6.1. The "harvest and then transmit" protocol is employed for the WPCN, where the users harvest energy from the broadcasted RF signals by the PS (downlink communication) during the WET phase and then transmit their information signals to the BS (uplink communication) during the WIT phase. For simplicity of implementation, the PS, the BS, and all the users are equipped with a single antenna and operate under orthogonal frequency multiple access scheme so that transmission interference is avoided (e.g., OFDMA [167]). The timeslot duration is denoted by T $[s]$.

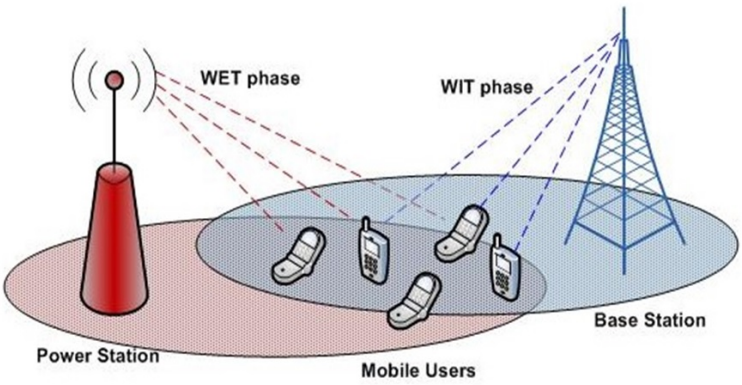

Figure 6.1: Wireless Powered Communication Network (WPCN) topology

We assume that each user is equipped with a rechargeable built-in battery, which initially may not be charged. The downlink channel power gain between the PS and the user k, $k \in N$, and the uplink channel power gain between user k, $k \in N$ and the BS are denoted as h_k and g_k, respectively and they both capture the joint effect of path loss, shadowing, and multipath fading.

During the WET phase, the PS broadcasts an RF signal for a time duration τ_h, $\tau_h \leq T$, at a transmission level P_s, $[Watt]$. In the energy harvesting duration τ_h $[s]$, the users charge their rechargeable built-in battery by collecting the energy of the RF signal radiated from the BS. The harvested energy by

the user k, $k \in N$ from the broadcasted RF signal in the τ_h time duration is given by:

$$E_k = \eta \tau_h P_s h_k \tag{6.1}$$

where $\eta \in \big(0, 1\big]$ is the energy conversion efficiency factor which depends on the type of the receivers.

During the WIT phase, each user transmits its information signal to the BS for a time duration τ_t, where $\tau_t = T - \tau_h$ at an uplink transmission power level p_k. The communication between the users and the BS is realized as mentioned before in an OFDMA manner. It should be clear that user's uplink transmission power p_k depends on the harvested energy by the PS during the WET phase and can be expressed as:

$$p_k = \frac{E_k}{\tau_t} = \frac{\eta h_k P_s \tau_h}{\tau_t} \tag{6.2}$$

The corresponding achieved uplink transmission data rate R_k is formulated as follows:

$$R_k = R_{ser} f\left(\gamma_k\right) \tag{6.3}$$

where R_{ser} is the fixed transmission rate depending on the type of service that the user requests and $f(\gamma_k)$ denotes the efficiency function as already described in Definition 2.3.2. The aforementioned signal-to-noise ratio from user k to the BS during the WIT phase is appropriately modified for this problem as below:

$$\gamma_k = \frac{g_k p_k}{\Gamma I_0} \tag{6.4}$$

where Γ characterizes the gap between the achievable rate and the channel capacity due to the use of practical modulation and coding schemes and I_0 denotes the noise variance. All key notations from this Chapter are summarized in the Table 6.1 below.

Table 6.1: Chapter 6 list of key notations

Symbol	**Description**
$\|N\|$	Number of backlogged users
N	User set
h_k	Downlink channel power gain between PS and user
g_k	Uplink channel power gain between user and BS
T	Timeslot duration
τ_h	Energy harvesting duration
P_s	PS transmission power
E_k	Harvested energy by the PS
η	Energy conversion efficiency factor
τ_t	Time duration of information signal to BS
p_k	Uplink transmission power level
R_k	Uplink transmission data rate
R_{ser}	Fixed transmission rate depending on the type of service
$f(\gamma_k)$	Efficiency function
γ_k	Signal-to-noise ratio
Γ	Gap between achievable rate and channel capacity
I_0	Noise variance
U_k	Utility function
a	Percentage factor of timeslot split between WET and WIT
A_k	Feasible interval of uplink transmission power levels
$P^*_{s,k}$	Optimal customized PS's transmission power
A, M	Efficiency function parameters
$\mu(\gamma_k)$	Auxiliary function

6.2.2 Problem Formulation and Solution

Aiming at expressing users' perceived satisfaction from the fulfillment of their QoS prerequisites and the corresponding battery consumption under a holistic framework, each user is associated with a well-designed utility function, which represents the tradeoff among the achievable data rate R_k depending on the type of service that the user requests and the corresponding consumed transmission power. The proposed utility function captures users' QoS demands and is aligned with the definition of energy-efficiency (EE), which represents (in $bits/Joule$) the amount of the information bits transmitted per each Joule of consumed energy. Therefore, user's k, $k \in N$ utility function can be expressed as:

$$U_k = \frac{R_k}{p_k} = \frac{(1-a)\, R_{ser}\big(1-e^{-A\gamma_k}\big)^M}{\eta h_k P_s a} \tag{6.5}$$

where $a \in (0,1)$ denotes the percentage factor of the timeslot split between the energy harvesting (WET) and information transmission (WIT), where $\tau_h = a \cdot T$ and $\tau_t = \big(1-a\big) \cdot T$.

Each user aims at maximizing its utility via determining its optimal uplink transmission power during the WIT phase, which however is interdependent on the optimal customized transmission power of the PS. Therefore, the corresponding adaptive resource management problem can be expressed as a distributed maximization problem of each user's utility function [168]:

$$\max_{p_k \in A_k} U_k\left(p_k\right) \tag{6.6}$$

where $A_k = \big(0, p_k^{Max}\big]$ denotes the feasible interval of user's k, $k \in N$ uplink transmission power levels and p_k^{Max} is the maximum available uplink transmission power of user k, which is determined based on the harvested energy during the WET phase. It should be noted that in case that a user during the WIT phase does not exhaust all of the energy harvested during the corresponding WET phase of the timeslot under consideration, it could store any excessive energy in a rechargeable built-in battery, in order to be available for use in future transmissions or for performing other processing tasks. For simplicity, we do not consider the potential exploitation of any excess energy in current timeslot. The consideration of this feature in turn would influence the value of the maximum available uplink transmission power of user k as the stored energy should be properly reflected in the calculation.

Combining equations (6.5) and (6.6), the adaptive resource management problem in turn can be formulated as a maximization problem of each user's utility function with respect to its customized need of PS's transmission power towards harvesting the necessary energy in order to meet its QoS prerequisites. The corresponding Energy Transfer and Transmission Adaptation (ENTRADA) optimization problem is expressed as follows:

ENTRADA Optimization Problem :

$$\max_{P_s \in A_s} U_k\left(P_s\right) \tag{6.7}$$

$A_s = \big(0, P_s^{Max}\big]$ and P_s^{Max} is the maximum available transmission power of the PS.

The maximization problem of each user's utility function with respect to user's customized need of PS's transmission power is solved in a distributed manner by each mobile node in the WPCN towards determining the optimal customized PS's transmission power $P_{s,k}^*$.

Theorem 33. ***(ENTRADA Critical Point:)*** *The distributed optimization problem formally expressed in relation (6.7) has a unique optimal customized PS's transmission power solution for each user:*

$$P_{s,k}^* = \max\left\{\hat{P}_{s,k}, P_s^{Max}\right\} \tag{6.8}$$

where $\hat{P_{s,k}} = \underset{P_s \in A_s}{argmax}\, U_k\big(P_s\big)$ and each user's SINR feasible interval is $\gamma_k \in \left(\frac{lnM}{A}, \frac{ln10^4 M}{A}\right)$.

Proof. Towards proving the existence and uniqueness of the optimal customized PS's transmission power for each user, we examine the properties of its utility function, as expressed in equation (6.5). Initially, we study its monotonicity via examining the sign of its first order derivative:

$$\frac{\partial U_k}{\partial P_s} = \frac{(1-a)\cdot R_{ser}}{\eta \cdot h_k \cdot a \cdot P_s^2}\big(1-e^{-A\gamma_k}\big)^{M-1} \cdot \mu(\gamma_k) \tag{6.9}$$

where $\mu(\gamma_k) = MAe^{-A\gamma_k}\gamma_k - \left(1 - e^{-A\gamma_k}\right)$. Bolzano Theorem is applied *(See definition 2.5.1)* by selecting an extremely small, i.e., $\gamma_k = \frac{lnM}{A}$, and an extremely large, i.e., $\gamma_k = \frac{ln10^4M}{A}$ value of SINR, which has an analogous relation (one-to-one) with P_s. Thus, the feasible interval of SINR values is not practically affected by the selected values.

For $\gamma_k = \frac{lnM}{A}$, we have $\mu(\gamma_k) = lnM + 1/M - 1 > 0$, and for $\gamma_k = \frac{ln10^4M}{A}$, we have $\mu(\gamma_k) = ln10^4M/10^4M + 1/10^4M - 1 < 0$, $\forall A \in (0.1, 100)$ and $\forall M \in (1, 1000)$. Therefore, there exists at least one critical point $\hat{\gamma_k} \in \left(\gamma_k = \frac{lnM}{A}, \gamma_k = \frac{ln10^4M}{A}\right)$ such that $\frac{\partial U_k}{\partial P_s} = 0$. Moreover, since $\mu(\gamma_k)$ is a continuous function in $\left(\frac{lnM}{A}, \frac{ln10^4M}{A}\right)$, it is concluded that $\mu(\gamma_k)$, $\left(\frac{\partial U_k}{\partial P_s}\right)$ changes its sign from positive to negative at least once within the interval $\left(\frac{lnM}{A}, \frac{ln10^4M}{A}\right)$. The above denotes that the monotonicity of U_k changes from increasing to decreasing, implying that the critical point leads to utility maximization within the modified space $\gamma_k = \left(\frac{lnM}{A}, \frac{ln10^4M}{A}\right)$. Finally, based on the second order derivative criterion, we identify from all the determined critical points the one that is the global maximum, i.e., $\hat{\gamma_k}$ and due to the one-to-one relationship we determine the optimal customized PS's transmission power $\hat{P_{s,k}}$. □

It is noted that each user determines the optimal customized PS's transmission power, thus we adopt the notation $\hat{P_{s,k}}$ instead of P_s.

6.2.3 Distributed Algorithm

In this section, we introduce a distributed and low complexity Energy Transfer and Transmission Adaptation (ENTRADA) algorithm, which determines the optimal customized PS's transmission power during the WET phase in order to guarantee the fulfillment of users' QoS prerequisites in the WIT phase. The fundamental novelty of the ENTRADA algorithm is that it allows the users to influence the wireless energy transfer from the power station via disclosing their transmission requirements for the following WIT phase. The aforementioned characteristic of ENTRADA algorithm is of great importance due to the fact that both WET and WIT phases will reserve and consume only the necessary resources towards fulfilling users' QoS demands, thus avoiding overconsumption or unfair allocation of power/energy among the users. In a nutshell, ENTRADA algorithm can be described as follows:

Algorithm 16 ENTRADA Algorithm

1: *WET Phase*
2: Each mobile user within the WPCN at the beginning of each timeslot T determines in a distributed manner the optimal customized PS's transmission power $P^{\star}_{s,k}$ towards maximizing its utility based on Equation (6.8).
3: Each user reports the optimal customized PS's transmission power $P^{\star}_{s,k}$ to the PS via a unicast signal.
4: The PS broadcasts an RF signal with power levels $P^{\star}_{s} = max\{P^{\star}_{s,1}, ..., P^{\star}_{s,|N|}\}$ during the WET phase ensuring adequate energy storage in the rechargeable built-in batteries of all users for the upcoming WIT.
5: *WIT Phase*
6: Each mobile user transmits its information signal with an optimal uplink transmission power $p_k = \frac{\eta h_k P^{\star}_{s} \tau_h}{\tau_t}$ to the BS during the WIT phase.

Based on the description of the ENTRADA algorithm, it becomes apparent that the WET phase is adapted to the WIT phase driven by the power requirements of the users of the WPCN. Finally, it should be highlighted that the ENTRADA algorithm is implemented in a distributed manner, meaning that the final outcome depends on the individual decision of each mobile user, thus eliminating any additional complexity as the number of users residing within the WPCN increases.

6.2.4 Numerical Results

In this section, we provide some numerical results illustrating the operation, features, and benefits of the proposed framework and the ENTRADA algorithm. Initially, we focus on the operation performance achievements of ENTRADA algorithm in terms of efficiently controlling the power station's optimal customized transmission power. The relation of PS's optimal customized transmission power to users'

devices' hardware characteristics (e.g., energy conversion efficiency factor), as well as application layer parameters (e.g., charging percentage time) is studied, while the total achievable data rate at the equilibrium operational point of the overall system is presented as well. Then, we provide a comparative evaluation of our proposed approach against other existing works in the literature with respect to the achieved energy-efficiency. For demonstration purposes, throughout our study, we consider a single WPCN cell with radius $r = 1000\ m$ and $|N = 50|$ users, a base station (BS) and a power station (PS) randomly placed within cell's coverage area. We model users' path gains from the BS and the PS using the simple path loss model $h_k = {}^{K_k}/_{d^{\theta}_{k,PS}}$, $g_k = {}^{K_k}/_{d^{\theta}_{k,BS}}$, respectively, where $d^{\theta}_{k,PS}$ and $d^{\theta}_{k,BS}$ is the distance of user k from the PS and BS, respectively, θ is the distance loss exponent (e.g., $\theta = 4$) and K_k is a log-normal distributed random variable with mean 0 and variance $\sigma^2 = 8dB$. We consider the following values of the system parameters: $a = 0.7$, $\eta = 0.9$, $R_{ser} = 256\ kbps$, $\Gamma = 0dB$, $P_s^{Max} = 50dBm$, $M = 80$, $A = 3.7$, $I_0 = -110dBm$

ENTRADA Properties and Operation

Towards presenting the inherent characteristics of ENTRADA framework and its ability to efficiently exploit the transmission power of the PS towards fulfilling users' QoS demand, we provide a detailed analysis of PS's transmission power with respect to the charging time and the energy conversion efficiency. Specifically, Fig. 6.2 and Fig. 6.3 present (horizontal axis) the optimal customized PS's transmission power levels $P_s^{\star}$ of the RF signal broadcasted by the PS during the WET phase, as a function (vertical axis) of the energy harvesting percentage a of the timeslot, as well as with respect to the energy-efficiency conversion factor η, respectively. The results reveal that the longer the users are able to harvest energy from the PS, i.e., higher values of a, the lower optimal customized PS's transmission power $P_s^{\star}$ is required in order to sufficiently charge the users and fulfill their QoS prerequisites for the following WIT phase.

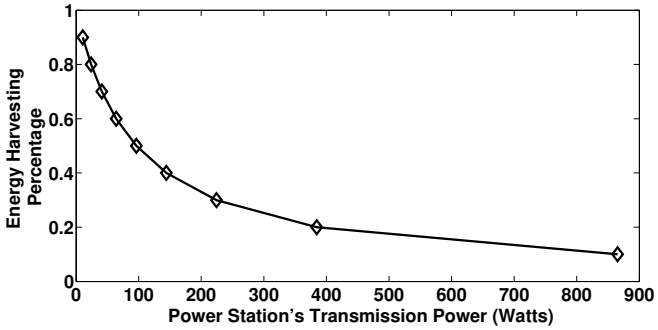

Figure 6.2: Optimal customized PS's transmission power as a function of the charging percentage time a

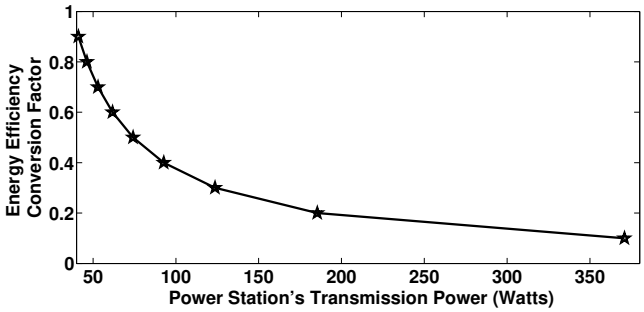

Figure 6.3: Optimal customized PS's transmission power as a function of the energy conversion efficiency factor η

Moreover, as expected, it is observed that superior energy conversion levels lead to decreased necessary PS's transmission power levels $P_s^{\star}$ in order the users to charge sufficiently their rechargeable built-in batteries and meet their QoS requirements during the following WIT phase. Based on the numerical results of Fig. 6.2 and Fig. 6.3, we observe that given the energy availability of the power station, i.e.,

P_s^{Max}, the technical characteristics of users' devices considering their energy conversion efficiency, we are able a priori to determine from the beginning of each timeslot T, the duration of the WET and WIT phase, towards guaranteeing the requested services to the users.

Furthermore, in Fig. 6.4 the total achievable data rate of all the users residing in the examined network is presented (vertical axis) as a function of the power station's transmission power level. As mentioned before, in the examined scenario it is considered that all the users request the same type of service with target achievable data rate $R_{ser} = 256$ $kbps$, ($a = 0.7$, $\eta = 0.9$). The results clearly reveal that as the transmission power levels of the PS increase, the total achievable data rate increases. Moreover, at the equilibrium value $P_s^{\star}$, as determined by the ENTRADA algorithm, the QoS prerequisites of all the users have been fulfilled, thus the power station should not spend additional power.

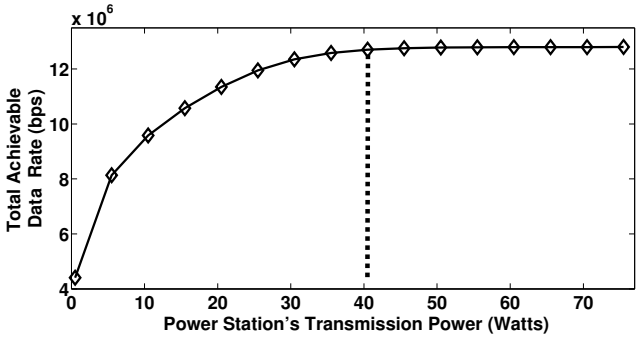

Figure 6.4: Total achievable data rate as a function of the PS's transmission power

Comparative Evaluation

Next, we provide a comparative study highlighting the benefits of the ENTRADA algorithm in terms of achieved energy-efficiency compared to other similar approaches from the recent literature. Specifically, we compare ENTRADA algorithm to two different approaches from the recent literature proposed for WPCNs: (a) the algorithm in [164], where a joint time allocation and power control problem is proposed targeting at maximizing network's energy-efficiency and (b) the algorithm in [165], where a joint energy and time allocation is proposed towards maximizing the uplink sum rate network performance. Fig. 6.5 presents user's energy-efficiency (in bits/Joule) as a function of user's ID, which is increasing as the distance of the user from the base station increases, for the three different examined approaches. It is noted that in order to preserve fairness among the different scenarios, all algorithm simulations were conducted under the same transmission conditions. It is clearly observed that the ENTRADA algorithm provides significantly higher energy-efficiency levels, reaching up to 98.28% and 94.77% improvement compared to [165] and [164], respectively. The above outcome stems from the specific adaptive design of the ENTRADA algorithm, where the users harvest the exact necessary energy according to their actual transmission requirements, in contrast to [165] and [164], where the users in order to meet their energy-efficiency and rate threshold targets, transmit with the maximum available transmission power, as determined by the harvested energy. On the other hand, the proposed scheme delivers additional gains for the Power Station's transmission during the WET phase, achieving a reduction up to 39.68% in PS's transmission power, in contrast to [164] and [165], due to the adjustment of the users' energy harvesting to the subsequent user transmission to the BS.

6.3 General Summary

In this Chapter, the problem of user-centric energy-efficient power control in wireless powered communication networks (WPCNs) was studied. A holistic energy-efficient power control framework within the WPCN was designed, where a generic utility function has been associated with each user capturing its QoS demands and energy harvesting requirements. An optimization problem of each user's utility function with respect to the optimal customized PS's transmission power was formulated and solved. The fundamental novelty of the proposed framework is that the PS considers users' actual needs in energy consumption during the wireless energy transfer (WET) phase, towards providing them the exact necessary

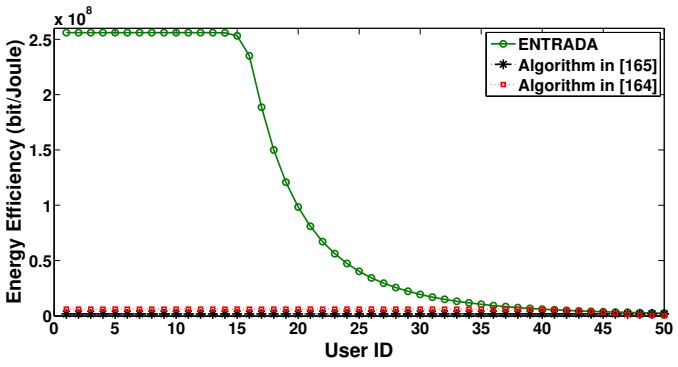

Figure 6.5: Users' energy-efficiency with increasing distance from the BS under three comparative scenarios

transmission power so as to achieve their QoS requirements during the wireless information transmission (WIT) phase. A distributed and low-complexity Energy Transfer and Transmission Adaptation (ENTRADA) algorithm was proposed aiming at determining the optimal customized PS's transmission power, and detailed numerical results show the increased energy-efficiency achieved by the proposed adaptable scheme.

Chapter 7

Dynamic Resource Management for Fragile Resources

As already discussed, the transition to 5G wireless networks is delivering a massive transformation from a conventional, static network structure where a limited amount of users requested voice-only services to a highly diverse and volatile environment where an increasing number of interconnected smart devices is requesting diverse services, with decisions changing rapidly based on the requirements at the time and the relevant information content to be exchanged. This realization dictates that modern networks need to develop techniques and algorithms to manage and allocate resources in a dynamic manner, adjusting each time to changing user preferences, allocating spectrum in real time conditions, and allowing user mobility, on-demand services or exchange between bands, among others. The above capabilities, expressed under the more holistic term *"Dynamic Resource Management"* refer to a complete set of actions ad-hoc and self-optimizable networks can adopt in order to allocate limited resources more efficiently and increase utilization, enhance energy-efficiency and manage interference, as well as adapt to varying network configurations, traffic trends, etc.

User behavior constitutes a key element of dynamic resource management, since user decisions play an ever growing role in how networks manage to distribute resources in terms of content preferences (e.g., streaming or video conference compared to voice calls) or traffic offloading (radio access technique or band selection). In this Chapter, we study in depth how user behavior and priorities can not only impact the way networks optimally distribute the available spectrum among them, but also design algorithms which integrate user strategies into the resource allocation process towards further improving network performance, instead of viewing customers as neutral agents who only consume bandwidth and cause interference.

Additionally, one of the major contributions of this work is the assumption that network resources which are shared can be *fragile*; implying that they may collapse or deliver diminishing returns if they are over exploited by the users. Examples of fragile resources include fisheries, forests [169], free parking, pollution [170] etc. Within this context, spectrum in wireless networks can also be fragile, since excessive utilization and an unexpected surge in traffic may result in severe outages (e.g., in cases of a natural disaster, terrorist attack or very high media demand for certain events like sports, elections etc). By perceiving spectrum as fragile and model systems under the appropriate theoretical tools, user behavior can considerably vary among different groups, helping WISPs better regulate traffic and enhance performance, while minimizing the probability of spectrum outage occurrences.

7.1 General on Prospect Theory

The majority of relevant research works in the literature concerning resource allocation problems in the area of telecommunications have adopted game theoretic approaches due to their distributed nature, relying mostly on Expected Utility Theory (EUT) maximization. In such a setting, users are viewed as neutral utility maximizers, ignoring decision making under conditions of uncertainty. Game Theory considers rational players whose behavior remains uninfluenced by risk, an assumption which deviates from real life decisions where individuals exhibit risk seeking behavior under losses and risk averse behavior under gains.

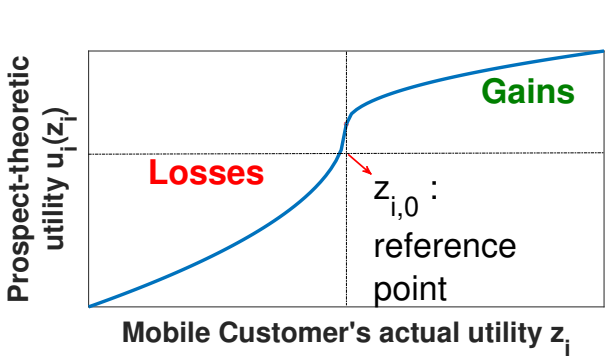

(a) Prospect-theoretic utility function

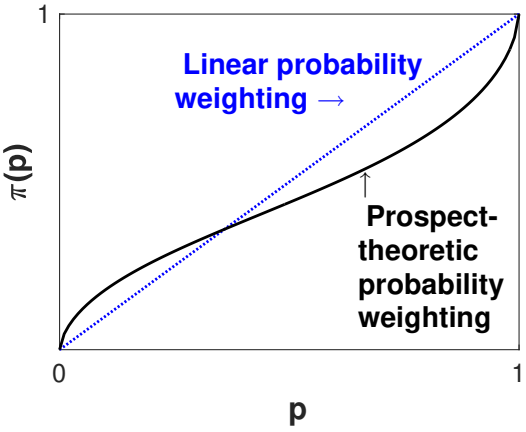

(b) Probability-weighting function

Figure 7.1: Prospect-theoretic users' behavioral model

Recognizing the highly volatile and uncertain environment under which wireless networks operate where player competition is fierce and often with conflicting strategies, Prospect Theory (PT) proposed by Kahneman and Tversky in their seminal paper [171], is a Nobel-prize-winning behavioral economics theory which can be identified as an interesting alternative in the modeling and formulation of optimization problems for telecommunications, where user decisions can define the performance and efficiency of resource distribution.

For such a user centric paradigms, Prospect Theory has emerged as a dominant behavioral model in formulating decision making under risk and probabilistic uncertainty. PT succeeds in integrating user subjectivity in decisions, and is characterized by four principal features: (i) *reference dependence:* individuals assess uncertain outcomes with respect to a reference point and exhibit different behavior between events of gain or loss; (Fig. 7.1a) (ii) *loss aversion:* the decrease in utility under losses is perceived greater than the increase in utility under a gains of the same magnitude; (iii) *diminishing sensitivity:* illustrated by an S-shaped utility function, with PT utility functions being concave for gains and convex for losses, suggesting that individuals behave as risk averse in positive outcomes and adopt a risk seeking behavior when negative outcomes are considered. Lastly, (iv) *probability weighting:* indicates that users overweight smaller probabilities and underweight larger ones (Fig. 7.1b) [172].

As the above points highlight, prospect theoretic modeling manages to integrate the above human behavior deviations which EUT has failed to incorporate in wireless network optimization problems. In view of including realistic user perceptions towards decision making in resource allocation problems, in this work two different types of resources have been identified, as defined below:

Definition 7.1.1. ***Safe Resources:*** *Resources which have a constant return on investment. Such resources do not fail and are usually of closed access nature [172].*

Definition 7.1.2. ***Common Pool of Resources:*** *Common Pool of Resources (CPR) refer to a wider class of resources which are shared among users and are non-excludable (i.e., it is not possible to prevent a user from accessing it) and rivalrous or subtractable (i.e., use of the resource by one user reduces the availability of the resource for the rest of the users) [172].*

CPR resources due to their open access and shared nature to users become susceptible to the phenomenon of the *"Tragedy of the Commons"*, which is formally defined below:

Definition 7.1.3. ***Tragedy of the Commons:*** *Users competing for a CPR (i.e., via over-congestion or over-investment) may often result to destruction of the resource or inferior or suboptimal outcomes, a situation popularized by Hardin as "Tragedy of the Commons", [170].*

7.2 User Behavior and Perceptions towards Risk

Against this background, it can be observed that the application of Prospect Theory in various domains such as lotteries, gambles or travellers' behavior is important in order to model events where user choices between alternatives or risky situations need to be captured [173]. In this thesis, we expand the use of Prospect Theory also in resource allocation problems by realizing the fragility and the challenges stemming from the over-utilization of the limited spectrum due to the rising congestion and the data hungry applications in future wireless networks.

The potential collapse of spectrum in networks induces increased uncertainty to users who are called upon taking decisions with incomplete or missing information, and respond accordingly by interpreting the involved risks. According to [173], human beings (e.g., taking the role of a traveller or a network user etc.) have been so far mostly been modeled as rational agents (*"homo economicus"*) who simply aim to maximize their satisfaction and minimize any negative aspects of their decisions. However, newest research trends towards modeling human behavior have concluded that under conditions of uncertainty humans tend to deviate from the expected rational decision making (*"homo psychologicus"*), and exhibit behavior closer to the theoretical framework included by Prospect Theory.

Specifically within the context of wireless network operation in pragmatic conditions, the high uncertainty and competition forcing different users to constantly assess the risks, makes obvious that they will not behave as blind and neutral agents but their behavior can significantly vary depending on their risk aversion and individual preferences. In this work, we put users and their actions at the centerpiece of the resource allocation process and the subsequent network performance optimization. Mobile customers are driven by their data greedy and interference causing transmissions targeting at maximizing their utility by capturing as much of the needed spectrum with as less consumed power as possible. However, this assumption does not fully captivate the parameters shaping human decision making. Hence, in the next sections we include in the theoretical modeling those diverse risk preferences of users and the trend to overweight the risk of shut-down of spectrum if over-exploited, also varying based on the type of service, the channel gains or the radio access technique architecture.

7.3 Dynamic Spectrum Management for Licensed and Unlicensed Bands

The emergence and upcoming deployment of 5G networks is drastically revolutionizing existing network infrastructure [174], with 5G projected to generate 4.7 times more traffic than existing 4G networks by 2021, with more than 75% of global data traffic being multimedia services (e.g., video, online gaming). Mobile data traffic has increased 18-fold in the last 5 years with no signs of slowing down, since the usage of smart devices is already generating almost 90% of total mobile traffic. Subsequently, 5G networks are expected to handle an ever increasing amount of data, foreseen to reach approximately 50 exabytes per month as smart phones, wearable devices, and Internet of Things evolution is intensifying [175]. At the same time already since 2016, fixed networks like Wi-Fi or femtocell, have been absorbing 60% of mobile data traffic, offloading heavily congested cellular networks [176]. The massive expansion of mobile devices and the mobile applications associated with changing trends in data use is shedding light to the problem of spectrum shortage, with mobile users being unable to exploit bandwidth resources based on lack of infrastructure, outdated regulation policies, or limited access to data sharing. The ongoing transformation of radio cellular networks towards heterogeneity, machine-to-machine communications, and small cell deployment has shifted the interest to schemes exploiting the coexistence and use of both licensed and unlicensed spectrum bands. Unlicensed bandwidth provided by supplementary communication sources (e.g., Wi-Fi) can support users with sufficient transmission conditions, creating a second parallel environment of operation besides licensed spectrum on a non-interference basis towards increasing spectral capacity and dealing with the emerging traffic demands.

Given the above developments, it has become visible that existing network infrastructure faces significant challenges in meeting this ever growing demand with WISPs exploring possible ways to boost spectrum capacity and respond to the ongoing proliferation of mobile connections. Heterogeneous networks integrating dense small cells of open or closed access with high power macrocells have been developed towards improving network performance and connectivity. Significant advances have been obtained throughout the recent years to extend capacity in licensed spectrum and increase the number of connected users, improve throughput, and broadening network coverage and data demand [17], through the use of

enhanced network architectures and technologies (e.g., femtocells, picocells, multi-carrier deployment and carrier aggregation, cell splitting or adaptive resource partitioning, etc.) Nevertheless, a holistic answer to the problem of spectral efficiency is still missing, and therefore additional challenges emerge. Severe intercell interference, deteriorating energy-efficiency as well as coverage holes have been associated with the operation of heterogeneous networks which further exacerbate congestion and inferior Quality of Service (QoS) provision problems. In view of this research and practical gap, regulators (e.g., Federal Communication Commission, FCC) [177, 178] are releasing several unlicensed bands for commercial purposes, hence facilitating the exploration of the use of commonly accessible and admission fee-free unlicensed spectrum in a shared platform with closed-access, subscription-based licensed bands. Additionally, so far, cellular networks and other wireless networking technologies such as Wi-Fi, WiMax, mmWave or television white-space have been studied and evolved following separate routes further intensifying the urgency for licensed and unlicensed spectrum convergence. Below we provide a brief overview of licensed and unlicensed spectrum basics.

Licensed Spectrum

Licensed spectrum, operating under a strict regulatory and legal framework has long been the foundation for cellular network evolution. Licensed bands provide wide range and superior signal-to-interference-plus-noise (SINR) communications, however due to their exclusivity are expensive to access and limited in resource availability. Licensed spectrum bands for radio access networks (RANs) have been granted to operators under exclusive rights and legal protection on dedicated frequencies. Communications in such bands take advantage of reliable and strong signal and guaranteed QoS thresholds, whereas geographical range and user mobility are facilitated through extensive network infrastructure and land investment. However, even when licensees are not transmitting, licensed bands block any opportunistic access to non-registered users with the spectrum being left unused. On the contrary due to the scarcity of the available resources, shortages and spectral misallocation have become a common phenomenon in incidents of overcrowding and congestion.

Unlicensed Spectrum

Given the non deniable push of existing networks to their theoretical licensed spectrum limits, it has been observed that unlicensed spectrum bands above $3\,GHz$ have been largely unutilized [179], with currently only the $2.4\,GHz$ band shared by users in Wi-Fi, Zigbee or Bluetooth being relatively in use. Typical utilization of bands above $3\,GHz$ has been less than 0.5% [179], despite the fact that the less congested $5\,GHz$ (Wi-Fi or LTE-U) or $28\,GHz$ (mmWave) bands provide abundant spectrum that could enable high broadband multimedia transmissions.

Moreover, with almost 90% of data services occurring within indoor environment or central public hotspots, the use of unlicensed spectrum for shorter range coverage (e.g., small cells or fixed networks) can provide seamless access and operation with limited infrastructure costs and admission fees, while also surpassing the considerations of physical power limitations and the need to develop sophisticated interference management techniques due to the coexistence with licensed bands on a non interference basis. The inclusion of unlicensed spectrum due to its free to access or low fee admission policy despite enabling connection scalability, comes at the risk of potential over-utilization and severe user spectrum competition. Unlicensed bands are considered: a) non-excludable, meaning that they are openly accessible to all users, and b) subtractable with regards to the available spectrum, due to the fact that exploitation from one user reduces the ability of the other users to utilize the remaining spectrum. The latter comes at the risk of potential unlicensed spectrum over-utilization and severe user spectrum competition. Unlicensed spectrum has recently started to attract increasing research attention with efforts to access and utilize unused unlicensed bands [179], [180] or combine them with existing licensed spectrum communications. For instance, in [181], unlicensed spectrum is split among Wi-Fi and femtocell networks, whereas in [182], a primary licensee and secondary users engage in collaborative spectrum sensing and sharing.

Unlicensed spectrum by virtue of its nature as a free to obtain resource, in combination with the absence of a supervisory body enforcing social welfare and monitoring consumption and competition, stresses the need for a different approach with respect to the fragility of the resource and its over-exploitation risks. The absence of regulations and the self-optimizing process of resource allocation in the unlicensed bands, shift the weight of decisions to the users, who need to consider and incorporate risk-based behaviors in their strategies in order meet their Quality of Service (QoS) prerequisites.

Coexistence

The availability of unlicensed bands alongside licensed ones comes with profound advantages which far exceed the significant spectral capacity increase. The flexibility of choice and potential bundling between licensed and unlicensed spectrum sources create a whole new vision in the field of efficient resource allocation and congestion management in modern wireless networks. The extensibility of this scheme is yet to be fully explored, since wireless connectivity is gaining attention as a factor of critical importance for the function of the emerging digital economy, the IoT evolution, or even in public safety domains. More fair resource allocation is enabled with congestion offloading from heavily utilized licensed bands by being redirected to the unlicensed spectrum which has been underutilized. The use and sharing of unlicensed bands among different WISPs, cannot only bring ameliorated performance and social welfare for the system overall, but it can increase operator and price competition [178], in favor of consumers. In particular, under user-centric operating models as the ones emerging in 5G wireless networks and beyond, the users can direct the nature of their transmission via the licensed and unlicensed bands according to their QoS requirements or the type of service they require (i.e., elastic or inelastic). Fig. 7.2 provides a conceptual illustration of a prospective network with licensed and unlicensed spectrum sharing. One cell with registered licensees coexists with unlicensed and access free sources, where users can opportunistically utilize the available spectrum. In a nutshell, aggregation of licensed and unlicensed bands in harmonious coexistence paves the way for a whole new perspective in areas like traffic offloading and utilization management. Efficient spectrum sharing and access technology preference are enabled, whilst the economic and market impact of such a framework cannot be underestimated in alignment with the deployment of 5G networks [183].

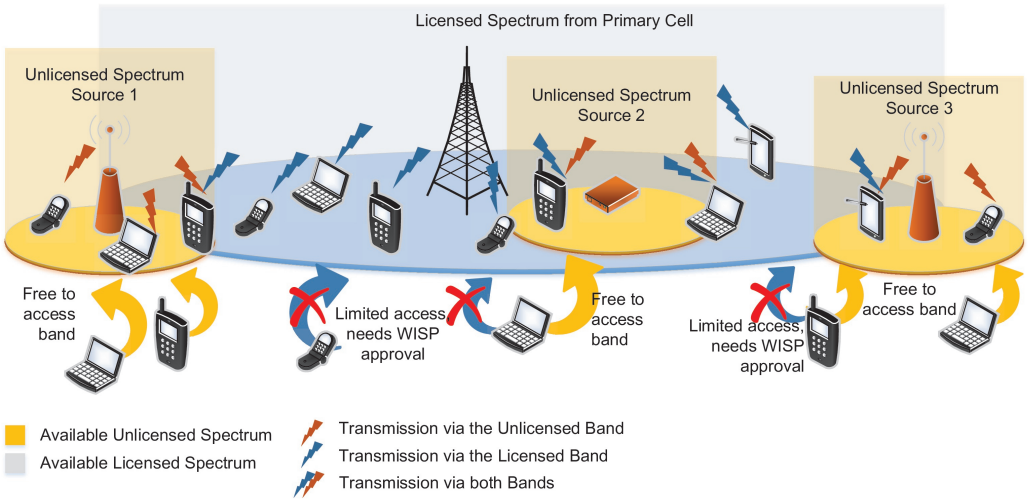

Figure 7.2: Conceptual network topology with both licensed and unlicensed spectrum access

7.3.1 Related Work on Band Coexistence and Prospect Theory

With the available spectrum capacity being at critical bottleneck, several problems referring to band coexistence and throughput optimization have been studied. In [184], Wi-Fi and LTE-U exist in the same band under a shared spectrum model, where a centralized approach delivers improvements in fair spectrum access and data throughput. In [185], the problem of direct transmission to unlicensed bands is considered. By merging band selection and data routing, an overall increase in data rates is observed, while [186] proposes a new transmission protocol for a joint utilization for licensed and unlicensed spectrum with gains in average user throughput compared to conventional Wi-Fi/LTE. [187] investigates the coexistence of unlicensed and licensed LTE, achieving superior performance in traffic balancing and data offloading.

At the same time, PT has also started gaining research attention also in the area of networked systems, spanning from smart grid networks [188], and communications systems [189], to transportation networks, [190], [191]. Although the research status of PT for resource management in wireless networks

is still at a very early stage, works have already used this theory in evaluating user or operator decisions in circumstances where risk induces serious challenges to the network's performance. In particular, the authors in [192] examine system's deviation from EUT under PT leading to potential degradations in terms of throughput, delay, and pricing pressure for a time slotted wireless random access network. Additionally, in [193] WISP profit attributes were examined, concluding in a loss aversion attitude of the providers in favor of lower gains with reduced risks, whereas in [194] users behave differently under reward and penalty cases, switching from a conservative to a more aggressive attitude depending on the loss and gain probabilities.

The work presented in this section bridges the gap between the ongoing trends in band coexistence and optimization with real life decisions that users are requested to take regarding their connectivity, given the risk of distorted access to a cellular network or to a wireless band with collapse dilemmas. In contrast to the above referenced research works, resource failure (i.e., fragility) due to uncontrolled investment becomes a reality addressing pragmatic situations with regards to increasing congestion under dense deployments and spectrum scarcity.

7.3.2 System Model

We consider the uplink of a NOMA wireless network consisting of a base station (BS) serving a region of radius R. Let $\aleph = \{1, ..., i, ..., N\}$ denote the set of users randomly placed within the topology, who are provided the option of transmitting in either one or simultaneously in both of the available licensed and unlicensed bands. Each band corresponds to a different independent fraction of the available spectrum with the users at the beginning of the timeslot indicating the structure and nature of their transmission. For instance, users are enabled to dynamically adjust the percentage of their available transmission power allocated to the unlicensed band, potentially streamlining their operation from fully operating within the unlicensed spectrum only, to adopting a shared scheme between the licensed and the unlicensed options.

In this work we distinguish the operation of the licensed and unlicensed bands with regards to their stability and spectral capacity. Both bands become available to users under the NOMA transmission technique, with the licensed band being regulated by the WISP where users transmit under predefined data target rates, while the unlicensed band captures a much larger portion of the overall spectrum attracting users due to the higher feasible data speeds, operating though without any regulatory framework or performance warranties. An illustrative representation of such a network structure is shown in Fig. 7.3. This means that an over-investment in the unlicensed spectrum by the users would eventually lead to the collapse of this band with none of them being able to retrieve any utility returns from their transmission. Thus, in the circumstance of band failure, a user who fully invested into the unlicensed spectrum will eventually receive zero return from this action (i.e., will eventually not transmit), whereas a user who decided to partially transmit in the licensed band will at least recover some utility surplus from this part of its operation. In this section, we adopt a scheme where all users are lured into transmitting via the unlicensed bandwidth due to the expected increased satisfaction from this resource, with some of them opting to minimize the unlicensed band collapse risk by still transmitting under the safer licensed spectrum.

Utility Functions Under Prospect Theoretic Perspective

We assume that individuals assess uncertain outcomes under a loss averse attitude, i.e., the utility detriment in the event of a loss is sensed as of greater magnitude in comparison to gains of equal extent given a reference point. This reference point is considered as the zero point (i.e., ground truth) of user perceived utility scale, and it is not necessarily common for all users. Additionally, the probability weighting effect is considered, implying that users tend to overweight events with small probabilities and underweight events with higher probabilities, thus instructing the formulation of a utility where value estimations and probabilistic outcomes are integrated under a common umbrella.

Specifically, the PT utility adopted is concave in positive outcomes and convex in negative outcomes, forming an S-curved shape, indicating user risk seeking or aversion behavior as follows:

$$v_i(z_i) = \begin{cases} (z_i - z_0)^{a_i} & when\ z_i > z_0 \\ -k_i(z_0 - z_i)^{\beta_i} & otherwise \end{cases} \tag{7.1}$$

where z_i and z_0 denote the relative per user i outcome and the reference point suggesting the boundary among an event of gain or loss, respectively. Parameters $a_i, \beta_i \in \big(0, 1\big]$ express and quantify the sensitivity

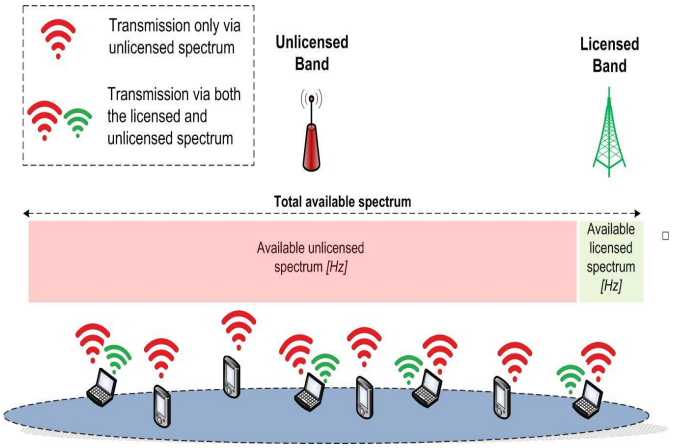

Figure 7.3: Licensed and unlicensed band spectrum split

of user i with regards to a gain or a loss, while $k_i \in [0, \infty)$ reflects the impact of losses compared to gains in user's utility. In other words, a value of $k_i > 1$ implies a loss aversion attitude, where users perceive utility losses under a steeper curve compared to earns in the event of an equivalent gain. For convenience and without loss of generality, we assume $a_i = \beta_i$. The above framework solidifies the alignment of PT to wireless networks, where users are called to decide how to maximize their utility under terms of probabilistic uncertainty. Licensed bandwidth is assumed to function as a safe option with lower data rate capacity, whereas the unlicensed band is regarded as a CPR available to all users offering a higher fraction of the overall spectrum, however delivering increasing risks of collapse due to high competition (if occurred). By treating unlicensed band as a CPR it means that it is non-excludable, i.e., all users have the right to access it, while simultaneously its rivalrous or subtractable, i.e., its utilization by one user reduces the degree that is exploited and utilized by another user. Subsequently, users viewed as competitive players, incorporate these estimations into their decisions directing their transmission and corresponding power through each band, depending on their perceptions towards risk.

It should be noted that in the current section the utility functions have been specifically designed in accordance with the Shannon log-based paradigm, indicating the maximum feasible rate for successful transmission under system's physical constraints and illustrating user greedy behavior towards the maximization of their QoS satisfaction, as follows:

$$U_i(x_i) = \begin{cases} \frac{W_l/N_l}{P'_i} ln(1+\gamma_i) & if\ x_i = 0 \\ \frac{W_l/N_l}{P'_i} ln(1+\gamma_i)(1-x_i) \ + \frac{W_u/N}{P''_i} x_i(2-e^{-x_\tau}) ln(1+\gamma_i) & otherwise \end{cases} \tag{7.2}$$

where W_l and W_u, $[Hz]$ correspond to the bandwidth segments of the licensed and unlicensed bands, N denotes the total number of users and N_l the number of users who choose to transmit not only in the unlicensed but also via the licensed band. In the following let $P'_i, P''_i \in [0, P_{max}], P'_i + P''_i = P_{max}$ refer to the fractions of the transmission power allocated to the licensed and the unlicensed band, respectively, and γ_i is the SINR:

$$\gamma_i = \begin{cases} \frac{W_l}{R_i} \frac{G_i P'_i}{\sigma^2 + \sum\limits_{i>k} G_k P'_k} & (licensed\ band) \\ \frac{W_u}{R_i} \frac{G_i P''_i}{\sigma^2 + \sum\limits_{i>k} G_k P''_k} & (unlicensed\ band) \end{cases} \tag{7.3}$$

where σ^2 denotes the Additive White Gaussian Noise (AWGN) at the receiver and user channel gain G_i reflects the corresponding path gain conditions.

Additionally, $x_i \in [0, 1]$ indicates the power investment of each user to the CPR and is defined as the percentage of maximum power P_{max} reserved for the transmission in the unlicensed band, thus, the

transmission power to the unlicensed band is determined as: $P_i'' = x_i P_{max}$, with the remaining power, $P_i' = P_{max} - P_i''$, allocated for transmission to the licensed band. Lastly, let $x_\tau = \sum_i x_i$ denote the aggregate investment of all users in the CPR. The first branch of (7.2) reflects a transmission only via the licensed (safe) band since the investment to the unlicensed is zero, (i.e., $x_i = 0$, although out of scope for our current investigation), whilst the second branch depicts the utility captured from a shared transmission scheme between the two available bands. Please note that in our setting, user aggregate investment x_τ is considered to be bounded due to the physical limitations of each user. Without loss of generality we normalize aggregate investment x_τ, $x_\tau \in [0, 1]$. Thus, CPR's failure probability increases with the rise of x_τ, with the unlicensed band to collapse with certainty once $x_\tau \to 1$.

In the following, for simplicity of notation, we set:

$$\theta_i = \frac{W_l/N_l}{P_i'} ln(1+\gamma_i) \; and \; \xi_i = \frac{W_u/N}{P_i''} ln(1+\gamma_i) \tag{7.4}$$

and we define the rate of return function of the CPR as follows:

$$r(x_\tau) = 2 - e^{-x_\tau} \tag{7.5}$$

Definition 7.3.1. ***Rate of Return:*** *The rate of return (RoR) indicates the gain or loss of the CPR with regards to aggregate investment.*

For demonstration purposes, we consider the rate of return from the unlicensed band to be increasing with total investment, providing higher returns than the licensed band unless the CPR fails, where zero returns are collected by the users. Nevertheless, similar analysis can be also devised by considering a decreasing rate of return function *(See next sections)*. Based on the above, we explicitly select a rate of return function increasing, concave, twice continuously differentiable, and greater than 1, $\forall x_\tau \in [0, 1]$, and assuming that all users decide to invest to the CPR, i.e., $x_i > 0$, by subtracting θ_i from (7.2) we obtain:

$$U_i(x_i) = \begin{cases} 0 & if \; x_i = 0 \\ x_i \xi_i r(x_\tau) - \theta_i x_i & otherwise \end{cases} \tag{7.6}$$

Subsequently, by adjusting (7.6) to the PT function in (7.1) and by normalizing the rate of return function so that $\theta_i = 1$, without loss of generality for $x_i > 0$ we obtain $U_i(x_i) = [x_i(\xi_i r(x_\tau) - 1)]^{a_i}$. For notational purposes we denote:

$$\overline{r_i}(x_\tau) = (\xi_i r(x_\tau) - 1)^{a_i} \tag{7.7}$$

If the CPR collapses, only users who invested into the safe resource will transmit, which prior to normalization refers to $\theta_i(1 - x_i) < \theta_i$. Thus, the utility obtained in case the CPR survives, is $U_i(x_i) = {x_i}^{a_i} \overline{r_i}(x_\tau)$. For any $r(x_\tau)$ increasing, concave, twice continuously differentiable, and greater than 1, $\forall x_\tau \in [0, 1]$, then for any $a_i \in (0, 1]$, $\overline{r_i}(x_\tau)$ is also increasing, concave, twice continuously differentiable, and positive [172].

At this point, we introduce the stochastic probabilistic framework under which the PT model has been designed. Failure probability reflects how close the CPR comes to failure and is increasing with the total investment, with $p(x_\tau = 1) = 1$ indicating a certain collapse of the CPR. Hence, the PT utility of the problem is formulated as:

$$U_i(x_i) = \begin{cases} {x_i}^{a_i} \overline{r_i}(x_\tau) & with \; prob. \; (1 - p(x_\tau)) \\ -k_i x_i^{a_i} & with \; prob. \; p(x_\tau) \end{cases} \tag{7.8}$$

where the first outcome of (7.8) denotes user gains from its investment when the CPR survives, and the second illustrates the negative return in case of CPR failure, due to the fact that total investment surpassed the size of the resource, leading to failure. Acknowledging the probabilities of failure for the CPR, the expected PT utility can be written as follows:

$$\mathbf{E}(U_i) = {x_i}^{a_i} \overline{r_i}(x_\tau)(1 - p(x_\tau)) - k_i x_i^{a_i} p(x_\tau) \tag{7.9}$$

Consequently, users' objective is to maximize the expected utility in (7.9), which can be formally expressed as the non-cooperative game for Allocation of Licensed and Unlicensed Resources under probabilistic Uncertainty (ALLURE-U), as follows:

$$\begin{gathered}\textbf{ALLURE} - \textbf{U Game}: \\ max\mathbf{E}(U_i) = max\{x_i^{a_i} f_i(x_\tau)\},\ \forall i \in \aleph \\ s.t.\ x_i \in [0,1]\end{gathered} \tag{7.10}$$

where $f_i(x_\tau) = \overline{r_i}(x_\tau)(1-p(x_\tau)) - k_i p(x_\tau)$ is defined as the *effective rate of return*. For convenience, the key parameters used throughout this section are summarized in Table 7.1.

Table 7.1: Section 7.3 list of key notations

Symbol	Description
R	Network radius
$\aleph$	User set
x_i	Player specific investment to unlicensed band
N_l	Users transmitting via the licensed band
N	Total number of users
W_l, W_u	Licensed and unlicensed band spectrum
σ^2	Additive White Gaussian Noise
γ_i	Signal-to-Interference-plus-Noise Ratio
P_i'	Transmission power via the licensed band
P_i''	Transmission power via the unlicensed band
x_τ	Aggregate player investment to unlicensed band
G_i	Channel gain
$r(x_\tau)$	Rate of return function
$\overline{r_i}(x_\tau)$	PT related rate of return
$p(x_\tau)$	Unlicensed band failure probability
a_i, β_i	Sensitivity parameters
k_i	Risk aversion parameter
$f_i(x_\tau)$	Effective rate of return
$g(x_\tau)$	Player specific optimal nonzero investment
Q	Pure Nash Equilibrium Support
R_i	User data rate
$BR_i(x_{-\tau})$	Player best response
S_i	Player investment strategy set
S_i'	Modified player investment strategy set
$\overline{S}_{-i}'$	Space of total investment excluding player i
θ_i, ξ_i	Auxiliary parameters

7.3.3 Problem Formulation and Solution

Towards treating the above optimization problem and obtaining a stable solution, we model it as a Fragile CPR game [172], since as mentioned before it is assumed to be: 1) non excludable, meaning that all users may access the available resources, and 2) rivalrous, i.e., users compete over claiming those scarce resources, where greedy utilization may eventually drive the system to an outcome of collapse, (*"Tragedy of the Commons"*).

Definition 7.3.2. ***Fragile & CPR Games:*** *A Fragile CPR game is based on the standard CPR game by introducing the potential for resource failure. In a CPR game, players start with an initial endowment and direct how they will invest in two types of resources; one that has a steady return of investment (i.e., safe resource), and another is a CPR resource with returns based on the RoR function [172], [195].*

Users have the dilemma of investing only to a commonly accessible resource (i.e., CPR) with high returns under however a high collapse risk, or split their operation including a safe resource, which despite its guaranteed operation status does not deliver gains of comparable magnitude. We consider a Fragile CPR game under the following properties:

Assumption:

1. The failure probability $p(x_\tau)$ is a convex, strictly increasing, and twice differentiable function of the normalized total investment $x_\tau = [0, 1)$ and $p(1) = 1$.
2. The rate of return $\overline{r_i}(x_\tau)$ in (7.7) is monotonic (increasing), concave, twice continuously differentiable, and positive $\forall x_\tau \in [0, 1]$.
3. The strategy set of each player i is defined as: $S_i = [0, 1], \forall i \in \aleph$.

Without loss of generality we adopt failure probability from aggregate user investment equal to $p(x_\tau) = {x_\tau}^2$. Subsequently, the effective rate of return is defined accordingly as:

$$f_i(x_\tau) = \overline{r_i}(x_\tau)(1 - {x_\tau}^2) - k_i {x_\tau}^2 \tag{7.11}$$

Let $BR_i(x_{-\tau}) = \text{argmax}\mathbf{E}(U_i(x_\tau, x_{-\tau}))$, $BR_i : \overline{S}_{-i} \rightrightarrows S_i$ be the best response correspondence of player i, where $\overline{S}_{-i}$ denotes the space of total investment by the players, excluding player i. Please note that in the following we use the terms user and player interchangeably. Any best response $BR_i(x_{-\tau}) \in br_i(x_{-\tau})$, $0 \leq BR_i(x_{-\tau}) < 1$ implies that the user i may invest only in the safe resource (i.e., $BR_i(x_{-\tau}) = 0$), or have a strictly positive return by investing in the CPR. Best response $BR_i(x_{-\tau})$ cannot be equal to one, otherwise it will lead to a certain failure of the CPR.

Theorem 34. ***(Existence of PNE:)*** *For Fragile CPR game, $G = [\aleph, \{S_i\}_{i\in\aleph}, \{U_i\}_{i\in\aleph}]$ there exists a player specific value $z \in [0, 1]$ such that $BR_i(x_{-\tau}) = 0, \forall x_\tau \geq z$ and an interval $\ell \subset [0, z]$ such that $BR_i(x_{-\tau}) > 0, \forall x_\tau < z$ with each best response $BR_i(x_{-\tau}) \in br_i(x_{-\tau})$ satisfying $BR_i(x_{-\tau}) + x_{-\tau} \in \ell$ [172].*

Proof. For $BR_i(x_{-\tau}) > 0$ the best response investment according to the first order condition of (7.9) is:

$$\frac{\partial \mathbf{E}(U_i)}{\partial x_i} = {x_i}^{a_i - 1}\phi(x_\tau) = 0 \tag{7.12}$$

where $\phi(x_\tau) = [x_i f_i'(x_\tau) + a_i f_i(x_\tau)]$. Towards proving that (7.12) equals zero, we examine $\phi(x_\tau)$. By applying Bolzano Theorem for $f_i'(x_\tau)$, we observe that $f_i'(0) > 0$ and $f_i'(1) < 0$. Since $f_i(x_\tau)$ in (7.10) is concave in x_τ, $f_i'(x_\tau)$ is monotone and decreasing, thus there exists a unique global maximum $y \in (0, 1)$ such that $f_i'(x_\tau) < 0, \forall x_\tau \in [y, 1]$. Similarly, we apply again Bolzano Theorem for $f_i(x_\tau)$, where $f_i(y) > 0$ (since $f_i(0) > 0$) and $f_i(1) < 0$. Hence, there exists a $z \in (y, 1)$ such that $f_i(x_\tau) > 0, \forall x_\tau \in [y, z]$. Subsequently, there exists the player specific interval $[y, z]$ where $\phi(x_\tau) = 0$ (due to the opposite signs of $f_i(x_\tau)$ and $f_i'(x_\tau)$), with subsequently all the best responses of the players being positive. We denote the new modified space $[y, z]$ as $S_i' \subset \ell \subset S_i$. □

Lemma 35. ***(Single Valued Best Responses:)*** *The best response correspondence $BR_i(x_{-\tau})$ is single valued $\forall x_\tau \in S_i'$.*

Proof. $\mathbf{E}(U_i)$ has a critical point in the modified space S_i', guaranteeing the existence of nonzero best responses. Given that $\overline{r_i}(x_\tau)$ is increasing, $\mathbf{E}(U_i)$ is concave, thus the critical point in S_i' is a unique maximum of $\mathbf{E}(U_i)$. □

Lemma 36. ***(Continuous Best Responses:)*** *The best response correspondence $BR_i(x_{-\tau})$ is continuous $\forall x_\tau \in S_i'$.*

Proof. Based on Berge's Maximum Theorem, $BR_i(x_{-\tau})$ is upper hemicontinuous and proven to be single valued from Lemma 35. This applies to each player $i \in \aleph$ by symmetry. □

Hence, for each player $i \in \aleph$ there exists a Pure Nash Equilibrium (PNE) for the Fragile CPR game G in the modified strategy space $S_i' \subset \ell, \forall x_\tau \in [y, z] \subset [0, 1]$.

Theorem 37. ***(Fragile CPR game Uniqueness of PNE:)*** *The Fragile CPR game G admits a unique PNE,* $x^* = \{x_i^*\}_{i\in\aleph}$ *for the total investment* $x_\tau^* = \sum_{I=1}^{N} x_i^*$.

Proof. Towards proving the uniqueness of game's PNE, we utilize the following two propositions:
Proposition 1: For simplicity of the proof, we define:

$$g(x_\tau) = -\frac{a_i f(x_\tau)}{f'(x_\tau)} \tag{7.13}$$

where $g(x_\tau)$ represents the optimal nonzero investment of a player and satisfies:

$$g(BR(x_{-\tau}) + x_{-\tau}) = BR(x_{-\tau}),\ when\ BR(x_{-\tau}) > 0 \tag{7.14}$$

It is easily proven that $\frac{\partial g(x_\tau)}{\partial x_\tau} = -a_i + a_i \frac{f(x_\tau)}{f'(x_\tau)^2} f''(x_\tau) < 0, \forall x_\tau \in S_i'$
Proposition 2: We determine the set of players with nonzero investment as the *"support"* of a PNE [172], as follows:

$$Q \triangleq \{i \in \aleph | x_\tau^* < z\} \tag{7.15}$$

We initially assume that the game admits two PNEs with $x_{\tau 1}^*$ and $x_{\tau 2}^*$ with supports Q_1, Q_2 for each PNE, respectively. Without loss of generality, we consider $x_{\tau 2}^* > x_{\tau 1}^*$, with supports stemming from (7.15) to be $Q_2 \subseteq Q_1$, respectively. The optimal nonzero investments of all players for the above PNEs are shown below:

$$\sum_{i\in Q_1} g_i(x_{\tau 1}^*) = x_{\tau 1}^*,\ and \sum_{i\in Q_2} g_i(x_{\tau 2}^*) = x_{\tau 2}^* \tag{7.16}$$

For the optimal nonzero investments we have $\sum_{i\in Q_2} g_i(x_{\tau 1}^*) \leq x_{\tau 1}^* < x_{\tau 2}^* = \sum_{i\in Q_2} g_i(x_{\tau 2}^*)$. However from Proposition 1, $g_i(x_\tau)$ is a strictly decreasing function, and given that $x_{\tau 1}^* < x_{\tau 2}^*$, then $g_i(x_{\tau 1}^*) > g_i(x_{\tau 2}^*)$ which contradicts the previous conclusion. Hence, we conclude that the PNE of the game is unique, and $x_{\tau 1}^* = x_{\tau 2}^*$.

□

Theorem 38. ***(Fragile CPR Game PNE:)*** *The vector* $\boldsymbol{x}^* = \{x_i^*\}_{i\in\aleph}$ *in the modified strategy set* S_i' *is a Pure Nash Equilibrium (PNE) of the Fragile CPR game G, if for each user i the following holds:*

$$U_i(\mathbf{x}^*) \geq U_i(x_i), \forall x_i \in S_i' \tag{7.17}$$

Remark 4. *A Pure Nash Equilibrium refers to a condition where each player of the game plays one specific strategy. This contrasts mixed Nash Equilibria, where at least one player of the game randomizes over some of its all pure strategies.*

Convergence

In this part, we discuss game's G convergence to its unique PNE $\mathbf{x}^* = \{x_i^*\}_{i\in\aleph}$. Fragile CPR games are categorized as Weak Strategic Substitutes games with aggregation [196], modeled as below:

Theorem 39. ***(Weak Strategic Substitutes game:)*** *A game* $\Gamma = [\aleph, \{S_i'\}_{i\in\aleph}, \{U_i\}_{i\in\aleph}]$ *is a Weak Strategic Substitutes game with aggregation, if the corresponding player utilities are defined as* $u_i : S_i' \times \overline{S'}_{-i} \to \mathbb{R}$ *and the best response correspondence satisfies the following:*

1. $BR_i(x_{-\tau}) = argmax\boldsymbol{E}(U_i(x_\tau, x_{-\tau}))$, $\forall x_{-}\tau \in \overline{S'}_{-i}$
2. $BR_i(x_{-\tau})$ *is continuous on* $\overline{S'}_{-i}$
3. $BR_i(x_{-\tau})$ *is decreasing in* $\overline{S'}_{-i}$

Properties 1 and 2 already hold as proven in Lemmas 35 and 36 respectively, therefore, in the following we focus only on the 3$^{\text{rd}}$ property.

Lemma 40. ***(Decreasing Best Responses:)*** *The best response correspondence $BR_i(x_{-\tau})$ is decreasing $\forall x_\tau \in \overline{S'}_{-i}$.*

Proof. Let $x_{\tau 1} = BR_i(x_{-\tau 1})$ and $x_{\tau 2} = BR_i(x_{-\tau 2})$ with $x_{-\tau 2} > x_{-\tau 1} \in \overline{S'}_{-i}$. As introduced in Proposition 1, $g(x_\tau)$ is strictly decreasing, thus, according to (7.14), $x_{\tau 1} = g(x_{\tau_1} + x_{-\tau_1})$ and $x_{\tau 2} = g(x_{\tau_2} + x_{-\tau_2})$. From Theorem 34, it is stated that $BR_i(x_{-\tau}) + x_{-\tau} \in \ell$. Hence, if $x_{\tau 2} > x_{\tau 1}$ then $x_{\tau 2} = g(x_{\tau 2} + x_{-\tau 2}) < g(x_{\tau 1} + x_{-\tau 1}) = x_{\tau 1}$ which is contradicting. □

Subsequently, the game's best response dynamics decrease in the aggregate strategies of the users, guaranteeing the convergence to the examined PNE.

7.3.4 Distributed Algorithm

In this section we present an iterative and low complexity algorithm reaching the game's unique PNE point, starting from any initial feasible set of investment values. The algorithm operates under a distributed manner, with each user to declare its behavioral specific parameters and selections for the upcoming transmission.

Algorithm 17 ALLURE-U Algorithm

Require:
User number N, specific constants k_i, a_i and topological coordinates
$ite \leftarrow 1$
$collapse^{(ite)} \leftarrow 0$
$convergence^{(ite)} \leftarrow 0$
$CPR\ Size \leftarrow$ *unlicensed bandwidth*
Calculate and sort channel gains G_i according to SIC
Assign random value to initial user investment $x_i^{(ite)}$
while $convergence^{(ite)}$=0 **and** $collapse^{(ite)}$=0 **do**
  Split transmission power $P_i^{\prime(ite)}, P_i^{\prime\prime(ite)}$ per band according to $x_i^{(ite)}$ and calculate intracell interference;
  Calculate utility $U_i^{(ite)}$ according to equation (7.9)
  for all $x_i \in [0,1]$ **do**
    x_i^*=$argmax_{x_i} U_i$
    if $U_i > U_i^{(ite)}$ **then**
      $x_i^{(ite+1)} \leftarrow x_i^*$ **and** $U_i^{(ite+1)} \leftarrow U_i$
    end if
  end for
  Calculate *normalized* $x_\tau = \dfrac{\sum_1^N x_i^{(ite+1)}}{N}$
  if $\sum R_i^{unlicensed} > CPR\ Size$ **then**
    $collapse^{(ite+1)} \leftarrow 1$
  end if
  if $x_i^{(ite+1)} - x_i^{(ite)} < \epsilon$ **then**
    $convergence^{(ite+1)} \leftarrow 1$
  end if
  $ite \leftarrow ite + 1$
end while
return
User investment to unlicensed resource x_i and *collapse* to confirm if the band still operates

The *"ALLURE-U"* algorithm, i.e., **Al**location of **L**icensed and **U**nlicensed **Re**sources under probabilistic **U**ncertainty, acts as the common interface between users and the WISP dynamically managing spectrum among the licensed and unlicensed bands, and integrates users' decision part with the resource allocation process. Initially users configure their topological and behavioral parameters in terms of exhibiting a risk seeking or averse behavior towards CPR failure. According to NOMA standards, the WISP applies the SIC technique and observes users' transmission based on their choice to invest in each band.

The WISP collects all the information from the power allocation of each user to the unlicensed band, and broadcasts (alongside the interference) the failure probability. Users depending on their unique preferences (determined by the parameters a_i and k_i) reconsider their decisions under the rising probability of collapse of the CPR and may accept to transmit also with the licensed band which however provides lower bandwidth, or decide to keep transmitting only via the unlicensed band.

Eventually the algorithm functions under two potential outcomes. The first being the convergence of the system to the PNE point, where all users manage to optimize their transmission given the strategies of the rest of the players, while on the other side the algorithm may terminate its operation due to CPR collapse from over-exploitation. In the latter case, only the users who partially invested to the licensed band manage to transmit, whilst the rest of the users reach a state of non operation, despite devoting all of their transmission power to the unlicensed band. Due to the non-centralized nature of the algorithm and the parallel execution of the decisions, as well as the low data exchange requirements, the algorithm converges very fast to the PNE point or identifies the collapse of the resource in very few steps, i.e., in practice in less than 10 iterations. The simplified arithmetic calculations performed, establish the convergence of the ALLURE-U framework with minimal demand for computational complexity. The algorithm was tested in an Intel(R) Core(TM) i7-7500U CPU @ 2.70 GHz 2.90 GHz laptop with 8.00 GB of available RAM and its average run time per user was less than 0.3 $msec$. The above result ensures the adaptability and applicability of the proposed scheme to realistic implementations, where low duration timeslots (i.e., 0.5 $msec$) are regarded.

7.3.5 Numerical Results

Evaluation Setting and Parameters

In this section we provide a series of numerical results evaluating the performance and the inherent attributes of the proposed prospect theoretic framework for a dual band wireless network operating under NOMA. Initially, we focus on a basic scenario where users exhibit common risk averse behavior (i.e., homogeneous population) regarding their preferences for the unlicensed band over the licensed one, in order to gain some insight about the process of optimal user power investment in each band, as well as the corresponding utility obtained. Subsequently, the effect of user heterogeneity is investigated in terms of both loss aversion and sensitivity parameters, by assuming that some users may modify their behavior towards a more risk seeking attitude, therefore impacting their competitor user decisions, and the overall system operation as a whole. Furthermore, the case of aggressive user investment leading to failure of the CPR due to the potential over-exploitation of the unlicensed band by the users, is also examined and evaluated. Finally, a direct comparison of our proposed prospect theoretic framework (i.e., ALLURE-U Algorithm) against a conventional EUT based framework is performed, clearly demonstrating its superiority, and stressing the fact that the realistic modeling empowered by PT, properly reflects user behavioral preferences against risk, indicating the deviations that EUT-based approaches fail to capture.

The uplink of a NOMA wireless network of radius $R = 2.5\ km$ is considered, with 20 users being accommodated within its range. System's total bandwidth is set at $W = 4\ MHz$, where for demonstration purposes 90% is allocated to the unlicensed band and the remaining 10% to the licensed band [197]. The user transmission power is set to $P_{max} = 0.2\ Watts$, with all users splitting it between the two bands.

Common User Behavior - Homogeneous Population

Originally, we examine users' investment considering common risk aversion and sensitivity parameters (i.e., $k_i = k = 20$ and $a_i = a = 0.1$, $\forall i \in \aleph$). This suggests a homogeneous perception of users against resource failure, hence the main factors affecting users' transmission being their channel conditions and sensed interference. Fig. 7.4 illustrates each user i investment x_i, as well as its normalized utility obtained from its transmission to the unlicensed band. We observe that users with intermediate distance from the BS almost fully transmit under the unlicensed band, whereas users closer to or further away from the BS choose to split their transmission power to both bands. The above stems from the application of the SIC technique in NOMA, where users with medium distance from the BS sense significant interference while they are also affected by their own channel conditions, which impacts their corresponding utility. This drove their decision towards transmitting almost fully via the unlicensed band given its higher bandwidth capacity and potential. On the contrary, the users closer to the BS due to their superior channel conditions, and the most distant ones who sense lower interference due to SIC, share the advantage of a less strenuous transmission extracting broader utility surplus. Hence, they invest less in the unlicensed

band and transmit via the licensed band as well, ensuring their operation even in case of CPR failure. Accordingly, Fig. 7.5 depicts the users' transmission power allocation between unlicensed and licensed bands.

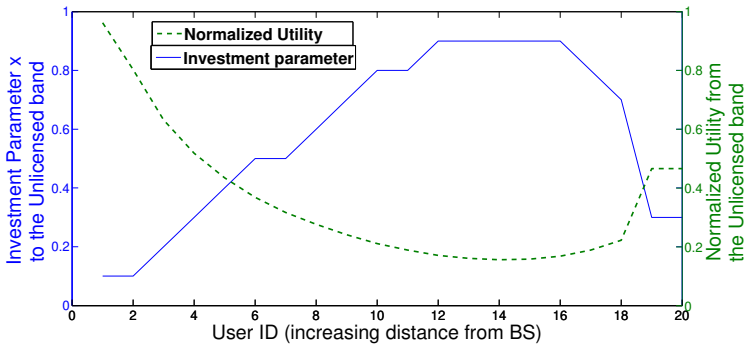

Figure 7.4: Investment parameter x_i and normalized utility per user

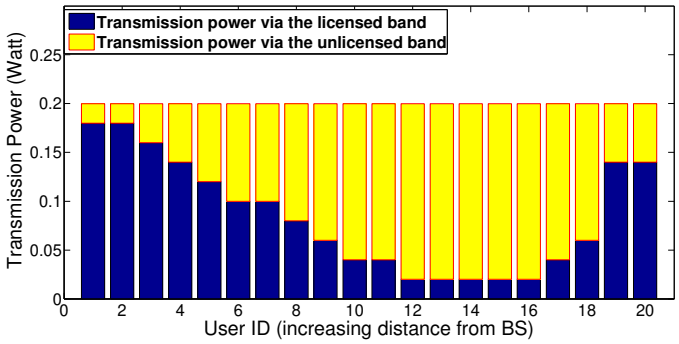

Figure 7.5: Power allocation among bands per user

Differentiating User Behavior - Heterogeneous Population

In this subsection we investigate a scenario under which some of the worse performing users become less risk averse and decide to excessively invest in the CPR. For demonstration purposes we consider that users 11-13 increase their sensitivity parameter a_i from 0.1 to 0.8, while the rest of the users retain their original risk perceptions. Specifically, in Fig. 7.6 we present achieved users' data rates in a comparative manner, under the heterogeneous scenario considered here (right graph) and the homogeneous one considered in previous subsection (left graph), aiming in particular at studying the impact of the increase of the sensitivity parameter a_i. All other things being equal, users 11-13 significantly improve their data rates due to fully investing their power to the higher capacity unlicensed band (no transmission with the licensed band). On the other hand, the rest of the users of the network are also impacted by this change of behavior of users 11-13, with data rates for some of them deteriorating (e.g., users 9 and 10) in the unlicensed band, while on the contrary a positive effect is observed through the rise in data rate per user in the licensed band. Subsequently, we adjust the loss aversion parameter k_i selectively for users 8 and 12, such as to eliminate the risk aversion for user 8, while increases it tenfold for user 12. As depicted in Fig. 7.7, user's 8 investment to the CPR reaches 100%, while user 12 becomes more conservative compared to the original scenario with its investment to the CPR dropping from approximately 90% to 40%.

Collapse of the Unlicensed band

Please note that in the previous subsections, all experiments were conducted under conditions which did not endanger the operation of the unlicensed band cumulatively. In the following, we address the case where aggregate investment possibly exceeds spectrum's capacity to address user demand, and therefore

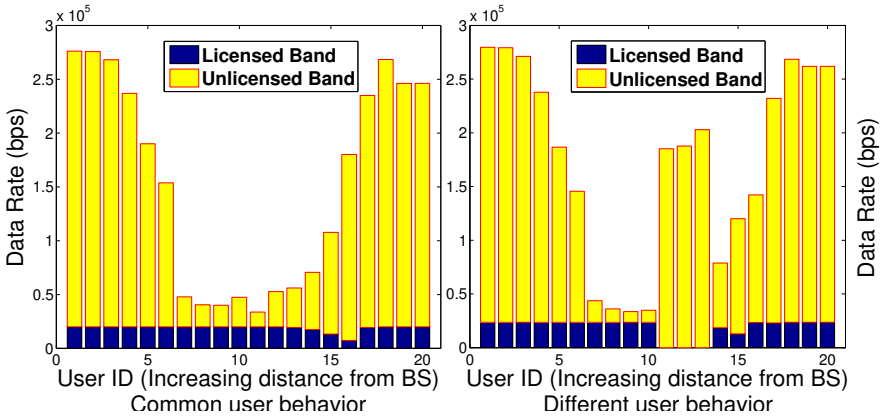

Figure 7.6: Data rates with (a) common user behavior and (b) diverging 11-13 user behavior

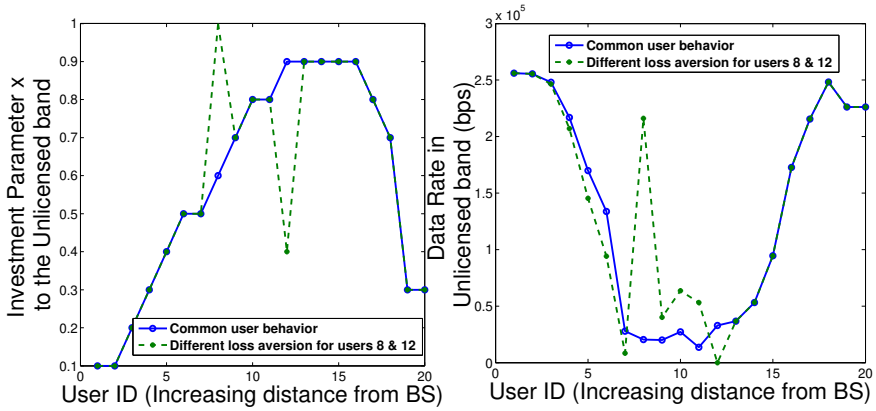

Figure 7.7: (a) Investment parameter x_i and (b) data rate per user under changing k_i for users 8 and 12

CPR may fail. Accordingly, we investigate the network's performance as users' average sensitivity gradually increases. Based on the results presented in Table 7.2, an increase in the average user sensitivity (i.e., parameter a_i) results in higher investment x_i by all users to the CPR. Users become more risk seeking, with the number of users of the licensed band dropping from twenty to just four, at the moment that the unlicensed band collapses. The unlicensed bandwidth utilization initially rises with higher investment as expected, however it eventually fails when demand surpasses the available spectrum. Therefore, only the four users who kept transmitting in the licensed band will still operate, whereas the remaining 80% of users investing to the unlicensed band eventually fail to transmit.

Comparison with EUT

It is noted that one of the key differentiating factors of our work and PT in general, is that it considers the user behavioral deviations from the traditional EUT, where the latter regards users as neutral agents who

Table 7.2: Unlicensed band collapse for ALLURE-U algorithm

Mean a_i	**Mean** x_i	**Licensed Users**	**Unlicensed Spectrum Utilization**	**Unlicensed Band Status**
0.10	0.58	20	74.86%	*active*
0.20	0.61	17	86.25%	*active*
0.24	0.74	9	97.02%	*active*
0.39	0.91	4	108.99%	*fails*

aim at selfishly maximizing their utility reflecting their degree of satisfaction from the QoS they receive. In this subsection, we present a comparative case between our proposed prospect theoretic framework and an EUT-based approach, with the latter characterized by the absence of user risk perceptions. From Table 7.3, it is clearly shown that EUT instructs users to invest in the CPR due to the higher available spectrum. Therefore, users' aggregate investment exceeds the threshold that the band can tolerate and since the utilization demand surpasses 100%, it collapses. On the contrary, according to our framework users follow a risk averse attitude and adopt a more conservative position considering the fragility of the CPR, and therefore decreasing the potential of failure.

In Fig. 7.8 we compare users' transmission power among our proposed prospect theoretic approach (i.e., ALLURE-U Algorithm) and two different cases of EUT realization, where in the first one the band collapses (fails) while in the second one, though it remains active it still operates with almost full utilization. ALLURE-U algorithm delivers lower power levels compared to both EUT cases, since users do not exhaust their full power transmission to the unlicensed band, thus protecting it from potential over-exploitation. On the other hand, under EUT realizations, users transmit at higher power in order to extract additional bandwidth and return from the available spectrum. This reverses (cancels) the positive impact of SIC for users far from the BS, while simultaneously increases the probability of CPR failure since users lack the sophistication of considering the potential risks in their final decisions.

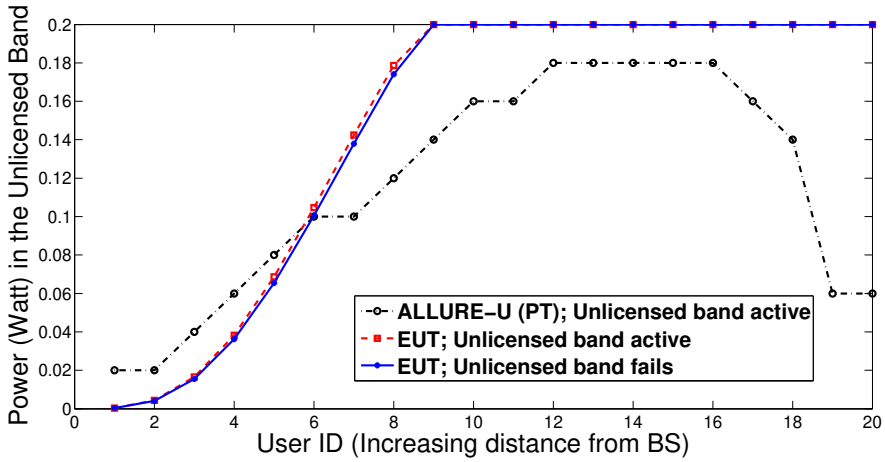

Figure 7.8: Transmission power per user ID under PT and EUT

7.4 Flexible Access Technology Interface Coexistence

In view of the challenges related to resource fragility, growing data demand, and spectrum scarcity, [198], a rethinking of how modern networks are addressing spectrum shortages should prioritize user integration into the self-optimization process of 5G networks. This should be aimed at achieving more efficient resource utilization and flexibility, vital elements for the future design and structure of wireless communication systems. This objective is expected to be further supported in future emerging wireless networks through the use of devices with flexible access technology interfaces, where more than one access technologies [11] (e.g., Orthogonal Frequency Division Multiple Access (OFDMA) and Non-Orthogonal Multiple Access (NOMA)), become simultaneously available to the users as potential options of communications and usage. We aim at introducing a novel, holistic, and yet realistic framework of treating the arising

Table 7.3: Unlicensed Band Transmission: PT (ALLURE-U) vs EUT

System Model	Mean Power (Watt)	Unlicensed Spectrum Utilization	Unlicensed Band Status
EUT	0.1467	101.65%	*fails*
PT	0.1160	74.86%	*active*

resource management problem in such wireless networks under the assumption of dual multiple access technology interfaces, while considering both user behaviors and actions and the resource sharing nature.

7.4.1 Related Work on Radio Access Technologies

NOMA technique has recently attracted widespread attention as a crucial means towards the design and implementation of 5G wireless networks [199]. As already described, NOMA-based cellular networks operate under the concept that multiple users are able to utilize the whole spectrum available to the WISP while employing the same code, in contrast to other existing technologies like orthogonal multiple access (OMA) and code division multiple access (CDMA) [200]. Another fundamental characteristic of NOMA is that despite the fact that the users may exploit the entire spectrum, intracell interference levels are significantly mitigated via the implementation of the Successive Interference Cancellation (SIC) technique at the receiver [136]. SIC technology dictates that a user can only decode the signals of other users with superior channel gains in the uplink communication, with the signals from other users to be treated as noise [201]. NOMA is considered as a preferred candidate for 5G networks due to its flexibility in spectrum management and its high degree of compatibility with other access technologies and numerous wireless systems (e.g., TV broadcasting) [155]. In the recent literature, multiple research methods have been proposed to deal with the resource management problem (e.g., power control, spectrum allocation) in the downlink [202] or uplink communication [137] of 5G NOMA-based networks.

Additionally, OFDMA technique has been also considered as a potential technology to be employed in the forthcoming 5G networks [203, 204]. OFDMA is based on the division of the bandwidth into subcarriers, organized into resource blocks. Each resource block can accommodate only one user, thus, only one fraction of the spectrum is accessible by each customer [205]. OFDMA has been widely adopted due to completely eliminating narrowband interference and channel equalization with limited complexity, despite simultaneous transmissions from users, thus ensuring operation continuity and transmission robustness. The problem of resource management in OFDMA networks has been studied in [205] targeting at the joint rate and power control in single-cell networks. Furthermore, the problem has been extended in the downlink communication of a multi-cell scenario [206], where a resource block is shared among multiple base stations. Specifically, the authors in [206] study the load management problem in a multi-cell OFDMA-based network, aiming at minimizing the total load of the base stations on the shared resource blocks and determining the number of users whose demands can be concurrently satisfied. A similar problem has been studied in [207] considering OFDMA two-tier femtocell networks via proposing a joint admission control and resource management approach. The problem is formulated via the integer nonlinear programming and its solution is determined by a graph-based algorithm with polynomial computational complexity.

Similar to the previous section where licensed and unlicensed bands were considered, this time, since under NOMA the entire spectrum may be simultaneously accessible and utilized by all the users, it can be characterized as the *Common Pool of Resources (CPR)*. NOMA has the potential to provide superior spectral capacity, however at the same time becomes as well susceptible to the phenomenon of the *Tragedy of the Commons* [208]. The latter may occur due to the potential over-exploitation of the available spectrum by all users, which will eventually lead to the collapse of the resource due to the increased interference. On the other hand, in the OFDMA-based communication, each resource block that is assigned to each user can be considered as the *safe resource* providing, through its interference-free and of relatively limited bandwidth transmission (assuming that interference from neighboring cells is trivial), a more constant return of satisfaction to the users. Additionally, when access technique topics and their suitability for users' transmission were under consideration, users and their behavior have again so far been considered under *Expected Utility Theory (EUT)* solving the resource allocation problem from only a utility maximization perspective [209]. However, this does not hold true in real life, where users make decisions regarding their connectivity and network access under various risks introduced by the environment's uncertainty, the limited available information and the spectrum's fragility, and based on their personal characteristics.

7.4.2 System Model

Dual Communication Interface Environment

In this work, we consider the coexistence of OFDMA and NOMA-based communication in wireless networks. Each User Equipment (UE) $i, i \in N$ has a dual communication interface to transmit data

either via using NOMA - or the CPR - (i.e., exploiting the entire available spectrum to this option) or via OFDMA (i.e., using its occupied resource block), as presented in Fig. 7.9. If the UEs selfishly decide their transmission power levels to satisfy their QoS prerequisites, this will result to suboptimal outcomes for the entire set of UEs that concurrently transmit with the NOMA technique. In contrast, the band operating over OFDMA - or the safe resource - is split into resource blocks, where only one cellular UE transmits per resource block, thus, the intracell interference is eliminated while each UE can obtain a guaranteed level of QoS given its personal characteristics (channel gain), and its transmission power level.

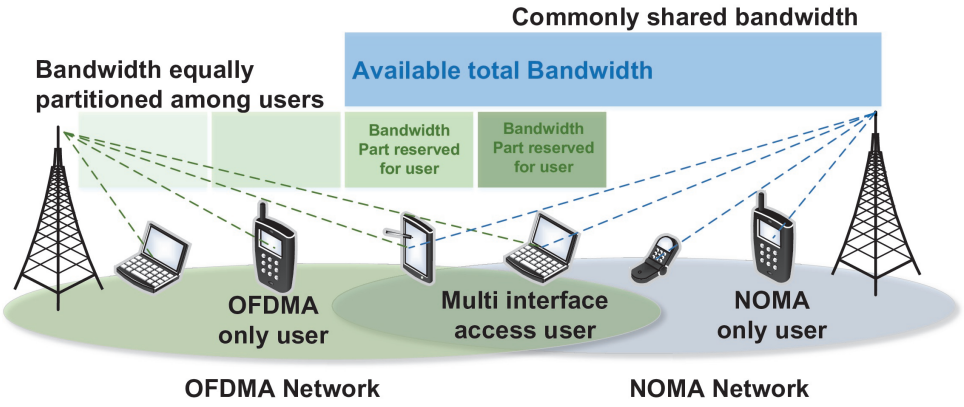

Figure 7.9: Conceptual dual access network with OFDMA and NOMA technologies

Each UE's goal is to opportunistically allocate its available power, and determine in an autonomous manner its optimal transmission power over the NOMA p_i^N, and over the OFDMA p_i^O, to fulfill its QoS prerequisites. Specifically, assuming that each UE $i, i \in N$ has a maximum transmission power p_i^{Max}, which can be invested to the OFDMA and NOMA-based transmissions, the percentage of transmission power investment to the NOMA is again denoted as x_i, $x_i \in [0,1]$, thus, the corresponding transmission power is $p_i^N = x_i p_i^{Max}$, while the transmission power over the OFDMA is the remaining amount, i.e., $p_i^O = (1-x_i)p_i^{Max}$.

Prospect-theoretic Utility Function

Users are assumed to exhibit a risk-aware behavior, as their decisions of their transmission power levels over the band operating over NOMA are characterized by uncertainty of the outcome and the corresponding enjoyed QoS. Thus, the users do not behave as risk-neutral expected utility maximizers following the EUT principles. To capture users' loss aversion or gain seeking behavior within the dual communication interface environment, Prospect Theory is again preferred as a powerful modeling tool towards formulating the above problem.

Based on Prospect Theory, the user's prospect-theoretic utility is defined as follows [171].

$$\mathscr{V}_i(z_i) = \begin{cases} (z_i - z_{0,i})^{a_i} & when\ z_i > z_{0,i} \\ -k_i(z_{0,i} - z_i)^{\beta_i} & otherwise \end{cases} \tag{7.18}$$

As in the previous chapter, the main behavioral elements of the prospect theoretic utility are summarized as below: the parameters $a_i, \beta_i \in (0,1]$, (without loss of generality, $a_i = \beta_i$) express the user's sensitivity to the gains and losses of its actual utility $z_i(x_i, x_T)$, respectively. The risk seeking behavior of a user in losses and its risk averse behavior in gains is reflected by small values of the parameter a_i. Small values of parameter β_i imply higher decrease of user's prospect-theoretic utility for small values of z_i and close to the reference point $z_{0,i}$. Moreover, the loss aversion parameter $k_i, k_i \in [0, +\infty)$ reflects the impact of losses compared to gains on user's prospect-theoretic utility (Eq. 7.18). If $k_i > 1$, the user i weighs the losses more than the gains, thus, it illustrates a loss averse behavior as it is resistant to lose part of its actual utility z_i. If $0 \leq k_i \leq 1$, the user weighs more or equal the gains than the losses, thus presenting an aggressive gain seeking behavior.

The total obtained actual utility $z_i(x_i, x_T)$, when the CPR (i.e., band operating over NOMA) does not fail, is defined as the summation of the energy-efficiency obtained by the OFDMA - safe resource (first term of Eq. (7.19)) and the NOMA - CPR (second term of Eq. (7.19)) transmission, while considering user's power investment to each choice, as follows.

$$z_i(x_i, x_T) = z_{0,i}(1 - x_i) + \zeta_i x_i \mathscr{R}(x_T) \tag{7.19}$$

where $\zeta_i = \frac{B_N/N_N}{p_i^N} ln(1 + \gamma_i^N)$, B_N denotes the spectrum of the band operating over NOMA, N_N is the number of UEs transmitting with the NOMA technique, and $\gamma_i^N = \frac{B_N}{R_i^N} \frac{h_i p_i^N}{\sigma^2 + \sum\limits_{i>k} h_k p_k^N}$ is the SINR of the UE i as it is measured at the receiver.

The function $\mathscr{R}(x_T)$ represents the rate of return of the CPR to the UEs, which is assumed to be a decreasing, concave function with respect to the UEs' total investment x_T, as the band operating over NOMA becomes congested. The latter holds true due to the fact that in this case the interference sensed by the UEs is increased, thus, the corresponding perceived satisfaction is decreased. Accordingly, without loss of generality and for demonstration purposes, the rate of return $\mathscr{R}(x_T)$ of the CPR is formulated as follows:

$$\mathscr{R}(x_T) = 2 - e^{x_T - 1} \tag{7.20}$$

The CPR has a probability of failure $Pr(x_T)$, i.e., fragility of the CPR, to serve the UEs which transmit with the NOMA technique, which is increasing with respect to the UEs aggregate investment x_T. In the following, for simplicity in our analysis we consider $Pr(x_T) = x_T^2$ and x_T is considered normalized. If the CPR does not fail, then each UE perceives an actual utility given by Eq. (7.19), which is greater than the reference point, i.e., $z_i > z_{0,i}$. Therefore, via subtracting the reference point $z_{0,i}$ from the actual utility (Eq. (7.19)), and shaping the result according to the first branch of the prospect-theoretic utility function (Eq. (7.18)), we have $\mathscr{V}_i(x_i) = x_i^{a_i}[\zeta_i \mathscr{R}(x_T) - z_{0,i}]^{a_i}$. For the simplicity of the notation, we normalize the rate of return function, so that $z_{0,i} = 1$ without loss of generality, and denote $\overline{\mathscr{R}_i}(x_T) \triangleq (\zeta_i \mathscr{R}(x_T) - 1)^{a_i}$ for notational convenience. Thus, $\mathscr{V}_i(x_i) = x_i^{a_i} \overline{\mathscr{R}_i}(x_T)$. On the other hand, if the CPR becomes overloaded and fails to provide satisfactory service to its UEs due the its over-exploitation by them, then no UE receives any satisfaction from its transmission with the NOMA technique, thus, the second term of Eq. (7.19) becomes zero and the UEs enjoy the transmission only over the safe resource (via investing $(1 - x_i)$ percentage of their maximum transmission power). In this case, the actual utility z_i is less or equal than the reference point, i.e., $z_i \leq z_{0,i}$, thus, by subtracting the actual utility from the reference point and reshaping the result based on the second branch of Eq. (7.18), we have $\mathscr{V}_i(x_i) = -k_i x_i^{a_i}$.

Following the aforementioned argumentation, we can rewrite Eq. (7.18), as the following UE's prospect-theoretic utility function.

$$\mathscr{V}_i(x_i) = \begin{cases} {x_i}^{a_i} \overline{\mathscr{R}_i}(x_T) & if\ z_i > z_{0,i} \\ -k_i x_i^{a_i} & otherwise \end{cases} \tag{7.21}$$

Given that the probability of failure of the CPR is $Pr(x_T)$, the probability that the band operating over NOMA survives and serves the UEs is $(1 - Pr(x_T))$. As a result, Eq. (7.21) can be written equivalently as:

$$\mathscr{V}_i(x_i) = \begin{cases} {x_i}^{a_i} \overline{\mathscr{R}_i}(x_T) & with\ probability\ (1 - Pr(x_T)) \\ -k_i x_i^{a_i} & with\ probability\ Pr(x_T) \end{cases} \tag{7.22}$$

7.4.3 Problem Formulation and Solution

The prospect-theoretic adjusted utility incorporates two potential outcomes with regards to network's operation, with the first quantifying UEs' satisfaction from the fulfillment of their QoS prerequisites, while also calculating the risk of failure of the band operating over NOMA. The second potential result depicts UE satisfaction in the event of collapse of the band under the NOMA technique due to excessive investment leading to congestion and overwhelming spectrum demand. Subsequently, for this scenario, UEs who invested in the NOMA transmission will cease to operate in the corresponding band, and will receive negative returns since the initial investment did not result in successful transmission. By integrating probabilistic uncertainty into user behavioral modeling (Eq. (7.22)), utility functions do not

Table 7.4: Section 7.4 list of key notations

Symbol	Description
N	User set
p_i^N	Transmission power over NOMA band
p_i^O	Transmission power over OFDMA band
x_i	Percentage of transmission power investment to NOMA band
$\mathscr{V}_i$	Prospect-theoretic utility function
a_i, β_i	User's sensitivity to gains and losses
$z_i(x_i, x_T)$	Actual utility
$z_{0,i}$	Reference point
x_T	Aggregate investment
k_i	Loss aversion
ζ_i	Auxiliary constant
B_N	Spectrum of band operating over NOMA
N_N	Number of users transmitting over NOMA
γ_i^N	NOMA signal-to-interference-plus-noise ratio
h	Channel gain
$\mathscr{R}(x_T)$	Rate of return of CPR
$Pr(x_T)$	CPR probability of failure
$\overline{\mathscr{R}_i}(x_T)$	PT related RoR
$\mathbf{E}(\mathscr{V}_i)$	Expected PT utility
$\mathscr{F}_i(x_T)$	Effective rate of return
$\mathscr{G}$	Fragile CPR game
$\mathscr{X}_i$	Investment strategy set
B_i	Best response strategy
$\overline{\mathscr{X}}_{-i}$	All users' investment excluding user i
ω	Constant below which all users have positive best responses
$\mathscr{X}_i'$	Modified strategy space
$\psi(x_T)$	Auxiliary function
y	Root of $\psi(x_T)$
$\mathbf{x}^*$	PNE investment vector
$\mathscr{H}(x_T)$	Optimal nonzero investment

simply represent the QoS as the amount of the exchanged data to the consumed energy, but also mirror specific attributes related to decision-making in real life cases, when resource failure dilemmas and user behavioral heterogeneity are considered.

Given the probabilistic formulation of the UEs' prospect-theoretic utility function (Eq. (7.22)), the UEs are expected utility maximizers for the following reformulated utility:

$$\mathbf{E}(\mathscr{V}_i) = {x_i}^{a_i}\overline{\mathscr{R}_i}(x_T)(1 - Pr(x_T)) - k_i x_i^{a_i} Pr(x_T) \tag{7.23}$$

Therefore, each UE targets at maximizing the above expected utility, with the examined Resource & Risk Efficient Access Technology Selection (REACTS) optimization problem stated as below:

REACTS Game

$$max\mathbf{E}(\mathscr{V}_i) = max\{x_i^{a_i}\mathscr{F}_i(x_T)\},\ \forall i \in N \tag{7.24}$$
$$s.t.\ x_i \in [0, 1]$$

where $\mathscr{F}_i(x_T) = \overline{\mathscr{R}_i}(x_T)(1 - Pr(x_T)) - k_i Pr(x_T)$ is referred to as the *effective rate of return*. For convenience, all notations met in this sections are summarized in Table 7.4.

The above presented problem is formulated as a *Fragile CPR* game in order to capture the different structural characteristics of each access technology and their imminent impact on user behavior [172].

The REACTS game $\mathscr{G} = [N, \{\mathscr{X}_i\}_{i\in N}, \{\mathscr{V}_i\}_{i\in N}]$ is assumed to satisfy the following properties:

1) Failure probability $Pr(x_T)$ is convex, strictly increasing, and twice continuously differentiable with regards to aggregate investment x_T.
2) The player's rate of return $\mathscr{R}_i(x_T)$ is monotonic (decreasing), concave, twice continuously differentiable, and positive (i.e., $\frac{\partial \mathscr{R}_i(x_T)}{\partial x_T} < 0$, and $\frac{\partial^2 \mathscr{R}_i(x_T)}{\partial x_T^2} < 0$)
3) Each player's investment strategy set is $\mathscr{X}_i = [0,1], \forall i \in N$
The effective rate of return $\mathscr{F}_i(x_T)$ is written as follows.

$$\mathscr{F}_i(x_T) = \overline{\mathscr{R}_i}(x_T)(1 - x_T^2) - (k_i x_T^2) \tag{7.25}$$

where for practical and realistic scenarios, it is $\zeta_i > 1$ and $a_i < 0.5$, so it holds that $\frac{\partial \mathscr{F}_i(x_T)}{\partial (x_T)} < 0$ and $\frac{\partial^2 \mathscr{F}_i(x_T)}{\partial x_T^2} < 0$.

Towards identifying a stable operating outcome for the considered optimization problem, we examine whether the studied CPR game admits a unique Pure Nash Equilibrium (PNE) point, which corresponds to a unanimous consensus among game's contestants in the following sense: a UE's utility would not obtain further gains by a unilateral strategy deviation, given that the other UEs' strategies remain unmodified.

We consider the best response strategy B_i of each UE as $B_i(\mathbf{x_{-i}}) = argmax\mathbf{E}(\mathscr{V}_i(x_i, \mathbf{x_{-i}}))$, $B_i : \overline{\mathscr{X}}_{-i} \rightrightarrows \mathscr{X}_i$, with $\overline{\mathscr{X}}_{-i}$ denoting all the UEs' investment excluding UE i. UEs' strategy selection to invest to each transmission is reflected via the UE specific best response strategy, with $B_i(\mathbf{x_{-i}}) = 0$ implying a UE is operating entirely via the OFDMA, and $0 < B_i(\mathbf{x_{-i}}) < 1$ delivers positive returns from the successful transmission via the NOMA technique. On the contrary, if $B_i(\mathbf{x_{-i}}) = 1$, then the band operating over NOMA is assumed to collapse with certainty due to being over-exploited by UEs who adopt a more risk seeking investment approach.

Theorem 41. ***(REACTS Game PNE Existence:)*** *For the Fragile CPR game $\mathscr{G}$, there exists a value $\omega \in (0,1)$ such that all UEs have positive best responses in $\mathscr{X}_i' = [0,\omega] \subset \mathscr{X}_i$, and $B_i(\mathbf{x_{-i}}) = 0$, $\forall x_T > \omega$.*

Proof. First, we examine the behavior of the effective rate of return function, $\mathscr{F}_i(x_T)$. By applying Bolzano's Theorem for a relatively small and large value of x_T, we observe that $\mathscr{F}_i(0) > 0$ and $\mathscr{F}_i(1) < 0$ and since $\mathscr{F}_i(x_T)$ is decreasing according to Eq. (7.25), there exists a unique value $\omega \in (0,1)$ such that $\mathscr{F}_i(x_T) > 0$, $\forall x_T \in (0,\omega)$.

Next, we demonstrate that $\mathbf{E}(\mathscr{V}_i)$ is concave in the modified strategy space $\mathscr{X}_i'$. According to the second order derivative criterion, we obtain:

$$\frac{\partial^2 \mathbf{E}(\mathscr{V}_i)}{\partial x_i^2} = a_i(a_i - 1){x_i}^{a_i - 2}\mathscr{F}_i(x_T) + 2a_i{x_i}^{a_i - 1}\mathscr{F}_i'(x_T) + {x_i}^{a_i}\mathscr{F}_i''(x_T) \tag{7.26}$$

Since $a_i < 0.5$ and $\mathscr{F}_i(x_T) > 0$ in $\mathscr{X}_i'$ and according to Eq. (7.25), $\mathscr{F}_i'(x_T) < 0$ and $\mathscr{F}_i''(x_T) < 0$, Eq. (7.26) is negative and $\mathbf{E}(\mathscr{V}_i)$ is concave in the modified space $\mathscr{X}_i'$.

Then, we examine the first order derivative of $\mathbf{E}(\mathscr{V}_i)$.

$$\frac{\partial \mathbf{E}(\mathscr{V}_i)}{\partial x_i} = {x_i}^{a_i - 1}\psi(x_T) = 0 \tag{7.27}$$

where $\psi(x_T) = x_i\mathscr{F}_i'(x_T) + a_i\mathscr{F}_i(x_T)$. Similarly to before, we apply Bolzano's Theorem to $\psi(x_T)$ for $x_T = 0$ and $x_T = \omega$. We notice that $\psi(0) = a_i\mathscr{F}_i(0) > 0$ since $\mathscr{F}_i(0)$ is positive in $\mathscr{X}_i'$, and $\psi(\omega) = \omega\mathscr{F}_i'(\omega) < 0$ due to $\mathscr{F}_i(\omega) = 0$ and Eq. (7.25). Hence, there exists a value $y \in (0,\omega)$ such that $\psi(y) = 0$ and subsequently $\frac{\partial \mathbf{E}(\mathscr{V}_i)}{\partial x_i} = 0$ and a critical value indicating an extremal point for $\mathbf{E}(\mathscr{V}_i)$ is identified.

Moreover, due to the concavity of $\mathbf{E}(\mathscr{V}_i)$, $\frac{\partial \mathbf{E}(\mathscr{V}_i)}{\partial x_i}$ is monotonic (decreasing) in $\mathscr{X}_i'$. Hence, $\frac{\partial \mathbf{E}(\mathscr{V}_i)}{\partial x_i}$ is changing its sign from positive to negative and $y \in (0,\omega)$ is a global (unique) maximum of $\mathbf{E}(\mathscr{V}_i)$.

□

Based on the existence and uniqueness of the critical point of $\mathbf{E}(\mathscr{V}_i)$, we conclude that the investment vector $\mathbf{x}^* = \{x_i^*\}$ for the modified strategy space $\mathscr{X}_i'$ is a unique PNE of game $\mathscr{G}$, [120]:

$$\mathscr{V}_i({x_i}^*, \mathbf{x}_{-i}^*) \geq \mathscr{V}_i(x_i, \mathbf{x}_{-i}^*), \forall x_i \in \mathscr{X}_i' \tag{7.28}$$

Convergence

Towards studying UEs' strategies' convergence to the above established unique PNE $\mathbf{x}^*$, we prove that the best response B_i is decreasing with respect to UEs' aggregate investment x_T [172]. We consider the following properties for the best response correspondence:

1. $B_i(\mathbf{x_{-i}}) = argmax\mathbf{E}(\mathscr{V}_i(x_i, \mathbf{x_{-i}}))$, $\forall \mathbf{x_{-i}} \in \overline{\mathscr{X}'}_{-i}$
2. $B_i(\mathbf{x_{-i}})$ is continuous on $\overline{\mathscr{X}'}_{-i}$
3. $B_i(\mathbf{x_{-i}})$ is decreasing in $\overline{\mathscr{X}'}_{-i}$

Similarly to previous section, Properties 1 and 2 already hold as proven by determining the critical point and the behavior of $\mathbf{E}(\mathscr{V}_i)$, therefore, in the following we focus on the third property.

Theorem 42. ***(Decreasing Best Responses:)*** *The best response correspondence $B_i(\mathbf{x_{-i}})$ is decreasing $\forall \mathbf{x_{-i}} \in \overline{\mathscr{X}'}_{-i}$.*

Proof. First, we define the optimal nonzero investment of a player, $\mathscr{H}(x_T) = -\frac{a_i \mathscr{F}_i(x_T)}{\mathscr{F}'_i(x_T)}$ satisfying $\mathscr{H}(B_i(\mathbf{x_{-i}}) + \mathbf{x_{-i}}) = B_i(\mathbf{x_{-i}})$, *when* $B(\mathbf{x_{-i}}) > 0$. We easily show that $\mathscr{H}(x_T)$ is decreasing since $\frac{\partial \mathscr{H}(x_T)}{\partial x_T} = -a_i + \frac{\mathscr{F}_i(x_T)}{\mathscr{F}'_i(x_T)^2} \mathscr{F}''_i(x_T) < 0$.

Let $x_1 = B_i(\mathbf{x_{-1}})$ and $x_2 = B_i(\mathbf{x_{-2}})$, where $\mathbf{x_{-1}}, \mathbf{x_{-2}} \in \overline{\mathscr{X}'}_{-i}$. Stemming from the definition of the optimal nonzero investment $\mathscr{H}$, $x_1 = \mathscr{H}(x_1 + \mathbf{x_{-1}})$ and $x_2 = \mathscr{H}(x_2 + \mathbf{x_{-2}})$. Assuming that $x_2 > x_1$ (and subsequently $B_i(\mathbf{x_{-2}}) > B_i(\mathbf{x_{-1}})$), then given that $\mathscr{H}$ is strictly decreasing, $x_2 = \mathscr{H}(x_2 + \mathbf{x_{-2}}) < \mathscr{H}(x_1 + \mathbf{x_{-1}}) = x_1$, which is contradicting. Thus, the game's best response correspondence is decreasing with the total investment of the UEs. □

Consequently, all three aforementioned properties hold true and the convergence to the determined PNE is established.

7.4.4 Distributed Algorithm

In the following, we present a distributed and low complexity algorithm designed to realize the above described overall theoretical framework. The algorithm aims at achieving optimal spectral efficiency, as well as determining UEs' decisions with respect to their transmission power distribution in the two available access technologies. In the following we describe the **R**esource & **R**isk **E**fficient **Ac**cess **T**echnology **S**election - *REACTS* - algorithm, which converges to game's unique PNE, starting from any initial investment values.

REACTS algorithm is sophisticated enough to encompass both the investment and resource allocation processes under a user-centric perspective. This happens since the UEs are able to dynamically adjust their behavior and strategic actions based not only on their QoS priorities, but also on constantly reassessing the failure probability of the CPR.

At the beginning of each timeslot, the UEs define their behavioral and channel conditions and announce them to the WISP. The WISP adjusts UEs' transmissions accordingly, by allocating each UE to a unique resource block for the OFDMA transmission and by applying SIC technique for the NOMA transmission. The flexible access technology interface allows the UEs to streamline their transmission in each band in a real time basis in line with their calculations with regards to a probable collapse event of the band operating over NOMA, while maximizing their corresponding utility. REACTS algorithm empowered from the decisions and actions of the UEs concludes its operation under two different outcomes: a) the first being the optimal spectrum allocation as a result of the convergence of the investment game; b) in the second case declaring the collapse of the CPR since aggregate demand for the band's spectrum surpassed its capacity to support the UEs (with the imminent transmission shut down). However, even in the second case, the UEs who selected to partially or fully transmit via OFDMA will continue their transmission (with possibly limited spectrum), since a guaranteed portion of the spectrum is reserved for the UEs in each resource block.

Given the fact that decision intelligence lies at the UE side allowing for decentralization of actions during the transmission phase, the complexity of calculations is dramatically reduced. As a result, the UEs within only a few iterations are capable of determining the optimal power investment to each transmission, i.e., over NOMA and OFDMA. Specifically, REACTS algorithm was tested in an Intel(R) Core(TM) i7-7500U CPU @ 2.70 GHz 2.90 GHz laptop with 8.00 GB RAM. As shown in Fig. 7.10, the transmission

Algorithm 18 REACTS Algorithm

Require:
User number N; constants k_i, a_i; band spectra B_O, B_N
$ite \leftarrow 1$; $fail^{(ite)} \leftarrow 0$; $converge^{(ite)} \leftarrow 0$
Apply SIC for NOMA band
Assign initial random $x_i^{(ite)}$
while $converge^{(ite)}$=0 **and** $fail^{(ite)}$=0 **do**
  Calculate p_i^N, p_i^O;
  Calculate utility $\mathbf{E}(\mathscr{V}_i)^{(ite)}$ according to equation (7.23)
  for all $x_i \in [0,1]$ **do**
    x_i^*=$argmax_{x_i}\mathbf{E}(\mathscr{V}_i)$
    if $\mathbf{E}(\mathscr{V}_i) > \mathbf{E}(\mathscr{V}_i)^{(ite)}$ **then**
      $x_i^{(ite+1)} \leftarrow x_i^*$ **and** $\mathbf{E}(\mathscr{V}_i)^{(ite+1)} \leftarrow \mathbf{E}(\mathscr{V}_i)$
    end if
  end for
  Calculate *normalized* $x_T = \dfrac{\sum_i^N x_i^{(ite+1)}}{N}$
  if $\sum R_i^N > B_N$ **then**
    $fail^{(ite+1)} \leftarrow 1$
  end if
  if $x_i^{(ite+1)} - x_i^{(ite)} < \epsilon$ **then**
    $converge^{(ite+1)} \leftarrow 1$
  end if
  $ite \leftarrow ite + 1$
end while
return
User investment x_i and $fail$ if NOMA band still active

power investment x_i per UE starting from a random initial value converges to the PNE investment vector within only 3 iterations, and the run-time per UE is 1.4 *msec* due to the simple calculations, implying that the proposed scheme can readily adapt to real life situations, where short timeslot duration is considered. Furthermore, REACTS algorithm is designed in a generic manner facilitating the application of varying access technologies and resources, where UE behavior is a key factor for the operation and performance evolution of the system.

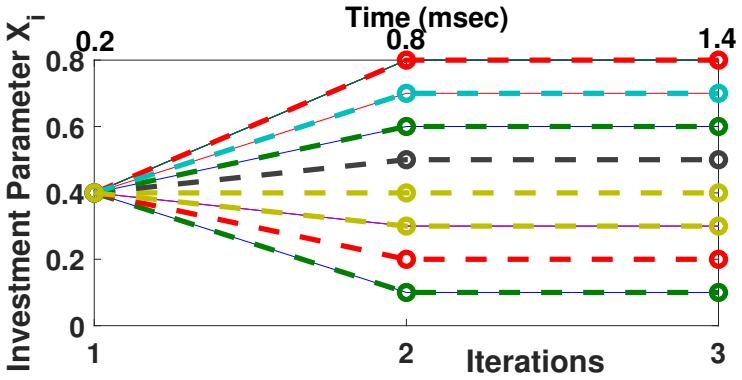

Figure 7.10: User specific investment parameter x_i calculation complexity as a function of time and number of iterations

7.4.5 Numerical Results

In this section we evaluate the operating efficiency of the preceding theoretical model via a series of extensive numerical simulations. Originally, different snapshots of the network with dual access technology interfaces are illustrated, demonstrating the optimality of the investment game in terms of both spectral and energy-efficiency, as well as the overall operation stability. Next, the impact of modifying UE behavior on network's performance is discussed, both for heterogeneous and homogeneous populations, as UE risk aversion preferences and sensitivities are evolving. Lastly, the potential and operation effectiveness of the proposed scheme is compared against single access technologies, indicating the benefits of dynamic technology access selection and decision-making at the level of the UEs, towards overall system's performance enhancement.

We consider the uplink of a wireless network of radius of $r = 2.5\ km$ with $N = 20$ UEs who can simultaneously access and transmit between the band operating over NOMA and OFDMA. For demonstration purposes only, increasing user IDs correspond to increasing distances from the base station. The total spectrum is indicatively set at 4 MHz, 80% of which is allocated to the band operating over NOMA, due to the ability of the UEs to utilize it in its entirety, and the remaining 20% is reserved by the band operating over OFDMA. UEs' maximum transmission power is set to 0.2 $Watts$.

Optimal Investment Game Basic Operation

Initially we assume a homogeneous population where all users have the same prospect-theoretic characteristics with $a_i = 0.1$ and $k_i = 20$. Fig. 7.11 depicts UEs' data rate (in bps) obtained only in the band operating over NOMA, as well as the overall UE data rate combining the achieved data rates under both NOMA and OFDMA operation, as determined by the optimal value of the investment parameter x_i. Due to the dominant spectrum size of the band operating over NOMA, middle distance (e.g users with ID ranging from 5 to 15) UEs with worsening channel conditions are also impacted by intracell interference, and consequently tend to invest mostly in the NOMA transmission. In contrast, UEs relatively close (e,g users with ID from 1 to 4) or far away from the base station (e.g., users with ID from 16 to 20) select to invest less aggressively to the NOMA transmission. This is due to the fact that the channel conditions for the first and the absence of any interference for the latter due to the application of SIC technique, are favorable enough to attain satisfactory data rates with low power investment, and hence mostly prefer to transmit via the safe option of OFDMA transmission.

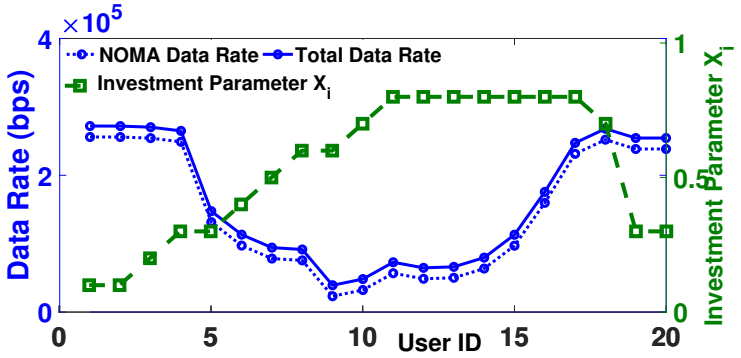

Figure 7.11: User data rate (under NOMA and total) and investment parameter x_i as a function of users' ID

Additionally, in Table 7.5 we compare the outcome of the optimal investment allocation game as obtained via the implementation of REACTS algorithm - in terms of achieved data rate, and energy-efficiency - against various fixed allocations of the user transmission power between the two access technologies and corresponding bands, where investment is predetermined. We observe that the optimal investment game where each UE defines its investment to the NOMA transmission based on its risk and transmission preferences, outperforms all other cases, both in terms of mean data rate and energy-efficiency. Moreover, the more aggressive cases where the UEs invest more in NOMA transmission eventually lead to its imminent collapse, due to over-exploitation, with only the OFDMA technique allowing UEs to transmit and obtain satisfaction, whereas when $x_i = 1$, none of the UEs manages to successfully transmit at all, in the specific scenario under consideration. Thus, we observe that by dynamically

Table 7.5: Investment allocation scenarios ($a = 0.1$, $k = 20$) for REACTS algorithm

Investment Strategy	**Investment Parameter** x_i	**Mean Rate (bps)**	**Mean Energy Efficiency (bit/Joule)**	**NOMA Band Status**
Optimal Investment	0.54	1.61×10^5	8.02×10^5	active
Equal Split	0.50	1.54×10^5	7.73×10^5	active
25% NOMA	0.25	1.39×10^5	6.95×10^5	active
75% NOMA	0.75	0.16×10^5	0.80×10^5	fails
100% NOMA	1.00	0	0	fails

enabling the UEs to contribute to system's self-optimization, it significantly improves utilization and delivery of service, compared to cases where fixed allocation and transmission decisions apply.

Diversifying User Behavior

In this section, we examine system's evolving behavior when the UEs follow heterogeneous prospect-theoretic risk assumptions as captured by the parameters a_i and k_i, and evaluate the corresponding effect on the spectrum fragility. Specifically, Fig. 7.12 illustrates system's average energy-efficiency as average UEs investment (i.e., x_i) to the band operating over NOMA gradually increases, via the adjustment of the sensitivity and loss aversion parameters (thus altering their risk-based behavior). In more detail, towards a more risk seeking approach on behalf of the UEs, sensitivity parameter a_i rises, resulting in higher fragility for the spectrum. At the same time, we gradually decrease the value of loss aversion parameter k_i indicating a tendency to underestimate the potential collapse of the band operating under the NOMA access technique. As a result, the UEs utilize the available spectrum in a more aggressive manner, which leads to the subsequent increase in the levels of the investment parameter, x_i. It becomes clear that as investment to the CPR originally rises, this enhances the energy-efficiency since the UEs benefit from their access the full and of higher capacity NOMA spectrum. However, after a critical value of the investment parameter x_i, the spectrum of the band operating over NOMA eventually fails due to its over-exploitation by the users. This justifies the significant drop in the energy-efficiency, while after that critical point any positive returns are obtained through UEs' transmission over OFDMA. However the latter are being restricted via the smaller fraction of the available spectrum, being split among separate resources blocks to realize the interference free communication. Finally, as user power investment reaches its maximum levels despite the collapse of the CPR, the returns are zero since all UEs would attempt to fully invest (x_i=1) in the failed CPR obtaining no returns, with the OFDMA transmission remaining idle.

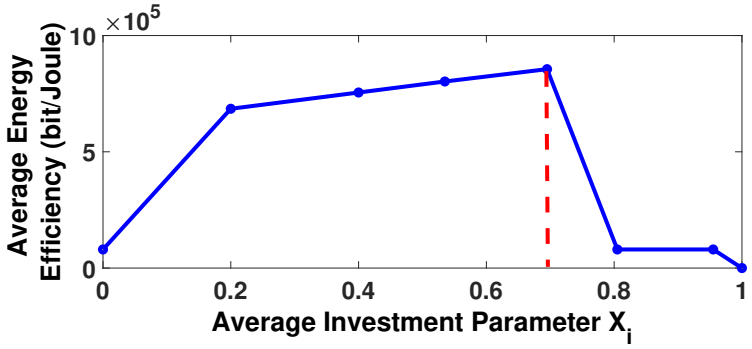

Figure 7.12: Average energy-efficiency for increasing investment x_i via adjustment of sensitivity and loss aversion parameter

Additionally, in Fig. 7.13a and Fig. 7.13b, we present the invested power in the NOMA transmission, as well as the attainable data rate (NOMA, OFDMA and total) for each UE and for varying values of the sensitivity parameter a_i. In Fig. 7.13a, we notice that low values of a_i are linked with moderate investment in the NOMA transmission and hence, lower values of corresponding transmission power

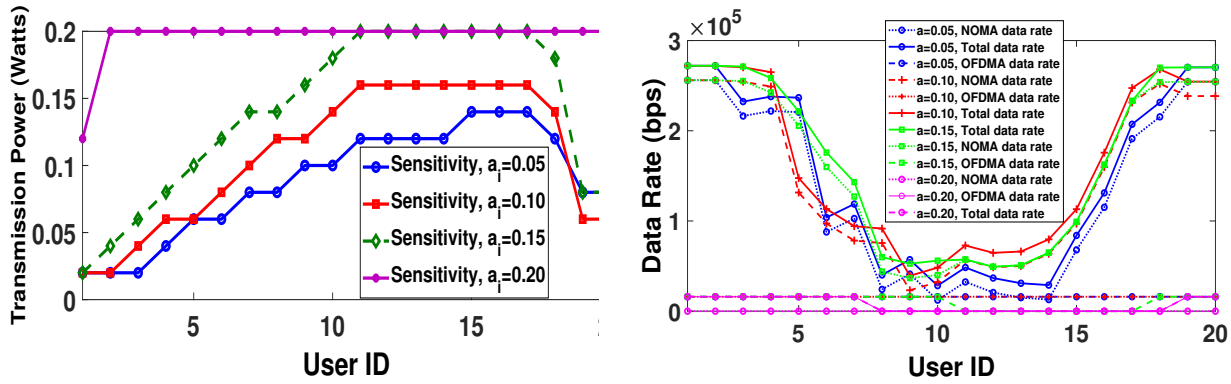

(a) NOMA transmission power

(b) User Data rate (NOMA, OFDMA, total)

Figure 7.13: (a) Transmission power and (b) data rate as a function of user ID for different sensitivity parameters a_i

under NOMA. Due to the SIC technique, middle distance UEs invest more intensively to the NOMA transmission due to its higher potential return. On the contrary, for high sensitivity levels, all UEs follow a more risk seeking approach resulting in almost all of them to invest in the NOMA transmission. From the data rate perspective, in Fig. 7.13b we present for different values of a_i, the NOMA and OFDMA components as well as the total data rate obtained per UE. Increasing sensitivity implies higher values of NOMA related data rate, however when $a_i = 0.20$, the NOMA band collapses with none of the UEs being able to transmit under NOMA. On the contrary, the UEs who still invested (even partially) to the OFDMA transmission will receive stable data rates, since each resource block remains unaffected by the increasing investment in the NOMA transmission. Moreover, as the sensitivity rises, the UEs tend to abandon OFDMA and invest in NOMA, and consequently their corresponding rate in this band is eliminated.

Lastly, in Fig. 7.14, we examine a case where only two UEs (ID=11 and 12) deviate from the common user risk attributes by selecting a lower risk aversion parameter k_i, falling from $k_i = 20$ to $k_i = 7$. In this case, we observe that UEs 11 and 12 increase their investment to the maximum possible value in the NOMA transmission as expected, since they underestimate the potential impact of spectrum collapse and more aggressively compete at claiming fraction of the available NOMA spectrum (Fig. 7.14a). Considering the band operating over NOMA, UEs 11 and 12 investment leads to a considerable amelioration in their NOMA related transmission, with more than doubling their data rates (Fig. 7.14b). On the other hand, SIC application indicates that the UEs who will sense the interference of UEs 11 and 12, exhibit deteriorating data rates, whereas UEs farther away (i.e., UEs 13 to 20), do not decode those signals with their transmission, thus they remain unaffected.

Dual Access Technology Benefits & Comparisons

To further assess the benefits of the proposed paradigm realizing coexisting access technology schemes, we compare REACTS approach against scenarios implementing a single only access technology, that is either exclusively NOMA or exclusively OFDMA, in terms of energy-efficiency for increasing number of connected UEs. For fairness in the comparison, in all examined cases the total available spectrum cumulatively is the same. For demonstration and benchmarking purposes, we have implemented two comparative cases of OFDMA, with a standard version of OFDMA of 50 fixed resource blocks to accommodate all UEs where only one RB is allocated for transmission to each user (denoted as OFDMA - single RB per UE), as well as an ideal version, where the resource blocks are rearranged each time in order to perfectly exhaust the available spectrum (denoted as OFDMA - multiple RBs per UE). When single access technology scenarios are assumed, Prospect Theory cannot be equally applied and therefore in those cases UEs utilities are modeled based on EUT.

Based on the corresponding results in Fig. 7.15 we observe that a dual access implementation scheme (i.e., REACTS algorithm) outperforms all other cases. This is due to the flexibility of the UEs to dynamically use both bands complementary, while streamlining their investment in each access technology in a real time manner. The latter is achieved by evaluating the increasing probability of spectrum

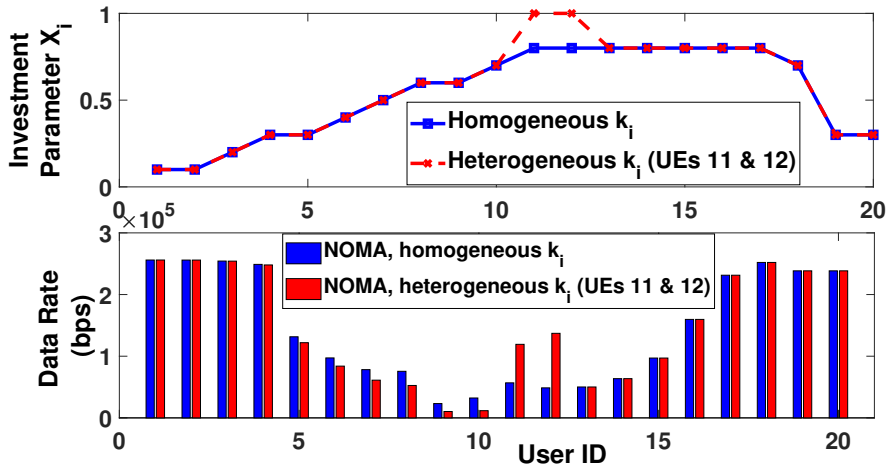

Figure 7.14: System modifying behavior per changing risk aversion k_i for UEs 11 and 12 - Data rate and investment parameter x_i as a function of UEs ID

collapse as allowed by the proposed prospect-theoretic modeling and accordingly adjusting the investment parameter x_i. As expected, the energy-efficiency decreases as more UEs are connected to the network due to increasing interference in the NOMA transmission.

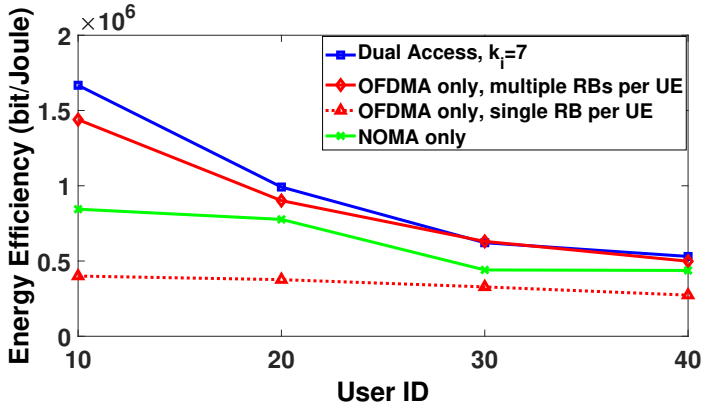

Figure 7.15: Energy-efficiency for dual access technology interface against single access technologies

It is noted that, for the standard case (i.e., OFDMA- single RB per UE), the utilization is relatively low, since a large part of the spectrum in OFDMA remains undernutilized, as a number of resource blocks stays inactive for small number of UEs. However the performance remains steady despite the increasing number of UEs, due to the absence of intracell interference owing to the operation nature of OFDMA. In the second ideal case (i.e., OFDMA - multiple RBs per UE), where the spectrum is assumed to be rearranged among the resource blocks based on UE numbers, energy-efficiency is significantly improved mainly due to the absence of interference and the UEs exhausting the entire available spectrum. Lastly, comparing NOMA against standard OFDMA it is noted that NOMA delivers superior results because the UEs are allowed to have access to the entire spectrum. However, its performance is still worse than REACTS algorithm, since in the latter the UEs are able to estimate the probability of band collapse, and take advantage of the synchronous OFDMA access.

7.5 Protecting Resource Fragility via Pricing

Based on the preceding analysis, it becomes apparent that resources where *congestion effects* are identified (in contrast to *network effects*), like spectrum in communication networks are associated with decreasing rate of returns stemming from over-crowding and excessive utilization. Such resources are bound to increasing probability of failure (or fragility) if over exploited by the users in a shared and competitive

environment, with the potential outcome being that none of them would eventually be able to extract any surplus from that resource. Understanding the above constraint, it becomes of great research important to investigate strategies under which the risk of resource failure can be mitigated and protect the fragility of the resource.

Pricing in wireless networks has already been extensively discussed in Chapter 3 as a means of controlling and trading resources in systems where the users have competitive and often even conflicting strategies. Thus, pricing (or taxation) is an efficient tool in order to control the utilization of a resource not only in terms of more fairly distributing it among the users and increase social welfare, but also as a means of safeguaring the accessibility of that resource and ensuring that it will remain available in cases of over-investmentnt from the consumers without disrupting the operation of the network. It is noted that, in the relevant literature, pricing schemes have been mainly adopted for power and rate control in wireless networks, without however considering or accounting for spectrum fragility [29], [10], [210].

In this section, we approach pricing from a different perspective, assuming it represents the cost of investment of the users to a specific scarce resource under a prospect theoretic model. This considerably differentiates user behavior against not only claiming that resource, but also it links their individual assessment of risk and preferences with the price that is applied in order to protect the resource from collapse. Eventually, it is shown that investment pricing is indeed increasing the utilization of a shared resource, since users can easier evaluate the criticality and the impact of their actions for the survival of the resource under consideration. Specifically for the case of wireless networks, we consider again the case of spectrum being available jointly via licensed and unlicensed bands. Users' investment to the unlicensed band (or simply the CPR) is priced, with the prospect theoretic utility function being modified accordingly. The results confirm that spectrum utilization and energy-efficiency increase when pricing is applied, since not only a collapse of the resource is avoided, but under an optimal pricing level, it supports the fairer allocation of the bandwidth among the users minimizing unnecessary consumption and more optimal traffic offloading among the licensed and unlicensed bands. As a result, this work provides a sharp innovation on linking network utilization, spectral stability, and user preferences, against the literature where spectrum was considered as unlimited or indestructible resource with homogeneous and neutral users who simply aim at maximizing their own utilities.

7.5.1 System Model

The uplink of a Non-Orthogonal Multiple Access (NOMA) wireless network is considered, with each user i from the user set $\mathcal{N}$, able to transmit via licensed or unlicensed bands, with the first operating under a closed access scheme and regulated by the WISP. The licensees are assumed to pay a flat based fee and are offered guaranteed QoS thresholds and target data rates, acting as the *safe resource* [172] providing a limited but constant return of satisfaction to users. On the contrary, unlicensed spectrum operates on the basis that can be exploited by any user without restrictions, however it comes at the risk of over-exploitation and collapse, where none of the users would be able to transmit. According to the standard modeling of this Chapter, each user $i \in \mathcal{N}$ invests a percentage of its maximum transmission power (denoted as the investment parameter x_i) P_i^{Max} to the unlicensed band i.e., $P_i^U = x_i P_i^{Max}$ with the remaining power directed to the licensed (or safe) transmission, hence, $P_i^L = (1 - x_i)P_i^{Max}$.

It is noted that different approaches of unlicensed traffic steering exist in the literature, such as carrier aggregation, dual connectivity and/or Licensed Assisted Access (LAA), with the objective of facilitating network densification and spectrum management optimization. The considered unlicensed band in our work is assumed to function independently of the licensed band, with some traffic routed via the licensed cellular band while the rest is sent over the unlicensed one. NOMA technique allows users to synchronously utilize the whole spectrum of the unlicensed band without prior checking of channel occupancy (e.g., listen-before-talk protocol) or applying any other admission control policy, enabling them to claim spectrum resources in a greedy manner based on their risk behavioral modeling. Consequently, traffic is being offloaded to the unlicensed band in an agile and load aware perspective, with the above structure functioning similar to the LTE-WLAN radio level Aggregation (LWA) paradigm [211], [212].

Investment Pricing

The concept of pricing is introduced as a means of controlling unlicensed spectrum utilization and fragility, by adding a convex usage based pricing mechanism on the amount of power investment of each user to the unlicensed band. Users are able to direct their transmissions within each band, given their risk perceptions

towards spectrum collapse and their QoS priorities. At the same time they may adjust their behavior according to the imposed pricing policy by lowering their investment to the common resource [213].

A convex or nonlinear pricing function, e.g., cx_i^b, in contrast to linear pricing can be used as means of more appropriate price discrimination within the range of resource investment while reflecting the criticality of the considered resources. This is due to the fact that the impact that one user causes by investing in the common resource to the rest of the users is not equivalent within the whole range of transmission power. Hence, a convex pricing policy better quantifies the cost of investment that a user should pay for capturing a high fraction of the CPR. To reflect this, we consider a convex pricing function of the form cx_i^b, where without loss of generality we assume $b = 2$.

It is noted that alternative solutions to spectrum fragility have recently emerged, including the use of mm-Wave frequencies. Such bands, operating between 10 and 300 GHz, provide abundant bandwidth and have arisen as a promising solution in 5G networks to address capacity shortages by unlocking spectrum of much higher magnitude [214], [215]. However, challenges of expanding to such bands, like mm-Wave communications (e.g., 60 GHz) are the high propagation loss, directivity, and sensitivity to blockage (e.g., physical obstacles) due to their order of magnitude wavelength difference against the 2.4 GHz (Wi-Fi) band. Directional mm-Wave transmissions can isolate users and lead to coverage holes with path losses changing rapidly, while processing power consumption can increase leading to more intense power drain [215].

Pricing network resources enhances decentralization of decisions towards self-optimization of the system, leading to more sophisticated and user centric outcomes without any additional infrastructure investment. Mitigating unnecessary resource over-consumption and managing spectrum fragility are achieved by allowing intelligent users to weigh risk and coordinate towards sharing scarce resources in an optimal and socially fair approach. It is also stressed that the introduction of pricing in wireless networks is complementary to the alternative frequency bands utilized, while its application is not constrained only in preserving spectrum utilization and fragility, but can also be used in other service and network management functions, such as interference and power management, areas of high relevance and importance to mm-Wave communications as well.

7.5.2 Problem Formulation and Solution

As similar to the previous topics, users exhibit a risk-aware behavior with respect to their transmission over the unlicensed band due to the uncertainty over its failure, if over-exploited. For convenience, we present again the PT utility formulated as follows:

$$\mathscr{U}_i(y_i) = \begin{cases} (y_i - y_{0,i})^{\lambda_i} & when\ y_i > y_{0,i} \\ -k_i(y_{0,i} - y_i)^{\mu_i} & otherwise \end{cases} \tag{7.29}$$

where $y_i(x_i, x_T)$ denotes user's actual utility, $x_T = \sum_{i=1}^{N} x_i$ is the aggregate power investment to the unlicensed band, and $y_{0,i}$ is the reference point or ground truth. Parameters $\lambda_i, \mu_i \in (0, 1]$ refer to user sensitivity to gains or losses, whereas $k_i \in [0, +\infty]$ corresponds to the loss aversion parameter depicting the impact of losses compared to gains. Without loss of generality, in this work we assume that $\lambda_i = \mu_i$ and normalize aggregate investment so that $x_T = [0, 1]$.

When a user opts to transmit only via the licensed band (i.e., $x_i = 0$), its achieved energy-efficiency is $y_{0,i} \triangleq \frac{W_L}{P_i^L} log_2(1 + \gamma_i^L), \forall i \in N$, where W_L is the licensed spectrum, $N_L \subseteq \mathscr{N}$, and $\gamma_i^L = \frac{h_i P_i^L}{\sigma^2 + \sum_{i>k} h_k P_k^L}$ refers to the Signal-to-Interference-plus-Noise Ratio (SINR) of user i. This operational status is perceived as the ground truth for the users according to the reference dependence property [171], [216].

Assuming that the spectrum of the unlicensed band does not collapse, the corresponding user's i utility is expressed as:

$$y_i(x_i, x_T) = y_{0,i}(1 - x_i) + \Xi_i x_i \mathscr{R}(x_T) - cx_i^2 \tag{7.30}$$

where $\Xi_i = \frac{W_U}{P_i^U} log_2(1 + \gamma_i^U)$, W_U is the unlicensed spectrum, N_U is the number of users transmitting to the unlicensed band, and γ_i^U reflects the user's i SINR in the unlicensed band, while c represents the imposed pricing factor. We denote $\mathscr{R}(x_T) = 2 - e^{x_T - 1}$ as the rate of return from the transmission via the unlicensed band, exhibiting congestion effects where the common resource is suppressed under increasing utilization with diminishing returns as investment rises, in line with communications systems modeling. Under formulating the unlicensed band as a CPR, the increasing risk of its collapse is expressed by its failure probability $Pr(x_T)$, which is increasing with respect to users' aggregate investment. For demonstration purposes we select $Pr(x_T) = x_T^2$.

Table 7.6: Section 7.5 list of key notations

Symbol	Description
$\mathscr{N}$	User set
P_i^{Max}	Maximum transmission power
x_i	Power investment percentage to unlicensed band
P_i^U, P_i^L	Transmission power to unlicensed and licensed band
c	Pricing factor
b	Pricing function constant
U_i	PT utility
$y_i(x_i, x_T)$	User's actual utility
x_T	Aggregate power investment to the unlicensed band
$y_{0,i}$	Reference point
λ_i, μ_i	User sensitivity to gains or losses
k_i	Loss aversion
W_L, W_U	Licensed and unlicensed spectrum
N_L, N_U	Users in licensed and unlicensed band
γ_i^L, γ_i^U	SINR in licensed and unlicensed band
σ^2	Variance of Additive White Gaussian Noise
h	Channel gain
Ξ_i	Auxiliary constant
$\mathscr{R}(x_T)$	Rate of return
$\overline{\mathscr{R}_i}(x_T)$	PT related rate of return
$Pr(x_T)$	Failure probability
$\mathscr{G}$	Fragile CPR game
$\mathscr{X}_i$	Users' strategy space
$\mathfrak{F}_i(x_T)$	Effective rate of return
ψ	Auxiliary function
ζ	Root of ψ
$\mathbf{x}^*$	Optimal investment vector
BR_i	Best response
$\overline{\mathscr{X}'}_{-i}$	Aggregate investment space excluding user i
$\mathscr{U}_i(x_i)$	Utility function
$\mathbf{E}(\mathscr{U}_i)$	Expected PT utility

Assuming that the CPR does not collapse, users are able to capture additional utility surplus by transmitting in the unlicensed band, surpassing their perceived satisfaction from the initial reference point. Instructed by PT modeling, we subtract the reference point $y_{0,i}$ from Eq. (7.29) and define $\overline{\mathscr{R}_i}(x_T) \triangleq (\Xi_i \mathscr{R}(x_T) - cx_i - y_{0,i})^{\lambda_i}$ as the PT specific rate of return, such that $\mathscr{U}_i = x_i^{\lambda_i} \overline{\mathscr{R}_i}(x_T)$. Alternatively, in the event of collapse of the CPR, no transmission is feasible via the unlicensed band, thus users will receive a negative return from their investment, expressed as $\mathscr{U}_i = -k_i x_i^{\lambda_i}$. Referring to the event of collapse of the CPR with probability $Pr(x_T)$ as the reference point, the PT utility is reformulated as:

$$\mathscr{U}_i(x_i) = \begin{cases} {x_i}^{\lambda_i} \overline{\mathscr{R}_i}(x_T) & \textit{with prob. } (1 - Pr(x_T)) \\ -k_i x_i^{\lambda_i} & \textit{with prob. } Pr(x_T) \end{cases} \tag{7.31}$$

Fragile CPR Game Formulation with Pricing

Under the fundamental assumption that common resources are fragile if overexploited and the PT modeling which integrates user subjectivity in decisions, in this section we formulate the problem as a Fragile CPR game $\mathscr{G} = [\mathscr{N}, \{\mathscr{X}_i\}_{i \in \mathscr{N}}, \{\mathscr{U}_i\}_{i \in \mathscr{N}}]$, where $\mathscr{X}_i = [0, 1]$ denotes users' strategy space. According to [213], in Fragile CPR games, failure probability function is considered convex, strictly increasing, and twice continuously differentiable, with $Pr(1) = 1$, where the CPR collapses with certainty, while the player specific rate of return $\overline{\mathscr{R}_i}(x_T)$ is monotonic (decreasing), concave, twice continuously differentiable,

and positive, $\forall x_i < \frac{\Xi_i - y_{0,i}}{c}$ [213]. The above formulation captures a wide range of resources, while also incorporates risk perceptions and pricing in user strategies. Users aim to maximize their expected PT utilities, which based on relation (7.31) are expressed as:

$$\mathbf{E}(\mathscr{U}_i) = {x_i}^{\lambda_i}\overline{\mathscr{R}_i}(x_T)(1 - Pr(x_T)) - k_i x_i^{\lambda_i} Pr(x_T) \tag{7.32}$$

Subsequently, the Investment in Network Spectrum via Pricing for Intelligent Resource Utilization (INSPIRE-U) game is constructed as the following maximization problem:

$$\begin{gathered}\textbf{INSPIRE} - \textbf{U Game} \\ max\mathbf{E}(\mathscr{U}_i) = max\{x_i^{\lambda_i}\mathfrak{F}_i(x_T)\},\ \forall i \in N \\ s.t.\ x_i \in [0,1]\end{gathered} \tag{7.33}$$

where $\mathfrak{F}_i(x_T) = \overline{\mathscr{R}_i}(x_T)(1 - Pr(x_T)) - k_i Pr(x_T)$ corresponds to the user's effective rate of return. For clarity, all key notations from this section are found in Table 7.6.

Solution via S-modular Games:

Convex pricing as a means of controlling spectrum fragility under conditions of competition and probabilistic uncertainty, has not been investigated in the context of PT modeling in relevant works (e.g., [216], [213]). Towards treating this modeling inefficiency, we utilize the class of *S-modular Games* [62]. Submodular games in particular as already discussed in Section 3.2, are characterized by strategic substitutes implying that an increase in the actions of one player leads other users to decrease their actions accordingly. Submodular games are well aligned with the problem of optimizing investment and pricing in Fragile CPR problems, since user strategies are shaped in accordance with increasing probability of spectrum fragility and rising transmission cost due to pricing.

Theorem 43. ***(Submodular fragile CPR game:)*** *The Fragile CPR Game $\mathscr{G}$ is submodular in the modified strategy space $\mathscr{X}_i' = (0, \omega) \subseteq \mathscr{X}_i$ if and only if [10]:*

$$\frac{\partial^2 \mathscr{U}_i}{\partial x_i \partial x_j} \leq 0 \tag{7.34}$$

Proof. According to Eq. (7.34), $\frac{\partial^2 \mathscr{U}_i}{\partial x_i \partial x_j} = x_i^{\lambda_i - 1}(\psi - 2\lambda_i x_T(\overline{\mathscr{R}_i} + k_i) + x_i \frac{\partial^2 \overline{\mathscr{R}_i}}{\partial x_i \partial x_j} - 2x_i(\overline{\mathscr{R}_i} + k_i))$, where $\psi = \frac{\partial \overline{\mathscr{R}_i}}{\partial x_j}(\lambda_i - \lambda_i x_T^2 - 2x_i x_T) - 2\frac{\partial \overline{\mathscr{R}_i}}{\partial x_i} x_i x_T$. By applying Bolzano's Theorem for ψ for a supposedly small and large value of x_T, we obtain that $\psi(0) < 0$ and $\psi(1) > 0$. Hence, there exists at least one $\zeta \in (0,1)$ such that $\psi(\zeta) = 0$. Since $\psi(0) < 0$, we assume that $\psi < 0, \forall x_i \in (0, \zeta)$. This implies that all terms of Eq. (7.34) are negative and $\mathscr{G}$ is submodular in $(0, \zeta)$.

Moreover, since $x_i < \frac{\Xi_i - y_{0,i}}{c}$, we further reduce the strategy space in which the game is submodular to $\mathscr{X}_i' = (0, \omega)$, where $\omega = min(\zeta, \frac{\Xi_i - y_{0,i}}{c})$ □

Lemma 44. *Fragile CPR, Submodular Game $\mathscr{G}$ with pricing admits at least one Nash Equilibrium (NE), identified as the optimal investment vector $\boldsymbol{x}^* = \{x_i^*\}$ such that $\mathscr{U}_i({x_i}^*, \boldsymbol{x}_{-i}^*) \geq \mathscr{U}_i(x_i, \boldsymbol{x}_{-i}^*), \forall x_i \in \mathscr{X}_i'$.*

Convergence:

$BR_i(\mathbf{x_{-i}}) = argmax\mathbf{E}(\mathscr{U}_i(x_i, \mathbf{x_{-i}}))$ is the best response of user i providing the most favorable outcome given the strategies of the other users, with $BR_i : \overline{\mathscr{X}'}_{-i} \rightrightarrows \mathscr{X}_i'$, where $\overline{\mathscr{X}'}_{-i}$ represents aggregate investment space excluding user i, with $BR_i = 1$ indicating failure of the CPR with certainty. Since game $\mathscr{G}$ is proven to be submodular, then it is dominance solvable with its best response strategies monotonically decreasing, converging to game's NE [10].

Algorithm 19 INSPIRE-U Algorithm

$ite \leftarrow 1$; $CPR_{down}^{(ite)} \leftarrow 0$; $CPR_{on}^{(ite)} \leftarrow 0$; $x_i^{(ite)}$; $c \leftarrow 0$
while $CPR_{down}^{(ite)} = 0$ **and** $CPR_{on}^{(ite)} = 0$ **do**
  Calculate $P_i^{L/U}$; $\mathbf{E}(\mathscr{U}_i)^{(ite)}$;
  for all $x_i \in [0,1]$ **do**
    x_i^*=$argmax_{x_i}\mathbf{E}(\mathscr{U}_i)$
    if $\mathbf{E}(\mathscr{U}_i) > \mathbf{E}(\mathscr{U}_i)^{(ite)}$ **then**
      $x_i^{(ite+1)} \leftarrow x_i^*$ **and** $\mathbf{E}(\mathscr{U}_i)^{(ite+1)} \leftarrow \mathbf{E}(\mathscr{U}_i)$
    end if
  end for
  if $sum\ of\ rates \sum R_i^U > W_U$ **then**
    $CPR_{down}^{(ite+1)} \leftarrow 1$
  end if
  if $x_i^{(ite+1)} - x_i^{(ite)} < \epsilon$ **then**
    $CPR_{on}^{(ite+1)} \leftarrow 1$
  end if
  $ite \leftarrow ite + 1$ **and** $c \leftarrow c + c_{step}$
end while

7.5.3 Distributed Algorithm

Concerning the practical implementation of game $\mathscr{G}$, we introduce the distributed and low complexity *INSPIRE-U* algorithm, i.e., **I**nvestment in **N**etwork **S**pectrum via **P**ricing for **I**ntelligent **RE**source **U**tilization. *INSPIRE-U* combines the resource allocation, pricing, and investment actions in a user-centric manner, where the WISP only imposes the pricing policy towards controlling unlicensed spectrum utilization whereas each user defines its investment to the unlicensed band given its PT risk perceptions. As the system evolves, the algorithm converges to game's optimal operational point for a certain price level, or announces the collapse of the unlicensed band due to excessive investment.

Owing to its distributed nature, the algorithm allows each user to calculate its power investment in a decentralized manner with no need to maintain historical data from previous allocations. Thus, data overhead and storage needs are rather limited, as only the pricing value and the cell interference are exchanged between WISP and users. The algorithm converges rapidly to the Nash Equilibrium (less than ten iterations), while in each iteration only algebraic calculations are performed, thus limiting processing power and CPU requirements.

7.5.4 Numerical Results

In this section we provide a series of numerical results evaluating the impact of pricing on spectrum fragility and the overall network performance. The uplink of a NOMA wireless network is considered, including a base station and 20 continuously backlogged users randomly placed within its radius (2 km). System's total spectrum is set at 4 MHz with 80% allocated to the unlicensed band, while the remaining part refers to the licensed spectrum. User maximum power is $P_i^{Max} = 0.2\ W$ which is split among the two bands depending on users' investment strategy. In the direction of introducing a first degree of regulation in the commonly accessible unlicensed band, the WISP applies a convex investment-based pricing, expressed by cx_i^2. At each timeslot, users based on their risk perceptions and QoS preferences estimate their preferred investment to the unlicensed spectrum. Depending on the probability of collapse for the unlicensed band, the WISP gradually increases the pricing level to the users, up to a value which guarantees that spectrum does not collapse, while also delivers the network optimal cumulative utility.

In Fig. 7.16, we observe spectrum fragility (or utilization) patterns for increasing pricing levels, for both risk averse or seeking users. We observe that fragility is significantly higher for risk seeking users (i.e., $k_i = 0$), since this class of users underestimate the impact of spectrum collapse in their effort to capture a higher portion of the available resources. As pricing levels increase, both classes of users affected by the higher price for their investment, claim the available spectrum in a less aggressive manner, hence spectrum fragility considerably falls. Fig. 7.17a depicts how transmission power to the unlicensed band is impacted, as a function of different risk behaviors as they are expressed by increasing values of k_i, and for

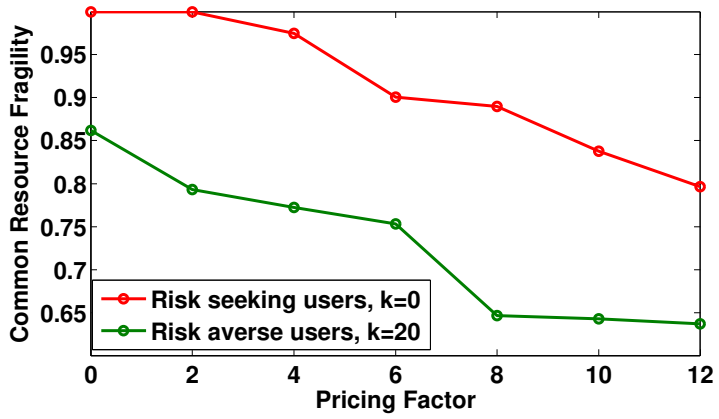

Figure 7.16: Spectrum fragility per pricing factor

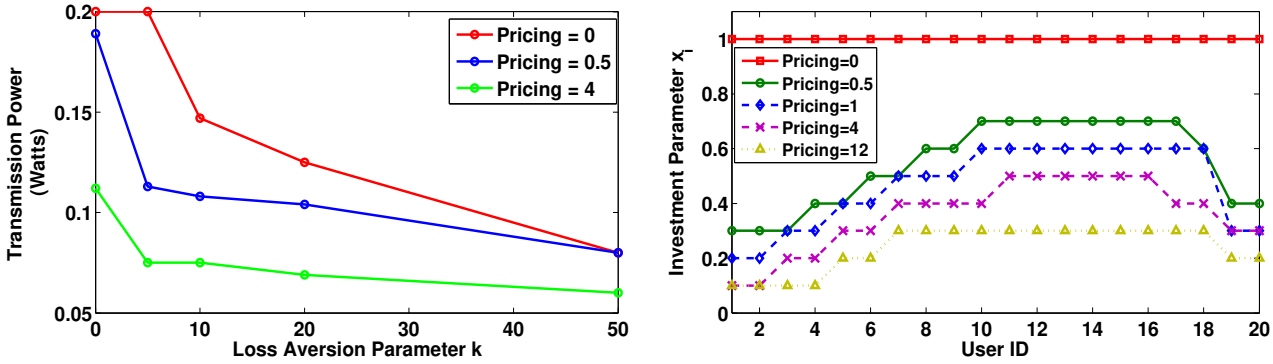

(a) (b)

Figure 7.17: (a) Transmission power per varying k_i and (b) Investment parameter per user ID

different pricing factors. It is shown that for higher pricing and higher values of k_i, i.e., more risk averse modeling, transmission power can significantly vary. For a steady pricing policy, as users become more risk averse, transmission power falls, since investment to the band becomes more costly, thus reducing congestion and competition within the unlicensed band.

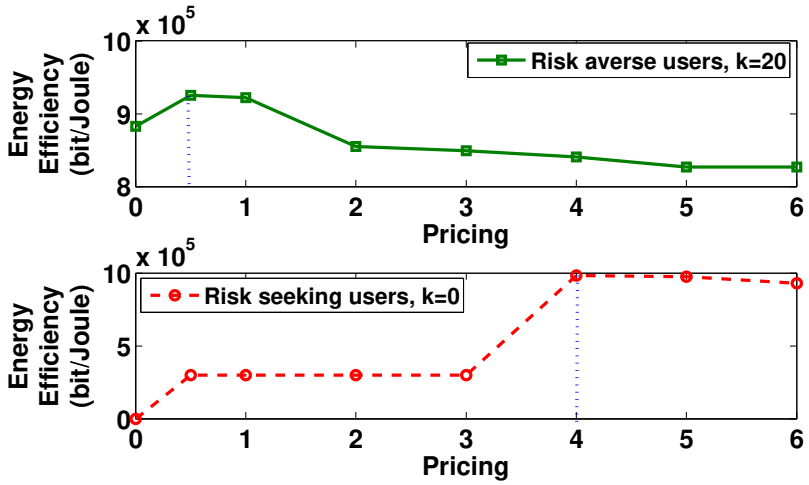

Figure 7.18: Energy-efficiency per pricing factor

The investment of each user with respect to different pricing values is presented in Fig. 7.17b, for a homogeneous value of k_i, ($k_i = 10$ for all users). When pricing is absent, all users invest the maximum of their power to the unlicensed band, hence eventually causing its failure. In this scenario, none of the users will transmit, since the unlicensed band fails due to over-exploitation, while the licensed band remains idle due to the fact that all users fully invested in the unlicensed spectrum. When pricing is introduced, users close or very far from the base station achieve their targeted QoS with low investment, stemming either from their favorable channel conditions, or the low interference. The latter is due to the Successive Interference Cancellation (SIC) property of NOMA, with each user decoding only signals from users with worse channel conditions. On the other hand, middle distance users invest more as they are simultaneously impacted by worsening channel conditions and rising interference levels. In overall, investment per user decreases when pricing rises, regardless of the position of a user in the network. In Fig. 7.18, the overall performance of the network is analyzed when pricing is applied with respect to energy-efficiency measured in bit/Joule. Risk averse users (upper plot) manage to optimize their performance for a relatively low pricing value. As pricing still rises, users radically reduce their investment in the unlicensed band, thus more traffic is routed to the limited licensed spectrum, therefore energy-efficiency falls. On the contrary, for risk seeking users, absence of pricing implies that the unlicensed band does not operate (i.e., fails) due to overinvestment. Gradually, as price levels increase, users transmit via the licensed band as well, while once the unlicensed presents reduced congestion the optimal allocation is achieved, this time for a much higher pricing value compared to the case of risk averse users.

Additionally, the impact of user mobility on its transmission characteristics, i.e., data rate and power, is examined. The duration of a timeslot is 0.5 $msec$, thus user's intracell mobility can be considered rather constrained per timeslot, and therefore it does not significantly affect the resource allocation process, and impact of pricing thereof. In order to gain some insight, we studied how user mobility influences user transmission for a time-window for movements up to 10 m. The results reveal that the change in pricing and rate allocation is negligible (practically 0%), whereas impact on power investment is very limited (approximately 0.1%), owing to slight changes in the relative channel gains. Also, the application of the NOMA SIC technique significantly mitigates interference, restricting the potential impact of user mobility on the overall interference, risk perceptions, and failure probability weighting.

7.6 General Summary

In this Chapter we provided a different perspective with respect to resource allocation problems by integrating the notions of resource fragility and user risk awareness of potential collapse of the involved resources due to over-exploitation. EUT, although extensively applied in wireless network optimization problems, lacks the sophistication to incorporate user subjectivity in decisions, hence, this work consists one of the first approaches to introduce the use of Prospect Theory in resource allocation problems in wireless networks. Prospect Theory has emerged as a powerful behavioral tool which manages to include uncertainty in user decision making which tends to violate rational behavior, since users overweight risks compared to gains.

As a result, in this part of the thesis user strategies and their unique preferences and assessment towards risk become the most crucial element in the effort to distribute resources in an efficient way and at the same time protect resources from collapse in cases of over-congestion or over-utilization. More specifically, the above theory is applied to allocate spectrum among users in wireless networks, which is split among different bands, a new trend and functionality emerging with the deployment of 5G networks. In order to model the problem in a realistic perspective, we consider that parts of the spectrum are considered as a closed access, *"safe resources"* delivering a stable (but low) return of investment, whereas the highest portion of the spectrum becomes available in an open access and commonly shared manner, known as *"Common Pool of Resources", (CPR)*, which are susceptible to failure if over-exploited. Users decide in which fraction of spectrum to invest by allocating part of their transmission power, while their utility functions are designed according to the prospect theoretic principles integrating their personal preferences towards risk aversion and sensitivity, creating a novel scheme with respect to how decision making becomes personalized and dependent on each user's transmission priorities.

In the first section, the subject of spectrum management in a wireless network supporting both licensed and unlicensed bands and operating under NOMA access technology was investigated, in line with rising trends in wireless networks to unlock additional sources of spectra by allowing the use of previously unregulated and unutilized bands of higher frequencies. Aiming at a pragmatic approach

towards resource management and decision making within this setting, the unlicensed band has been considered as a CPR, subject to the risk of collapse from potential over-exploitation, with the failure probability rising with user aggregate investment. Taking into account the potential interdependence of users' decisions with respect to their transmissions, the problem was treated as a non-cooperative fragile CPR game among the users, while its convergence to a unique Pure Nash Equilibrium has been proven, and an algorithm (i.e., ALLURE-U) that determines the optimal power investment of each user to the corresponding bands in a distributed manner, was designed. Detailed numerical results were presented highlighting the operation and superiority of the proposed framework, while providing useful insights about user decisions under realistic conditions and behaviors and demonstrating the benefits stemming from the proper shared optimization of both bands.

Following, motivated by the functionalities of modern intelligent mobile devices able to simultaneously transmit via multiple access techniques, we discuss a risk-aware transmission power control framework considering an environment supporting dual multiple access technology interfaces, that is both OFDMA and NOMA. The UEs invest their available transmission power to the NOMA transmission - treated as the CPR due to its commonly shared spectrum utilization - and/or the OFDMA transmission treated as the safe resource, as it splits the spectrum in distinct resource blocks - in order to facilitate their information transmission and satisfy their QoS prerequisites. The UEs exhibit risk-aware behavior while determining their optimal power investment, owing to the uncertainty of the perceived satisfaction due to the shared nature of the network's resources. The problem was again modeled as a fragile CPR non-cooperative power control game among the UEs under PT, confirming the existence and uniqueness of a Pure Nash Equilibrium (PNE) point as well as the convergence of the UEs' best response strategies to the PNE. The operation and performance of our proposed framework were extensively evaluated via modeling and simulation, while the presented detailed numerical results demonstrated its superior energy-efficiency and stability properties accounting for UEs' realistic behavioral scenarios.

In the last section of Chapter 7, the problem of protecting resource fragility was studied by examining the impact of resource pricing on spectrum utilization within a NOMA wireless network, supporting both licensed and unlicensed band access. Similarly to the first section of this Chapter, we treated the unlicensed band as the CPR which might collapse if over-exploited or not properly controlled, with the users exhibiting risk-aware behavior by sensing the probability of the unlicensed spectrum failure. The corresponding problem was solved this time via the principles of Prospect Theory and Fragile CPR non-cooperative games with pricing, and convergence to Nash Equilibrium was determined based on S-modular games. Eventually it was identified that the application of pricing can impact user decision making for preserving resource stability while efficiently managing spectral scarcity, an important achievement in view of the application of dynamic resource management in conditions of uncertainty and competition in wireless networks.

Chapter 8

Resource Management in Challenging Environments

8.1 General on Public Safety Networks

Public Safety Networks (PSNs) are utilized to ensure resilient and reliable exchange of data in disaster-struck areas (e.g., natural disasters, terrorist attacks). PSNs are expected to be deployed in extreme communication environments and are characterized by their fast deployment, adaptive operation, coverage guarantee, low latency, and extended energy availability for their users. Unmanned Aerial Vehicles (UAVs) support PSNs towards improving system adaptability and resilience by providing coverage extension, and enhanced bandwidth availability, while also gaining increasing research and commercial popularity due to their salient attributes such as flexible and effortless deployment, mobility, strong line-of-sight (LoS) connection links, adaptive altitude, low-cost, adjustable usage, and hovering ability [217, 218] especially during public safety threatening events [219].

Emphasizing on the usage of UAVs for wireless communications over existing network infrastructure, their main benefits and advantages include: cost effectiveness compared to a fixed ground base stations' deployment, low power requirements, maneuverability to improve the signal reception, enhanced connectivity, improved performance, massive data transmission, etc. [220]. Many key industrial vendors have invested on deploying UAVs to improve the wireless connectivity, especially in disaster-struck areas after a natural disaster has occurred. Compared to other alternative strategies such as the ones that provide ground movable base stations [221], UAV-based solutions bypass associated deployment inefficiencies due to possible physical ground infrastructure damages, while allow for more efficient communication with the rest of system (i.e., backhauling). Indicative examples include Facebook's Aquila UAV project [222] and Google's Project Loon, where the latter has deployed UAVs in a disaster response scenario in Puerto Rico [223]. This new reality motivates and demands the examination of the major challenging research problems of resource management and security in UAV-assisted wireless networks due to the critical missions that the UAVs can undertake.

8.2 Related Work on UAV-assisted PSNs

Among the key challenges related to the deployment and operation of the UAVs to support the communication demands in PSNs that have attracted significant interest in the literature are: (a) the intelligent resource management to support the PSNs' energy-efficient operation, and (b) the efficient bandwidth allocation to improve users' achievable data rate. Efficient resource management in UAV-assisted wireless networks affects various network performance metrics, such as connectivity, energy saving, throughput, coverage, and revenue. In [224], the authors formulate and solve a non-convex joint optimization problem towards determining the users' optimal transmission power, achievable data rate, the optimal position of the UAV, and the optimal bandwidth usage. In this case, the UAV acts as a relay, enabling the communication of the ground users with the macro base station (MBS), who are either far away from a base station or simply obstructed. Traditional PSN architectures that were based on dedicated cellular networks, such as the narrowband time-division multiple access (TDMA)-based Terrestrial Trunked Radio (TETRA) [225], and the Project 25, [226], require specialized hardware and offer low data rates [227],

and consequently they are even less used nowadays [220]. On the other hand in modern PSNs, UAVs are adopted to improve the wireless connectivity during a disaster, and this new reality motivates and demands the study of the dynamic spectrum management in UAV public safety networks, where the victims' communication-related decisions are taken under risk and uncertainty, stemming primarily from the scarcity of the communication resources and the limited only information availability. Moreover, UAV-assisted PSNs can target at various objectives, such as network's energy-efficient operation, prolongation of the humans' mobile devices' battery life [228], efficient bandwidth allocation to improve users' achievable data rate, or even addressing simultaneously several of the aforementioned challenges [143,229].

Furthermore, a centralized resource allocation problem is studied in [230], towards maximizing the overall users' throughput in a UAV relay system, while considering that the users adopt the NOMA technique for their communication. In [231], the problem of maximizing the uplink minimum throughput of all the ground users during a specific period of the UAV's flight is studied, while considering the UAV's maximum speed constraint and the users' energy availability. The problem of joint aerial-terrestrial resource management in mobile radio networks supported by a UAV is studied in [232], and the authors show that significant improvement in users' achievable data rate and energy-efficiency can be obtained, by properly optimizing the system's parameters related to the UAV flight.

The uplink resource allocation regarding the power and transmission timeslots allocation among the ground users is investigated in [233] to optimize the users' uplink sum rate. The authors decompose the joint sum rate optimization problem into the individual problems of energy allocation and transmission timeslots allocation, which subsequently are solved separately. Furthermore, in [234], the authors propose a game-theoretic mechanism for load balancing between Wi-Fi access points and LTE unlicensed base stations mounted on a UAV, utilizing a no-regret learning algorithm. The optimal location of a UAV when Device-to-Device (D2D) underlay links are present is studied in [235]. Moreover, in [236], a coalition formation mechanism among the users based on reinforcement learning is proposed, and the optimal UAV's position, energy harvesting levels of the users from the UAV, and the users' optimal transmission power are determined following a game-theoretic approach.

The theory of minority games is used in [237] to create clusters among the users based on their physical characteristics (energy availability, communication distance from the UAV) and determine their optimal transmission power to communicate with the UAV. A non-cooperative power control problem is formulated in [238] to calculate the users' optimal transmission power to the UAV in a distributed manner. In this model, the users create coalitions among each other by exploiting their socio-physical characteristics and following the Chinese Restaurant Process.

Moreover, the authors in [239] *(See Section 8.4)*, introduce a risk-aware resource management problem considering a static and a mobile UAV serving the ground users, and accordingly they determine the optimal power transmission of each user via a game-theoretic approach, in order to communicate with the two available receivers. This work is further extended in [240] *(See Section 8.3)* towards determining the users' optimal transmission power in order to communicate with the macro base station or the flying UAV, following a risk-aware analysis, where risk stems from the incomplete available information in the users' decision-making process. The authors in [241] focus on the application of structural inspection services assisted by the UAVs and they propose an algorithm to enable the Unmanned Aerial System to provide uninterrupted services considering the feasible flying time of the UAVs. In [242], the open challenges regarding the resource management problem in the UAV-assisted public safety systems are presented. Moreover, in [243] a zero-sum network interdiction game is formulated between a vendor, operating a drone delivery system, and a malicious attacker in order to study the cyber-physical security challenges in drone delivery systems. This work has been extended in [244] to study the cyber-physical security challenges of time-critical UAV applications.

Additional research efforts have been devoted to the problem of UAV positioning to improve the resource management process. In [245] the multi-UAV optimal placement to support the data aggregation in an Internet of Things (IoT) setting is examined. Also, the problem of UAV optimal positioning for system's throughput optimization is studied in [246], where a heuristic and an approximation method have been proposed.

On another note, the problem of detecting attacks in UAV-based communication networks has not been well addressed in the literature. UAVs are vulnerable to attacks, as they are highly exposed technical systems, while gaining illegitimate entry into the UAVs' operation and network can cause an enormous amount of losses regarding data confidentiality, money, and reputation. Wireless attacks are the most common form of UAVs' hacking, such as password theft, Wireshark, Global Positioning System (GPS) spoofing, man-in-the-middle attacks, Trojan horse viruses, and distributed denial of service (DDoS)

attacks [247]. A very well-known GPS spoofing example (however, the legitimacy of this attack has not been confirmed) occurred in 2011, when an Iranian engineer reported that they have spoofed false GPS coordinates to a US UAV, and they guided it to land safely on an Iranian airfield [248]. Examples and events like that raise concerns regarding the state of UAV-based communication security. Some indicative mechanisms in order to detect and/or defend against the hacking of the UAVs are: encryption and cryptography, anomaly detection, defense techniques against DDoS attacks, and the development of intrusion detection (IDS) and intrusion ejection systems (IES) [249].

In [250], a risk assessment scheme for UAVs is developed based on the UAVs' provided services, equipped communication infrastructures and sensor systems, as well as the existing UAVs' fault handling mechanisms. In [251], the authors discuss the security and privacy challenges of the UAVs' systems and networks. In [252], the Bayesian game theory is adopted to design an intrusion detection system (IDS) for monitoring the network and an intrusion ejection system for excluding the malicious nodes that are anticipated to instigate an attack is presented. In [253], the authors proposed a differential game-theoretic approach to determine the optimal strategies of multiple UAVs evading the attack of an aerial jammer on the communication channel. In [254], an intrusion detection and response scheme is implemented focusing on the most lethal cyber-attacks (i.e., false information dissemination, GPS spoofing, jamming, and black and gray hole attacks) and identifying the UAVs' behavior as normal, abnormal, suspect, or malicious. In [255], the authors introduce a prototype UAV monitoring system that captures UAVs' flight data and it detects anomalies by performing real-time behavioral modeling. A survey summarizing the state of the art intrusion detection systems which identify attacks under networked UAV environments is presented in [256], while in [257], a survey of the game-theoretic approaches that study UAV-assisted wireless communication network security is introduced.

It is noted that advanced devices have already become available in the market in recent years [11,258], which can opportunistically access and utilize bandwidth resources even from distinct cells or providers. Such a multi-communication interface environment immensely modifies the flexibility enjoyed by the users who are not restricted in selecting only one receiver but can proportionally split their invested transmission power to multiple ones. The above assumptions are largely used in the following sections as a means of streamlining the operation of PSNs where multiple UAVs are simultaneously considered as alternative spectrum sources.

8.3 On the Prospect of UAV-assisted PSNs

The previous examined research works have demonstrated that the UAV provides additional bandwidth and communication flexibility to the users. The majority of the literature has regarded that the users in PSNs act as neutral expected utility maximizers, thus the Expected Utility Theory (EUT) has been used to solve the emerging resource management problems [209], where implicitly or explicitly the users in a PSN, i.e., victims and first responders, make decisions regarding their communication in a rational manner aiming at maximizing their perceived Quality of Service (QoS). However, this does not hold true in real PSNs, where users make decisions: a) under risks introduced by the extreme and uncertain communication environment, the limited information availability and bandwidth limitations and b) based on their personal characteristics and reactions under risks.

Despite the extensive existing literature with respect to the resource allocation problem in UAV-assisted PSNs, to the best of our knowledge, the resource orchestration considering users' risk-aware behavior in terms of communicating either over the UAV and/or the MBS has not been studied so far. The novelty of this work is the design of a novel flexible users' power control framework, where the users exploit both the MBS and UAV, while exhibiting risk-based behavior. The goal of the proposed framework is to enable the rethinking of the QoS provisioning problem in the UAV-assisted PSNs via opportunistically exploiting any available communication alternative of the users, while capturing their realistic risk-aware behavior in the PSNs extreme communication environment.

The bandwidth's fragility in the UAV-based communication is examined regarding its exploitation by the users. Based on the above, a user-centric power control problem is formulated as a maximization problem of each user's expected prospect-theoretic utility, and it is confronted as a non-cooperative game. The specific decision at stake refers to the users' investment of their transmission power in the two available communication alternatives. The existence and uniqueness of a Pure Nash Equilibrium (PNE) is shown and the convergence of the users' power strategies to the unique PNE is proven delivering an optimal allocation in terms of users' transmission power investment, achievable data rate, and fragility

of the UAV's available bandwidth stemming from users' risk-aware behavior on the system's operation. Moreover, the concept of the freshness of information is adopted and numerically evaluated, in order to capture the need and criticality of fast data exchange that can be achieved through the UAV-based communication, and thus contribute to the greater rate of return and corresponding satisfaction for the users.

8.3.1 System Model

In the UAV-assisted PSN, each ground user $i, i \in N$, where N denotes the set of users, can communicate over the UAV and/or the MBS. The UAV-based communication is characterized by limited available bandwidth (as the UAV acts as an ad-hoc communication solution in the disaster area) compared to the MBS-based communication. However, due to the UAV's proximity to the users and respectively improved channel gain, the UAV-based communication becomes more attractive to them as they can achieve higher data rates with lower transmission power. Similarly, the close distance between the users and the UAV contributes to the fast exchange of data, thus, improving the *freshness of information*, which is critical in many requested services especially during a catastrophic event. Thus, the available bandwidth in the UAV-based communication is considered in this case as the CPR, since it is non-excludable (i.e that is accessible by all users), rivalrous, and subtractable, prone to failure due to increased interference at the receiver.

In contrast, the MBS usually resides far away from the majority of the users and higher transmission power levels are required by the ground users to achieve their QoS satisfaction. Thus, the MBS-based communication becomes less attractive as it results to lower energy-efficiency transmissions. On the other hand, assuming that usually a greater portion of bandwidth is available by the MBS to support the ground users' communication and considering that more processing capabilities are offered by the MBS, in our system model the MBS's available bandwidth is treated as the safe resource alternative, due to the fact that each user can obtain a guaranteed level of QoS given its personal characteristics (e.g., channel gain, transmission power).

Within the considered UAV-assisted PSN, each user $i, i \in N$ has a maximum transmission power P_i^{Max}, which is invested to the UAV and MBS-based communication towards fulfilling its QoS demands. Each user's goal is to determine in an autonomous manner its transmission power investment, $(x_i, x_i \in [0,1])$ to the UAV-based communication P_i^{UAV} and to the MBS-based communication P_i^{MBS}, hence, $P_i^{UAV} = x_i P_i^{Max}$ and $P_i^{MBS} = (1 - x_i) P_i^{Max}$.

The ground users are assumed to exhibit risk-aware behavior towards determining their transmission power levels P_i^{UAV}. This behavior stems from the uncertainty of the outcome and the enjoyed QoS, due to the UAV's limited available bandwidth, communication traffic congestion, and the increased interference. To capture users' risk-aware behavior, we follow the Prospect Theory principles, and the users' prospect-theoretic utility $\mathscr{U}_i(y_i)$ is defined accordingly to equations (7.1) and (7.22), [171] from previous sections, where $y_i(x_i, x_T)$ indicates the user's i actual utility and x_T is the total power investment to the UAV-based communication.

The users' satisfaction is determined with respect to a reference point $y_{0,i}$, [171], which is considered as the ground truth of the users' actual utility $y_i(x_i, x_T)$. We define $y_{0,i} \triangleq \frac{B_{MBS}/N_{MBS}}{P_i^{MBS}} ln(1+\gamma_i^{MBS}), \forall i \in N$, as the achieved energy-efficiency, if the users were exploiting only the safe resource (transmission only to the MBS), where B_{MBS} is the MBS's bandwidth, N_{MBS} the number of users transmitting to the MBS, $\gamma_i^{MBS} = \frac{B_{MBS}}{R_i^{MBS}} \frac{h_i^{MBS} P_i^{MBS}}{\sum_{j>i} h_j^{MBS/UAV} P_j^{MBS/UAV} + \sigma^2}$ represents the user's i Signal-to-Interference-plus-Noise Ratio (SINR), R_i^{MBS} is the users' requested service data rate, h_i^{MBS} reflects the user's channel gain to the MBS, $\sum_{j>i} h_j^{MBS/UAV} P_j^{MBS/UAV}$ is the interference considering the NOMA technique, and σ^2 is the variance of the noise power.

As previously, we denote user's sensitivity to the gains and losses of its actual utility $y_i(x_i, x_T)$, via the parameters $\lambda_i, \mu_i \in (0, 1]$ respectively. The risk seeking behavior of a user in losses and its risk averse behavior in gains is reflected by small values of the parameter λ_i. Small values of parameter μ_i imply higher decrease of user's prospect-theoretic utility for small values of y_i and close to the reference point $y_{0,i}$. Without loss of generality, we assume $\lambda_i = \mu_i$. Moreover, $k_i, k_i \in [0, +\infty)$ reflects the already mentioned loss aversion parameter.

If the UAV's bandwidth is not over-exploited (CPR survives), the user enjoys the utility (measured in energy-efficiency units) of transmitting data to the MBS (first term of Eq. (8.1)) and the UAV (second

term of Eq. (8.1)) as follows.

$$y_i(x_i, x_T) = y_{0,i}(1 - x_i) + E_i x_i \mathfrak{R}(x_T) \tag{8.1}$$

where $E_i = \frac{B_{UAV}/N_{UAV}}{P_i^{UAV}} ln(1+\gamma_i^{UAV})$, B_{UAV} is the UAV's bandwidth, N_{UAV} is the number of users transmitting to the UAV, and $\gamma_i^{UAV} = \frac{B_{UAV}}{R_i^{UAV}} \frac{h_i^{UAV} P_i^{UAV}}{\sigma^2 + \sum_{j>i} h_j^{MBS/UAV} P_k^{MBS/UAV}}$ reflects the user's i SINR measured at the UAV. The function $\mathfrak{R}(x_T)$ represents the rate of return of the UAV-based communication to the users, which is a decreasing concave function with respect to $x_T = \sum_{i=1}^{N} x_i$. For demonstration purposes, the rate of return $\mathfrak{R}(x_T)$ of the CPR is formulated as follows:

$$\mathfrak{R}(x_T) = 2 - e^{x_T - 1} \tag{8.2}$$

The UAV spectrum has a probability of failure $Pr(x_T)$ (CPR's fragility), which is increasing with respect to users' aggregate power investment x_T. In the following, we consider $Pr(x_T) = x_T^2$ and x_T is considered normalized. If the CPR survives, then each user perceives an actual utility (Eq. (8.1)) greater than the reference point ($y_i > y_{0,i}$). Via subtracting the reference point $y_{0,i}$ from the actual utility (Eq. (8.1)), and shaping the result according to the first branch of $\mathscr{U}_i$ *(See Eq. (7.1) and (7.22))* we have $\mathscr{U}_i(x_i) = x_i^{\lambda_i}[E_i \mathfrak{R}(x_T) - y_{0,i}]^{\lambda_i}$. For the simplicity of the notation, we normalize the rate of return function, so that $y_{0,i} = 1$, and denote $\overline{\mathfrak{R}_i}(x_T) \triangleq (E_i \mathfrak{R}(x_T) - 1)^{\lambda_i}$, where $\overline{\mathfrak{R}_i}(x_T)$ is concave, decreasing, twice continuously differentiable, and positive. Thus, $\mathscr{U}_i(x_i) = x_i^{\lambda_i} \overline{\mathfrak{R}_i}(x_T)$. On the other hand, if the UAV's bandwidth is over-exploited by the users' transmissions, then no user receives any satisfaction from its transmission to the UAV. Thus, the second term of Eq. (8.1) becomes zero and the users enjoy the transmission only to the MBS. In this case, the actual utility is $y_i \leq y_{0,i}$, thus, by subtracting the actual utility from the reference point and reshaping the result based on the second branch of PT utility $\mathscr{U}_i$, we have $\mathscr{U}_i(x_i) = -k_i x_i^{\lambda_i}$.

Based on the previous analysis, the ground users' prospect-theoretic utility function can be rewritten as follows.

$$\mathscr{U}_i(x_i) = \begin{cases} {x_i}^{\lambda_i} \overline{\mathfrak{R}_i}(x_T) & if\ y_i > y_{0,i} \\ -k_i x_i^{\lambda_i} & otherwise \end{cases} \tag{8.3}$$

Given the CPR's probability of failure $Pr(x_T)$, the probability that the UAV's bandwidth serves the users is $(1 - Pr(x_T))$. As a result, Eq. (8.3) can be written equivalently as:

$$\mathscr{U}_i(x_i) = \begin{cases} {x_i}^{\lambda_i} \overline{\mathfrak{R}_i}(x_T) & with\ prob.\ (1 - Pr(x_T)) \\ -k_i x_i^{\lambda_i} & with\ prob.\ Pr(x_T) \end{cases} \tag{8.4}$$

8.3.2 Problem Formulation and Solution

The sophisticated design of the prospect-theoretic utility functions sufficiently represents real life outcomes of ground users' operation in the UAV-assisted PSNs. In view of this realization, user behavioral modeling and actions become the key element for the self-optimization of the PSN. The users incorporate multiple parameters in shaping their strategic decision-making (e.g., QoS, transmission power, probability of CPR failure, heterogeneous risk and gain perceptions etc.) and define their expected prospect-theoretic utilities, under a probabilistic perspective, as follows.

$$\mathbf{E}(\mathscr{U}_i) = {x_i}^{\lambda_i} \overline{\mathfrak{R}_i}(x_T)(1 - Pr(x_T)) - k_i x_i^{\lambda_i} Pr(x_T) \tag{8.5}$$

Subsequently, the optimization of the operation of the PSN via the resource allocation and simultaneous risk management is formulated as a distributed Prospect-theoretic Autonomous Resource Investment maximization problem for public Safety (PARIS) maximization problem:

PARIS Game

$$\begin{gathered} max \mathbf{E}(\mathscr{U}_i) = max\{x_i^{\lambda_i} f_i(x_T)\},\ \forall i \in N \\ s.t.\ x_i \in [0, 1] \end{gathered} \tag{8.6}$$

Table 8.1: Section 8.3 list of key notations

Symbol	Description
N	Set of users
P_i^{Max}	Maximum transmission power
x_i	Power investment to its transmission to UAV
P_i^{UAV}	Transmission power to UAV
P_i^{MBS}	Transmission power to MBS
$\mathscr{U}_i(y_i)$	PT utility
x_T	Aggregate investment
$y_i(x_i, x_T)$	Actual utility
$y_{0,i}$	Reference point
B_{MBS}, B_{UAV}	UAV's and MBS's bandwidth
N_{MBS}, N_{UAV}	Number of users transmitting to MBS and UAV
γ_i^{MBS}, γ_i^{UAV}	SINR measured at MBS and UAV
R_i	Requested service data rate
h_i	Channel gain to MBS
σ^2	Variance of noise power
λ_i, μ_i	Sensitivity to the gains and losses of actual utility
k_i	Loss aversion parameter
E_i	Auxiliary constant
$\mathfrak{R}(x_T)$	Rate of return of the UAV-based communication
$Pr(x_T)$	Probability of failure
$\overline{\mathfrak{R}_i}(x_T)$	PT rate of return
$\mathbf{E}(\mathscr{U}_i)$	Expected PT utility
$f_i(x_T)$	Effective rate of return
Γ	Fragile CPR Game
$\mathscr{X}_i$	User's investment strategy
$\mathbf{x}^*$	Optimal investment vector
b_i	Best response
$\overline{\mathscr{X}}_{-i}$	Aggregate investment space excluding user i
ϱ	Maximum point of $\mathbf{E}(\mathscr{U}_i)$
$\phi(x_i)$	Auxiliary function
ξ	Root of $\phi(x_i)$
$\mathscr{X}_i'$	Reduced strategy space
$\mathscr{I}(x_T)$	Optimal nonzero investment
t_i	Freshness of information

where $f_i(x_T) = \overline{\mathfrak{R}_i}(x_T)(1 - Pr(x_T)) - k_i Pr(x_T)$ corresponds to the user's effective rate of return. All parameters from this section are summarized in Table 8.1.

The above problem can be treated and solved as a *Fragile CPR game* which captures not only the rising opportunity of supporting the performance of the PSN via the commonly shared bandwidth of the UAV, but also the potential implications of resource fragility. A Fragile CPR game is defined as $\Gamma = [N, \{\mathscr{X}_i\}_{i\in N}, \{\mathscr{U}_i\}_{i\in N}]$, where each user's strategy is $\mathscr{X}_i \in [0, 1]$. In Fragile CPR games, the probability of resource failure $Pr(x_T)$ is considered convex, increasing, and twice continuously differentiable with respect to x_T.

In this work as well, the notion of Pure Nash Equilibrium *(PNE)* provides a stable and predictable solution for the non-cooperative game, under which no user has the incentive to deviate from the concluded strategy, since its utility cannot be improved by a unilateral strategy change, given that the strategies of all other users remain unmodified. For game Γ, the PNE is the optimal investment vector $\mathbf{x}^* = \{x_i^*\}$ such that $\mathscr{U}_i({x_i}^*, \mathbf{x}_{-i}^*) \geq \mathscr{U}_i(x_i, \mathbf{x}_{-i}^*)$, $\forall x_i \in \mathscr{X}_i$, under which the UAV's bandwidth does not collapse and the users enjoy sufficient returns through their transmission to the UAV.

Concerning the best response of the investigated topic, b_i is considered as the strategy of each user

providing the most favorable outcome given the actions of the other users, and is defined as, $b_i(\mathbf{x_{-i}}) = argmax\mathbf{E}(\mathscr{U}_i(x_i, \mathbf{x_{-i}}))$, $b_i : \overline{\mathscr{X}}_{-i} \rightrightarrows \mathscr{X}_i$, where $\overline{\mathscr{X}}_{-i}$ represents aggregate investment space excluding user i. For the game Γ, $0 < b_i < 1$ reflects a joint transmission scheme to the MBS and the UAV, whereas $b_i = 1$ indicates a failure state of the UAV's bandwidth, since all users transmitted their data directly to the UAV.

Theorem 45. ***(Global Maximum Point of PT utility:)*** *There exists at least one point $\varrho \in \mathscr{X}_i$ which is a maximum point $\boldsymbol{E}(\mathscr{U}_i)$.*

Proof. An extremal point for $\mathbf{E}(\mathscr{U}_i)$ can be identified by applying the first order derivative criterion:

$$\frac{\partial \mathbf{E}(\mathscr{U}_i)}{\partial x_i} = {x_i}^{\lambda_i - 1}\phi(x_i) = 0 \tag{8.7}$$

where $\phi(x_i) = (x_i f_i'(x_T) + \lambda_i f_i(x_T))$. Towards facilitating the study of the above equation, we first examine $f_i(x_T)$ and its behavior. Since $\overline{\mathfrak{R}_i}(x_T)$ is decreasing and concave, then $f_i(x_T) = \overline{\mathfrak{R}_i}(x_T)(1 - Pr(x_T)) - k_i Pr(x_T)$ is proven to be decreasing and concave for $E_i > 1$, $\lambda_i < 0.5$, i.e., $\frac{\partial f_i(x_T)}{\partial (x_T)} < 0$, $\frac{\partial^2 f_i(x_T)}{\partial x_T^2} < 0$. By examining the monotonicity of $f_i(x_T)$, we observe that it changes its sign from positive to negative within $(0, 1)$, hence there exists a unique value $\xi \in (0, 1)$ such that $f_i(\xi) = 0$. By considering the above, from (8.7), $\phi(x_i)|_{x_i=0} > 0$ and $\phi(x_i)|_{x_i=\xi} < 0$, since $f_i' < 0, \forall x_i \in \mathscr{X}_i$ and $f_i(\xi) = 0$. As a result, by applying and extending Bolzano's theorem for $\frac{\partial \mathbf{E}(\mathscr{U}_i)}{\partial x_i}$, there exists at least one extremal point $\varrho \in (0, \xi)$ for $\mathbf{E}(\mathscr{U}_i)$ such that $\frac{\partial \mathbf{E}(\mathscr{U}_i)}{\partial x_i} = 0$.

□

Lemma 46. ***(PARIS Game Existence of PNE:)*** *The extremal point ϱ in the reduced strategy space $\mathscr{X}_i' = (0, \xi)$ is a local maximum point for $\boldsymbol{E}(\mathscr{U}_i)$ and is identified as a PNE of game Γ.*

Proof. We apply the second order derivative criterion for $\mathbf{E}(\mathscr{U}_i)$, that is, $\frac{\partial^2 \mathbf{E}(\mathscr{U}_i)}{\partial x_i^2} = \lambda_i(\lambda_i - 1){x_i}^{\lambda_i - 2} f_i(x_T) + 2\lambda_i {x_i}^{\lambda_i - 1} f_i'(x_T) + {x_i}^{\lambda_i} f_i''(x_T)$. By tracking the sign of all terms of the above equation, we observe that in the reduced space $\mathscr{X}_i'$ are negative, and hence $\mathbf{E}(\mathscr{U}_i)$ is concave, that is $\frac{\partial^2 \mathbf{E}(\mathscr{U}_i)}{\partial x_i^2} < 0$ and ϱ is a local maximum of $\mathbf{E}(\mathscr{U}_i)$. □

Theorem 47. ***(PARIS Game PNE Uniqueness:)*** *The point $\varrho \in \mathscr{X}_i'$ is a unique PNE for the game Γ.*

Proof. Since $\mathbf{E}(\mathscr{U}_i)$ is concave, $\frac{\partial \mathbf{E}(\mathscr{U}_i)}{\partial x_i}$ is decreasing in $\mathscr{X}_i'$. Hence, the point ϱ, $(\frac{\partial \mathbf{E}(\mathscr{U}_i)}{\partial x_i}|_{x_i=\varrho} = 0)$ is unique due to the monotonicity of $\frac{\partial \mathbf{E}(\mathscr{U}_i)}{\partial x_i}$ and ϱ is a unique global maximum point for $\mathbf{E}(\mathscr{U}_i)$ and Γ admits a unique PNE. □

Theorem 48. ***(PARIS Game Decreasing Best Responses:)*** *Convergence of game Γ to its unique PNE is established if b_i is decreasing in x_T [172].*

Proof. We determine optimal nonzero investment of a player as $\mathscr{I}(x_T) = -{\lambda_i f_i(x_T)}/{f_i'(x_T)}$ for which $\mathscr{I}(b_i(\mathbf{x_{-i}}) + \mathbf{x_{-i}}) = b_i(\mathbf{x_{-i}})$, when $b_i(\mathbf{x_{-i}}) > 0$. It is proven that $\mathscr{I}'(x_T) < 0$, thus, $\mathscr{I}$ is decreasing. We assume $x_1 = b_i(\mathbf{x_{-1}})$, $x_2 = b_i(\mathbf{x_{-2}})$, with $\mathbf{x_{-1}}, \mathbf{x_{-2}} \in \overline{\mathscr{X}'}_{-i}$. If b_i is increasing, then for $x_2 > x_1$, then $b_i(x_{-2}) > b_i(x_{-1})$. However, due to $\mathscr{I}$ being decreasing, for $x_2 > x_1$, $\mathscr{I}(b_i(\mathbf{x_{-2}}) + \mathbf{x_{-2}}) = b_i(x_{-2}) < b_i(x_{-1}) = \mathscr{I}(b_i(\mathbf{x_{-1}}) + \mathbf{x_{-1}})$, which is a contradiction. Hence, b_i is decreasing in x_T. □

8.3.3 Distributed Algorithm

In this section, we introduce a low complexity and iterative **P**rospect-theoretic **A**utonomous **R**esource **I**nvestment algorithm for public **S**afety (*PARIS*) which determines the PNE of the game Γ. The primary novelty of the algorithm lies in the multifaceted execution of different actions of distinct network stakeholders during the investment and resource allocation phases, allowing for decision decentralization which enables the self-optimization dynamics of the network. Each user interacts with the UAV and independently defines its investment to the UAV's bandwidth, stemming from its prospect-theoretic modeling, as described above. As the system evolves, PARIS confirms the convergence of the UAV-assisted PSN to a stable operational point, or announces the collapse of UAV's bandwidth due to excessive user resource demand.

Algorithm 20 PARIS Algorithm

Require:
UAV, MBS, user coordinates & $B_{MBS/UAV}, k_i, \lambda_i$
$step \leftarrow 1$; $UAV_{fails}^{(step)} \leftarrow 0$; $UAV_{active}^{(step)} \leftarrow 0$
Calculate $h_i^{MBS/UAV}$, apply SIC, set random $x_i^{(step=1)}$
while $UAV_{fails}^{(step)} = 0$ **and** $UAV_{active}^{(step)} = 0$ **do**
  Calculate $P_i^{MBS/UAV}$; $\mathbf{E}(\mathscr{U}_i)^{(step)}$;
  for all $x_i \in [0, 1]$ **do**
    x_i^*=$argmax_{x_i}\mathbf{E}(\mathscr{U}_i)$
    if $\mathbf{E}(\mathscr{U}_i) > \mathbf{E}(\mathscr{U}_i)^{(step)}$ **then**
      $x_i^{(step+1)} \leftarrow x_i^*$ **and** $\mathbf{E}(\mathscr{U}_i)^{(step+1)} \leftarrow \mathbf{E}(\mathscr{U}_i)$
    end if
  end for
  if $\sum R_i^{UAV} > B_{UAV}$ **then**
    $UAV_{fails}^{(step+1)} \leftarrow 1$
  end if
  if $x_i^{(step+1)} - x_i^{(step)} < \epsilon$ **then**
    $UAV_{active}^{(step+1)} \leftarrow 1$
  end if
  $step \leftarrow step + 1$
end while
return
User investment x_i and UAV_{fails} if PSN has failed

8.3.4 Numerical Results

Experiment Setup and User Behavior Analysis

In this section, we provide an extensive numerical evaluation of the operating features and the performance of the presented prospect-theoretic framework in the UAV-assisted PSNs via modeling and simulation. We consider a UAV-assisted PSN topology with 20 ground users. The MBS-based network covers an area of approximately 6 km, whereas the UAV hovers close to the users (from 0.2 to 1.5 km) ensuring more reliable connections and superior channel gain conditions, both operating under the NOMA transmission technique. The total available bandwidth is 4 MHz, 70% of which is offered by the MBS and the remaining fraction becomes available from the UAV. We set $P_i^{Max} = 0.2$ $Watts$ and the users request emergency services, e.g., $R_i^{UAV} = 64$ $kbps$. We examine the case where the UAV is located above a homogeneous population with respect to the users' risk preferences and behaviors ($\lambda_i = 0.1$ and $k_i = 20$). Specifically, Fig. 8.1 shows the users' achieved data rate from the UAV and MBS-based communication versus their distance from the MBS. It is shown that only the users closer to the MBS manage to achieve high data rates from the MBS, due to their good channel gain conditions, taking advantage of the highly MBS's under-exploited bandwidth, while the more distant ones do not manage to transmit via the MBS at all. On the contrary, all the users exchange data with the UAV, due to its close proximity and superior communication channel gains. The impact from the application of the Successive Interference Cancellation technique in the NOMA communication environment is evident, with the users farthest away (deteriorated communication channel conditions) to successfully operate due to the absence of interference. Regarding the users' investment to the UAV-based communication, in Fig. 8.2a it is shown that users closer and farthest away from the UAV do not need to invest heavily in the CPR since they achieve to obtain their target data rates by taking advantage of the NOMA communication environment. On the other hand, middle distant users from the UAV, select to fully invest their transmission power in the UAV-based communication, however they still do not reach their target data rate since they are simultaneously impacted by the high interference levels and the limited UAV's bandwidth.

Following, we modify users' behavior regarding their risk aversion perception, reflected via $k_i = k$. Fig. 8.2b presents users mean transmission power and energy-efficiency for increasing values of k. For low values of k, users underestimate the CPR's probability to fail and transmit with maximum power to communicate with the UAV, leading to the inevitable collapse of the UAV's bandwidth due to its

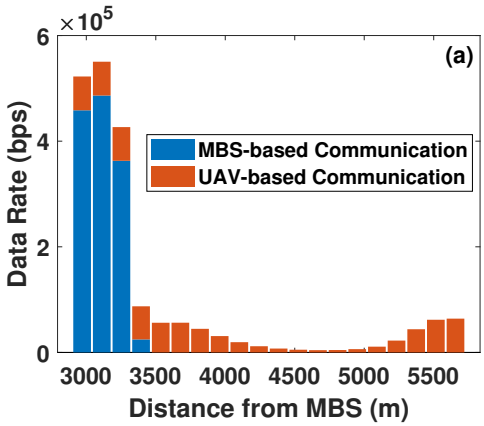

Figure 8.1: Users' data Rate vs Distance from the MBS

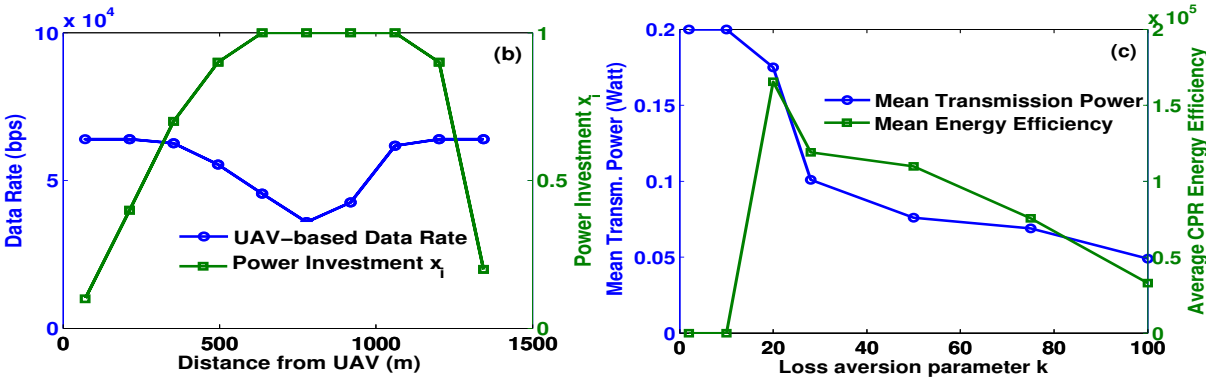

(a) (b)

Figure 8.2: (a) Users' data rate and power investment vs distance from the UAV, and (b) mean transmission power and average CPR energy-efficiency vs loss aversion parameter k

over-exploitation, thus, energy-efficiency is zero since users are practically unable to communicate. With the gradual increase of k, users become more conservative, hence, their transmission power decreases and the CPR does not fail with energy-efficiency reaching its highest average value, since the UAV bandwidth is fully utilized. For even higher values of k, users further reduce their investment to the CPR as they become more risk averse and subsequently their energy-efficiency decreases.

UAV Positioning

In this subsection we examine impact of UAV's positioning on the overall system performance, by allowing UAV to re-position itself above the users towards improving the communication efficiency of the PSN. Specifically, in Fig. 8.3a, we study users' average power investment and average data rates for increasing average distance of the UAV from the users. We conclude that when the UAV has greater proximity to the examined population, the users invest less power to their UAV-based communication, since their favorable channel conditions ensure that they can sufficiently communicate with the UAV. However, as the UAV moves away (especially when the average distance surpasses 1 km), the users' power investment x_i increases rapidly, while the average attainable data rates significantly decrease.

The same hold true in Fig. 8.3b as well, where we observe that the average energy-efficiency of all users significantly deteriorates with the increase of the distance of the UAV from the users, since the average energy-efficiency decreases by 67.27% at 1.5 km when compared to an average distance of 0.7 km.

Freshness of Information

When considering special multimedia services during the public safety events, e.g., geolocation data collection, evacuee coordinates report, etc., the freshness of the transmitted information to the UAV

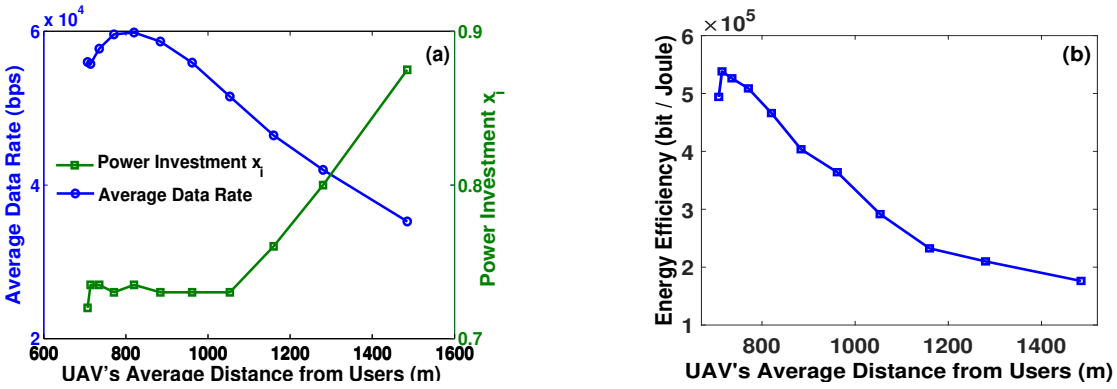

(a) (b)

Figure 8.3: (a) Average data rate and power investment, and (b) Energy-efficiency, vs UAV's average distance from the users.

or the MBS becomes of high criticality. Given that the UAV is located close to the users, the latter are attracted to transmit their data to the UAV, since in addition to the significantly better channel conditions, the information may arrive to the UAV much faster, when compared to the MBS that is located far away from the ground users, resulting in high transmission and propagation delays. To capture the impact of the information freshness, we introduce the parameter $t_i, t_i \in [0, +\infty)$, in the CPR's rate of return (Eq. (8.2)), which is reformulated accordingly as follows: $\mathfrak{R}(x_T) = t_i(2 - e^{x_T - 1})$. If $t_i = 1$, this means that the freshness of information is not critical for the ground user i, while if $t_i > 1$, the user enjoys superior satisfaction from sending its data to the UAV in a fast manner. Fig. 8.4 shows that when the parameter $t_i = t, \forall i \in N$ representing that the PSN importance of information freshness increases, the average user perceived utility from the UAV-based communication (first term of Eq. (8.5)) as well as the users' power investment to the UAV increase. As a result, users have the incentive to invest more in the UAV-based communication not only due to the more favorable channel conditions, but also due to the importance of the data from this transmission. However, as the value of the parameter t further increases, this can lead to the imminent collapse of the UAV's bandwidth, since users' aggregate investment surpasses the capacity of the UAV to meet total demand.

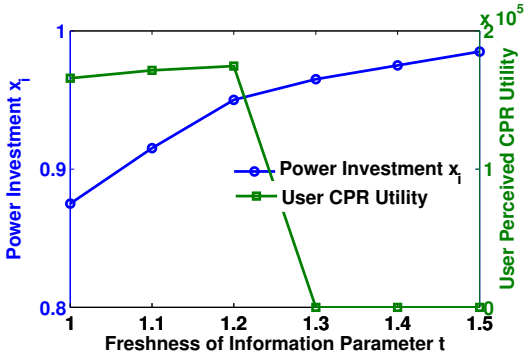

Figure 8.4: Users' power investment and CPR perceived utility as a function of the freshness of information parameter t

8.4 Dynamic Spectrum Management in multi UAV-assisted PSNs

This part of the thesis extends the problem of uplink energy-efficient resource allocation in UAV-assisted PSNs considering users' risk-aware behavior in terms of communicating over a mobile UAV and/or a static UAV that hovers above the disaster-struck area. The static UAV hovers above an area in a specific altitude, i.e., 1000 m acting as a flying base station. Examples of static UAVs are the Boeing Insitu

ScanEagle [259], and the Aerovel Flexrotor [260]. The mobile UAV also flies in a specific altitude, but closer to the end-users, i.e., 360 m. Examples of mobile UAVs are the AeroVironment RQ-11 Raven [261] and WASP AE Micro Air Vehicle [262]. The users exploit their devices' dual communication interface to transmit their data to the two available receivers, i.e., static and mobile UAV, thus realizing a dynamic spectrum management. The static UAV hovers above the disaster area having a smaller portion of the total spectrum available to serve the users' QoS requirements compared to the mobile UAV, based on the spectrum allocation that the Emergency Control Center (ECC) has planned. A representative high-level topology of the considered UAV-assisted PSN is presented in Fig. 8.5. The aforementioned spectrum allocation is motivated by the fact that the mobile UAV has greater probability to fly closer to the users compared to the static UAV, thus the greater portion of allocated spectrum enables the mobile UAV to better serve the users, who have improved channel conditions when communicating with the mobile UAV compared to the static UAV.

Adopting such a multi-UAV environment delivers additional flexibility in the design of wireless networks which can accommodate larger areas or regions with significant topological constraints where infrastructure is not available or has been damaged. By allowing users to weigh the risks and connect to more than one of the UAVs, wireless networks can be instantly established serving users with urgent needs where limited service coverage is provided. Moreover, due to the mobility potential and the ability to split spectrum in UAV-assisted networks, additional means to optimize network performance can be identified towards improving user experience and resource utilization.

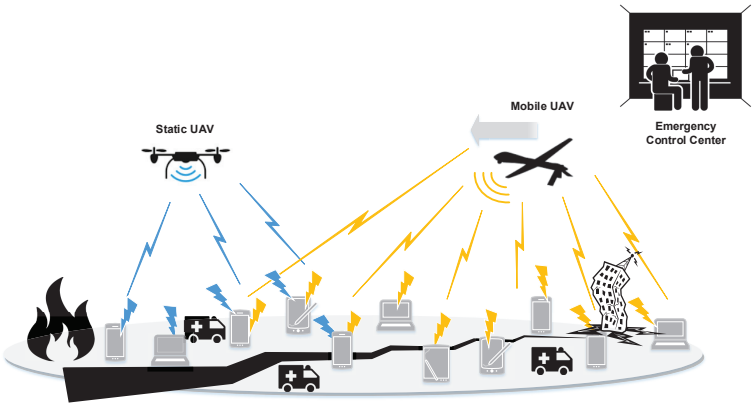

Figure 8.5: UAV-assisted public safety network topology

8.4.1 System Model

A PSN at this part is considered consisting of a static UAV s that hovers in a fixed position above the disaster-struck area, and a mobile UAV m that moves over the disaster area to better serve the users, i.e., victims and first responders. The disaster area has dimensions $L \times L$ $[m^2]$ and the set of users is denoted as $U = \{1, \ldots, u, \ldots, |U|\}$. Each user is assumed to be equipped with dual communication interface devices capable of transmitting data to the two available receivers (i.e., mobile and static UAV) simultaneously, if needed. The Emergency Control Center (ECC) allocates a portion y (where $0 \leq y \leq 1$) of the overall available spectrum W to the static UAV, while the rest of the available spectrum for the public safety operations is allocated to the communication through the mobile UAV, i.e., $(1-y)W$. Typically a larger portion of spectrum is allocated to the mobile UAV compared to the static one, due to the fact that given the capability and flexibility of movement the mobile UAV has better chances to be closer to the users compared to the static UAV. Noting that the mobile UAV flies at a lower altitude compared to the static UAV, the users are expected to experience superior channel conditions by communicating with the mobile UAV. The latter in combination with the greater available spectrum allocated to the mobile UAV, will result in improved QoS for the users that will be associated with the mobile UAV. Given this setting, the mobile UAV acts as the Common Pool of Resources since all the users will be keen on communicating through it. Therefore, the mobile UAV may fail to serve users due to the increased levels of interference, if the users over-exploit their communication through the mobile UAV. On the other hand, the static

UAV acts as the "safe resource" providing more predictable rewards to the users due to the lower levels of interference, as the users tend to invest low levels of transmission power to communicate with it due to the limited returns (i.e., data rate) that they can achieve through this type of communication, and due to the fact that the channel conditions remain almost the same over the time given that both the UAV and the trapped users in the disaster area are static. A representative example is the Tham Luang Nang Non cave disaster event in Chiang Rai Province, Thailand, where a junior football team was trapped in a disaster area [263].

Each user u located in the disaster area has a distance $d_{u,i}$ $[m]$, where $i, i \in \{s, m\}$, from the static UAV s and the mobile UAV m. The channel gain between the user u and the receiver i is defined as $G_{u,i} = \frac{k}{d_{u,i}^2}$, where k is a positive constant that expresses the channel fading for a time slot t (i.e., $t = 0.5\ msec$). The non-orthogonal multiple access (NOMA) technique is adopted for the communication with the static and the mobile UAV [264]. Accordingly, the receivers perform the Successive Interference Cancellation technique at the reception of the users' signals. Without loss of generality and mainly for presentation purposes, the users' channel gains are sorted as $G_{|U|,i} \leq \cdots \leq G_{u,i} \leq \ldots G_{1,i}$ and the corresponding sensed interference from the user u is denoted as $I_u = (\mathbf{P_{-u,i}}) = \sum_{u' \geq u+1}^{|U|} G_{u',i} P_{u'} + I_0$, where I_0 is the background noise and $\mathbf{P_{-u,i}}$ is the transmission power vector of all the users communicating with the receiver i except for user u. It is noted that the users communicating with the static UAV do not sense the interference from the transmissions to the mobile UAV, as the static and the mobile UAV are considered to operate in different frequency bands of the spectrum, as explained above. Therefore, the user's u SINR as it is measured at the receiver $i, i \in \{s, m\}$ is given as follows.

$$\gamma_{u,i}(P_{u,i}, \mathbf{P_{-u,i}}) = \frac{G_{u,i} P_{u,i}}{I_u} \tag{8.8}$$

Given that each user u has a total uplink transmission power P_u^{Max}, its goal is to determine the power investment portion (i.e., distribution) that will be allocated for the communication with the static and the mobile UAV. Letting $x_u, x_u \in [0, 1]$ denote the percentage of user's power investment to the communication with the mobile UAV, then its corresponding transmission power is $x_u P_u^{Max}$, and consequently the corresponding transmission power for the communication with the static UAV is $(1 - x_u) P_u^{Max}$. At this point, it should be clarified that the problem of optimally positioning the mobile UAV is not part of our study, as much work has already been devoted to the optimal UAV positioning [217, 218]. At each time slot t, the mobile UAV changes position, and its coordinates are considered to be known in the following analysis.

The problem of users'/victims' risk-aware decision making during disaster events has been extensively studied in the literature of Public Safety Systems. Current research on Public Safety Systems dealing with dynamically evolving disaster scenarios focuses mostly on the crowd evacuation dynamics. While macroscopic models treat the crowd as a flowing continuum based on the physical features of liquid flow [265], microscopic models based on the cellular automata model [266] and social force model [267], treat the human as a self-driving particle. Indeed, human behavioral models capture individuals' characteristics and peculiarities during disasters. For example, the Nomad model focuses on humans' daily activities [268]; the social identity theory recognizes the impact of belonging to a group on human behavior [269]; and the elaborated social identity model identifies that human social behavior can rapidly change during an emergency [270]. Self-organization phenomena have also been studied in the context of Public Safety Systems [271], such as the herding effect [272], zipper effect [273], Faster-is-Slower effect [274], and so on. In this Chapter, as already discussed, we focus on the users'/victims' risk-aware decisions regarding their communication with the static and/or the mobile UAV by adopting the principles of Prospect Theory. The proposed framework is in line with the existing research initiative of 5G networks to support users' autonomy and develop user-centric approaches that will be implemented in a distributed manner without requiring a centralized entity to control the communication environment and impose additional signaling overhead [275].

The considered wireless communication environment is characterized by high levels of uncertainty, stemming from the dynamically changing communication, the probability of the mobile UAV to be unable to serve the users due to its over-exploitation, i.e., increased levels of interference, and the partial available information to the users. Within this uncertain environment, the users are making decisions under risk regarding their communication with the UAVs based on their behavioral characteristics.

According to the prospect theoretic formulation paradigm, the users experience greater dissatisfaction from a potential outcome of losses, compared to their corresponding satisfaction from gains of the same

amount. Also, the users' prospect-theoretic payoff, i.e., utility, is estimated with respect to a reference point $U_{0,u}$, which acts as the ground truth for users' satisfaction. Based on the above, the user's prospect-theoretic utility for convenience is again presented below:

$$\mathcal{U}_u(x_u, x_T) = \begin{cases} (U_u - U_{0,u})^{a_u}, & if\ U_u > U_{0,u} \\ -k_u(U_{0,u} - U_u)^{b_u}, & otherwise \end{cases} \tag{8.9}$$

where $U_u(x_u, x_T)$ is the user's u actual utility expressed as the user's achieved energy-efficiency and $x_T = \sum_{u=1}^{|U|} x_u$ is the total power investment of all the users to their communication with the mobile UAV. The reference point $U_{0,u}$ is defined as the user's u achieved energy-efficiency if the user was only exploiting its communication with the static UAV and is given as follows.

$$U_{0,u} = \frac{y \cdot W \cdot log(1 + \gamma_{u,s}(P_{u,s}, \mathbf{P_{-u,s}}))}{P_{u,s}} \tag{8.10}$$

The user u has the potential to experience superior actual perceived utility U_u by opportunistically exploiting its communication and data transmission to the mobile UAV. In this case, the user achieves greater payoff than the reference point and thus, the user enjoys improved performance and in a personalized manner (through parameters a_u, b_u, and k_u explained below), as expressed by the first branch of Eq. (8.9). However, if the users cumulatively over-exploit their communication to the mobile UAV by investing increased transmission power, then the levels of interference at the receiver increase, and the user can experience less payoff than the reference point, i.e., loss, as expressed by the second branch of Eq. (8.9).

The way that each user experiences its personalized gains and losses, as well as how much risk-seeking it can become regarding its power investment for the data transmission to the mobile UAV, are captured by the user's customized behavioral parameters a_u, b_u, and k_u. In particular, the parameters a_u and b_u, $a_u, b_u \in (0, 1]$ capture the users' perception of the gains and losses, respectively. A user becomes more risk-seeking and tends to invest more transmission power to the mobile UAV communication for increasing values of a_u. Also, for decreasing values of b_u, the user experiences greater dissatisfaction from its losses, thus, it becomes more risk-averse. Without loss of generality in the following we assume $a_u = b_u$. The loss aversion parameter $k_u, k_u \in [0, +\infty)$ reflects the impact of losses compared to gains on user's prospect-theoretic utility. If $k_u > 1$, the user u weighs the losses more than the gains, while if $0 \leq k_u \leq 1$, the user weighs more or equal the gains than the losses, thus presenting an aggressive gain seeking behavior.

As mentioned before, each user exploits its dual communication interface in order to transmit its data to the static and the mobile UAV via intelligently investing its transmission power, and dynamically managing the available spectrum. Therefore, the user's actual utility is given as follows.

$$U_u(x_u, x_T) = U_{0,u}(1 - x_u) + F_u \cdot x_u \cdot RoR(x_T) \tag{8.11}$$

The first term of Eq. (8.11) expresses the user's utility, in terms of energy-efficiency units, by its transmission to the static UAV. The second term of Eq. (8.11) captures the user's satisfaction by transmitting its data to the mobile UAV, where $F_u = \frac{(1-y) \cdot W \cdot log(1+\gamma_{u,m}(P_{u,m}, \mathbf{P_{-u,m}}))}{P_{u,m}}$. The function $RoR(x_T)$ expresses the Rate of Return (RoR) of the mobile UAV-based communication and is a decreasing function with respect to the users' total power investment for communication with the mobile UAV. The latter is justified and motivated by the fact that, as the more the users' increase their transmission power investment to their mobile UAV-based communication, the less the mobile UAV is able to serve them due to the increased interference at the reception of their signals and its limited spectrum. Without loss of generality, also here we adopt the rate of return:

$$RoR(x_T) = 2 - e^{x_T - 1} \tag{8.12}$$

Following the previous reasoning, the mobile UAV has a probability of not being able to serve the users (let us refer to as probability of failure), which is an increasing function with respect to the users' total transmission power investment to their mobile UAV-based communication. For demonstration purposes and without limiting the following analysis, we adopt a probability of failure function $\mathcal{P}(x_T)$ for the mobile UAV, as follows: $\mathcal{P}(x_T) = x_T^2$. If the mobile UAV is able to serve the users, then each user perceives an actual utility U_u greater than the reference point, i.e., the user gains from investing to the mobile UAV-based communication. Thus, by calculating the difference $U_u - U_{0,u}$ via using Eq. (8.10) and Eq. (8.11),

we have $\mathcal{U}(x_u, x_T) = x_u^{a_u} \cdot [F_u \cdot RoR(x_T) - U_{0,u}]^{a_u}$. For the simplicity of the notation, we normalize the rate of return function, so that $U_{0,u} = 1$, and denote $\overline{RoR_u}(x_T) \triangleq (F_u \cdot RoR(x_T) - 1)^{a_u}$, where $\overline{RoR_u}(x_T)$ is assumed concave, decreasing, twice continuously differentiable, and positive. Thus, we conclude that $\mathcal{U}_u(x_u, x_T) = x_u^{a_u}\overline{RoR_u}(x_T)$. In the opposite case that the mobile UAV is not able to serve the users, then the user achieves less utility than its reference point. Thus, by calculating the difference $(U_{0,u} - U_u)$, and shaping the result following the second branch of Eq. (8.9), we have $\mathcal{U}_u(x_u, x_T) = -k_u x_u^{a_u}$. It is noted that in this case, the second term of Eq. (8.11) is zero, as the user gets zero satisfaction from the mobile UAV-based communication, even if invested some power in this communication effort.

Summarizing the above analysis, the users' prospect-theoretic utility function is written as follows.

$$\mathcal{U}_u(x_u, x_T) = \begin{cases} x_u^{a_u}\overline{RoR_u}(x_T), & if\ U_u > U_{0,u} \\ -k_u x_u^{a_u}, & otherwise \end{cases} \tag{8.13}$$

Furthermore, by incorporating the probability of the mobile UAV to fail serving the users' QoS requests, the user's prospect-theoretic utility is reshaped as follows.

$$\mathcal{U}_u(x_u, x_T) = \begin{cases} x_u^{a_u}\overline{RoR_u}(x_T), & with\ probability\ (1 - \mathcal{P}(x_T)) \\ -k_u x_u^{a_u}, & with\ probability\ \mathcal{P}(x_T) \end{cases} \tag{8.14}$$

Table 8.2: Section 8.4 list of key notations

Symbol	Description
U	Set of users
W	Spectrum
y	Portion of spectrum allocated to static UAV
$d_{u,i}$	Distance from disaster area
$G_{u,i}$	Channel gain
k	Channel fading
t	Time slot
I_0	Background noise
$\mathbf{P_{-u,i}}$	Transmission power vector of all the users i except for user u
$\gamma_{u,i}(P_{u,i})$	SINR
P_u	Uplink transmission power
x_u	Percentage of user's power investment to mobile UAV
$U_{0,u}$	Reference point
$\mathcal{U}_u(x_u, x_T)$	PT utility
x_T	Total power investment to mobile UAV
k_u	Loss aversion parameter
a_u, b_u	Personalized behavioral parameters
F_u	Auxiliary constant
$RoR(x_T)$	Rate of Return of mobile UAV-based communication
$\mathcal{P}(x_T)$	Probability of failure function
$\mathbb{E}(\mathcal{U}_u)$	Expected prospect-theoretic utility function
$h_u(x_T)$	Effective rate of return of the mobile UAV-based communication
G	DYNAMISM Game
X_u	Strategy space
$\mathbf{x}^*$	Optimal investment vector
$BR_u(\mathbf{x_{-u}})$	Best response strategy
X'_u	Modified strategy space
$g(x_T)$	Auxiliary function
ϵ_1, ϵ_2	Constants
$H(x_T)$	Optimal non zero investment

8.4.2 Problem Formulation and Solution

In this section, we formulate the distributed resource management problem to enable the users, to autonomously determine their uplink transmission power investment to the static and mobile UAV-based communication. This in turn allows the realization of a dynamic spectrum methodology. Given the probabilistically defined user's prospect-theoretic utility function (Eq. (8.14)), the user's expected prospect-theoretic utility function is derived as follows.

$$\mathbb{E}(U_u) = x_u^{a_u}\overline{RoR_u}(x_T)(1-\mathcal{P}(x_T)) - k_u x_u^{a_u}\mathcal{P}(x_T) \tag{8.15}$$

Therefore, the corresponding distributed DYNAMIc Spectrum Management (DYNAMISM) problem is formulated as a maximization problem of each user's expected prospect-theoretic utility function, as follows.

DYNAMISM Game

$$\max_{x_u\in[0,1]}\{\mathbb{E}(\mathcal{U}_u) = x_u^{a_u}h_u(x_T)\},\ \forall u \in U \tag{8.16}$$

where $h_u(x_T) = \overline{RoR_u}(x_T)(1-\mathcal{P}(x_T)) - k_u\mathcal{P}(x_T)$ and $h_u(x_T)$ is the effective rate of return of the mobile UAV-based communication considering the users' personal behavioral characteristics and the probability of the mobile UAV to fail serving the users. All key notations are summarized in Table 8.2.

The maximization problem of Eq. (8.16) can be addressed as a non-cooperative game among the users. The non-cooperative game is defined as $G = [U, \{X_u\}_{u\in U}, \{\mathbb{E}(\mathcal{U}_u)\}_{u\in U}]$, where U denotes the set of users, $X_u = [0,1], \forall u \in U$ is the strategy space of user u (i.e., its percentage power investment to the mobile UAV-based communication), and $\mathbb{E}(\mathcal{U}_u)$ is the user's payoff as expressed by its expected prospect-theoretic utility function (Eq. (8.15)). Our goal is to determine the existence and uniqueness of a Pure Nash Equilibrium (PNE) point representing users' power investment to their mobile UAV-based communication. The PNE is denoted as $\mathbf{x}^* = [x_1^*, \ldots, x_u^*, \ldots, x_{|U|}^*]$ and at the PNE point no user can further improve its achieved expected prospect-theoretic utility by unilaterally changing its uplink transmission power investment given the strategies of the rest of the users, i.e., $\mathbb{E}(\mathcal{U}_u(x_u^*, \mathbf{x}_{-\mathbf{u}}^*)) \geq \mathbb{E}(\mathcal{U}_u(x_u, \mathbf{x}_{-\mathbf{u}}^*)),\ \forall x_u \in X_u$. Before proving the existence and uniqueness of the PNE point in the following subsection, we provide some useful mathematical properties regarding the probability of failure $\mathcal{P}(x_T)$ and the normalized rate of return function $\overline{RoR_u}(x_T)$. The probability of the mobile UAV failing to serve the users is strictly increasing, twice differentiable, and convex in the normalized total power investment $x_T = [0,1]$ and $\mathcal{P}(x_T \geq 1) = 1$. The normalized rate of return function $\overline{RoR_u}(x_T) \triangleq (F_u \cdot RoR(x_T) - 1)^{a_u}$ is twice-differentiable, monotonic decreasing ($\frac{\partial \overline{RoR_u}(x_T)}{\partial x_T} < 0$), concave ($\frac{\partial^2 \overline{RoR_u}(x_T)}{\partial x_T^2} < 0$), and positive $\forall x_T \in [0,1]$.

In this section, we prove the existence and uniqueness of the PNE for the game G, as well as the convergence of all the users' strategies to the PNE. The concept of best response strategy $BR_u(\mathbf{x}_{-\mathbf{u}})$ is adopted, where $BR_u(\mathbf{x}_{-\mathbf{u}}) = argmax\mathbb{E}(\mathcal{U}_u), BR_u : \overline{X_{-u}} \rightrightarrows X_u$, where $\overline{X_{-u}}$ denotes the aggregate investment of all the users except for user u. The users' best response strategy BR_u lies in the interval $[0,1]$, where $BR_u(\mathbf{x}_{-\mathbf{u}}) = 0$ means that the user communicated only through the static UAV and if $BR_u(\mathbf{x}_{-\mathbf{u}}) = 1$, then the user invested its maximum uplink transmission power to the communication with the mobile UAV. In the following theorem, we examine the properties of the effective rate of return function $h_u(x_T) = \overline{RoR_u}(x_T)(1-\mathcal{P}(x_T)) - k_u\mathcal{P}(x_T)$.

Theorem 49. ***(Effective Rate of Return:)*** *The effective rate of return function $h_u(x_T)$ is decreasing, concave, and positive in the modified strategy space $X_u' = [0, \mu],\ \forall a_u < 0.5$.*

Proof. The first order derivative of $h_u(x_T)$ with respect to each user's power investment x_u is given as follows.

$$\frac{\partial h_u(x_T)}{\partial x_u} = \frac{\partial \overline{RoR_u}(x_T)}{\partial x_u}(1-x_T^2) - 2x_T\overline{RoR_u}(x_T) - 2k_u x_T \tag{8.17}$$

Based on Eq. (8.12) and the normalized rate of return function $\overline{RoR_u}(x_T) = (F_u \cdot RoR(x_T) - 1)^{a_u}$, we have $\overline{RoR_u}(x_T) > 0$ and $\frac{\partial \overline{RoR_u}(x_T)}{\partial x_T} < 0$. Thus, $\frac{\partial h_u(x_T)}{\partial x_u} < 0$ and the effective rate of return function is decreasing. Considering the second order derivative of $h_u(x_T)$, we have:

$$\frac{\partial^2 h_u(x_T)}{\partial x_u^2} = \frac{\partial^2 \overline{RoR_u}(x_T)}{\partial x_u^2}(1 - x_T^2) + g(x_T) - 2k_u \tag{8.18}$$

where $g(x_T) = -4x_T \frac{\partial \overline{RoR_u}(x_T)}{\partial x_u} - 2\overline{RoR_u}(x_T)$. Given that $\frac{\partial^2 \overline{RoR_u}(x_T)}{\partial x_T^2} < 0$, the normalized aggregate investment is $x_T \leq 1$, and $g(x_T) < 0$ in X_u, $\forall a_u < 0.5$, thus we show that $\frac{\partial^2 h_u(x_T)}{\partial x_u^2} < 0$. Therefore, the effective rate of return function $h_u(x_T)$ is concave.

Towards showing that the effective rate of return function $h_u(x_T)$ is positive, we apply Bolzano's Theorem within $X_u = [0, 1]$ which is an important specialization of Intermediate Value Theorem [81]. We observe that $h_u(0) > 0$ and $h_u(1) < 0$, hence there exists a value $\mu \in X_u$, such that $h_u(\mu) = 0$. Thus, h_u is positive in the modified strategy space $X'_u = [0, \mu] \subseteq [0, 1] = X_u$. □

In the following theorem, we prove the existence of the PNE for the non-cooperative game G.

Theorem 50. ***(DYNAMISM Game PNE Existence:)*** *For the non-cooperative game $G = [U, \{X_u\}_{u\in U}, \{\mathbb{E}(\mathcal{U}_u)\}_{u\in U}]$, there exists a PNE $x_u^*, x_u^* \in X'_u, \forall u \in U$.*

Proof. Initially, we examine the first order derivative of the user's expected prospect-theoretic utility $\mathbb{E}(\mathcal{U}_u(x_u, x_T))$, as follows.

$$\frac{\partial \mathbb{E}(\mathcal{U}_u(x_u, x_T))}{\partial x_u} = {x_u}^{a_u - 1}(x_u \frac{\partial h_u(x_T)}{\partial x_T} + a_u h_u(x_T)) \tag{8.19}$$

For $x_u = 0$, we have $(x_u \frac{\partial h_u(x_T)}{\partial x_T} + a_u h_u(x_T))|_{x_u=0} > 0$, since $h_u(x_T) > 0$. Considering a very small value $\epsilon_1 \to 0, \epsilon_1 > 0$, we have $(x_u \frac{\partial h_u(x_T)}{\partial x_T} + a_u h_u(x_T))|_{x_u=\epsilon_1} > 0$, thus $\frac{\partial \mathbb{E}(\mathcal{U}_u(x_u, x_T))}{\partial x_u}|_{x_u=\epsilon_1} > 0$. For a very large value $\epsilon_2 = \mu \in X'_u$, we have $h_u(\epsilon_2) = 0$, thus $(x_u \frac{\partial h_u(x_T)}{\partial x_T} + a_u h_u(x_T))|_{x_u=\epsilon_2} < 0$, and subsequently $\frac{\partial \mathbb{E}(\mathcal{U}_u(x_u, x_T))}{\partial x_u}|_{x_u=\epsilon_2} < 0$. Given that $\frac{\partial \mathbb{E}(\mathcal{U}_u(x_u, x_T))}{\partial x_u}|_{x_u=\epsilon_1} > 0$ and $\frac{\partial \mathbb{E}(\mathcal{U}_u(x_u, x_T))}{\partial x_u}|_{x_u=\epsilon_2} < 0$ and by applying the Intermediate Value Theorem, we prove that there exists at least one x_u^* value, $x_u^* \in X'_u$, such that $\frac{\partial \mathbb{E}(\mathcal{U}_u(x_u, x_T))}{\partial x_u}|_{x_u=x_u^*} = 0$. Given also the properties of $\mathcal{P}(x_T)$ and $\overline{RoR_u}(x_T)$, we conclude that $x_u^*, x_u^* \in X'_u, \forall u \in U$ is a PNE of the game $G = [U, \{X_u\}_{u\in U}, \{\mathbb{E}(\mathcal{U}_u)\}_{u\in U}]$. □

In the following theorem, we prove the uniqueness of the PNE point for the game G.

Theorem 51. ***(DYNAMISM Game PNE Uniqueness:)*** *The PNE point $x_u^*, x_u^* \in X'_u, \forall u \in U$ of the non-cooperative game $G = [U, \{X_u\}_{u\in U}, \{\mathbb{E}(\mathcal{U}_u)\}_{u\in U}]$ is unique.*

Proof. Initially, we study the concavity of $\mathbb{E}(\mathcal{U}_u(x_u, x_T))$ by examining its second order derivative with respect to x_u.

$$\frac{\partial^2 \mathbb{E}(\mathcal{U}_u(x_u, x_T))}{\partial x_u^2} = a_u(a_u - 1){x_u}^{a_u - 2} h_u(x_T) + 2a_u {x_u}^{a_u - 1} \frac{\partial h_u(x_T)}{\partial x_u} + {x_u}^{a_u} \frac{\partial^2 h_u(x_T)}{\partial x_u^2} \tag{8.20}$$

All the terms of the above equation are negative given that $x_u > 0 \in X'_u$, h_u is positive, decreasing, and concave in X'_u, and $a_u < 0.5$. Thus, we conclude that $\frac{\partial^2 \mathbb{E}(\mathcal{U}_u(x_u, x_T))}{\partial x_u^2} < 0$, therefore $\mathbb{E}(\mathcal{U}_u(x_u, x_T))$ is concave. Based on the above analysis, the point $x_u^*, x_u^* \in X'_u, \forall u \in U$ is a unique global maximum of $\mathbb{E}(\mathcal{U}_u(x_u, x_T))$ and a unique PNE point of the non-cooperative game $G = [U, \{X_u\}_{u\in U}, \{\mathbb{E}(\mathcal{U}_u)\}_{u\in U}]$. □

Towards providing the convergence of the users' strategies of uplink transmission power to the PNE point, we use the best response dynamics $BR_u(\mathbf{x_{-u}})$. In the following theorem, we prove that the users' best response dynamics $BR_u(\mathbf{x_{-u}}), \forall u \in U$ monotonically decrease with users' aggregate power investment x_T and converge to the PNE point.

Theorem 52. ***(Decreasing best responses:)*** *The user's best response strategy $BR_u(\mathbf{x_{-u}}), \forall u \in U$ in the non-cooperative game $G = [U, \{X_u\}_{u\in U}, \{\mathbb{E}(\mathcal{U}_u)\}_{u\in U}]$ is decreasing in x_T and converges to the PNE point $x_u^*, x_u^* \in X'_u, \forall u \in U$.*

Proof. Let $H(x_T) = -a_u \frac{h_u(x_T)}{\partial h_u(x_T)/\partial x_u}$ be defined as the optimal non zero investment of each user $u, u \in U$, where $H(BR_u(\mathbf{x_{-u}}) + \mathbf{x_{-u}}) = BR_u(\mathbf{x_{-u}})$, when $BR_u(\mathbf{x_{-u}}) > 0$. Identical to Theorem 48 it is proven by contradiction the BR_u is decreasing in x_T, confirming the convergence of game's G to a unique PNE. □

8.4.3 Distributed Algorithm

In the following, we present and discuss a distributed and low complexity algorithm, namely **DYNAMI**c **S**pectrum **M**anagement in risk-aware UAV networks (i.e., DYNAMISM), which undertakes the practical implementation of the previously described theoretical framework. DYNAMISM algorithm enables the optimal user's power investment determination for the spectrum usage of both UAVs.

Transmission is differentiated for each user given its relative position from both UAVs, with the static UAV to provide a stable channel gain environment due to its steady position, while the mobile UAV offers varying channel gain conditions since its movement impacts the quality of communication among itself and the users. DYNAMISM algorithm is executed per timeslot, with its duration range (i.e., 0.5 $msec$) to allow to capture a snapshot of the network's operation. Hence, the users are able to optimize their power investment to each UAV's spectrum during this timeslot, an outcome which may be modified in the upcoming timeslots, if the transmission via the mobile UAV becomes more favorable or strenuous.

The algorithm promotes a highly decentralized approach with regards to decision making, since each user is responsible for streamlining its power investment in order to optimize its prospect-theoretic expected utility during the resource allocation process. At the beginning of the algorithm's implementation, the users define their behavioral characteristics reflecting their QoS preferences and their perceptions towards risk. Based on their topological and prospect-theoretic modeling, the users identify the optimal power investment to each UAV's spectrum, starting from any initial feasible point. Eventually, the algorithm converges into an optimal allocation of users' power investment among the UAVs indicating a successful transmission, otherwise if excessive congestion and over-exploitation of mobile UAV's spectrum is identified, then the algorithm will terminate and only the users who transmitted via the static UAV will be able to communicate. During the entire process, the role of the system administrator is rather limited, as only the overall interference in the network is required to be exchanged from the UAVs to the users. The user-centric design of the DYNAMISM algorithm and the parallel execution of actions significantly mitigate the computational complexity required to determine the game's optimal operational point (i.e., Pure Nash Equilibrium).

The low duration of each timeslot ensures that the movement of the mobile UAV within the timeslot duration is not significant with limited impact on the channel gain determination. However, since DYNAMISM algorithm is timeslot based, each iteration for a consecutive timeslot is capable of capturing the trajectory of the mobile UAV, and repeat the resource allocation process for the new topological coordinates. Thus, the algorithm manages to address the challenge of changing positions of the UAV above the users and identify the optimal power investment and spectrum allocation for the system.

8.4.4 Numerical Results

In this section, we present a detailed evaluation of the performance and the operational characteristics of the proposed framework, obtained via modeling and simulation. Furthermore, a detailed comparative evaluation of the proposed framework against other approaches with respect to user selection policies to multiple UAV spectrum sources, is provided. All simulations have been conducted under the MATLAB computing environment in an Intel(R) Core(TM) i7-7500U CPU @ 2.70 GHz 2.90 GHz laptop with 8.00 GB RAM.

In the tested operational scenario, we assume a wireless network covering an area of radius $\Re = 3.5\ km$, and consisting of two UAV aircrafts flying above a number of $|U| = 20$ ground users randomly distributed within the wireless network. The first UAV (i.e., static UAV) is hovering in a steady position and provides stable transmission conditions to the users of the network, while the second UAV (i.e., mobile UAV) moves above the users resulting in changing channel gains depending on its relative position towards them. For demonstration purposes we assume that the spectrum of the network is $W = 4\ MHz$, 80% of which is allocated to the mobile UAV and 20% allocated to the static UAV. Both UAVs operate under the NOMA transmission paradigm, and acknowledging system's physical limitations, user maximum feasible transmission power is set at $P_u^{Max} = 0.2\ Watts$, being split between the communication with the two UAVs.

We examine system's behavior under various transmission scenarios considering initially homogeneous population where all users present common behavior characteristics, while following, a heterogeneous set of users is considered where the impact of diversifying risk characteristics - as modeled via Prospect Theory - is evaluated. Moreover the impact of the mobility and repositioning of the mobile UAV on the achievable user data rate and system spectrum utilization is examined.

Algorithm 21 DYNAMISM Algorithm

Require:
constants k_u, a_u; user & UAV position coordinates; UAV spectra $W_{UAV}^{mobile} = (1-x)W$, $W_{UAV}^{static} = xW$

1: $ite \leftarrow 1$; $convergence^{(ite)} \leftarrow 0$; $system\ fail \leftarrow 0$
2: Calculate channel gains per user and apply SIC
3: Assign initial random $x_u^{(ite)}$
4: **while** $convergence^{(ite)}$=0 **do**
5: Calculate $P_{u,s}, P_{u,m}$;
6: Overall interference per UAV broadcasted and each user calculates its own sensed interference
7: Calculate utility $\mathbb{E}(\mathcal{U}_u)^{(ite)}$
8: **for all** $x_u \in [0,1]$ **do**
9: x_u^*=$argmax_{x_u}\mathbb{E}(\mathcal{U}_u)$
10: **if** $\mathbb{E}(\mathcal{U}_u) > \mathbb{E}(\mathcal{U}_u)^{(ite)}$ **then**
11: $x_u^{(ite+1)} \leftarrow x_u^*$ **and** $\mathbb{E}(\mathcal{U}_u)^{(ite+1)} \leftarrow \mathbb{E}(\mathcal{U}_u)$
12: **end if**
13: **end for**
14: Calculate *mobile UAV Spectrum utilization*, $util = \frac{\sum_{u=1}^{|U|}(1-y)\cdot W \cdot log(1+\gamma_{u,m}(P_{u,m}, \mathbf{P_{-u,m}}))}{(1-y)W}$
15: **if** $util > 1$ **then**
16: $system\ fail \leftarrow 1$
17: **end if**
18: **if** $x_u^{(ite+1)} - x_u^{(ite)} < \epsilon$ **then**
19: $convergence^{(ite+1)} \leftarrow 1$
20: **end if**
21: $ite \leftarrow ite + 1$
22: **end while**
23: **return**
The DYNAMISM algorithm returns each user's investment x_u, if the mobile UAV achieves to serve the users and the flag "$system\ fail$", if the mobile UAV fails to serve the users.

Finally, we illustrate some comparative results in order to assess the performance of the DYNAMISM algorithm against two other alternative approaches: one performing a fixed user allocation to each UAV under the Expected Utility Theory without considering risk behavioral modeling, and a second one providing exclusive UAV selection by enabling the users' devices to select each UAV based on their most favorable channel conditions at each timeslot.

The key simulation parameters that have been adopted in the following numerical results are summarized in Table 8.3.

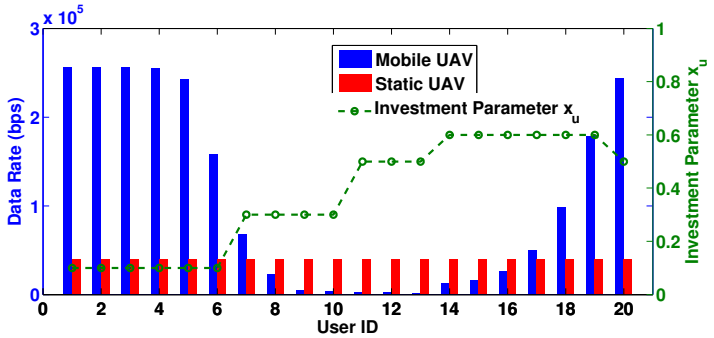

Figure 8.6: Data rates and power investment per user ID

Homogeneous Population: Common User Behavior

Initially, we consider that the users have common prospect-theoretic parameters, that is the same risk aversion parameter $k_u = 20$ and sensitivity parameter $a_u = 0.1$. Fig. 8.6 depicts users' achievable data rates from each UAV, as well as the relative investment x_u to the mobile UAV, for a case where both UAVs are placed very close to each other. Please also note that for presentation purposes, the user IDs are assigned such that increasing user ID corresponds to an increasing distance from the mobile UAV. We observe that due to the higher spectrum availability from the mobile UAV, the obtained data rates for users who are very close to the mobile UAV or far away from it are quite high, owing either to their very favorable channel gain conditions (for the close ones) or to the absence of interference as a consequence of the application of SIC technique (for the distant ones) adopted by NOMA. On the contrary, middle distance users are severely impacted by their worsening channel conditions in conjunction with the rising interference levels sensed from the users with worse channel gains than them. The overall above discussion is also reflected on the values of the power investment parameter, with the users close to the mobile UAV to obtain high data rates even with small investment values. Distant users on the contrary do not further increase their investment significantly (e.g., observe for example users with IDs 14-20), since they manage to achieve satisfactory communication with the mobile UAV due to the low sensed interference as explained above. The static UAV since it operates under a stricter framework with each user transmitting with steady channel conditions, delivers much more stable achievable data rate to all users, with all of them managing to split the limited spectrum in a more balanced manner.

Heterogeneous Population: Diversifying User Behavior

In this part, we study how system utilization is impacted, when a subset of users modify their behavior towards investing in the mobile UAV (which is assumed to have higher spectrum availability), in an attempt to further improve their benefits (i.e., heterogeneous population).

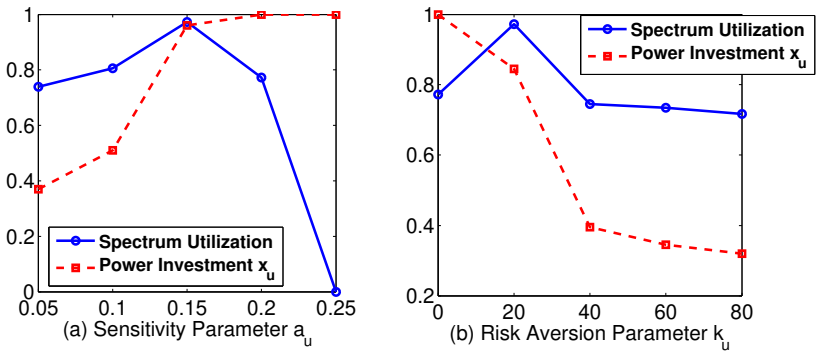

Figure 8.7: Average spectrum utilization and power investment for varying: (a) sensitivity (i.e., parameter a_u); and (b) risk aversion (i.e., parameter k_u)

Particularly, Fig. 8.7a presents system's overall spectrum utilization and the respective power investment x_u for communicating with the mobile UAV, for a user group that modifies its perceptions towards risk through its prospect-theoretic parameters (a) sensitivity parameter a_u, and (b) the risk aversion parameter k_u. Based on the results we notice that when parameter a_u increases, initially this

Table 8.3: Simulation parameters values for DYNAMISM algorithm

Parameter	Description	Value
y	Portion of the overall available spectrum allocated to the static UAV	0.2 (20%)
$\Re$	Radius of the PSN	3.5 km
$\|U\|$	Number of users	20
W	Network's spectrum	4 MHz
P_u^{Max}	User's maximum transmission power	0.2 W

leads to higher levels of investment to the mobile UAV spectrum, while the investment to the static UAV is correspondingly reduced. However, there is a certain level ($a_u = 0.15$ in our case) where utilization reaches a peak (almost 100%), while subsequently further increasing the sensitivity value makes the users become very aggressive against the mobile UAV spectrum due to its higher expected returns and fully invest in it. As a result, spectrum utilization decreases rapidly as the mobile UAV spectrum collapses due to over-exploitation. At this point users have fully invested their power to the mobile UAV, as observed by the trend of the corresponding curve presenting the power investment parameter (i.e., $x_u = 1$), and therefore they do not receive any return from the spectrum of the static UAV either.

Similarly, with reference to the risk aversion parameter, lower values of k_u indicate that users are more risk seeking, hence investing more heavily to the mobile UAV spectrum. Consequently, as observed from the results in Fig. 8.7b, when $k_u = 0$, users do not invest in the static UAV at all, while by rising risk aversion parameter users become more conservative and reduce their investment to the mobile UAV, thus unlocking the additional spectrum of the static UAV, with the utilization eventually reaching 100% at certain point of parameter k_u. However, for even higher values of k_u, users keep investing less to the mobile UAV (i.e., CPR) due to their more conservative approach against its probability of failure, and therefore the overall spectrum utilization decreases again.

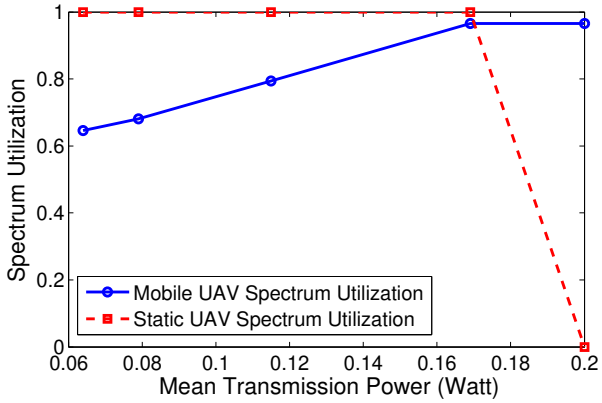

Figure 8.8: Average mobile and static spectrum utilization per mean transmission power investment

Additionally, in Fig. 8.8 we demonstrate the achieved spectrum utilization - separately for the mobile and static UAV - as a function of increasing values of transmission power investment to the mobile UAV (x_u), obtained through properly altering in a combined manner both user prospect-theoretic parameters, that is sensitivity parameter a_u, and risk aversion parameter k_u. The combinations of (a_u, k_u) are $(0.05, 40), (0.10, 40), (0.10, 20), (0.15, 20), (0.15, 10)$, where the users' behavior becomes more risk-seeking in the latter choices. For low values of x_u, users do not invest intensively to the mobile UAV, with the respective spectrum utilization (blue curve) remaining slightly above 60%, while for increasing levels of power, utilization gradually rises until the point that transmission power reaches its upper bound (e.g., 0.2 Watts as assumed here), where utilization to the mobile UAV has reached almost 96.5%. Please note that here we have considered a scenario and respective parameters where the CPR does not collapse. On the contrary, utilization for the static UAV (red curve) follows an opposite trend. For low transmission power levels to the mobile UAV, users invest more in the static UAV, and therefore its utilization remains close to 100%, as an outcome of the safe nature of this resource, as explained before. In the extreme case where users only transmit via the mobile UAV, users do not opt to communicate with the static UAV, and therefore the respective spectrum utilization eventually drops to zero.

UAV Mobility and Utilization

In Fig. 8.9 we present the achievable average user data rates for both the mobile UAV and the static UAV, for different snapshots of the system with changing positions of the mobile UAV. The latter is reflected by moving the mobile UAV such that the distance between the static and mobile UAV is increasing (the horizontal axis of this figure reflects exactly this distance). It is expected that the relative position of the mobile UAV against the users in the ground impacts their channel gain conditions. Consequently, this in combination with the application of the NOMA SIC technique, will impact and influence the user decision in their power investment. It is evident that indeed different positions of the mobile UAV result

in diverse obtained data rates for the users and the system as a whole, while the average data rate of the static UAV remains practically stable, or is slightly reduced in some cases due to the potential higher investment of the users to the mobile UAV. Specifically, when the distance between the two UAVs reaches approximately 2.3 km, then the majority of the users takes advantage of the most favorable channel gain conditions and they obtain the highest data rates, which are 33.53% higher than the base case (zero distance between the two UAVs).

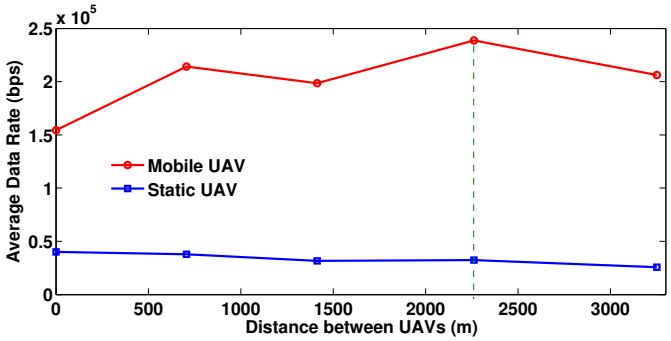

Figure 8.9: Average user data rate for mobile and static UAV for increasing distance between the UAVs

Comparative Evaluation

In this subsection the advantages and superiority of the DYNAMISM algorithm compared to other approaches with regards to UAV selection and spectrum utilization are demonstrated and analyzed. In particular, the proposed framework is compared against: a) an approach where the users follow a fixed UAV allocation under Expected Utility Theory (EUT) - in the following referred to as EUT-fixed allocation approach - and b) an approach where users can dynamically connect to the best UAV option (mobile or static) based on their optimal channel gain condition at that specific timeslot. It should be noted that under the examined comparative scenario of the EUT-fixed allocation approach, each user aims at maximizing its utility function, as expressed by its energy-efficiency in Eq. (8.10), where the available bandwidth is $y \cdot W$ for the static UAV and $(1-y) \cdot W$ for the mobile UAV. In the EUT-fixed allocation approach, each user can communicate only with one UAV, i.e., the static or the mobile UAV. The user initially selects the UAV that it will communicate with based on the criterion of the best channel conditions. Then, each user keeps the same communication choice, i.e., the UAV initially selected.

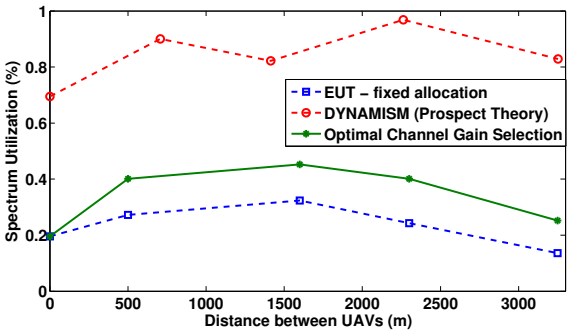

Figure 8.10: Average total spectrum utilization for increasing distance between the UAVs under different resource management approaches

Specifically, in Fig. 8.10 we present the average spectrum utilization (from both UAVs) for different positions of the mobile UAV, reflected by the increasing distance between the static and mobile UAV (horizontal axis) for the various approaches considered.

Firstly, we notice that the EUT-fixed allocation (blue curve) delivers the worst utilization, since users do not have the capability to dynamically switch between the available bands, and they are forced to stay with the UAV they have been originally assigned to. The approach under which users can dynamically connect to a UAV based on their superior channel gain conditions (green curve), gives an additional

degree of freedom to users in order to improve their transmission compared to a fixed allocation and therefore presents a slightly improved utilization compared to the EUT-fixed allocation.

Specifically, under the optimal channel gain selection scenario, while the mobile UAV is moving away from the constant position of the static UAV, each user checks the communication channel gain conditions with each UAV and selects to connect with the one that has the best communication channel gain conditions. However, it is noted that this scenario results in worse spectrum utilization compared to our proposed framework, due to the fact that in the latter the users can jointly exploit their communication with both the UAVs, while in the optimal channel gain selection scenario the user will exploit only the available bandwidth of the UAV that it selected to communicate with, while letting idle and unused the bandwidth of the non-selected UAV. Also, the optimal channel gain selection scenario leads to better spectrum utilization results compared to the EUT-fixed allocation approach, as in the latter the user keeps its initial UAV selection without dynamically exploiting the channel gain conditions. Lastly, we notice that the DYNAMISM algorithm following the principles of Prospect Theory (red curve), outperforms all other cases, since the users enjoy multiple degrees of freedom with regards to their transmission and are capable of: a) dynamically splitting their transmission power between both UAVs, b) investing intelligently in the higher spectrum capacity mobile UAV in a more aggressive manner, while still routing some traffic to the static UAV, and c) dynamically managing the spectrum utilization of the system in a decentralized and distributed manner, since they are able to modify their behavior based on the risk of the spectrum failure.

The overall performance gains are summarized in Table 8.4. The proposed prospect theory based approach (DYNAMISM) manages to increase the average user data rate by almost 260% compared to a fixed allocation under EUT-fixed allocation. Also note that, though the approach based on the channel gain selection also delivers some improvements (approximately 45%) in the attained user data rates compared to the EUT-fixed allocation, its performance remains significantly lower than the DYNAMISM algorithm.

8.5 On Security Aspects of PSN-based Communications

So far, the related literature examines the resource management and security aspects of the UAV-assisted wireless networks, assuming that all the users have rational characteristics and aim at maximizing their perceived utility, i.e., benefit from communicating with the UAV, regardless if they are normal or malicious users. Nevertheless, in real life networking scenarios, the users demonstrate a risk-aware behavior, which is driven by their personal characteristics, the actions and behavior of the other users, and the conditions in the UAV-assisted network [239], [240].

At this section the above gap is filled by exploring user behavioral insights and incorporating behavioral factors into modeling normal and malicious users' decisions. The latter consideration enables to determine the users' optimal transmission power allocation in the two available communication alternatives, that is UAV-based and MBS-based communication, towards improving their utility, while capitalizing on this to devise a sophisticated intrusion detection and ejection process. Towards capturing normal and malicious users' behavior in a more pragmatic manner, Prospect Theory (PT) is adopted for this case as well [216, 276].

In such a setting, a malicious user can take advantage of the vulnerability of the UAV-based communication to failure, due to the over-exploitation of the UAV's bandwidth, and thus perform a Distributed Denial of Service (DDoS) type of attack. During the attack, the malicious users demonstrate a risk-seeking behavior and they over-invest their available transmission power to the UAV-based communication, driving the UAV's bandwidth to failure, thus the service of the normal users is denied. We propose an

Table 8.4: DYNAMISM algorithm vs other approaches

Scenario/Approach	**Average Data Rate per User (bps)**	**% Increase in Average Data Rate**
EUT-fixed allocation	6.55×10^4	-
Channel Gain Selection	9.53×10^4	45.50%
DYNAMISM (Prospect Theory)	23.60×10^4	260.22%

intrusion detection process that considers users' behavioral characteristics and transmission power levels to identify the malicious users. Additionally, by intelligently exploiting the Successive Interference Cancellation (SIC) technique at the UAV-receiver that characterizes the NOMA technology, we propose a novel intrusion ejection methodology. An example of the topology under consideration where malicious users participate in the resource allocation process is shown in Fig. 8.11.

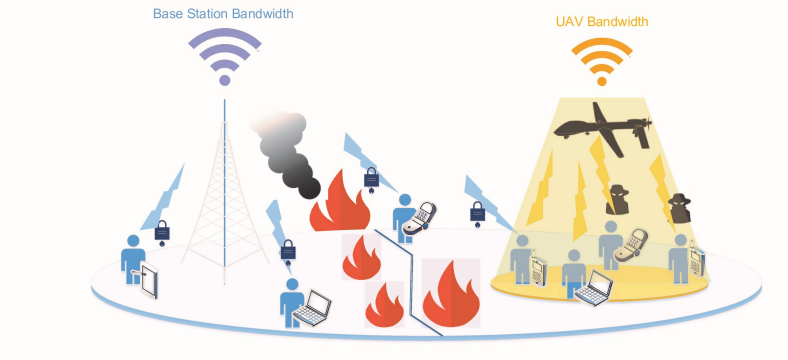

Figure 8.11: UAV-assisted wireless network consisting of risk-aware users

The main contributions of this research work are summarized as follows:

1. A holistic approach based on the Prospect Theory and the theory of the Tragedy of the Commons is introduced to capture and model normal and malicious users' risk-aware behavioral characteristics in representative prospect-theoretic utility functions. Specifically, novel and generic enough prospect-theoretic utility functions are used, which do not simply represent the trade off between the number of transmitted bits to the corresponding consumed power, but on the contrary reflect normal and malicious users' risk-aware choices and priorities in the NOMA-based UAV-assisted wireless network. The bandwidth's fragility in the UAV-based communication is examined by reviewing the bandwidth's exploitation by the normal users, and its over-exploitation by the malicious users.

2. Based on the above modeling, a user-centric power control problem is formulated as a maximization problem of each normal and malicious user's expected prospect-theoretic utility, and it is treated as a non-cooperative game among the users. The goal of each user (either normal or malicious) is to accordingly determine its optimal transmission power investment in the two available communication alternatives, i.e., UAV-based and MBS-based communication. The existence and uniqueness of a Pure Nash Equilibrium (PNE) is shown and the convergence of the users' power strategies to the unique PNE is proven.

3. Capitalizing on the proposed prospect-theoretic resource management framework, a risk-aware and transmission-based intrusion detection process is introduced. Subsequently, a novel intrusion ejection methodology is proposed based on the salient characteristics of the Non-Orthogonal Multiple Access (NOMA) technology and the Successive Interference Cancellation (SIC) technique.

8.5.1 System Model

We study the uplink communication of a UAV-assisted wireless network consisting of $|N_N|$ normal users and $|N_M|$ malicious users, where their corresponding sets are $N_N = \{1, \ldots, i, \ldots, |N_N|\}$ and $N_M = \{1, \ldots, i, \ldots, |N_M|\}$, respectively, and $N = N_N \cup N_M$. Each user $i, i \in N$ exploits both the MBS and UAV connectivity, while exhibiting risk-aware behavior. For convenience of presenting the model, we assume that the UAV-based communication is characterized by greater portion of available bandwidth compared to the MBS-based communication. Due to the UAV's proximity to the users and respectively improved channel gain, the users tend to communicate over the UAV in order to achieve higher data rates, while transmitting at low power levels, thus, extending their battery life. However, the UAV has an upper limit capacity in terms of available bandwidth. Thus, if an increased number of users transmit over the UAV, its corresponding bandwidth becomes over-exploited, and consequently the UAV presents an increased probability of failure in serving the users, primarily due to the increased levels of interference

at the reception of the users' signals. On the other hand, the bandwidth that is available at the MBS-based communication is considered as a safe resource, and the user may achieve a more limited but guaranteed level of Quality of Service (QoS) given its personal characteristics, i.e., channel conditions, transmission power.

Considering the described dual communication environment, each user i, has a maximum transmission power P_i^{Max}, which it invests to both the UAV-based and MBS-based communication to satisfy its goals (i.e., QoS prerequisites if a normal user, or its negative impact if a malicious user). Given the complexity of the dual UAV/MBS communication environment, a centralized resource management approach would introduce increased signaling overhead and would require a centralized entity to obtain and maintain a global view and control of the communication system. Thus, a distributed resource management approach is followed enabling both the normal and malicious users to determine in an autonomous manner their transmission power investment to the UAV-based communication P_i^{UAV} and to the MBS-based communication $P_i^{MBS}, \forall i \in N = N_N \cup N_M$. The percentage of normal and malicious user's i power investment to its transmission to the UAV is assumed to be $x_i, x_i \in [0,1]$, thus, $P_i^{UAV} = x_i P_i^{Max}$, and accordingly, $P_i^{MBS} = (1 - x_i) P_i^{Max}$.

Given the considered communication environment, the malicious users perform a Distributed Denial of Service (DDoS) attack by simply investing high transmission power levels to their UAV-based communication, thus, over-exploiting the UAV's available bandwidth and introducing high levels of interference to the reception of the normal users' signals at the UAV. The outcome of the malicious users' attack is the failure of the UAV's available bandwidth to serve the normal users.

In the examined UAV-assisted wireless network, the normal and malicious users exhibit risk-aware behavior regarding their decisions of investing their transmission power to the UAV-based and MBS-based communication. The users' risk-aware behavior in terms of their decision-making stems from the fact that the individuals assess uncertain outcomes under a loss averse attitude (instead of neutral) in real life communication environments. Thus, the users' utility (i.e., perceived satisfaction) in the event of a loss (i.e., UAV's bandwidth failure) is sensed as of greater magnitude compared to the gains of equal extent given a reference point. This reference point is considered as the ground truth of user perceived utility scale, and it is not necessarily common for all the users. Furthermore, the users tend to overweight events, e.g., UAV's bandwidth failure, with small probabilities, and underweight events with higher probabilities, thus, instructing the formulation of the utility function following the probability weighting effect. Accordingly, the users' cognitive risk-aware behavior is transformed in representative prospect-theoretic utility functions as follows (for convenience notations through this section are explained again):

$$\mathscr{V}_i(y_i) = \begin{cases} (y_i - y_{0,i})^{a_i} & if\ y_i > y_{0,i} \\ -\kappa_i (y_{0,i} - y_i)^{\delta_i} & otherwise \end{cases} \tag{8.21}$$

where $y_i(x_i, x_T)$ is the user's $i, i \in N = N_N \cup N_M$ actual utility, $x_T = \sum_{i=1}^{|N|} x_i$ denotes the total power investment of all users to the UAV-based communication, $|N| = |N_N| + |N_M|$ is the total number of users in the examined network including both the normal and the malicious users, and $y_{0,i}$ the reference point. The reference point is defined as the corresponding user's achieved energy-efficiency point, if the user was exploiting only the safe resource, i.e., if it was transmitting its data only to the MBS by solely investing all of its transmission power to the MBS-based communication. Thus, the reference point is given as follows:

$$y_{0,i} \triangleq \frac{W_{MBS}/N_{MBS}}{P_i^{MBS}} log_2(1 + \gamma_i^{MBS}), \forall i \in N \tag{8.22}$$

where W_{MBS} is the available bandwidth at the MBS-based communication, N_{MBS} is the number of normal and malicious users transmitting to the MBS, $P_i^{MBS} = P_i^{Max}$ presents the user's transmission power (if the user was solely investing its available power to the MBS-based communication), and γ_i^{MBS} denotes the Signal-to-Interference-plus-Noise Ratio (SINR), as measured at the MBS receiver, given as follows:

$$\gamma_i^{MBS} = \frac{h_i^{MBS} P_i^{MBS}}{\sum_{j>i} h_j^{MBS/UAV} P_j^{MBS/UAV} + \sigma^2} \tag{8.23}$$

where h_i^{MBS} is the user's communication channel gain to the MBS, and the interference sensed by user i during its transmission considering the NOMA technology is $\sum_{j>i} h_j^{MBS/UAV} P_j^{MBS/UAV}$, while σ^2 is the variance of the noise power. The communication system of the examined UAV-assisted wireless network is assumed to operate under the NOMA technology that utilizes the Successive Interference Cancellation (SIC) technique at the receiver, which decodes first the signals from the users with better channel gains. Assuming, without loss of generality, that the channel gains pertaining to user i are sorted, then the SIC technique first decodes the signals received from the best channel. Thus, the users with better channel gains experience interference from users with worse channel conditions, while the transmissions of lower channel gain users receive less interference by removing the already decoded signals [151]. The above functionality of SIC will be later discussed as a crucial element for the protection of the network against attacks.

Given the definition of the reference point in Eq. (8.22) and the users' prospect-theoretic utility function as introduced in Eq. (8.21), it is concluded that the users' perceived satisfaction (Eq. (8.21)) is determined with respect to the reference point (Eq. (8.22)), which acts as the ground truth of the user's actual utility $y_i(x_i, x_T)$. The users' risk-aware behavior is further captured by the personalized parameters $\alpha_i, \delta_i, \kappa_i, i \in N = N_N \cup N_M$. Specifically, the risk seeking behavior of a normal or malicious user in losses and its risk averse behavior in gains is reflected by small values of the parameter $\alpha_i, \alpha_i \in (0, 1]$. Furthermore, small values of parameter $\delta_i, \delta_i \in (0, 1]$ imply higher decrease of user's prospect-theoretic utility for small values of y_i and close to the reference point $y_{0,i}$. Without loss of generality, we assume $\alpha_i = \delta_i$. Additionally, the loss aversion parameter $\kappa_i, \kappa_i \in [0, +\infty)$ reflects the impact of losses compared to gains on user's prospect-theoretic utility. If $\kappa_i > 1$, the user i weighs the losses more than the gains, while if $0 \leq \kappa_i \leq 1$, the user weighs more or equal the gains than the losses, thus presenting an aggressive gain seeking behavior.

Based on Eq. (8.21) and Eq. (8.22), it is noted that the user's prospect-theoretic utility is expressed in terms of achieved energy-efficiency. Taken into account that the normal and malicious users exploit the dual communication environment consisting of the MBS and UAV receivers, their perceived actual utility $y_i(x_i, x_T)$ is expressed as the summation of the perceived satisfaction by the MBS-based communication, i.e., first term of Eq. (8.24), and the corresponding satisfaction by the UAV-based communication, i.e., second term of Eq. (8.24). Therefore, the user's actual utility is defined as follows:

$$y_i(x_i, x_T) = y_{0,i}(1 - x_i) + \mathscr{E}_i x_i \mathscr{R}(x_T) \tag{8.24}$$

where $\mathscr{E}_i$ is the achieved energy-efficiency by the UAV-based communication and is defined as follows.

$$\mathscr{E}_i = \frac{W_{UAV}/N_{UAV}}{P_i^{UAV}} log_2(1 + \gamma_i^{UAV}) \tag{8.25}$$

where W_{UAV} is the UAV's bandwidth, N_{UAV} is the number of normal and malicious users transmitting to the UAV, and γ_i^{UAV} is the SINR of user i as measured at the UAV receiver and is given as follows.

$$\gamma_i^{UAV} = \frac{h_i^{UAV} P_i^{UAV}}{\sigma^2 + \sum_{j>i} h_j^{MBS/UAV} P_k^{MBS/UAV}} \tag{8.26}$$

where h_i^{UAV} is the channel gain of user i communicating with the UAV. The function $\mathscr{R}(x_T)$ in Eq. (8.24) represents the rate of return of the UAV-based communication to the normal and malicious users, which is a decreasing concave function with respect to $x_T = \sum_{i=1}^{|N|} x_i$, as the more the users exploit the UAV's available bandwidth, the less the UAV is able to meet the users' QoS prerequisites. For demonstration purposes, in this work the rate of return $\mathscr{R}(x_T)$ of the CPR is formulated as follows.

$$\mathscr{R}(x_T) = 2 - e^{x_T - 1} \tag{8.27}$$

As discussed above, the UAV's bandwidth may fail to address all the normal and malicious users' service requests. Thus, the UAV's bandwidth, acting as the CPR, has a probability of failure $\mathscr{P}(x_T)$ (i.e., CPR's fragility) to serve the users who transmit to the UAV, which is increasing with respect to users' aggregate power investment x_T. In the following, we consider $\mathscr{P}(x_T) = x_T^2$ while x_T is considered normalized. At this point, it is highlighted that the malicious users have the intention to over-invest their transmission

power to the UAV-based communication via performing a DDoS attack in order to drive the UAV's bandwidth to failure, thus, none of the normal users would enjoy the UAV's services.

If the CPR does not fail due to the over-exploitation and the transmission power over-investment by the users, then each user perceives an actual utility given by Eq. (8.24). In this case, the actual perceived utility is greater than the reference point $y_{0,i}$, i.e., $y_i > y_{0,i}$. Therefore, via subtracting the reference point (Eq. (8.22)) from the actual utility (Eq. (8.24)), and shaping the result according to the first branch of Eq. (8.21), we have:

$$\mathscr{V}_i(x_i) = x_i^{a_i}[\mathscr{E}_i\mathscr{R}(x_T) - y_{0,i}]^{a_i} \tag{8.28}$$

For the simplicity of the notation, we normalize the rate of return function, so that $y_{0,i} = 1$, and denote $\overline{\mathscr{R}_i}(x_T) \triangleq (\mathscr{E}_i\mathscr{R}(x_T) - 1)^{a_i}$, where $\overline{\mathscr{R}_i}(x_T)$ is concave, decreasing, twice continuously differentiable, and positive. Thus, $\mathscr{V}_i(x_i) = x_i^{a_i}\overline{\mathscr{R}_i}(x_T)$. In the opposite case, where the CPR becomes over-exploited and fails to serve the normal and the malicious users' service requests, then no user receives any satisfaction from its transmission to the UAV. Therefore, the rate of return from the UAV is extremely small, and the second term of Eq. (8.24) is zero, while the user perceives satisfaction only by its transmission to the MBS, i.e., first term of Eq. (8.24). In this case, the actual utility is $y_i \leq y_{0,i}$, thus, by subtracting the actual utility from the reference point and reshaping the result based on the second branch of Eq. (8.21), we have $\mathscr{V}_i(x_i) = -\kappa_i x_i^{\alpha_i}$.

Following the above detailed argumentation, we can rewrite the normal and malicious user's prospect-theoretic utility function as follows.

$$\mathscr{V}_i(x_i) = \begin{cases} {x_i}^{a_i}\overline{\mathscr{R}_i}(x_T) & if\ y_i > y_{0,i} \\ -\kappa_i x_i^{a_i} & otherwise \end{cases} \tag{8.29}$$

The UAV's bandwidth (CPR) probability of failure is $\mathscr{P}(x_T)$, thus, the probability that the CPR survives and serves the users' service requests is $(1 - \mathscr{P}(x_T))$. As a result, considering the UAV's bandwidth probability of failure, Eq. (8.29) can be written equivalently as follows

$$\mathscr{V}_i(x_i) = \begin{cases} {x_i}^{a_i}\overline{\mathscr{R}_i}(x_T), & with\ prob.\ (1 - \mathscr{P}(x_T)) \\ -\kappa_i x_i^{a_i}, & with\ prob.\ \mathscr{P}(x_T) \end{cases} \tag{8.30}$$

All key involved notations are summarized in Table 8.5.

8.5.2 Problem Formulation and Solution

Given the above modeling, the normal users empowered by Prospect Theory are able to sense the increasing probability of UAV's bandwidth collapse in the incident of a DDoS attack. Towards safeguarding their transmission in uncertain conditions prevailing within the UAV network, normal users aim to maximize their expected prospect-theoretic utilities, defined below:

$$\mathbf{E}(\mathscr{V}_i) = \begin{cases} {x_i}^{a_i}\overline{\mathscr{R}_i}(x_T)(1 - \mathscr{P}(x_T)) - \kappa_i x_i^{a_i}\mathscr{P}(x_T) & for\ normal\ users,\ i \in N_N \\ {x_i}^{\beta_i}\overline{\mathscr{R}_i}(x_T)(1 - \mathscr{P}(x_T)) - \lambda_i x_i^{\beta_i}\mathscr{P}(x_T) & for\ malicious\ users,\ i \in N_M \end{cases} \tag{8.31}$$

where a_i, κ_i and β_i, λ_i are the personalized risk-aware parameters following the principles of Prospect Theory for the normal and malicious users. For notational convenience, we define $\mathscr{F}_i(x_T) = \overline{\mathscr{R}_i}(x_T)(1 - \mathscr{P}(x_T)) - \kappa_i\mathscr{P}(x_T)$ and $\mathscr{F}'_i(x_T) = \overline{\mathscr{R}_i}(x_T)(1 - \mathscr{P}(x_T)) - \lambda_i\mathscr{P}(x_T)$ as each normal and malicious user's effective rate of return, respectively. Thus, the expected prospect-theoretic utility can be re-written as follows:

$$\mathbf{E}(\mathscr{V}_i) = \begin{cases} {x_i}^{a_i}\mathscr{F}_i(x_T) & for\ normal\ users,\ i \in N_N \\ {x_i}^{\beta_i}\mathscr{F}'_i(x_T) & for\ malicious\ users,\ i \in N_M \end{cases} \tag{8.32}$$

Fragile Common Pool Resource (CPR) games have been used in this thesis as a convenient class of games capturing investment in both safe and fragile resources, with the latter prone to collapse if over-exploited. Users have an initial endowment enabling them to invest by splitting it to each resource (i.e., power investment to allocate their transmission power to the MBS and the UAV). A fundamental characteristic of fragile CPR games is incorporating the probabilistic resource failure of the CPR (i.e., UAV's bandwidth) if the aggregate user investment surpassed system's capacity to address demand.

A Fragile CPR game adjusted for the resource allocation process between normal and malicious users is assumed to satisfy the following properties:

Table 8.5: Section 8.5 list of key notations

Symbol	Description
$\Re$	Network radius
N, $\|N\|$	Set of all users, Cardinality of the set
x_i	User specific investment to UAV
N_{UAV}, N_{MBS}	Users transmitting via the UAV and the MBS
N_N, $\|N_N\|$	Set of normal users, Cardinality of the Set
N_M, $\|N_M\|$	Set of malicious users, Cardinality of the set
W_{UAV}, W_{MBS}	UAV and MBS bandwidth
γ_i	Signal-to-Interference-plus-Noise Ratio
P_i^{UAV}, P_i^{MBS}	Transmission power via the UAV and the MBS
x_T	Aggregate users investment to UAV-based communication
h_i	Channel gain
$\mathscr{R}(x_T)$	Rate of return function
$\overline{\mathscr{R}_i}(x_T)$	PT related rate of return
$\mathscr{P}(x_T)$	UAV's bandwidth probability of failure
a_i, δ_i, β_i	Sensitivity parameters
κ_i, λ_i	Risk aversion parameters
$\mathscr{F}_i(x_T)$	Effective rate of return
$\mathscr{J}(x_T)$	User specific optimal non zero investment
R_i	User data rate
$\mathscr{B}_i(\mathbf{x_{-i}})$	User best response
$\mathscr{X}_i$	User power investment strategy set
$\mathscr{V}_i(y_i)$	PT utility
$y_i(x_i, x_T)$	Actual utility
$\mathscr{E}_i$	Achieved energy-efficiency by UAV
$\mathbf{E}(\mathscr{V}_i)$	Expected PT utility
$\theta(x_T)$, $\Phi(x_i)$	Auxiliary functions
ζ	Root of $\mathscr{F}_i$
ξ	Critical point of $\mathbf{E}(\mathscr{V}_i)$
$\mathscr{X}_i'$	Reduced strategy space
ϵ	Constant

- The probability of failure $\mathscr{P}(x_T)$ is a convex, strictly increasing, and twice differentiable function of the normalized total investment $x_T = [0, 1)$ and $\mathscr{P}(1) = 1$.

- The rate of return $\overline{\mathscr{R}_i}(x_T)$ in Eq. (8.27) is monotonic decreasing, i.e., $\frac{\partial \overline{\mathscr{R}_i}(x_T)}{\partial x_T} < 0$, concave ($\frac{\partial^2 \overline{\mathscr{R}_i}(x_T)}{\partial x_T^2} < 0$), twice continuously differentiable, and positive $\forall x_T \in [0, 1]$.

- The strategy set of each user i is defined as: $\mathscr{X}_i = [0, 1], \forall i \in N$.

Stemming from the ability of Fragile CPR games to reflect how rivalrous and non excludable resources can be allocated among competing users, in this work we denote $\mathscr{G} = [N, \{\mathscr{X}_i\}_{i\in N}, \{\mathscr{V}_i\}_{i\in N}]$ as the corresponding Security Aware Power Investment for Efficient Network Spectrum Sharing (SAPIENSS) Game in UAV-assisted communication networks under DDoS attack, where as mentioned before, N denotes the index set of both normal and malicious users.

Each of the normal users aims at the maximization of its expected prospect-theoretic utility jointly targeting for the optimal allocation of its power investment across the MBS and the UAV, while at the same time adjusting its band preference based on the probability of failure of the UAV's available bandwidth. Thus, the corresponding optimization problem is formulated as the maximization of each normal user's expected prospect-theoretic utility, as follows.

SAPIENSS Game (normal users)

$$max\mathbf{E}(\mathscr{V}_i) = max\{x_i^{a_i}\mathscr{F}_i(x_T)\},\ \forall i \in N_N \quad s.t.\ x_i \in [0,1] \tag{8.33}$$

On the other hand, malicious users follow a different prospect-theoretic behavior through the sensitivity and risk aversion parameters, with their expected prospect-theoretic utility maximization model as follows:

SAPIENSS Game (malicious users)

$$max\mathbf{E}(\mathscr{V}_i) = max\{x_i^{\beta_i}\mathscr{F}'_i(x_T)\},\ \forall i \in N_M \quad s.t.\ x_i \in [0,1] \tag{8.34}$$

The solution of the SAPIENSS Game $\mathscr{G}$ determines a Pure Nash Equilibrium (PNE), where both the normal and the malicious users have determined their power investment to the MBS-based and UAV-based communication, while each user type aims at achieving its own personal goals, i.e., satisfy their QoS prerequisites for the normal users and deny the service of the normal users by the malicious users who over-invest their transmission power to the UAV-based communication.

For the examined game $\mathscr{G}$, PNE is a stable power investment vector $\mathbf{x}^* = \{x_i^*\}$ where no user can witness an improved utility from its transmission, i.e., $\mathscr{V}_i({x_i}^*, \mathbf{x}^*_{-i}) \geq \mathscr{V}_i(x_i, \mathbf{x}^*_{-i})$, $\forall x_i \in \mathscr{X}_i$. On the other hand, the inability of the game to converge to a PNE would suggest an unstable state for the network which would be associated to the collapse of the UAV's bandwidth with no normal user being able to transmit properly via the UAV network, since only the users who invested in communicating with the MBS will be able to transmit, however at the expense of very low returns (i.e., low data rates and inferior channel gains) in comparison to the UAV-based communication.

Let $\mathscr{B}_i$ be the best response correspondence of each user $i, i \in N$ where $\mathscr{B}_i(\mathbf{x_{-i}}) = argmax\mathbf{E}(\mathscr{V}_i(x_i, \mathbf{x_{-i}}))$, $\mathscr{B}_i : \overline{\mathscr{X}}_{-i} \rightrightarrows \mathscr{X}_i$, where $\overline{\mathscr{X}}_{-i}$ represents the aggregate investment from all users (both normal and malicious users), excluding user i. User's selected strategy for its joint transmission via both the MBS and the UAV is reflected through its best response, where a value $\mathscr{B}_i(\mathbf{x_{-i}}) = 0$ would imply that the user did not invest in communicating with the UAV and opted to transmit only with the MBS preferring to minimize any risks by utilizing only the safe resource. On the other hand, the case where a user opts to communicate only through the UAV-based communication without considering the fragility of the resource, mirrors a malicious user's desire to claim more aggressively the bandwidth from the UAV due to its favorable channel conditions compared to the MBS and thus perform a DDoS attack. This increased power investment of the malicious users to the UAV-based communication will lead to the UAV's bandwidth collapse with certainty due to excessive aggregate demand compared to its overall capacity. Thus, the users that exhibit abnormally aggressive behavior towards claiming data rate from the UAV can reveal malicious user actions aiming to disrupt UAV network's operation, an incident which can be of high criticality, especially in events where public safety is jeopardized, e.g., Public Safety Networks (PSNs).

Following, we examine the existence and uniqueness of a PNE point for the SAPIENSS game $\mathscr{G}$. Without loss of generality and for simplicity of the proof, we assume $a_i = \beta_i$, $\kappa_i = \lambda_i$, and $\mathscr{F}_i = \mathscr{F}'_i$.

Theorem 53. ***(Effective Rate of Return:)*** *The effective rate of return $\mathscr{F}_i$ function is decreasing, concave, and positive in the modified strategy space $\mathscr{X}'_i$, $\forall a_i < 0.5$.*

Proof. We examine the behavior of $\mathscr{F}_i$, via calculating its first (monotonicity) and second (concavity) order derivatives:

$$\frac{\partial \mathscr{F}_i(x_T)}{\partial x_i} = \frac{\partial \overline{\mathscr{R}_i}(x_T)}{\partial x_i}(1 - x_T^2) - 2x_T\overline{\mathscr{R}_i}(x_T) - 2\kappa_i x_T \tag{8.35}$$

$$\frac{\partial^2 \mathscr{F}_i(x_T)}{\partial x_i^2} = \frac{\partial^2 \overline{\mathscr{R}_i}(x_T)}{\partial x_i^2}(1 - x_T^2) + \theta(x_T) - 2\kappa_i \tag{8.36}$$

where $\theta(x_T) = -4x_T\frac{\partial \overline{\mathscr{R}_i}(x_T)}{\partial x_i} - 2\overline{\mathscr{R}_i}(x_T)$.

The solution approach is identical to the proof of Theorem 49, hence for convenience purposes it is omitted. Eventually, we conclude that $\mathscr{F}_i$ is decreasing, concave, and positive in the reduced strategy space $\mathscr{X}'_i = [0, \zeta]$, $\mathscr{X}'_i \subset \mathscr{X}_i$, where $\zeta \in \mathscr{X}_i = [0,1]$. □

Theorem 54. ***(SAPIENSS Game PNE Existence:)*** *For the Fragile CPR SAPIENSS game $\mathscr{G}$, there exists a value $\xi \in \mathscr{X}_i'$ which is a critical point for $\boldsymbol{E}(\mathscr{V}_i)$.*

Proof. Towards proving the existence of a PNE, we investigate the first order condition for $\mathbf{E}(\mathscr{V}_i)$, as follows.

$$\frac{\partial \mathbf{E}(\mathscr{V}_i)}{\partial x_i} = {x_i}^{a_i-1}\Phi(x_i) = 0 \tag{8.37}$$

where $\Phi(x_i) = (x_i \frac{\partial \mathscr{F}_i(x_T)}{\partial x_i} + a_i \mathscr{F}_i(x_T))$. The proof is identical to the proof of Theorem 50, hence for convenience purposes it is omitted. By examining the first order derivative and apply Bolzano's Theorem for $\epsilon \to 0$, $\epsilon > 0$ and ζ, we conclude that there exists at least one $\xi, \xi \in \mathscr{X}_i'$ such that $\frac{\partial \mathbf{E}(\mathscr{V}_i)}{\partial x_i}|_{x_i=\xi} = 0$ and the first order condition is satisfied, indicating that ξ is a critical point of $\mathbf{E}(\mathscr{V}_i)$.

□

Theorem 55. ***(SAPIENSS Game PNE Uniqueness:)*** *The critical point $\xi \in \mathscr{X}_i'$ is a unique PNE for the SAPIENSS game $\mathscr{G}$.*

Proof. In order to prove that the above determined critical point is a unique PNE for SAPIENSS game $\mathscr{G}$, we examine the concavity of $\mathbf{E}(\mathscr{V}_i)$. The second order derivative of $\mathbf{E}(\mathscr{V}_i)$ is given as follows:

$$\frac{\partial^2 \mathbf{E}(\mathscr{V}_i)}{\partial x_i^2} = a_i(a_i-1){x_i}^{a_i-2}\mathscr{F}_i(x_T) + 2a_i{x_i}^{a_i-1}\frac{\partial \mathscr{F}_i(x_T)}{\partial x_i} + {x_i}^{a_i}\frac{\partial^2 \mathscr{F}_i(x_T)}{\partial x_i^2} \tag{8.38}$$

From Eq. (8.38), since we assume that $a_i < 0.5$, $x_i > 0 \in \mathscr{X}_i'$, and $\mathscr{F}_i$ is positive, decreasing, and concave in $\mathscr{X}_i'$, then all terms of $\frac{\partial^2 \mathbf{E}(\mathscr{V}_i)}{\partial x_i^2}$ are negative, and $\mathbf{E}(\mathscr{V}_i)$ is concave, so that the critical point $\xi \in \mathscr{X}_i'$ is a unique global maximum and a unique PNE for SAPIENSS game $\mathscr{G}$ is identified.

□

Convergence

In this section we prove the convergence of the normal and malicious users' decisions to the above unique PNE. According to [172], concerning the class of Fragile CPR games, convergence is established sufficiently via proving that users' best response dynamics $\mathscr{B}_i(\mathbf{x_{-i}})$ monotonically decrease with users' aggregate investment x_T to the CPR.

Theorem 56. ***(Decreasing Best Responses:)*** *The Best Response (BR) strategies of SAPIENSS game $\mathscr{G}$ are monotonically decreasing in x_T.*

Proof. Let $\mathscr{J}(x_T) = -a_i \frac{\mathscr{F}_i(x_T)}{\partial \mathscr{F}_i(x_T)/\partial x_i}$ be defined as the optimal non zero investment of each player $i, i \in N$, where $\mathscr{J}(\mathscr{B}_i(\mathbf{x_{-i}}) + \mathbf{x_{-i}}) = \mathscr{B}_i(\mathbf{x_{-i}})$, when $\mathscr{B}_i(\mathbf{x_{-i}}) > 0$. Identical to Theorems 48 and 52 it is proven by contradiction that the $\mathscr{B}_i$ is decreasing in x_T, confirming the convergence of game's $\mathscr{G}$ to a unique PNE.

□

8.5.3 Distributed Algorithm

In this section we present the distributed and low complexity algorithm for the practical implementation of the SAPIENSS game. The SAPIENSS algorithm is executed in an iterative manner where the normal and malicious users configure their topological and behavioral characteristics and in each step they are allowed to adjust their transmission power levels between the MBS and the UAV towards maximizing their expected prospect-theoretic utility. The algorithm is able to identify intrusive behavior and DDoS attacks within the UAV network, by tracking abnormally high transmission power and interference with regards to the UAV-based communication and notifies the system administrator about the potential network DDoS attack in case counter active defensive actions are necessary.

SAPIENSS algorithm ultimately operates under two potential outcomes: The first is the optimal power investment allocation of all users between the MBS and the UAV, reflecting a successful transmission from the normal users in the UAV network (also considering the case that defensive actions against attackers were applied or no malicious behavior was detected). The above suggests that game's PNE was determined implying a stable outcome for the resource allocation process where no user wishes to deviate with regards to its perceived QoS satisfaction from its transmission. On the contrary, the algorithm can also conclude to the loss of communication between the UAV and the normal users due to excessive

investment from the users in the UAV network, potentially due to malicious behavior of attackers and a corresponding DDoS attack. The system is able to track harmful user behavior during the transmission (which can also be confirmed by the prospect-theoretic modeling of the users' behavior), however if no actions are taken or if the overall demand is significantly higher compared to the available bandwidth from the UAV, then SAPIENSS algorithm announces the cease of UAV's operations, and only the users who partially transmitted via the MBS will be able to exchange information in the overall considered communication environment.

Implementation Steps

The practical execution of SAPIENSS algorithm is based on users informing the system of their topological and behavioral parameters as instructed by the prospect-theoretic modeling. Users initiate their transmission with a randomly selected power investment value x_i within the physical limitations of the network, with the algorithm being able to converge to the PNE or to conclude the collapse of UAV's bandwidth due to a performed DDoS attack. Given the principles of the NOMA access technique, Successive Interference Cancellation is applied based on users channel gains in the UAV network and the overall interference is calculated.

Based on the initial power investment, the normal and malicious users split their transmission among the MBS and the UAV and calculate their expected prospect-theoretic utilities accordingly. UAV is considered to be active during this stage, with the above process being iterated until system converges to stable transmission power allocation between the MBS and the UAV. In the event that malicious behavior is identified via the calculation of overall interference in the communication environment, SAPIENSS algorithm notifies the system administrator of the UAV network and asks for input if counter defensive actions will be taken or not. Eventually, if the system does not manage to address the demand comparative to the UAVs' bandwidth, the algorithm changes the operation status of the UAV to inactive and concludes its execution.

Complexity

SAPIENSS algorithm functions under a decentralized approach where the main decision steps affecting the transmission power (i.e., MBS or UAV) as well as the resource allocation process lie at the users' level. This parallel execution of actions and the reduced data exchange between the users and the system administrator (e.g., only the overall interference is broadcasted by the MBS and UAV) contribute to the fast convergence of the algorithm to the PNE of the game or the identification of the UAV collapse within only a few iterations.

Moreover, the user-centric design allows users to differentiate their transmission priorities according to their QoS requirements or their behavioral modeling. Hence, the algorithm can also quickly track users who are attacking the UAV network without spending additional resources via calculating the intracell interference. The simplified arithmetic calculations and the absence of maintaining historical data minimize computational and storage requirements as well as data overhead, reducing the complexity of the involved calculations. The algorithm was run in an Intel(R) Core(TM) i7-7500U CPU @ 2.70 GHz 2.90 GHz laptop with 8.00 GB RAM, with its average run time per user being approximately 0.3 $msec$, a figure close to realistic timeslot durations (e.g., 0.5 $msec$), allowing the implementation of SAPIENSS algorithm in practical application scenarios. The aforementioned convergence of the SAPIENSS algorithm is guaranteed by the Best Response dynamics approach that is followed to determine the PNE [120].

8.5.4 Intrusion Detection and Ejection

Exploiting the SAPIENSS distributed algorithm presented is Section 8.5.3, in this section we introduce a sophisticated joint intrusion detection and ejection process. As mentioned before, the UAV-receiver is able to measure the overall sensed interference by all the users, i.e., normal and malicious users. If the measured interference exceeds a predefined acceptable level of interference to successfully perform the decoding of the received signals, then the SAPIENSS algorithm raises an alarm flag that a failure is observed, potentially due to the presence of malicious behavior or extremely selfishly acting users, where both cases conclude to the failure of the UAV to serve the users. This mechanism consists a simple intrusion detection process that autonomously operates at the UAV's receiver without requesting any human intervention.

Algorithm 22 SAPIENSS Algorithm

Require:

Number of users $|N_N|$; constants κ_i, a_i, λ_i, β_i; users position coordinates; W_{UAV}, W_{MBS}, $Bound_{interference}$

1: $ite \leftarrow 1$; $UAV_{active}^{(ite)} \leftarrow 1$; $convergence^{(ite)} \leftarrow 0$
2: Apply SIC for NOMA band
3: Assign initial random $x_i^{(ite)}$
4: **while** $convergence^{(ite)}$=0 **and** $UAV_{active}^{(ite)}$=1 **do**
5: Calculate P_i^{UAV}, P_i^{MBS};
6: UAV and MBS broadcast the overall interference and each user calculates its own sensed interference
7: **if** interference> $Bound_{interference}$ **then**
8: Apply defense mechanisms (Go To Step 1) or take no action*
9: **end if**
10: Calculate utility $\mathbf{E}(\mathscr{V}_i)^{(ite)}$ according to Eq. (8.32)
11: **for all** $x_i \in [0,1]$ **do**
12: x_i^*=$argmax_{x_i}\mathbf{E}(\mathscr{V}_i)$
13: **if** $\mathbf{E}(\mathscr{V}_i) > \mathbf{E}(\mathscr{V}_i)^{(ite)}$ **then**
14: $x_i^{(ite+1)} \leftarrow x_i^*$ **and** $\mathbf{E}(\mathscr{V}_i)^{(ite+1)} \leftarrow \mathbf{E}(\mathscr{V}_i)$
15: **end if**
16: **end for**
17: Calculate *normalized* $x_T = \dfrac{\sum_{1}^{|N|} x_i^{(ite+1)}}{|N|}$
18: **if** $\sum R_i^{UAV} > W_{UAV}$ **then**
19: $UAV_{active}^{(ite+1)} \leftarrow 0$
20: **end if**
21: **if** $x_i^{(ite+1)} - x_i^{(ite)} < \epsilon$ **then**
22: $convergence^{(ite+1)} \leftarrow 1$
23: **end if**
24: $ite \leftarrow ite + 1$
25: **end while**
26: **return**

User investment x_i and UAV_{active} if UAV still active

** more details in Sections 8.5.5 and 8.5.4*

After detecting a potential malicious behavior, an efficient mechanism should exist to protect the UAV network from concluding to a probability of UAV's bandwidth failure close to one, thus, the UAV being unable to serve the normal users' QoS requests. Therefore, an intrusion ejection methodology is proposed to isolate the suspicious malicious user and enable the smooth operation of the UAV network. The proposed approach is based on the principles and characteristics of NOMA technology and SIC technique. It is highlighted that the SIC technique decodes first the signals of the users with better channel conditions, thus the users with worse channel conditions are able to cancel the interference stemming from the transmissions of the users with better channel conditions. Therefore, it is evident that if the malicious users have the worse channel conditions in the wireless network, then they can cause the maximum damage. Based on this observation and exploiting the capabilities of the SIC technique, we argue that as the UAV decodes the received signals, it can identify the signal with the greater contribution to the overall sensed interference. Hence, for the specific transmitter (i.e., potential malicious user), the UAV-receiver sets a virtual malicious user's channel gain, which is close to infinity. Following this strategy, the malicious user's signal will be decoded first at the receiver based on the SIC technique and the contribution to the overall interference provided by the potential malicious user's signal is cancelled. Therefore, the transmissions and communication of the rest of the normal users in the examined UAV network are protected. Detailed numerical results showing the operation and efficiency of the proposed methodology are presented in Section 8.5.5.

8.5.5 Numerical Results

In this section, we provide a series of numerical results to evaluate the operational features and the performance of the proposed SAPIENSS algorithm. We consider a UAV-assisted wireless network supporting $N = 20$ continuously backlogged users and it consists of a standard MBS and a mobile UAV which hovers close to the users, both operating under the NOMA transmission technology. The MBS-based wireless network is of radius $\Re = 6\ km$, while the UAV covers an area of approximately 2.5 km within the network. For simplicity of the simulation, we assume that the users are gathered around a specific area of the network with their ID denoting increasing distance from both the MBS and the UAV. The UAV positions itself closer to the users towards providing more favorable channel conditions, in comparison to the static MBS which is impacted by inferior channel gains especially for the distant users. Additionally, the total available bandwidth is 4 MHz, 80% of which is offered by the UAV and the rest provided by the MBS. Given the technical and physical limitations of the system, we set the maximum feasible transmission power $P_i^{Max} = 0.2\ Watts$, while the users request emergency services up to $R_i = 256\ kbps$.

In the aim of covering a wide array of potential operational scenarios for the function of the UAV network from the security perspective, we assume that during the simulations a number of users exhibit malicious behavior with their main objective to disrupt the function of the UAV communication part. Since the UAV based transmission delivers a critical mission for the data exchange, especially under conditions where human life or public safety is at risk (i.e., critical missions), we investigate how malicious or intrusive user behavior can be identified, as well as how the system can cope with such attacks by establishing and utilizing effective defensive mechanisms, i.e., IDS and IES. In the examined scenarios, malicious users attack the UAV bandwidth with a DDoS attack by transmitting at abnormally high transmission power levels which deteriorate the quality of transmission for all other normal users especially via increasing the overall interference, while also by claiming a higher portion of the available UAV's bandwidth, restricting other users for having access to very valuable data rates. The above does not exclude other types of malicious user behaviors such as data eavesdropping, spread of malware, GPS spoofing, which however are considered out of scope for the presented research work.

In the next sections we present different stages of the operation of the UAV network starting with a baseline scenario where the system operates without any disruptions from intruders, and following we examine how system adjusts to cases of user attacks, how their behavior can be identified both from the practical and theoretical perspective of the model, as well as how the UAV network can sustain such incidents protecting the rest of the normal users with regards to ensuring reliable transmission conditions.

Normal Operation

Fig. 8.12a depicts user power investment x_i to the UAV bandwidth per their ID in the UAV network (assuming also increasing distance from the UAV and MBS position). We observe that due to the relatively high value of the loss aversion parameter κ_i the users are conservative enough towards transmitting via the UAV magnifying the probability of the potential risk of the collapse of its bandwidth. As a result, the maximum investment in the UAV bandwidth is below 50%, while the users also to select the safe communication with the MBS. Moreover, we observe that users closer to the MBS and the UAV select a very low investment to the UAV since their favorable channel conditions allow them to obtain satisfactory data rates without devoting a high portion of their transmission power to the collapse prone UAV-based communication. The same applies for the very distant users (i.e., 19 and 20) who sense almost no interference since it has been significantly cancelled due to the application of the NOMA SIC technique. Hence, they manage to still transmit without raising their investment despite their unfavorable channel conditions. On the other hand, middle distance users are simultaneously affected by worsening channel conditions and rising interference levels, and subsequently they are attracted to invest more transmission power to the UAV communication, since it provides high return and free to access bandwidth resources.

The above analysis is confirmed also in Fig. 8.12b illustrating the achievable data rates of each user from both its communication with the UAV and the MBS. As described before, very close or distant users manage to obtain high data rates from the UAV (blue bars) without excessive investment, where middle distance users achieve lower data speeds since their transmission conditions (i.e., channel gain and interference) hinder meeting their QoS targets. On the other hand, all users obtain the same data rate from their transmission via the MBS (red curve). The lower magnitude of MBS's bandwidth and the higher distance of the MBS from the users in comparison to the UAV delivers significantly lower data rates, which however are considered as a safe and guaranteed return due to the closed access scheme of the MBS and the strict bandwidth monitoring policies implemented by the Service Provider.

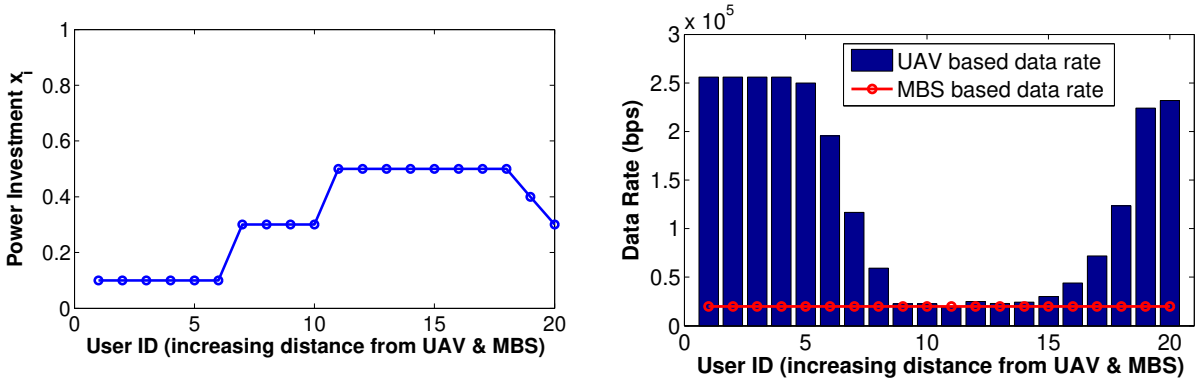

(a) (b)

Figure 8.12: (a) User power investment x_i vs user ID: Case of absence of malicious users, (b) User data rate vs user ID: Case of absence of malicious users

Identifying Malicious User Behavior

Next, we discuss the case that users with ID 11-13 are considered as malicious (i.e., $|N_M| = 3$) with their objective not necessarily being to satisfy their QoS prerequisites, but to disrupt the UAV network's operation by transmitting with abnormally high transmission power levels to the UAV causing interference and claiming significant bandwidth resources in expense of the rest of the normal users (i.e., $|N_N| = 17$), whose behavior is considered unmodified compared to the previous scenario. Specifically, users with ID 11-13 are assumed to eliminate their risk aversion parameter (i.e., $\lambda_i = 0$) and at the same time present a threefold increase of their sensitivity parameter towards the CPR (i.e., $\beta_i = 0.15$). As shown in Fig. 8.13, the power investment of users with ID 11-13 rises to the upper value (i.e., $x_i = 1$), implying that they solely try to transmit via the UAV-based communication. Under this scenario, we assume the case that the UAV's bandwidth sustains the attack both in terms of the higher interference levels and bandwidth distribution among the users. In Fig. 8.14, it is clearly observed that users with ID 11-13 due to their considerably risk seeking behavior managed to significantly increase their data rates in the CPR (i.e., the UAV-based communication), while they stopped transmitting via the MBS. The impact to the rest of the normal users has been mostly visible for users with ID 6-10 since they are the ones sensing the additional interference from the malicious users while also they have to manage their low quality channel gains. On the other hand, normal users still investing in the safe resource (i.e., the MBS-based communication) experienced a small increase in their attainable data rates since the malicious users with ID 11-13 stopped transmitting via the MBS, thus they reduced the competition in this part of the UAV network.

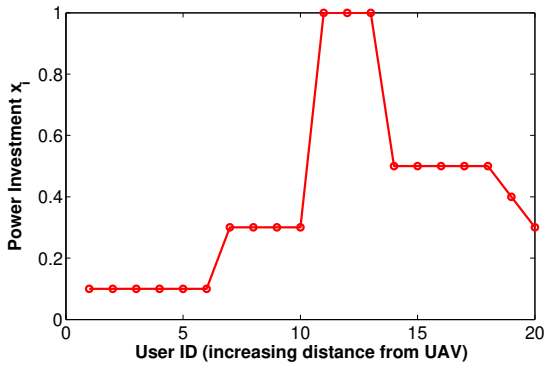

Figure 8.13: User power investment x_i vs user ID: Case of presence of malicious users 11-13

On another case, we assume the scenario that the UAV network is under a wide scale of DDoS attack from multiple malicious users. In this situation, users with ID 10-18 are considered malicious (i.e., $|N_N| = 9$), with all of them completely investing in the UAV-based communication, hence driving the commonly shared UAV's bandwidth to collapse due to excessive demand and rising interference

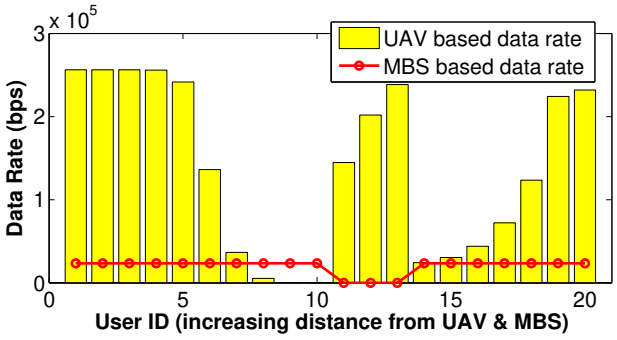

Figure 8.14: User data rate vs user ID: Case of presence of malicious users 11-13

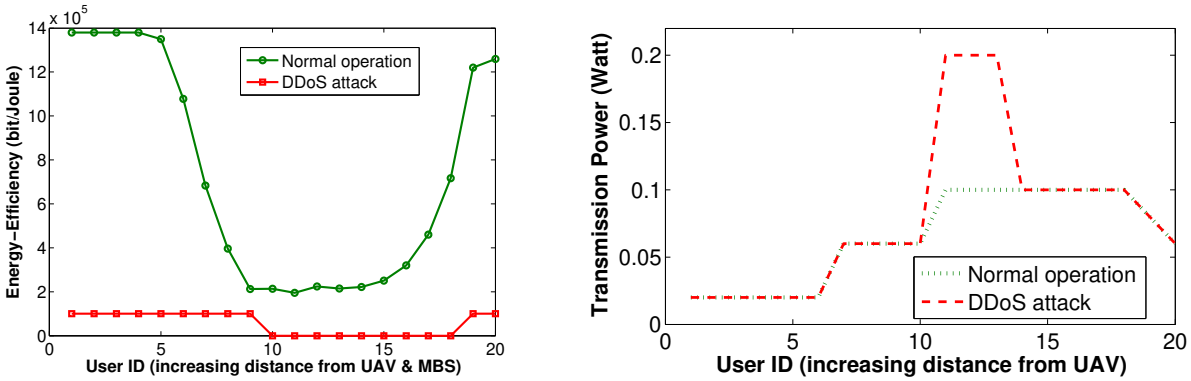

(a) (b)

Figure 8.15: (a) Energy-efficiency vs user ID: Case of intensive attack due to presence of malicious users 10-18 and collapse of UAV bandwidth, (b) Detecting malicious user behavior: Transmission power vs user ID

levels. This has immediate impact on the achieved energy-efficiency of the system, representing the transmitted data bits per Joule of consumed energy, measured in [bits/Joule]. In Fig. 8.15a, we compare the energy-efficiency of each user for increasing distance from the UAV and the MBS. In the case where the system operates normally without any DDoS attack (green curve), we notice the trend explained before, with close and far away users to have significantly higher energy-efficiency levels due to their favorable transmission in comparison to the middle distance users. On the other hand, in the incident of the intensive DDoS attack against the UAV network (red curve), the energy-efficiency is significantly lower due to the failure of the UAV's bandwidth to serve the users' QoS requests. In this case, the malicious users do not manage to transmit at all, while the rest of normal users manage to obtain some returns only from their communication with the MBS. It is highlighted that based on the IDS and IES systems proposed in Section 8.5.4, the NOMA SIC technique enables the cancellation of the malicious users' imposed interference, thus even if they transmit through the UAV, their transmission does not affect the rest of the normal users in the network. In that case, the normal users sense no transmission (Fig. 8.15a) and corresponding interference from the malicious users.

Stemming from the above simulation examples, the importance of early detecting the malicious users' behavior via the IDS and IES systems towards protecting the operation of the UAV is evident. The above can be identified both from the practical implementation of the SAPIENSS algorithm, as well as from the theoretical system model based on the principles of Prospect Theory. Fig. 8.15b compares user transmission power when the system operates normally (green curve) and the case where the users with ID 11-13 are malicious. It is shown that in the case that the UAV network is under attack, the malicious users transmit with maximum power (i.e., $P_i^{Max} = 0.2$ Watts), which acts as an obvious and quick identifier for the system administrator in view of detecting suspicious users' activity and to take counter actions towards protecting the UAV network following the operation of the autonomous IDS and IES systems. Furthermore, the above conclusions can be confirmed by the theoretical background presented in

the previous sections of this research work. In more detail, the user specific utilities designed according to the behavioral model of Prospect Prospect allowing heterogeneous user preferences and risk perceptions, corroborate the trends found from the transmission powers of the attackers. By studying the values of loss aversion and sensitivity parameters, malicious user behavior is reflected by their risk seeking attitude with regards to aggressively claiming bandwidth from the UAV. In Fig. 8.16 the behavioral deviation of normal and malicious users is easily noticed via the elimination of risk aversion from the latter, ($\kappa_i > 0$, $\lambda_i = 0$) and the increase in sensitivity ($a_i = 0.05$, $\beta_i = 0.15$), implying an aggressive stance of attackers ignoring the impact of UAV's bandwidth failure which could result in an interruption of the UAV communication. On the other hand, normal users are concerned over the potentiality of system collapse so they tend to overweight the probability of failure of the UAV's bandwidth and subsequently adopt a more conservative behavior when transmitting via the UAV-based communication so that it does not collapse and prefer to maintain an additional guaranteed data rate via investing in communicating with the MBS.

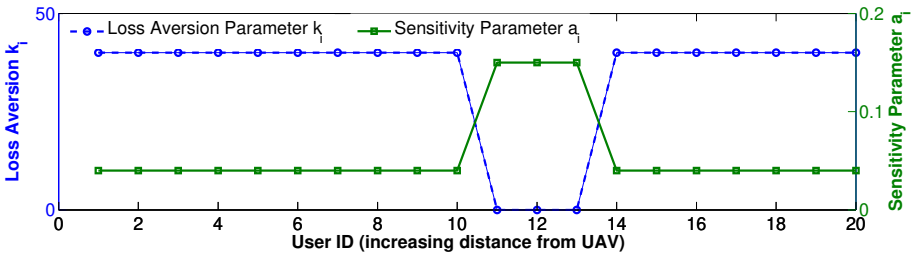

Figure 8.16: Detecting malicious user behavior: Prospect-theoretic parameters vs user ID

Defense Mechanisms

At this point it becomes of paramount importance for the PSN to develop additional defense mechanisms besides SIC against malicious users who can put network operation at stake in case not only NOMA networks are considered. In this subsection we discuss two indicative counter measures when suspicious user activity is concerned in order to ensure that the network will continue its operation with the highest possible QoS delivered to the users following the principles of the proposed IDS and IES systems. The SAPIENSS framework generally allows the integration of defense and intrusion ejection mechanisms from the UAV network during its implementation, hence the resource allocation process is not distorted or modified.

Admission Control: As previously identified, one of the basic operational characteristics of the malicious users in this work which can be easily recognized is the considerably higher transmission power towards the UAV-based communication. The above feature can be used as an instant autonomous detection and intrusion ejection tool that the UAV can utilize when the criticality of conditions intensifies the need to preserve the fragility of UAV's bandwidth. In this direction, in Fig. 8.17 we show the application of the proposed IDS and IES systems under which the SAPIENSS algorithm expels potentially malicious users from the network during its implementation steps in case their transmission power is abnormally high compared to their closer neighbors. In more detail, in the red curve, the original attack scenario is shown where the users with 11-13 are considered as malicious, since all the rest of the users transmit with less than the half of their transmission power. Concerning this case, the SAPIENSS algorithm since it already receives this information towards calculating the intracell interference in the UAV network, raises an alarm flag and in its next iteration blocks those users from transmitting following the principles of the NOMA SIC technique. This is shown in the green curve of Fig. 8.17, where we observe that the UAV has cancelled the interference caused by them to the rest of the normal users, thus the malicious users appear to the rest of the users like they do not transmit at all. Interestingly enough, this impacts the rest of the users of the network, since users with ID 7-10 reduce their investment to the UAV-based communication since their sensed interference has decreased according to the NOMA protocol, while the users with ID 14-20 increase their investment to the UAV due to the reduced competition after the transmission cancellation of the users with ID 11-13.

UAV Mobility: Another alternative targeting at maintaining the UAV-assisted communication is to adjust the transmission conditions of the users within the PSN in order to minimize the impact of

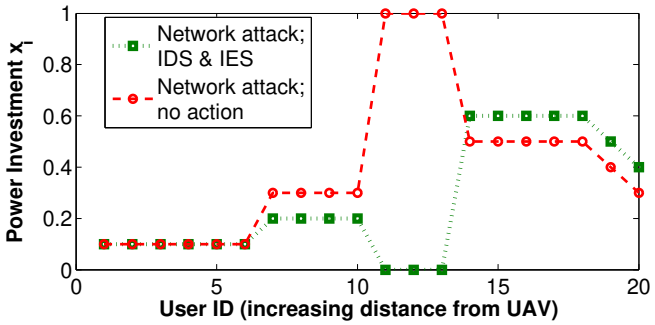

Figure 8.17: Power investment vs user ID implementing intrusion detection and ejection

suspicious behavior via worsening the channel conditions for the transmission of malicious users. In this point, SAPIENSS algorithm would again identify risky user activity through higher transmission power and during its implementation will reposition the UAV in the PSN in order to prevent the malicious user to achieve high data rates and discourage continuing its interference causing transmission. In Fig. 8.18 we developed a holistic overview of the system behavior with regards to user data rates when the network operates normally (green bars), when user 8 changes its behavior and adopts a much more aggressive behavior which would characterize it as malicious (red bars) and lastly, the counter action mechanism from the PSN where the UAV moved in order to confront the attack (blue bars). In more detail, under the normal operation of the PSN, data rates follow the general trend we described in a previous section (*See Fig. 8.12b as well*), while when user 8 attacks, it manages to rapidly increase its achieved data rate, however considerably damaging the transmission of users 5-7. In the last case where the UAV moves in order to reduce the impact of the attack, in this scenario we assume that SAPIENSS instructs the UAV to move close to user 20 (who originally was the most distant) in order to worsen the channel conditions of user 8. As we observe from the blue bars of Fig. 8.18, indeed the attainable data rate of user 8 is reduced, hence defending the network against the alleged attack. Additionally, since users 11-20 are much closer to the UAV, they manage to significantly increase their data rates since their channel gains are much improved under the new coordinates of the UAV. Lastly, users 1-7 still manage to transmit with sufficient data rates, in contrast to users 9 and 10 who are very heavily affected by the new position of the UAV and can no longer transmit.

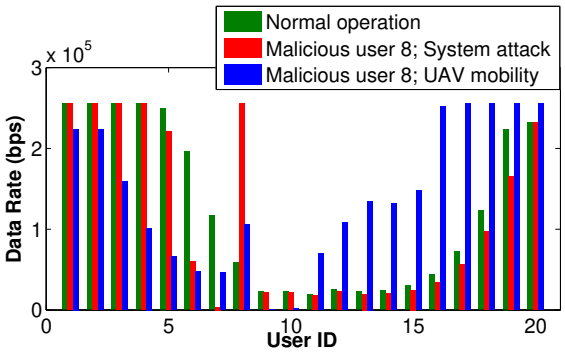

Figure 8.18: Data rate in case of UAV mobility

8.6 General Summary

Chapter 8 broadens the scope of dynamic resource management under conditions of uncertainty in challenging environments posing significant constraints in the resource allocation process. Public Safety Networks constitute a special category of wireless networks which are especially deployed to support transmissions in cases of an unexpected external event or in severe environments, via utilizing Unmanned Aerial Vehicles. Additionally, the case of malicious user behavior and the potential impact of intrusive

actions in the fragility of spectrum was examined. In each case, the use of Prospect Theory offers the appropriate background in order to model such problems, since PSNs and networks where security concerns are raised operate under even higher volatility and fragility risks. Subsequently, in this thesis we provide a new fresh point of view on how users by properly selecting their strategies can impact not only the performance of the network, but more importantly its own survival and operational continuity, while also develop proper threat identification and ejection techniques.

Regarding PSNs, in the first two sections of this Chapter, a risk-aware transmission power control framework is proposed, considering a UAV-assisted PSN with a macro BS and a UAV, or involving multiple UAVs (both static and mobile). The ground users can invest their transmission power to the MBS or the UAVs, with the (mobile) UAV-based communication considered as the CPR, where the users compete with each other for the UAV's limited bandwidth, while the Macro MBS (or the static UAV) to be viewed as a safe resource. The UAV spectrum's exploitation, while promising higher satisfaction, introduces uncertainty to users' power investment decisions, as the potentially increased levels of interference if over-exploited can make it fail to serve the users. Furthermore, the resource-constrained environment and the partial information availability introduce risk to users' decisions regarding their transmission power investment. Respecting the need for developing distributed solutions for the users' risk-aware behavior in the created competitive communication environment, non-cooperative games among the involved players have been formulated, where each user aims at maximizing its prospect-theoretic utility function by autonomously deciding its power investment x_i. The existence and uniqueness of Pure Nash Equilibrium points was shown and distributed algorithms were introduced to converge to those PNE points. Finally, the performance of our proposed frameworks in terms of several metrics were examined via modeling and simulation, while accounting for users' realistic behavioral scenarios.

Lastly, we also introduced a novel framework towards ensuring the efficient and smooth operation of a UAV-assisted NOMA wireless network consisting of both normal and malicious risk-aware users. User devices are assumed capable of splitting their transmission power in two different communication alternatives - that is UAV-based and MBS-based communication links. Again, the UAV's bandwidth was considered as a CPR accessible by everyone offering potentially high rate of return, but being susceptible to failure due to its potential over-exploitation. In contrast, the MBS's bandwidth was designed as the safe resource offering to the users a more limited but guaranteed level of service, due to the fact that though it has less available total bandwidth, it operates under a more controlled access and monitoring scheme. In this case as well, malicious users' risk-aware behavior was reflected via Prospect Theory, while the potential failure of the CPR due to the attacks was captured by the Tragedy of the Commons. The problem was formulated as a non-cooperative power control game whose existence and convergence to its PNE was analytically shown. Based on the normal and malicious users' risk-aware behavioral characteristics, their corresponding transmission power investments as an outcome of the power control game, and the operational principles of the NOMA technology and the SIC technique, a novel intrusion detection and ejection methodology was introduced. The performance and inherent attributes of the proposed user-centric risk-aware operational framework were assessed under several different operation scenarios, in terms of its capability to effectively utilize the available system and user resources (i.e., bandwidth and power), while succeeding in identifying potential abnormal or malicious user behaviors.

Chapter 9

Conclusions and Future Work

In this chapter, the main takeaways of this doctoral work are discussed and its key contributions are summarized (Section 9.1). Additionally, we briefly present some indicative further research directions stemming from this work (Section 9.2). Lastly, in Appendices A and B the list of publications that the author contributed are presented, as well as the awards received in relation to this work.

9.1 Conclusions

The upcoming adoption of 5G networks in wireless telecommunications is expected to deliver fundamental and disruptive changes in the architecture, infrastructure, and operational attributes of wireless networks. Massive connectivity and diversifying user requirements are forming a highly competitive and volatile communication environment, which poses significant challenges to Wireless Internet Service Providers (WISPs) towards designing wireless networks able to provide a seamless user experience with superior Quality of Service (QoS). Intelligent mobile devices under the dawn of the Internet of Things (IoT) era, new communication standards as well as the rapid increase of data hungry applications have been associated with skyrocketing traffic levels and congestion, bringing existing networks to their operational and capacity limits.

Future cellular networks cannot evolve in the direction of simply increasing spectral capacity or adopting new access technologies, but should be structurally redesigned, placing the user at the core of their operation. In view of this, a plethora of research tools and algorithms are already being developed to tackle the topic of the efficient allocation of network's principal resources, i.e., bandwidth and transmission power, in a socially fair, energy-aware, and market sustainable approach. Diversification of services, standards, and applications alongside network densification and mass connectivity create a disruptive and new landscape in wireless communications which is expected to magnify data and traffic volumes, boost data rates and provide a whole new user experience away from the conventional voice-only cellular networks that dominated telecommunications in the past decades.

Against those developments, in this thesis we proposed a holistic and multi-faceted framework for optimizing network performance from the perspective of both Service Providers and users alike. Ameliorating user satisfaction and customer surplus have been key objectives of this work, achieved by empowering users to control multiple aspects of their transmission in an interactive communication with the WISP, instead of being simply instructed on how to mitigate interference and excessive data consumption. Users are not considered as uniform and neutral nodes requesting identical services, but are viewed as heterogeneous players with different preferences and priorities, consuming simultaneously diverse applications in terms of delay tolerance and data volumes. In that sense, resource allocation in wireless networks becomes a dynamic mechanism which supports network evolution, expansion, and constant adjustment to changing user requirements, functioning in a decentralized and user-oriented manner. In parallel, motivated by the need to transition into energy-efficient and sustainable communications, this work focused on developing all those methodologies to reduce unnecessary over-utilization of resources and minimize energy consumption, hence accomplishing the optimal transfer of information with respect to both data exchange and the corresponding transmission power requirements.

In order to ensure a concrete theoretical foundation for this work, user satisfaction was quantified via the use of network utility maximization, while the involved resource allocation problems have been modeled as non-cooperative games whose stable outcomes have been confirmed via solid mathematical

proofs ensuring the determination of the games' corresponding Nash Equilibria, representing stable outcomes for the operation of the network from which no user wishes to deviate. Novel solutions have been adopted including multi variable optimization, using elements from S-modular games, quasi-concavity of utility functions and optimization theory, etc. Thorough investigation of the existing literature allowed to identify the research gaps in the respective fields, while the results obtained within this work have been practically implemented via distributed algorithm sets and tested via extensive series of simulations, evaluating the operation of the proposed schemes under varying scenarios and also against other state of the art approaches in the literature. Due to the user-centric approach and the resource flexible allocation, notable performance advantages have been identified in terms of energy-efficiency, resource utilization, power, and interference mitigation as well as data speed superiority, among others.

The structure of the thesis with regards to the identified problems and their respective solutions is summarized below:

After a brief introduction of the research state of the art and the thesis motivation as a first new paradigm for the resource allocation in wireless networks, the use of multi-tier architectures and network layers was introduced in Chapter 2. Heterogeneous wireless networks consisting of the macrocell, multiple femtocells, and Visible Light Communication (VLC) cells were examined, [23]. The initial distributed power allocation problem for real and non-real time services for both macro users (MUs) and femto users (FUs) was investigated (Section 2.3), [68]. Expanding the study to include more complicated resource allocation problems, in Section 2.4, [80], the joint power and rate control was examined for a double tier multi-service network, consisting of a macrocell and a varying number of femto access points. The original two variable problem was converted to a single pseudo variable optimization by considering the ratio of data rate to its corresponding transmission power. Following, the real two parameter power and rate allocation problem was confronted and solved in Section 2.5, [119], delivering significant performance improvements with regards to the previous approaches, as well as compared to the literature, due to the distributed and actual control of two distinct degrees of freedom by the users. The Chapter is closed with Section 2.6, [277], where the power control and the optical access point allocation problems are comparatively examined for both the OFDMA and NOMA access techniques in VLC networks, offering additional insights on how multi-tier structures can support complex resource allocation cases with notable performance gains.

Next, in Chapter 3, the topic of personalized pricing policies in resource allocation problems was studied with respect to multiple resources. The impact of pricing on the behavior of the users and the network performance in total was tested, while the user populations are accordingly clustered into different segments to reduce computational complexity. More specifically, in Section 3.2, [120], the power and price control problem is for the first time considered as a joint resource allocation problem with the users correlating their power consumption with their willingness to pay for their transmission instead of centrally having prices being enforced to the users as penalties by the network administrator. Examining the problem from a different angle and considering a economic dimension for resource utilization, in Section 3.3, [121], we proposed a mechanism for rate allocation where users are similarly expressing their willingness to pay, however for the respective fraction of the available bandwidth this time. Lastly, the last part of Chapter 3, (Section 3.4), [210], investigated for the first time the triple resource allocation problem of power, rate, and price, with the users ultimately optimizing their entire energy-efficiency performance by adjusting the corresponding price for the service they receive and the power they transmit. They results reveal that pricing schemes can act as an effective tool towards a Pareto optimal outcome for the network in general in terms of social welfare, and for the users to enjoy superior QoS as they determine the basic aspects of their transmission and reveal the relevant charges they accept in order to operate.

Following, the power control and pricing policy implementation are combined with the Provider Selection problem assuming a competitive wireless network environment (Chapter 4), [200]. In order to adapt to the new trends in pattern recognition and big data management, an autonomous and decentralized Machine Learning mechanism was built, operating in parallel with the resource allocation process. Users are modeled as learning automata and select the WISP that better addresses their QoS requirements in terms of both transmission quality and pricing, based on a price and service reputation scheme. The results indicate that the respective pricing strategy as well as the automated decision process of the users, heavily impact the ability of each WISP to penetrate the market and the network's resource allocation efficiency under conditions of severe competition.

The scope of resource allocation problems was further broadened in Chapter 5, by integrating bundling

schemes through the accumulations of multiple telecommunication services in one package under a market driven perspective, which is shaped by the user in a customized manner. In Section 5.1, [151], the resource allocation problem for the first time considers the simultaneous receipt and use of both real and non-real time services by the users, who have the capacity to determine the percentage of their transmission power referring to each service type. The problem is considerably enlarged in Section 5.2, [152] via the aggregation of numerous services into a single product, with the users to define at each time which options they prefer in a modular architecture concept. The potential synergies among the diverse services significantly differentiate the overall user experience, with simulations to confirm the superior user satisfaction, while at the same time providing WISPs with more tools towards unlocking new market segments and boosting their revenue prospects.

In parallel, aiming at delivering a different point of view in the resource allocation problem, the topic of wireless energy harvesting before the actual resource allocation process takes place has been analyzed in Chapter 6, by utilizing Wireless Powered Communication Networks (WPCNs), [278]. In this Chapter, the resource allocation (or Wireless Information Transfer - WIT) phase is connected with the preceding Wireless Energy Transfer - WET - phase between a Power Station and the users, with the objective that the energy consumption is ideally adjusted to the users' transmission requirements. Hence users' batteries are sufficiently charged for the subsequent communication with the base station, by determining the time duration of the WET phase. In that sense, energy-efficiency is improved, and unnecessary energy spend is eliminated since the users specifically define how much energy is required for the WIT phase according to their QoS preferences.

All the above problems were solved under the assumption that user utilities are uniform, while also resource fragility and probabilistic uncertainty have not been considered. This thesis delivered a major breakthrough in the fundamental understanding of dynamic resource management problems instructing that user strategies are not a consequence but a major driving factor for network's operation. The use of Nobel winning Prospect Theory as the main modeling tool of user behavior allowed the introduction of user subjectivity in decisions when probabilistic uncertainty of the risk of resource collapse or shut down of the network are considered, under the concept of the Tragedy of the Commons. In particular, network's spectrum has been modeled as a fragile resource, with one part of it being commonly shared and accessible to all users functioning as a Common Pool of Resources (CPR), which may collapse if over-exploited due to being rivalrous and non-excludable, while another part was regarded safe, due to closed access and strict traffic management. Subsequently, in Chapter 7 the above framework has found fertile ground for application in areas where user decisions are crucial between different connectivity options, such as bundling of licensed and unlicensed spectrum (Section 7.3, [216]) as well as joint transmission of different access techniques, such as NOMA and OFDMA (Section 7.4, [264]). Moreover, the use of pricing was checked this time from a different perspective, not as a penalizing force or an expression of customers' willingness to pay, but as a taxation mechanism whose mission is to protect resource (spectrum) fragility against over-utilization, and maintain the highest possible social welfare and utility surplus among the users of the network (Section 7.5, [276]).

Capitalizing on the sophisticated practical and theoretical tools and methodologies developed for solving resource allocation problems under diverse conditions and technologies, in Chapter 8 the problem was also expanded to extreme communication environments. Public Safety Networks, or simply PSNs (Sections 8.3, [240] and 8.4, [239]) with the use of Unmanned Aerial Vehicles (UAVs) have made telecommunications feasible in cases of urgent external events (such as natural disasters, infrastructure destruction or terrorist attacks etc.), that in the past was not possible to manage. In this work, user-centric resource management becomes part of those networks by facilitating traffic control and congestion offloading, towards minimizing the risk of spectrum over-utilization and ensuring that the operation of the PSNs remains uninterrupted, especially in cases where human life or public security is at stake. Additionally, aiming at analyzing users' behavior and integrating it within the resource distribution process, advanced security mechanisms were designed towards identifying malicious user activity which could jeopardize the operation of the PSN (Section 8.5). In the last part of the thesis, potential attacks and excessive utilization of spectrum were studied in depth via using Prospect Theory and the SIC technology of NOMA networks, as well as taking advantage from the flexibility and mobility of UAVs to allow to stabilize and eject from PSNs any users whose malicious or suspicious activities may disrupt the fair distribution of resources and downgrade user satisfaction.

Based on the previous overview, via this thesis a series of novelties and breakthrough approaches have been introduced, aiming at leading to a rethinking of how resource allocation can enhance network

performance and lead to optimal outcomes of utilization, sustainability, and superior user satisfaction. As already claimed in the introductory Section 1.2, a brief summary of the contributions of this work is as follows:

- Resource allocation has been applied in multi-layered, multi-service, multi-resource, self-optimizable systems. Users can now control various parameters of the transmission and are able to select the interface, tier or service based on their individual preferences. The network becomes a decentralized structure which reaches optimal communication outcomes based on the strategy of each user without the intervention of an external administrator or regulator.

- Novel resource management methodologies under new technology schemes and standards have been implemented (e.g., VLC, femtocells, use of unlicensed bands, NOMA, SIC etc.), taking advantage of the new functionalities and their enhanced capacity towards ameliorating QoS provision and data speed.

- Tangible gains in energy-efficiency and spectrum utilization have been provided. Realizing the importance of energy savings, battery autonomy, and prolonged wireless network on-time durability, tools have been designed for the reduction of transmission power reduction and interference mitigation. Moreover, a more rational utilization of spectrum and its fair distribution among users has been proposed, leading to increased social welfare and more reasonable data use, further lowering energy requirements.

- Resource allocation and service composition become correlated. Services are considered heterogeneous and diverse data exchange modules which are differentiated based on their delay tolerance and data volume characteristics. Mobile customers are given the freedom to pick the service options they prefer, shaping personalized telecommunication bundles in a market oriented perspective.

- Resource pricing in wireless networks is viewed from a fresh new perspective as an independent, bounded user resource to be allocated. Price becomes customized and is optimized in accordance to users' willingness to pay based on their transmission and data consumption prerequisites, instead of a flat external penalty targeting at interference mitigation.

- In this thesis, for the first time spectrum is considered as fragile resource allowing for a more pragmatic approach against resource management in wireless networks, easily adjusted to real life situations. Users are not any more blind and homogeneous agents, but they are able to assess risks and take decisions on how to optimize their transmission and protect the operation of the network in overall.

- Multidisciplinary approach encompassing elements from Machine Learning, Service Bundling, Microeconomics, Game Theory and Behavioral Economics, among others, provide a wide array of tools in order to tackle resource management problems where users interact with each other. Subsequently resource allocation can be expanded in managing increasing amounts of data, user heterogeneity, and energy conservation, while also being established in environments where harsh telecommunication conditions prevail (Public Safety Networks).

- This thesis introduced a scalable resource allocation framework both from the practical implementation and theoretical modeling, being adjustable to new technologies and architectures, user requirements, and different resource types. Hence, it is constructed to solve a broad range of problems and be easily transferred in different scientific domains not necessarily related to telecommunications.

9.2 Future Work

The work summarized in this thesis proposes a meaningful and general framework, where the control intelligence and decision making process lie at the users towards applying agile resource allocation methodologies for enhancing energy-efficiency, distribution fairness, and superior QoS delivery in 5G wireless networks. The future researcher can derive interesting extensions stemming from this work in fields related to topics with respect to resource allocation and optimization in decentralized and ad-hoc network designs, where users' interdependent behaviors and decisions play a key role in system's self-optimization, applicable in many aspects of the upcoming deployment and research for 5G networks and beyond.

We identify below some interesting directions for further research as a continuation of this work. The list is by no means exhaustive, as ongoing technology advancements and changing user requirements provide interesting opportunities to apply the proposed approach in other fields of wireless networking or in other scientific disciplines.

Mobile Edge Computing: Mobile Edge Computing (MEC) suggests a new network architecture paradigm identified as a key enabler for future 5G networks. Under the MEC concept, computing tasks in congested cellular networks are offloaded partially or entirely at the edge of the network in a distributed computing environment [279, 280]. Resources are shared and utilized via the use of servers integrated as elements of the radio access network (RAN), enabling the more sophisticated traffic management and ease the demand for data hungry applications at the backhaul of the network [281], [282]. Applying the approaches described in this work becomes of great practical and research interest, since resource allocation between the mobile devices and the MEC servers can be efficiently orchestrated and synchronized via game theoretic models under an energy and risk-aware manner. In this case as well, users are emerging as the key stakeholders towards controlling resource management and enabling the improvement of network's performance in diverse activities, such as edge video caching, content delivery, connected and self-driving vehicles etc.

Machine-to-Machine and Device-to-Device Communications: Machine-to-Machine (M2M) and Device-to-Device (D2D) technologies allow for omnipresent connectivity between smart devices with minimal human intervention [283–287]. In alignment with the Internet of Things (IoT) evolution, devices become able to exchange data in an autonomous manner, either overlaying or underlaying the cellular network, using dedicated or common resources within the wireless environment. Resource block allocation, access technology selection or power and rate control management are problems of paramount importance in this field of wireless communications as well. The schemes presented in this work can facilitate the resource allocation process in such networks aiming at ameliorating QoS serving different purposes such as eHealth applications, security and surveillance or city automation, among others [288], [289]. Given the exploding number of connected devices and the densification of wireless networks, improving the data exchange and ameliorating the energy-efficiency among autonomous devices is of profound significance.

Light Fidelity communications: Light Fidelity (Li-Fi) technology suggests a novel optical communication interface towards addressing the spectral shortages in heavily congested wireless networks via the use of LEDs. Li-Fi as a VLC based communication standard is expected to further expand transmissions by shifting radio signals to optical technologies and unlock additional fractions of the visible spectrum, allowing mobile devices to exchange data via the light in indoor facilities (museums, airplanes etc.) in high data speeds with low energy requirements where Wi-Fi does not effectively operate [290]. The framework proposed in this work delivers great potential of application in this area, since the presented resource allocation algorithms and theoretical modeling can easily be adjusted in such environments allowing users to maximize their QoS satisfaction in multi-tier architectures, switch between access technologies or adapt their strategies accordingly in order to reduce their transmission power levels.

Prospect Theory in personalized communications: The use of Prospect Theory in wireless communication problems suggest a major breakthrough on how resource allocation problems are modeled and user interactions are perceived in general. Prospect Theory proposes a shift from the static behavioral modeling of Expected Utility Theory (EUT) [291], allowing user heterogeneity and assessment of risk as in real life scenarios. Further applying prospect theoretic behaviors in wireless network optimization problems appears as an essential path towards comprehending how actually user satisfaction is structured moving from a plain quantification of Quality of Service to a real identification of users' experience and decision making. Prospect Theory emerges as a tool applicable in a wide range of resource allocation problems capturing critical user choices under conditions of uncertainty such as accessing already congested networks, WISP revenue, and pricing models within fierce provider competition, investing in high data rates while battery levels are low etc. [192], [194].

Automation, pattern recognition, and big data analytics in telecommunications: The rapidly rising volumes of data and the need to provide reliable and low latency communications indicate that actions to automate, evaluate information, take decisions, and keep human involvement to a minimum become a necessity [292, 293]. The Machine Learning mechanism presented in this work consists only a

fraction of the potential of merging Artificial Intelligence with emerging wireless communication technologies [294]. Wireless systems are evolving to *Artificial Neural Networks (ANNs)*, offering numerous development directions for more efficient resource allocation. Examples include designing models for prediction and inference via ML algorithms, user clustering and computational caching, data compression and recovery, virtual reality and intelligent UAV-based self-organized networks (e.g., path planning, trajectory prediction etc), among others. All the above require multidisciplinary approaches for more agile and scalable resource allocation methodologies, to overcome the challenges in managing increased traffic and computational power in a proactive manner, so that over-utilization of network's capacity is avoided [122].

Use of new sources of spectrum: The initiatives towards increasing spectral capacity in wireless communications by the use of unlicensed bands of higher frequencies, mm-Wave communications or coexistence of multiple radio access technologies (multi-RAT) offer interesting research possibilities towards exploring massive deployments with limited infrastructure costs, simultaneous connectivity, and convergence among different spectrum sources etc. Those new trends allow for bold resource allocation concepts to be implemented with the users to be able to flexibly and dynamically decide the major parameters of their transmission. This work can provide the foundation for exploring new energy-efficient schemes and resource sharing functionalities when multiple sources of spectrum become available in a user-centric manner aiming at providing low latency, high quality, and multimedia communications.

New product designs and smart data pricing: The pricing research conducted in this work proves that innovative pricing schemes can reinvent the way wireless communications take place, not only as a corrective measure in the direction of more rational resource utilization, but also as a means of stimulating service consumption and unveil customers' willingness to pay for their transmission. The rise of IoT provides new opportunities for enhancing network performance and promote pricing incentives in order to control congestion, traffic, and excessive interference. Combining different pricing models with resource allocation schemes similar to this work offers interesting applications for future wireless networks due to the increasing diversity in services and data requirements of users. Auction and packet pricing, pricing for cloud computing, or token pricing all constitute important costing variations serving different purposes depending on distinct business and data consumption models. Moreover, bundling of services alongside resource allocation as presented in this work, is well aligned with ongoing trends for accumulating multiple information services in single offers to customers. Designing flexible, synergetic, and superior telecommunications products paves the way for the evolution of wireless networks offering multiple further research opportunities. Also addressing computation requirements and complexity with regards to price calculations is of great importance for WISPs, as a crucial element of their revenue generation strategies [295], [9].

Resource allocation in B5G and 6G communications: Network evolution is a never stopping process. Despite the imminent implementation of 5G networks, researchers and the industry alike have already started to identifying the key enabling technologies towards the so called "Beyond 5G" (B5G) and sixth generation (6G) communications [296]. 6G is assumed to be benefiting from various 5G technologies integrating Artificial Intelligence in network operation, 3D coverage, semantic communication, and enhanced computational and caching capabilities [297]. All the above dictate that resource allocation processes need to evolve accordingly in order to meet those new network requirements. The methodologies of this work can be considered as generic and flexible enough to be used for various access technologies, resource types, and service categories compatible with the envisioned B5G and 6G networks aiming at an even more holistic and comprehensive communication experience [298, 299].

Network security, privacy, and cyberphysical systems: In this thesis we briefly studied the topic of Public Safety Networks and how communications and efficient resource allocation can become a critical element for society in cases of extreme external events. Further capitalizing on the presented framework and in alignment with the growing research trends in the literature, developing new resource management techniques for coordinating physical communications and cyber-computing is important in various areas like aerospace, defence, factory automation, healthcare etc. [300]. Moreover, as UAV-assisted communications are expected to further grow for fast network deployments, resource allocation methodologies need to address issues like limited flying time and UAV localization, data fusion, and maintaining the relay network in order to sustain more reliable communications in cases of disasters [301]. In addition to the

above, responding to security threats and privacy issues is crucial towards protecting data exposure and compromising network operation. Cyber warfare, data theft in the cloud, phishing, etc. are just a few examples of the challenges future wireless networks are facing, heavily impacting how resource allocation is conducted and how data exchange can be safeguarded both in terms of fairness and privacy. Various ongoing approaches are currently being investigated, with blockchain, fog computing or software defined networks (SDN) technologies to offer various opportunities for reinventing how resource management is perceived and applied in new network architectures in a more reliable way.

Energy management, wireless charging, and more: Efforts to improve energy management, prolong battery lifetime, and extend network autonomy are only intensifying. All the techniques studied in this thesis with regards to distributed interference management, Wireless Powered Communication Networks (WPCNs) where charging is correlated and adapted to the transmission phase as well as the different power control algorithms, offer meaningful additions in the existing literature with regards to more energy-efficient communications. Expanding the above techniques to wireless sensor and RF identification (RFID) networks as well as exploring green WPCN schemes via harvesting renewable energy sources [160], are all assumed to reduce energy requirements from fixed power sources in the direction of more sustainable and autonomous communications. Moreover, new battery technologies offer promising solutions towards ultra fast charging Wireless Rechargeable Sensor Networks (WRSNs) [302], extended in areas like the Electrical Vehicle industry, smart devices charging or implant charging in medical applications.

Broader resource allocation applications: In the wider use of the term, resource allocation problems refer to a wide array of topics stepping far beyond wireless networking and telecommunications. User or device interactions are found in multiple fields of human activities with a great degree of similarity to the problems examined in this thesis. The algorithms and theoretical schemes developed in our work have been purposely designed to be generic enough facilitating their application in other disciplines in a flexible manner. Resource allocation and data exchange by capturing users' utility and satisfaction from the quality of the services they receive are found in transportation networks, smart grid or in emerging smart city environments, among others. The algorithms and modeling schemes in this work can provide interesting alternatives in studying resource allocation in those areas, again prioritizing energy-efficient and customer centric solutions.

Appendix A

Author Publications

International Peer Reviewed Journals

1. **Vamvakas, Panagiotis**, Eirini Eleni Tsiropoulou, and Symeon Papavassiliou. "Exploiting Prospect Theory and Risk-awareness to Protect UAV-assisted Network Operation." submitted to *EURASIP Journal on Wireless Communications and Networking* (2019), *(under revision)*

2. **Vamvakas, Panagiotis**, Eirini Eleni Tsiropoulou, and Symeon Papavassiliou. "On Controlling Spectrum Fragility via Resource Pricing in 5G Wireless Networks." *IEEE Networking Letters* (2019).

3. **Vamvakas, Panagiotis**, Eirini Eleni Tsiropoulou, and Symeon Papavassiliou. "Risk-aware Resource Management in Public Safety Networks." *Sensors* 2019, 19, 3853.

4. **Vamvakas, Panagiotis**, Eirini Eleni Tsiropoulou, and Symeon Papavassiliou. "A user-centric economic-driven paradigm for rate allocation in non-orthogonal multiple access wireless systems." *EURASIP Journal on Wireless Communications and Networking* 2018, no. 1 (2018): 129.

5. **Vamvakas, Panagiotis**, Eirini Eleni Tsiropoulou, and Symeon Papavassiliou. "Dynamic provider selection power resource management in competitive wireless communication markets." *Mobile Networks and Applications* 23, no. 1 (2018): 86-99.

6. Tsiropoulou, Eirini Eleni, **Panagiotis Vamvakas**, and Symeon Papavassiliou. "Joint customized price and power control for energy-efficient multi-service wireless networks via S-modular theory." *IEEE Transactions on Green Communications and Networking* 1, no. 1 (2017): 17-28.
   Remark 5. *The first two authors of this publication have had equal scientific and editiorial contribution, appearance of names is solely based on alphabetical order.*

7. Tsiropoulou, Eirini Eleni, **Panagiotis Vamvakas**, and Symeon Papavassiliou. "Supermodular game-based distributed joint uplink power and rate allocation in two-tier femtocell networks." *IEEE Transactions on Mobile Computing* 16, no. 9 (2016): 2656-2667.
   Remark 6. *The first two authors of this publication have had equal scientific and editiorial contribution, appearance of names is solely based on alphabetical order.*

8. Tsiropoulou, Eirini Eleni, **Panagiotis Vamvakas**, Georgios K. Katsinis, and Symeon Papavassiliou. "Combined power and rate allocation in self-optimized multi-service two-tier femtocell networks." *Computer Communications* 72 (2015): 38-48.
   Remark 7. *The first two authors of this publication have had equal scientific and editiorial contribution, appearance of names is solely based on alphabetical order.*

9. Tsiropoulou, Eirini Eleni, **Panagiotis Vamvakas**, and Symeon Papavassiliou. "Joint utility-based uplink power and rate allocation in wireless networks: A non-cooperative game theoretic framework." *Physical Communication* 9 (2013): 299-307.

International Conferences

1. **Vamvakas, Panagiotis**, Eirini Eleni Tsiropoulou, and Symeon Papavassiliou. "A market-based modular service composition approach for flexibility and adaptability in future wireless networks." *In IEEE INFOCOM 2019 - IEEE Conference on Computer Communications Workshops (INFOCOM WKSHPS)*, pages 252–257, April 2019.

2. **Vamvakas, Panagiotis**, Eirini Eleni Tsiropoulou, and Symeon Papavassiliou. "On the prospect of UAV-assisted communications paradigm in public safety networks." In *IEEE INFOCOM 2019 - IEEE Conference on Computer Communications Workshops (INFOCOM WKSHPS)*, pages 762–767, April 2019.

3. **Vamvakas, Panagiotis**, Eirini Eleni Tsiropoulou, and Symeon Papavassiliou. "Risk-Aware Resource Control with Flexible 5G Access Technology Interfaces." In *2019 IEEE 20th International Symposium on "A World of Wireless, Mobile and Multimedia Networks"(WoWMoM)*, pp. 1-9. IEEE, 2019.

4. **Vamvakas, Panagiotis**, Eirini Eleni Tsiropoulou, and Symeon Papavassiliou. "Dynamic Spectrum Management in 5G Wireless Networks: A Real-Life Modeling Approach." In *IEEE INFOCOM 2019-IEEE Conference on Computer Communications*, pp. 2134-2142. IEEE, 2019.

5. **Vamvakas, Panagiotis**, Eirini Eleni Tsiropoulou, and Symeon Papavassiliou. "Personalized pricing for efficient user-centric multi-resource control in 5G wireless networks." In *2018 IEEE 19th International Symposium on" A World of Wireless, Mobile and Multimedia Networks"(WoWMoM)*, pp. 1-6. IEEE, 2018.

6. **Vamvakas, Panagiotis**, Eirini Eleni Tsiropoulou, Marinos Vomvas, and Symeon Papavassiliou. "Adaptive power management in wireless powered communication networks: A user-centric approach." In *2017 IEEE 38th Sarnoff Symposium*, pp. 1-6. IEEE, 2017.

7. **Vamvakas, Panagiotis**, Eirini Eleni Tsiropoulou, Symeon Papavassiliou, and John S. Baras. "Optimization and resource management in NOMA wireless networks supporting real and non-real time service bundling." In *2017 IEEE Symposium on Computers and Communications (ISCC)*, pp. 697-703. IEEE, 2017.

8. Tsiropoulou, Eirini Eleni, Iakovos Gialagkolidis, **Panagiotis Vamvakas**, and Symeon Papavassiliou. "Resource allocation in visible light communication networks: NOMA vs OFDMA transmission techniques." In *International Conference on Ad-Hoc Networks and Wireless*, pp. 32-46. Springer, Cham, 2016.

9. Tsiropoulou, Eirini Eleni, Georgios K. Katsinis, **Panagiotis Vamvakas**, and Symeon Papavassiliou. "Efficient uplink power control in multi-service two-tier femtocell networks via a game theoretic approach." In *2013 IEEE 18th International Workshop on Computer Aided Modeling and Design of Communication Links and Networks (CAMAD)*, pp. 104-108. IEEE, 2013.

10. Tsiropoulou, Eirini Eleni, **Panagiotis Vamvakas**, and Symeon Papavassiliou. "Energy efficient uplink joint resource allocation non-cooperative game with pricing." In *2012 IEEE Wireless Communications and Networking Conference (WCNC)*, pp. 2352-2356. IEEE, 2012.

Book Chapters

1. Tsiropoulou, Eirini Eleni, **Panagiotis Vamvakas**, and Symeon Papavassiliou. "Resource Allocation in Multi-tier Femtocell and Visible-Light Heterogeneous Wireless Networks." In *Resource Allocation in Next-Generation Broadband Wireless Access Networks*, pp. 210-246. *IGI Global*, 2017.

Appendix B

Honors and Awards

1. Student Travel Grant Award IEEE INFOCOM 2019, by IEEE Communications Society (IEEE ComSoc).
2. Best Paper Award for Mobile and Wireless Networks, *IEEE Wireless Communications and Networking Conference* - Paris, France, April, 2012.

Bibliography

[1] AB Ericsson. Ericsson mobility report: On the pulse of the networked society. *Ericsson, Sweden, Tech. Rep. EAB-14*, 61078, 2015.

[2] Statistics. https://www.itu.int/en/ITU-D/Statistics/Pages/stat/default.aspx. (Accessed on 08/17/2019).

[3] Cisco Visual Networking Index. Global mobile data traffic forecast update, 2011–2016. *White Paper, February*, 14, 2012.

[4] Cisco Visual Networking Index. Cisco visual networking index: Global mobile data traffic forecast update, 2016–2021 white paper. *URL: http://www. cisco. com/c/en/us/solutions/collateral/serviceprovider/visual-networking-index-vni/mobile-white-paper-c11-520862. html*, 2017.

[5] Jeffrey G Andrews, Stefano Buzzi, Wan Choi, Stephen V Hanly, Angel Lozano, Anthony CK Soong, and Jianzhong Charlie Zhang. What will 5G be? *IEEE Journal on Selected Areas in Communications*, 32(6):1065–1082, 2014.

[6] Jose F Monserrat, Irene Alepuz, Jorge Cabrejas, Vicente Osa, Javier López, Roberto García, María José Domenech, and Vicent Soler. Towards user-centric operation in 5G networks. *EURASIP Journal on Wireless Communications and Networking*, 2016(1):6, 2016.

[7] Zhu Han and KJ Ray Liu. *Resource allocation for wireless networks: basics, techniques, and applications*. Cambridge University Press, 2008.

[8] Ruogu Li, Atilla Eryilmaz, Lei Ying, and Ness B Shroff. A unified approach to optimizing performance in networks serving heterogeneous flows. *IEEE/ACM Transactions On Networking*, 19(1):223–236, 2010.

[9] Soumya Sen, Carlee Joe-Wong, Sangtae Ha, and Mung Chiang. Smart data pricing (SDP): Economic solutions to network congestion. *Recent advances in networking*, 1:221–274, 2013.

[10] Cem U Saraydar, Narayan B Mandayam, David J Goodman, et al. Efficient power control via pricing in wireless data networks. *IEEE Transactions on Communications*, 50(2):291–303, 2002.

[11] Alan Jones, Peter Darwood, and Paul Howard. Simultaneous dual mode operation in cellular networks, October 4 2007. US Patent App. 11/398,255.

[12] Patrick Maillé, Peter Reichl, and Bruno Tuffin. Competition among telecommunication providers. In *Telecommunication Economics*, pages 179–187. Springer, 2012.

[13] Xin-Lin Huang, Xiaomin Ma, and Fei Hu. Machine learning and intelligent communications. *Mobile Networks and Applications*, 23(1):68–70, 2018.

[14] Samson Lasaulce and Hamidou Tembine. *Game theory and learning for wireless networks: fundamentals and applications*. Academic Press, 2011.

[15] Zhu Han, Dusit Niyato, Walid Saad, Tamer Başar, and Are Hjørungnes. *Game theory in wireless and communication networks: theory, models, and applications*. Cambridge University Press, 2012.

[16] Eirini-Eleni Tsiropoulou, Timotheos Kastrinogiannis, and Symeon Papavassiliou. Non-cooperative power control in CDMA wireless networks. In *Game Theory for Wireless Communications and Networking*, pages 205–240. CRC Press, 2011.

[17] Aleksandar Damnjanovic, Juan Montojo, Yongbin Wei, Tingfang Ji, Tao Luo, Madhavan Vajapeyam, Taesang Yoo, Osok Song, and Durga Malladi. A survey on 3GPP heterogeneous networks. *IEEE Wireless Communications*, 18(3):10–21, 2011.

[18] V Chandrasekhar, J Andrews, and A Gatherer. Femtocell networks: A survey, IEEE Communications Magazine. 2008.

[19] Anthony Cuthbertson. LiFi internet: First real-world usage boasts speed 100 times faster than WiFi, 2015.

[20] Alain Richard Ndjiongue, Hendrik C Ferreira, and Telex MN Ngatched. Visible light communications (VLC) technology. *Wiley Encyclopedia of Electrical and Electronics Engineering*, pages 1–15, 1999.

[21] Chetna Singhal and Swades De. *Resource allocation in next-generation broadband wireless access networks*. IGI Global, 2017.

[22] Kaiyun Cui, Jinguo Quan, and Zhengyuan Xu. Performance of indoor optical femtocell by visible light communication. *Optics Communications*, 298:59–66, 2013.

[23] Eirini Eleni Tsiropoulou, Panagiotis Vamvakas, and Symeon Papavassiliou. Resource allocation in multi-tier femtocell and visible-light heterogeneous wireless networks. In *Resource Allocation in Next-Generation Broadband Wireless Access Networks*, pages 210–246. IGI Global, 2017.

[24] Eirini Eleni Tsiropoulou, Timotheos Kastrinogiannis, and Symeon Papavassiliou. Realization of QoS provisioning in autonomic CDMA networks under common utility-based framework. In *2009 IEEE International Symposium on a World of Wireless, Mobile and Multimedia Networks & Workshops*, pages 1–7. IEEE, 2009.

[25] Antonio De Domenico, Emilio Calvanese Strinati, and Antonio Capone. Enabling green cellular networks: A survey and outlook. *Computer Communications*, 37:5–24, 2014.

[26] Guillaume De La Roche, Alvaro Valcarce, David López-Pérez, and Jie Zhang. Access control mechanisms for femtocells. *IEEE Communications Magazine*, 48(1):33–39, 2010.

[27] Eirini Eleni Tsiropoulou and Symeon Papavassiliou. Utility-based uplink joint power and subcarrier allocation in SC-FDMA wireless networks. *International Journal of Electronics*, 98(11):1581–1587, 2011.

[28] Eirini Eleni Tsiropoulou, Georgios K Katsinis, and Symeon Papavassiliou. Distributed uplink power control in multiservice wireless networks via a game theoretic approach with convex pricing. *IEEE Transactions on Parallel and Distributed Systems*, 23(1):61–68, 2011.

[29] Mehdi Rasti, Ahmad R Sharafat, and Babak Seyfe. Pareto-efficient and goal-driven power control in wireless networks: A game-theoretic approach with a novel pricing scheme. *IEEE/ACM Transactions on Networking (TON)*, 17(2):556–569, 2009.

[30] Madhusudhan R Musku, Anthony T Chronopoulos, and Dimitrie C Popescu. Joint rate and power control using game theory. In *CCNC 2006. 2006 3rd IEEE Consumer Communications and Networking Conference, 2006.*, volume 2, pages 1258–1262. IEEE, 2006.

[31] Madhusudhan R Musku, Anthony T Chronopoulos, and Dimitrie C Popescu. Joint rate and power control with pricing. In *GLOBECOM'05. IEEE Global Telecommunications Conference, 2005.*, volume 6, pages 5–pp. IEEE, 2005.

[32] Mohammad Hayajneh and Chaouki T Abdallah. Distributed joint rate and power control game-theoretic algorithms for wireless data. *IEEE Communications Letters*, 8(8):511–513, 2004.

[33] Madhusudhan R Musku, Anthony T Chronopoulos, Dimitrie C Popescu, and Anton Stefanescu. A game-theoretic approach to joint rate and power control for uplink CDMA communications. *IEEE Transactions on Communications*, 58(3):923–932, 2010.

[34] Eirini Eleni Tsiropoulou, Panagiotis Vamvakas, and Symeon Papavassiliou. Joint utility-based uplink power and rate allocation in wireless networks: A non-cooperative game theoretic framework. *Physical Communication*, 9:299–307, 2013.

[35] Eirini Eleni Tsiropoulou, Panagiotis Vamvakas, and Symeon Papavassiliou. Energy efficient uplink joint resource allocation non-cooperative game with pricing. In *2012 IEEE Wireless Communications and Networking Conference (WCNC)*, pages 2352–2356. IEEE, 2012.

[36] V Chandrasekhar, JG Andrews, T Muharemovic, Zukang Shen, and A Gatherer. Power control in two-tier femtocell networks. *IEEE Transactions on Wireless Communications*, 8(8):4316–4328, 2009.

[37] Tao Su, Wei Zheng, Wei Li, Dabing Ling, and Xiangming Wen. Energy-efficient power optimization with Pareto improvement in two-tier femtocell networks. In *2012 IEEE 23rd International Symposium on Personal, Indoor and Mobile Radio Communications-(PIMRC)*, pages 2512–2517. IEEE, 2012.

[38] Vaggelis G Douros, Stavros Toumpis, and George C Polyzos. Power control under best response dynamics for interference mitigation in a two-tier femtocell network. In *2012 10th International Symposium on Modeling and Optimization in Mobile, Ad Hoc and Wireless Networks (WiOpt)*, pages 398–405. IEEE, 2012.

[39] Vikram Chandrasekhar, Jeffrey G Andrews, Zukang Shen, Tarik Muharemovic, and Alan Gatherer. Distributed power control in femtocell-underlay cellular networks. In *GLOBECOM 2009-2009 IEEE Global Telecommunications Conference*, pages 1–6. IEEE, 2009.

[40] Jingfang Liu, Wei Zheng, Wei Li, Xidong Wang, Yuanbao Xie, and Xiangming Wen. Distributed uplink power control for two-tier femtocell networks via convex pricing. In *2013 IEEE Wireless Communications and Networking Conference (WCNC)*, pages 458–463. IEEE, 2013.

[41] Zhenping Lu, Yong Sun, Xiangming Wen, Tao Su, and Dabing Ling. An energy-efficient power control algorithm in femtocell networks. In *2012 7th International Conference on Computer Science & Education (ICCSE)*, pages 395–400. IEEE, 2012.

[42] Wei Zheng, Tao Su, Wei Li, Zhenping Lu, and Xiangming Wen. Distributed energy-efficient power optimization in two-tier femtocell networks. In *2012 IEEE International Conference on Communications (ICC)*, pages 5767–5771. IEEE, 2012.

[43] Eun Jin Hong, Se Young Yun, and Dong-Ho Cho. Decentralized power control scheme in femtocell networks: A game theoretic approach. In *2009 IEEE 20th International Symposium on Personal, Indoor and Mobile Radio Communications*, pages 415–419. IEEE, 2009.

[44] Duy Trong Ngo, Long Bao Le, Tho Le-Ngoc, Ekram Hossain, and Dong In Kim. Distributed interference management in two-tier CDMA femtocell networks. *IEEE Transactions on Wireless Communications*, 11(3):979–989, 2012.

[45] Rebeca Estrada, Abdallah Jarray, Hadi Otrok, Zbigniew Dziong, and Hassan Barada. Energy-efficient resource-allocation model for OFDMA macrocell/femtocell networks. *IEEE Transactions on Vehicular Technology*, 62(7):3429–3437, 2013.

[46] Yanhui Ma, Tiejun Lv, and Yueming Lu. Efficient power control in heterogeneous femto-macro cell networks. In *2013 IEEE Wireless Communications and Networking Conference (WCNC)*, pages 4215–4219. IEEE, 2013.

[47] Peng Xu, Xuming Fang, Meirong Chen, and Yang Xu. A Stackelberg game-based spectrum allocation scheme in macro/femtocell hierarchical networks. *Computer Communications*, 36(14):1552–1558, 2013.

[48] Debalina Ghosh and Prasant Mohapatra. Resource allocation using link state propagation in OFDMA femto networks. *Computer Communications*, 46:3–9, 2014.

[49] Reza Banirazi, Edmond Jonckheere, and Bhaskar Krishnamachari. Heat-diffusion: Pareto optimal dynamic routing for time-varying wireless networks. In *IEEE INFOCOM 2014-IEEE Conference on Computer Communications*, pages 325–333. IEEE, 2014.

[50] Michael J Neely, Eytan Modiano, and Charles E Rohrs. Dynamic power allocation and routing for time varying wireless networks. In *IEEE INFOCOM 2003. Twenty-second Annual Joint Conference of the IEEE Computer and Communications Societies (IEEE Cat. No. 03CH37428)*, volume 1, pages 745–755. IEEE, 2003.

[51] Li Li, Changqing Xu, and Meixia Tao. Resource allocation in open access OFDMA femtocell networks. *IEEE Wireless Communications Letters*, 1(6):625–628, 2012.

[52] Yu-Shan Liang, Wei-Ho Chung, Guo-Kai Ni, Yi Chen, Hongke Zhang, and Sy-Yen Kuo. Resource allocation with interference avoidance in OFDMA femtocell networks. *IEEE Transactions on Vehicular Technology*, 61(5):2243–2255, 2012.

[53] Long Bao Le, Dusit Niyato, Ekram Hossain, Dong In Kim, and Dinh Thai Hoang. QoS-aware and energy-efficient resource management in OFDMA femtocells. *IEEE Transactions on Wireless Communications*, 12(1):180–194, 2012.

[54] Duy Trong Ngo, Suman Khakurel, and Tho Le-Ngoc. Joint subchannel assignment and power allocation for OFDMA femtocell networks. *IEEE Transactions on Wireless Communications*, 13(1):342–355, 2013.

[55] Xin Kang, Rui Zhang, and Mehul Motani. Price-based resource allocation for spectrum-sharing femtocell networks: A Stackelberg game approach. *IEEE Journal on Selected areas in Communications*, 30(3):538–549, 2012.

[56] Azamossadat Hosseinzadeh Salati, Masoumeh Nasiri-Kenari, and Parastoo Sadeghi. Distributed subband, rate and power allocation in OFDMA based two-tier femtocell networks using fractional frequency reuse. In *2012 IEEE Wireless Communications and Networking Conference (WCNC)*, pages 2626–2630. IEEE, 2012.

[57] Jianmin Zhang, Zhaoyang Zhang, Kedi Wu, and Aiping Huang. Optimal distributed subchannel, rate and power allocation algorithm in OFDM-based two-tier femtocell networks. In *2010 IEEE 71st Vehicular Technology Conference*, pages 1–5. IEEE, 2010.

[58] Jun Zhao, Wei Zheng, Xiangming Wen, Xiaoli Chu, Haijun Zhang, and Zhaoming Lu. Game theory based energy-aware uplink resource allocation in OFDMA femtocell networks. *International Journal of Distributed Sensor Networks*, 10(3):658158, 2014.

[59] Rami Langar, Stefano Secci, Raouf Boutaba, and Guy Pujolle. An operations research game approach for resource and power allocation in cooperative femtocell networks. *IEEE Transactions on Mobile Computing*, 14(4):675–687, 2014.

[60] Jongwon Yoon, Mustafa Y Arslan, Karthikeyan Sundaresan, Srikanth V Krishnamurthy, and Suman Banerjee. Self-organizing resource management framework in OFDMA femtocells. *IEEE Transactions on Mobile Computing*, 14(4):843–857, 2014.

[61] ITURM Recommendation. 1225. *Guidelines for evaluation of radio transmission technologies for IMT-2000*, 69, 1997.

[62] Drew Fudenberg and Jean Tirole. Game theory, 1991. *Cambridge, Massachusetts*, 393(12):80, 1991.

[63] John Nash. Non-cooperative games. *Annals of Mathematics*, pages 286–295, 1951.

[64] Donald M Topkis. Equilibrium points in nonzero-sum n-person submodular games. *Siam Journal on Control and Optimization*, 17(6):773–787, 1979.

[65] Xavier Vives. Complementarities and games: New developments. *Journal of Economic Literature*, 43(2):437–479, 2005.

[66] Robert Gibbons et al. A primer in game theory. 1992.

[67] Eirini Eleni Tsiropoulou, Timotheos Kastrinogiannis, and Symeon Papavassiliou. A utility-based power allocation non-cooperative game for the uplink in multi-service CDMA wireless networks. In *Proceedings of the 2009 International Conference on Wireless Communications and Mobile Computing: Connecting the World Wirelessly*, pages 365–370. ACM, 2009.

[68] Eirini Eleni Tsiropoulou, Georgios K Katsinis, Panagiotis Vamvakas, and Symeon Papavassiliou. Efficient uplink power control in multi-service two-tier femtocell networks via a game theoretic approach. In *2013 IEEE 18th International Workshop on Computer Aided Modeling and Design of Communication Links and Networks (CAMAD)*, pages 104–108. IEEE, 2013.

[69] Eirini Eleni Tsiropoulou, John S Baras, Symeon Papavassiliou, and Surbhit Sinha. RFID-based smart parking management system. *Cyber-Physical Systems*, 3(1-4):22–41, 2017.

[70] Sarma Gunturi and Fernando Paganini. Game theoretic approach to power control in cellular CDMA. In *2003 IEEE 58th Vehicular Technology Conference. VTC 2003-Fall (IEEE Cat. No. 03CH37484)*, volume 4, pages 2362–2366. IEEE, 2003.

[71] Tansu Alpcan, Tamer Başar, Rayadurgam Srikant, and Eitan Altman. CDMA uplink power control as a non-cooperative game. *Wireless Networks*, 8(6):659–670, 2002.

[72] Jang-Won Lee, Ravi R Mazumdar, and Ness B Shroff. Joint resource allocation and base-station assignment for the downlink in CDMA networks. *IEEE/ACM Transactions on Networking (TON)*, 14(1):1–14, 2006.

[73] Jang-Won Lee, Ravi R Mazumdar, and Ness B Shroff. Downlink power allocation for multi-class wireless systems. *IEEE/ACM Transactions on Networking (TON)*, 13(4):854–867, 2005.

[74] Eirini Eleni Tsiropoulou, Georgios K Katsinis, and Symeon Papavassiliou. Utility-based power control via convex pricing for the uplink in CDMA wireless networks. In *2010 European Wireless Conference (EW)*, pages 200–206. IEEE, 2010.

[75] Daquan Feng, Chenzi Jiang, Gubong Lim, Leonard J Cimini, Gang Feng, and Geoffrey Ye Li. A survey of energy-efficient wireless communications. *IEEE Communications Surveys & Tutorials*, 15(1):167–178, 2012.

[76] Eirini Eleni Tsiropoulou, Timotheos Kastrinogiannis, and Symeon Papavassiliou. Uplink power control in QoS-aware multi-service CDMA wireless networks. *Journal of Communications*, 4(9):654–668, 2009.

[77] Timotheos Kastrinogiannis, Eirini-Eleni Tsiropoulou, and Symeon Papavassiliou. Utility-based uplink power control in cdma wireless networks with real-time services. In *International Conference on Ad-Hoc Networks and Wireless*, pages 307–320. Springer, 2008.

[78] Ziqiang Feng, Lingyang Song, Zhu Han, Xiaowu Zhao, et al. Cell selection in two-tier femtocell networks with open/closed access using evolutionary game. In *2013 IEEE Wireless Communications and Networking Conference (WCNC)*, pages 860–865. IEEE, 2013.

[79] Eirini Eleni Tsiropoulou, Georgios K Katsinis, Alexandros Filios, and Symeon Papavassiliou. On the problem of optimal cell selection and uplink power control in open access multi-service two-tier femtocell networks. In *International Conference on Ad-Hoc Networks and Wireless*, pages 114–127. Springer, 2014.

[80] Eirini Eleni Tsiropoulou, Panagiotis Vamvakas, Georgios K Katsinis, and Symeon Papavassiliou. Combined power and rate allocation in self-optimized multi-service two-tier femtocell networks. *Computer Communications*, 72:38–48, 2015.

[81] Tom M Apostol. *Calculus, Volume I, One-variable Calculus, with an Introduction to Linear Algebra*, volume 1. John Wiley & Sons, 2007.

[82] Roy D. Yates et al. A framework for uplink power control in cellular radio systems. *IEEE Journal on Selected Areas in Communications*, 13(7):1341–1347, 1995.

[83] E Won. PHY and MAC standard for short-range wireless optical communication using visible light, 2008.

[84] Zhe Chen, Dobroslav Tsonev, and Harald Haas. Improving SINR in indoor cellular visible light communication networks. In *2014 IEEE International Conference on Communications (ICC)*, pages 3383–3388. IEEE, 2014.

[85] Svilen Dimitrov and Harald Haas. Information rate of OFDM-based optical wireless communication systems with nonlinear distortion. *Journal of Lightwave Technology*, 31(6):918–929, 2012.

[86] Eirini Eleni Tsiropoulou, Ioannis Ziras, and Symeon Papavassiliou. Service differentiation and resource allocation in SC-FDMA wireless networks through user-centric distributed non-cooperative multilateral bargaining. In *International Conference on Ad Hoc Networks*, pages 42–54. Springer, 2015.

[87] Eirini-Eleni Tsiropoulou, Ioannis Ziras, and Symeon Papavassiliou. A non-cooperative approach to the joint subcarrier and power allocation problem in multi-service SC-FDMA networks. *ICST Trans. Mobile Communications Applications*, 2(7):e1, 2016.

[88] Nirzhar Saha, Ratan Kumar Mondal, and Yeong Min Jang. Opportunistic channel reuse for a self-organized visible light communication personal area network. In *2013 Fifth International Conference on Ubiquitous and Future Networks (ICUFN)*, pages 131–134. IEEE, 2013.

[89] Dima Bykhovsky and Shlomi Arnon. Multiple access resource allocation in visible light communication systems. *Journal of Lightwave Technology*, 32(8):1594–1600, 2014.

[90] Nirzhar Saha, Ratan Kumar Mondal, Md Shareef Ifthekhar, and Yeong Min Jang. Dynamic resource allocation for visible light based wireless sensor network. In *The International Conference on Information Networking 2014 (ICOIN2014)*, pages 75–78. IEEE, 2014.

[91] Ratan Kumar Mondal, Nirzhar Saha, Nam-Tuan Le, and Yeong Min Jang. SINR-constrained joint scheduling and optimal resource allocation in VLC based WPAN system. *Wireless Personal Communications*, 78(4):1935–1951, 2014.

[92] Birendra Ghimire and Harald Haas. Self-organising interference coordination in optical wireless networks. *EURASIP Journal on Wireless Communications and Networking*, 2012(1):131, 2012.

[93] Woo-Chan Kim, Chi-Sung Bae, Soo-Yong Jeon, Sung-Yeop Pyun, and Dong-Ho Cho. Efficient resource allocation for rapid link recovery and visibility in visible-light local area networks. *IEEE Transactions on Consumer Electronics*, 56(2):524–531, 2010.

[94] Ratan Kumar Mondal, Mostafa Zaman Chowdhury, Nirzhar Saha, and Yeong Min Jang. Interference-aware optical resource allocation in visible light communication. In *2012 International Conference on ICT Convergence (ICTC)*, pages 155–158. IEEE, 2012.

[95] Hanaa Marshoud, Vasileios M Kapinas, George K Karagiannidis, and Sami Muhaidat. Non-orthogonal multiple access for visible light communications. *IEEE Photonics Technology Letters*, 28(1):51–54, 2015.

[96] Liang Yin, Xiping Wu, and Harald Haas. On the performance of non-orthogonal multiple access in visible light communication. In *2015 IEEE 26th Annual International Symposium on Personal, Indoor, and Mobile Radio Communications (PIMRC)*, pages 1354–1359. IEEE, 2015.

[97] Joseph M Kahn and John R Barry. Wireless infrared communications. *Proceedings of the IEEE*, 85(2):265–298, 1997.

[98] Dusit Niyato and Ekram Hossain. Competitive pricing for spectrum sharing in cognitive radio networks: Dynamic game, inefficiency of Nash Equilibrium, and collusion. *IEEE Journal on Selected Areas in Communications*, 26(1):192–202, 2008.

[99] Christos A Gizelis and Dimitrios D Vergados. A survey of pricing schemes in wireless networks. *IEEE Communications Surveys & Tutorials*, 13(1):126–145, 2010.

[100] Qipeng Song, Loutfi Nuaymi, and Xavier Lagrange. Survey of radio resource management issues and proposals for energy-efficient cellular networks that will cover billions of machines. *EURASIP Journal on Wireless Communications and Networking*, 2016(1):140, 2016.

[101] Shuang Wu, Xu Wang, and Jian Liu. A power control game via new pricing with dynamic coefficient in cognitive radio. In *2011 Third International Conference on Communications and Mobile Computing*, pages 262–265. IEEE, 2011.

[102] Jinho Choi. On the power allocation for a practical multiuser superposition scheme in NOMA systems. *IEEE Communications Letters*, 20(3):438–441, 2016.

[103] Anthony T Chronopoulos, Madhusudhan R Musku, Satish Penmatsa, and Dimitrie C Popescu. Spectrum load balancing for medium access in cognitive radio systems. *IEEE Communications Letters*, 12(5):353–355, 2008.

[104] Yi Zhang, Hui-Ming Wang, Qian Yang, and Zhiguo Ding. Secrecy sum rate maximization in non-orthogonal multiple access. *IEEE Communications Letters*, 20(5):930–933, 2016.

[105] Zhenyu Na, Xiaotong Li, Xin Liu, and Zhian Deng. Subcarrier allocation based simultaneous wireless information and power transfer for multiuser OFDM systems. *EURASIP Journal on Wireless Communications and Networking*, 2017(1):148, 2017.

[106] Chao Yang and Scott Jordan. Power and rate allocation for video conferencing in cellular networks. *EURASIP Journal on Wireless Communications and Networking*, 2013(1):31, 2013.

[107] Symeon Papavassiliou and Chengzhou Li. Joint throughput maximization and fair uplink transmission scheduling in CDMA systems. *EURASIP Journal on Wireless Communications and Networking*, 2009(1):564692, 2009.

[108] Qi Sun, Shuangfeng Han, Zhikun Xu, Sen Wang, I Chih-Lin, and Zhengang Pan. Sum rate optimization for mimo non-orthogonal multiple access systems. In *2015 IEEE Wireless Communications and Networking Conference (WCNC)*, pages 747–752. IEEE, 2015.

[109] Srinivas Shakkottai, Rayadurgam Srikant, Asuman Ozdaglar, and Daron Acemoglu. The price of simplicity. *IEEE Journal on Selected Areas in Communications*, 26(7):1269–1276, 2008.

[110] Chi-Kin Chau, Qian Wang, and Dah-Ming Chiu. On the viability of Paris metro pricing for communication and service networks. In *2010 Proceedings IEEE INFOCOM*, pages 1–9. IEEE, 2010.

[111] Sangtae Ha, Soumya Sen, Carlee Joe-Wong, Youngbin Im, and Mung Chiang. Tube: Time-dependent pricing for mobile data. *ACM SIGCOMM Computer Communication Review*, 42(4):247–258, 2012.

[112] Liang Zheng, Carlee Joe-Wong, Chee Wei Tan, Sangtae Ha, and Mung Chiang. Customized data plans for mobile users: Feasibility and benefits of data trading. *IEEE Journal on Selected Areas in Communications*, 35(4):949–963, 2017.

[113] Matthew Andrews. Understanding the effects of quota trading on mobile usage dynamics. In *2016 14th International Symposium on Modeling and Optimization in Mobile, Ad Hoc, and Wireless Networks (WiOpt)*, pages 1–8. IEEE, 2016.

[114] Xiaowen Gong, Lingjie Duan, Xu Chen, and Junshan Zhang. When social network effect meets congestion effect in wireless networks: Data usage equilibrium and optimal pricing. *IEEE Journal on Selected Areas in Communications*, 35(2):449–462, 2017.

[115] Nguyen Cong Luong, Ping Wang, Dusit Niyato, Yonggang Wen, and Zhu Han. Resource management in cloud networking using economic analysis and pricing models: A survey. *IEEE Communications Surveys & Tutorials*, 19(2):954–1001, 2017.

[116] Nguyen Cong Luong, Dinh Thai Hoang, Ping Wang, Dusit Niyato, Dong In Kim, and Zhu Han. Data collection and wireless communication in Internet of Things (IoT) using economic analysis and pricing models: A survey. *IEEE Communications Surveys & Tutorials*, 18(4):2546–2590, 2016.

[117] Lin Gao, George Iosifidis, Jianwei Huang, and Leandros Tassiulas. Hybrid data pricing for network-assisted user-provided connectivity. In *IEEE INFOCOM 2014-IEEE Conference on Computer Communications*, pages 682–690. IEEE, 2014.

[118] Eitan Altman and Zwi Altman. S-modular games and power control in wireless networks. *IEEE Transactions on Automatic Control*, 48(5):839–842, 2003.

[119] Eirini Eleni Tsiropoulou, Panagiotis Vamvakas, and Symeon Papavassiliou. Supermodular game-based distributed joint uplink power and rate allocation in two-tier femtocell networks. *IEEE Transactions on Mobile Computing*, 16(9):2656–2667, 2016.

[120] Eirini Eleni Tsiropoulou, Panagiotis Vamvakas, and Symeon Papavassiliou. Joint customized price and power control for energy-efficient multi-service wireless networks via S-modular theory. *IEEE Transactions on Green Communications and Networking*, 1(1):17–28, 2017.

[121] Panagiotis Vamvakas, Eirini Eleni Tsiropoulou, and Symeon Papavassiliou. A user-centric economic-driven paradigm for rate allocation in non-orthogonal multiple access wireless systems. *EURASIP Journal on Wireless Communications and Networking*, 2018(1):129, 2018.

[122] Mingzhe Chen, Ursula Challita, Walid Saad, Changchuan Yin, and Mérouane Debbah. Artificial neural networks-based machine learning for wireless networks: A tutorial. *IEEE Communications Surveys & Tutorials*, 2019.

[123] Timothy O'Shea and Jakob Hoydis. An introduction to deep learning for the physical layer. *IEEE Transactions on Cognitive Communications and Networking*, 3(4):563–575, 2017.

[124] Tim O'Shea, Kiran Karra, and T Charles Clancy. Learning approximate neural estimators for wireless channel state information. In *2017 IEEE 27th International Workshop on Machine Learning for Signal Processing (MLSP)*, pages 1–7. IEEE, 2017.

[125] Walid Saad, Mehdi Bennis, and Mingzhe Chen. A vision of 6G wireless systems: Applications, trends, technologies, and open research problems. *arXiv preprint arXiv:1902.10265*, 2019.

[126] Ejaz Ahmed and Mubashir Husain Rehmani. Mobile edge computing: opportunities, solutions, and challenges, 2017.

[127] Stefania Sardellitti, Gesualdo Scutari, and Sergio Barbarossa. Joint optimization of radio and computational resources for multicell mobile-edge computing. *IEEE Transactions on Signal and Information Processing over Networks*, 1(2):89–103, 2015.

[128] Hyogi Jung. Cisco visual networking index: Global mobile data traffic forecast update 2010–2015. Technical report, Technical Report, Cisco Systems Inc. 2011. Available online: https://www ..., 2011.

[129] M Bylehn, S Carson, P Cerwall, R Moller, and S Bavertoft. Ericsson mobility report on the pulse of the networked society. *Ericsson, Stockholm, Sweden, Tech. Rep. EAB-14*, 61078, 2016.

[130] Vojislav Gajić, Jianwei Huang, Bixio Rimoldi, et al. Competition of wireless providers for atomic users: Equilibrium and social optimality. In *2009 47th Annual Allerton Conference on Communication, Control, and Computing (Allerton)*, pages 1203–1210. IEEE, 2014.

[131] Prashanth Hande, Mung Chiang, Robert Calderbank, and Junshan Zhang. Pricing under constraints in access networks: Revenue maximization and congestion management. In *2010 Proceedings IEEE INFOCOM*, pages 1–9. IEEE, 2010.

[132] Luca Delgrossi and Domenico Ferrari. Charging schemes for reservation-based networks. *Telecommunication Systems*, 11(1-2):127–137, 1999.

[133] Patrick Loiseau, Galina Schwartz, John Musacchio, and Saurabh Amin. Incentive schemes for internet congestion management: Raffles versus time-of-day pricing. In *2011 49th Annual Allerton Conference on Communication, Control, and Computing (Allerton)*, pages 103–110. IEEE, 2011.

[134] Jeffrey K MacKie-Mason, Liam Murphy, and John Murphy. Responsive pricing in the internet. *Internet Economics*, pages 279–303, 1997.

[135] Richard J Gibbens and Frank P Kelly. Resource pricing and the evolution of congestion control. *Automatica*, 35(12):1969–1985, 1999.

[136] Mohamed M El-Sayed, Ahmed S Ibrahim, and Mohamed M Khairy. Power allocation strategies for non-orthogonal multiple access. In *2016 International Conference on Selected Topics in Mobile & Wireless Networking (MoWNeT)*, pages 1–6. IEEE, 2016.

[137] Fei Liu, Petri Mähönen, and Marina Petrova. Proportional fairness-based user pairing and power allocation for non-orthogonal multiple access. In *2015 IEEE 26th Annual International Symposium on Personal, Indoor, and Mobile Radio Communications (PIMRC)*, pages 1127–1131. IEEE, 2015.

[138] Lei Lei, Di Yuan, Chin Keong Ho, and Sumei Sun. Joint optimization of power and channel allocation with non-orthogonal multiple access for 5G cellular systems. In *2015 IEEE Global Communications Conference (GLOBECOM)*, pages 1–6. IEEE, 2015.

[139] Shamik Sengupta, Mainak Chatterjee, and Samrat Ganguly. An economic framework for spectrum allocation and service pricing with competitive wireless service providers. In *2007 2nd IEEE International Symposium on New Frontiers in Dynamic Spectrum Access Networks*, pages 89–98. IEEE, 2007.

[140] Sajal K Das, Haitao Lin, and Mainak Chatterjee. An econometric model for resource management in competitive wireless data networks. *IEEE Network*, 18(6):20–26, 2004.

[141] Eirini Tsiropoulou, George Kousis, Athina Thanou, Ioanna Lykourentzou, and Symeon Papavassiliou. Quality of experience in cyber-physical social systems based on reinforcement learning and game theory. *Future Internet*, 10(11):108, 2018.

[142] Pavlos Athanasios Apostolopoulos, Eirini Eleni Tsiropoulou, and Symeon Papavassiliou. Demand response management in smart grid networks: A two-stage game-theoretic learning-based approach. *Mobile Networks and Applications*, pages 1–14, 2018.

[143] Georgios Fragkos, Pavlos Athanasios Apostolopoulos, and Eirini Eleni Tsiropoulou. ESCAPE: Evacuation strategy through clustering and autonomous operation in public safety systems. *Future Internet*, 11(1):20, 2019.

[144] Navid Abedini and Srinivas Shakkottai. Content caching and scheduling in wireless networks with elastic and inelastic traffic. *IEEE/ACM Transactions on Networking (TON)*, 22(3):864–874, 2014.

[145] Osman NC Yilmaz, Carl Wijting, Petteri Lundén, and Jyri Hämäläinen. Optimized mobile connectivity for bandwidth-hungry, delay-tolerant cloud services toward 5G. In *2014 11th International Symposium on Wireless Communications Systems (ISWCS)*, pages 6–10. IEEE, 2014.

[146] Ashwin Rao, Arnaud Legout, Yeon-sup Lim, Don Towsley, Chadi Barakat, and Walid Dabbous. Network characteristics of video streaming traffic. In *Proceedings of the Seventh Conference on emerging Networking EXperiments and Technologies*, page 25. ACM, 2011.

[147] William E Halal. Forecasting the technology revolution: Results and learnings from the techcast project. *Technological Forecasting and Social Change*, 80(8):1635–1643, 2013.

[148] Angeliki Alexiou. Wireless world 2020: Radio interface challenges and technology enablers. *IEEE Vehicular Technology Magazine*, 9(1):46–53, 2014.

[149] Stefan Stremersch and Gerard J Tellis. Strategic bundling of products and prices: A new synthesis for marketing. *Journal of Marketing*, 66(1):55–72, 2002.

[150] Yannis Bakos and Erik Brynjolfsson. Bundling information goods: Pricing, profits, and efficiency. *Management Science*, 45(12):1613–1630, 1999.

[151] Panagiotis Vamvakas, Eirini Eleni Tsiropoulou, Symeon Papavassiliou, and John S Baras. Optimization and resource management in NOMA wireless networks supporting real and non-real time service bundling. In *2017 IEEE Symposium on Computers and Communications (ISCC)*, pages 697–703. IEEE, 2017.

[152] Panagiotis Vamvakas, Eirini Eleni Tsiropoulou, and Symeon Papavassiliou. A market-based modular service composition approach for flexibility and adaptability in future wireless networks. In *IEEE INFOCOM 2019 - IEEE Conference on Computer Communications Workshops (INFOCOM WKSHPS)*, pages 252–257, April 2019.

[153] Samson Lasaulce, Merouane Debbah, and Eitan Altman. Methodologies for analyzing equilibria in wireless games. *IEEE Signal Processing Magazine*, 26(5):41–52, 2009.

[154] Melissa A Schilling. Toward a general modular systems theory and its application to interfirm product modularity. *Academy of Management Review*, 25(2):312–334, 2000.

[155] Linglong Dai, Bichai Wang, Yifei Yuan, Shuangfeng Han, I Chih-Lin, and Zhaocheng Wang. Non-orthogonal multiple access for 5G: solutions, challenges, opportunities, and future research trends. *IEEE Communications Magazine*, 53(9):74–81, 2015.

[156] William James Adams and Janet L Yellen. Commodity bundling and the burden of monopoly. *The Quarterly Journal of Economics*, pages 475–498, 1976.

[157] Chenghuan Sean Chu, Phillip Leslie, Alan Sorensen, et al. Bundle-size pricing as an approximation to mixed bundling. *American Economic Review*, 101(1):263, 2011.

[158] Dimitrios Sikeridis, Eirini Eleni Tsiropoulou, Michael Devetsikiotis, and Symeon Papavassiliou. Energy-efficient orchestration in wireless powered internet of things infrastructures. *IEEE Transactions on Green Communications and Networking*, 3(2):317–328, 2018.

[159] Dimitrios Sikeridis, Eirini Eleni Tsiropoulou, Michael Devetsikiotis, and Symeon Papavassiliou. Socio-spatial resource management in wireless powered public safety networks. In *MILCOM 2018-2018 IEEE Military Communications Conference (MILCOM)*, pages 810–815. IEEE, 2018.

[160] Suzhi Bi, Yong Zeng, and Rui Zhang. Wireless powered communication networks: An overview. *IEEE Wireless Communications*, 23(2):10–18, 2016.

[161] Hyungsik Ju and Rui Zhang. Throughput maximization in wireless powered communication networks. *IEEE Transactions on Wireless Communications*, 13(1):418–428, 2013.

[162] Yue Ling Che, Lingjie Duan, and Rui Zhang. Spatial throughput maximization of wireless powered communication networks. *IEEE Journal on Selected Areas in Communications*, 33(8):1534–1548, 2015.

[163] Eirini Eleni Tsiropoulou, Giorgos Mitsis, and Symeon Papavassiliou. Interest-aware energy collection & resource management in machine to machine communications. *Ad Hoc Networks*, 68:48–57, 2018.

[164] Qingqing Wu, Meixia Tao, Derrick Wing Kwan Ng, Wen Chen, and Robert Schober. Energy-efficient resource allocation for wireless powered communication networks. *IEEE Transactions on Wireless Communications*, 15(3):2312–2327, 2015.

[165] Hoon Lee, Kyoung-Jae Lee, Hanjin Kim, Bruno Clerckx, and Inkyu Lee. Resource allocation techniques for wireless powered communication networks. In *2016 IEEE International Conference on Communications (ICC)*, pages 1–6. IEEE, 2016.

[166] Hoon Lee, Kyoung-Jae Lee, Hanjin Kim, Bruno Clerckx, and Inkyu Lee. Resource allocation techniques for wireless powered communication networks with energy storage constraint. *IEEE Transactions on Wireless Communications*, 15(4):2619–2628, 2015.

[167] Hanjin Kim, Hoon Lee, Minki Ahn, Han-Bae Kong, and Inkyu Lee. Joint subcarrier and power allocation methods in full duplex wireless powered communication networks for OFDM systems. *IEEE Transactions on Wireless Communications*, 15(7):4745–4753, 2016.

[168] Eirini Eleni Tsiropoulou, Surya Teja Paruchuri, and John S Baras. Interest, energy and physical-aware coalition formation and resource allocation in smart IoT applications. In *2017 51st Annual Conference on Information Sciences and Systems (CISS)*, pages 1–6. IEEE, 2017.

[169] David Feeny, Fikret Berkes, Bonnie J McCay, and James M Acheson. The tragedy of the commons: twenty-two years later. *Human Ecology*, 18(1):1–19, 1990.

[170] Garrett Hardin. The tragedy of the commons. *Science*, 162(3859):1243–1248, 1968.

[171] Daniel Kahneman and Amos Tversky. Prospect theory: An analysis of decision under risk. In *Handbook of the Fundamentals of Financial Decision Making: Part I*, pages 99–127. World Scientific, 2013.

[172] Ashish R Hota, Siddharth Garg, and Shreyas Sundaram. Fragility of the commons under prospect-theoretic risk attitudes. *Games and Economic Behavior*, 98:135–164, 2016.

[173] Erel Avineri and Piet HL Bovy. Identification of parameters for a prospect theory model for travel choice analysis. *Transportation Research Record*, 2082(1):141–147, 2008.

[174] Qualcomm. Making 5G NR a reality: Leading the technology inventions for a unified, more capable 5G air interface. *White paper*, 2016.

[175] Cisco Visual Networking Index. Global mobile data traffic forecast update, 2016–2021 white paper. *Cisco: San Jose, CA, USA*, 2017.

[176] Cisco Visual Networking Index. Global mobile data traffic forecast update, 2016-2021 white paper [internet].

[177] Haijun Zhang, Xiaoli Chu, Weisi Guo, and Siyi Wang. Coexistence of Wi-Fi and heterogeneous small cell networks sharing unlicensed spectrum. *IEEE Communications Magazine*, 53(3):158–164, 2015.

[178] Thanh Nguyen, Hang Zhou, Randall A Berry, Michael L Honig, and Rakesh Vohra. The impact of additional unlicensed spectrum on wireless services competition. In *New Frontiers in Dynamic Spectrum Access Networks (DySPAN), 2011 IEEE Symposium on*, pages 146–155. Citeseer, 2011.

[179] Danijela Cabrić, Shridhar Mubaraq Mishra, Daniel Willkomm, Robert Brodersen, and Adam Wolisz. A cognitive radio approach for usage of virtual unlicensed spectrum. In *14th IST Mobile and Wireless Communications Summit*. Citeseer, 2005.

[180] Ian F Akyildiz, Won-Yeol Lee, and Kaushik R Chowdhury. Spectrum management in cognitive radio ad hoc networks. *IEEE Network*, 23(4), 2009.

[181] Sima Hajmohammad and Halima Elbiaze. Unlicensed spectrum splitting between femtocell and WiFi. In *Communications (ICC), 2013 IEEE International Conference on*, pages 1883–1888. IEEE, 2013.

[182] Amir Ghasemi and Elvino S Sousa. Collaborative spectrum sensing for opportunistic access in fading environments. In *New Frontiers in Dynamic Spectrum Access Networks, 2005. DySPAN 2005. 2005 First IEEE International Symposium on*, pages 131–136. IEEE, 2005.

[183] Coleman Bazelon. Licensed or unlicensed: The economic considerations in incremental spectrum allocations. *IEEE Communications Magazine*, 47(3), 2009.

[184] Shweta Sagari, Samuel Baysting, Dola Saha, Ivan Seskar, Wade Trappe, and Dipankar Raychaudhuri. Coordinated dynamic spectrum management of LTE-U and Wi-Fi networks. In *2015 IEEE International Symposium on Dynamic Spectrum Access Networks (DySPAN)*, pages 209–220. IEEE, 2015.

[185] Yue Wu, Weisi Guo, Hu Yuan, Long Li, Siyi Wang, Xiaoli Chu, and Jie Zhang. Device-to-device meets LTE-unlicensed. *IEEE Communications Magazine*, 54(5):154–159, 2016.

[186] Taras Maksymyuk, Maryan Kyryk, and Minho Jo. Comprehensive spectrum management for heterogeneous networks in LTE-U. *IEEE Wireless Communications*, 23(6):8–15, 2016.

[187] Ran Zhang, Miao Wang, Lin X Cai, Zhongming Zheng, Xuemin Shen, and Liang-Liang Xie. LTE-unlicensed: the future of spectrum aggregation for cellular networks. *IEEE Wireless Communications*, 22(3):150–159, 2015.

[188] Liang Xiao, Narayan B Mandayam, and H Vincent Poor. Prospect theoretic analysis of energy exchange among microgrids. *IEEE Transactions on Smart Grid*, 6(1):63–72, 2014.

[189] Liang Xiao, Jinliang Liu, Yan Li, Narayan B Mandayam, and H Vincent Poor. Prospect theoretic analysis of anti-jamming communications in cognitive radio networks. In *2014 IEEE Global Communications Conference*, pages 746–751. IEEE, 2014.

[190] Agachai Sumalee, Richard D Connors, and Paramet Luathep. Network equilibrium under cumulative prospect theory and endogenous stochastic demand and supply. In *Transportation and Traffic Theory 2009: Golden Jubilee*, pages 19–38. Springer, 2009.

[191] Song Gao, Emma Frejinger, and Moshe Ben-Akiva. Adaptive route choices in risky traffic networks: A prospect theory approach. *Transportation Research Part C: Emerging Technologies*, 18(5):727–740, 2010.

[192] Tianming Li and Narayan B Mandayam. When users interfere with protocols: Prospect theory in wireless networks using random access and data pricing as an example. *IEEE Transactions on Wireless Communications*, 13(4):1888–1907, 2014.

[193] Junlin Yu, Man Hon Cheung, and Jianwei Huang. Spectrum investment with uncertainty based on prospect theory. In *2014 IEEE International Conference on Communications (ICC)*, pages 1620–1625. IEEE, 2014.

[194] Tianming Li and Narayan B Mandayam. Prospects in a wireless random access game. In *2012 46th Annual Conference on Information Sciences and Systems (CISS)*, pages 1–6. IEEE, 2012.

[195] James M Walker, Roy Gardner, and Elinor Ostrom. Rent dissipation in a limited-access common-pool resource: Experimental evidence. *Journal of Environmental Economics and Management*, 19(3):203–211, 1990.

[196] Pradeep Dubey, Ori Haimanko, and Andriy Zapechelnyuk. Strategic complements and substitutes, and potential games. *Games and Economic Behavior*, 54(1):77–94, 2006.

[197] Yochai Benkler. Open wireless vs. licensed spectrum: Evidence from market adoption. *Harv. JL & Tech.*, 26:69, 2012.

[198] Ericsson Mobility. Ericsson mobility report, 2018.

[199] Zhiguo Ding, Xianfu Lei, George K Karagiannidis, Robert Schober, Jinhong Yuan, and Vijay K Bhargava. A survey on non-orthogonal multiple access for 5G networks: Research challenges and future trends. *IEEE Journal on Selected Areas in Communications*, 35(10):2181–2195, 2017.

[200] Panagiotis Vamvakas, Eirini Eleni Tsiropoulou, and Symeon Papavassiliou. Dynamic provider selection & power resource management in competitive wireless communication markets. *Mobile Networks and Applications*, 23(1):86–99, 2018.

[201] Mohammed Al-Imari, Pei Xiao, Muhammad Ali Imran, and Rahim Tafazolli. Uplink non-orthogonal multiple access for 5G wireless networks. In *2014 11th International Symposium on Wireless Communications Systems (ISWCS)*, pages 781–785. IEEE, 2014.

[202] Boya Di, Siavash Bayat, Lingyang Song, and Yonghui Li. Radio resource allocation for downlink non-orthogonal multiple access (NOMA) networks using matching theory. In *2015 IEEE global communications conference (GLOBECOM)*, pages 1–6. IEEE, 2015.

[203] Eirini Eleni Tsiropoulou, Aggelos Kapoukakis, and Symeon Papavassiliou. Uplink resource allocation in SC-FDMA wireless networks: A survey and taxonomy. *Computer Networks*, 96:1–28, 2016.

[204] Eirini Eleni Tsiropoulou, Aggelos Kapoukakis, and Symeon Papavassiliou. Energy-efficient subcarrier allocation in SC-FDMA wireless networks based on multilateral model of bargaining. In *2013 IFIP Networking Conference*, pages 1–9. IEEE, 2013.

[205] Yashuang Guo, Qinghai Yang, and Kyung Sup Kwak. Quality-oriented rate control and resource allocation in time-varying OFDMA networks. *IEEE Transactions on Vehicular Technology*, 66(3):2324–2338, 2016.

[206] Fahime Khoramnejad, Mehdi Rasti, Hossein Pedram, and Ekram Hossain. On resource management in load-coupled OFDMA networks. *IEEE Transactions on Communications*, 66(5):2295–2311, 2018.

[207] Feifei Zhao, Wenping Ma, Momiao Zhou, and Chengli Zhang. A graph-based QoS-aware resource management scheme for OFDMA femtocell networks. *IEEE Access*, 6:1870–1881, 2017.

[208] Garrett Hardin. Extensions of "the tragedy of the commons". *Science*, 280(5364):682–683, 1998.

[209] Michał Lewandowski. Prospect theory versus expected utility theory: Assumptions, predictions, intuition and modelling of risk attitudes. *Central European Journal of Economic Modelling and Econometrics*, 2017.

[210] Panagiotis Vamvakas, Eirini Eleni Tsiropoulou, and Symeon Papavassiliou. Personalized pricing for efficient user-centric multi-resource control in 5G wireless networks. In *2018 IEEE 19th International Symposium on "A World of Wireless, Mobile and Multimedia Networks"(WoWMoM)*, pages 1–6. IEEE, 2018.

[211] Ning Zhang, Shan Zhang, Shaohua Wu, Ju Ren, Jon W Mark, and Xuemin Shen. Beyond coexistence: Traffic steering in LTE networks with unlicensed bands. *IEEE Wireless Communications*, 23(6):40–46, 2016.

[212] Marcin Dryjanski and Michal Szydelko. A unified traffic steering framework for LTE radio access network coordination. *IEEE Communications Magazine*, 54(7):84–92, 2016.

[213] Ashish R Hota and Shreyas Sundaram. Controlling human utilization of shared resources via taxes. In *2016 IEEE 55th Conference on Decision and Control (CDC)*, pages 6984–6989. IEEE, 2016.

[214] Mattia Rebato, Marco Mezzavilla, Sundeep Rangan, Federico Boccardi, and Michele Zorzi. Understanding noise and interference regimes in 5G millimeter-wave cellular networks. In *European Wireless 2016; 22th European Wireless Conference*, pages 1–5. VDE, 2016.

[215] Sundeep Rangan and Elza Erkip. Millimeter-wave cellular wireless networks: Potentials and challenges. *Proceedings of the IEEE*, 102(3), 2014.

[216] Panagiotis Vamvakas, Eirini Eleni Tsiropoulou, and Symeon Papavassiliou. Dynamic spectrum management in 5G wireless networks: A real-life modeling approach. In *IEEE INFOCOM 2019-IEEE Conference on Computer Communications*, pages 2134–2142. IEEE, 2019.

[217] Lav Gupta, Raj Jain, and Gabor Vaszkun. Survey of important issues in UAV communication networks. *IEEE Communications Surveys & Tutorials*, 18(2):1123–1152, 2015.

[218] Samira Hayat, Evşen Yanmaz, and Raheeb Muzaffar. Survey on unmanned aerial vehicle networks for civil applications: A communications viewpoint. *IEEE Communications Surveys & Tutorials*, 18(4):2624–2661, 2016.

[219] Ali Masood, Navuday Sharma, Muhammad Mahtab Alam, Yannick Le Moullec, Davide Scazzoli, Luca Reggiani, Maurizio Magarini, and Rizwan Ahmad. Device-to-device discovery and localization assisted by UAVs in pervasive public safety networks. In *Proceedings of the ACM MobiHoc workshop on innovative aerial communication solutions for FIrst REsponders network in emergency scenarios*, pages 6–11. ACM, 2019.

[220] Reza Shakeri, Mohammed Ali Al-Garadi, Ahmed Badawy, Amr Mohamed, Tamer Khattab, Abdulla K. Al-Ali, Khaled A. Harras, and Mohsen Guizani. Design challenges of multi-UAV systems in cyber-physical applications: A comprehensive survey, and future directions. *CoRR*, abs/1810.09729, 2018.

[221] Mamta Narang, William Liu, Jairo Gutierrez, and Luca Chiaraviglio. A cyber physical buses-and-drones mobile edge infrastructure for large scale disaster emergency communications. In *2017 IEEE 37th International Conference on Distributed Computing Systems Workshops (ICDCSW)*, pages 53–60. IEEE, 2017.

[222] Mark Zuckerberg. The technology behind Aquila. *Available: https://www.facebook.com/notes/mark-zuckerberg/the-technology-behind-aquila/10153916136506634/*, 2016. accessed on Apr. 22, 2019.

[223] Alastair Westgarth. Turning on Project Loon in Puerto Rico. *Available: https://blog.x.company/turning-on-project-loon-in-puerto-rico-f3aa41ad2d7f.* accessed on Apr. 22, 2019.

[224] Rongfei Fan, Jiannan Cui, Song Jin, Kai Yang, and Jianping An. Optimal node placement and resource allocation for UAV relaying network. *IEEE Communications Letters*, 22(4):808–811, 2018.

[225] John Dunlop, Demessie Girma, and James Irvine. *Digital mobile communications and the TETRA system*. John Wiley & Sons, 2013.

[226] Pete Lunness. P25 radio systems training guide. *TG-001*, pages 1–74 (available at: https://www.dvsinc.com/papers/p25_training_guide.pdf), 2007.

[227] Abhaykumar Kumbhar, Farshad Koohifar, Ismail Güvenç, and Bruce Mueller. A survey on legacy and emerging technologies for public safety communications. *IEEE Comm. Surveys & Tutorials*, 19(1):97–124, 2017.

[228] Dimitrios Sikeridis, Eirini Eleni Tsiropoulou, Michael Devetsikiotis, and Symeon Papavassiliou. Context-aware wireless-protocol selection in heterogeneous public safety networks. *IEEE Transactions on Vehicular Technology*, 68(2):2009–2013, 2018.

[229] E Tsiropoulou, K Koukas, and S Papavassiliou. A socio-physical and mobility-aware coalition formation mechanism in public safety networks. *EAI Endorsed Trans. Future Internet*, 4:154176, 2018.

[230] Jaeuk Baek, Sang Ik Han, and Youngnam Han. Optimal resource allocation for non-orthogonal transmission in UAV relay systems. *IEEE Wireless Communications Letters*, 7(3):356–359, 2018.

[231] Meng Hua, Chunguo Li, Yongming Huang, and Luxi Yang. Throughput maximization for UAV-enabled wireless power transfer in relaying system. In *2017 9th International Conference on Wireless Communications and Signal Processing (WCSP)*, pages 1–5. IEEE, 2017.

[232] Roberto Verdone and Silvia Mignardi. Joint aerial-terrestrial resource management in UAV-aided mobile radio networks. *IEEE Network*, 32(5):70–75, 2018.

[233] Sixing Yin, Zhaowei Qu, and Lihua Li. Uplink resource allocation in cellular networks with energy-constrained UAV relay. In *2018 IEEE 87th Vehicular Technology Conference (VTC Spring)*, pages 1–5. IEEE, 2018.

[234] Dasun Athukoralage, Ismail Guvenc, Walid Saad, and Mehdi Bennis. Regret based learning for UAV assisted LTE-U/WiFi public safety networks. In *2016 IEEE Global Communications Conference (GLOBECOM)*, pages 1–7. IEEE, 2016.

[235] Mohammad Mozaffari, Walid Saad, Mehdi Bennis, and Mérouane Debbah. Unmanned aerial vehicle with underlaid device-to-device communications: Performance and tradeoffs. *IEEE Transactions on Wireless Communications*, 15(6):3949–3963, 2016.

[236] Dimitrios Sikeridis, Eirini Eleni Tsiropoulou, Michael Devetsikiotis, and Symeon Papavassiliou. Wireless powered public safety IoT: A UAV-assisted adaptive-learning approach towards energy efficiency. *Journal of Network and Computer Applications*, 123:69–79, 2018.

[237] Dimitrios Sikeridis, Eirini Eleni Tsiropoulou, Michael Devetsikiotis, and Symeon Papavassiliou. Self-adaptive energy efficient operation in UAV-assisted public safety networks. In *2018 IEEE 19th International Workshop on Signal Processing Advances in Wireless Communications (SPAWC)*, pages 1–5. IEEE, 2018.

[238] Dimitrios Sikeridis, Eirini Eleni Tsiropoulou, Michael Devetsikiotis, and Symeon Papavassiliou. Socio-spatial resource management in wireless powered public safety networks. In *MILCOM 2018-2018 IEEE Military Communications Conference (MILCOM)*, pages 810–815. IEEE, 2018.

[239] Panagiotis Vamvakas, Eirini Eleni Tsiropoulou, and Symeon Papavassiliou. Risk-aware resource management in public safety networks. *Sensors*, 19(18):3853, 2019.

[240] Panagiotis Vamvakas, Eirini Eleni Tsiropoulou, and Symeon Papavassiliou. On the prospect of UAV-assisted communications paradigm in public safety networks. In *IEEE INFOCOM 2019 - IEEE Conference on Computer Communications Workshops (INFOCOM WKSHPS)*, pages 762–767, April 2019.

[241] Milan Erdelj, Osamah Saif, Enrico Natalizio, and Isabelle Fantoni. UAVs that fly forever: Uninterrupted structural inspection through automatic UAV replacement. *Ad Hoc Networks*, 2017.

[242] Milan Erdelj, Enrico Natalizio, Kaushik R Chowdhury, and Ian F Akyildiz. Help from the sky: Leveraging UAVs for disaster management. *IEEE Pervasive Computing*, 16(1):24–32, 2017.

[243] Anibal Sanjab, Walid Saad, and Tamer Başar. Prospect theory for enhanced cyber-physical security of drone delivery systems: A network interdiction game. In *2017 IEEE International Conference on Communications (ICC)*, pages 1–6. IEEE, 2017.

[244] Anibal Sanjab, Walid Saad, and Tamer Başar. A game of drones: Cyber-physical security of time-critical UAV applications with cumulative prospect theory perceptions and valuations. *arXiv preprint arXiv:1902.03506*, 2019.

[245] Mohammad Mozaffari, Walid Saad, Mehdi Bennis, and Mérouane Debbah. Mobile unmanned aerial vehicles (UAVs) for energy-efficient internet of things communications. *IEEE Transactions on Wireless Communications*, 16(11):7574–7589, 2017.

[246] Shams Rahman and You-Ze Cho. UAV positioning for throughput maximization. *EURASIP Journal on Wireless Communications and Networking*, 2018(1):31, 2018.

[247] Eirini Eleni Tsiropoulou, John S Baras, Symeon Papavassiliou, and Gang Qu. On the mitigation of interference imposed by intruders in passive RFID networks. In *International Conference on Decision and Game Theory for Security*, pages 62–80. Springer, 2016.

[248] Adam Rawnsley. Iran's alleged drone hack: Tough, but possible. *Available: http://www.wired.com/dangerroom/2011/12/irandrone-hack-gps.* accessed on Apr. 22, 2019.

[249] Chaitanya Rani, Hamidreza Modares, Raghavendra Sriram, Dariusz Mikulski, and Frank L Lewis. Security of unmanned aerial vehicle systems against cyber-physical attacks. *The Journal of Defense Modeling and Simulation*, 13(3):331–342, 2016.

[250] Kim Hartmann and Christoph Steup. The vulnerability of UAVs to cyber attacks-an approach to the risk assessment. In *2013 5th international conference on cyber conflict (CYCON 2013)*, pages 1–23. IEEE, 2013.

[251] Thomas Lagkas, Vasileios Argyriou, Stamatia Bibi, and Panagiotis Sarigiannidis. UAV IoT framework views and challenges: Towards protecting drones as "things". *Sensors*, 18(11):4015, 2018.

[252] Hichem Sedjelmaci, Sidi Mohammed Senouci, and Nirwan Ansari. Intrusion detection and ejection framework against lethal attacks in UAV-aided networks: A bayesian game-theoretic methodology. *IEEE Transactions on Intelligent Transportation Systems*, 18(5):1143–1153, 2016.

[253] Sourabh Bhattacharya and Tamer Başar. Game-theoretic analysis of an aerial jamming attack on a UAV communication network. In *Proceedings of the 2010 American Control Conference*, pages 818–823. IEEE, 2010.

[254] Hichem Sedjelmaci, Sidi Mohammed Senouci, and Nirwan Ansari. A hierarchical detection and response system to enhance security against lethal cyber-attacks in UAV networks. *IEEE Transactions on Systems, Man, and Cybernetics: Systems*, 48(9):1594–1606, 2017.

[255] Zachary Birnbaum, Andrey Dolgikh, Victor Skormin, Edward O'Brien, Daniel Muller, and Christina Stracquodaine. Unmanned aerial vehicle security using behavioral profiling. In *2015 International Conference on Unmanned Aircraft Systems (ICUAS)*, pages 1310–1319. IEEE, 2015.

[256] Gaurav Choudhary, Vishal Sharma, Ilsun You, Kangbin Yim, Ray Chen, and Jin-Hee Cho. Intrusion detection systems for networked unmanned aerial vehicles: A survey. In *2018 14th International Wireless Communications & Mobile Computing Conference (IWCMC)*, pages 560–565. IEEE, 2018.

[257] Mbazingwa E Mkiramweni, Chungang Yang, Jiandong Li, and Zhu Han. Game-theoretic approaches for wireless communications with unmanned aerial vehicles. *IEEE Wireless Communications*, 25(6):104–112, 2018.

[258] Kamran Etemad, Vivek Gupta, Nageen Himayat, and Shilpa Talwar. Opportunistic carrier aggregation for dynamic flow switching between radio access technologies, August 25 2015. US Patent 9,119,154.

[259] Boeing Insitu ScanEagle. *Available: https://www.insitu.com/information-delivery/hardware2*, 2019. Accessed on Aug. 14, 2019.

[260] Aerovel. About the flexrotor unmanned aerial system. *Available: https://aerovel.com/flexrotor/*, 2019. Accessed on Aug. 14, 2019.

[261] AeroVironment RQ-11 Raven. *Available: https://www.avinc.com/uas/view/raven*, 2019. Accessed on Aug. 14, 2019.

[262] WASP AE Micro Air Vehicle. *Available: https://www.avinc.com/uas/view/wasp*, 2019. Accessed on Aug. 14, 2019.

[263] Tham Luang cave rescue - wikipedia. https://en.wikipedia.org/wiki/Tham_Luang_cave_rescue. (Accessed on 09/14/2019).

[264] Panagiotis Vamvakas, Eirini Eleni Tsiropoulou, and Symeon Papavassiliou. Risk-aware resource control with flexible 5G access technology interfaces. In *2019 IEEE 20th International Symposium on "A World of Wireless, Mobile and Multimedia Networks" (WoWMoM)*, pages 1–9, June 2019.

[265] RL Hughes. The flow of large crowds of pedestrians. *Mathematics and Computers in Simulation*, 53(4-6):367–370, 2000.

[266] Ansgar Kirchner, Katsuhiro Nishinari, and Andreas Schadschneider. Friction effects and clogging in a cellular automaton model for pedestrian dynamics. *Physical Review E*, 7(5):1–10, 2003.

[267] DR Parisi and CO Dorso. Microscopic dynamics of pedestrian evacuation. *Physica A: Statistical Mechanics and its Applications*, 354:606–618, 2005.

[268] Serge Hoogendoorn and Piet HL Bovy. Simulation of pedestrian flows by optimal control and differential games. *Optimal Control Applications and Methods*, 24(3):153–172, 2003.

[269] Catherine E Amiot, Roxane De la Sablonniere, Deborah J Terry, and Joanne R Smith. Integration of social identities in the self: Toward a cognitive-developmental model. *Personality and Social Psychology Review*, 11(4):364–388, 2007.

[270] Chris Cocking, John Drury, and Steve Reicher. The psychology of crowd behaviour in emergency evacuations: Results from two interview studies and implications for the fire and rescue services. *The Irish Journal of Psychology*, 30(1-2):59–73, 2009.

[271] Herbert H Tsang, Andrew J Park, Mengting Sun, and Uwe Glässer. Genius: A computational modeling framework for counter-terrorism planning and response. In *2010 IEEE International Conference on Intelligence and Security Informatics*, pages 71–76. IEEE, 2010.

[272] Dirk Helbing, Lubos Buzna, Anders Johansson, and Torsten Werner. Self-organized pedestrian crowd dynamics: Experiments, simulations, and design solutions. *Transportation science*, 39(1):1–24, 2005.

[273] Serge P Hoogendoorn and Winnie Daamen. Pedestrian behavior at bottlenecks. *Transportation science*, 39(2):147–159, 2005.

[274] Dirk Helbing and Anders Johansson. Pedestrian, crowd and evacuation dynamics. In *Encyclopedia of Complexity and Systems Science*, pages 6476–6495. Springer, 2009.

[275] Mamta Agiwal, Abhishek Roy, and Navrati Saxena. Next generation 5G wireless networks: A comprehensive survey. *IEEE Communications Surveys & Tutorials*, 18(3):1617–1655, 2016.

[276] Panagiotis Vamvakas, Eirini Eleni Tsiropoulou, and Symeon Papavassiliou. On controlling spectrum fragility via resource pricing in 5G wireless networks. *IEEE Networking Letters*, 2019.

[277] Eirini Eleni Tsiropoulou, Iakovos Gialagkolidis, Panagiotis Vamvakas, and Symeon Papavassiliou. Resource allocation in visible light communication networks: NOMA vs OFDMA transmission techniques. In *International Conference on Ad-Hoc Networks and Wireless*, pages 32–46. Springer, 2016.

[278] Panagiotis Vamvakas, Eirini Eleni Tsiropoulou, Marinos Vomvas, and Symeon Papavassiliou. Adaptive power management in wireless powered communication networks: A user-centric approach. In *2017 IEEE 38th Sarnoff Symposium*, pages 1–6. IEEE, 2017.

[279] Pavlos Athanasios Apostolopoulos, Eirini Eleni Tsiropoulou, and Symeon Papavassiliou. Game-theoretic learning-based QoS satisfaction in autonomous mobile edge computing. In *2018 Global Information Infrastructure and Networking Symposium (GIIS)*, pages 1–5. IEEE, 2018.

[280] Giorgos Mitsis, Pavlos Athanasios Apostolopoulos, Eirini Eleni Tsiropoulou, and Symeon Papavassiliou. Intelligent dynamic data offloading in a competitive mobile edge computing market. *Future Internet*, 11(5):118, 2019.

[281] Yuyi Mao, Changsheng You, Jun Zhang, Kaibin Huang, and Khaled B Letaief. A survey on mobile edge computing: The communication perspective. *IEEE Communications Surveys & Tutorials*, 19(4):2322–2358, 2017.

[282] Pavel Mach and Zdenek Becvar. Mobile edge computing: A survey on architecture and computation offloading. *IEEE Communications Surveys & Tutorials*, 19(3):1628–1656, 2017.

[283] Georgios Katsinis, Eirini Tsiropoulou, and Symeon Papavassiliou. Multicell interference management in device to device underlay cellular networks. *Future Internet*, 9(3):44, 2017.

[284] Georgios Katsinis, Eirini Eleni Tsiropoulou, and Symeon Papavassiliou. Joint resource block and power allocation for interference management in device to device underlay cellular networks: A game theoretic approach. *Mobile Networks and Applications*, 22(3):539–551, 2017.

[285] Georgios Katsinis, Eirini Eleni Tsiropoulou, and Symeon Papavassiliou. A game theoretic approach to the power control in D2D communications underlay cellular networks. In *2014 IEEE 19th International Workshop on Computer Aided Modeling and Design of Communication Links and Networks (CAMAD)*, pages 208–212. IEEE, 2014.

[286] Georgios Katsinis, Eirini Eleni Tsiropoulou, and Symeon Papavassiliou. On the problem of resource allocation and system capacity evaluation via a blocking queuing model in D2D enabled overlay cellular networks. In *International Conference on Ad-Hoc Networks and Wireless*, pages 76–89. Springer, 2015.

[287] Georgios Katsinis, Eirini Eleni Tsiropoulou, and Symeon Papavassiliou. On the performance evaluation of distributed resource block and power allocation in D2D-enabled multi-cell networks. In *Proceedings of the 14th ACM Symposium on Performance Evaluation of Wireless Ad Hoc, Sensor, & Ubiquitous Networks*, pages 77–84. ACM, 2017.

[288] Monowar Hasan, Ekram Hossain, and Dusit Niyato. Random access for machine-to-machine communication in LTE-advanced networks: Issues and approaches. *IEEE Communications Magazine*, 51(6):86–93, 2013.

[289] Klaus Doppler, Mika Rinne, Carl Wijting, Cássio B Ribeiro, and Klaus Hugl. Device-to-device communication as an underlay to LTE-advanced networks. *IEEE Communications Magazine*, 47(12):42–49, 2009.

[290] Dr Simmi Dutta, Kameshwar Sharma, Naman Gupta, and Tenzen Lovedon Bodh. Li-Fi (light fidelity)-a new paradigm in wireless communication. *International Journal of Innovative Research in Computer and Communication Engineering*, 1(8), 2013.

[291] Athina Thanou, Eirini Eleni Tsiropoulou, and Symeon Papavassiliou. Quality of experience under a prospect theoretic perspective: A cultural heritage space use case. *IEEE Transactions on Computational Social Systems*, 6(1):135–148, 2019.

[292] Pavlos Athanasios Apostolopoulos, Marcos Torres, and Eirini Eleni Tsiropoulou. Satisfaction-aware data offloading in surveillance systems. In *Proceedings of the 14th Workshop on Challenged Networks*, pages 21–26. ACM, 2019.

[293] Nathan Patrizi, Pavlos Athanasios Apostolopoulos, Kelly Rael, and Eirini Eleni Tsiropoulou. Socio-physical human orchestration in smart cities. In *2019 IEEE International Conference on Smart Computing (SMARTCOMP)*, pages 115–120. IEEE, 2019.

[294] My T Thai, Weili Wu, and Hui Xiong. *Big Data in Complex and Social Networks*. CRC Press, 2016.

[295] Dusit Niyato, Dinh Thai Hoang, Nguyen Cong Luong, Ping Wang, Dong In Kim, and Zhu Han. Smart data pricing models for the internet of things: a bundling strategy approach. *IEEE Network*, 30(2):18–25, 2016.

[296] Faisal Tariq, Muhammad Khandaker, Kai-Kit Wong, Muhammad Imran, Mehdi Bennis, and Merouane Debbah. A speculative study on 6G. *arXiv preprint arXiv:1902.06700*, 2019.

[297] Emilio Calvanese Strinati, Sergio Barbarossa, José Luis Gonzalez-Jimenez, Dimitri Kténas, Nicolas Cassiau, and Cédric Dehos. 6G: The next frontier. *arXiv preprint arXiv:1901.03239*, 2019.

[298] Michail Fasoulakis, Eirini Eleni Tsiropoulou, and Symeon Papavassiliou. Satisfy instead of maximize: Improving operation efficiency in wireless communication networks. *Computer Networks*, 159:135–146, 2019.

[299] Michail Fasoulakis, Eirini-Eleni Tsiropoulou, and Symeon Papavassiliou. A new theoretical evaluation framework for satisfaction equilibria in wireless networks. *arXiv preprint arXiv:1806.01905*, 2018.

[300] Edward A Lee. Cyber physical systems: Design challenges. In *2008 11th IEEE International Symposium on Object and Component-Oriented Real-Time Distributed Computing (ISORC)*, pages 363–369. IEEE, 2008.

[301] Milan Erdelj and Enrico Natalizio. UAV-assisted disaster management: Applications and open issues. In *2016 International Conference on Computing, Networking and Communications (ICNC)*, pages 1–5. IEEE, 2016.

[302] Yuanyuan Yang, Cong Wang, and Ji Li. Wireless rechargeable sensor networks—current status and future trends. *Journal of Communications*, 10(9):696–706, 2015.